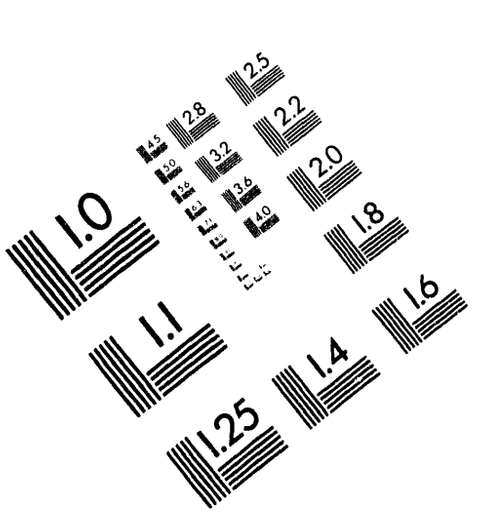

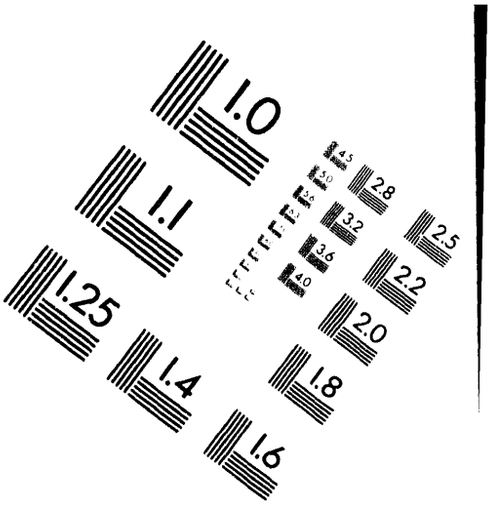

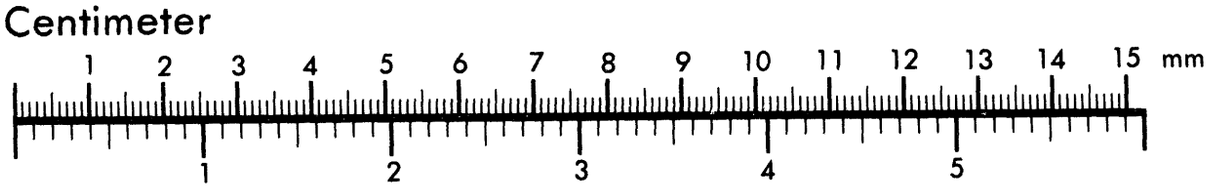

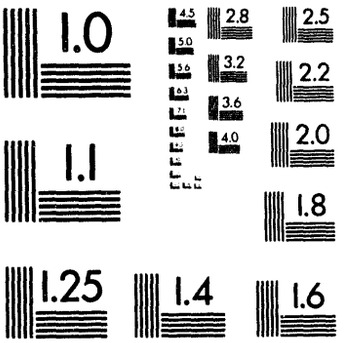

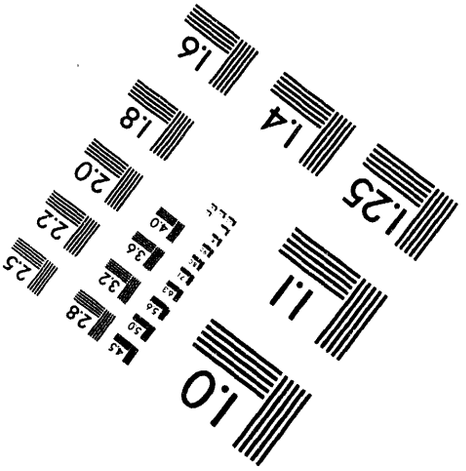

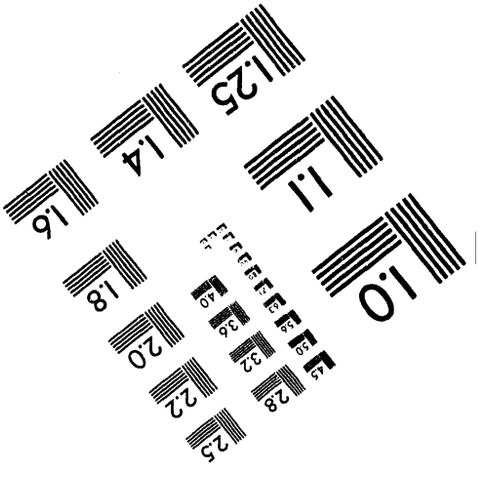

AIIM

Association for Information and Image Management

1100 Wayne Avenue, Suite 1100
Silver Spring, Maryland 20910
301/587-8202

MANUFACTURED TO AIIM STANDARDS
BY APPLIED IMAGE, INC.

1 of 5

EGG-WM-8773

Radioactive Waste Management Complex Low-Level Waste Radiological Performance Assessment

Steven J. Maheras
Arthur S. Rood
Swen O. Magnuson
Mary E. Sussman
Rajiv N. Bhatt

Published April 1994

Idaho National Engineering Laboratory
EG&G Idaho, Inc.
Idaho Falls, Idaho 83415

Prepared for the
U.S. Department of Energy
Office of Environmental Restoration and Waste Management
Under DOE Idaho Operations Office
Contract DE-AC07-76ID01570

ABSTRACT

This report documents the projected radiological dose impacts associated with the disposal of radioactive low-level waste at the Radioactive Waste Management Complex at the Idaho National Engineering Laboratory. This radiological performance assessment was conducted to evaluate compliance with applicable radiological criteria of the U.S. Department of Energy and the U.S. Environmental Protection Agency for protection of the public and the environment. The calculations involved modeling the transport of radionuclides from buried waste, to surface soil and subsurface media, and eventually to members of the public via air, groundwater, and food chain pathways. Projections of doses were made for both offsite receptors and individuals inadvertently intruding onto the site after closure. In addition, uncertainty and sensitivity analyses were performed. The results of the analyses indicate compliance with established radiological criteria and provide reasonable assurance that public health and safety will be protected.

EXECUTIVE SUMMARY

This report documents the projected radiological dose impacts associated with the disposal of radioactive low-level waste (LLW) at the Idaho National Engineering Laboratory (INEL) Radioactive Waste Management Complex (RWMC). The impacts were compared with applicable radiological dose criteria of the U.S. Department of Energy (DOE) and the U.S. Environmental Protection Agency (EPA).

The LLW radiological performance assessment for the RWMC presents a comprehensive, systematic analysis of the long-term impacts of LLW disposal in an arid, near-surface environment. Occupational radiological doses and impacts of nonradioactive hazardous constituents are beyond the scope of this radiological performance assessment and will be considered in other assessments.

For the purpose of assessing the performance of LLW disposed of at the RWMC, three time periods are of concern:

1. The operational period, 1984 through 2020, during which radioactive waste is actively disposed of at the facility.

2. The institutional period, 2021 through 2120, which follows site closure and during which periodic maintenance and monitoring activities are conducted. The facility is assumed to be closed, stabilized, and maintained but is still part of the INEL reservation and is fenced and patrolled.

3. The post-institutional period, from 2120 to the future, during which the facility is no longer maintained by the DOE and may be accessible to the public.

Two receptor types were assessed. The first was a member of the public. During the operational and institutional periods this individual resided at the INEL Site boundary. During the post-institutional control period, the member of the public resided 100 m from the RWMC Subsurface Disposal Area (SDA) boundary.

The second type of receptor evaluated was an intruder. This hypothetical receptor was assumed to inadvertently intrude onto the RWMC SDA during the post-institutional control period. Two general kinds of intruder scenarios were evaluated. The first was a chronic exposure scenario, which included an agricultural scenario and a radon scenario. In the agricultural scenario, the receptor obtained a portion of their food from farming at the RWMC SDA and used water from a well drilled at the edge of the waste. In the radon scenario, the receptor excavated a basement and was exposed to radon and its short-lived progeny that diffused through the basement foundation. The second was an acute exposure scenario, which included a construction scenario and a well-drilling scenario. In the acute construction scenario, the receptor was an individual who built a house at the RWMC SDA and was exposed to contaminated soil while excavating a basement. In the well-drilling scenario, the receptor was exposed to contaminated drill cuttings that are spread over the ground.

The performance assessment process consists of conceptual models that link radionuclide inventory, release (or source term), environmental transfer, and impact assessment (see Figure ES-1) and culminate in radiological doses to receptors. The waste inventory used in the performance assessment was derived from the Radioactive Waste Management Information System (RWMIS) and consists of the LLW buried since 1984 and LLW projected for future disposal through 2020. Transuranic (TRU) waste and LLW intermixed with TRU waste that was buried before 1984 were not included because they are planned for assessment by the Environmental Restoration Program. Where possible, site-specific data and parameters were used in the analyses.

Results of the monitoring, special studies, and modeling efforts to date indicate that the greatest potential for transport of radionuclides from the RWMC to offsite receptors (now and in the future) is via airborne transport of resuspended contaminated near-surface soil particles from biointrusion and groundwater transport of radionuclides leached from buried waste. For this reason, the performance assessment focuses on these two transport pathways for members of the public.

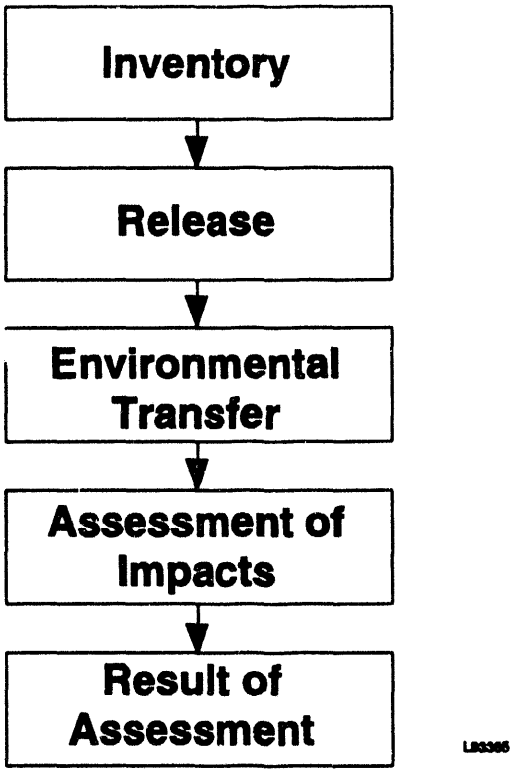

Figure ES-1. Performance assessment process.

The exposure pathways evaluated include ingestion of contaminated food and water, inhalation of contaminated airborne particulates, and external exposure to radionuclides in the air and on the ground (or soil) surface. The agricultural products consumed by members of the public are contaminated via food chain transport of radionuclides deposited from air onto soil or plant surfaces or from irrigation water.

The source of radionuclides for airborne transport was biointrusion by plant roots and harvester ants. Radioactivity was brought to the surface by plant roots and harvester ants and dispersed downwind to a receptor. The GENII computer code was used to calculate the dose to the offsite receptor using annual average atmospheric dispersion conditions. Radioactive progeny were included in the calculations.

The GWSCREEN and PORFLOW computer codes were used to determine the impacts of subsurface migration of radionuclides. For purposes of simplifying

the transport calculations, the RWMC was assumed to be an area source of uniform thickness in which the waste was uniformly mixed with the backfill. The waste was assumed to be released from waste containers or waste forms and leach at an exponentially decreasing rate into the unsaturated zone beneath the RWMC as a result of a low constant moisture infiltration. Radionuclides were assumed to migrate through the unsaturated zone, reach the aquifer, and be transported to a downgradient receptor. Physical processes, such as decay and sorption, were allowed to reduce or slow this downward movement of radionuclides.

This representation of subsurface transport is undoubtedly greatly simplified over the true processes that occur, reflecting the lack of definitive understanding of water movement in the subsurface beneath the RWMC. As a result, the predictive concentrations used in this radiological performance assessment are affected by the uncertainties regarding these processes. Site-specific data were used where available, and conservative assumptions were made where the processes were uncertain, such as the use of a constant infiltration rate that maximizes waste release and a relatively instantaneous water travel time through fractured basalt. The assumptions represent our best current professional opinion and are used as such. The results of this radiological performance assessment analyses are, thus, more likely to overestimate rather than underestimate doses. Periodic review and revision of this radiological performance assessment is planned to incorporate new data from future studies concerning subsurface water movement.

The results of the groundwater, atmospheric, and inadvertent intruder analyses indicate compliance with the performance objectives shown in Table ES-1. The highest dose contributor for members of the public was through the groundwater pathway. The groundwater dose is dominated by C-14, H-3, and I-129, with peak dose occurring at approximately year 2160. The results for the performance assessment analyses provide reasonable assurance that public health and safety will be protected.

Table ES-1. Regulatory requirements and performance assessment results.

Regulatory requirement	Limit	RWMC performance
Protection of the public Air (40 CFR 61)	10 mrem/yr	0.86 mrem/yr
Protection of the public All pathways but air (DOE Order 5820.2A)	25 mrem/yr	0.57 mrem/yr during operational and institutional control 17 mrem/yr during post-institutional control
Inadvertent intrusion Chronic (DOE Order 5820.2A)	100 mrem/yr	**Soil vaults** 53 mrem/yr direct contact 17 mrem/yr groundwater all pathways 4.5 mrem/yr radon 75 mrem/yr total **Pits** 28 mrem/yr direct contact 12 mrem/yr groundwater all pathways 12 mrem/yr radon 52 mrem/yr total
Inadvertent intrusion Acute (DOE Order 5820.2A)	500 mrem	190 mrem (soil vaults) 11 mrem (pits)
Public Drinking Water (40 CFR 141)	4 mrem/yr	0.2 mrem/yr
	15 pCi/L (adjusted alpha)	0.035 pCi/L

CONTENTS

FIGURES

TABLES

ACRONYMS AND INITIALISMS

AEC	Atomic Energy Commission
ALARA	as low as reasonably achievable
ANC	Aerojet Nuclear Company
ANL-E	Argonne National Laboratory-East
ANL-W	Argonne National Laboratory-West
ATR	Advanced Test Reactor
BWR	boiling water reactor
CERCLA	Comprehensive Environmental Response, Compensation, and Liability Act
CEDE	committed effective dose equivalent
CFA	Central Facilities Area
CFR	Code of Federal Regulations
CR	concentration ratio
DCF	dose conversion factor
DCG	derived concentration guide
DOE	U.S. Department of Energy
DOE-ID	U.S. Department of Energy Idaho Operations Office
EBR-I	Experimental Breeder Reactor No. 1
EDE	effective dose equivalent
EPA	U.S. Environmental Protection Agency
ESRP	Eastern Snake River Plain
FFA/CO	Federal Facilities Agreement and Consent Order
ICPP	Idaho Chemical Processing Plant
ICRP	International Commission on Radiological Protection
ILTSF	Intermediate Level Transuranic Storage Facility
INC	Idaho Nuclear Corporation
INEL	Idaho National Engineering Laboratory
ISU	Idaho State University
LLW	low-level waste
MAP	mixed activation products
MFP	mixed fission products
MLLWDF	Mixed and Low-Level Waste Disposal Facility
NEA	Nuclear Energy Agencies
NESHAP	National Emission Standards for Hazardous Air Pollutants
NOAA	National Oceanic and Atmospheric Administration
NRC	U.S. Nuclear Regulatory Commission
NRF	Naval Reactor Facilities
OSCC	outer shim control cylinder
PWR	pressurized water reactor
RESP	Radiological Environmental Surveillance Program
RCRA	Resource Conservation and Recovery Act

RESL	Radiological and Environmental Sciences Laboratory
RWMC	Radioactive Waste Management Complex
RWMIS	Radioactive Waste Management Information System
SDA	Subsurface Disposal Area
SWEPP	Stored Waste Examination Pilot Plant
TLD	thermoluminescent dosimeter
TSA	Transuranic Storage Area
TRA	Test Reactor Area
TRU	transuranic
USDA	U.S. Department of Agriculture
USGS	U.S. Geological Survey
WAC	Waste Acceptance Criteria
WAG	Waste Area Group
WERF	Waste Experimental Reduction Facility
WVRF	Waste Volume Reduction Facility

RADIOACTIVE WASTE MANAGEMENT COMPLEX
LOW-LEVEL WASTE RADIOLOGICAL PERFORMANCE ASSESSMENT

1. INTRODUCTION

1.1 Purpose and Scope

This report documents the projected radiological dose impacts associated with the disposal of low-level radioactive waste (LLW) at the Radioactive Waste Management Complex (RWMC) at the Idaho National Engineering Laboratory (INEL). The projected effects are used to demonstrate compliance with applicable radiological dose criteria of the U.S. Department of Energy (DOE) and the U.S. Environmental Protection Agency (EPA) for protection of the public and the environment. The radiological performance assessment is being conducted to fulfill the requirements of DOE Order 5820.2A, "Radioactive Waste Management" (DOE 1988a).

A performance assessment is "a systematic analysis of the potential risks posed by waste management systems to the public and environment, and a comparison of those risks to established performance objectives" (DOE 1988a). Performance objectives include public and intruder radiological dose limits and drinking water radiological dose limits established by DOE orders and EPA requirements. In the context of this radiological performance assessment, the waste management system consists of the disposed LLW, the LLW disposal facility, and its environs. This radiological performance assessment is a tool used to predict the potential environmental consequences of the LLW disposal facility; its intent is to determine whether waste management activities will accomplish the goal of effectively containing LLW. This goal is accomplished if compliance with performance objectives is demonstrated in the performance assessment.

The LLW radiological performance assessment for the RWMC presents a comprehensive, systematic analysis of the long-term impacts of LLW disposal in an arid near-surface environment. Related assessment activities (e.g., safety assessments, risk assessments, characterizations for siting or construction, engineering evaluations, and cost/design studies) are outside the scope of this document. Potential radiological doses to workers at the RWMC are not

assessed in this document. Although occupational doses to workers are an important area of concern for facility operations, they are covered by regulations and guidance different than those covering performance assessments. Furthermore, compliance with occupational criteria is not necessarily demonstrated by the type of calculations performed for radiological performance assessments. Additionally, this document excludes the potential impacts of chemical toxicity of radiological constituents and nonradiological hazardous constituents that may be in the waste.

Waste has been buried in the Subsurface Disposal Area (SDA) since 1952 in trenches, pits, and soil vault rows. LLW buried since 1984 and projected for the future are assessed in this report. Buried transuranic (TRU) waste, stored TRU waste, and buried commingled TRU and LLW are not included in the report. Although DOE Order 5820.2A applies only to LLW disposed of after September 26, 1988, LLW disposed of before this date was included in the radiological performance assessment. The Environmental Restoration Program at the INEL will assess waste buried in the SDA from 1952 through 1983 in accordance with the National Contingency Plan under the Comprehensive Environmental Response, Compensation, and Liability Act (CERCLA). The year 1983 was selected as the cutoff date for waste to be assessed under CERCLA because waste containing the hazardous materials mercury and cadmium were disposed of in the SDA as late as June 1983. Therefore, the trenches, pits, and soil vault rows that were open before this date could potentially contain mixed waste, which falls under the domain of the Environmental Restoration Program and will be assessed under CERCLA.

Because it is impractical to remediate only part of a pit or soil vault row, all waste buried in Pit 16 and Soil Vault Row 13 will be assessed under CERCLA even though Pit 16 closed October 25, 1984, and Soil Vault Row 13 closed on December 21, 1984. Soil Vault Row 14 opened on October 16, 1984, and Pit 17 opened on May 5, 1984; they should only contain LLW, not the mixed waste described previously. Therefore, Soil Vault Row 14 and Pit 17 (1984) are a logical point from which to begin the radiological performance assessment, and it provides an effective point of interface with the Environmental Restoration Program. This will ensure that all waste is accounted for either in the radiological performance assessment performed

under DOE Order 5820.2A or in the baseline risk assessments performed under CERCLA.

The remainder of this introductory section provides background information relating to the RWMC and regulations, guidelines, and criteria (i.e., performance objectives) applicable to the LLW radiological performance assessment of the RWMC.

1.2 General Description of the RWMC

The INEL is a DOE facility occupying approximately 2,315 km^2 of land in southeastern Idaho (see Figure 1-1). Activities conducted at the INEL primarily involve nuclear research and development projects and experiments. The RWMC is one of several waste management facilities at the INEL; it is the only operating LLW disposal area for solid radioactive wastes at the INEL.

The RWMC provides a near surface disposal site for solid LLW generated almost exclusively by INEL activities. The RWMC opened in 1952 near the southwestern corner of the INEL Site (see Figure 1-1). The initial tract of land used as a burial ground for radioactive waste was 13 acres. This tract became the SDA and was later expanded to 97 acres. In 1970, the 58-acre Transuranic Storage Area (TSA) was added to the RWMC. Over the years, service and operations buildings have been constructed. The SDA and TSA are surrounded by a security fence. A drainage system at the RWMC diverts runoff away from the facility.

Most of the LLW arrives at the RWMC packed in containers such as large wooden boxes with plastic liners. Incineration, compaction, melting, and sizing activities have been conducted on portions of the waste. Waste is buried in large pits that are excavated to a depth of 9 m. After the waste is emplaced, it is covered with 1 to 2 m of soil. Small quantities of LLW with higher radiation levels are placed in cylindrical soil vaults.

LLW generated at the INEL primarily consists of contaminated or potentially-contaminated protective clothing, paper, rags, packing material, glassware, tubing, and other general-use items. Also included is contaminated

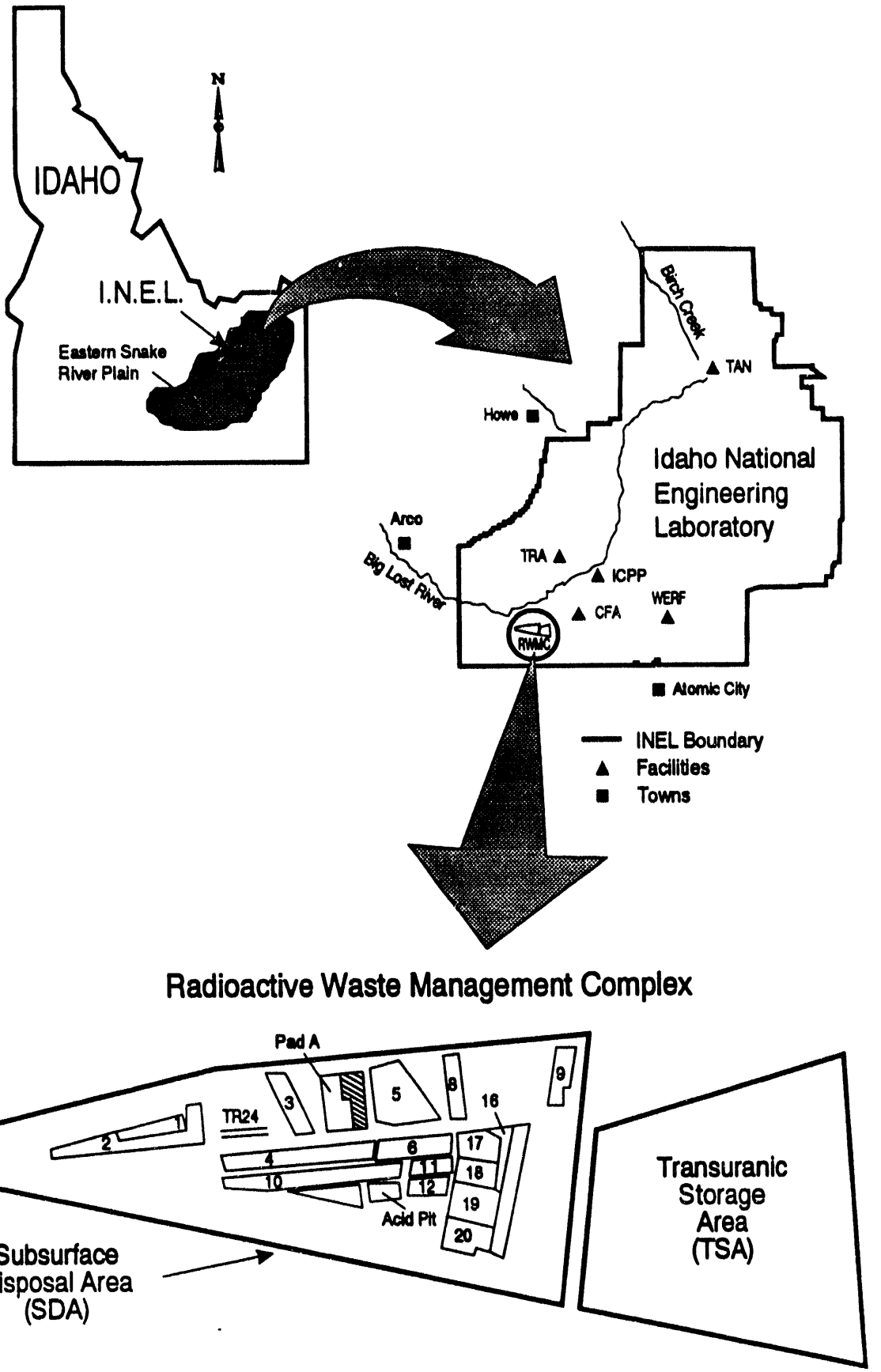

Figure 1-1. Overview of the INEL, RWMC, and the SDA.

equipment (such as gloveboxes and ventilation ducts) and process waste (such as filter cartridges and sludges). These materials are either surface contaminated with radionuclides or are activated from nuclear reactions. Most of the radioactivity in the LLW at the time of receipt stems from short-lived radionuclides. Most of this waste has an external exposure rate <500 mR/h at 0.9 m from the container surface.

Environmental surveillance programs are conducted onsite and offsite to monitor for any inadvertent release of radioactivity from the RWMC and the INEL.

1.3 Performance Objectives

The specific radiological performance objectives for LLW disposed of at the RWMC are summarized in Table 1-1. These performance objectives, contained in DOE orders and EPA regulations, are described below.

1.3.1 DOE Order 5820.2A

DOE Order 5820.2A, "Radioactive Waste Management," dated September 26, 1988, contains policies, guidelines, and minimum requirements including performance objectives by which DOE manages LLW (DOE 1988a). Chapter III of this order is applicable to managing DOE LLW. The order contains general policy statements regarding protection of the public health and safety and specific performance objectives for DOE LLW disposal operations. This order also requires a site-specific performance assessment to demonstrate compliance with the objectives.

The specific performance objectives set forth in DOE Order 5820.2A state that DOE LLW disposed of after the order was issued shall be managed to accomplish the following:

- Protect public health and safety in accordance with standards specified in applicable Environmental Health Orders and other DOE orders

Table 1-1. Summary of regulations and radiological performance objective limits applicable to the RWMC LLW performance assessment.

Regulations	Exposure group	Performance objectives limit (annual)	Compliance point	Compliance period
DOE orders				
5820.2A, Ch. III	Public	25 mrem EDE[a] (all pathways but air)	Point of restricted access (fence, guards, signs, etc.) at the INEL Site boundary	During operations and institutional control
			Point of restricted access (fence, guards, signs, etc.) 100 m from the RWMC facility boundary	During post-institutional control
	Inadvertent intruder	100 mrem/yr EDE (chronic exposure) 500 mrem EDE (acute exposure)	Disposal facility	During post-institutional control
EPA				
40 CFR 61 Subpart H	Public	10 mrem EDE (air emissions)	Point of maximum annual air concentration in an unrestricted area where the public resides or abides	During operations, institutional control, and post-institutional control
EPA and State of Idaho				
IDAPA 16.01.08000 40 CFR 141	Public	4 mrem EDE[b,c] (community drinking water system)	Any community drinking water system at the INEL boundary	During operations, institutional control, and post-institutional control

a. Effective dose equivalent (EDE) is the summation of the products of the dose equivalent received by specified tissues of the body and a tissue-specific weighting factor. This sum is a risk-equivalent value and can be used to estimate the health-effects risk of the exposed individual. The tissue-specific weighting factor represents the fraction of the total health risk resulting from uniform whole-body irradiation that would be contributed by that particular tissue. The EDE includes the committed effective dose equivalent (CEDE) from internal deposition of radionuclides and the external EDE due to penetrating radiation from sources external to the body. EDE is expressed in units of rem or sievert (DOE Order 5400.5) (DOE 1990).

b. Beta and photon emitters.

c. 15 pCi/L for adjusted gross alpha (including Ra-226; excluding uranium and radon); 5 pCi/L Ra-226, Ra-228.

- Assure that external exposure to the waste and concentrations of radioactive material that may be released into surface water, groundwater, soil, plants, and animals results in an effective dose equivalent (EDE) that does not exceed 25 mrem/yr to any member of the public. Releases to the atmosphere shall meet the requirements of 40 CFR 61 (CFR 1992).

  Reasonable effort should be made to maintain releases of radioactivity in effluents to the general environment to levels as low as reasonably achievable (ALARA).

- Assure that the committed effective dose equivalent (CEDE) received by individuals who inadvertently intrude into the facility after the loss of active institutional control (100 years) will not exceed 100 mrem/yr for continuous exposure or 500 mrem for a single acute exposure.

- Protect groundwater resources consistent with Federal, State, and local requirements.

1.3.2 40 CFR 61

Subpart H of the "National Emission Standards for Hazardous Air Pollutants (Clean Air Act)" contains EPA dose limits for members of the public resulting from airborne effluents from DOE facilities. This regulation requires preparing and submitting a request for construction or modification of any DOE facility demonstrating compliance with the regulation. The following performance objective is contained in 40 CFR 61 (CFR 1992): the airborne effluent pathway shall not result in any member of the public receiving, in a year, a dose equivalent >10 mrem EDE.

It is not clear whether the performance objective contained in 40 CFR 61 as implemented in DOE Order 5820.2A applies to just the LLW disposal facility or to the entire INEL. The EPA approach to 40 CFR 61 compliance considers the entire INEL in the 10 mrem/yr compliance determination. However, in

"Clarification of Requirements of DOE Order 5820.2A,"[a] it is specifically stated that "the performance objectives are intended to apply to each LLW facility on a reservation rather than to the reservation as a whole." Because of these contradictory regulatory positions, it was decided to evaluate atmospheric emission on a single facility basis and on an INEL-wide basis, using the present levels of INEL emissions as a baseline. No attempt was made to derive emission estimates for new facilities that may be built at the INEL or for projects that may take place in the future.

1.3.3 40 CFR 141

Compliance with the performance objective for protecting groundwater resources has been interpreted in this radiological performance assessment to mean that concentrations of radioactive contaminants should not exceed standards for public drinking water supplies as established by EPA. The National Primary Drinking Water Regulations require that all community drinking water systems that have at least 15 connections or serve 25 people meet the following requirements:

- Beta and photon emitters <4 mrem EDE/yr
- Adjusted gross alpha emitters <15 pCi/L (including Ra-226; excluding uranium and radon)
- Radium-226 and radium-228 <5 pCi/L.

1.3.4 IDAPA 16.01.08000, Idaho Regulations for Public Drinking Water Systems

All states are required to comply with the Safe Drinking Water Act set forth by EPA, and state regulations must be at least as stringent as the Federal regulations to be in compliance. The Idaho regulations incorporate the requirements for maximum contaminant levels listed in 40 CFR 141.

---

a. Letter from T. B. Hindman to Distribution, February 28, 1989, and letter from T. B Hindman to P. Saxman et al., March 28, 1989. These letters are contained in Dodge et al. (1991).

1.4 Time Periods of Concern

For the purpose of assessing the performance of the LLW disposed of at the RWMC, three time periods are of concern: the operational period, the institutional control period, and the post-institutional control period. These periods are defined as follows:

- The operational period was assumed to last from 1984 to 2020, at which time the RWMC was assumed to be closed. Although current plans are to replace the existing RWMC by approximately 2002, anticipated disposals of LLW through CY 2020 were included in the RWMC radiological performance assessment to provide future flexibility because of uncertain funding levels needed to support developing a new disposal facility. The waste inventory includes the amount accumulated from 1984 through 1993 plus the amount projected to accumulate until 2020.

- The period of institutional control was assumed to last for 100 years, 2021 through 2120, during which time maintenance and surveillance monitoring of the RWMC continued and no additional waste was received. During this time, the INEL Site boundary was maintained, restricting public access to the RWMC.

- The post-institutional control period, beginning in the year 2120, was the period during which no maintenance or surveillance monitoring occurred, and the area was available for unrestricted access and use by the public. The period has an indefinite ending point; analyses were made out to the point in time of maximum potential impact.

1.5 Receptors

Two receptor types were assessed in this radiological performance assessment: (1) a member of the public and (2) an intruder. During the operational and institutional period, the member of the public resided at the INEL Site boundary. During the post-institutional control period, the member of the public resided 100 m from the RWMC SDA boundary.

The intruder was assumed to inadvertently intrude onto the RWMC SDA during the post-institutional control period. Two general kinds of intruder scenarios were evaluated: (1) a chronic exposure scenario and (2) an acute exposure scenario. The chronic exposure scenario was based on a receptor who obtained a portion of his food from farming at the RWMC SDA. The intruder also used water from a well drilled at the edge of the waste and was exposed to radon and its short-lived progeny that diffused through a basement foundation. The acute exposure scenario included both a construction scenario and a well-drilling scenario. The scenario was based on a receptor who built a house at the RWMC SDA and was exposed to contaminated soil while he excavated the basement. In the well-drilling scenario, the receptor was exposed to contaminated drill cuttings spread over the ground.

2. SITE BACKGROUND AND FACILITY DESCRIPTION

This chapter describes the existing conditions at the INEL Site, RWMC description and waste characteristics, and planned RWMC environmental restoration activities.

2.1 Site Description

This section describes the INEL environment, which includes the RWMC. The description includes climate and meteorology, geology and soils, geochemistry, hydrology, biotic resources, demography, land use, and cultural resources. This description provides the information necessary to understand how the INEL environment impacts the results of the radiological performance assessment.

The INEL is located along the northwestern edge of the eastern Snake River Plain in southeastern Idaho (Figure 2-1). Lying at the foot of the Lost River, Lemhi, and Bitteroot-Centennial Mountain ranges, the INEL comprises 2,315 km^2 of arid shrub steppe.

Most of the land withdrawn from public domain for use by DOE lies in Butte County, Idaho, although it extends into Bingham, Bonneville, Jefferson, and Clark Counties.

The INEL was established in 1949 as the National Reactor Testing Station (NRTS), a place where the Atomic Energy Commission (AEC) could build, test, and operate various types of nuclear reactors, support facilities, and equipment with maximum safety. As of April 1991, 52 reactors were built at the INEL; of which, 13 were operating or operable (DOE 1991).

In 1952, the SDA of the RWMC was opened on a 13-acre tract in the southwestern corner of the INEL. In 1957, the SDA was expanded to its present size of 97 acres. The RWMC was expanded in 1970 by adding the TSA, covering 58 acres. Several service and support buildings have been constructed over the years.

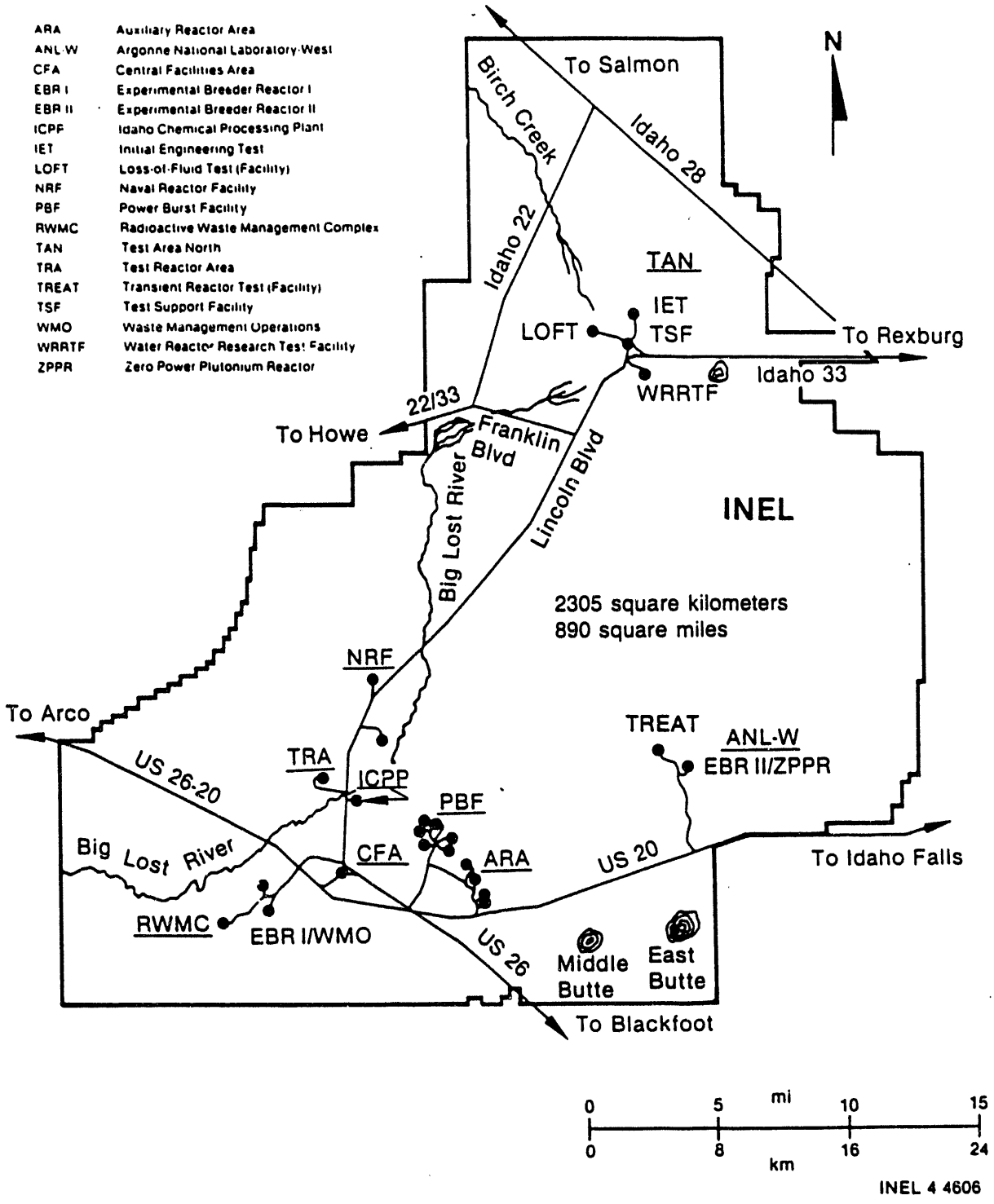

Figure 2-1. Location and principal INEL features.

2.1.1 Climate and Meteorology

This section describes the RWMC climate and meteorology (which includes the temperature, wind, precipitation, evaporation, relative humidity, and severe weather conditions).

The INEL climate is arid, with sagebrush-steppe characteristics. The topographic features that affect local weather patterns are the northeast-southwest orientation of the Snake River Plain and the mountain ranges to the north and west. Air masses entering the Snake River Plain must first cross mountain barriers, where much of the air moisture is precipitated. Thus, annual rainfall at the INEL is light.

Meteorological and climatological data summarized in this subsection are from a monitoring program conducted by the National Oceanic and Atmospheric Administration (NOAA).[a] Temperature, wind, precipitation, evaporation, relative humidity, and severe weather conditions measured at locations near the RWMC are included.

2.1.1.1 Temperature. The daily air temperature extremes at the INEL vary from -44°C in January to 38°C in July. During the winter (November through March), the average monthly temperature varies from -9 to -1°C. During the summer (April through October), the average monthly temperature varies from 5 to 20°C.

Normal weather at the INEL includes lapse conditions (the air temperature decreases with height above the ground surface) during daylight hours and inversion conditions (temperature increases with height) from about sunset until shortly after sunrise. Winds and clouds associated with stormy weather may prevent nighttime inversions. Daytime inversions may occur during winter and early spring if there is snow cover. Annual averages show lapse conditions 52% of the time and inversion conditions 48% of the time. However,

---

a. Data were recorded from January 1950 through December 1988 (Clawson et al. 1989). Most of the data reported in this section were gathered at the Central Facilities Area, approximately 8 km northeast of the RWMC.

a nocturnal inversion can be expected to form on almost every day of the year (96.2% of the time) (Clawson et al. 1989).

2.1.1.2 Wind. The INEL is in a belt of prevailing westerly winds that is channeled by local terrain into a prevailing southwest-to-northeast direction. In summer a very sharp reversal in wind direction occurs daily; winds from the southwest predominate during daylight hours, and northeasterly winds predominate at night. The reversals normally occur shortly after sunrise and sunset.

Wind roses (Figure 2-2) recorded at the Central Facilities Area (CFA) at the 6-m level indicate the percentage of time that the wind blows from a given direction and the associated windspeeds. Although the wind roses are similar for the four seasons, there is a fundamental difference between the forces controlling the winds in winter and those in the other three seasons. Winter winds are controlled almost exclusively by either large-scale weather systems or stagnation, and they show no significant diurnal characteristics in response to relatively strong local buoyancy forces resulting from the ground heating. Because of the absence of mountain-valley wind circulation in winter, there are frequent calms during periods of high atmospheric pressure.

The average monthly windspeed varies from 8 km/h in December to 15 km/h in April and May. The greatest hourly-average speed was 82 km/h from the west-southwest. On the average, 2 or 3 thunderstorm days per month occur during June, July, and August. Strong wind gusts can occur in the immediate vicinity of thunderstorms. The highest instantaneous speed, recorded 6 m aboveground at CFA, was 126 km/h, with the wind from the west-southwest. Calm conditions prevail 11% of the time.

Atmospheric particulate matter is routinely monitored using low-volume air sampling stations at various locations across the INEL and a total suspended particulate monitor at CFA. In 1989 and 1990, the INEL mean value from the low-volume air samplers ranged from 17 to 20 $\mu g/m^3$, and the CFA annual average ranged from 28 to 40 $\mu g/m^3$ (Hoff et al. 1990, 1991). A study completed in 1953 (Humphrey et al. 1953) recorded a seasonal variation in the airborne dust concentration of 14 $\mu g/m^3$ in the winter and 77 $\mu g/m^3$ in the

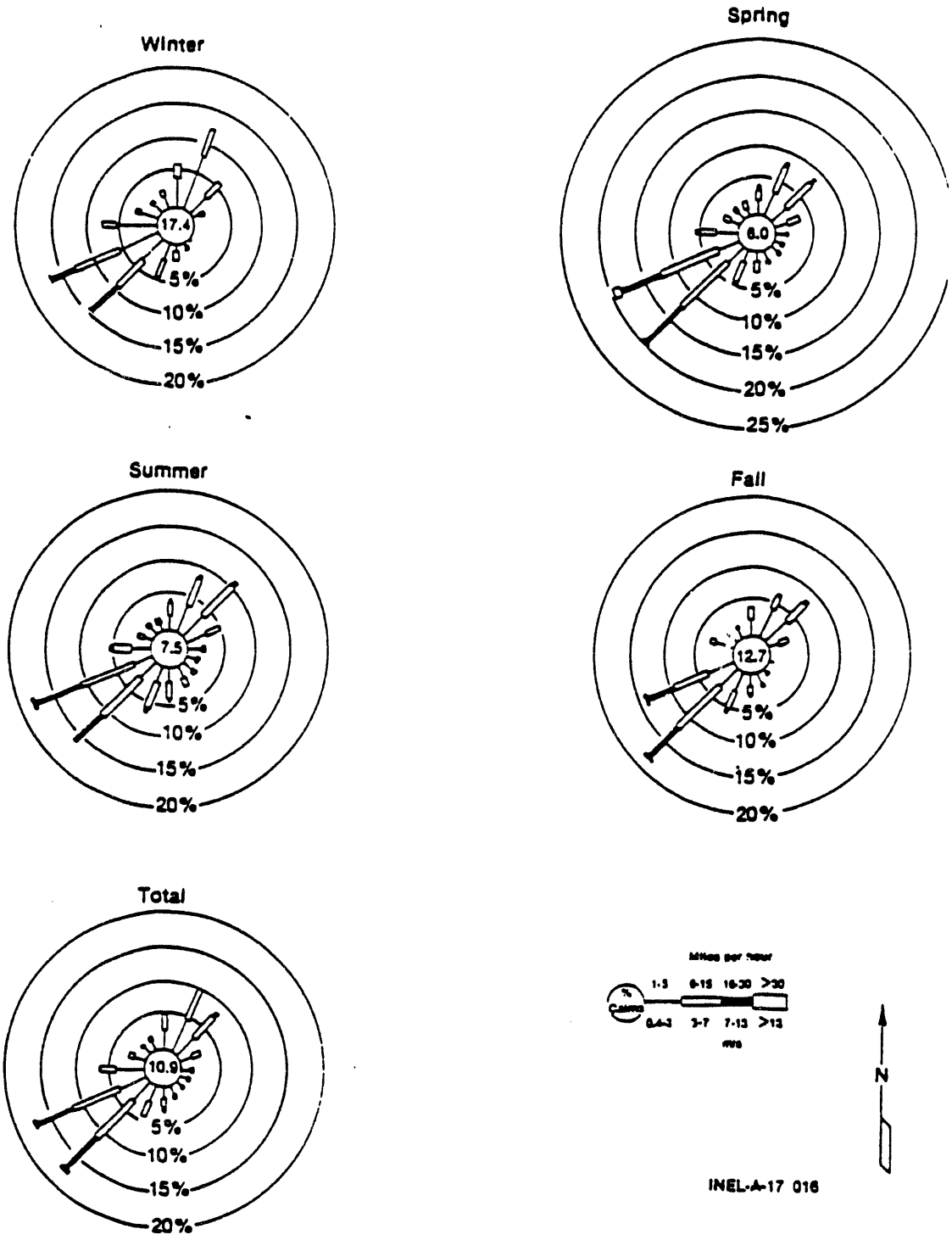

Figure 2-2. Wind rose for the INEL CFA at the 6.1-m level.

summer. This study found a maximum concentration in dust devils of 150 $\mu g/m^3$ and that less than 1% of the particles were larger than 10 μm in diameter.

2.1.1.3 Precipitation. The average annual precipitation at the INEL is 22 cm. From 1950 through 1988, the highest annual amount of precipitation recorded was 36.6 cm, and the lowest amount was 11.4 cm. A precipitation peak of approximately 3 cm/mo occurs in May and June each year. Other months generally receive one-half or less of these amounts. There have been eight occasions from 1950 through 1988 when 2.5 cm or more of rain fell within a 24-hour period at CFA. The greatest rainfall recorded within a 24-hour period was 4.2 cm in June 1969.

Snowfall ranges from 17 to 152 cm/yr, with an annual average of 70 cm. Although snow occurs mostly during November through April, it does occasionally fall during May, September, and October (Clawson et al. 1989).

2.1.1.4 Evaporation. The potential annual evaporation from a saturated ground surface at the INEL is approximately 91 cm, with 80% of the evaporation occurring between May and October. During the warmest month (July), the daily potential evaporation rate is approximately 0.6 cm (Hull 1989). From December through February, potential evaporation is small and may be insignificant. Actual evaporation rates are much lower than potential rates because the ground surface is rarely saturated. Transpiration by the native vegetation of the Snake River Plain is estimated to be 15 to 23 cm/yr. From late winter to spring, precipitation is most likely to infiltrate into the ground because of the low evapotranspiration rates (Mundorff et al. 1964). For evaporation from surface water bodies (ponds), a pan evaporation rate of approximately 109 cm/yr has been estimated (Clawson et al. 1989).

2.1.1.5 Relative Humidity. The relative humidity at the INEL Site ranges from a monthly average minimum of 15% in August to a monthly average maximum of 89% in February and December. On a daily basis, humidity reaches a maximum just before sunrise, at the time of the lowest temperature, and a minimum late in the afternoon, near the time of the highest temperature.

2.1.1.6 Severe Weather Conditions. On the average, two or three thunderstorm days occur at the INEL during June, July, and August. The surface effects from thunderstorms over the Snake River Plain are usually much less severe than those east of the Rocky Mountains or even in the mountains surrounding the Plain. Although small hailstones frequently accompany the thunderstorms, damage from hail to buildings and facilities has not occurred at the INEL.

2.1.2 Geology and Soils

2.1.2.1 Regional Setting. The INEL is located near the northern margin of the Eastern Snake River Plain (ESRP) in southeastern Idaho (Figure 2-3). The Snake River Plain is a low-lying area of late Tertiary and Quaternary volcanism and sedimentation that extends from the Idaho-Oregon border to the Island Park area of southeastern Idaho. Early silicic volcanism of the ESRP is related to the Yellowstone mantle plume passing beneath the INEL area approximately 6.5 to 4.3 million years ago. During the past 4 million years the INEL area has undergone regional subsidence, basaltic volcanism, and terrigenous-clastic sedimentation (Pierce and Morgan 1992; Hackett and Smith 1992). In the vicinity of the INEL, ESRP elevations range from 1,460 m at the Big Lost River Sinks to approximately 1,650 m along the axis of the ESRP. The elevation is approximately 1,500 m at the RWMC.

The northwest-trending mountain ranges to the north and south of the ESRP developed concurrently with volcanism on the ESRP and are part of the northern Basin and Range Province (Figure 2-3). The ranges are comprised of Paleozoic and Mesozoic sedimentary rocks, which are mostly marine carbonates that were folded and thrust faulted during Mesozoic and early Tertiary time. The ranges have been uplifted into their present configuration along major Quaternary normal faults, which terminate at the margins of the ESRP. Between the ranges are downfaulted, sediment-filled valleys from which streams flow southward onto the ESRP.

A broad volcanic highland (the Axial Volcanic Zone; see Section 2.1.2.6) extends northeasterly along the axis of the ESRP, preventing streams draining the basin and range mountains to the north of the ESRP from reaching the Snake River, which flows along the southern margin of the ESRP. Instead, streams

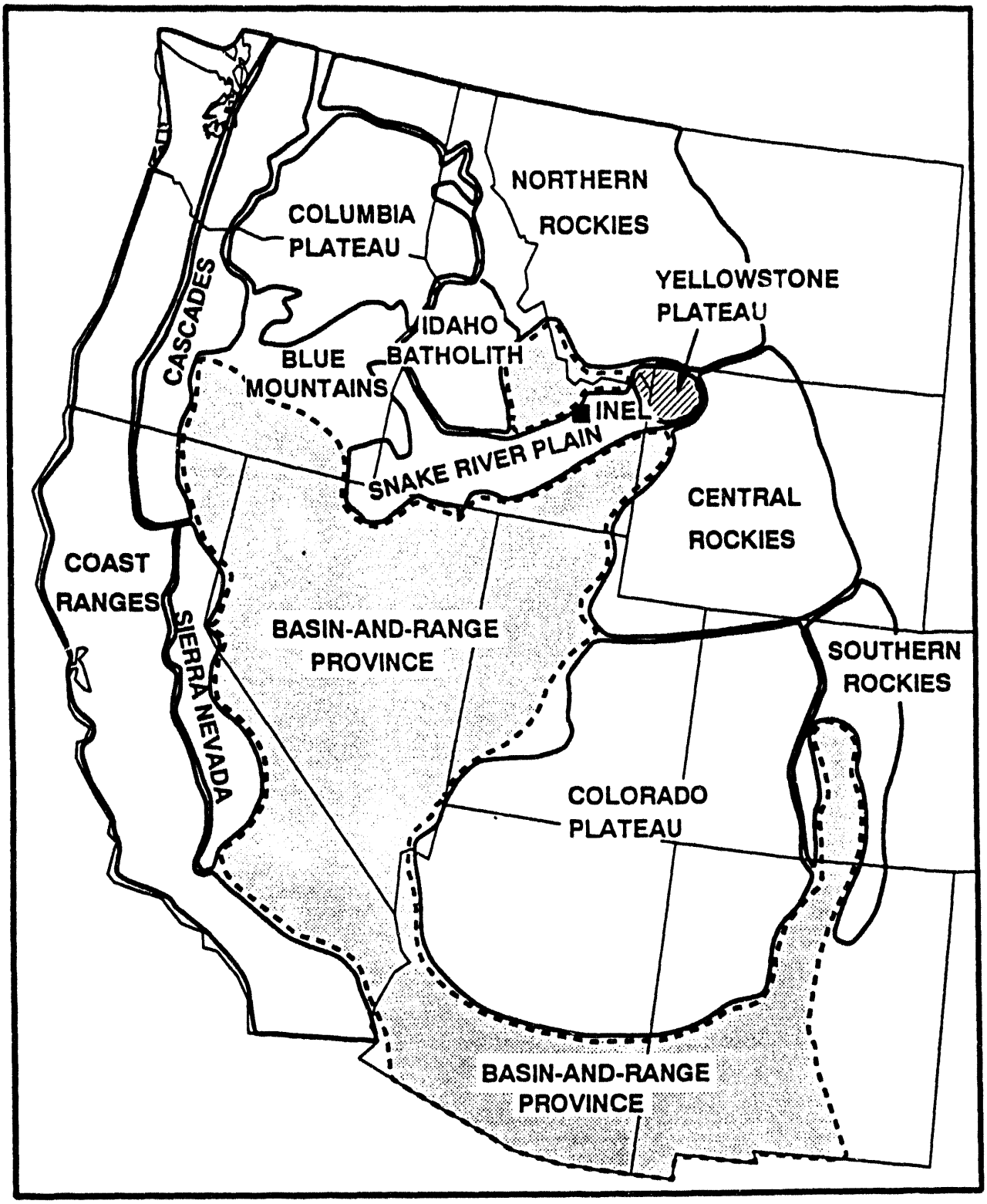

Figure 2-3. Location of INEL with respect to regional geologic and physiographic provinces.

draining onto the INEL from the north are diverted into shallow basins on the northern and central INEL, and the surface water percolates into fractured lava and permeable sediment.

Erosion has not established regular drainage patterns in the INEL area because of repeated surfacing of the ESRP by basaltic-lava flows during the past several million years and the permeable lava and surficial sediments. Streams are intermittent, wandering and blind as they follow the edges of lava flows and lava channels, commonly ending in small closed depressions. Mass wasting processes are not important in ESRP landscape evolution because of the low relief of the terrain and the absence of a well-integrated surface drainage pattern. Local exceptions to this generalization are the three steep-sided volcanic buttes along the central axis of the ESRP to the south and east of the RWMC, which are surrounded by talus aprons and alluvial-fan deposits.

Overviews of the regional physiography and tectonics of the Snake River Plain and its surrounding area are given in Blackwell (1989), Malde (1991), and Pierce and Morgan (1992). The general geology, volcanism, and tectonics of the INEL region are discussed in Kuntz et al. (1990, 1992) and Hackett and Smith (1992). Scott (1982) presents a map of the surficial geology of the ESRP. Barraclough et al. (1976) describes the hydrogeoloic setting of the RWMC area.

2.1.2.2 Subsurface Geology. The subsurface stratigraphy of the RWMC area has been studied using borehole-geophysical logs (Anderson and Lewis 1989) and the geochronometry and paleomagnetic properties of basalt cores (Champion et al. 1988). Figure 2-4 depicts a geologic cross section through the RWMC area showing the interlayering of basalt lava flows and sedimentary deposits. Groups of basalt flows are labeled A to I, with increasing depths, following the nomenclature of Anderson and Lewis (1989). This nomenclature is used throughout this report. Surficial sediments covering the basalts at the surface are wind deposited loess and minor alluvial silts and sands, which range from 1 to 7.5 m thick and have an average thickness of 4.5 m (see Figure 2-5).

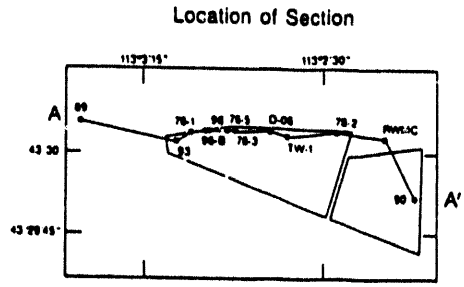

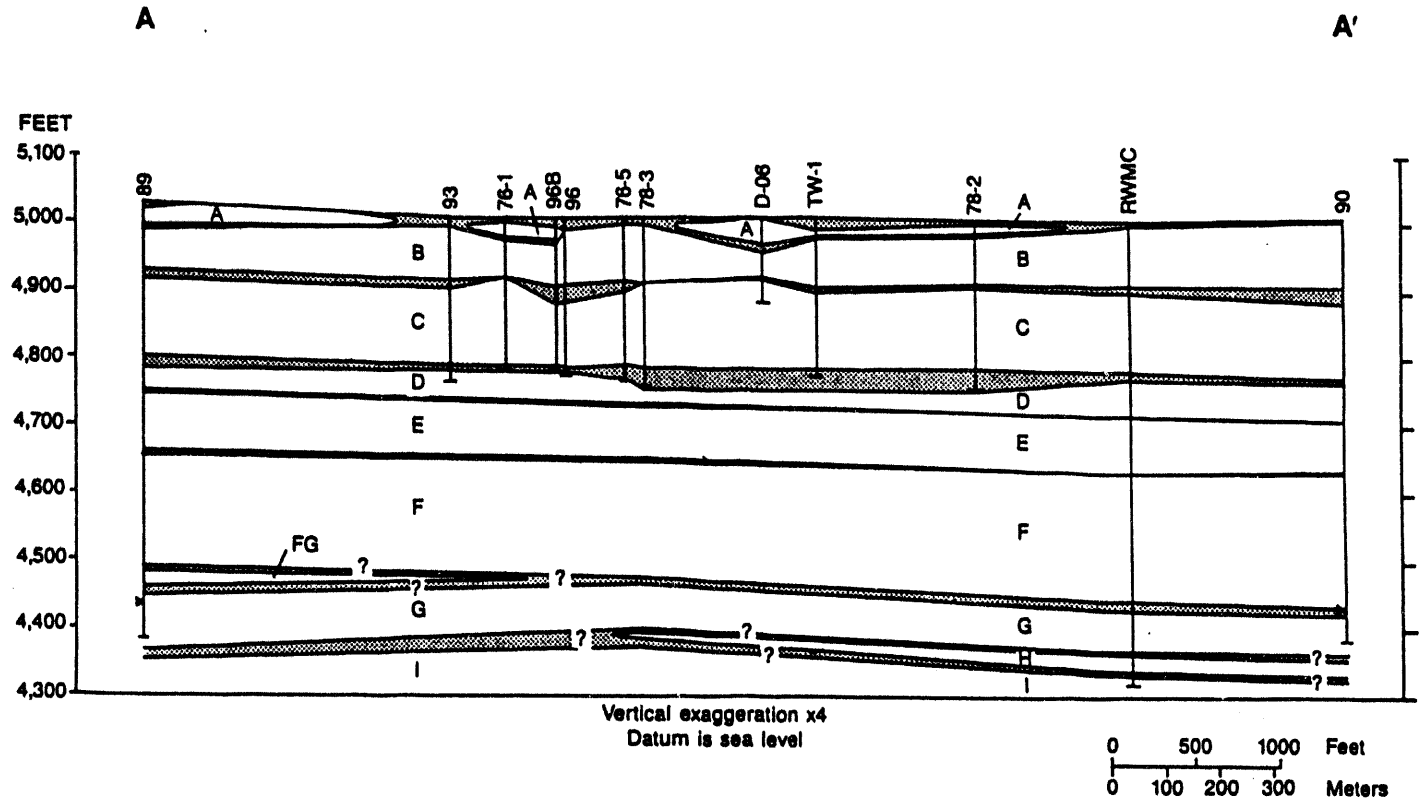

Figure 2-4. East-west geologic cross section A-A′ across the northern RWMC, showing the general stratigraphy of the unsaturated zone (Anderson and Lewis 1989). White areas depict basalt; dark areas represent sedimentary interbeds.

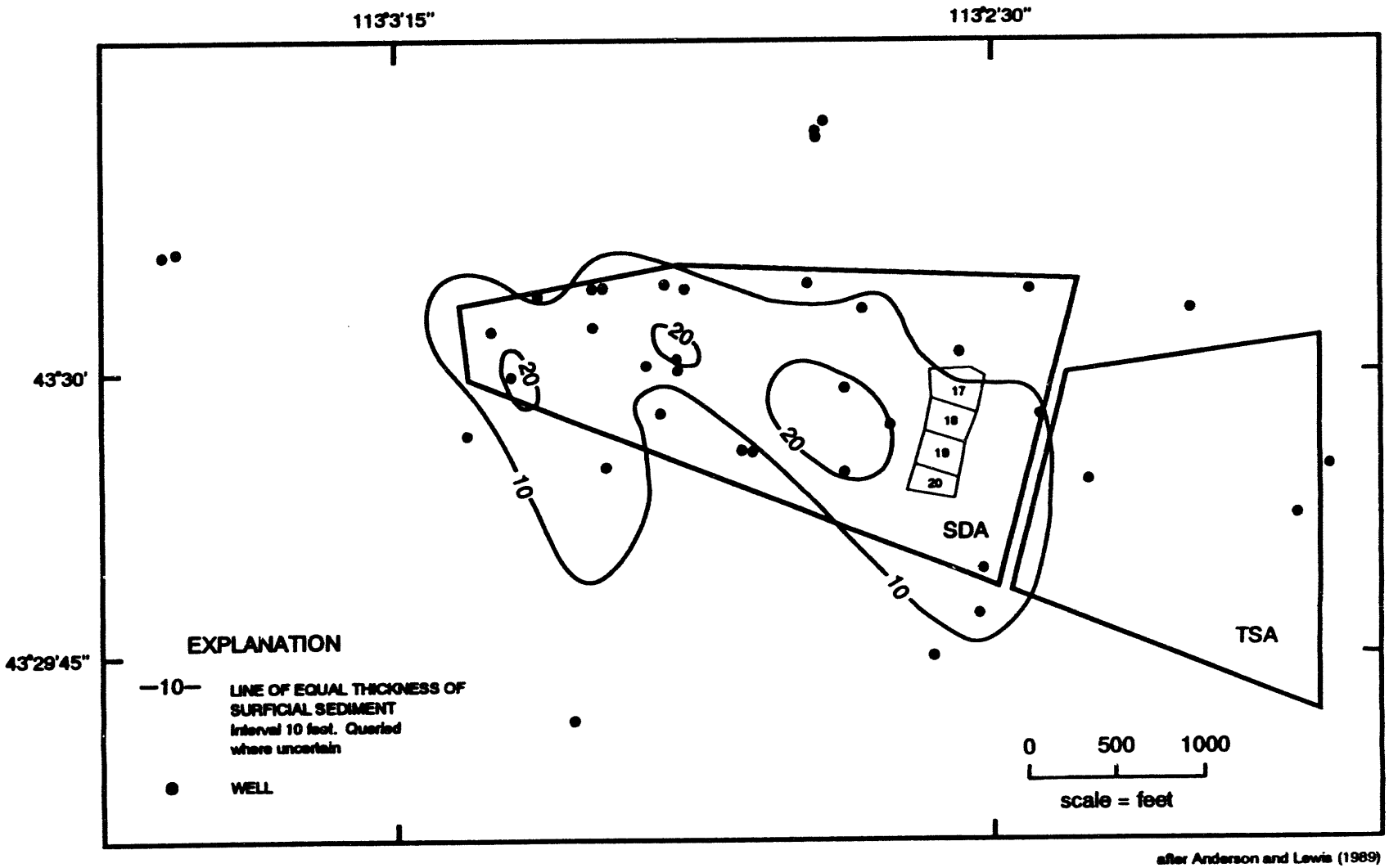

Figure 2-5. Isopach map of surficial sediment thickness for the SDA.

Sedimentary interbeds occur above the water table beneath the RWMC at various depths. These interbeds are referred to in relation to the basalts above and below them as indicated on Figure 2-4. Three major interbeds (A-B, B-C, and C-D) are observed in wells drilled to the C-D interbed inside the SDA. They occur at depths of approximately 9, 34, and 73 m; the 34- and 73-m interbeds have in the past been referred to as the 110- and 240-ft interbeds. The A-B and B-C interbeds are discontinuous, while the C-D interbed has been found in all wells drilled inside and in the vicinity of the SDA. Isopach maps show the thickness of the A-B, B-C, and C-D interbeds in the vicinity of the SDA (Figures 2-6, 2-7, and 2-8). The location of the LLW Pits 17 through 20 is shown on each figure. Anderson and Lewis (1989) reports average thicknesses for the A-B, B-C, and C-D interbeds of 1.5, 4.0, and 5.2 m, respectively. These interbeds have a slight slope from west to east. The tops of the B-C and C-D interbeds slope on the average 3.8 and 4.7 m/km to the east, respectively (Anderson and Lewis 1989; Barraclough et al. 1976). Two other interbeds, D-E and E-F, have been observed in wells drilled outside the SDA. The operational policy inside the SDA is to not drill wells through the C-D interbed to avoid possibly creating preferential pathways to the aquifer. The D-E and E-F interbeds have reported average thicknesses of 1.8 and 1.5 m, respectively (Anderson and Lewis 1989).

Knutson et al. (1992) reported the thickness of lava flows ranges from 3 to 30 m. Because of their emplacement mechanisms and cooling phenomena, the flows are strongly fractured and fissured. They typically have a rubbly base, a lower vesicular zone, a medial massive and columnar jointed zone, an upper vesicular zone, and an upper zone of platy horizontal fractures near the lava flow top. Fractures are almost always coated with fine sediments washed in from overlying interbeds or surficial sediments. Knutson et al. (1992) characterized fractures in Box Canyon, which is approximately 14 km west of the RWMC. At this location, fracture spacing ranges from 0.25 m near the surface of individual flows to 3 m in the central portion of a flow. Measured apertures on fractures range from 0.5 to 2.5 mm.

RWMC basalt-lava flows range in age from 100,000 years at the surface to more than 500,000 years at depth, and they occur as subsurface lava-flow groups separated by fine-grained sedimentary interbeds. No conclusive evidence has been found from the RWMC subsurface to suggest major faulting or

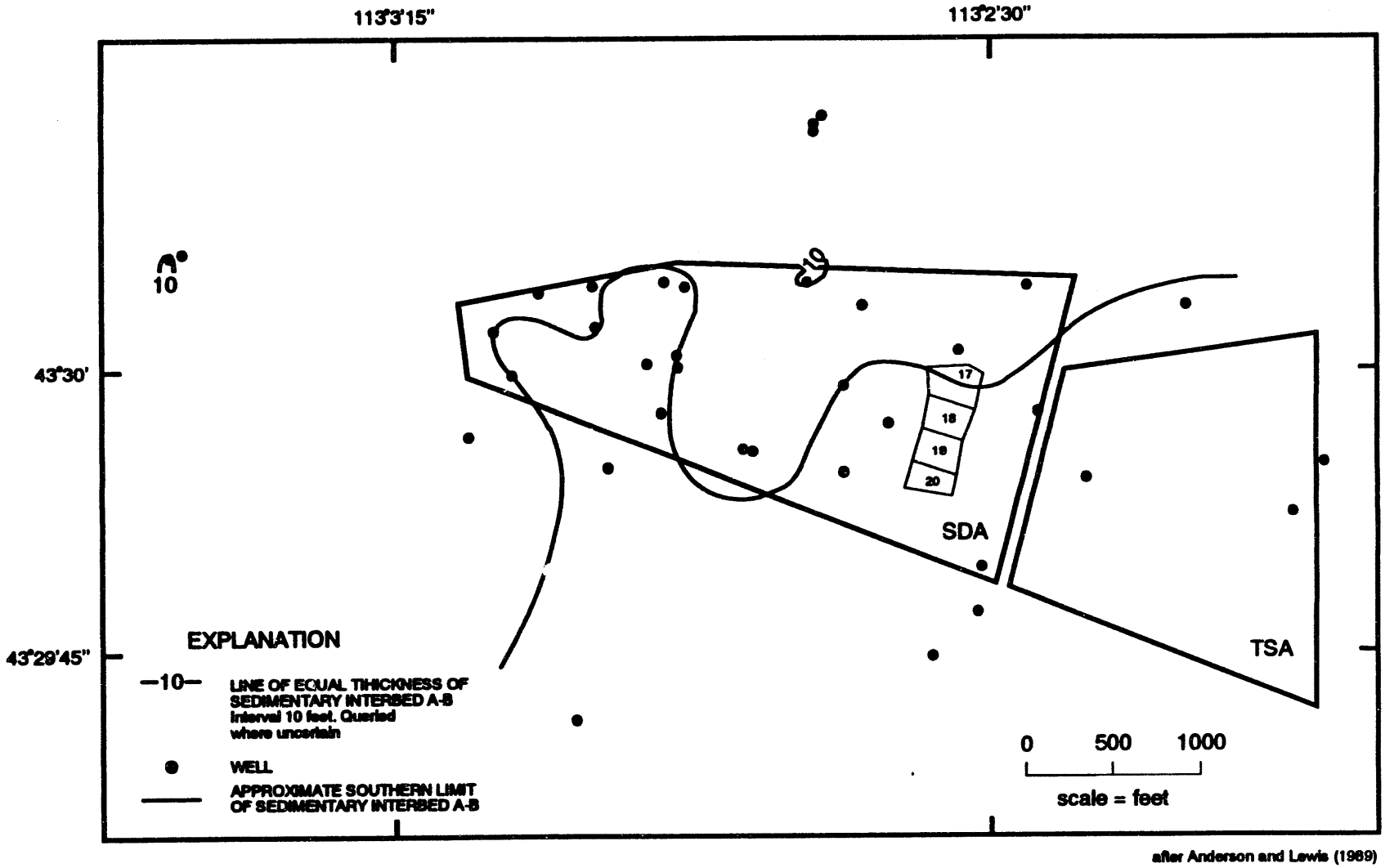

Figure 2-6. Isopach map of Interbed A-B thickness beneath the SDA.

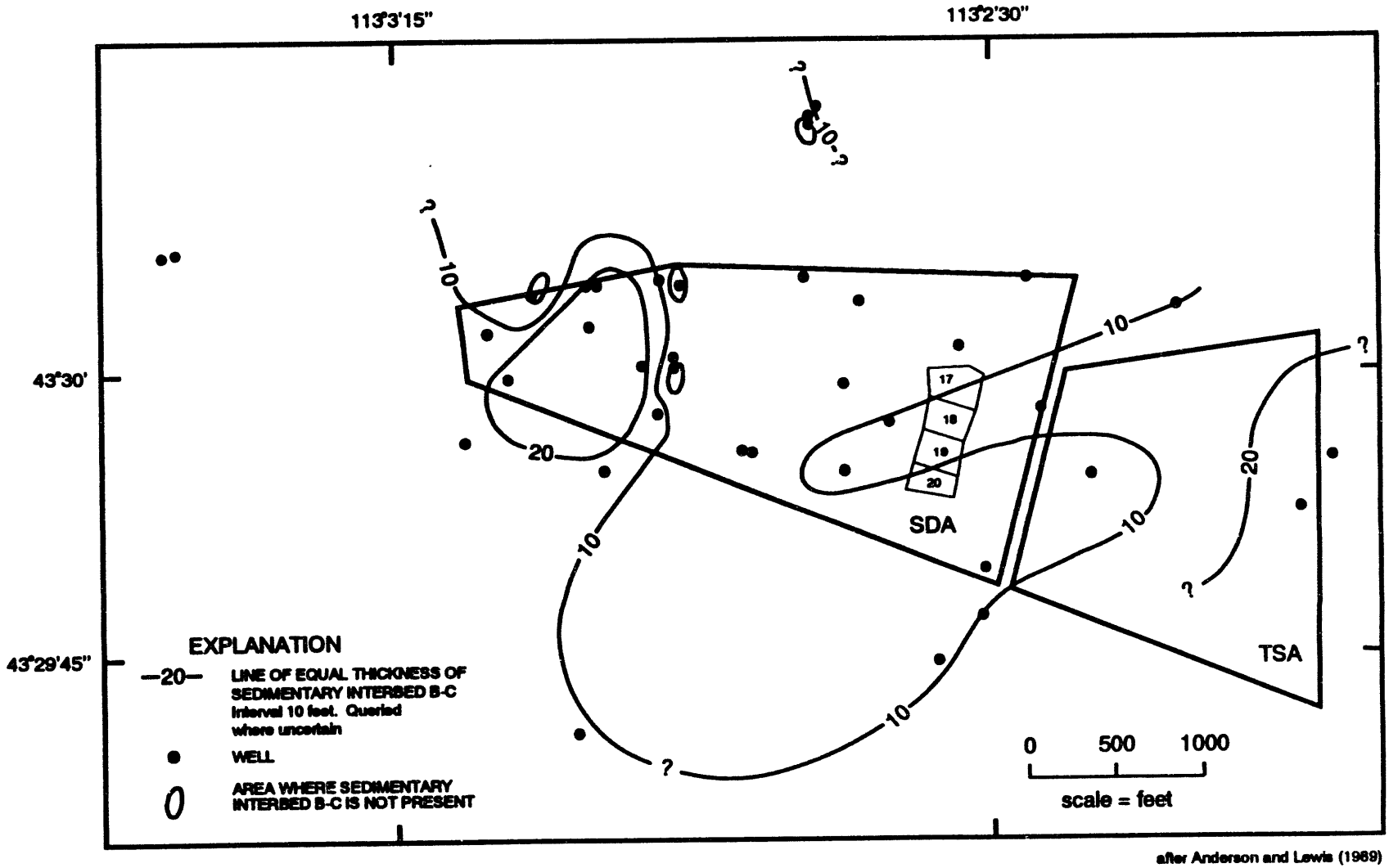

Figure 2-7. Isopach map of Interbed B-C thickness beneath the SDA.

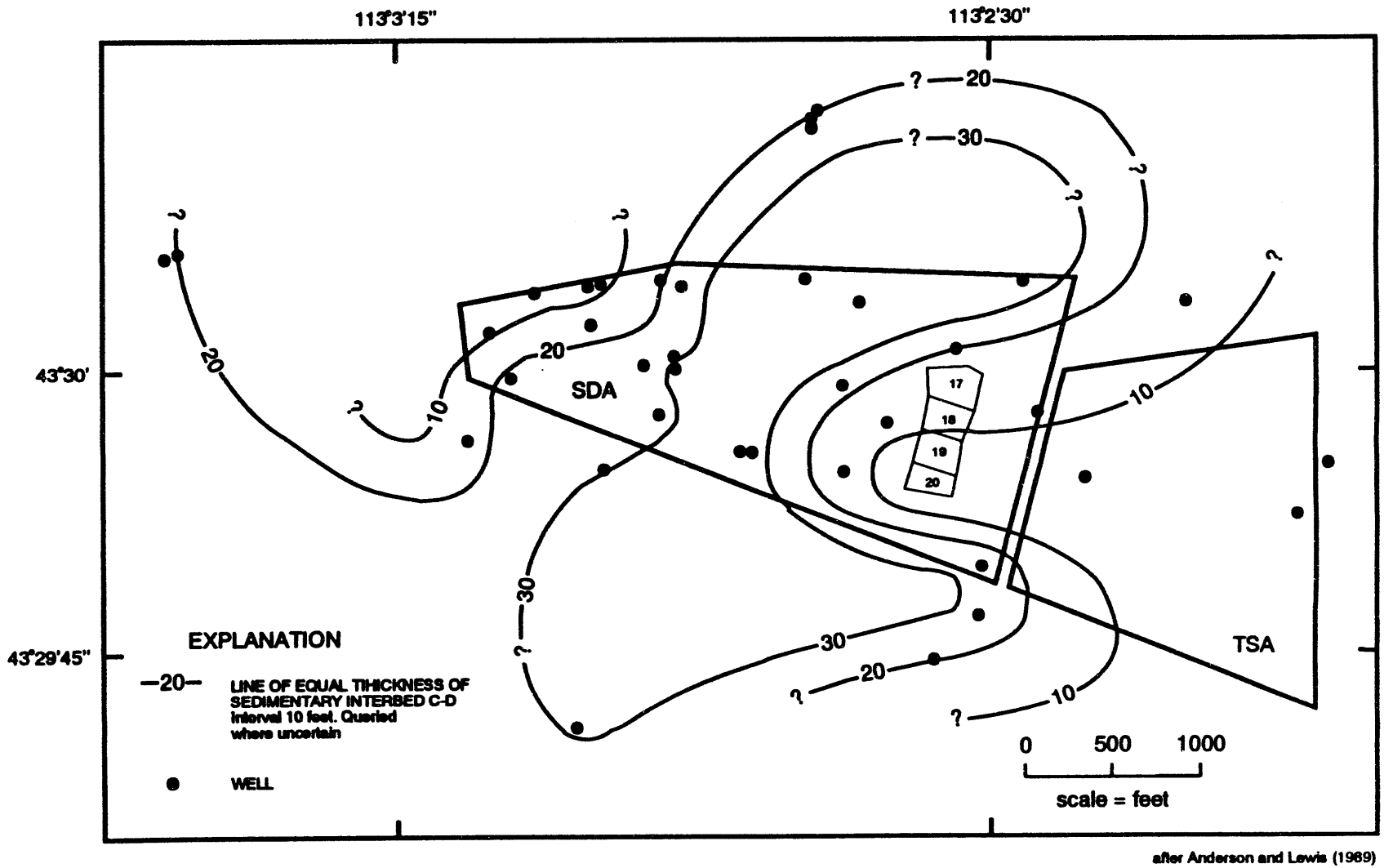

Figure 2-8. Isopach map of Interbed C-D thickness beneath the SDA.

other basalt and sediment deformation or buried erosional surfaces. The available evidence at the RWMC and elsewhere on the INEL Site indicates that the ESRP is an area of ongoing regional subsidence, which has been accumulating basalts and sediments for more than 4 million years. The average rate of INEL basalt and sediment accumulation is derived by compiling the depths (cumulative thickness) and ages of lava flows intersected in boreholes. The subsurface data from the RWMC (Champion et al. 1988) suggest several relatively brief periods of basaltic volcanism, each lasting 1,000 to 10,000 years and each represented by emplacement of a subsurface lava-flow group. Periods of volcanism were separated by longer intervals of sedimentation, each lasting up to several hundred thousand years and each represented by deposition of a major sedimentary interbed. The overall accumulation rate, which also approximates the regional-subsidence rate at the RWMC, is about 1 ft/1,000 yr or 0.3 mm/yr. Therefore, subsurface-geologic relations indicate that the RWMC, like much of the ESRP, is situated in an area of long-term subsidence, involving the continuous accumulation of volcanic and sedimentary material over several million years.

2.1.2.3 Surface Geology and Archaeology. Much of the land surface near the RWMC is underlaid by unconsolidated, silty clastic sedimentary deposits up to 7.5 m thick (Rightmire and Lewis 1987). The sediments were deposited onto the irregular surfaces of underlying basalt lava flows, which form rubbly outcrops throughout the area (Scott 1982). North of the RWMC, the Big Lost River channel is incised into mainstream alluvial deposits and basalt lava flows. Pleistocene alluvial fan deposits surround Big Southern Butte, a large rhyolite dome 7 km south of the RWMC. Several Holocene basalt lava fields occur 10 km southeast of the RWMC. The surficial deposits of the RWMC area indicate long-term deposition of fine-grained eolian and fluvial materials in the RWMC area for at least the past 100,000 years (Scott 1982; Forman et al. 1993; Tullis 1993). RWMC surficial deposits include loess (wind-blown slit), lacustrine (playa deposits), sand and pebble horizons, buried soils, and carbonate-accumulation horizons (Dechert et al. 1993). The carbonate accumulations and paleosols indicate that many buried land surfaces were exposed for periods that allowed weathering and soil formation and that they did not undergo substantial erosion. The formation of each paleosol required several thousand to ten thousand years of subaerial exposure before burial by younger sediment.

The rim of basalt around the RWMC basin is breached by two "wind gaps" immediately west of the RWMC, which have been filled in to improve waste disposal operations. Trains of basalt cobbles and boulders up to 1.5 m in diameter extend eastward from these gaps 75 to 100 m into the RWMC basin. The gaps and boulder trains are probably the result of late-Pinedale, glacial outburst flood(s) from the Pioneer Mountains of central Idaho (Rathburn 1991). The most recent of these catastrophic events may have occurred 10,000 to 12,000 years ago at the end of Pinedale glaciation (Hackett et al. 1993), and an earlier flood event may have occurred about 19,000 years ago (Poreda and Cerling 1992). Glacial flooding has stripped the surficial-sediment cover from much of the land surface higher than approximately 1,529 m in elevation, producing upland areas of relatively bare basalt. Land surfaces below 1,529 m in elevation, including the RWMC basin itself, were areas of glacial flood sedimentation.

The RWMC area contains much evidence of prehistoric human occupation, and archaeological artifacts are present that date back 10,000 years or more. These sites provide evidence of lack of erosion and support assumptions used in the performance assessment because 10,000-year-old materials are found on the ground surface, together with much younger materials only a few millennia or centuries old. The oldest materials are stone projectiles, known as Folsom points, which have been recovered together with production flakes from a surface site at the base of the basalt ridge to the west of the RWMC (Ringe 1992). Many INEL sites are relatively fragile in content and relationship of materials, and their in situ preservation indicates that archaeological materials have not generally been affected by the destructive erosional or soil-forming processes that characterize more humid regions. The effects of Holocene erosion and deposition are apparently limited to the upper 0.1 to 0.2 cm of surficial sediment because archaeological materials are either maintained at the surface or are buried to depths less than approximately 20 cm. Repeated covering and uncovering of the materials by eolian sediment (predominately fine sand) suggest that ESRP erosion and deposition during the past 10,000 years have been nearly in net balance on open terrain. The main causes of archaeological site disturbance through time are not the removal of artifacts by erosion, but rather the biological redistribution of near-surface materials by burrowing insects, small mammals, and plant roots.

2.1.2.4 Geochemistry. Knowledge of the sorptive properties of contaminants is key to understanding contaminant movement at the RWMC. The subsurface is comprised of surficial sediments, sedimentary interbeds, and fractured basalt. The surficial and interbed sediments provide the majority of the contaminant retardation at the RWMC. Currently, there is limited site-specific adsorption information for contaminants in the subsurface environment at the INEL (Del Debbio and Thomas 1989; Schmalz 1972). Distribution coefficients are available for cobalt, chromium, strontium, cesium, cadmium, mercury, and selenium for alluvium and cadmium, mercury, selenium, and strontium for interbed sediments and basalt. Limited availability of site-specific adsorption information for other radionuclides for sediments and basalts at the INEL has resulted in the use of adsorption parameters measured for sediments and basalts from other sites. Table 2-1 summarizes the measured K_d values with those used in the performance assessment.

Table 2-1. Summary of sorption coefficients measured at the INEL.

	K_d values (mL/g)				
Element	Alluvium	Interbed sediment	Basalt	This study	Reference for measured K_d
Sr	35-52 24	110-186	1.1-2.7	2	Del Debbio and Thomas (1989) Schmalz (1972)
Se	63-5.8	17-4.9	3.4-0.29	1	Del Debbio and Thomas (1989)
Hg	1921-236	673-72	87-9.2	10	Del Debbio and Thomas (1989)
Cd	4891-2864	10,115-8622	2319-785	650[a]	Del Debbio and Thomas (1989)
Cs	950	--	--	20[b]	Schmalz (1972)
Co	56	--	--	50	Schmalz (1972)
Cr	1.2	--	--	1	Schmalz (1972)

a. Value based on Baes et al. (1984)

b. Value based on EG&G Idaho (1984).

Several investigators have published compendia of soil and sediment distribution coefficient data (Baes and Sharp 1983; Coughtrey et al. 1985; Sheppard and Thibault 1990). The most thorough of these compendia is Sheppard and Thibault (1990), which contains a breakout of the distribution coefficients by major soil types (i.e., sand, loam, clay, and organic). Past compendia grouped all soil types together. The major source of basalt adsorption information is from investigations conducted during the Basalt Waste Isolation Project at Hanford, Washington, documented in the Nuclear Energy Agencies (NEA) sorption data base (Ticknor and Ruegger 1989).

Distribution coefficients were identified for cesium, strontium, and technetium on site-specific sediments. Distribution coefficient values for radionuclides with no site-specific K_d values were taken from the Sheppard and Thibault (1990) analysis, which allowed a more realistic selection of the K_ds based on soil type similar to that at the INEL. The surficial and interbed sediments at the INEL are classified as a sandy loam and silty loam, respectively (Del Debbio and Thomas 1989). The sand category was selected to represent both the surficial and interbed sediments to conservatively estimate adsorption.

Figure 2-9 compares the values used in the performance assessment with the range and geometric mean from Sheppard and Thibault (1990). The K_d values used generally fall within the range of values from the literature. The majority of values used in the performance assessment fall at or below the geometric mean of sand values with the exceptions of plutonium, uranium, and neptunium. The sensitivity of these nuclides to lower K_ds is discussed in the groundwater sensitivity analysis in Chapter 4.

Distribution coefficient data for basalts (Figure 2-10) are not as readily available as data for soils and sediments. The main source of K_ds is basalts from the Hanford Reservation. The appropriateness of using these K_ds values at the INEL is difficult to assess. The mineralogic differences have not been addressed, and the secondary minerals (e.g., clays and iron oxides) that form in the fractures may have a major impact on the adsorption of many radionuclides have not been quantified. Also, it is unclear if equilibrium is maintained during flow through the unsaturated zone. If local equilibrium is

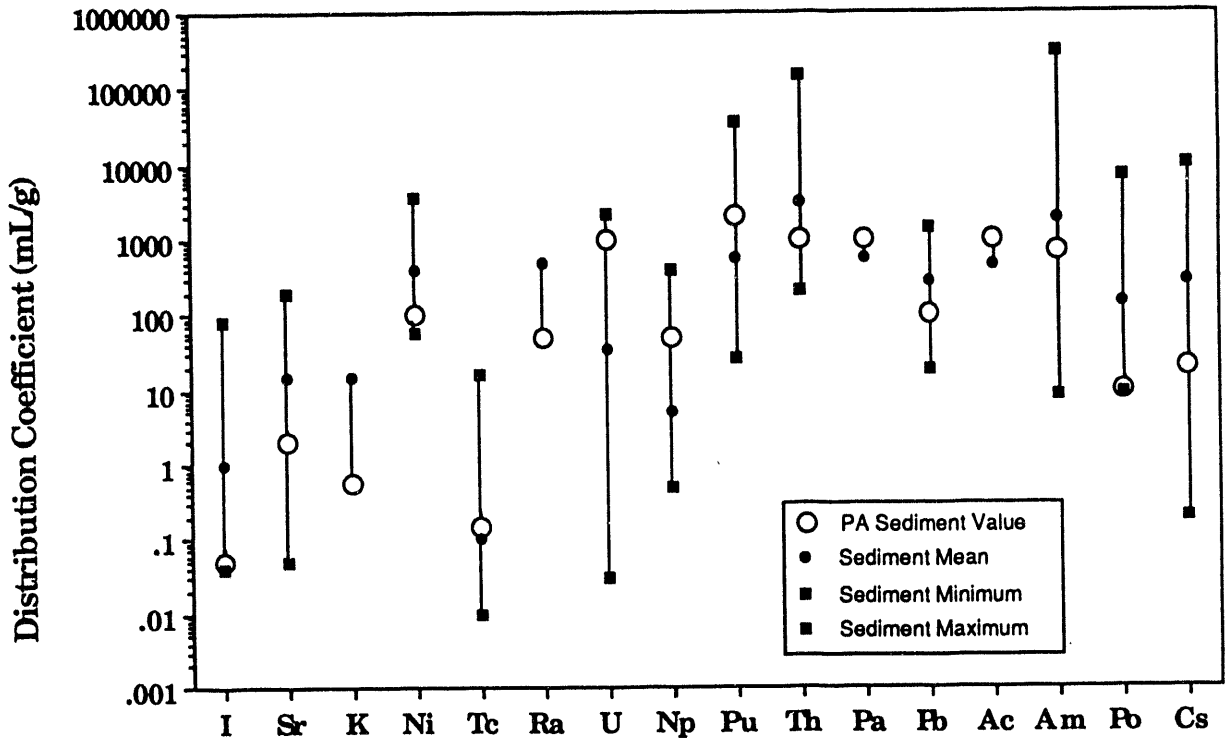

PA values are from Track 1 Guidance.
Other values are from Sheppard and Thibault, 1990.

Figure 2-9. Sediment K_d comparison.

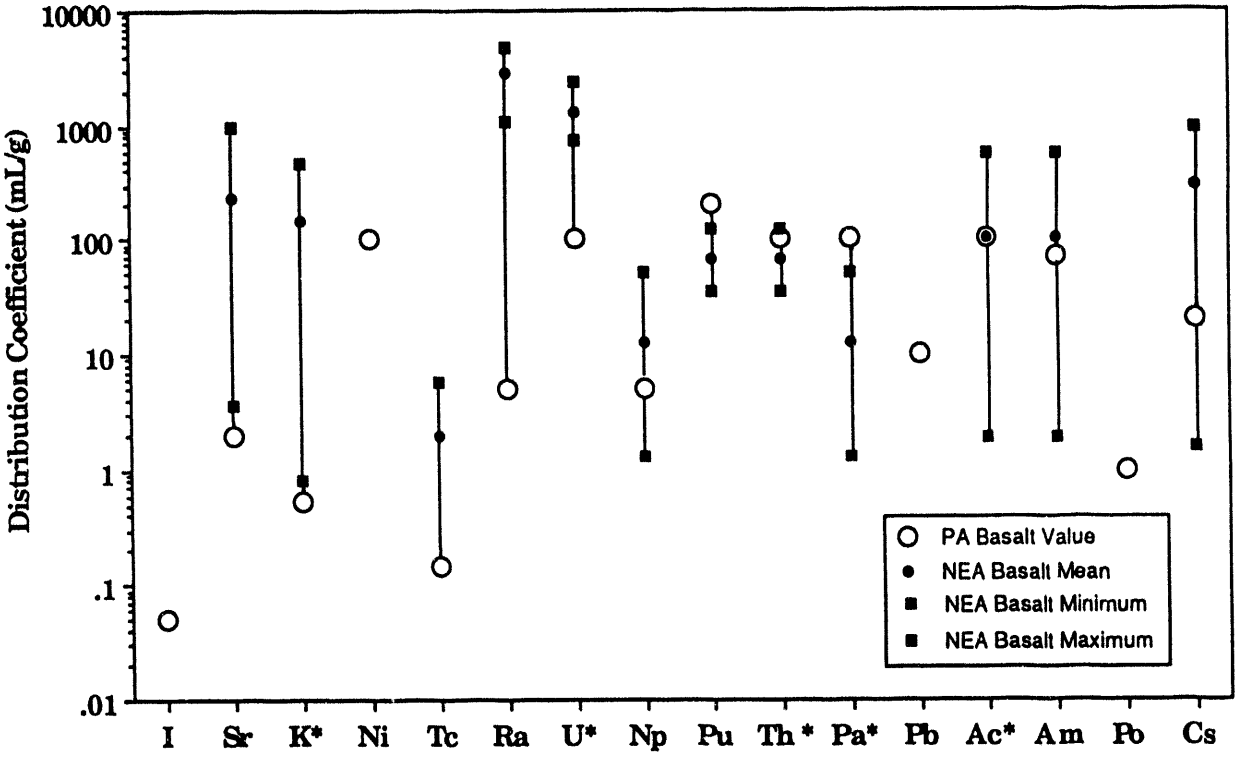

* Uranium values determined for basalt and alteration products. Thorium, protactinium, and actinium values based on plutonium, neptunium, and americium values, respectively. Cesium values divided by two to estimate potassium adsorption.

Figure 2-10. Basalt K_d comparison.

not a valid assumption, the K_d will overestimate the retardation of contaminants. Several radionuclides did not have basalt K_d information available in the literature. If possible, an analog was used to estimate the radionuclides adsorption on basalt. Potassium, thorium, protactinium, and actinium K_d values were estimated based on cesium, plutonium, neptunium, and americium, respectively. The basis for these analogs is that the elements are in the same group, and in the case of the actinides, that the elements are present in the same oxidation state. Nickel, lead, and polonium do not have available values, nor are values available for analogs.

Basalt K_d values used in the performance assessment calculations are near to slightly below Hanford basalt K_ds with the exception of plutonium and protactinium. Distribution coefficients used for plutonium and protactinium are higher than the maximum values contained in the NEA data base (Figure 2-10). Column studies like those conducted by Del Debbio and Thomas (1989) show a strontium K_d value for basalt ranging from 1.1 to 2.7 mL/g. This is significantly lower than the mean value from the NEA sorption data base (Ticknor and Ruegger 1989). The origin of this discrepancy cannot be explained with the current level of information. The difference in adsorption is possibly the result of differences in the secondary mineralization of the basalt.

Mineralogic data of the soil (alluvium) at the SDA that can be used to estimate contaminant behavior is provided in Rightmire and Lewis (1987). The alluvium ranges from 0 to 7.6 m thick, with an average thickness of 4 m, and it is comprised of airborne and waterlain sediments. The sediments are primarily silt size, but they may contain up to 50% clay-size particles. The average modal mineralogy (volume %) of the silt-size fraction is 30% quartz, 13% calcite, 17% feldspar, and 40% clay minerals. The clay minerals include approximately 32% illite, 30% mixed-layers illite-smectite, 26% smectite, and 12% kaolinite. The average mineralogy of the clay-size fraction is 27% quartz, 1% calcite, 16% feldspar, and 56% clay minerals. The clay minerals are dominantly smectite and illite with minor kaolinite.

This mineralogic information implies contaminant migration at the RWMC is affected in two ways. First, significant calcite in the soils and sediments

indicates the pH of the sediments is in the range of 8 to 9. This pH means that the actinides important in the radiological performance assessment would be at minimum solubilities. Second, the high clay content of the soils, up to 50%, shows the potential for significant adsorption within the sediments and interbeds. Further evidence of high sorptive capacity is given in Barraclough et al. (1976), which documents cation exchange capacities measured in 56 subsurface samples collected from wells drilled in and around the RWMC. The average cation exchange capacity from RWMC subsurface soils was 15 meq/100 g of soil. Cation exchange capacity in surface soils at the CFA and Power Burst Facility areas ranged from 8.2 to 16.5 meq/100 g (Martin et al. 1992). Studies of INEL surface sediments demonstrate that significant sorption of plutonium and americium occurs depending on the characteristics of the specific soils and actinide solutions (Glover et al. 1976). Considering available mineralogic information, the soils and sediments will provide significant adsorption capacity, and reasonable adsorption estimates can be made based on literature values such as those found in Sheppard and Thibault (1990).

2.1.2.5 Seismicity. The ESRP is surrounded by the seismically active Intermountain and Centennial seismic belts (Figure 2-11). The Intermountain seismic belt is a zone of concentrated seismicity that extends from northwestern Montana through eastern Idaho and Utah into southern Nevada. The Centennial seismic belt, also a seismically active zone, extends from the Hebgen Lake, Montana, area westward into central Idaho.

Earthquake data for 1884 to 1989, shown in Figure 2-11, have been compiled by the INEL, U.S. Geological Survey (USGS), Montana Bureau of Mines and Geology, United States Bureau of Reclamation, University of Utah Seismograph Stations, and Decade of North American Geology. The distribution of epicenters indicates that the Snake River Plain is devoid of earthquakes relative to the active areas surrounding it with the possible exception of the 1905 earthquake located at Shoshone, Idaho. Historical records suggest that the epicenter for the 1905 earthquake is not located within the Snake River Plain but rather near the Idaho-Utah border.

A large earthquake in the vicinity of the INEL occurred in the Centennial seismic belt on October 28, 1983, and it had a surface-wave magnitude of 7.3.

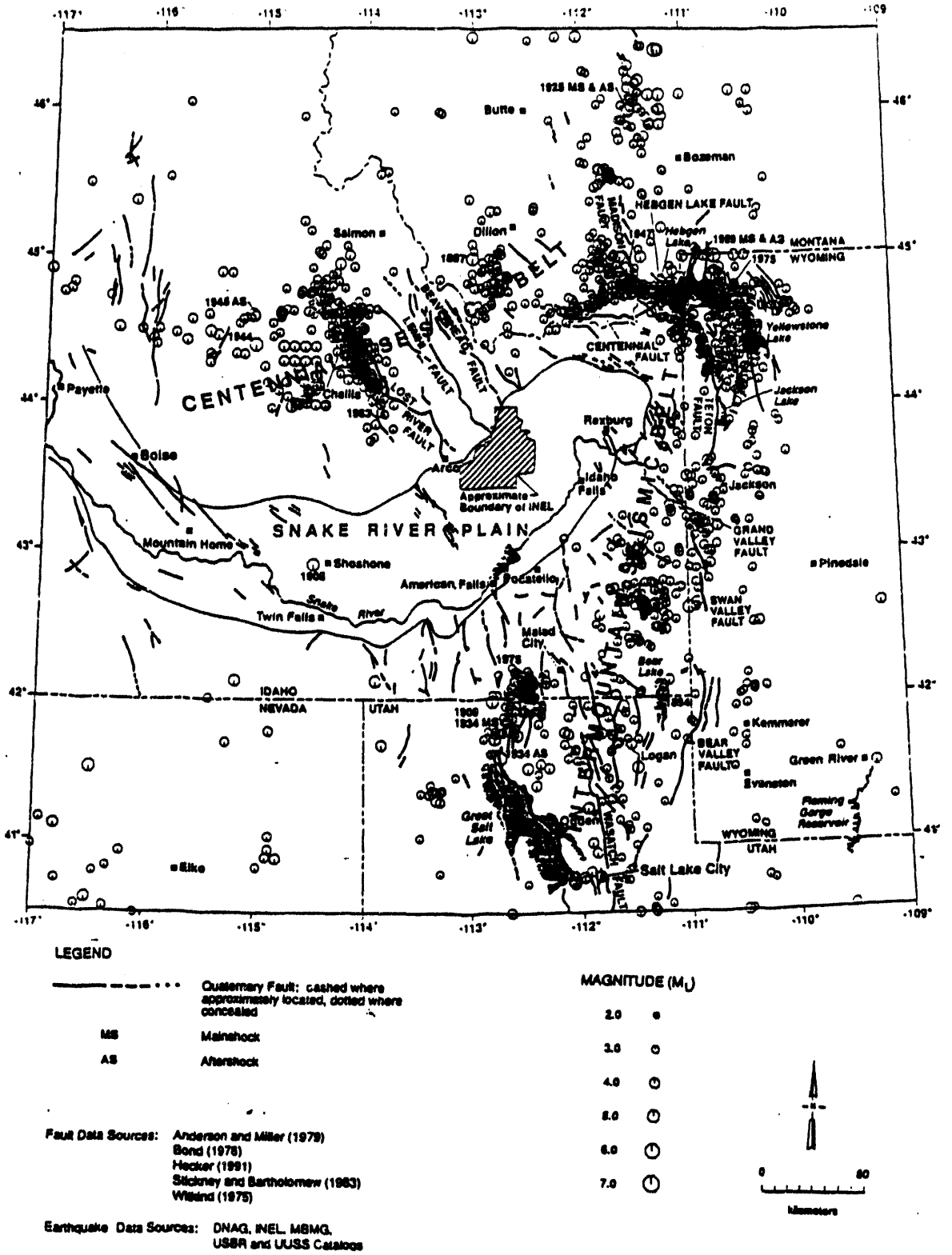

Figure 2-11. Historical seismicity map of earthquakes (M $\geq$2.5) for 1884 to 1989 and Quaternary faults of the Intermountain and Centennial seismic belts and the Snake River Plain.

The earthquake resulted from slippage along the Lost River fault--a northwest rupture along a normal fault with relative vertical movement downward to the west. The epicenter for this event was located in the Thousand Springs valley near the western flank of Borah Peak, approximately 89 to 97 km from INEL facilities. Substantial damage occurred to masonry structures in the local communities of Mackay and Challis near the epicentral area. Although the earthquake ground motions were felt at the INEL Site, only minor nonnuclear building damage occurred in the form of hairline cracks and settlement (Gorman and Guenzler 1983). The RWMC did not experience structural failures or waste spills as a result of the earthquake, and waste storage facilities do not show evidence of permanent movement or resulting damage. Peak ground accelerations ranging from 0.022 to 0.078 g were recorded at several INEL facility areas, and the INEL was located in Modified Mercalli Intensity Zone VI during the earthquake (Jackson 1985).

The largest earthquake in the region occurred on August 17, 1959, at Hebgen Lake, Montana, located approximately 193 km northeast of the INEL Site. The event had a surface-wave magnitude (M) of 7.5 and was felt at the INEL, but it caused no damage at the INEL.

The INEL has maintained a seismic network for monitoring earthquake activity on and around the ESRP since December 1971. Currently, the seismic network consists of 24 seismic stations and 21 strong-motion accelerographs. The seismic stations continually record seismic data, and their data are used to calculate the locations and magnitudes of microearthquakes ($M \leq 3.5$) that occur locally. When triggered, the strong-motion accelerographs record earthquake ground motions from local moderate to large earthquakes.

Earthquake data have been compiled by the INEL seismic network for 18-years, from 1972 to 1990. During this period, approximately 15 microearthquakes have been located within the ESRP, indicating that infrequently-occurring, small magnitude earthquakes ($M \leq 1.3$) are characteristic of ESRP seismicity (Jackson et al. 1993; Pelton et al. 1990). These data are in agreement with the historical earthquake data compiled for the surrounding region (Figure 2-11). Recent modifications to the seismic network, such as placing sensors in 18 to 21-m boreholes, will lower the magnitude threshold of detecting microearthquakes within the ESRP.

Because the ESRP is surrounded by the seismically-active Intermountain and Centennial seismic belts and several Quaternary faults are located near the western boundary of the INEL, seismic hazards assessments are being updated for all facility areas at the INEL. These assessments are being performed to quantitatively estimate peak ground motions that INEL facilities may experience from nearby large magnitude earthquakes. Most of the INEL is located in Seismic Zone 2B, and a small portion is located in Zone 3. The seismic design levels for INEL facilities exceed those required for these classifications.

Uplift and erosion of the RWMC area could result from faulting and uplift of the southern Lost River fault if the fault encroached southward onto the ESRP to a position several kilometers west of the RWMC. Assuming immediate initiation of this faulting and maximum-uplift rates from the most recently active fault segments of the nearby Basin and Range Province (1 to 2 m/1,000 yr), significant uplift and erosion of the RWMC area would require times of 10,000 to 100,000 years.

2.1.2.6 Volcanic Activity. Most of the INEL is underlain by a 0- to 1-km thick sequence of late Tertiary and Quaternary basalt lava flows and interbedded sediments. Based on drill hole information, regional mapping along the margins of the ESRP, and geophysical information, the basalt/sediment sequence is underlain by an older section (up to several kilometers thick) of late Tertiary rhyolitic volcanic rocks. These two volcanic sequences are a consequence of the passage of the Yellowstone mantle plume (hotspot) through the INEL area of the ESRP in late Tertiary time (Malde 1991).

The Tertiary rhyolitic volcanic rocks were erupted at 6.5 to 4.3 Ma, when the hotspot resided beneath the INEL area. They are comprised mostly of ash-flow tuffs erupted during large, violent explosive episodes and large rhyolitic lava flows. They are analogous to the ash flow tuffs and lava flows that were erupted from calderas in the Yellowstone Plateau at 2.0 to 0.6 Ma. These types of large-scale explosive eruptions can occur only directly over the mantle hotspot because large inputs of heat into the lower and middle crust are required to generate such large volumes of rhyolitic magma. Because

the hotspot is now situated beneath the Yellowstone National Park, recurrence of this type of volcanic activity in the INEL area is nearly impossible.

Residual heat in the upper mantle after passage of the hotspot has continued to produce basaltic magmas that have risen to the surface and erupted onto the subsiding ESRP. Basaltic eruptions in the INEL area began at about 4 Ma, soon after passage of the hotspot, and have continued with the most recent activity occurring along the Great Rift about 2,100 years ago.

Basalt vents on the ESRP include broad, nearly circular, low-relief shield volcanoes; small spatter cones; and spatter ramparts along eruptive fissures. Lava fields related to single vents range in surface area from 2 to 400 km^2 and in volume from 0.05 to 7 km^3 (Kuntz et al. 1992). Volcanic vents are not randomly distributed on the ESRP, but they are concentrated in northwest-trending linear zones known as volcanic rift zones (Figure 2-12). In addition, vents are concentrated in a northeast-trending zone, known as the Axial Volcanic Zone, along the central axis of the ESRP. The Axial Volcanic Zone is a constructional highland caused by more voluminous magma output along the axis of the ESRP.

The RWMC lies near the northeast margin of the Arco Volcanic Rift Zone (Figure 2-12). Based on radiometric age determinations of basalt lava flows, the Arco Volcanic Rift Zone north of Big Southern Butte was active between 600 and 100 kilo annum (Ka) (Kuntz et al. 1990). The Cerro Grande and North and South Robbers flows (10,500 to 12,000 Ka) near Big Southern Butte occur at the intersection of the Arco Volcanic Rift Zone with the Axial Volcanic Zone. Except for volcanism along the Great Rift, all of the Holocene volcanic fields of the ESRP occur along the Axial Volcanic Zone (Figure 2-12). Recurrence of volcanism in the ESRP has a greater likelihood of occurring along the Great Rift and along the Axial Volcanic Zone than elsewhere, and volcanism on the INEL is an improbable event.

Holocene surficial geology and archaeology suggest that eolian deposition and erosion in the INEL area have been in approximate net balance for at least the past 10,000 years. A reversal of the long-term, regional pattern of ESRP subsidence, sedimentation, and volcanism into an erosional rather than a

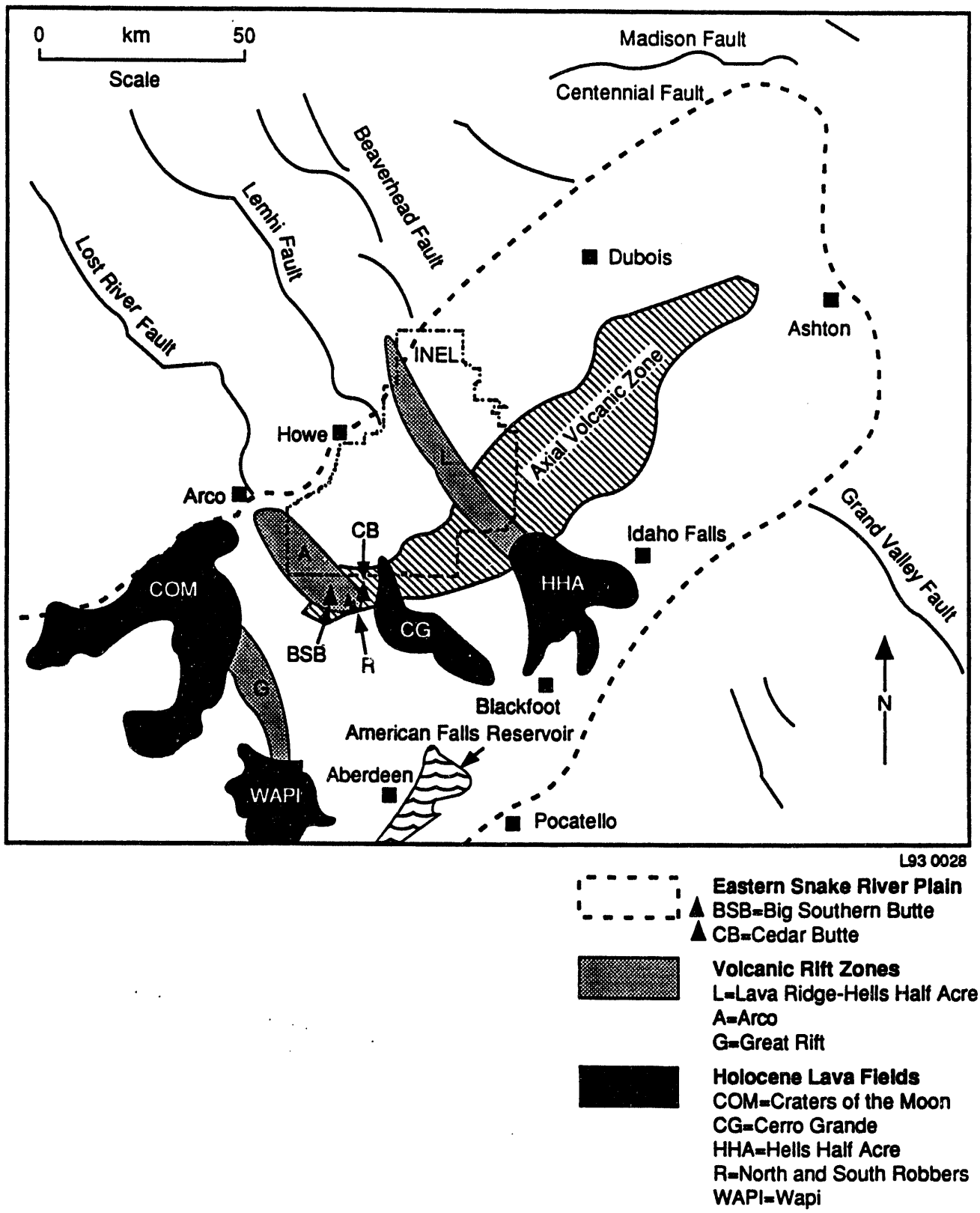

Figure 2-12. Volcanic rift zones and Holocene lava fields of the ESRP.

depositional regime would require major changes from the Holocene tectonic or climatic configuration of the ESRP. Worldwide geologic evidence indicates that the Quaternary epoch (approximately the past 2 millions years) has been a time of major climatic fluctuations. During colder and wetter periods, glaciers occupied high-elevation areas, and lowland areas such as the ESRP received thick, widespread loess blankets. Lowland areas were also periodically impacted by local catastrophes [such as the large, late-Pleistocene, glacial outburst flood(s) that traveled down the Big Lost River valley], eroded upland surfaces on the ESRP, and deposited sediment in the RWMC area. If the future ESRP climate were to become warmer and more arid, the probable consequences would be decreased vegetation and increased eolian transport of fine-grained sediment, mainly as longitudinal dunes of fine sand.

The following impacts from volcanic activity are relevant to RWMC radiological performance assessment:

1. During the past 4 million years, the ESRP and the RWMC area have undergone regional subsidence, basaltic volcanism, and fluvial and eolian sedimentation. Erosion has not been a significant process on the ESRP.

2. Surficial- and subsurface-geologic data indicate that the RWMC area has both subsided and accumulated basalt lava flows and sediments at an average rate of 0.3 mm/yr. This long-term trend has not been interrupted by significant uplift or erosion.

3. Lava inundation or magma intrusion associated with volcanism from the nearby Arco Volcanic Rift Zone is improbable considering the volcanic history of the area, and lava inundation or magma intrusion would not likely result in the release of radionuclides to the environment.

4. The RWMC lies in a small basalt-rimmed basin, more than 7 km from the nearest major river (Big Lost River), and this basin has existed in its largely uneroded configuration for approximately the past 100,000 years. During that time, the RWMC basin has received up to 7 m of fine-grained sediment, mainly of eolian origin. The

preservation of multiple paleosols and caliche horizons within these sediments indicates that numerous RWMC land surfaces were subaerially exposed and weathered, but they remained largely uneroded for 1,000 to 10,000 years.

5. Erosion by wind, surface water, or mass wasting is not anticipated to extend below the original RWMC ground surface in the areas of the pits and soil vault row covers because the ESRP is a low-lying region where Quaternary sedimentation and volcanism (not erosion) have been the dominant processes of landscape evolution. As a local basin within the ESRP, the RWMC basin is distant from the eroded channel of the Big Lost River or other surface drainages, and it has been a place of Quaternary eolian sediment deposition and soil formation.

6. Future climate fluctuations on the ESRP, to either colder/wetter or warmer/drier conditions, are not expected to erode the RWMC land surface. Quaternary geologic and Holocene archaeological data suggest the INEL area will probably continue its long-term history of regional subsidence and net accumulation of sedimentary and volcanic materials, although sedimentation patterns on the ESRP will change in response to future climate fluctuations.

7. RWMC soil cover erosion could occur as a consequence of faulting and uplift, but this erosion would involve a major change in the Quaternary tectonic configuration of the ESRP. Therefore, this scenario is improbable within the next 10,000 years considering the regional seismicity and tectonic history of the INEL area, the absence of Quaternary tectonic faults on the ESRP in the vicinity of the INEL, and the long response time for significant erosion to occur as a result of protracted faulting and uplift.

2.1.3 Hydrology

2.1.3.1 The INEL. Surface water at the INEL Site comes from streams draining through intermountain valleys to the west and north, localized snowmelt, and rain. Streams entering the INEL Site include the Big Lost

River, Little Lost River, and Birch Creek. Flows from the Little Lost River and Birch Creek are diverted for irrigation before reaching the INEL Site. Birch Creek is also diverted for electrical production. Thus, during dry years, water from those streams does not reach the INEL Site. These three drainages are part of a closed basin without an outlet. The drainages terminate in four playas, collectively called the Big Lost River Sinks, in the north-central part of the INEL Site (Figure 2-13). As a result of the closed basin, when water does flow onto the INEL, it either evaporates or infiltrates into the ground. However, water from the Little Lost River and Birch Creek does not normally reach the playas. The INEL Site is not crossed by any perennial streams. All surface outflows are a result of localized runoff.

Except for evaporation, all water from the Big Lost River in the Snake River Plain is recharged to the ground. Water infiltrates from the Big Lost River and can form perched groundwater beneath the river before eventually reaching the Snake River Plain Aquifer. This infiltration has been significant during wet years. There are also zones of perched water, the exact extent and volume of which are not known, near large water sources [such as the TRA and Idaho Chemical Processing Plant (ICPP) infiltration ponds] within the INEL Site.

The Snake River Plain Aquifer is a continuous body of groundwater that underlies nearly all of the ESRP. It is approximately 320 km long, 48 to 97 km wide, and 25,000 km^2 in area. The depth to the aquifer at the INEL Site varies from 61 m in the north to 270 m in the southwest corner. Most of the permeable zones in the aquifer occur in highly fractured basalt or in rubble zones beneath basaltic flows.

The thickness of the aquifer is difficult to estimate. Deep drilling of the INEL-1 well northeast of Test Reactor Area (TRA) indicated the base of the aquifer is defined by sand, silt, and clay intervals that begin at either 260 or 370 m below land surface (Mann 1986). Hydraulic conductivity measurements of basalt samples from this well indicate the upper 60 to 240 m of basalt rocks have a higher permeability than basaltic rocks below the sedimentary intervals. The depth to the regional aquifer at this location is 120 m below land surface, so the estimated thickness of the aquifer at this location

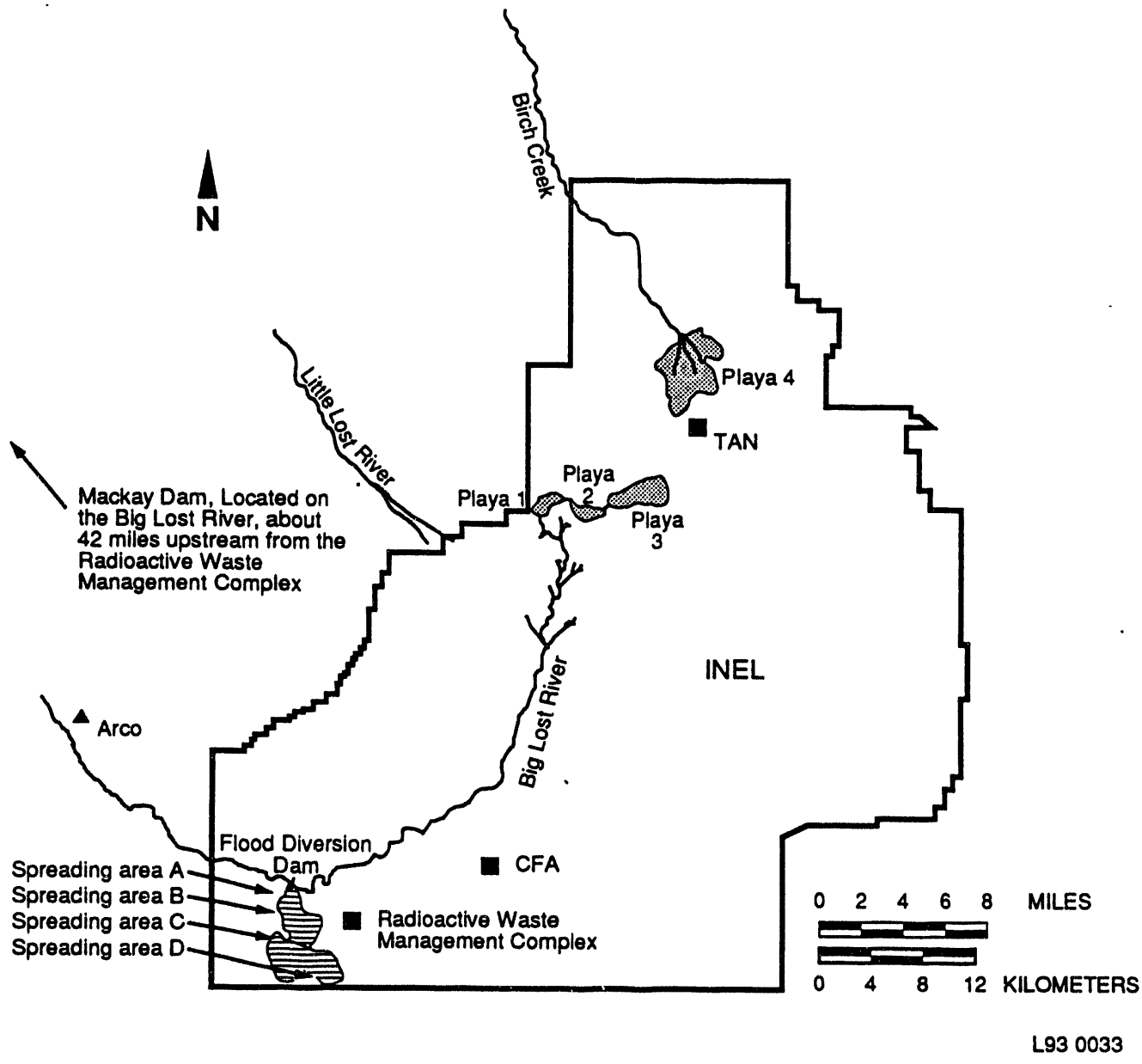

Figure 2-13. Surface water features at or near the INEL.

ranges from 140 to 250 m. Anderson (1991) indicates the base of the aquifer at the TRA-DISP well is at 370 m below land surface. While the aquifer may extend down to 370 m below land surface on the INEL, the effective thickness and most permeable portion through which the majority of water movement occurs has been estimated to be 76 m (Robertson 1974). This estimate was derived, in part, from the maximum depth that tritium was found in the regional aquifer after its disposal in the ICPP injection well.

Groundwater in the aquifer flows generally southwest (Figure 2-14). Tracer studies at the INEL Site indicate natural flow rates of 1.5 to 6.1 m/day, with an average near 3 m/day. However, these locally-measured rates are not necessarily representative of flow rates throughout the aquifer (Robertson et al. 1974). Tracer concentrations of waste products in the southern portion of the INEL migrate about 1.3 to 2.1 m/day. A stock-watering well is located 16 km downgradient from the RWMC, and a domestic well is located 29 km in the same direction. Both of these wells are outside the southern boundary of the INEL. The nearest community public water supply (15 or more connections servicing residents year-round) to the RWMC is located 18 km distant at Atomic City, which is also outside the southern INEL boundary. Depending on variations in flow in the regional aquifer, the well at Atomic City is either offgradient or even slightly upgradient from the RWMC.

The aquifer may contain 2,500 billion m^3 of water, of which 630 billion m^3 might be recoverable. The aquifer discharges about 8 billion m^3 of water annually through springs in the Hagerman area and in the region west of Pocatello. About 1.8 billion m^3 of water is withdrawn from the aquifer through irrigation well pumpage. The discharges from the Hagerman springs significantly contribute to the flow of the Snake River downstream of Twin Falls, Idaho.

In addition to providing water for INEL Site operations, the aquifer supplies water for other industries. Water from springs in the Twin Falls-Hagerman area is used to raise fish commercially. The spring water flow of 47 m^3/s constitutes 76% of the water used for the commercial production of

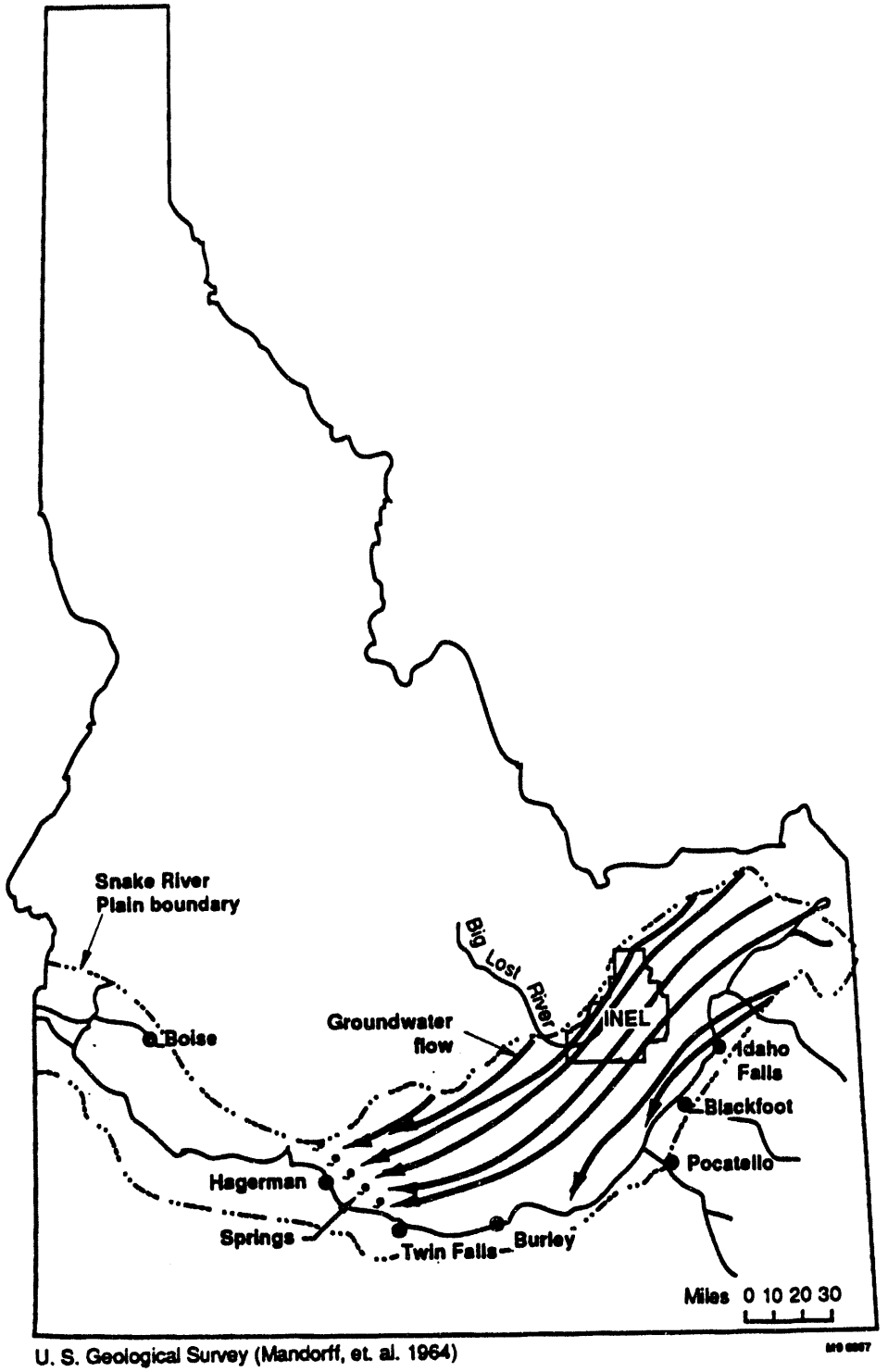

Figure 2-14. Location of generalized groundwater flow lines for the Snake River Plain Aquifer.

fish in Idaho. Most of these fish farms discharge water directly into the Snake River.

2.1.3.2 The RWMC

2.1.3.2.1 Surface Water--The principal surface water body near the RWMC is the Big Lost River, approximately 3 km northwest of the RWMC (see Figure 2-15). The Big Lost River drains mountain watersheds to the northwest of the INEL. The river is an important source of irrigation water for agricultural areas west and northwest of the INEL. A significant portion of the streamflow is controlled by Mackay Dam, which stores runoff for irrigation. Streamflows are often depleted by irrigation withdrawals and infiltration losses along the river channel. During periods of high streamflows, the river flows to its terminus in the Big Lost River Sinks in the northwest central portion of the INEL.

A flood-control system was constructed on the Big Lost River in 1958 to control downstream flooding that was occurring as a result of ice accumulation in the main channel during the winter months. The flood-control system consists of a diversion dam, diversion channel, two 1.8-m diameter gated culverts, three dikes, four spreading areas on the INEL Site, and interconnecting channels (Figure 2-15). The flood-control system was upgraded in 1984 by raising the dikes to allow for a total diversion capacity of 263 m^3/s (Bennett 1986). The gated culverts control flow into the main channel, with a total culvert capacity of 25 m^3/s (Lamke 1969). The last significant discharge to the spreading areas occurred in 1984 and 1985. The elevation of the Big Lost River just upstream from the diversion dam is 1,544 m (5,066 ft) (see Figure 2-15). The elevation of Spreading Areas A and B vary, but is approximately 1,536 m (5,040 ft).

The SDA is located in a natural topographic depression at an average elevation of 1,527 m. This natural depression holds precipitation and collects additional runoff water from the surrounding slopes. The SDA has been flooded at least three times (in 1962, 1969, and 1982) by local basin runoff. These floods were the consequence of rapid snowmelt combined with heavy rains and warm winds, resulting in runoff water from the surrounding

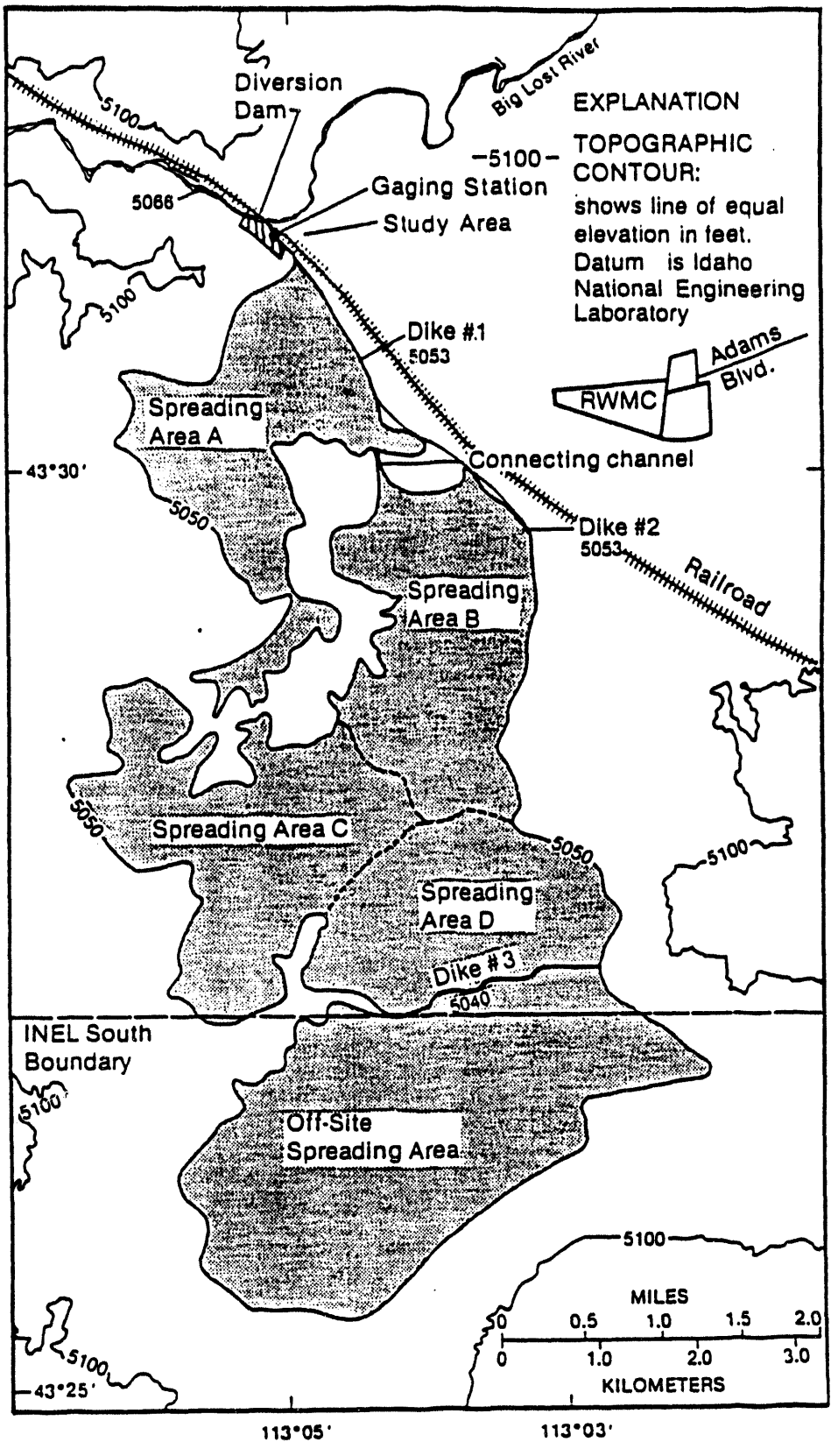

Figure 2-15. Location of the study area and enlarged Spreading Areas A, B, C, and D.

areas entering the SDA. In response to the 1962 flood, dikes were constructed around the perimeter of the SDA to prevent local runoff from entering the SDA. After the 1969 flood, the dike around the SDA was raised and the perimeter drainage ditch was enlarged.

In 1971, the SDA was graded and drainage channels were provided to control surface water runoff. An outlet pipe with a flap valve was placed through the dike in the northeast corner of the SDA to allow surface water to flow out and to prevent water from entering the SDA.

In February 1982, a warm front characterized by strong winds and heavy rains moved into the RWMC area. Runoff from the surrounding area accumulated in the southeast corner of the SDA, causing a rupture of the perimeter dike. This rupture resulted in floodwaters entering Pits 16, 17, and 18. The following flood-control measures were then taken at the SDA: (a) the perimeter drainage channel was widened and deepened, (b) the perimeter dike was raised and rip-rap was added to prevent scouring, and (c) the SDA cover was recontoured and new fill material was brought in to fill depressions to improve surface water drainage.

In spite of the contouring efforts within the SDA, several small depressional areas with minimal drainage to the channels often result in precipitation ponding. A final cover design will be considered to prevent further infiltration of precipitation and snowmelt from entering the SDA cover.

Flooding studies at the RWMC can be divided into two categories: (1) flooding related to the Big Lost River and (2) flooding from within the local basin because of snowmelt and precipitation. Tullis and Koslow (1983) documents a study of recorded discharge data from several USGS streamflow stations along the Big Lost River that suggested a history of low-magnitude floods. Flooding in the Big Lost River basin is associated with peak flows during snowmelt season and occasional flooding caused by ice jams in the stream channel. A detailed flood-routing analysis of a hypothetical failure of Mackay Dam resulting from hydrologic and seismic failures showed the RWMC would not be affected by this severe flooding (Koslow and Van Haaften 1986). The RWMC, located 3.2 km south of the Big Lost River, is disconnected from the

river by a lava ridge that serves as a hydraulic barrier. Therefore, there is little danger of flooding from the Big Lost River affecting the RWMC.

A study documented in Martineau et al. (1990) investigated the effect of a hypothetical failure of Dike 2 on flooding the SDA. The study concluded that there was potential for overtopping of the SDA perimeter dike. Subsequent upgrades to the SDA perimeter drainage ditch have reduced this possibility. An additional study should be conducted to address the likelihood of flooding of the SDA to include the upgraded perimeter drainage ditch. This study should address the hypothetical failure of Dike 2 and investigate the possibilities of flooding from maximum predicted precipitation events within the local basin.

A study using meteorological data from CFA from 1950 through 1990 was compiled, and a statistical analysis was performed to determine the 25- and 100-year, 24-hour precipitation, and the 25- and 100-year snow depths on the ground for the RWMC (Sagendorf 1991). Results from the study indicate 3.43 cm of precipitation for a 25-year, 24-hour storm event and 4.06 cm of precipitation for a 100-year, 24-hour storm event. The expected 25- and 100-year snow depth is 57.40 and 77.72 cm, respectively.

2.1.3.2.2 Subsurface--This section contains measurements and interpretation about water movement in surficial sediments, perched water, interbeds, and the aquifer at the RWMC. The information presented here is drawn on in discussion of the hydrologic flow conceptual model in Section 3.2.

Surficial Sediments--Garabedian (1989) presented an annual estimate of net infiltration of less than 1.3 cm for the entire southern portion of the INEL. This estimate was based on measurements of precipitation, soil type, and soil depth.

Miller et al. (1990) presented estimates of annual net infiltration at the CFA landfills. The methodology combined an estimate of daily evapotranspiration obtained from meteorological records with a description of the vegetation on the landfills. The estimated daily evapotranspiration was subtracted from the daily precipitation and accumulated over each year of a 30-year period, which resulted in an annual cumulative distribution function

of the net amount of water available for infiltration into the cover material. This net infiltration was then reduced by an estimate of the storage capacity of the cover. The average net annual infiltration of 2.5 to 5.2 cm was taken from the median of the cumulative distribution. By assigning a dry year as the 0.1 quantile and a wet year as the 0.9 quantile from the cumulative distribution, net infiltration was estimated to be 0.0 to 1.9 cm in a dry year and 8.9 to 10.2 cm in a wet year.

The statistical results in Miller et al. (1990) assume that the maximum storage capacity was always available to prevent net infiltration. However, an appreciable amount of melting in the spring could deplete this storage and still result in net drainage because of low evapotranspiration. Another way to interpret their results is to assume net changes in storage over the long term are negligible and estimate net infiltration as the difference between measured precipitation and estimated daily evapotranspiration accumulated over an annual period. Miller et al. (1990) reported an average estimated evapotranspiration of 14.6 cm. Subtracting this from the annual precipitation of 22 cm results in a net infiltration estimate of 7.4 cm.

Cecil et al. (1992) estimated annual water infiltration rates through the surficial sediments ranging from 0.4 cm based on neutron logging to 1.1 cm based on isotopic tracers at a site immediately adjacent to the SDA boundary. However, this study was conducted in undisturbed, vegetated soils; therefore, it is not likely to represent infiltration rates in disturbed soils over the waste pits inside the SDA.

McElroy (1990) presented soil moisture monitoring data and matric potentials from two locations inside the SDA within the surficial sediments. These locations (shown in Figure 2-16) are both in undisturbed regions, with Well W06 possibly having been affected by surface disturbances because of its relative proximity to waste pits and access roads. Measurements made from 1986 to 1990 indicate that there was a substantial infiltration event associated with snowmelt during the early spring of 1989. The neutron probe used for these measurements was inadequately calibrated for the observed range of moisture contents, therefore, preventing quantitative infiltration estimates. Furthermore, monitoring was conducted monthly, which was inadequate because of the rapid infiltration events.

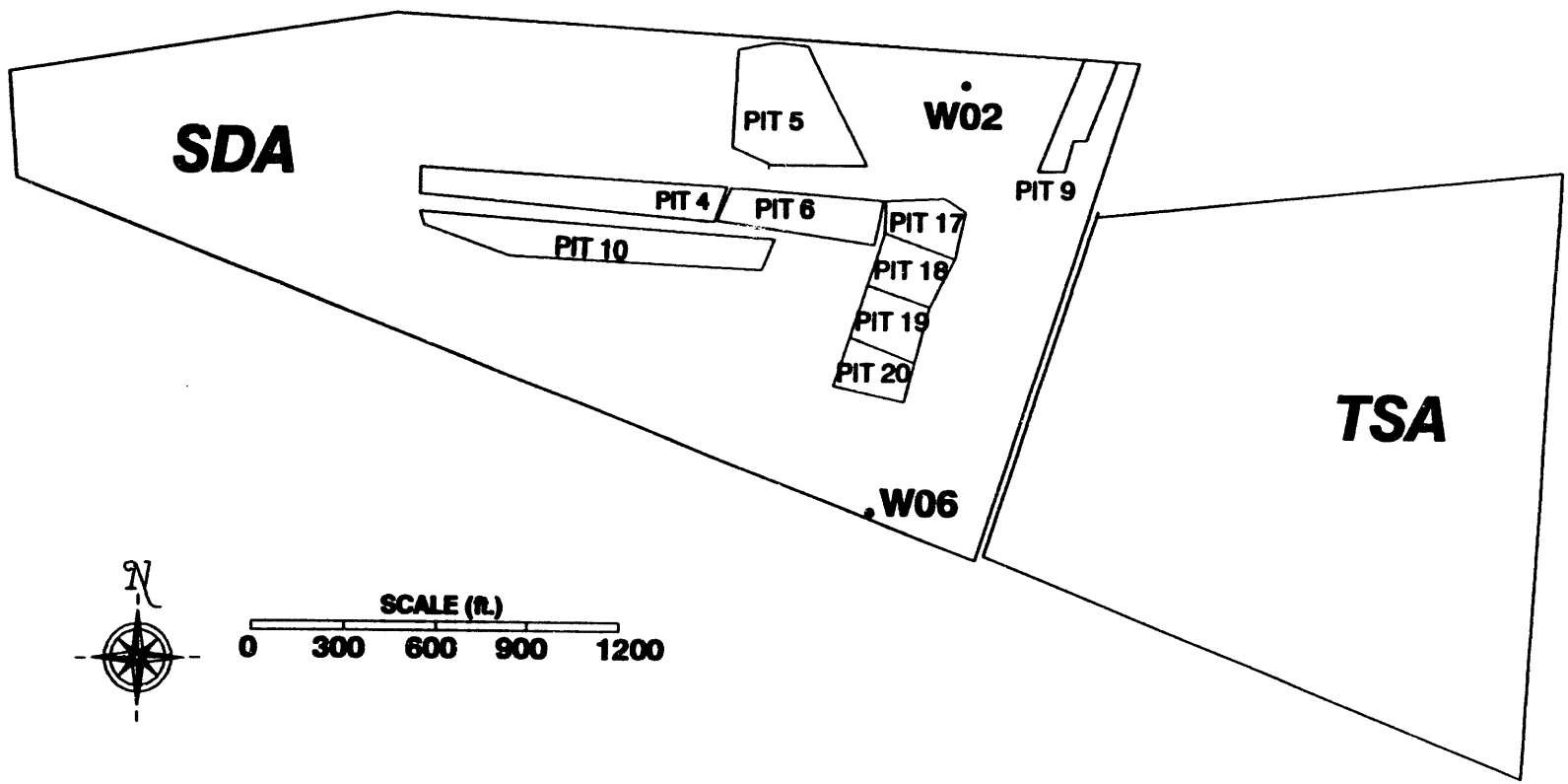

Figure 2-16. Two neutron access tube locations for monitoring soil water movement (McElroy 1993).

McElroy (1993) presented additional monitoring data collected from December 1992 into the summer of 1993. The calibration range of the neutron probe was expanded, and the measurement frequency was increased to obtain quantitative infiltration estimates. During this period, an estimated 24 cm of water infiltrated into the surficial soils at Well W02 to a depth of 1.1 m in 14 days. A coarse, sandy layer at 1.1 m depth in Well W02 inhibited infiltration of the majority of this water deeper into the surficial soils and allowed most of the water to be brought back to the surface by evapotranspiration. Through the end of July, the amount of water that drained into the underlying basalts beneath Well W02 was estimated to be less than 3 cm.

At Well W06, an estimated 56 cm of water infiltrated in 7 days during the spring of 1993 to 3.2 m, the depth to basalt. Subsequent evaporation brought about half of this water back to the surface. Through the end of July, an estimated 28 cm of water infiltrated into the underlying basalts.

Water equivalent measurements in the snowpack in the vicinity of the two neutron access tubes made before the beginning of the snowmelt ranged from 13 to 21 cm (McElroy 1993). These water equivalent measurements provide a partial explanation of the large amounts of infiltration (24 and 56 cm) observed at Wells W02 and W06. The remainder of the water observed in the surficial sediments at Well W06 was a result of lateral influx within the surficial sediments, probably from a snow berm 2 m away. For purposes of comparison, precipitation records collected by NOAA at CFA show 27.4 cm of water precipitation from November 1992 through August 1993--about 9.6 cm above the normal amount of precipitation.

McElroy (1993) also presented soil water tension measurements made at a tensiometer nest located 1 m east of Well W06. The measurements both corroborated the advance of water observed through moisture content measurements and indicated the water moved downward between the 0.9- and 1.8-m depths until the end of July. For the 1.8- to 2.7-m-depth interval, the gradient remained downward until the end of August.

Hubbell (1993) presented measurements of water levels of perched water within the surficial sediments that were also taken during spring 1993.

Perched water was observed in 6 out of 20 shallow monitoring locations inside the SDA (Figure 2-17). The thickness of the perched water measured up to approximately 1.1 m. Greater perched water thicknesses were observed in one well that had a suspect casing, indicating a possible lack of seal between the monitoring well and the surrounding sediments. Hubbell (1993) indicated there is a correlation between the 1.1-m rise in water levels and a cumulative precipitation of 5.9 cm during the previous 8-day period. This calculation was based on an assumption that an increase in moisture content of 0.05 saturated the soil and raised the perched water level.

Magnuson and McElroy (1993) presented estimates of annual infiltration into surficial sediments based on in situ moisture content measurements and representative moisture characteristic curves for the A-B and C-D interbeds. They used a unit gradient assumption in their estimates, which implied the hydraulic conductivity at the in situ moisture content was the same as the Darcy flux or net infiltration. Available hydraulic characterization data for the interbeds were used individually and were averaged by interbeds, which resulted in infiltration estimates that ranged from 0.014 to 55 cm/yr. If only averaged measurements from noncompacted samples taken from the deeper C-D interbed were considered, the range narrowed to 3.8 to 9.2 cm/yr. This latter range was identified in Magnuson and McElroy (1993) as a better estimate of the infiltration rate because it was from a greater depth, and transient water movement nearer the surface was more likely to have been dampened out.

This last net infiltration estimate in Magnuson and McElroy (1993) is not strictly based on information from within surficial sediments. However, infiltration estimated from measurements at depth most likely passed through the surficial sediments.

In summary, the measurements and estimates of infiltration from anywhere within the INEL region, including the SDA, vary widely. The hydrologic conceptual model outlined in Section 3.2 puts the most weight or confidence in the Magnuson and McElroy (1993) estimate because it is based on measurements from depth.

Perched Water-- This section presents information about perched water occurring above the B-C or C-D interbeds.

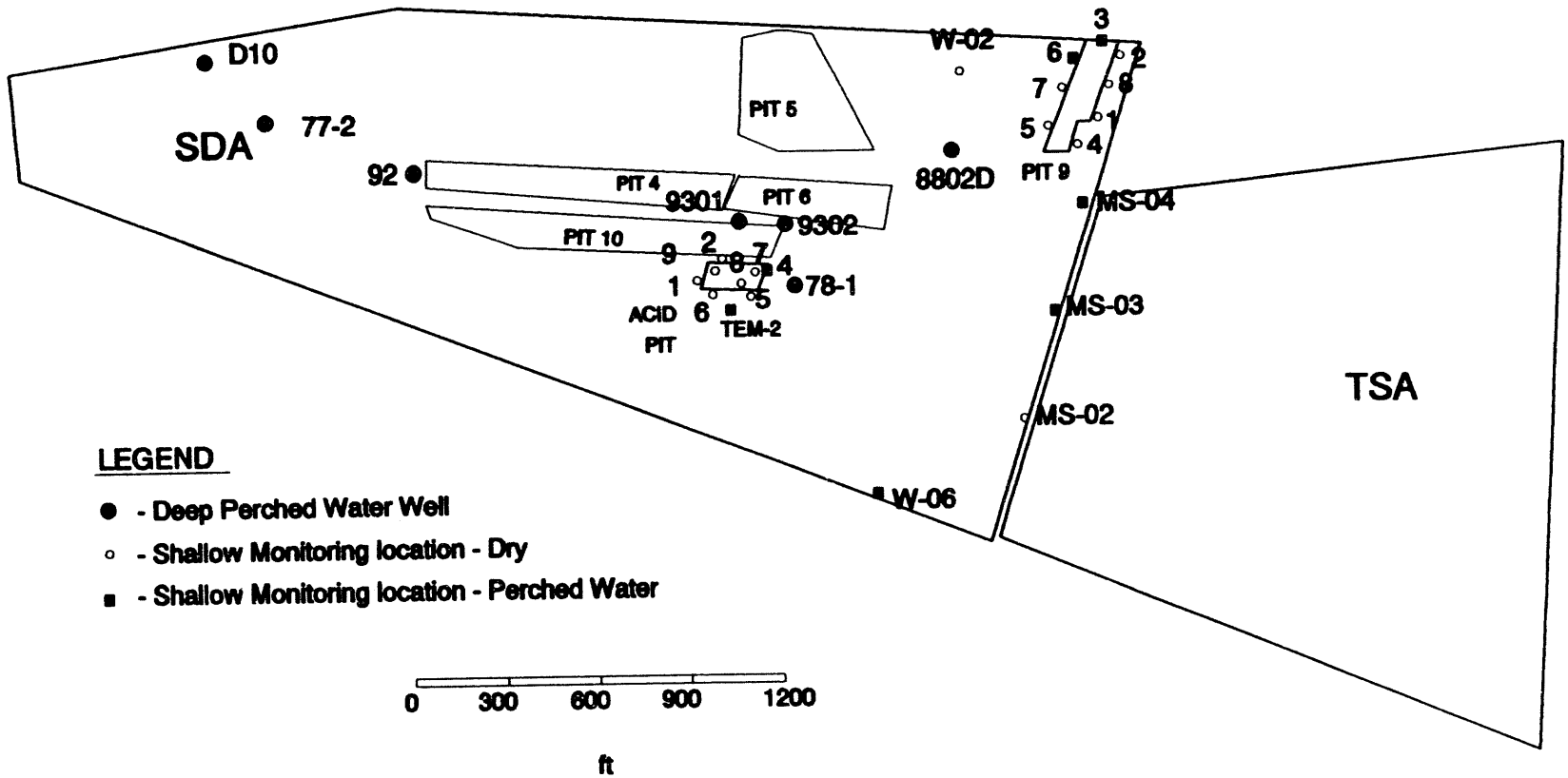

Figure 2-17. Location of perched water detected in shallow surficial sediments wells and in deep interbed monitoring wells (Hubbell 1993).

Hubbell (1990a, 1992, 1993) presented hydrographs for wells with perched water above the B-C and C-D interbeds. Figure 2-18 identifies the locations of wells referred to in the following discussion. Figure 2-19 shows several of the locations in cross section where perched water has been detected. Perched water was not detected in all wells drilled down to the C-D interbed, indicating that the perched water bodies are discontinuous. In Wells 92 and D10 (not on the cross section) the B-C interbed is not present. In these wells, perched water levels above the C-D interbed are believed to demonstrate a seasonal response and indicate that infiltrating water reached a depth of approximately 67 m in 2 months. Hubbell (1990a) also correlated the rate of recovery of the perched water level in Well 92 and observed discharges of water to the INEL diversion system. This indicates that the source of perched water in Well 92 is seasonal recharge of snowmelt as well as recharge water originating in the spreading areas.

The perched water zone in Well 92 was slug tested and showed a low horizontal permeability (Hubbell 1992). Water that recharges the perched zone in Well 92 from the spreading areas does not likely travel horizontally through this low conductivity zone. Rather, it moves horizontally through high permeability interflow or rubble zones that occur between individual basalt flows above the low horizontal permeability region.

As Well 92 was drilled, perched water was observed before the C-D interbed was penetrated. Immediately after the C-D interbed was penetrated, the perched water in the well bore drained into the interbed (Barraclough et al. 1976). This indicated that a low vertical permeability region above the interbed was responsible for the perched water at this location, not the interbed itself.

Perched water has been intermittently present in Well 77-2, above the B-C interbed in the western part of the SDA (Hubbell 1990a). This perched water is also believed to be related to seasonal recharge. Monitoring in Well 77-2 has been sporadic, preventing definitive conclusions.

Perched water levels in Well 88-02, above the C-D interbed in the eastern part of the SDA, have not shown a seasonal influence. Elevated concentrations

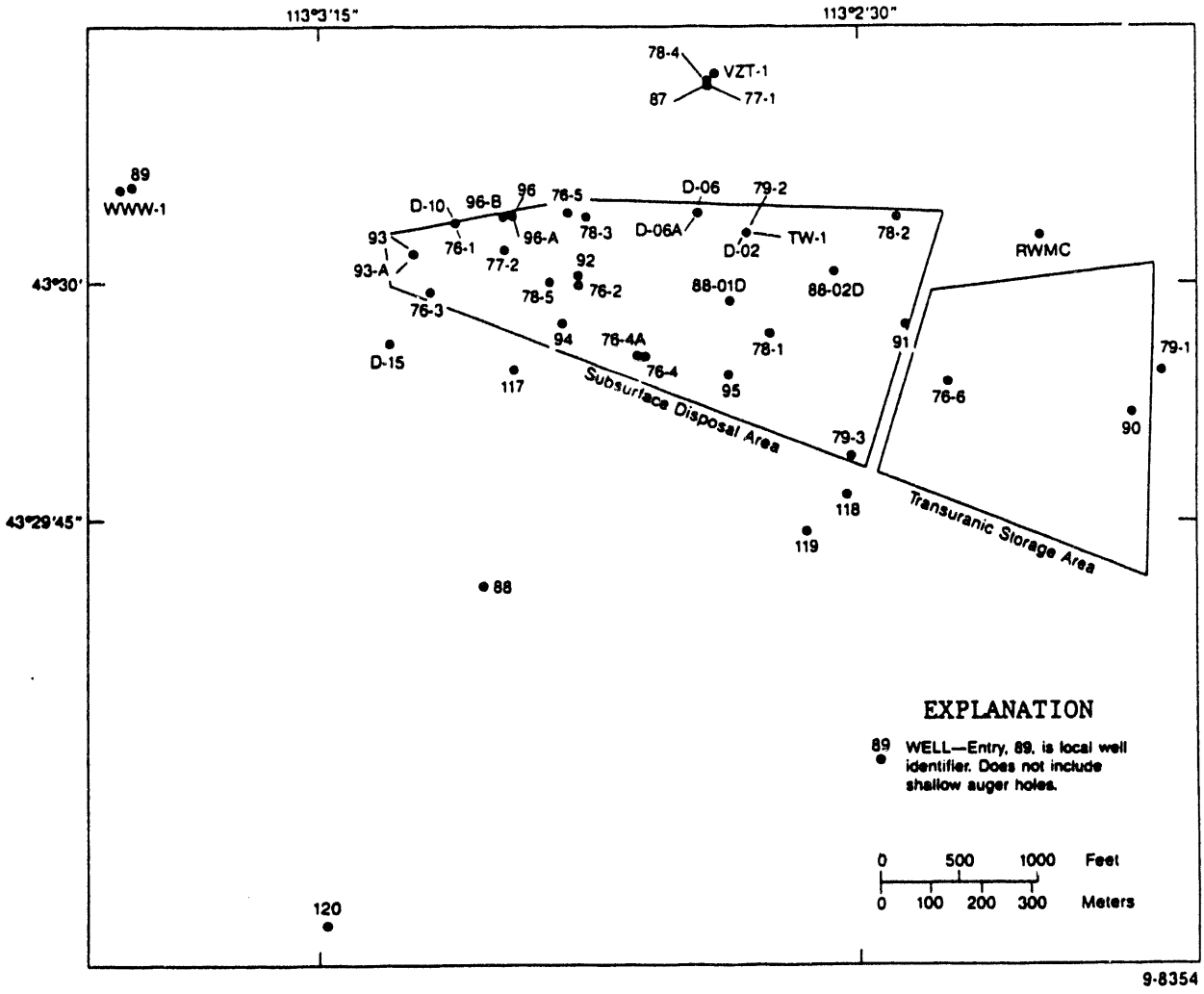

Figure 2-18. Well locations at the RWMC.

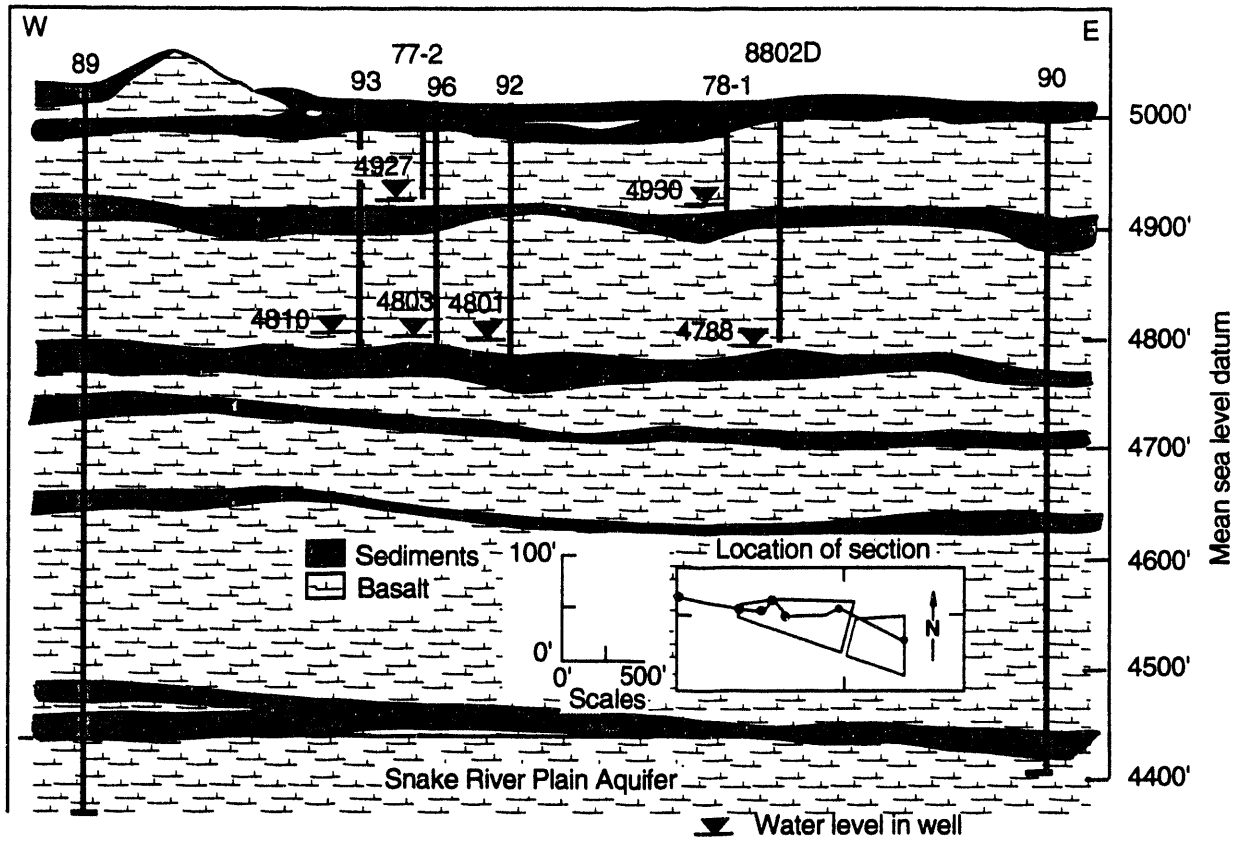

Geologic Section W-E at the Radioactive Wast Management Complex

Q94 0022

Figure 2-19. Geologic cross section at the RWMC showing locations and elevations of observed perched water.

of magnesium chloride have been found in this well. Hubbell (1992) hypothesized that these elevated levels were related to the salt used on roads inside the SDA. Magnesium chloride was used from 1984 to 1985 and again in 1990. Hubbell (1992) presented estimates of net water velocity of 12 m/yr down to the perched water in Well 88-02 based on the 1984 to 1985 use of magnesium chloride. This velocity estimate does not account for the mitigating presence of the B-C interbed that is present at this location.

Hubbell (1990a) presented a summary of chemical analyses of perched water samples. In addition to the magnesium chloride mentioned previously, tritium is the only radionuclide detected at the 3-sigma confidence level that is not subject to possible down-hole contamination. The 3-sigma confidence level refers to concentrations at least three times greater than the standard deviation of the concentration; with the standard deviation determined by propagating all uncertainties associated with the analytic process. This 3-sigma confidence level accounts for false positive detections that occur when the reported nuclide concentrations are of the same order of magnitude as the measurement error. Cobalt-60, Sr-90, and Cs-137 have been detected at the 3-sigma level in Well 92, but the samples may have been contaminated with drilling sediments from the sidewall of the well (Hubbell 1990a).

Rightmire and Lewis (1987) presented an analysis of stable isotopes in perched water samples obtained from Wells 77-2 and 92. They used deuterium and O-18 ratios to make inferences related to water movement in the RWMC subsurface. They concluded that water in Well 77-2, above the B-C interbed, was influenced by evaporation and likely infiltrated from the surface of the SDA. The water in Well 92, above the C-D interbed, did not show any evaporative influence. They hypothesized that the source of water in Well 92 was predominantly from the spreading areas that had rapidly infiltrated.

Three deep neutron access tube monitoring wells were installed by the USGS in 1989 near Spreading Areas A and B (Paarmann et al. 1991). The wells are labeled NA-89-1, NA-89-2, and NA-89-3 and were installed to monitor the effects of recharge from the spreading areas on the moisture regime in the unsaturated zone and to determine the likelihood of lateral spreading toward the SDA. Based on geophysical logs presented in Paarmann et al. (1991), the B-C interbed was absent in one of the three wells, while the C-D interbed was

present in the two wells drilled deep enough to contact the C-D interbed. Essentially no water has been diverted to the spreading areas since these well were installed, which prevents identifying spreading area recharge effects on the SDA flow regime. Big Lost River water was diverted for several days during spring 1993. Only the monitoring well in immediate proximity to the river showed any response at depth.

Interbeds--This section presents information about water movement within the B-C and C-D interbed.

McElroy (1990) presented measurements of hydraulic gradients across the B-C and C-D interbeds at two locations from 1986 to 1990. The hydraulic gradient across the B-C interbed at Well D15 ranged from -1 to -2 m/m, indicating the top of the interbed was slightly wetter than the bottom. At Well TW-1, the gradient across the C-D interbed remained relatively constant and ranged from -4 to -5 m/m, indicating the top of the interbed was substantially wetter than the bottom. Water contents and soil matric tension monitoring at these two locations were inconclusive in determining the seasonal affect on infiltration. The change in water contents was not large enough to conclude that a pulse of water infiltrated each year. One possible explanation for this lack of response is the affect of a regional drought that occurred during the majority of the monitoring period. However, as mentioned previously, monitoring within the surficial sediments in the spring of 1989 indicated an infiltration event occurred.

McElroy and Hubbell (1990) hydraulically characterized sediment core samples from the A-B, B-C, and C-D interbeds. The measured saturated hydraulic conductivities ranged from 1×10^{-8} to 7×10^{-3} cm/s--a range of almost six orders of magnitude. Magnuson and McElroy (1993) grouped and averaged the results from McElroy and Hubbell (1990) to estimate in situ moisture contents and representative moisture characteristic curves for each of the interbeds. The estimated moisture contents ranged from 0.38 for the C-D interbed to 0.59 for the A-B interbed.

No measurements related to water movement have been made in the basalts or deeper interbeds beneath the C-D interbed in or near the SDA. Any

inference regarding water movement in this region would have to be related to observations made in or above the C-D interbed.

Regional Aquifer--The depth to the Snake River Plain Aquifer at the RWMC is approximately 177 m. Water movement in the aquifer beneath the INEL is generally from the northeast to the southwest. Figure 2-20 shows the direction of groundwater movement based on water levels measured in July 1988. Similar maps for different times show approximately the same interpreted flow direction (Barraclough et al. 1967; Pittman et al. 1988). The sources of water driving regional flow beneath the INEL come from either the perimeter of the Snake River Plain or from irrigation seepage to the east and north of the INEL. Wood (1989) presented results from an investigation of the aquifer beneath the RWMC. Wood estimated a horizontal water average linear velocity in the Snake River Plain Aquifer beneath the RWMC under static conditions (4th quarter, 1980) of 1.5 m/day using a hydraulic conductivity of 210 m/day, an effective porosity of 0.10, and a water table gradient of 1.0 m/mi to the south-southwest. The effective porosity has been estimated to range from 0.05 (Garabedian 1989) to 0.15 (Arnett et al. 1990).

At the RWMC, Wylie and Hubbell (1993) used an effective base of the aquifer 370 m below land surface to interpret pumping tests conducted in monitoring wells just outside the SDA. This estimate was based on an evaluation of samples from a new borehole, C1A, which was drilled 600 m north of the SDA (Burgess et al. 1993). At this location there was no indication a more permeable zone existed in the upper portion of the aquifer.

The flow direction in the Snake River Plain Aquifer beneath the RWMC is not always constant. Barraclough et al. (1976) and Wood (1989) present hydraulic gradient maps that indicate the effect of water in the spreading areas to the west and southwest of the SDA. The resulting water mound in the regional aquifer deflected the local flow direction under the SDA to the east or southeast.

2.1.4 Biotic Resources

In 1975, the INEL Site was dedicated as one of five DOE National Environmental Research Parks. It is an outdoor laboratory used to study

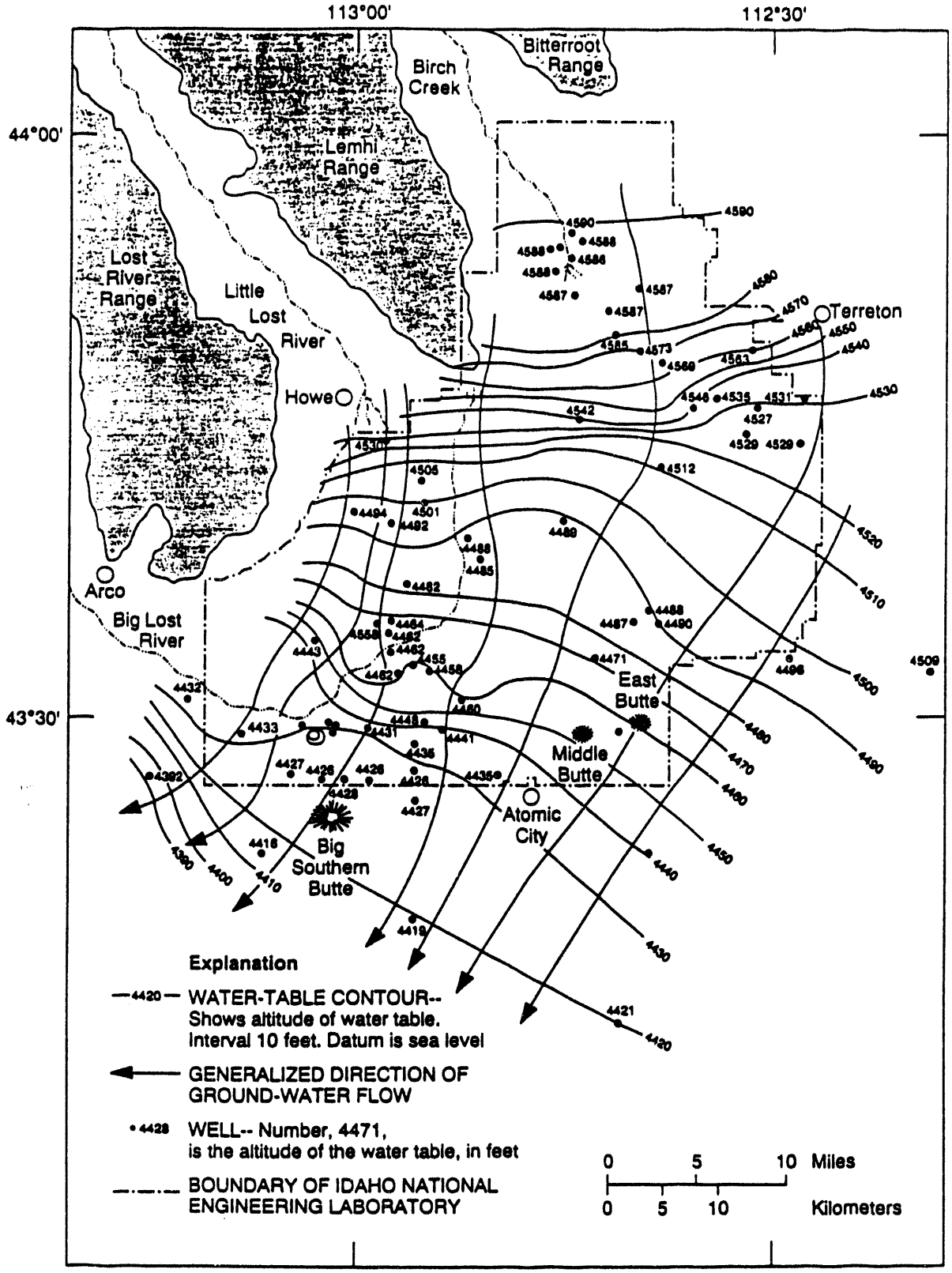

Figure 2-20. Altitude of the water table, Snake River Plain Aquifer, and general direction of groundwater movement (Orr and Cecil 1991).

ecological relationships and the effects of human activities on natural systems. In addition, it provides a unique setting for scientific investigation because the public has been excluded from much of the area for the past 25 years. Ecological data collected from the Idaho National Environmental Research Park provide a basis for analyzing environmental changes over time and assessing the effect of human influence on the environment.

Research on the flora and the fauna of the INEL Site has largely been conducted by or in conjunction with the DOE Radiological and Environmental Sciences Laboratory (RESL). The physical aspects of the INEL Site and its flora and fauna are typical of cold, high altitude, sagebrush ecosystems found in many parts of the western United States.

The discussion of the flora and fauna at the INEL is from the Environmental Document for the Idaho National Engineering Laboratory (Irving 1993). Irving (1993) contains more information and references to specific studies.

2.1.4.1 Flora. The common and scientific names for the flora discussed here are presented in Table 2-2. For ease of reading, only the common names are used in this discussion.

Extensive surveys of INEL vegetation were carried out in 1952, 1958, and 1967 using 150 permanent transects established and maintained for this purpose (Harniss and West 1973). Vegetation has also been described by McBride et al. (1978) and Jeppson and Holte (1978).

The common vegetation type, found on approximately 80% of the INEL Site, is a mixture of big sagebrush, green rabbitbrush, and perennial grasses. Most of the trees on the INEL Site are scattered along the Big Lost River and in the Twin Buttes area.

Vegetation in low-lying areas and along playa borders consists primarily of alkaline-tolerant species including shadscale saltbush, nuttal saltbush, and winterfat. Important associated grasses are bottlebrush squirreltail, giant wildrye, and Indian ricegrass.

Table 2-2. Flora at the INEL Site.[a]

Common Name	Latin Name
Cactus Family--Cactaceae	
Coryphantha	Coryphantha sp.
Prickly pear cactus	Opuntia polyacantha
Goosefoot Family--Chenopodiaceae	
Shadscale saltbush	Atriplex confertifolia
Nuttall saltbush	Atriplex nuttallii
Winterfat	Ceratoides lanata
Summer cypress	Kochia scoparia
Povertyweed	Monolepsis nuttalliana
Russian thistle	Salsola kali
Composite or Aster Family--Compositae	
Big sagebrush	Artemisia tridentata
Threetip sagebrush	Artemisia tripartita
Hoary false-yarrow	Chaenactis douglasii
Green rabbitbrush	Chrysothamnus viscidiflorus
Skeleton weed	Lygodesmia grandiflora
Common dandelion	Taraxacum officinale
Gray horsebrush	Tetradymia canescens
Goatsbeard or yellow salsify	Tragopogon dubius
Mustard Family--Cruciferae	
Flixweed tansy mustard	Descurainia sophia
Grass Family--Gramineae	
Crested wheatgrass	Agropyron cristatum
Bluebunch wheatgrass	Agropyron spicatum
Cheatgrass	Bromus tectorum
Giant wildrye	Elymus cinereus
Indian ricegrass	Oryzopsis hymenoides
Bottlebrush squirreltail	Sitanion hystrix
Rush Family--Juncaceae	
Baltic rush	Juncus balticus
Pea Family--Leguminosae	
Painted milkvetch	Astragalus ceramicus Sheld. var. apus Barneby
Thistle milkvetch	Astragalus kentrophyta Gray var. kentrophyta
Woolly-pod milkvetch	Astragalus purshii Dougl. var. ophiogenes Barneby

Table 2-2. (continued).

Common Name	Latin Name
Phlox Family--Polemoniaceae	
Large-flowered gymnosteris	Gymnosteris nudicaulis Greene
Longleaf phlox	Phlox longifolia
Buckwheat Family--Polygonaceae	
Buckwheat	Oxytheca dendroides[a], Nutt.
Willow Family--Salicaceae	
Willows	Salix sp.
Parsley Family--Umbelliferae	
Desert parsley	Lomatium sp.

a. Hitchcock and Cronquist (1974).

Prickly-pear, painted milkvetch, and skeletonweed are common in sandy areas in the north. Willows, baltic rush, and povertyweed grow along the Big Lost River channel.

At the RWMC, most of the SDA has been seeded with crested wheatgrass. Russian thistle, summer cypress, and halogeton (invader species) grow over many recently disturbed sites that were not seeded with wheatgrass. Other plants observed within the SDA include threetip sage, tansy mustard, common dandelion, bushy birdsbeak, cheatgrass, rabbitbrush, desert parsley, longleaf phlox, gray horsebrush, hoary false yarrow, and goatsbeard.

Vegetation studies of plant uptake of radionuclides at the INEL have focused primarily on (a) determining if deep rooted plants are a mechanism for waste pit intrusion and subsequent uptake of radionuclides and (b) analyzing inventories of radionuclides in aerial portions of plants. Aerial portions of

plants are important because they can potentially transport subsurface contaminants through dispersal of leaves, consumption by herbivores, and use by birds as nesting materials.

Knowledge of the rooting depth of SDA vegetation is important in evaluating which plants should be used for reseeding and which should be monitored for radionuclide concentrations. One SDA study comparing radionuclide uptake by crested wheatgrass (rooting depth 1 to 1.5 m) with that by Russian thistle (rooting depth 1 to 5 m) showed higher radionuclide concentrations in the deeper-rooted species (Arthur 1982). Examples of other deep-rooting species are rabbitbrush and sagebrush. General examples of shallow-rooting plant types are grasses and annual forbs.

Reynolds and Fraley (1989) found that the roots of big sagebrush extended to a depth of 2.3 m, and Great Basin wildrye had roots up to 2.0 m deep at the SDA. Maximum lateral spread of the roots of both of these species was 0.9 m and occurred at a depth of 0.4 m. In addition, preliminary findings of studies in progress indicate root penetration of up to 1.6 m for sodar and crested wheatgrass at the INEL (Markham 1987). A variety of biological barriers are being tested to determine more effective ways of preventing intrusion by deep rooted plants (Markham 1987).

Because of the significance of deep-rooted plants as transport vectors for radionuclides at the RWMC, DOE and the EG&G Idaho Environmental Monitoring organization are presently monitoring radionuclide uptake by vegetation at the SDA and SL-1 facilities. These studies primarily monitor radionuclide concentrations in aboveground portions of Russian thistle and crested wheatgrass (INEL 1992).

A survey of rare plants on the INEL Site was initiated in 1980 (Cholewa and Henderson 1984). The survey identified the following: painted milkvetch and woolly-pod milkvetch (which were under Federal review for endangered or threatened status); coryphantha, large-flowered gymnosteris, and oxytheca (on the Idaho State Watch List); and thistle milkvetch, which was previously unknown to occur in Idaho. Since then, the two species of milkvetch have been removed from candidate status (Mosely and Groves 1990).

2.1.4.2 Fauna. The INEL Site supports a variety of wildlife including small mammals, birds, reptiles, and a few large mammals. The common and scientific names for the fauna discussed here are presented in Table 2-3. For ease of reading, only the common names are used in this discussion.

The mammals include chipmunks, ground squirrels, several species of mice, kangaroo rats, cottontail rabbits, bats, jackrabbits, coyotes, and long-tailed weasels. Commonly occurring game animals are sage grouse, mourning dove, elk, pronghorn, and mule deer.

Limited data are available on the number of game animals seasonally inhabiting the INEL Site and on the harvest of these animals by hunters. Pronghorn inhabit the INEL Site during the entire year; however, many are migratory and summer to the north of the INEL Site. Pronghorn often bear young within the INEL Site.

Aquatic life on the INEL Site is limited and depends mainly upon the flow of the Big Lost River. During several months of the year, and even during some entire years, the river does not flow. However, during spring runoff and periods of high rainfall, the diversion system (at the southern boundary of the INEL Site) and the Big Lost River sinks (at the northern boundary of the INEL Site) support water flow during periods of water accumulation. This normally occurs less than 2 or 3 months in the spring.

Fish species observed in the Big Lost River on the INEL Site include rainbow trout, mountain whitefish, eastern brook trout, dolly varden char, Kokanee salmon, and the shorthead sculpin (Overton et al. 1976).

An investigation of amphibians and reptiles within the INEL was conducted from May through September 1975. The Great Basin spadefoot toad was the only amphibian recorded, typically associated with the Big Lost River, the Big Lost River sinks, and the spreading areas near the RWMC (Reynolds et al. 1986).The sagebrush lizard and the short-horned lizard are common; the sagebrush lizard is the most abundant reptile. The western skink and the leopard lizard have also been observed. Four species of snakes, including the Great Basin rattlesnake and Great Basin gopher snake, were recorded. The western

Table 2-3. Fauna at the INEL Site.

Common Name	Latin Name
Fish[a]	
Rainbow trout	Salmo gairdneri
Eastern brook trout	Salvelinus fontinalis
Dolly varden char	Salvelinus malma
Kokanee salmon	Oncorhynchus nerka
Mountain whitefish	Prosopium williamsoni
Shorthead sculpin	Cottus confusus
Reptiles and Amphibians[b]	
Leopard frog	Rana pipiens
Great Basin spadefoot toad	Spea intermontanus
Leopard lizard	Gambelia wislizenii
Sagebrush lizard	Sceloporus graciosus
Short-horned lizard	Phrynosoma douglassi
Western skink	Eumeces skiltonianus
Desert striped whipsnake	Masticophis taeniatus
Great Basin gopher snake	Pituophis melanoleucus
Terrestrial garter snake	Thamnophis elegans
Great Basin rattlesnake	Crotalus viridis
Mammals[c]	
Family--Canidae	
Coyote	Canis latrans
Family--Felidae	
Bobcat	Lynx rufus
Family--Antilocapridae'	
Pronghorn	Antilocapra americana
Family--Cervidae	
Mule deer	Odocoileus hemionus
Elk	Cervus canadensis
Family--Vespertilionidae	
Big-brown bat	Eptesicus fuscus
Townsend's big-eared bat	Plecotus townsendii

Table 2-3. (continued)

Common Name	Latin Name
Family--Leporidae	
White-tailed jackrabbit	Lepus townsendii
Black-tailed jackrabbit	L. californicus
Nuttall's cottontail	Sylvilagus nuttallii
Family--Sciuridae	
Least chipmunk	Tamias minimus
Townsend's ground squirrel	Spermophilus townsendii
Family--Geomyidae	
Northern pocket gopher	Thomomys talpoides
Family--Heteromyidae	
Ord's kangaroo rat	Dipodomys ordii
Family--Cricetidae	
Western harvest mouse	Reithrodontomys megalotis
Deer mouse	Peromyscus maniculatus
Birds[d]	
Family--Accipitridae	
Golden eagle	Aquila chrysaetos
Ferruginous hawk	Buteo regalis
Bald eagle	Haliaeetus leucocephalus
Family--Falconidae	
Merlin	Falco columbarius
Prairie falcon	Falco mexicanus
Peregrine falcon	Falco peregrinus
Family--Phasianidae	
Sage grouse	Centrocercus urophasianus
Family--Scolopacidae	
Long-billed curlew	Numenius americanus

Table 2-3. (continued)

Common Name	Latin Name
Family--Strigidae	
Burrowing owl	Athene cunicularia
Family--Columbidae	
Mourning dove	Zenaida macroura
Family--Mimidae	
Sage thrasher	Oreoscoptes montanus
Family--Tyrannidae	
Say's phoebe	Sayornis saya
Family--Alaudidae	
Horned lark	Eremophila alpestris
Family--Emberizidae	
Western meadowlark	Sturnella neglecta
Sage sparrow	Amphispiza belli
Brewer's sparrow	Spizella breweri

a. Simpson and Wallace (1978).

b. Nussbaum et al. (1983).

c. Jones et al. (1979).

d. American Ornithologist's Union (1983).

terrestrial garter snake and the desert striped whipsnake are present in lesser numbers and have more restricted distributions.

A total of 740 insect species have been recorded at the INEL Site; 226 of these species have not yet been identified beyond the family level. The majority of the abundant species belong to the orders Hymenoptera (wasps and ants) and Diptera (flies). About half of the abundant species are parasitic or predatory.

Over 185 species of birds have been recorded on the INEL Site, and about 60 of these species probably breed on the INEL Site. However, many of the bird species are relatively uncommon, and only a few species are very abundant. The most common species are the Brewer's sparrow, sage thrasher, sage sparrow, horned lark, sage grouse, mourning dove, western meadowlark, blackbilled magpie, and robin (Reynolds et al. 1986).

Species on the INEL Site that merit special consideration because of their sensitivity to disturbance or their threatened status include the ferruginous hawk, merlin, long-billed curlew, Townsend's big-eared bat, common loon, white pelican, great egret, and trumpeter swan (Reynolds et al. 1986; Mosely and Groves 1990). The bald eagle and peregrine falcon are on the Federal Endangered Species List and occasionally visit the INEL Site.

Radioecological research was initiated at the SDA in October 1977 to determine the role of ecological components in radionuclide uptake and transport throughout the RWMC area. This ongoing research is being directed by RESL.

Initial research efforts, directed toward determining the seasonal and relative abundance and distribution of wildlife at the RWMC, identified 34 species of vertebrates (Arthur and Markham 1978; Keller 1978; Groves 1978). The results of those studies indicated that cottontail rabbits, deer mice, ground squirrels, montane voles, kangaroo rats, and pocket mice were the primary species inhabiting the SDA. Thus, subsequent ecological studies focused on those species.

Subsequent studies have evaluated small mammal species composition, diversity, local movements, and densities (Groves and Keller 1983); small mammal radiation doses (Arthur et al. 1986); the effects of chronic radiation exposure on small mammals inhabiting the SDA (Evenson 1981); radionuclide concentration in coyote feces (Arthur and Markham 1982); and radionuclide concentrations in vegetation (Arthur 1982).

Studies have also been performed on burrowing characteristics of small mammals such as ground squirrels, deer mice, and voles (Arthur et al. 1983;, Markham 1987; Reynolds and Laundre 1988). Results of the studies indicate burrows no deeper than 1.4 m at the INEL.

Since 1978, the Environmental Monitoring organization of EG&G Idaho in conjunction with RESL have collected and analyzed tissue samples from mourning doves, sage grouse, cottontail rabbits, small mammals, Russian thistle, and crested wheatgrass. The biotic monitoring program at the RWMC is part of an INEL-wide comprehensive environmental monitoring program. It was instituted to (a) determine if biota are transporting radionuclides from buried waste or contaminated soil, (b) provide guidance to RWMC operations regarding general biotic conditions that may compromise waste containment, and (c) detect significant trends in the radionuclide concentrations in biotic samples. The results of the monitoring activities are used as indicators of the biotic conditions at the RWMC to determine if radionuclides in buried waste are being brought to the surface by burrowing animals or deep-rooted plants. Results of the monitoring program are published annually (Wilhelmsen et al. 1993) and are discussed in Chapter 5.

2.1.5 Demography

The population distribution around the INEL Site is shown in Figure 2-21 by distance and direction from the RWMC. This figure shows the population distribution centered at the RWMC based on 1990 census data.

The nearest town is Atomic City, which is less than 1.5 km from the southern boundary and has about 25 residents. In 1990, the population residing within an 80-km radius of the INEL boundary was 74,899. The larger

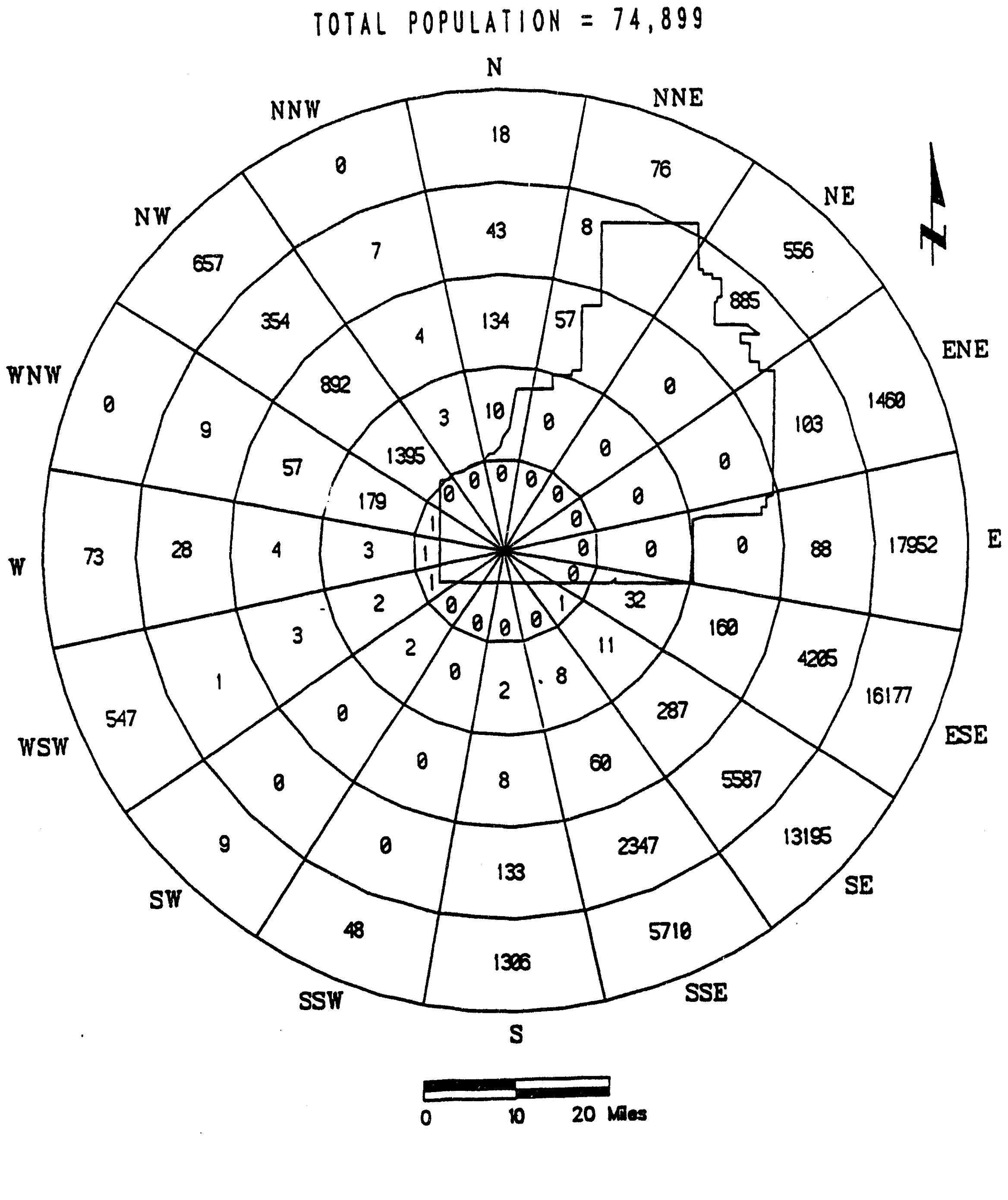

Figure 2-21. Population distribution within 80 km of the RWMC based on 1990 census data.

towns within 80 km of the RWMC are shown in Figure 2-22. The populations of those towns having more than 300 inhabitants are given in Table 2-4.

Total population growth rate in the region surrounding the INEL has exceeded the growth rate for the State of Idaho since 1980 according to the 1990 Census. This area has become the second fastest growing region in the State, with most of the growth centered in Bonneville (9%), Jefferson (8%), and Madison (21.5%) counties. Some rural counties and smaller communities, however, have lost population as housing has become more available in larger towns such as Idaho Falls (Table 2-4). This reverses the trend of the early 1980s of building more housing in the country where more affordable land was available.

There are no permanent residents at the INEL Site. The work force at the INEL Site varies depending on the levels of construction and research being performed at the facilities. Table 2-5 shows the INEL work force distribution for each INEL Site facility based on 1992 employment data.

A survey taken in 1991 indicated that approximately 60% of the INEL employees lived in Idaho Falls (Zelus et al. 1991). The majority of the remainder live in Ammon, Blackfoot, Pocatello, Shelley, Rigby, Rexburg, and other communities surrounding the INEL Site.

2.1.6 Land Use

The INEL Site, which is a National Environmental Research Park, has been dedicated to energy research and development. Approximately 95% of the land in the INEL Site has been withdrawn from the public domain and is controlled by DOE. The remainder consists of public highways crossing the INEL and Experimental Breeder Reactor No. 1 (EBR-I) [a historical landmark administered by the DOE Idaho Operations Office (DOE-ID)]. Existing facilities on the INEL Site lands are widely spaced for increased safety. They occupy a very small percentage of the available land.

Approximately 1,373 km^2 of the INEL Site is open to controlled grazing by cattle or sheep. Those grazing areas are mutually agreed on by the DOE and

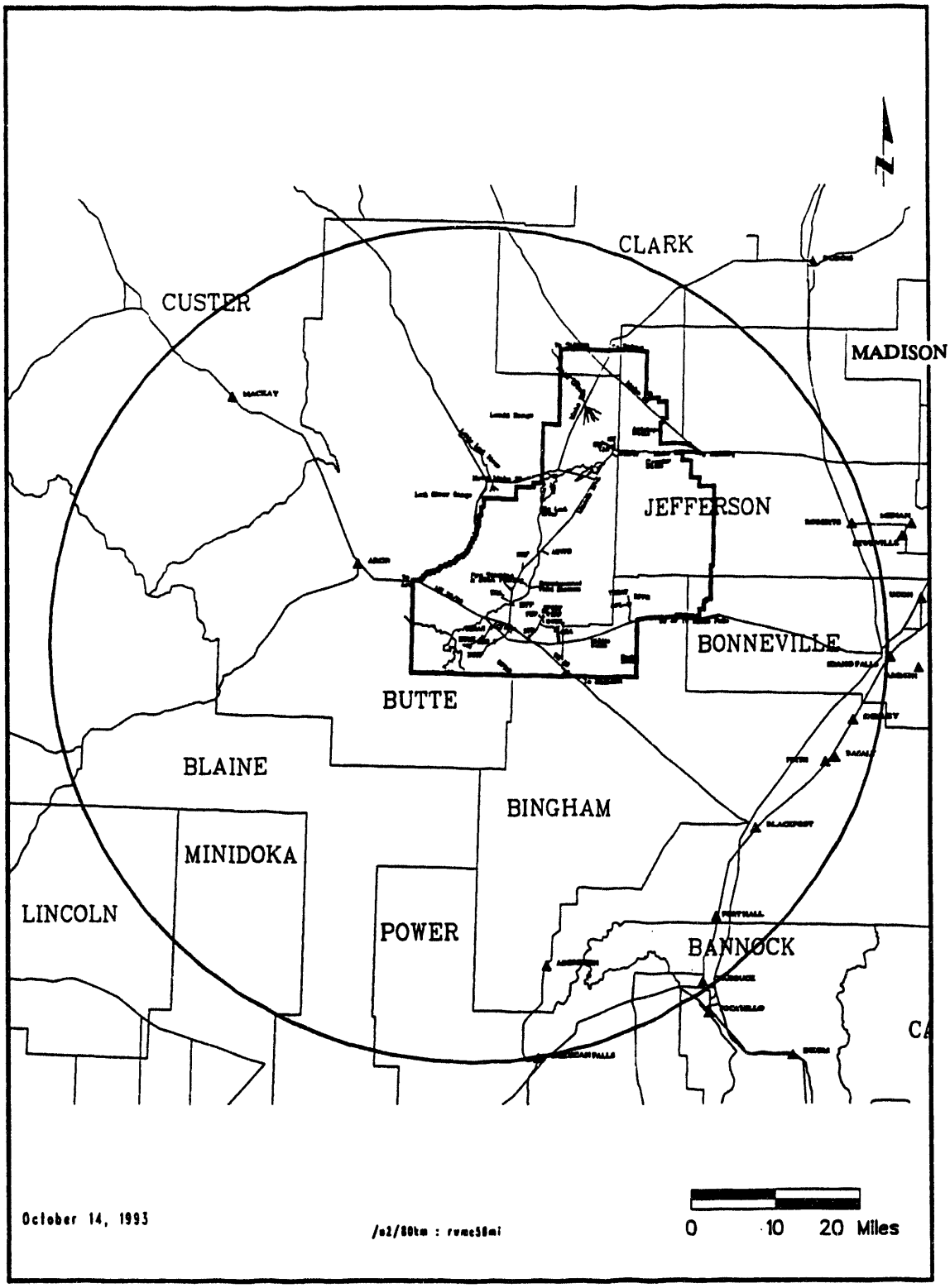

Figure 2-22. INEL vicinity map of communities within 80 km of the RWMC boundary.

Table 2-4. City population within 80 km of the RWMC.

City[b]	Population[a] 1970	1980	1990
Aberdeen	1,542	1,528	1,406
American Falls[c]		3,626	3,757
Arco	1,244	1,241	1,016
Basalt	349	414	407
Blackfoot	8,716	10,065	9,646
Chubbuck	2,927	7,052	7,791
Firth	362	460	429
Idaho Falls[c]	35,776	39,739	43,929
Mackay	539	541	574
Roberts	393	466	557
Shelley	2,674	3,300	3,536

a. Source: 1970-1980, 1990 U.S. Census.

b. Cities with more than 300 inhabitants.

c. Portions of these communities are outside the 80-km radius.

Table 2-5. INEL work force distribution as of January 1993.

Facility	Total employees[a,b,c]
Test Area North	664
Naval Reactors Facility	2,256
Argonne National Laboratory-West	944
Waste Experimental Reduction Facility Special Power Excursion Reactor Test, and Power Burst Facility	154
Central Facilities Area	1,149
Idaho Chemical Processing Plant	2,031
Test Reactor Area	681
Radioactive Waste Management Complex	119
TOTAL	7,998

a. Values are for employees working within INEL Site boundaries, Figure 2-1, including construction workers.

b. Includes day and night shifts.

c. Does not include workers assigned to facilities in Idaho Falls.

the Department of the Interior, and grazing permits are administered through the Bureau of Land Management. Grazing is prohibited within 3.2 km of any nuclear facility, and no dairy cows are allowed. When a domestic animal or a group of animals enters and remains in an active portion of the INEL beyond the designated grazing boundaries, security personnel contact the Bureau of Land Management.

According to the Office of Budget and Policy Planning, State of Idaho, the State does not have plans or policies specifically related to land use either adjacent to or within the boundaries of the INEL Site. The East-Central Idaho Planning and Development Association is a regional economic planning agency serving a nine-county region, most of which encompasses the INEL Site. Like the State of Idaho, the Association does not have any policies or plans that involve lands or activities near the INEL Site. Butte County, which encompasses most of the INEL Site land, is sparsely populated. Because the County does not have a policy plan, comprehensive plan, or zoning ordinance, no plans or policies specifically related to land use are available.

Future uses of the land are limited because of the climate, lava flows, and general desert soil characteristics. The only lands suitable for farming are near the end of the Big and Little Lost Rivers, near the town of Howe, and at a distance 13 km southeast from Howe. Arable land (with moderate irrigation) is present on both sides of the Big Lost River and between Mud Lake and Howe. The remainder of the INEL Site, approximately 65% of the surface area, has a low water-holding capacity, is rocky or covered with basalt, or is classified as having moderate-to-severe limitations for agriculture irrigation.

Because of the limitations of the land, it is not probable that a community would be established in the future at the RWMC. It is more likely that the area could be used for grazing livestock, such as cattle or sheep, and a well could be used for watering stock. The scenarios discussed in later chapters are unlikely cases selected for dose calculations.

2.1.7 Cultural Resources

In response to Federal environmental legislation, investigations of INEL cultural resources were initiated in the late 1960s. Since that time, approximately 4% of the facility has been systematically surveyed and over 1,500 localities have been identified. This inventory includes prehistoric resources representing a span of approximately 12,000 years; historic resources representing the period from 1805 to the late 1920s; important nuclear facilities like EBR-I, which was the first reactor in the world to produce useable amounts of electricity and is recognized as a National Historic Landmark; paleontological localities; and areas of special importance to local Native American groups. Comprehensive histories of INEL cultural resource management and the results of several decades of compliance-driven research can be found in the INEL Environmental Resource Document (Irving 1993) and the INEL Draft Management Plan for Cultural Resources (Miller 1992).

The majority of cultural resources identified on the INEL are prehistoric (94%). The remaining 6% are from the Historic period, and the majority of these are from agricultural activities. Work is currently being performed on inventories of important nuclear facilities, Native American sacred sites, and important paleontological localities.

The earliest known occupants of southeastern Idaho were big game hunters who used spears to hunt now-extinct forms of mammoth, camel, bison, horse, and mountain sheep. During the Middle Prehistoric period, groups of hunter-gatherers using atlatls (spear throwers) ranged widely across the region in pursuit of modern forms of bison, deer, mountain sheep, and other big game. Evidence also suggests that plant foods also gained increased importance in the economy. A proliferation of artifacts from the Middle Prehistoric period indicates that this was a time of some cultural recrganization and mobility, perhaps stimulated by warmer and dryer climatic conditions. The Late Prehistoric period is marked by full-scale adoption of the bow and arrow and aboriginal ceramics. Like their predecessors, Late Prehistoric populations were actively hunting and gathering throughout the region. Groups appear to have been relatively specialized, focusing on deer, mountain sheep, bison, and root plants such as camas.

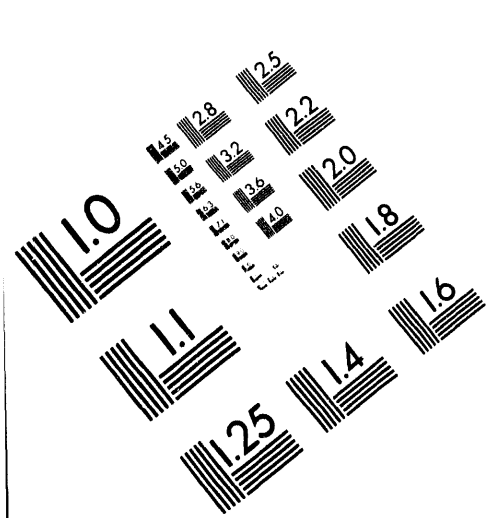

Association for Information and Image Management
1100 Wayne Avenue, Suite 1100
Silver Spring, Maryland 20910
301/587-8202

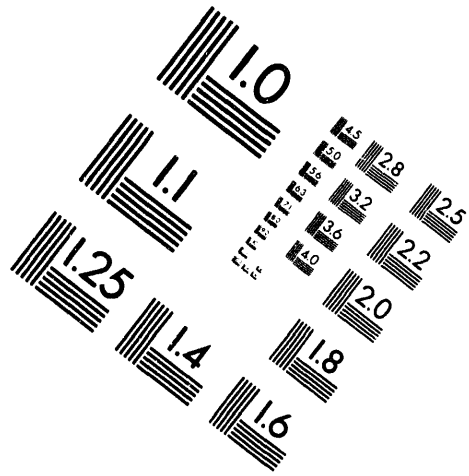

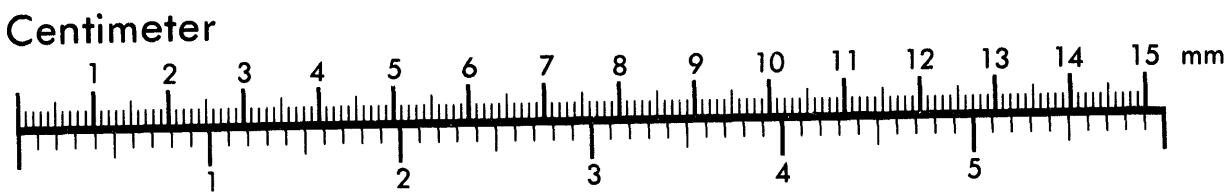

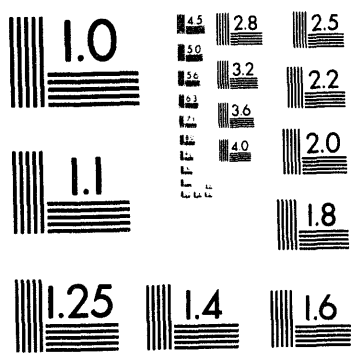

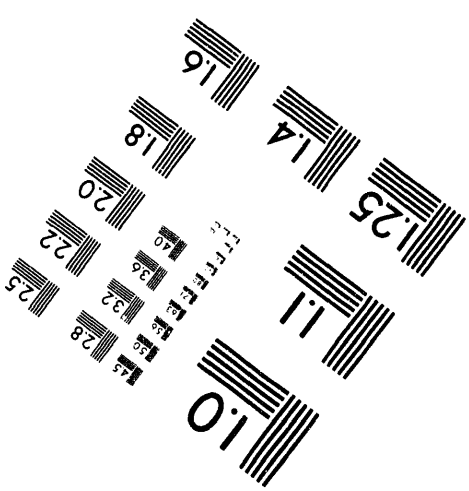

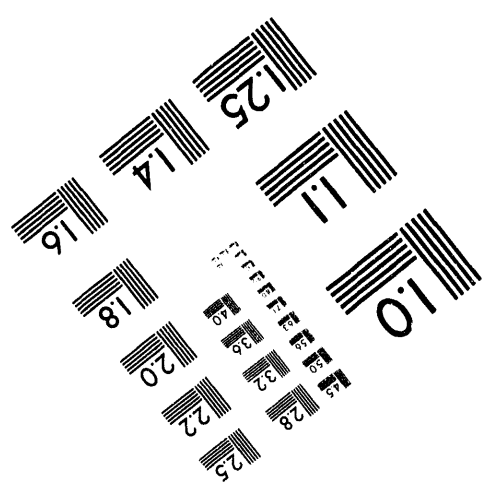

2 of 5

Southeastern Idaho is included in a large territory once inhabited by two linguistically distinct, but highly interactive Native American groups--the Shoshone and Bannock. The common lifeway of these groups, expanded by using horses for transportation, reportedly included sedentary winter occupation along major river drainages (such as the Snake River) and widely dispersed spring, summer, and fall occupations to exploit game animals, fish, and plant foods. This pattern reflects the small-scale hunting and gathering lifestyle that was prevalent during prehistoric times. In the late 1860s, treaties put an end to the autonomous lifestyle of the Shoshone and Bannock, and they began to adapt with mixed success to life on local Indian Reservations.

The Historic period in southeastern Idaho began with infrequent visits by explorers and fur trappers in the early 1800s. By the mid 1800s, some emigrants were moving through the INEL area as they made their way to the Oregon Territory via Goodales Cutoff, a northern spur of the Oregon Trail. In the 1860s, gold strikes in the Lost River Mountains drew many miners into the region, and many stage and wagon routes were established. Small family farms appeared along the Big Lost River by 1880 and several large ranching operations were also established in what is now the northern portion of the INEL. However, gross miscalculations of potential water flow led to the abandonment of most agricultural projects, even those that were Federally sponsored. Since 1940, the INEL area has been under the control of the U.S. Government. Initially used during World War II as a test firing range, it was purchased by the AEC in 1949, expanded, and set aside for nuclear research. Many of the scientific facilities developed on the INEL are historically important for their contribution to the overall development of U.S. nuclear science.

2.2 RWMC Description and Waste Characteristics

The RWMC includes the 97-acre SDA, the 58-acre TSA, and the Administrative Area. Within the SDA and TSA areas are smaller specialized disposal and storage areas. Solid waste is routed to the different areas depending on the waste's content. LLW received at the RWMC is buried in the SDA or stored at the RWMC. LLW contaminated with TRU isotopes $\leq$10 nCi/g is buried in the SDA. LLW contaminated with TRU isotopes <100 nCi/g but >10 nCi/g are excluded from disposal at the RWMC; it is stored in interim

storage at the RWMC. The layout of the RWMC areas and facilities is shown in Figure 2-23.

2.2.1 History of Waste Management at the RWMC

This section reviews past practices of waste management at the RWMC.

2.2.1.1 Original Burial Ground (1951 to 1957). In 1951, the AEC and the USGS selected a site for evaluation as a waste disposal area. An area of 100 acres near the southwestern corner of the INEL Site was chosen. After drilling 10 exploratory holes in the area and analyzing core samples, the USGS found acceptable geologic and hydrologic conditions. Some of these conditions were

- Several feet of clay sediment to slow water movement and to adsorb nuclides
- Sufficient sediment in the vicinity for fill and cover
- An area not directly upstream from existing or potential reactor sites or other places where water production wells may be drilled
- Good surface drainage leading away from existing or potential installations or water production sites.

In 1952, development of the SDA began on a 13-acre tract of the site. That same year the first shipments of radioactive waste from the INEL were received and buried in trenches at the SDA. This initial work was the beginning of the RWMC. The management of the RWMC was then the responsibility of the Site Survey Branch, Health and Safety Division, of the AEC-Idaho Operations Office. The National Industrial Maintenance Company conducted burial operations in 1952 and part of 1953. It was succeeded in 1953 by the Phillips Atomic Energy Division, a subsidiary of Phillips Petroleum Company, which continued burial operations.

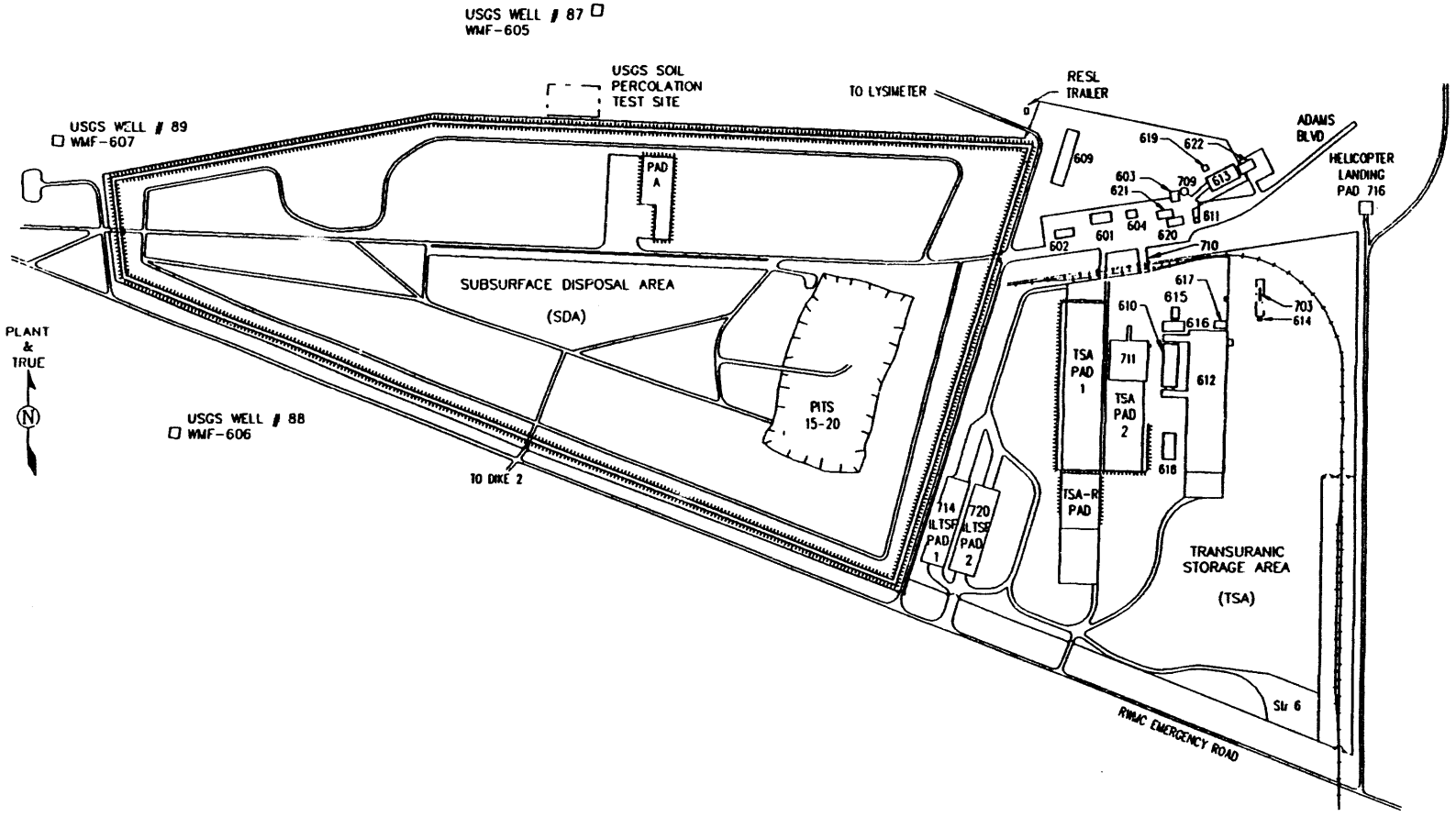

Figure 2-23. Layout of the RWMC areas and facilities.

Generally, the waste received from 1952 through 1957 was buried in trenches. On July 8, 1952, the first trench was opened for the waste generated at the INEL Site. Between 1952 and 1957, Trenches 1 through 10 were excavated to depths that sometimes encountered the top of the first basalt layer. Pits were also excavated starting in 1957 because of the large size of some containers and the amount of waste being received. The onsite low-level solid radioactive waste was placed in cardboard boxes and sealed with tape. The sealed boxes were placed in metal dumpsters that were labeled and used only for radioactive waste. The dumpsters were transported to the SDA, and the waste was dumped into the pits or trenches. LLW was periodically covered with soil. Waste that could cause excessive personnel exposure was transported in special containers and transfer vehicles to reduce worker exposure. That waste was deposited into the trenches and was immediately covered with soil.

In 1953, the AEC decided that solid radioactive waste from the Rocky Flats Fabrication Facility near Golden, Colorado, would be sent to the RWMC. The first shipment of Rocky Flats waste was authorized in March 1954. This shipment was a trial run to provide (a) handling and shipping experience and (b) cost information to compare with alternative disposal methods. The first drums containing TRU waste from Rocky Flats arrived on April 22, 1954. The trial run proved that these shipments could be handled satisfactorily, and the AEC authorized the shipment of Rocky Flats waste to the INEL. Between April 1954 and November 1957, the waste from Rocky Flats was interspersed with INEL waste in Trenches 1 through 10. In 1957, Rocky Flats waste destined for the pits was packed in steel 30- or 55-gal drums or, if bulky, in wooden crates. Waste arrived by railcar at CFA and was then transferred to the RWMC via truck. The drums were hand-stacked in the pits. The wooden crates were lifted from the trailer by crane and stacked around the edges of the pit. The waste in the pits was covered with soil periodically but on no set schedule.

2.2.1.2 Expanded SDA (1957 to 1970). The original 13-acre SDA was nearly filled by 1957. The SDA was then expanded to the immediate east and south of the original area to its present size, encompassing 97 acres of the original site evaluated by the USGS. The expansion also enclosed an acid pit that had been used for disposal of nonradioactive laboratory acids since January 1, 1954.

Trenches were used for the disposal of LLW, frequently waste with high radiation levels. The Rocky Flats waste was placed in the pits during this period because of the large volume being received and the low radiation level. In 1958, a flood control project was constructed on the Big Lost River adjacent to the RWMC to protect downstream INEL facilities and to protect the RWMC from flood waters. The project involved constructing a diversion dam and spreading areas for runoff water. The diversion system was later enlarged to protect the RWMC from runoff in the local drainage basin.

Between May 1960 and August 1963, the RWMC served as an interim burial ground for waste generated by AEC licensees. Waste from a number of offsite generators was received. In October 1962, the responsibility for the RWMC was transferred from the Site Survey Branch, AEC Idaho Operations Office, to Phillips Petroleum Company, which had been operating the RWMC. Beginning in November 1963, Rocky Flats waste was no longer stacked; it was dumped in pits to reduce labor costs and minimize personnel radiation exposures. Random dumping continued until 1969. In 1966, the Idaho Nuclear Corporation, a joint subsidiary of Aerojet-General Company and Allied Chemical Corporation, assumed responsibility for the RWMC.

Numerous changes in waste-handling practices took place from 1966 to 1970. The minimum required soil cover over buried waste was increased from 0.6 to 0.9 m. Minimum trench depth for future trenches was increased from 0.9 to 1.5 m. A heavy metal plate was dropped onto waste in trenches to compact the waste. Stacking of the waste containers within trenches and pits in the SDA was reinstated in 1969.

2.2.1.3 SDA and TSA (1970 to present). On March 20, 1970, the AEC issued Immediate Action Directive No. 0511-21, "Policy Statement Regarding Solid Waste Burial." That policy required segregation of all waste contaminated with TRU nuclides and storage of that waste to permit retrieval of contamination-free waste containers for 20 years. In support of the directive, a decision was made to store and cover TRU waste aboveground on pads. The 58-acre TSA was established at the RWMC for storage; thus, the RWMC was expanded to its present size, 165 acres. In 1971, Aerojet Nuclear Company replaced Idaho Nuclear Corporation as the operations contractor for the RWMC. In 1976, EG&G Idaho, Inc. replaced Aerojet Nuclear Company as a INEL prime

contractor and assumed responsibility for operating the RWMC. A change in disposal methods for LLW occurred early in the 1970s with the beginning of waste volume reduction by compaction. Since then, radioactive waste has been separated into compactible and noncompactible waste. Early in the 1970s, the Naval Reactors Facility (NRF) began compacting waste, reducing the volume of compactible waste by approximately 10:1. In 1974, a hydraulic bale-type compactor (like the NRF compactor) was installed in the Waste Volume Reduction Facility (WVRF) at the RWMC to reduce the volume of INEL waste. The volume reduction varies because of the heterogeneous mixture of compactible waste. INEL-generated, compactible LLW was placed in polyethylene bags, deposited in dumpsters designated for this type of waste, and transported to the RWMC. At the WVRF, the waste was compacted into plastic-lined cardboard bales, which were steel-banded, wrapped in plastic, and placed in a disposal pit. This operation was transferred to the Waste Experimental Reduction Facility (WERF) in 1986.

2.2.2 Description of the SDA

The SDA is a fenced, 97-acre area on the western part of the RWMC. Included in the SDA are pits, trenches, soil vault rows, and Pad A, all of which have been used to dispose of LLW. Figure 2-24 illustrates the layout of the SDA. Support facilities are located east of the SDA. Table 2-6 lists the opening and closing dates of the trenches, pits, soil vault rows, and Pad A.

2.2.2.1 Pits. Pits are normally used for routine, solid, low-level beta-gamma contaminated waste with radiation levels below 500 mR/h at 0.9 m. Current pits are excavated into rock to a depth of 9 m, then backfilled with 0.6 m of soil over rock. After the waste is emplaced, the pits are backfilled with at least 0.9 m of soil. In FY 1985, geotextile fabric was incorporated in the upper portion of the pit floor soil cover to add stability for the waste stack and for mobile equipment. After the flooding in 1982, the earth berm around Pit 17 was raised and serves as radiation shielding, firebreaks, and dikes. A crane pad was constructed for the bulk disposal area of the pit in FY 1985. Corners of the pits are marked by concrete monuments. A brass plate on each monument includes the pit number, boundary directions, and the opening and closing dates.

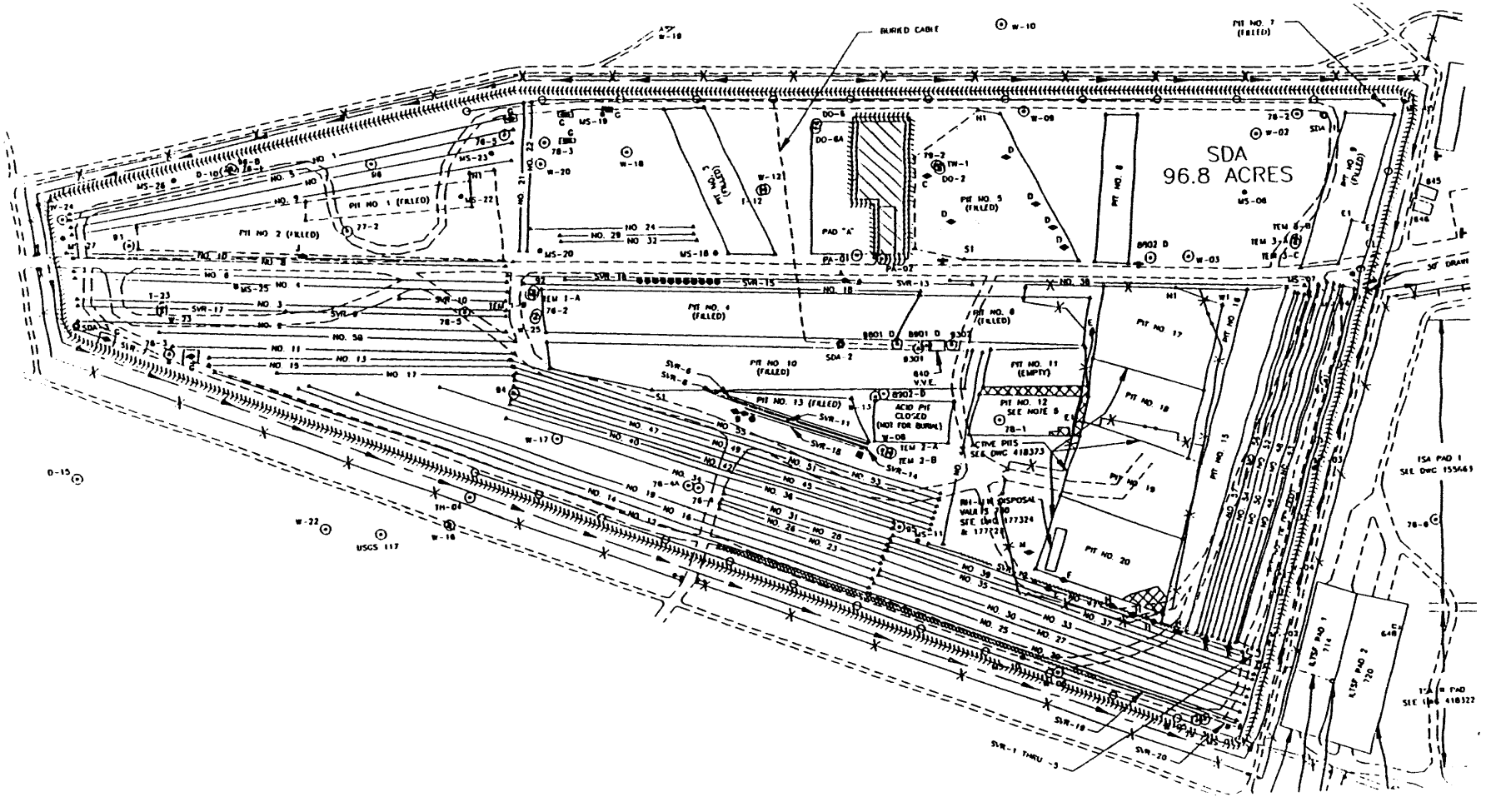

Figure 2-24. Layout of the SDA.

Table 2-6. Opening and closing dates for waste locations in the SDA.

Trench	Opened	Closed	Trench	Opened	Closed	Pit	Opened	Closed	Soil vault row	Opened	Closed	Pad	Opened	Closed
1	07-08-52	10-01-54	30	03-02-63	09-12-63	1	11-01-57	10-01-59	1	03-03-77	09-07-77	A	09-26-72	11-17-78
2	10-01-54	12-21-54	31	03-25-63	11-22-63	2	10-01-59	07-01-63	2	03-16-77	10-28-77	–	–	–
3	12-22-54	04-22-55	32	04-01-63	11-18-63	3	12-15-61	01-03-63	3	03-14-77	10-27-77	–	–	–
4	04-22-55	11-21-55	33	10-11-63	08-11-64	4	01-03-63	09-26-67	4	03-17-77	11-01-77	–	–	–
5	11-04-55	03-29-56	34	03-18-64	08-27-64	5	06-18-63	12-22-66	5	03-15-77	09-02-77	–	–	–
6	03-22-56	09-04-56	35	08-28-64	01-19-65	6	05-18-67	10-22-68	6	03-25-78	02-27-81	–	–	–
7	08-14-56	12-20-56	36	12-01-64	07-24-65	7	09-19-66	10-05-68	7	05-08-78	01-23-79	–	–	–
8	12-13-56	05-07-57	37	12-24-64	07-01-65	8	03-06-67	11-xx-69	8	02-12-78	09-08-81	–	–	–
9	01-07-57	09-06-57	38	05-15-65	09-16-65	9	11-08-67	06-09-69	9	02-06-79	07-15-81	–	–	–
10	07-19-57	02-07-58	39	07-20-65	11-05-65	10	08-07-68	07-08-71	10	06-09-81	11-03-82	–	–	–
11	02-11-58	07-25-58	40	10-07-65	01-13-66	11	04-14-70	10-16-70	11	08-07-81	12-12-84	–	–	–
12	01-03-58	01-16-59	41	01-04-66	10-04-66	12	07-02-70	09-12-72	12	05-05-82	07-24-83	–	–	–
13	01-09-58	04-24-59	42	05-09-66	01-17-67	13	07-20-71	07-29-74	13	04-04-83	12-21-84	–	–	–
14	04-16-59	07-30-59	43	10-20-66	06-01-67	14	07-01-74	03-31-76	14	10-16-84	05-08-89	–	–	–
15	07-31-59	10-16-59	44	01-13-67	03-24-67	15	06-25-75	07-03-84	15	10-16-84	03-07-87	–	–	–
16	10-17-59	04-12-60	45	02-28-67	09-27-67	16	05-22-78	10-25-84	16	10-16-84	01-22-90	–	–	–
17	11-01-59	07-01-60	46	09-25-67	03-14-68	17	05-05-84	–	17	04-24-87	–	–	–	–
18	05-10-60	07-20-60	47	02-28-68	08-05-68	18	09-01-88	–	18	02-12-87	–	–	–	–
19	07-05-60	11-29-60	48	08-08-68	05-02-69	19	09-01-88	–	19	01-22-90	–	–	–	–
20	12-01-60	06-30-61	49	11-18-68	06-30-69	20	03-01-89	–	20	09-12-91	–	–	–	–
21	12-13-60	01-10-61	50	07-01-69	11-01-69	–	–	–	–	–	–	–	–	–
22	02-01-61	04-25-61	51	10-30-69	04-08-70	–	–	–	–	–	–	–	–	–
23	06-20-61	09-15-61	52	03-04-70	07-04-70	–	–	–	–	–	–	–	–	–
24	10-01-61	07-31-62	53	07-01-70	10-12-70	–	–	–	–	–	–	–	–	–
25	08-01-61	07-27-62	54	09-23-70	05-04-71	–	–	–	–	–	–	–	–	–
26	04-13-62	08-17-62	55	04-07-71	03-12-82	–	–	–	–	–	–	–	–	–
27	08-20-62	01-04-63	56	12-29-71	02-01-73	–	–	–	–	–	–	–	–	–
28	12-26-62	03-12-63	57	12-28-72	06-11-74	–	–	–	–	–	–	–	–	–
29	11-19-62	03-20-63	58	02-20-74	08-17-81	–	–	–	–	–	–	–	–	–

2.2.2.2 Trenches. Trenches were dug along predetermined centerlines and were separated from adjacent centerlines by no more than 4.9 m. This allowed maximum use of available space without disturbing previously buried waste. The average width of the trenches was 3.1 m (those with collapsing walls were wider). Trench operation employed two metal trench liners that were placed over each other down the trench as they were filled. The liners performed two functions: they prevented the trench from sloughing off and they provided shielding. Trenches were used for all ranges of radioactive waste. Waste with high radiation levels was handled remotely using special shielded containers and boom cranes. As waste disposal became more rigorously controlled, the trenches were used more frequently for high radiation waste until they were replaced by the soil vault concept. When the trenches were full, they were covered with a minimum of 0.6 to 0.9 m of soil. Locations of all trenches and soil vaults are identified by concrete monuments. A brass plate on each monument is stamped with trench number and the opening and closing dates. All LLW packages exceeding 500 mR/h at 0.9 m were deposited in trenches or soil vaults. In July 1981, trench disposals were discontinued, and the unfilled trench area was redesignated for soil vault disposals.

2.2.2.3 Soil Vaults. Beginning in 1977, areas not suited for pits were set aside for drilling of soil vaults. This practice not only helped to conserve SDA space, but it also reduced personnel exposure to radiation. High radiation (greater than 500 mR/h) beta-gamma waste is normally deposited in the soil vaults. Rows of these vaults are drilled along predetermined centerlines and each vault is separated from previously buried waste by approximately 0.6 m. Soil vault diameters vary from 0.4 to 2 m; vault minimum depth is 2 m. If the drilling exposes basalt, 0.6 m of soil is placed on the vault floor. Open soil vaults are surrounded by barriers denoting the hazard. Vault liners are used to prevent vault collapse during disposal activities and are removed when the vault is closed. A shield cover is also placed over open vaults to provide shielding and protection when the vault is open for disposals. Earth fill (0.9 m minimum) provides shielding to personnel and the environment after the vault is filled and closed.

2.2.2.4 Pad A. Pad A was constructed in September 1972 in the north central part of the SDA that was not suited for pits or trenches because of near-surface basalt outcroppings. Pad A was established to dispose of uranium

waste and waste that was not TRU but did contain >0.1 nCi/g but <10 nCi/g of TRU alpha-emitting nuclides and had radiation levels <200 mR/h at the container surface. From 1972 through 1978, this waste was disposed of on Pad A. Boxes were stacked around the periphery and drums were stacked horizontally in staggered layers. Waste on the pads was covered with earth so that no more than one row of boxes or two rows of drums were exposed at anytime. Sufficient earth was placed around the pad to give at least a 0.9-m cover and a 3:1 maximum final slope. Since 1978, additional soil has been placed on top of the berm to correct for subsidence. The soil cover now ranges from 1 to 2 m deep. Pad A was closed to waste disposal in 1978.

2.2.2.5 Support Facilities. Operations within the SDA are supported by personnel and equipment housed in the structures and buildings located outside of the SDA, including material storage areas and health physics offices; facilities for temporary storage, vehicle monitoring, and equipment maintenance; guardhouse for security personnel staffed 24 h/day; office space and change areas for RWMC personnel; and shift manager and area manager offices.

2.2.3 Description of the Waste

The RWMC contains LLW and TRU waste, including some that could pose nonradiological hazards. Early waste management practices allowed intermixing of LLW and TRU waste in pits and trenches. Since 1970, waste has generally been segregated, depending on the type, with TRU waste stored on pads in the TSA and LLW buried in the SDA.

2.2.3.1 LLW. Operations at the INEL that produce LLW include research and development programs associated with reactor designs at Argonne National Laboratory-West facilities, fuel processing activities at ICPP, reactor development and training facilities at NRF, a production facility for the Army at Test Area North, and development, testing, and analysis of materials and fuels used in nuclear reactor applications at TRA. It is expected that decontamination and decommissioning operations and environmental restoration actions will become a major generator of LLW in the future.

Disposal of contact-handled LLW since 1984 has averaged approximately 2,000 m^3/yr. In addition, an average of 73 m^3/yr of remote-handled LLW has been received from waste generators; containers of this waste have been disposed of at the RWMC in waste disposal pits or in soil vaults.

Beginning in 1977, soil vaults were used to dispose of beta-gamma waste with high radiation levels (>500 mR/h at 0.9 m); before then, trenches were used for waste with high radiation levels. The trenches were closed in 1981. Pits are used for routine, solid low-level beta-gamma contaminated waste with radiation levels <500 mR/h at 0.9 m.

Waste disposed of in the older trenches and the pits included plastics, paper, cloth, a variety of metals (stainless steel and aluminum), wood, contaminated soil, asphalt, gravel, concrete, glass, construction equipment and materials, filters, resins, rubber, biological waste, reactor core components, and absorbed liquids. Soil vaults and the newer pits contained waste from irradiated reactor and reactor core components and irradiated samples.

2.2.3.2 TRU Waste. Receipt and shallow-land disposal of TRU waste began in 1954 and ended in 1970. About 62,000 m^3 of TRU waste was buried in pits and trenches at the RWMC SDA. In 1987, ongoing studies to address long-term management of buried TRU waste were accelerated in response to environmental monitoring that indicated migration of low concentrations of plutonium and organic chemicals from the buried waste. Remedial action requirements are currently being addressed to allow recommendation of an alternative for long-term management.

Since 1970, solid TRU waste received at the RWMC has been segregated from non-TRU solid waste and placed into interim retrievable storage at the RWMC TSA. Contact-handled wastes were either (a) stored on aboveground asphalt pads and protected by covering with plywood, plastic, and an earthen overburden or (b) placed on asphalt pads under an air supported weather shield. The majority of stored contact-handled TRU waste was generated by the Rocky Flats Plant. Lesser amounts were generated by the Mound Laboratory, Argonne National Laboratory-East, Battelle Columbus Laboratory, Bettis Atomic

Power Laboratory, and INEL onsite generators. Remote-handled TRU wastes are stored in specially designed steel vaults at the Intermediate Level Transuranic Storage Facility (ILTSF) within the TSA. The primary generator of remote-handled TRU waste in storage at the INEL Site is Argonne National Laboratory-East and Argonne National Laboratory-West; smaller amounts are generated by INEL onsite generators.

About 65,000 m^3 of additional contact-handled TRU waste (containing about 470,000 Ci) has accumulated from 1970 to the present in retrievable storage at the TSA of the RWMC. This 65,000 m^3 of stored waste is planned to undergo reexamination in the Stored Waste Examination Pilot Plant (SWEPP) facility located at the TSA. Principal findings thus far are

- Most (about 90%) of this stored waste in the TSA also contains EPA-hazardous constituents; therefore, it is classified as mixed waste.

- Many of these containers of waste have been found to contain TRU concentrations <100 nCi/g; therefore, they do not fit the present definition for TRU waste. Projections indicate that when the reexaminations are completed, about 40% of the total number of containers of waste will have been found to contain TRU concentrations <100 nCi/g.

Thus, it appears that about 27,000 m^3 of this stored waste would be reclassified to LLW-mixed waste. Plans for disposal of this waste have not yet been made, and the waste is not included in the inventory for this LLW radiological performance assessment.

2.2.4 Present Waste Management Practices

The major burial areas presently open are Pits 17, 18, 19, and 20 and Soil Vault Rows 17 through 20. Pits and soil vaults are excavated and backfilled with 0.6 m of soil over the basalt. Containers of waste are stacked in the pit or soil vault. An earth cover is then applied to provide a minimum cover of 0.9 m over all waste during the operational period.

Additional earth covering is applied during operations if the radiation level of the covered waste is greater than 1 mrem/h at 0.9 m above the ground.

Activities are in progress for the new Mixed and Low-Level Waste Disposal Facility (MLLWDF). The MLLWDF is planned to be an engineered disposal facility and is currently planned to begin operations in 2002. The MLLWDF is intended to be a replacement facility for the RWMC. A radiological performance assessment is planned to be performed for the MLLWDF as design activities progress. Assessing the impact from LLW disposal through 2020 in this RWMC radiological performance assessment provides future flexibility because of uncertain funding levels needed to support developing a new disposal capacity.

2.2.4.1 RWMC Waste Acceptance Criteria. Generators of LLW must be approved to ship LLW to the RWMC for disposal in the SDA. If new waste streams develop that have characteristics different than those allowed in the Waste Acceptance Criteria (WAC), the waste stream is not accepted for disposal at the RWMC until an analysis ensures the limitations of the WAC and the RWMC are not exceeded. To obtain and/or maintain this approval, the waste generator must comply with the requirements of the INEL Reusable Property, Recyclable Materials, and Waste Acceptance Criteria (DOE 1994). The criteria implement the requirements and philosophy of DOE Order 5820.2A, Chapter III, "Management of LLW." The criteria are also consistent with applicable EPA and U.S. Nuclear Regulatory Commission (NRC) requirements. The WAC requires each generator to have an approved waste certification plan and an approved waste minimization plan. Waste generators are also required by the WAC to submit an annual waste forecast and characterize their waste.

As specified by the WAC, waste characterization data must be included to

- Ensure that no Resource Conservation and Recovery Act (RCRA) toxicity characterization leaching procedure threshold limits are exceeded and EPA-listed or -characterized wastes are not in the waste form.

- Determine correct radiological characterization of the waste in each waste stream/package (it is no longer acceptable to report

radionuclides as unidentified, mixed fission product, or mixed activation product).

- Quantify each radionuclide and calculate its concentration.

- Define the waste's chemical and physical characteristics.

If a waste generator does not comply with the WAC, the RWMC facility manager may suspend the waste generator's authorization to ship until issues have been resolved and compliance has been reestablished.

Site-specific limitations for waste disposal at the RWMC, including limits resulting from performance assessment calculations are incorporated into the WAC. As noted in the WAC, the RWMC receiving organization is responsible to ensure that material or waste forms are within the RWMC's safety analysis and performance assessment limits and are within the technical capacity of the RWMC. Based on the draft performance assessment, limitations were incorporated into the WAC for disposal of LLW contaminated with TRU isotopes (Maheras and Rood 1991a, 1991b). LLW received at the RWMC that is contaminated with TRU isotopes <100 nCi/g but >10 nCi/g is excluded from disposal and is placed in interim storage. LLW contaminated with TRU isotopes ≤10 nCi/g can be disposed of in the SDA and is managed in one of several ways depending on the waste type, physical configuration, radioactivity, and container. The four categories of LLW are nonprocessible waste, compactible waste, incinerable waste, and WERF sizing waste as described below.

2.2.4.1.1 Nonprocessible Waste (Direct Disposal)--LLW that currently cannot be processed at WERF because of radiation levels, size, or composition is directly disposed of at the RWMC SDA. This waste comes to the RWMC in containers such as wooden boxes, metal bins, and 55-gal drums. The current LLW acceptance criteria document prohibits disposal of free liquids, hazardous materials, and pyrophorics. They also require physical and chemical waste characterization and encourage void space minimization. Studies confirm concrete boxes can be used for some wastes that have radiation levels greater than allowed for contact handling (i.e., >500 mR/h) to reduce the use of soil vaults, which may interfere with RWMC remedial actions. Plans for 1994 include using concrete boxes for disposal at the RWMC.

2.2.4.1.2 Compactible Waste--LLW that cannot be incinerated but can be compacted generally contains halogens or sulfur and some rubber materials, with a radiation level <200 mR/h at the surface. The waste is sent to WERF where it can be compacted into 1.2 × 1.2 × 1.8-m metal boxes and achieves a volume reduction ratio of about 5:1. The compacted waste is shipped to the RWMC for disposal. Current plans are to start up compaction operations at WERF after signing of the WERF Environmental Assessment Finding of No Significance in July 1994.

2.2.4.1.3 Incinerable Waste--Incinerable LLW material consists of rags, plastics, wood, and other combustible material with a radiation level currently limited to <20 mR/h at contact. Most incinerable waste is packaged in cardboard boxes at the generator, shipped to WERF in cargo containers so that it can be burned in the WERF incinerator. The incinerator achieves a volume reduction ratio of 50:1 to 300:1 depending on the type of material incinerated. The resulting fly ash is mixed waste because it contains leachable toxic metals (lead and cadmium). The incinerator fly ash is treated by solidification with cement in 71-gal drums to stabilize the chemically hazardous levels of lead and cadmium and sent for toxicity characterization leaching procedure testing. After it passes the toxicity characterization leaching procedure test, the stabilized fly ash is shipped to the RWMC for disposal. Incineration at WERF will not be conducted until the INEL Environmental Restoration and Waste Management Environmental Impact Statement Record of Decision, currently scheduled for July 1995.

2.2.4.1.4 WERF Sizing Waste--WERF sizing waste is defined as metal (aluminum, stainless and carbon steel, copper, and others with wall-thickness too great for compaction with the 200-ton compactor) having radiation levels <100 mR/h at contact and free of toxic and hazardous material. Metallic waste is shipped to WERF in bins. These bulk metal shipments are then reduced in size (achieving a volume reduction of about 4:1), packaged, and shipped to the RWMC for disposal. Current plans are to start up sizing operations at WERF after signing of the WERF Environmental Assessment Finding of No Significance in July 1994.

2.2.5 Waste Inventory Determination

Inventories of past burials and predictions for the future are discussed in this section. The information for the inventories generally comes from the available shipping records.

2.2.5.1 Radioactive Waste Management Information System Data Base The INEL Radioactive Waste Management Information System (RWMIS) was developed in 1971 for DOE-ID Waste Management. The system was designed to provide timely and accurate information on the amount of radioactive wastes stored or disposed of at the INEL. Information reported in the INEL RWMIS includes all gaseous, liquid, and solid radioactive wastes. Environmental Programs, EG&G Idaho, maintains and operates the INEL RWMIS for DOE-ID.

An effort was undertaken in 1976 to enter shipment data for waste sent to the INEL from 1954 to 1970 into the RWMIS using existing shipping invoices and other records. In 1984, when the INEL RWMIS data base language was converted from COBOL to NOMAD, these data were excluded. In 1987, the 1954 to 1970 data were added to the NOMAD environment.

Data on current shipments to the RWMC are furnished by the waste generator and include waste type, container type, shipment date, waste generator location, waste description, gross volume and weight, gross radioactivity, and nuclide identification including amount or percent of gross radioactivity. The burial or storage location and date of placement in the RWMC for each shipment are provided to the RWMIS by RWMC operating personnel.

Several improvements to the data base system and data reporting have taken place since data collection was computerized. One of these improvements is tracking of solid radioactive waste by waste package rather than by shipment. Since the inception of solid radioactive waste reporting and monitoring at the INEL, records were kept on shipments. A shipment could have consisted of anywhere from 1 to 500 waste packages. In January 1986, solid radioactive waste tracking at the INEL was changed to monitor waste packages. Tracking solid waste flow on the INEL is now more accurate. It is possible to pinpoint the location of an individual container, and information can be obtained on the waste package type and weight, total curies, and radionuclides

present. These kinds of waste package-specific details were unavailable when monitoring solid waste shipments.

DOE contractors routinely report information on gaseous and liquid radioactive effluents and solid radioactive waste that is stored, disposed of, and sent to the INEL for reduction. The RWMIS is the official repository for these data. An annual report is written to incorporate waste management data for the current year and to reflect changes from previous annual reports to more accurately reflect the current status of waste operations at the INEL.

2.2.5.2 RWMC Inventory for Modeling Analysis. The RWMC radiological performance assessment evaluates LLW disposed of in the SDA from 1984 through 1993. In addition, it evaluates projected LLW that will be disposed of in the SDA from 1994 through 2020. The LLW disposed of in the SDA from 1984 through 1993 is buried in Pits 17 through 20 and Soil Vault Rows 14 through 20. No trench burial occurred during this time period; the last open trench, Trench 55, closed in 1982. Although DOE Order 5820.2A applies only to LLW disposed of after September 26, 1988, LLW disposed of before this date was included in the radiological performance assessment. The Environmental Restoration Program at the INEL will assess wastes buried in the SDA from 1952 through 1983 in accordance with the National Contingency Plan under CERCLA.

The year 1983 was selected as the cutoff date for the waste to be assessed under CERCLA based on the following rationale. High-efficiency particulate air filters from the Waste Calcining Facility, located at the Idaho Chemical Processing Plant, containing the hazardous materials mercury and cadmium were disposed of in the SDA at late as June 1983. Therefore, the trenches, pits, and soil vaults rows that were open before June 1983 could potentially contain mixed waste, which falls under the domain of the Environmental Restoration Program and will be assessed under CERCLA.

In terms of disposal locations, this includes waste buried in Trenches 1 through 58, Soil Vault Rows 1 through 13, and Pits 1 through 16. Because it is impractical to remediate only part of pit or soil vault row, all wastes buried in Pit 16 and Soil Vault Row 13 will be assessed under CERCLA even though Pit 16 closed on October 15, 1984, and Soil Vault Row 13 closed on December 21, 1984.

Soil Vault Row 14 and Pit 17 opened on October 16, 1984, and May 5, 1984, respectively. Therefore, they should contain only LLW, not the mixed waste described previously and are a logical point to begin the radiological performance assessment. Using this date will ensure that all waste is accounted for either in the radiological performance assessment performed under DOE Order 5820.2A or in the baseline risk assessments performed under CERCLA.

Recent studies have improved knowledge of the waste disposal inventory buried at the RWMC. A study conducted during 1991 and 1992 improved the information about radionuclides in LLW buried at the RWMC (Plansky and Hoiland 1992). A questionnaire and a RWMIS LLW inventory printout was sent to LLW generators, requesting their review of that data. As a result of this study, generators either indicated agreement with their RWMIS inventory data or noted changes on the questionnaire and inventory data printout. The generators also provided the needed changes to RWMIS personnel for update to the RWMIS data base.

In 1992, the shipment-specific waste information in the historical data bases (for pre-1971 shipments) was verified with the RWMIS data base by comparing the original shipping manifests that accompanied the waste shipments for the years 1961 through 1984 with fields on printouts of the RWMIS data base (Barnard 1992). Inconsistencies were noted, and proposed amendments to the RWMIS data base were reviewed and discrepancies resolved. The RWMIS data base was updated to incorporate the new information from this task.

RWMIS data base personnel supplied information from the RWMIS for LLW disposed of from 1984 to 1993 for use in the radiological performance assessment. The information included radionuclide identification, curie quantities by radionuclide, container types and quantities, disposal location, disposal year, volume of LLW disposed by year, waste generator identification, and waste form description (Culbertson-Arendts 1993). The RWMIS information was input to the ORIGEN2 computer code used to decay and ingrow the inventory data as described in Section 2.2.5.4. RWMIS personnel also provided the forecast data forms filled out by the waste generators for LLW projected to be disposed of at the RWMC. The forecast data form were analyzed (Anderson 1993)

and used to derive the LLW disposal inventory for the RWMC from 1994 through 2020, as discussed in Section 2.2.5.3.

During the time period evaluated in the radiological performance assessment, 1984 through 2020, unidentified activity accounts for only 0.12% of the activity disposed of in the pits and 0.033% of the activity disposed of in the soil vault rows. For the purposes of analyses, unidentified activity (denoted mixed activation products, mixed fission products, and unidentified beta-gamma in the RWMIS data base) was assumed to be 50% Sr-90 and 50% Cs-137. The use of other radionuclides for unidentified activity was evaluated in the uncertainty analysis.

2.2.5.3 Radionuclide Forecasts. The RWMC LLW radiological performance assessment includes projected disposal through 2020. Although current plans are to replace the existing RWMC approximately by 2002, anticipated disposals through 2020 are included to provide future flexibility because of uncertain funding levels needed to support developing a new disposal capacity. The future disposal of tritium-containing beryllium reflector blocks was not included in the forecast pending the development of a suitable disposal technology or waste form for this waste. The Environmental Restoration and Decontamination and Decommissioning organizations have submitted radionuclide forecast information to the RWMIS by individual Waste Area Group (WAG). This information is included as part of the radiological performance assessment forecast information. Two methods are commonly used to forecast inventory. In the first method, generator forecasts are combined to yield an annual inventory to be disposed of in the future. In the second method, the past. several years of historical disposal data are used to arrive at an annual inventory to be disposed of in the future. Both methods have their drawbacks. For example, waste generators may not report all radionuclides of importance in a performance assessment. Past operations may also not be representative of future operations, especially when considering the changing role of DOE and the changing mission of the INEL. To address this uncertainty in projecting future LLW inventories, a combination of the two methods was used to forecast inventory to be disposed of from 1994 through 2020. First, an annual disposal rate based on the past 5 years of historical data was calculated. Second, an annual disposal rate based on 3 years of generator forecast data was calculated. The annual disposal rate calculated from 5 years of historical

data was weighted by 5/8, and the annual disposal rate calculated from 3 years of generator forecast data was weighted by 3/8. These two quantities were then added to arrive at an 8-year weighted average annual disposal rate.

$$\text{8 year weighted average} = \frac{5}{8}\left[\text{5 year historical average}\right] + \frac{3}{8}\left[\text{3 year generator average}\right] \quad (2\text{-}1)$$

Five years (1989 to 1993, inclusive) was chosen for the historical data average because radionuclide reporting requirements for these years were more comprehensive than for earlier years. In addition, the past 5 years of data should more accurately reflect future operations than data collected 10 or 15 years ago. Three years (1994 to 1996, inclusive) was chosen for generator forecast data because waste generators are able to forecast 1 to 3 years with reasonable accuracy, but forecasts for longer time periods have been unreliable. Tables listing the historical 5-year average, the 3-year forecast average, and the weighted average for pits and trenches and soil vaults are contained in Appendix A.

2.2.5.4 Decay and Ingrowth of Inventory. The ORIGEN2 computer code was used to decay and ingrow the inventory and forecast data. The decay and ingrowth was calculated based on time. For example, the inventory for pits in 1984 was decayed and ingrown for 1 year and added to the inventory disposed of in 1985. This sum was decayed and ingrown for 1 year and then added to the inventory disposed of in 1986. This process was continued until the year 2020, using actual data for 1984 through 1993 and forecast data for 1994 through 2020. After 2020, there were no more inventory additions because the SDA was assumed to be closed. The inventory in 2020 was decayed and ingrown for 10,000 years after SDA disposal ends, the year 12,020.

Appendix A contains the decayed and ingrown inventory for pits and soil vault rows.

2.2.5.5 Volumes and Containers. A total of 20,730 m^3 of waste disposed of from 1984 through 1993 is covered in the performance assessment. Pits

account for 20,000 m^3 (or an annual average of 2,000 m^3) of this waste. Soil vault rows account for 730 m^3 (or an annual average of 73 m^3) of this waste. The total volume of LLW was calculated to be 75,600 m^3 in the pits and 2,700 m^3 in the soil vault rows based on 27 additional years of disposal (1994 through 2020). Appendix A contains the waste volume disposed of by year from pits and soil vault rows.

LLW is disposed of in a wide variety of containers. From 1984 to 1993, of the 16,334 containers disposed of in pits, waste compacted into bales are the largest number (8,302), followed by wooden boxes (5,038), and metal barrels (1,576). For the same time period, of the 450 containers disposed of in soil vault rows, inserts are the largest number (419).

2.3 Environmental Restoration Activities

On December 21, 1989, the INEL was added to the EPA's National Priorities List of Superfund sites. Under CERCLA or Superfund of 1980, as amended, Federal agencies that have facilities included on the EPA's National Priorities List are required to enter into agreements with the EPA. The goal for this agreement is to ensure that INEL releases or potential releases of hazardous substances are thoroughly investigated in accordance with the National Contingency Plan and that appropriate response actions are taken as necessary to protect human health and the environment.

On December 9, 1991, a Federal Facility Agreement and Consent Order (FFA/CO) for the INEL was signed. The FFA/CO is a comprehensive environmental cleanup agreement between the DOE, EPA, and the State of Idaho. The FFA/CO requires DOE to perform specific remediation activities and meet certain legally enforceable deadlines. Major INEL facilities and waste management units scheduled for environmental restoration by DOE-ID are identified as WAGs and are generally grouped by facility area. Environmental restoration activities include an assessment phase to characterize the nature and extent of contamination and a cleanup/remediation phase. The cleanup/remediation phase begins when the extent and nature of the contamination constitutes a potential threat to human health and safety or the environment. Each WAG is subdivided into separate Operable Units, which are groupings of potential

release sites that are considered together for assessment and cleanup activities.

One of the WAGs defined under the FFA/CO is WAG-7, the RWMC. The Environmental Restoration Program at the INEL is planning to assess all the wastes buried in the SDA from start of operation in 1952 through 1983 in accordance with the National Contingency Plan under CERCLA. This includes waste buried in Trenches 1 through 58, Soil Vault Rows 1 through 13, and Pits 1 through 16.

3. ANALYSIS OF PERFORMANCE

This chapter summarizes the conceptual model for the movement of contaminants at the RWMC. It describes potential exposure pathways and provides detailed descriptions of how important pathways were analyzed.

3.1 RWMC Conceptual Model Summary

The conceptual model for the RWMC is divided into three parts: (1) the hydrologic flow conceptual mode, (2) the hydrologic transport model, and (3) the conceptual model used for the intruder and atmospheric scenarios. The hydrologic flow and transport conceptual models are discussed in Sections 3.2 and 3.3, respectively, followed by a description of the pathways and scenarios in Section 3.4. The conceptual model used for the intruder and atmospheric scenario is briefly described below.

For the performance assessment analyses, the RWMC SDA was modeled for disposal of LLW in pits and soil vaults from 1984 to 2020, at which time the SDA was closed. Upon closure, a thick soil barrier, which includes a vegetative cover, was emplaced over the operational cover and maintained during the period of institutional control. The total thickness of the cover at closure is 5 m. This maintenance includes keeping the vegetative cover intact and preventing animal burrowing. After the institutional control period, no maintenance is performed on the cover, and erosion is assumed to occur down to the existing RWMC grade. At the time of maximum erosion, this results in 2.4 m of cover remaining over the waste for pits and 3.3 m of cover remaining over the soil vaults. Figures 3-1 and 3-2 present the conceptual profile of a pit and a soil vault.

3.2 Hydrologic Flow Conceptual Model

This section describes the hydrologic conceptual model used to predict flow and transport within the unsaturated zone and regional aquifer for the LLW facility in the SDA. The section defines terms used in the modeling discussion, summarizes the hydrologic conceptual model, and provides a

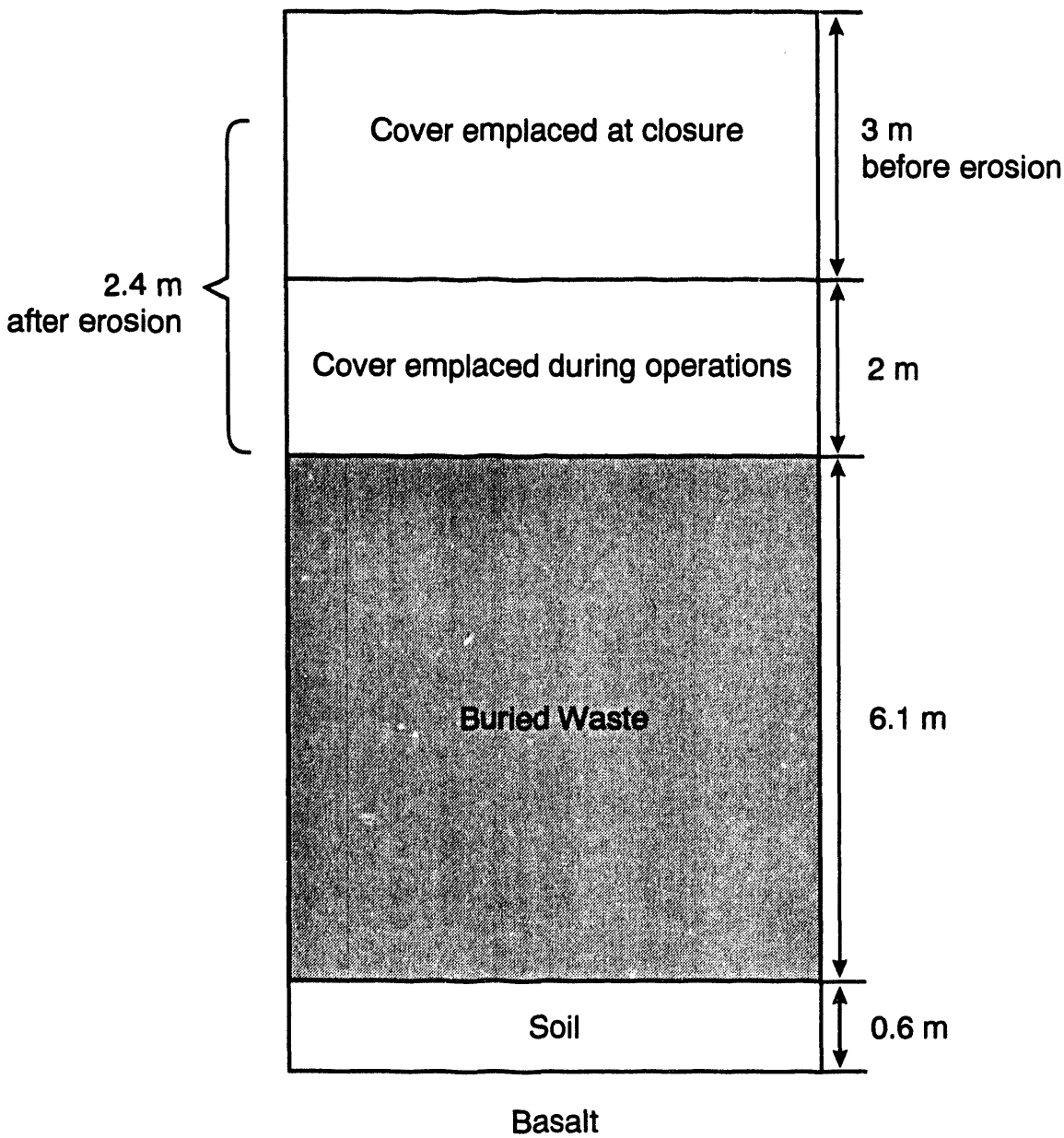

Figure 3-1. Conceptual profile of pits.

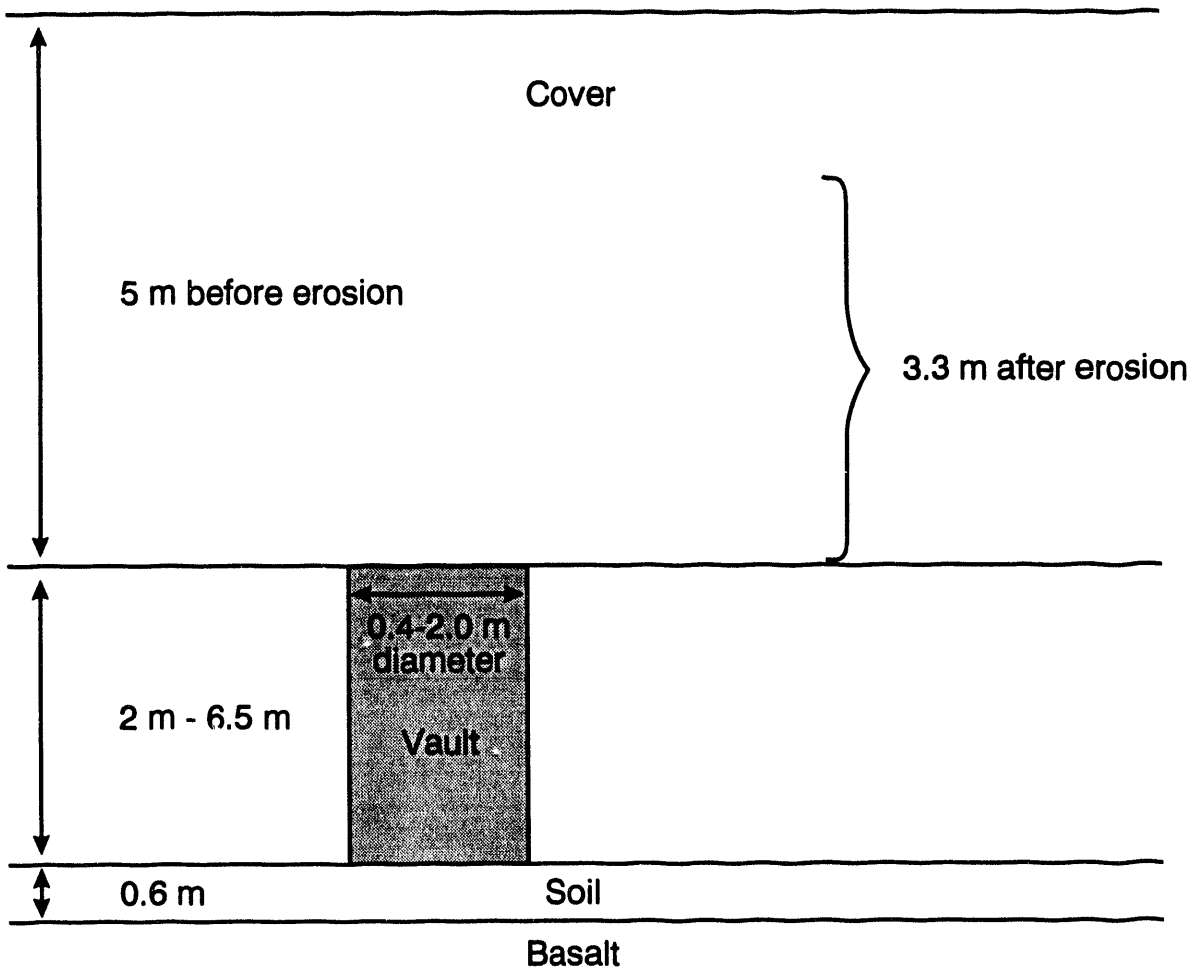

Figure 3-2. Conceptual profile of a soil vault.

detailed basis for calculating water travel times down through the unsaturated zone and within the regional aquifer. This section also describes implementing the conceptual model into a numerical simulation.

3.2.1 Definitions

This section defines terms used in flow and transport simulations in this radiological performance assessment.

A conceptual model describes the significant physical and chemical processes controlling movement of water and contaminants in a groundwater system. A conceptual model is based on site-specific data and a fundamental understanding of flow and transport.

A mathematical model is a set of governing equations that describe the processes incorporated in the conceptual model.

A numerical model is a numerical method used to solve the governing equations incorporated in the mathematical model. Numerical models can be analytic, if the governing equations have a closed-form solution, or they can be embedded in simulation codes.

The role of conservatism in performance assessment flow and transport calculations is important. To represent actual conditions, observations or field data that describe water movement are included as a basis for the conceptual model. When observations or field data are not available, conservative assumptions are used. For water movement analyses in this performance assessment, a conservative assumption estimates faster downward water movement than would be expected based on knowledge of water movement in porous media. By using a conservative assumption, water movement and dissolved radionuclide concentrations are thought to be overpredicted. The magnitude of the overprediction depends on the degree of conservatism used in the assumptions. Professional judgment ensures the assumptions are reasonable and appropriately conservative.

3.2.2 Hydrologic Conceptual Model Overview

This section provides an abbreviated picture of how flow, and to a degree transport, in the subsurface of the SDA is described and quantified for this radiological performance assessment. The topic of transport is covered in detail in Section 3.3. Readers interested in the detailed basis for the hydrologic conceptual model should read all of Section 3.2.3.

In general, water is thought to infiltrate at the land surface, contact emplaced waste, percolate downward through the surficial sediments, continue percolating downward through the fractured basalts and sedimentary interbeds, and enter into the regional Snake River Plain Aquifer. The actual hydrological flow regime in the subsurface at the SDA is not completely understood because of its complexity. This complexity is due to (a) a poor definition of the net amount of water that percolates, (b) uncertainty about the mechanism by which water enters into and flows through the fractured basalts that likely enhances retardation of radionuclides, (c) the effect of sediment infilling in the fractured basalts that likely enhances retardation of radionuclides, (d) gaps or intervals where the sedimentary interbeds are absent, and (e) recharge water from the spreading areas that appears to contribute to the flow regime beneath the SDA.

Because of these complications, flow and transport predictions are based on a simplified representation of the unsaturated zone and aquifer that relies heavily on an estimated amount of time required for infiltrating water and leached contaminants to travel from beneath the emplaced wastes down to and within the regional aquifer. Estimated radionuclide concentrations resulting from this simplified representation should be viewed as an upper bound on expected concentrations and not expected concentrations. Because of the limited hydrological data, no attempt is made to hydrologically mass-balance water movement within the unsaturated zone.

Table 3-1 summarizes the processes that are likely affecting flow and transport beneath the SDA and how they are used in the conceptual model for flow and transport. This table indicates whether the processes were included in the conceptual model. Processes that were not included could not be reasonably quantified given the current understanding of the hydrologic

Table 3-1. Processes in the RWMC hydrologic flow and transport conceptual models.

Process	Included/ not included	Comments
Infiltration into surface soil and waste zone	Included	Infiltration was modeled as a steady state process using a constant infiltration rate of 7 cm/yr from an estimated range of 4 to 10 cm/yr inside the SDA for the operational and post-institutional control periods. Infiltration during the period of institutional controi was 1 cm/yr through the engineered barrier based on previous modeling studies.
Degradation of engineered barrier	Included	The cover was assumed to uniformiy degrade over a 5-year period following the end of institutional control and maintenance. Cover integrity is a function of erosion rate, plant intrusion, and burrowing animal impacts. The net impacts of these processes were not evaluated; therefore, the value was conservatively selected to be relatively small.
Movement of infiltrating water through the burial grounds	Included	Steady state, unit gradient conditions at the prescribed infiltration rate were assumed for movement of the water downward through the burial grounds.
Movement of perched water in surficial sediments (see Figure 3-3)	Included	During the period of institutional control, the infiltration rate outside the covered waste pit was still 7 cm/yr. It was assumed horizontal movement of shallow perched water within the surficial sediments partially circumvents the engineered barrier and prevents using the reduced infiltration rate for any region except in the waste zone immediately beneath the cover. This perched water is assumed to not contact the waste.
Movement of infiltrating water in unsaturated basalts	Not included	Water travel times through unsaturated fractured basalt may vary from days to years depending on the local presence and spacing of fractures and the net water flux. Little site-specific data exist on unsaturated basalts below the RWMC, and as a result, water flow through fractured basalt is poorly understood. For these reasons, flow through basalt was conservatively assumed to be instantaneous.
Movement of infiltrating water through sedimentary interbeds	Included	There are limited characterization data for sedimentary interbeds below the RWMC. Unit gradient conditions were assumed for the B-C, D-E, and E-F interbed while a measured gradient was used for flow across the C-D interbed.
Recharge water from the spreading areas contributing to flow regime in the unsaturated zone beneath the SDA (see Figure 3-4)	Included	The possible effects of this additional water were included by using a measured gradient across the C-D interbed that was greater than would be expected because of gravity-driven flow alone. Whether this increased gradient is due to recharge from the spreading areas or from local preferential flow is uncertain.
Dilution because of shallow perched water or from spreading area recharge water	Not included	The dilution of radionuclides by shallow perched water or from spreading area recharge has little impact on the overall nuclide concentration in the aquifer because the volume of water entering the aquifer from the unsaturated zone is insignificant relative to the volume of water flowing in the aquifer.
Sorption reactions in burial grounds	Included	Instantaneous equilibrium between the liquid and aqueous phases was assumed in the backfilled soil immediately following release of radionuclides from the waste containers. Therefore, the linear sorption coefficient (K_d) could be used.

Table 3-1. (continued).

Process	Included/ not included	Comments
Sorption reactions in unsaturated zone	Included	Sorption reactions were only modeled in the sedimentary interbeds. Sorption reactions were conservatively not modeled in the unsaturated fractured basalt. Instantaneous equilibrium between the solid and aqueous phases was assumed.
Sorption reactions in aquifer	Included	Sorption reactions were modeled in the fractured basalts in which the majority of regional groundwater flow is thought to occur. Instantaneous equilibrium between the solid and aqueous phases was assumed.
Release of radionuclides from waste containment vessels to backfilled soil	Included	Site-specific data indicate the average metal container lifetime is about 10 years. Wood and cardboard containers lifetimes are considerably less (~2 years). Little data exist on nuclide leach rates from failed waste containers. For this reason, nuclides were assumed to transfer to the soil backfill immediately following container failure and redistribute homogeneously throughout the pits.
Release of radionuclides from activated metals	Included	Radionuclide inventories reported to be in activated metals were released to the backfilled soil based on the corrosion rate of the activated metal component.
Release of radionuclides from backfilled soil to unsaturated zone	Included	Radionuclides were leached from soil backfill to the unsaturated zone using a first order leach rate constant that was a function of the infiltration rate, porosity, and radionuclide-specific sorption coefficient.
Advection in the unsaturated zone	Included	Advection was modeled as plug flow through the sedimentary interbeds. Relatively instantaneous transport was assumed for the fractured basalts.
Dispersion in unsaturated zone	Not included	Little data exist on unsaturated water movement below the RWMC and virtually no data exist on dispersivity values in this environment. Adding dispersion in the unsaturated zone would tend to smear the pulse out, thereby reducing the instantaneous contaminant flux at the saturated-unsaturated zone interface. Including dispersion would not result in a significant change in the results (less than a factor of 2). Dispersion in the unsaturated zone was ignored because of the lack of defensible data and assuming no dispersion simplifies the model and is conservative.
Advection in the aquifer	Included	A pore velocity of 560 m/yr was incorporated. Water movement was assumed to be constant and unidirectional and to occur primarily within the permeable portions of basalt flows.
Dispersion in the aquifer	Included	Dispersion was modeled in the two horizontal directions (lateral and transverse). Values for dispersivity were based on site-specific measurements and model calibration data.
Vertical mixing in the aquifer	Included	Uniform mixing was assumed in the vertical direction in the aquifer. For the RWMC facility boundary receptor, concentrations were averaged over the 12-m well screen length because at that distance (100 m south of the facility), little mixing would have occurred. For the INEL Site boundary receptor, the mixing thickness was assumed to be the effective aquifer thickness of 76 m because almost complete mixing in the aquifer would have occurred at that distance downgradient (5,500 m).

Table 3-1. (continued).

Process	Included/ not included	Comments
Flooding events	Included	A flooding event was assumed to occur after the end of institutional control and complete degradation of the engineered cover. This process was addressed and simulated in the uncertainty analysis. Flooding before the end of institutional control was assumed to be prevented by flood mitigation activities at the SDA.
Transport because of nonequilibrium partitioning, colloidal, or organic complexation during flooding events	Not included	Radionuclides present in the soils underlying waste pits and in the B-C interbed were thought to have been transported by other than equilibrium partitioning during flooding events (Bishoff and Hudson 1979; McKinley and McKinney 1978). Estimated radionuclide movement and concentrations based on constant water velocities in this performance assessment do not attempt to match observed nuclide concentrations in the unsaturated zone.

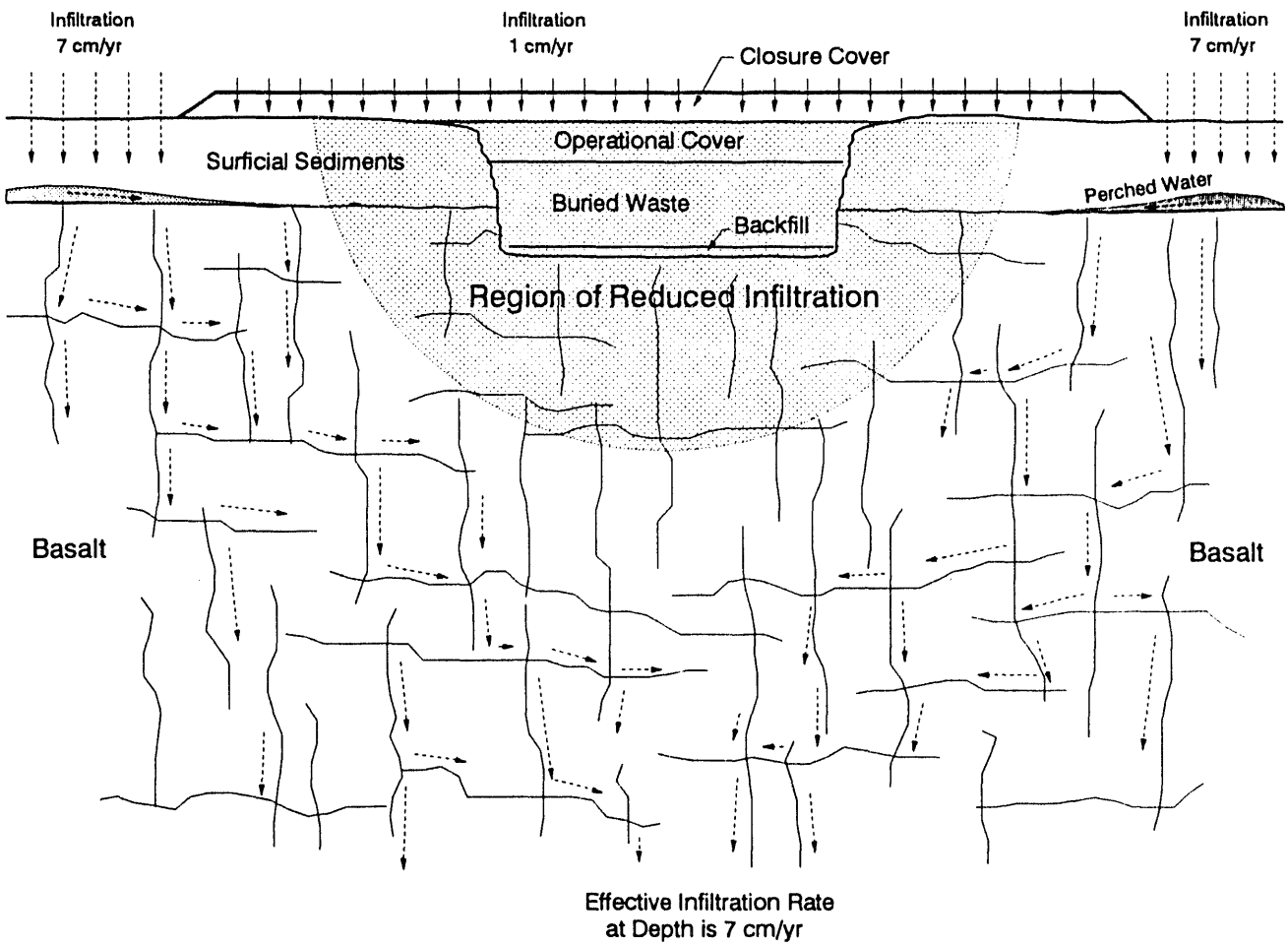

Figure 3-3. Conceptual movement of water in the vicinity of the LLW facility during institutional control.

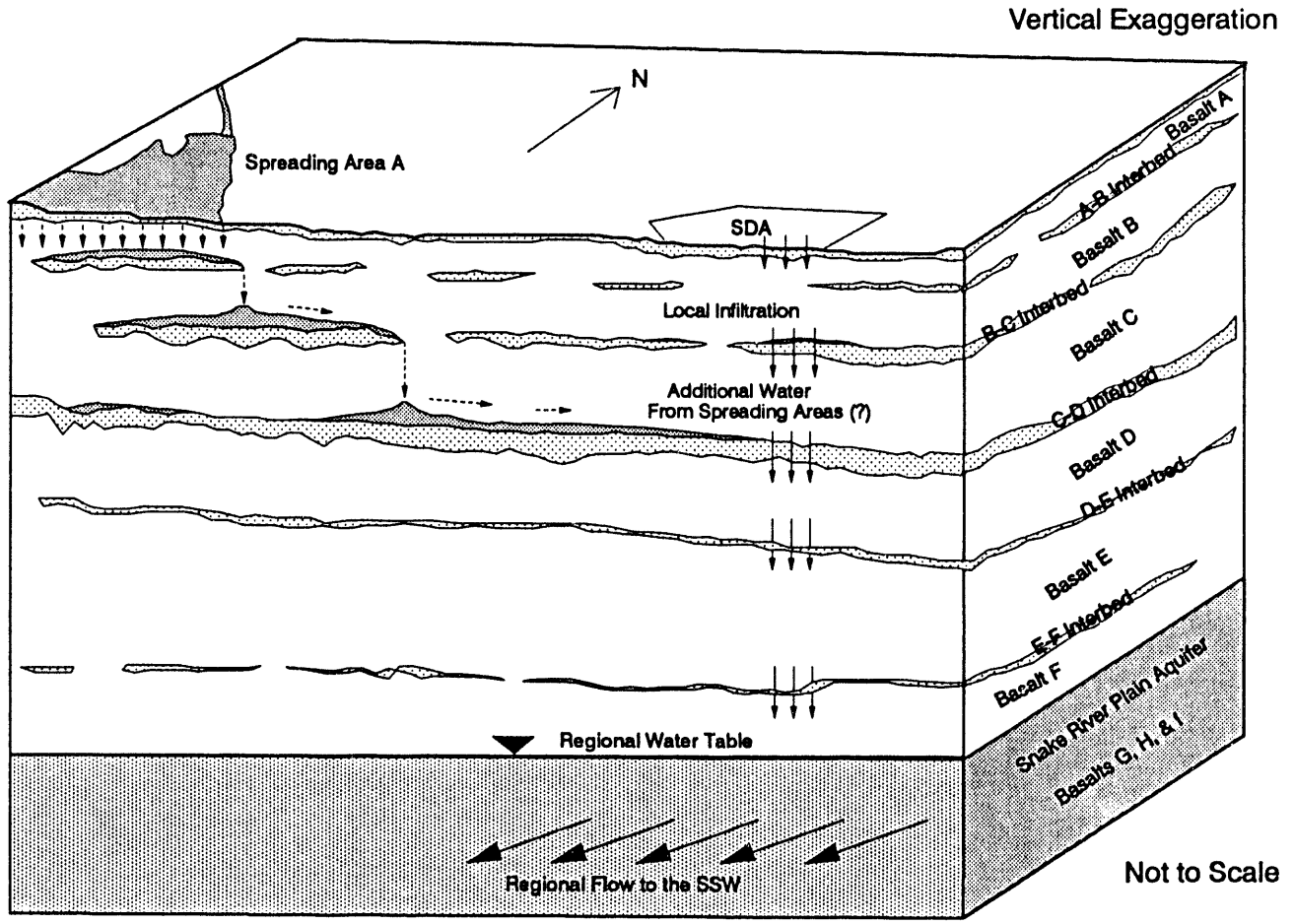

Figure 3-4. Conceptual movement of water in the subsurface beneath the SDA.

system. Some processes that were included could only be included conceptually. Transport processes are included in Table 3-1 and are discussed in detail in Section 3.3. The principle result of this conceptual model is a unsaturated zone water travel time of approximately 30 years.

3.2.3 Detailed Basis for Estimating Unsaturated Zone Water Travel Time and Velocities Within the Regional Aquifer

This section provides detailed information about how water velocities and travel time in the unsaturated zone and regional aquifer were estimated. The estimate generally begins with water infiltration at the land surface and ends with water velocities in the regional aquifer (see Figures 3-3 and 3-4).

3.2.3.1 Infiltration Rate Through Operational Cover. The best estimate of the current net infiltration rate into cover soils, waste pits, and the rest of the SDA ranges from 4 to 10 cm/yr. This estimate is based on observations and studies described in Section 2.1.3.2.2, primarily. The estimated infiltration rate given by Magnuson and McElroy (1993) of 3.8 to 9.2 cm/yr. For purposes of this performance assessment, their estimate was conservatively rounded up to the nearest whole integer. Infiltration at the SDA has been observed to be a transient process. The resulting pulses of water are believed to be dampened at depth by imbibition into smaller basalt fractures, the basalt matrix, and by interbeds. Therefore, measurements of moisture states at depth, such as those used in the Magnuson and McElroy (1993) estimate, are less subject to transient effects and are more representative of the average infiltration.

This 4 to 10 cm/yr infiltration range is consistent with the estimates of Miller et al. (1990) for CFA landfill covers. If storage in the CFA soil cover is assumed to be the same from year to year, the resulting average annual infiltration of 7.4 cm (Miller et al. 1990) is in very good agreement with the intermediate value of the 4 to 10 cm range presented by Magnuson and McElroy (1993).

The much lower infiltration rate estimate of 0.4 to 1.1 cm/yr in Cecil et al. (1992) does not represent conditions inside the SDA. The location Cecil et al. used, although immediately adjacent to the SDA, is undisturbed

and vegetated. The location is also on a slight topographic high relative to the surrounding area.

The monitoring results from McElroy (1993) and Hubbell (1993) showed an appreciable amount of water infiltrating rapidly down to the basalts at a number of locations inside the SDA. The amount of infiltrating water varied from 3 to 28 cm. Perched water level measurements within the surficial sediments showed increases up to 1.1 m, which could be approximately accounted for by precipitation received in a wet period during June 1993.

These four estimates of infiltration taken together indicate that an appreciable amount of water enters the subsurface of the SDA during the spring when evapotranspiration rates are low. This water is believed to move downward into the basalts before it can be brought back to the surface by higher evapotranspiration rates later in the summer. The infiltration rate range of 4 to 10 cm bounds the net long-term infiltration rates. This estimated range could change as the surficial sediment monitoring network inside the SDA is expanded and more detailed information is collected.

This estimated infiltration rate range is applicable for both pits and soil vaults during the current operational and post-institutional control periods in the analysis. In the post-institutional control period, the additional thickness of closure cover is assumed to have eroded down to the original grade (see Figures 3-1 and 3-2). Furthermore, because the cover is not maintained after institutional control ends, the vegetative cover cannot be guaranteed to remain and burrowing cannot be prevented. It is unlikely that the infiltration rate will return to the 0.4 to 1.1 cm/yr that was measured just outside the SDA because the natural processes that deposited the soil have been disrupted, increasing the effective permeability.

Compaction because of settling over time could reduce the permeability of the cover soils. However, this differential settling would likely result in increased infiltration because water accumulating in the resulting surface depressions could cause locally saturated conditions. The formation of a caliche or hardpan layer over time could also reduce permeability and infiltration. However, it takes hundreds to thousands of years to form a caliche layer--limiting the use of this process to reduce infiltration.

Additionally, caliche layers can also have significant fractures; therefore, their ability to reduce infilitration is limited. Considering the uncertainties in estimating infiltration rates during the operational period, there is no reason to suppose a better estimate can be made during the post-institutional control period. Therefore, the infiltration rates are considered to be likely to remain in the 4 to 10 cm/yr range for the post-institutional control period.

To determine compliance, an intermediate value of 7 cm/yr was used as the infiltration rate in this radiological performance assessment. The effect of this decision is addressed in the uncertainty and sensitivity sections in Chapter 4.

3.2.3.2 Infiltration Rate Through Engineered Barrier. This radiological performance assessment assumes that during closure of the LLW facility an engineered barrier, including a vegetative cover, will be emplaced over the operational cover and maintained during the period of institutional control. This maintenance includes keeping the vegetative cover intact and preventing animal burrowing. A preliminary estimate of the net infiltration through this engineered cover is 1 cm/yr, occurring at a relatively constant rate throughout the year. This estimate is based on a simulation study (Magnuson 1993) that used site-specific meteorological data and included the effect of an annual snowmelt event. The study was conducted to provide guidance in designing small-scale field test plots to demonstrate barrier performance (McElroy et al. 1992). A thick soil barrier and a capillary barrier are planned to be tested (see Figure 3-5). The 1 cm/yr net infiltration estimate is for the thick soil barrier. Simulations for the capillary barrier indicated that the net infiltration could be even lower. The higher infiltration rate from the thick soil barrier simulation provides a conservative estimate.

Because the field test plots have not been built, there were no measurements against which to calibrate the engineered barrier simulations. However, the simulations were made using estimates of hydraulic properties for

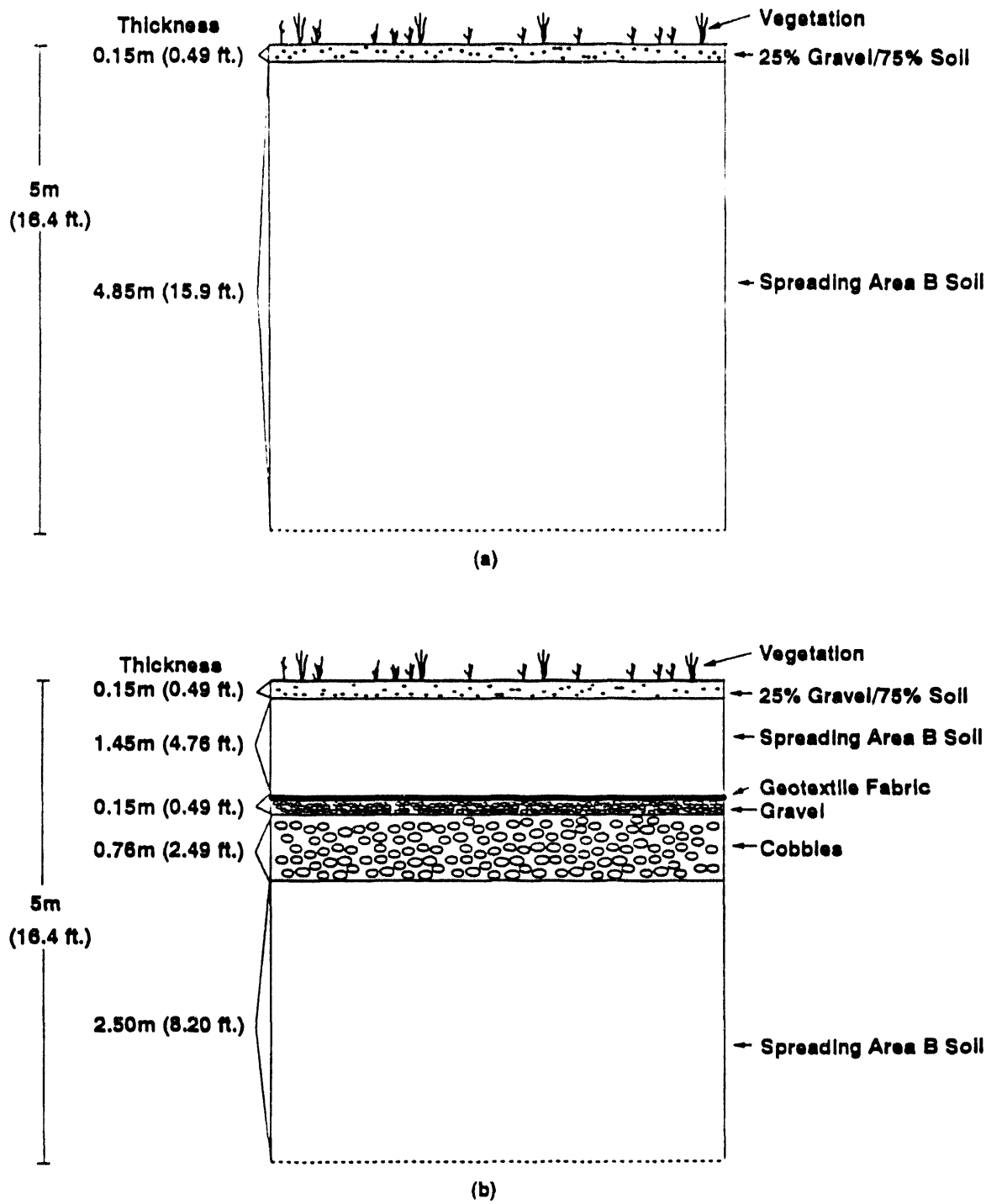

Figure 3-5. Two engineered barrier designs proposed for use in closure of the LLW facility (McElroy et al. 1992)--a thick soil barrier denoted by (a) and a capillary barrier denoted as (b).

the barrier materials and site-specific meteorologic data. These data are reasonable to use until a field-based estimate becomes available.

After institutional control and maintenance end, the barrier will begin to degrade by erosion and animal burrowing. In a least favorable scenario, decay of plant roots present as part of the barrier could also contribute to decreased performance in limiting the amount of water that infiltrates to the waste zone. These plants are more likely to remain living and transpiring, however. Erosion would take hundreds to thousands of years to remove the additional soil added as part of the engineered barrier. Rodent burrowing would likely occur much faster and would provide routes for water to rapidly infiltrate to depth and cause the barrier to fail. While it is possible to estimate the rate at which rodents burrow, the time of complete hydraulic failure of the engineered barrier was conservatively estimated to be 5 years after institutional control ends. At this time, the infiltration rate through the remaining cover over the waste returned to 7 cm/yr, the same rate used during the operational period.

3.2.3.3 Shallow Perched Water. In addition to providing evidence of rapid infiltration, the shallow perched water level measurements within the surficial sediments provide information about subsurface water movement.

Perched water typically originates as a result of areally-distributed infiltrating water being focused into a smaller region. As more water is added to a perched water body, its lateral extent and thickness increase. Thus, perched water within sediments creates a potential for lateral movement of water within the sediments. Although Hubbell (1993) indicated shallow perched water was not observed everywhere, its possible spreading effect is included to be conservative. The effect of shallow perched water is included conceptually by assuming (a) partial circumvention of the engineered barriers because of lateral spreading within the surficial sediments (see Figure 3-3 and the remainder of this section) and (b) substantial lateral movement along preferential flow channels in the basalts (see Section 3.2.3.4). The result of including both of these assumptions is that the infiltration rate at depth is equal to the infiltration rate without the engineered cover.

The presence of perched water at the surficial sediment-basalt contact indicates how water moves into the underlying fractured basalts. Water in a partially saturated medium is held under negative pressure or tension. This capillary tension prevents water from moving from a region with small pore spaces into a region of larger pore spaces until the tension is nearly reduced to zero pressure or equivalently, reaches saturation. Open fractures in basalt immediately beneath the surficial sediments impede water movement into the basalt until there are nearly saturated conditions in the overlying sediments. Under these conditions, water enters the open fractures more easily than the much lower permeability basalt matrix. As a result, the water movement into the fractured basalts is likely dominated by fracture frequency. Fracture spacing measurements documented in Knutson et al. (1992) indicate that near perimeter zones of basalt flows, the spacing between fractures decreases to 0.25 m. Because the uppermost portion of Basalt A, which underlies the surficial sediments, is the perimeter of a basalt flow, it will likely have this same frequent fracture spacing. This degree of fracturing will likely limit the lateral extent of perched water bodies within the surficial sediments. Under these assumptions, it is reasonable to further assume that a cover can be engineered so that the horizontal movement of shallow perched water is prohibited from contacting the waste covered by the barrier. However, as illustrated in Figure 3-3, perched water within the surficial sediments may spread underneath the cover part of the distance to the waste and contribute to an increased water flux in the basalts beneath the waste. The control on water movement of saturated conditions in the surficial sediment and infiltration into fractures is not known. This subject is further addressed in Section 5.2, "Enhancements to Environmental Monitoring and Data Needs."

3.2.3.4 Basalt Flows A and B. Water movement in basalts is assumed to be rapid. This assumption was based on data from Hubbell (1990a, 1992, 1993) that indicated perched water levels above the B-C interbed (and from above the C-D interbed where the B-C interbed is absent) show responses to seasonal pulses of water. Although the monitoring period using downhole data loggers was too short to make a conclusive determination, an upper bound for water movement in basalt is as much as 30 m/mo. The water travel times resulting from this velocity are negligible, and as a result are conservatively assumed to be zero. However, it is not an overly-conservative assumption based on the

limited number of water levels observed in perched water bodies existing at depths to 65 m below the surface. While there has been and continues to be extensive research about unsaturated fracture flow, there are still large uncertainties associated with theoretical descriptions. Also, theoretical descriptions would have to be demonstrated through field validation within the unsaturated zone at the RWMC before they could be used and defended for this radiological performance assessment. A field study of basalt hydrologic and transport properties, scheduled for summer 1994, is discussed in Section 5.2, "Enchancements to Environmental Monitoring and Data Needs."

In addition to moving rapidly downward, water also moves easily horizontally within the basalts along fractures or zones of increased horizontal conductivity. Bishop (1991) describes numerous horizontal flow channels of 1 to 2 cm width in a basalt block taken from the SDA. These horizontal channels resulted from gas bubbles concentrating in horizontal bands as they rose through the molten interiors of the extruded basalt flows. During experiments conducted to characterize the matrix flow in the basalt block, these horizontal flow channels had to be sealed to prevent horizontal water movement out of the block. The high horizontal conductivity allows infiltrating water to easily move horizontally through the basalts into the region below the LLW pits, as indicated in Figure 3-3. So infiltration water is assumed to circumvent the closure cover at depth and move downward rapidly as if there were no closure cover. As a result of assumptions regarding shallow perched water and horizontal movement with Basalt Flows A and B, the amount of infiltrating water at depth was 7 cm/yr with or without the closure cover.

3.2.3.5 B-C Interbed. Infiltrating water contacts the B-C interbed, which is continuous in the region of Pits 17 to 20 and Soil Vault Rows 14 to 20 (see Figures 2-7 and 2-24). Because perched water is observed at Well 78-1, west of the pits, perched water likely forms above the B-C interbed beneath Pits 17 to 20. This perched water spreads laterally until infiltration downward through the aquitard equals or exceeds the water percolation down from above. The perched water bodies observed beneath the SDA, including those above the B-C interbed, are discontinuous. The low permeability layer (aquitard) that causes the perching has been hypothesized to be either the contact between the overlying basalts and the interbeds or a

dense fracture-infilled basalt above the interbeds or both (Figure 3-6). The mechanism responsible for causing more water to percolate down in one region and create perched water zones is not known. It is hypothesized to be related to either increased infiltration through the surficial sediments because of topography and disturbed sediments or to preferential pathways in the fractured basalts.

Measurements in the basalts in the perched zones above the C-D interbed generally indicate low horizontal permeabilities. There is no reason to believe the horizontal permeabilities will be different in perched zones above the B-C interbed. This low horizontal permeability limits the likelihood of extensive horizontal movement within the perched water bodies to lateral discontinuities or "holes" in the B-C interbed, which are observed primarily in the western half of the SDA (see Figure 2-7).

The result of a continuous aquitard and a low horizontal permeability within the perched zone is that infiltrating water in the regions of Pits 17 to 20 must pass through the B-C interbed on the way down to the regional aquifer.

A unit-gradient condition was used to estimate the water velocity across the B-C interbed. This velocity calculation is performed using Darcy's law for unsaturated flow and is given by

$$v = \frac{q}{\theta_v} = \frac{K(\theta_v)}{\theta_v}\frac{\partial H}{\partial z} = \frac{K(\theta_v)}{\theta_v}\left(\frac{\partial \psi}{\partial z} \pm 1\right) \qquad (3\text{-}1)$$

where

v = average linear velocity

q = Darcy flux (cm/s)

θ_v = volumetric moisture content (cm^3/cm^3)

$K(\theta_v)$ = hydraulic conductivity as a function of θ_v (cm/s)

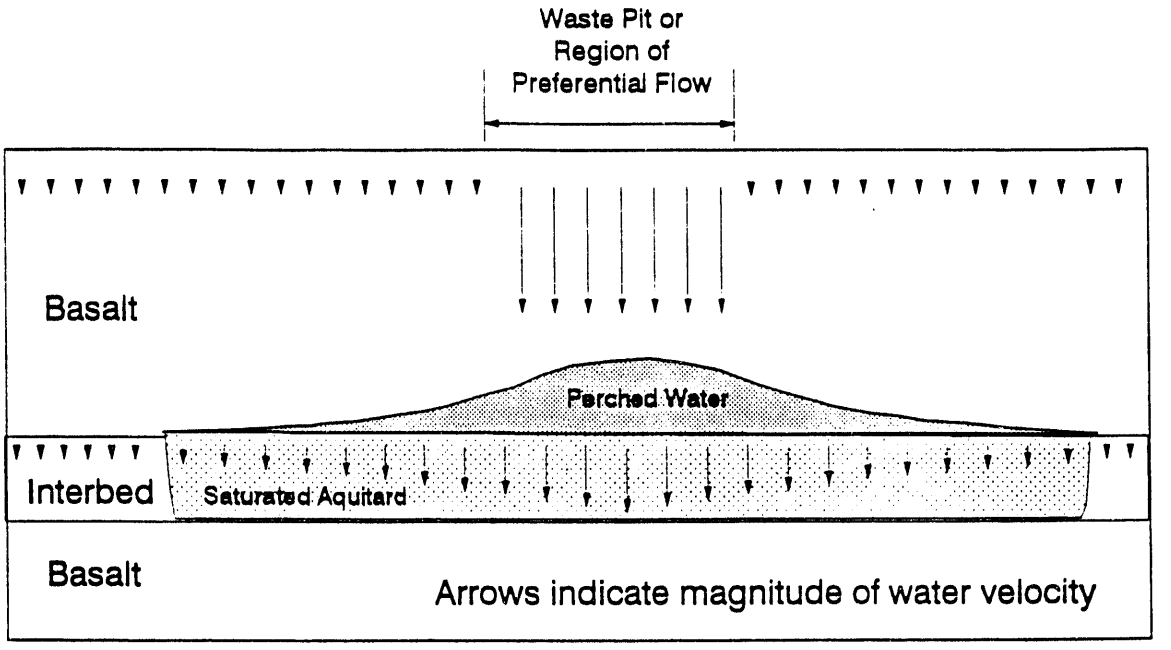

OR

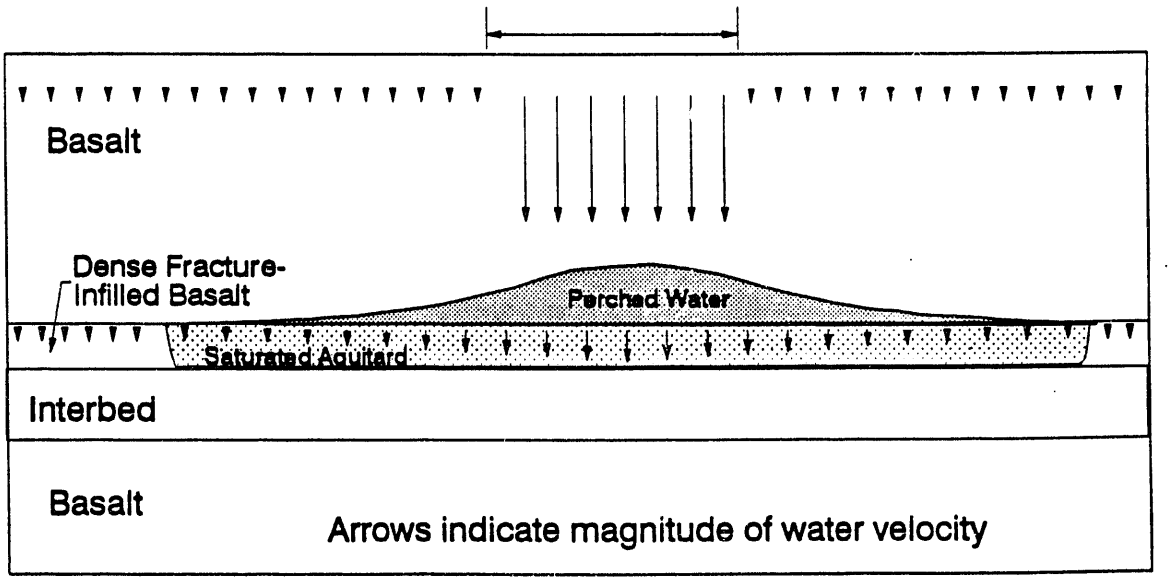

Figure 3-6. Conceptual drawings of perched water bodies.

H = total hydraulic head (cm)

z = vertical distance (cm)

ψ = matrix potential (cm).

The ± indicates that the coordinate, z, can be either up or down. This equation represents the mathematical model used to describe flow in this and other interbeds. In the case of unit gradient conditions, the moisture flux moving down through the soil column moves strictly in response to gravity. No capillary forces act to move the water. The matric potential, ψ, is the same at any vertical location within the profile, and the last term on the right of the equation becomes unity. Under this unit gradient condition, the Darcy flux is equivalent to the infiltration rate, which is also equivalent to the conductivity at that moisture content.

The moisture characteristic curve parameters describing the nonlinear relationship between ψ, θ, and K(ψ or θ) for both the B-C and C-D interbeds are given in Table 3-2. These parameters are for the commonly used van Genuchten (1980) curves. The parameters in the table result from curves fitted to water release data determined from core samples retrieved during drilling activities at the SDA (McElroy and Hubbell 1990; Magnuson and McElroy 1993).

Table 3-2. Fitted van Genuchten moisture characteristic curve parameters for the B-C and C-D interbeds.[a]

Interbed	Hydraulic conductivity (cm/s)	Saturated moisture content (cm^3/cm^3)	Residual moisture content (cm^3/cm^3)	Fitting parameters	
				Alpha (1/cm)	N
B-C	6.25×10^{-3}	0.48	0.04	0.03195	2.5338
C-D	1.53×10^{-4}	0.57	0.14	0.01775	1.3753

a. Source: Magnuson and McElroy (1993).

Using the assumption of unit gradient conditions, the Darcy flux was the 7 cm/yr net infiltration rate. Using this Darcy flux and an estimated corresponding moisture content of 0.082 from the assumed representative B-C interbed moisture characteristic curve from Magnuson and McElroy (1993), a water velocity of 0.9 m/yr across the B-C interbed was estimated. The average thickness of the B-C interbed is 4 m (Anderson and Lewis 1989), and this average was used for estimating travel times. The resulting travel time across the B-C interbed was 5 years given by

$$Water\ travel\ time = \frac{B\text{-}C\ interbed\ thickness}{water\ velocity} . \qquad (3\text{-}2)$$

The assumption of unit gradient conditions is consistent with measured gradients in the B-C interbed at Well D15, southeast of the SDA (McElroy 1990). If gradients are measured across the B-C interbed in the region of Pits 17 to 20, they may be higher than unity as a result of perched water above the interbeds. This will result in wetter conditions at the top of the interbed and drier conditions at the bottom where water can easily drain away into the basalt. In this case, unit gradient assumptions would not apply, and velocities estimated with unit gradient assumptions would be nonconservative when estimating water travel times through the B-C interbed. However, no credit was taken for the time necessary for water to travel through the perched water body within the basalt. This, to some unknown degree, balances the possibility of greater than unit-gradient conditions across the B-C interbed.

The lateral extents and thicknesses of perched water bodies and the exact mechanism that causes the perched water bodies are currently unknown, making defensible estimates of the water velocities not possible. Thus, the hydrological conceptual model neglects perched water bodies and aquitards causing them. In addition, perched water bodies are not considered because they are not thought to represent a shorter pathway around the B-C interbed.

3.2.3.6 Basalt Flow C. Although it is likely that perched water bodies above the B-C interbed and the B-C interbed itself will slow down transient pulses of water, rapid movement of water within Basalt C must be assumed. Theoretically, because of infiltration pulse damping by the B-C interbed,

there is a greater likelihood that the basalt matrix and smaller fractures will control water movement and result in appreciably slower downward water velocities within Basalt C than are observed in Basalts A and B. However, this slower movement has not been substantiated through field measurements. Therefore, water movement in Basalt C is assumed to be rapid with negligible travel times.

3.2.3.7 Perched Water Above the C-D Interbed. Similar logic was applied to the perched water zones above the B-C and C-D interbeds. The difference is that the C-D interbed is known to be continuous in every well drilled inside and in the vicinity of the SDA. Therefore, there is no shorter water travel path through a perched water body that is laterally limited because of a discontinuity of the C-D interbed. Rather, all water infiltrating to the aquifer must pass through the C-D interbed. Like the B-C interbed, the shapes and extent of the perched water bodies are not known for this region; therefore, the perched water bodies and time it takes water to pass through them are neglected.

3.2.3.8 Source of Additional Water Above the C-D Interbed. Three pieces of information are used together to conclude that recharge from the spreading areas likely contributes additional water above the C-D interbed.

First, Hubbell (1990a, 1992) indicated that the rate of recovery of perched water in Well 92 was correlated to discharges into the spreading areas. Second, McElroy (1990) presented unit gradient measurements in Well D15 across the B-C interbed southwest of the SDA and gradients of -4 to -5 m/m in Well TW1 in the C-D interbed in eastern portion of the SDA. The unit gradient conditions indicate a constant source of water passes through the interbeds, and the higher gradients indicate wetter conditions at the top of the interbed, which could be caused by an additional source of water. This additional water could come from the spreading areas, but it could also come from local focusing of the flow system caused by heterogeneity or fractures within the overlying basalt.

Third, the stable isotope data from Rightmire and Lewis (1987) indicated the water in Well 77-2, above the B-C interbed, had been influenced by evaporation and the water in Well 92, above the C-D interbed, had not. The

implication was that water in Well 77-2 was recharged locally within the SDA and underwent evaporation as it entered into the subsurface. Water in Well 92 was hypothesized to have entered the subsurface under saturated conditions during infiltration in the spreading areas.

A constant source of water does not exist from the spreading areas that moves horizontally to reach underneath the SDA. Rather, the source of water occurs when water is discharged to the spreading areas. This water could stair-step along preferential horizontal pathways within the basalt flows and in perched zones on top of the eastward-dipping B-C and C-D interbeds. However, the discontinuous nature of the B-C interbed makes it unlikely that this spreading area recharge would reach beneath the SDA on top of the B-C interbed. The next section discusses the impact of this additional water and how it was incorporated into estimating water travel times across the C-D interbed.

3.2.3.9 C-D Interbed. There currently is no basis for quantitatively estimating the amount of water from the spreading areas that may reach underneath the SDA. The effect of this likely additional water appears to persist and was conservatively included in the model by using the measured gradients across the C-D interbed at Well TW1 to estimate downward velocities and travel times for the whole C-D interbed. Whether this elevated gradient was due to recharge from the spreading areas or to locally-focused preferential flow cannot be determined from the existing data. The gradient ranged from -4 to -5 m/m during the 1985 to 1990 measurement period. A gradient of -4.5 m/m, an average measured in situ moisture content of 0.38, and the average of estimated unsaturated hydraulic conductivities at that moisture content of 0.07 m/yr (Magnuson and McElroy 1993) were used to predict a water velocity of 0.8 m/yr across the C-D interbed. Using the average C-D interbed thickness of 5 m (Anderson and Lewis 1989), the resulting travel time across the C-D interbed was 6 years.

Assuming the higher gradient applies everywhere across the C-D interbed beneath the LLW pits is conservative when estimating water travel times across the C-D interbed. There are some locations where perched water is not present that would have slower velocities and longer travel times. Additionally, perched water is not continuously available from the spreading areas because

water is not always being discharged to them. However, emphasis was placed on available data rather than hypothesis, so the higher gradient was used in this radiological performance assessment.

The effect of likely additional water from the spreading areas was included by using the higher measured gradients and increasing the velocity of water across the C-D interbed. Dilution resulting from either additional water from the spreading areas or from horizontal movement of shallow perched water back up in the surficial sediments is reasonably neglected.

The decision to neglect this dilution can be understood by considering the amount of water movement within a 1 × 1-m column extending from the land surface down into the regional aquifer. With an infiltration rate of 0.07 m/yr, 0.07 m^3/yr of water would enter the aquifer. Within the aquifer, water would flow horizontally through the column because of regional flow. Using the estimated average linear velocity of 560 m/yr, a effective porosity of 0.10 (these values are explained in Section 3.2.3.12), and a conservatively small effective aquifer thickness of 12 m, 672 m^3/yr of water would flow horizontally through this column. This amount of water is approximately four orders of magnitude greater than the amount of water entering from the unsaturated zone on a per unit area basis, justifying the approach of neglecting dilution within the unsaturated zone because only radionuclide concentrations within the aquifer are considered for determining compliance in this radiological performance assessment for the groundwater pathway.

3.2.3.10 Basalt Flows D, E, and F. As with Basalt C, the continuous C-D interbed above Basalts D, E, and F will further dampen pulses of water from either the spreading areas or seasonal infiltration. Theoretically, because of this increased damping, there is even greater likelihood that the basalt matrix and smaller fractures control water movement and result in appreciably slower downward water velocities within the basalts beneath the C-D interbed. However, there is no observed behavior of water in this region to substantiate this assumption. As a result, the only defensible description of water movement in the deeper unsaturated zone basalts is rapid with negligible travel times.

3.2.3.11 Interbeds D-E and E-F. These two interbeds are assumed to be present based on observations in wells drilled outside the SDA. This assumption is nonconservative, and its effect is considered in the uncertainty and sensitivity analysis (Section 4.2.2). No samples have been hydrologically characterized from the two deeper interbeds beneath or outside the SDA. As a result, the two deeper interbeds are estimated to be hydrologically similar to the C-D interbed, and the representative moisture characteristic curve for the C-D interbed from Magnuson and McElroy (1993) was used for the D-E and E-F interbeds. As stated in the previous section, the C-D interbed will dampen pulses from either seasonal infiltration or spreading area recharge and result in a relatively constant infiltration rate through the D-E and E-F interbeds. This flux is assigned the same 7 cm/yr value estimated in Magnuson and McElroy (1993) for the infiltration through the C-D interbed.

Under the constant infiltration assumption, unit gradient conditions were appropriately assumed. The 7 cm/yr infiltration rate and moisture characteristic curves from the C-D interbed were used to estimate the corresponding moisture contents of 0.40 for calculating the water velocity. Again, using average reported thickness of approximately 2 m from Anderson and Lewis (1989), the resulting velocity was 0.2 m/yr and the travel times were 10 and 9 years for the D-E and E-F interbeds, respectively.

3.2.3.12 Regional Aquifer. The conceptual model for flow within the fractured basalts of the Snake River Plain Aquifer in the vicinity of the RWMC was that water movement occurs uniformly with a horizontal velocity of 560 m/yr to the south-southwest (Wood 1989). The effective porosity of 0.1 was assigned based on previous modeling studies (Robertson 1974; Rood et al. 1989), and an effective aquifer thickness of 76 m was assigned (Robertson 1974). Actual hydraulic effective thickness was estimated to be from 75 to 330 m (Arnett et al. 1990) For consistency with previous modeling studies and lack of additional data, 76 m was used as the aquifer thickness.

Water movement within the aquifer is affected by local-scale heterogeneities just as it was in the unsaturated zone. However, the effects of this heterogeneity are not known well enough to incorporate into the conceptual model. As water moves further away from the SDA, this local

heterogeneity has even less effect, and the assumption of uniform flow is even more appropriate.

The conceptual model does not consider the effects of varying flow directions. This is the conservative approach. Variations in flow result in increased dilution of radionuclides within the aquifer. This dilution is caused both by adding the recharge water and by increasing dispersion that would result from longer pathways toward any potential downgradient receptors.

3.2.4 Summary of Water Velocity and Travel Times Across Interbeds

This section summarizes the parametric information that was used to estimate velocities and travel times across each interbed. Darcy's Law was used to calculate velocities and is given by

$$v = \frac{q}{\theta_v} = \frac{K(\theta_v)}{\theta_v} \frac{\partial H}{\partial z} \quad . \tag{3-3}$$

Table 3-3 summarizes parameters and calculated results for each interbed. For interbed C-D, the $K(\theta_v)$ entry is the unsaturated hydraulic conductivity at that moisture content and is not equivalent to the Darcy flux through the interbed because of the higher gradients across the interbed. As stated previously in Section 3.2.2, no attempt is made to hydrologically mass-balance water movement within the unsaturated zone.

3.2.5 Numerical Implementation of the Hydrologic Conceptual Model

A key parameter from Table 3-3 is the water travel time. This value represents the estimated time required for water released from the base of the near-field or waste region to reach the regional water table. This water movement was assumed to occur through the entire sedimentary interbed sequence. Each interbed sequence was assumed to have the same transport characteristics (see Section 3.3.2). Therefore, the individual interbeds can be modeled as one equivalent interbed that yields the same total travel time given the same infiltration rate.

Table 3-3. Interbed hydrologic parameters, estimated velocities, and travel times.

Interbed	Thickness[a] (m)	$K(\theta_v)$ (m/yr)	θ_v (cm^3/cm^3)	$\frac{\partial H}{\partial z}$ (m/m)	Velocity (m/yr)	Travel time (yr)
B-C	4.0	0.07[b]	0.082[c]	1[d]	0.86	5
C-D	5.2	0.07[e]	0.38[f]	4.5[g]	0.83	6
D-E	1.8	0.07[b]	0.40[c]	1[d]	0.18	10
E-F	1.5	0.07[b]	0.40[c]	1[d]	0.18	9
Total	12.5	---	---	---	---	30

a. Average thicknesses from Anderson and Lewis (1989).

b. Assigned intermediate infiltration from 4 to 10 cm range.

c. Based on unit-gradient assumption, assigned infiltration rate, and estimated representative moisture characteristic curves from Magnuson and McElroy (1993).

d. Assumed, based on measured gradients southeast of the SDA (McElroy 1990).

e. Intermediate value of estimated unsaturated conductivities at in situ moisture content from representative moisture characteristic curves from Magnuson and McElroy (1993).

f. Estimated representative value from Magnuson and McElroy (1993).

g. Measured value in well TW1 from McElroy (1990).

The resulting model consists of uniform flow down through one interbed with uniform properties for the unsaturated zone and horizontal flow in the regional aquifer. This model matches the conceptual model implemented in the GWSCREEN code (Rood 1993a). Therefore, the GWSCREEN code was used to perform flow and transport calculations for the radiological performance assessment. GWSCREEN did not simulate the movement of water. Rather, water velocities are assigned in the unsaturated and aquifer portions of the model, and transport is calculated using semi-analytical equations.

The net infiltration rate and the thickness and moisture content under unit gradient conditions for both the waste and equivalent sedimentary interbed are required to use the GWSCREEN code. The net infiltration rate, discussed previously, was assigned a value of 7 cm/yr. Using a combined interbed thickness of 12.5 m, the moisture content that resulted in a net 30-year water travel time was 0.168 cm^3/cm^3. This was used as an assigned input parameter in GWSCREEN simulations. Moisture content only affects advective transport. Using a moisture content that does not match any of the field-measured moisture contents does not affect contaminant retardation as shown in the full expansion of the equation for contaminant travel time through the unsaturated zone:

$$
\begin{aligned}
T_a &= \frac{X}{V} R_d \\
&= \frac{X \theta_v}{q} \left(\frac{1 + K_d \rho}{\theta_v} \right) \\
&= \frac{X \theta_v}{q} + \frac{X K_d \rho}{q}
\end{aligned}
\qquad (3\text{-}4)
$$

where

T_a = contaminant travel time (yr)

X = interbed sediment thickness (m)

V = average linear velocity (m/yr)

R_d = contaminant retardation factor

θ_v = volumetric moisture content (cm^3/cm^3)

q = Darcy flux or infiltration rate (m/yr)

K_d = contaminant distribution coefficient (cm^3/g)

ρ = interbed density (g/cm^3).

3.3 Hydrologic Transport Conceptual Model

The conceptual model for release from the source and transport in the unsaturated zone and aquifer is illustrated in Figure 3-7. Radionuclides are transported from the source zone as dissolved substances in pore water. Because the transport time in the basalt is not considered in the hydrologic conceptual model, the unsaturated zone is comprised of interbeds only. The pore water moves through the unsaturated zone and radionuclides in solution are allowed to sorb and desorb on sediments. After radionuclides in solution travel the length of the unsaturated zone, they are transported immediately to the aquifer where sorption and desorption reactions also occur. Radionuclides in the aquifer are mixed vertically in the mixing thickness denoted as aquifer well screen in Figure 3-7. Therefore, the concentration is uniform in the aquifer from the surface to the depth of the mixing thickness. Concentrations of radionuclides in the aqueous phase at the receptor well are assumed to be the same concentrations in the water extracted from the well by the hypothetical receptor. These concentrations are then evaluated for radiological dose impacts.

The GWSCREEN user's manual (Rood 1993a) describes the conceptual and mathematical model for hydrologic transport in the unsaturated zone and aquifer, and this section describes key assumptions and mathematical models used in the code. Release and transport of radionuclides from the RWMC disposal pits and soil vaults were modeled outside the GWSCREEN code, and a detailed description of the methodology is presented in Section 3.3.1. Section 3.3.2 discusses transport in the unsaturated zone, and transport in the aquifer is addressed in Section 3.3.3. Groundwater transport parameters are

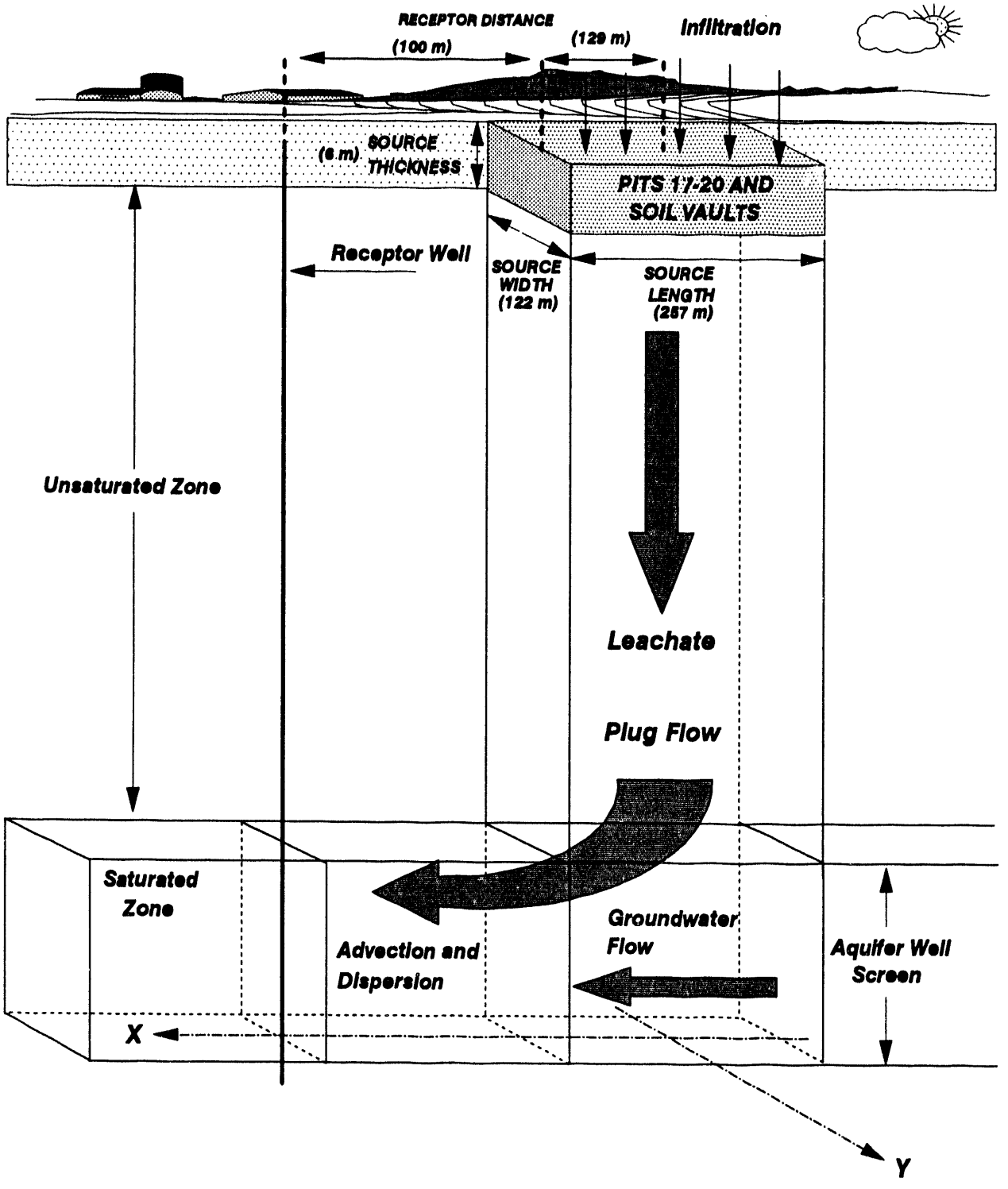

Figure 3-7. Conceptual model of the RWMC, Pits 17 to 20 for transport in the source and unsaturated (vadose) and saturated zones.

described in Section 3.3.4, and the groundwater screening methodology used for the analyses is detailed in Section 3.3.5.

3.3.1 Conceptual Model for Release from the Source Term

The RWMC is roughly triangular in shape (Figures 2-23 and 2-24), elongated in the east west direction. The facility is divided into the SDA and the TSA. The SDA comprises about 2/3 of the facility. Past disposal occurred in the western part of the SDA, and more recent and current disposal pits are located in the southeastern part of the SDA. The active disposal pits are Pits 17, 18, 19, and 20 (Figure 2-24). Combined dimensions of Pits 17, 18, 19, and 20 are estimated to 257 × 122 m with an average thickness of 6 m (Figure 3-7). Soil vaults have been interspersed throughout the SDA. For conservatism and model simplicity, all soil vault inventory was assumed to be placed in the active disposal pits. In addition, all inventory reported to be disposed of in pits from 1984 through 1993 and forecast from 1994 to 2020 was assumed to be disposed of in this composite active pit. This assumption is conservative because it does not account for the areal extent of disposal in the SDA and concentrates the waste in a smaller volume. The "composite" pit was assumed to have the combined dimensions of Pits 17, 18, 19, and 20. All waste was assumed to be homogeneously mixed in the active pit volume (257 × 122 × 6.1 m). Release from the source volume was modeled as a series of first order compartments with variable, time dependent input rates (Figure 3-8). The model begins in 1984--at the time Pit 17 is opened (1984).

Two waste forms were considered: (1) activated metals and (2) surface contaminated material. Activated metals were stainless and carbon steel core structural components and beryllium reflector blocks that were known to contain neutron activation products in the metal (not a surficial contamination of metal components). Release from these materials resulted from corrosion of these materials along with diffusion of tritium from beryllium reflector blocks.

Two types of waste containment vessels were considered: (1) waste contained in steel drums or metal boxes and (2) waste contained in wooden boxes, bales, and cardboard boxes.

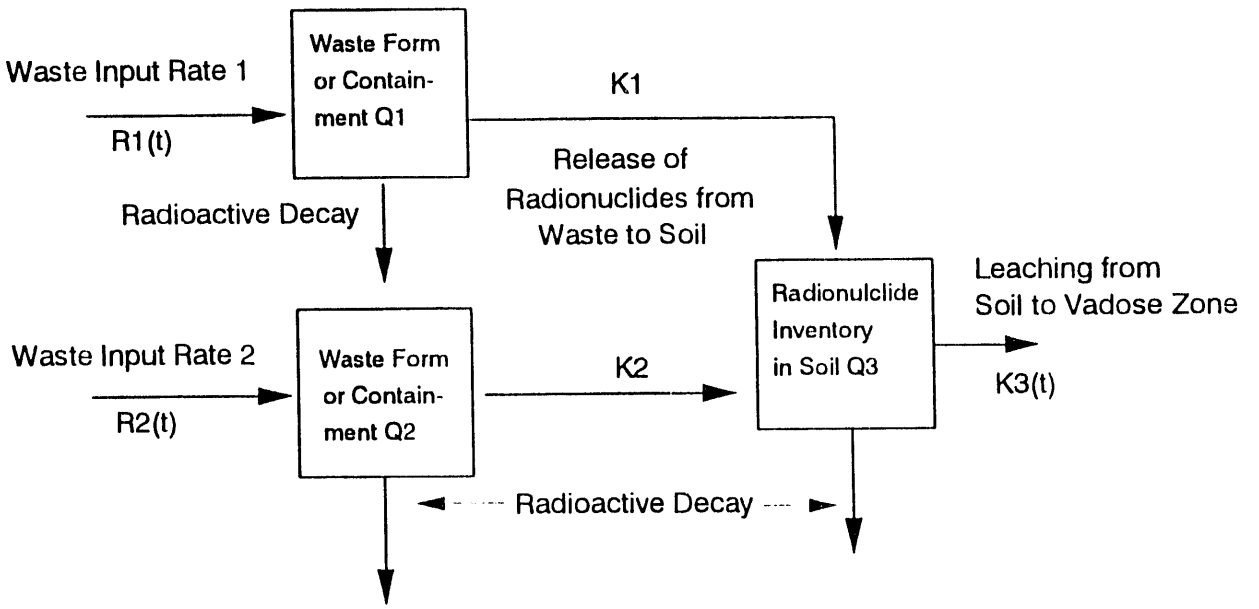

Figure 3-8. Conceptual model of the source release model for the RWMC performance assessment.

Radionuclides in each waste form and each waste containment vessel were released over time to the backfilled soil in the pits. Infiltrating water leached radionuclides from the backfilled soil and transported it to the unsaturated zone. Three infiltration rates were considered: 4, 7, and 10 cm/yr. The 4 and 10 cm/yr cases were run as sensitivity cases, and the 7 cm/yr case was run as the base case. For all three cases, an engineered cover was installed at 2020 and assumed to be maintained for 100 years. The cover reduced the infiltration to 1 cm/yr (see discussion in Section 3.2.3.2). The mass balance equations for activity in the three compartments is given by

$$\frac{dQ_1}{dt} = R_1(t) - (K_1 + \lambda) Q_1$$

$$\frac{dQ_2}{dt} = R_2(t) - (K_2 + \lambda) Q_2 \qquad (3\text{-}5)$$

$$\frac{dQ_3}{dt} = K_1 Q_1 + K_2 Q_2 - [K_3(t) + \lambda] Q_3$$

where

Q_1 = radionuclide inventory in the waste form or containment 1 (Ci)

t = time (yr)

$R_1(t)$ = waste input rate for waste form or containment 1 (Ci/yr)

K_1 = waste to soil rate constant for containment or waste form 1 (per yr)

λ = radioactive decay rate constant (per yr)

Q_2 = radionuclide inventory in the waste form or containment 2 (Ci)

$R_2(t)$ = waste input rate for waste form or containment 2 (Ci/yr).

K_2 = waste to soil rate constant for containment or waste form 2 (per yr)

Q_3 = radionuclide inventory in the soil backfill in the pits and trenches (Ci)

$K_3(t)$ = soil backfill to unsaturated zone (soil leaching) rate constant (per yr).

The rate constant, $K_3(t)$, may be given as a function of time based on variations in the infiltration rate over time. Variations in the infiltration rate result from the presence or absence of a cover or a hypothetical flooding event. The rate constant $K_3(t)$ is given by

$$K_3(t) = \frac{I(t)}{T\theta(t)\left[1 + \frac{K_d \rho}{\theta(t)}\right]} \qquad (3\text{-}6)$$

where

$I(t)$ = net infiltration rate as a function of time (m/yr)

T = backfill soil thickness (m)

$\theta(t)$ = volumetric water content as a function of time (m^3/m^3). For the three infiltration rates considered:

θ = 0.281 for I = 1 cm/yr
θ = 0.329 for I = 7 cm/yr
θ = 0.340 for I = 10 cm/yr

K_d = radionuclide specific sorption coefficient (mL/g)

ρ = density (g/cm^3).

The flux of the contaminant (J_s) from the source to the unsaturated zone is given by

$$J_s(t) = K_3 Q_3(t) \quad . \tag{3-7}$$

Equation (3-5) is solved numerically using a Runga-Kutta solving routine adapted from Press et al. (1992). Radionuclide fluxes at the source-unsaturated zone interface are output as a function of time, and these data are used as input in the GWSCREEN simulation. Note that infiltration rate (I) is a function of time in the governing equations. The infiltration rate was adjusted during the period of institutional control to account for the presence of an engineered cover. The infiltration rate was reduced to 1 cm/yr (Figure 3-9) during the period of institutional control where the cover was maintained. After institutional control, the cover degrades after 5 years and the infiltration returns to its precover rate of 7 cm/yr. Figure 3-9 also includes the infiltration rates for the sensitivity cases that were performed for 4 and 10 cm/yr infiltration. See Section 3.2 for background on the infiltration rates.

Activity input rates as a function of time for C-14, Sr-90, and H-3 are illustrated in Figures 3-10 through 3-12. For most nuclides evaluated, the waste form or containment was usually a single type of material or form. For example, all of the Ni-59 inventory was in the form of activated metal core components. Some of the actinides (plutonium) had significant inventories in metal drums and wooden boxes. Waste containment has little effect on nuclides like these that have long half-lives (>24,000 years) and high sorption coefficients (2,000 mL/g). A discussion of release rates for the two waste forms and waste containment vessels follows. Table 3-4 summarizes the waste to soil rate constants (K_1 and K_2) used in the analysis.

3.3.1.1 Corrosion Leaching--Activated Metals Components. In the corrosion leach model, not to be confused with corrosion of a containment vessel, the radionuclides are assumed to be present in the lattice structure of a metallic waste and are released only when corrosion (degradation) of the metallic waste occurs. Diffusion of radionuclides from the metallic component was not considered. Significant quantities of C-14 and Ni-59 in the RWMC waste inventory are reported to be in core structural components. Carbon-14 is formed primarily from an n-p reaction with nitrogen impurities in the steel [N-14(n,p)C-14]. Nickel-59 is produced from an n-γ reaction [Ni-58(n,γ)Ni-59]

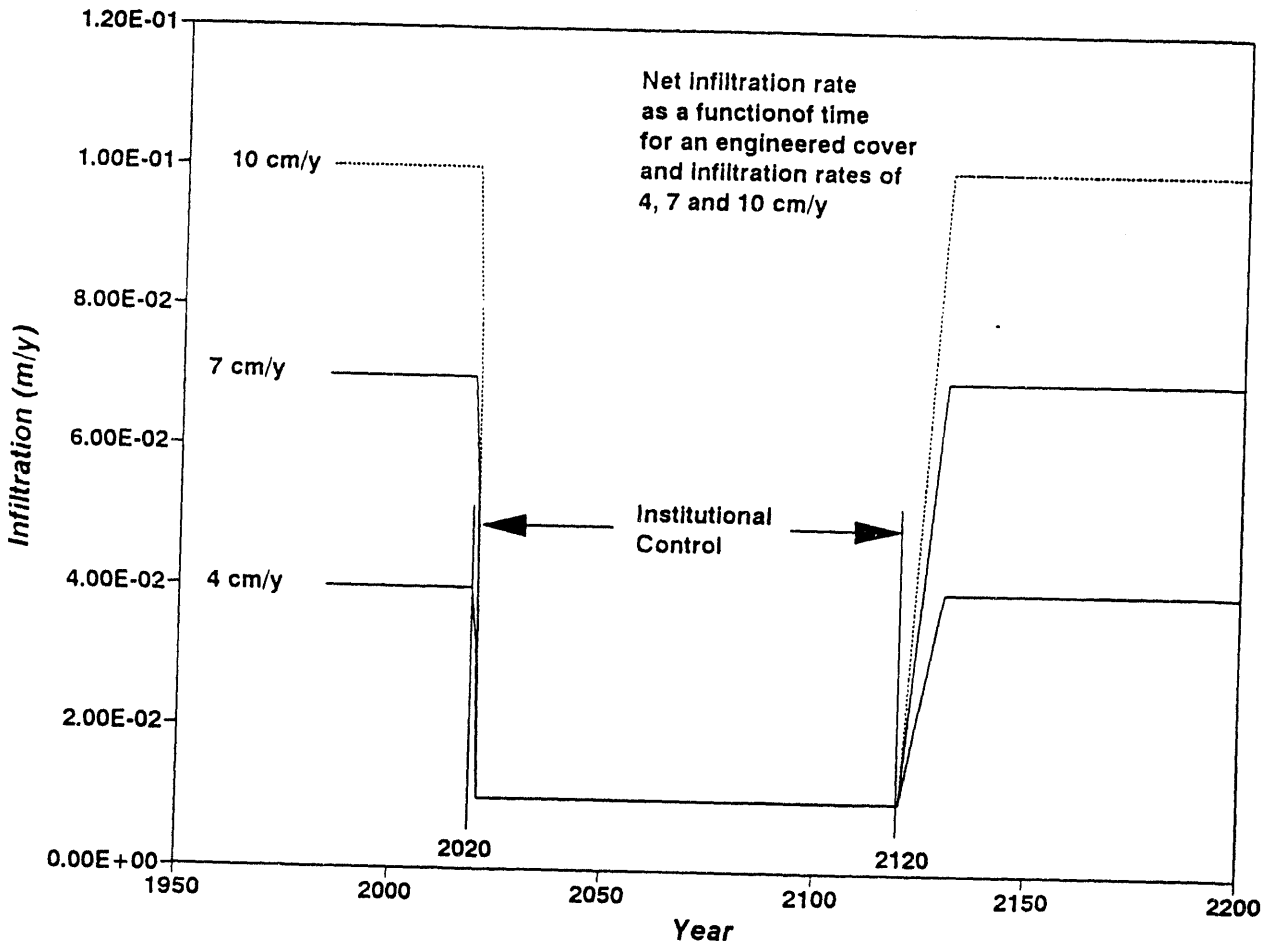

Figure 3-9. Infiltration rates as a function of time for the base case and two sensitivity cases (4 and 10 cm/yr).

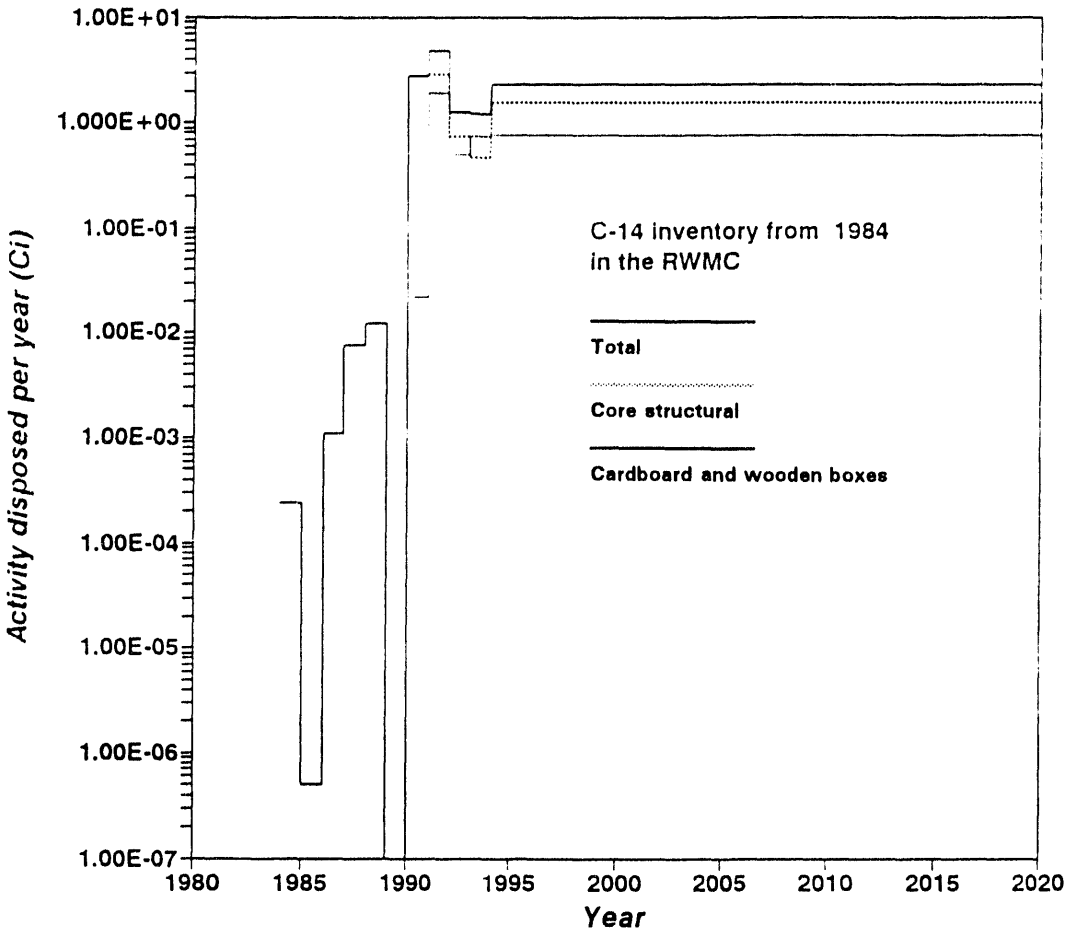

Figure 3-10. Carbon-14 inventory disposed of in the RWMC.

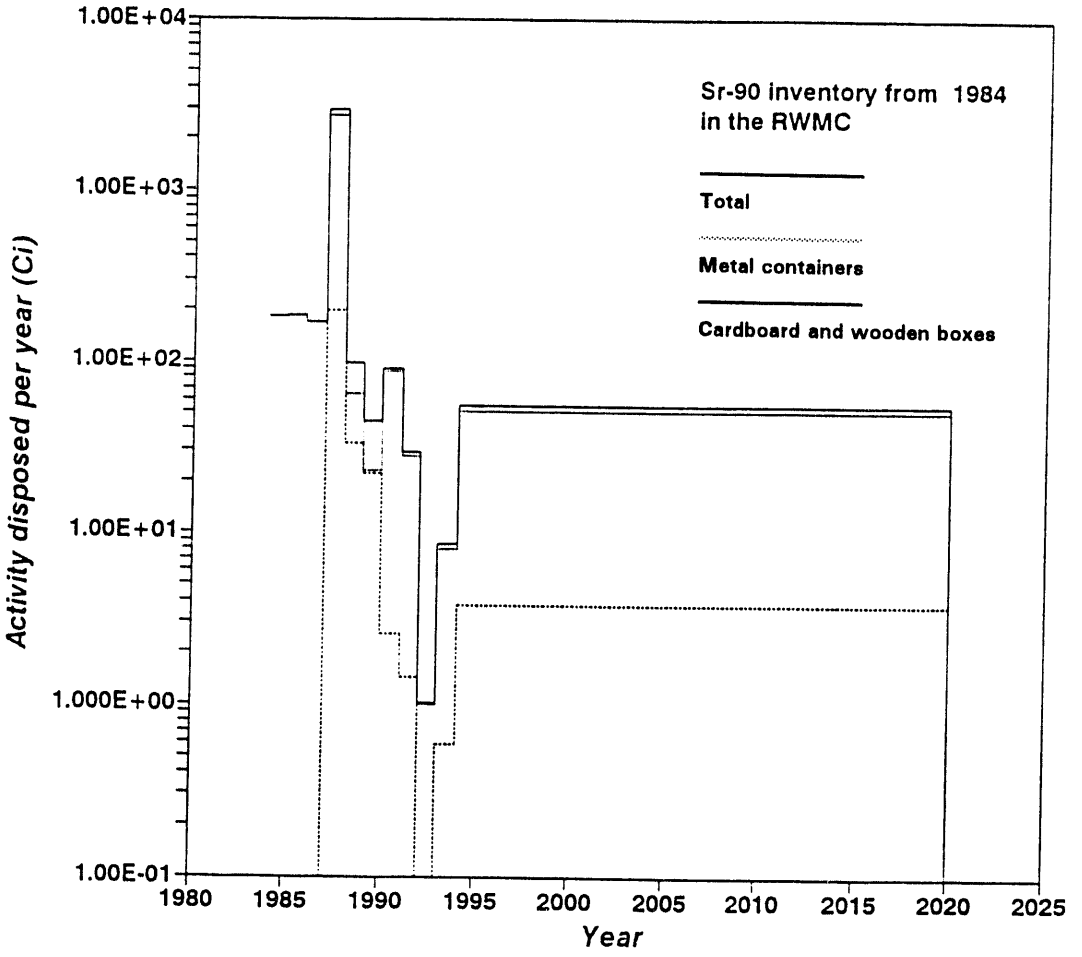

Figure 3-11. Strontium-90 inventory disposed of in the RWMC.

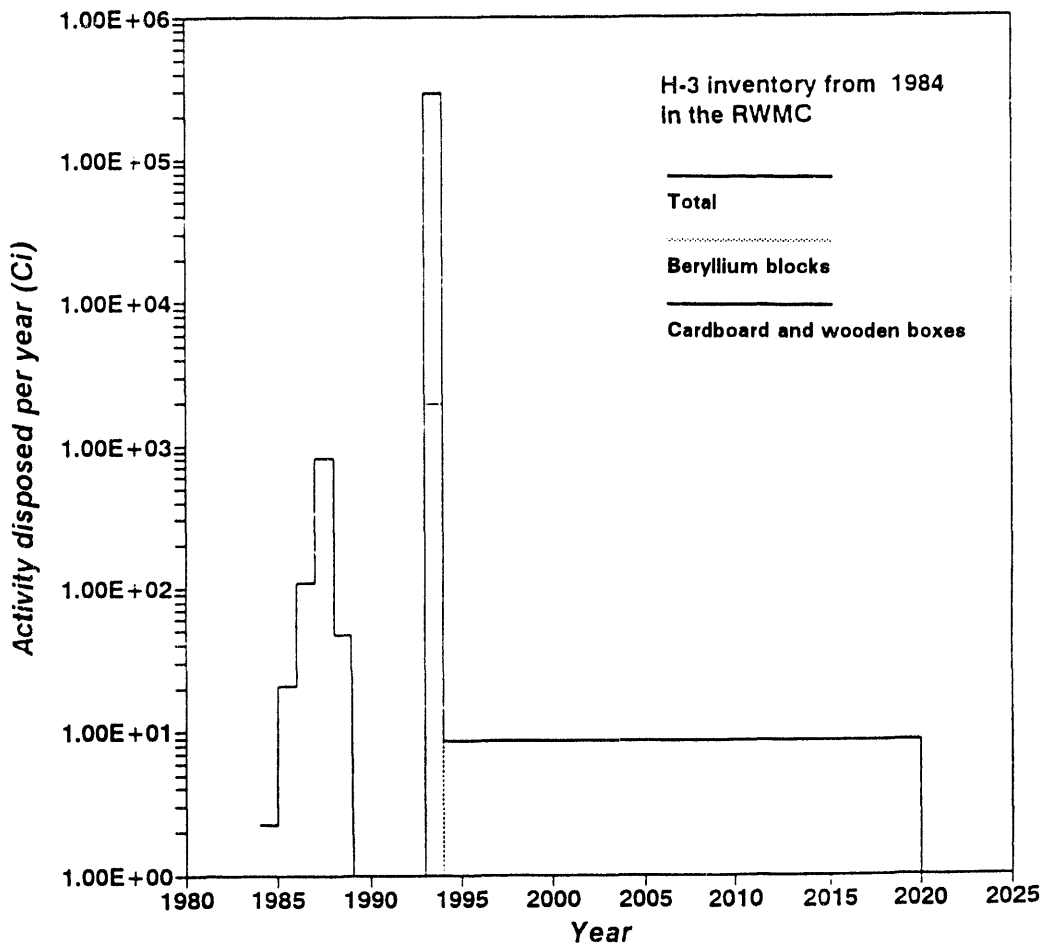

Figure 3-12. Tritium inventory disposed of in the RWMC.

Table 3-4. Waste to soil rate constants (K_1 and K_2) used in the RWMC source model.

Release process	Rate constant value (per yr)	Applicable nuclides/inventory
Release from metal containers to soil	0.1	All inventory stored in metal containers
Release from cardboard boxes to soil	0.5	All inventory in cardboard or wooden boxes or bales
Release from activated metals	4.17×10^{-4}	All activated metal inventory (C-14 and Ni-63)
Release from activated beryllium reflector blocks	9.27×10^{-4}	Tritium in beryllium reflector blocks

with Ni-58. Corrosion times for various core components are dependent on the material type (i.e., carbon steel or stainless steel); water chemistry; and geometry of the component. The RWMIS data base does not differentiate specific metallic material types or geometries; therefore, a generic corrosion time was applied to all radionuclide inventories reported to be in core structural materials. The corrosion rate was based on the corrosion times for various reactor core components as reported in the IMPACTS methodology (Oztunali and Roles 1986). Generally, there are two types of corrosion: uniform and pitting. Uniform corrosion means the surface of the material is uniformly penetrated a certain distance and is usually reported in mils per year (1 mil = 0.001 in.). This form of corrosion is most common in carbon steel. Pitting corrosion means that certain spots on the surface of the material corrode and is usually expressed in weight loss per unit time. Some stainless steels are only affected by pitting corrosion. In the IMPACTS methodology, pitting corrosion is expressed as a uniform corrosion rate because uniform corrosion rates are easier to incorporate into a calculational methodology.

The IMPACTS methodology conservatively assumes that all exposed surfaces of the activated metal waste stream corrode at a constant corrosion rate. Two corrosion rates in IMPACTS were considered: 4 mils per year (1.02×10^{-4} m/yr) for carbon steel and 0.3 mil per year (7.62×10^{-6} m/yr) for stainless steel. The other factor affecting the release rate is the

geometry of the waste stream. A waste stream with a large surface area will corrode faster than a low surface area waste stream. Corrosion of waste streams that have specific geometries (such as rods, plates, or pipes) are characterized by the corrosion time. IMPACTS assumes a geometry for the various reactor core component waste streams. The corrosion time is defined as the inverse of the fraction of material that corrodes per year as given by

$$C_{time} = \frac{1}{\frac{M_1}{M_o}} \qquad (3\text{-}8)$$

where

C_{time} = corrosion time

M_1 = mass of material corroded in one year

M_o = initial mass of material at beginning of year.

The corrosion time is analogous to the mean lifetime of a radionuclide; therefore, the rate constant that describes releases because of corrosion is $1/C_{time}$. For this analysis, the corrosion times for activated core shroud materials and activated reactor internals for boiling water reactors (BWRs) and pressurized water reactors (PWRs) were averaged so that an average corrosion time could be applied to all activated core structural components. The corrosion times reported in IMPACTS (in years) were as follows, which resulted in an average corrosion time for shroud and reactor internals of 2,400 years.

	BWRs	PWRs	Average
Activated core shroud	3,350	1,840	2,595
Activated reactor internals	2,190	2,190	2,190
			≅ 2,400

The corrosion rate constant for activated metals is then 1/2,400 years or 4.17×10^{-4}/yr. This value was used for the K_2 rate constant to describe release from activated metals to the soil.

3.3.1.2 Release from Beryllium Reflector Blocks. The Advanced Test Reactor (ATR) at the INEL uses beryllium reflector blocks to control the neutron flux in the reactor core. These reflector blocks periodically need to be replaced because of swelling that makes the blocks inoperable. Tritium is formed in the blocks by the reactions

$$^{9}_{4}Be + {}^{1}_{0}n \rightarrow {}^{4}_{2}\alpha + {}^{6}_{2}He$$
$$^{6}_{2}He \rightarrow {}^{6}_{3}Li + \beta$$
$$^{6}_{3}Li + {}^{1}_{0}n \rightarrow {}^{4}_{2}\alpha + {}^{3}_{1}H \quad .$$

Other activation products found in smaller quantities in the blocks include Co-60 and Ni-63, but by far, the largest inventory is tritium. As of April 1991, inventories of H-3, Co-60, and Ni-63 were 55,000, 141, and 510 Ci/block, respectively.[a] The H-3 inventory decayed to the 1993 disposal time was 48,830 Ci. The estimated tritium inventory is believed to be accurate within a factor of 2.[b] Release of activation products, Co-60, and Ni-63 were not considered because these nuclides were eliminated from consideration during the screening process as described in Section 3.3.5.

Two release processes were considered: (1) corrosion of the beryllium and subsequent release of tritium from the corrosion product and (2) diffusion of tritium out of the block. Release of tritium because of corrosion is discussed in Section 3.3.1.3, and diffusion of tritium out of the blocks is discussed in Section 3.3.1.4. Corrosion release was determined to be the dominant release mechanism, and diffusion was neglected because the estimated diffusive release was small, about 1×10^{-16} Ci compared to a cumulative corrosion release of approximately 500 Ci. Corrosion release was influenced by the presence of chloride ions in the pore water. Chloride ions are known to increase the corrosion rate of beryllium (Miller and Boyd 1967), and measurements taken in the vicinity of the soil vaults where the disposal took place show chloride concentrations as high as one-third of that for seawater

---

a. Personal communication T. A. Tomberlin, EG&G Idaho, Inc., with R. N. Beatty, EG&G Idaho, April 19, 1991.

b. Personal communication T. A. Tomberlin, EG&G Idaho, Inc., with D. E. Sheldon, EG&G Idaho, Inc., December 22, 1986.

(20,000 mg/L). Diffusive releases were limited by an oxide layer that is likely to be present for the entire evaluation period. The release rate constant for corrosion release was 9.27×10^{-4} per year for the base case of 7 cm/yr infiltration and a chloride concentration of 2,653 mg/L. All tritium released from the blocks was assumed to partition into the soil pore water and migrate toward the aquifer (Section 3.3.1.2.4).

3.3.1.2.1 Description of Beryllium Blocks and Disposal--The beryllium blocks considered in this performance assessment were disposed of in July 1993. The blocks were removed from the ATR reactor core in 1986 and had been stored in the ATR canal from 1986 to July 1993. Three shipments of two blocks each were made to the RWMC. The maximum tritium inventory in a single reflector block, corrected for decay (to 1993), was estimated to be 48,830 Ci per block for a total of 293,000 Ci for the entire shipment. The blocks are 122 cm long (Figure 3-13), have a surface area of 4.85×10^4 cm^2, a volume of 4.52×10^4 cm^3 and a roughly triangular cross section approximately 45 cm across. Holes drilled parallel to the long side of the block are used to hold the outer shim control cylinders (OSCCs) in place. The OSCCs also contain significant quantities of tritium, but they were not included in the 1993 shipment to the RWMC. The activity concentration as of 1991 was estimated to be about 3 Ci/cm^3, and it decreased by a factor of 2 for every 2.54 cm away from the fuel-beryllium interface. The average concentration in the blocks was estimated to be 1.14 Ci/cm^3 as of 1991 and 1.08 Ci/cm^3 as of 1993.

The blocks were shipped to the RWMC in Waste Calcining Facility filter cask inserts. The casks were rectangular, measuring 122 x 73.6 x 85 cm. The top of the cask was open except for a lifting I beam welded to the top where a cable was attached. The bottom consisted of a perforated metal plate welded to the base. Three inserts were disposed of in a soil vault, and each insert contained two blocks. The soil vault was 6.5 m deep. Soil was backfilled in the base of the vault to a depth of 0.6 m, making the base of the vault even with the surface sediment and basalt contact. The three inserts were then placed one on top of another in the vault with about 0.3 m of soil separating each insert. To protect the transport container, a plastic sheet was placed on top of each insert before backfilling began. However, this sheet probably did not prevent soil from entering the insert through the top and filling in

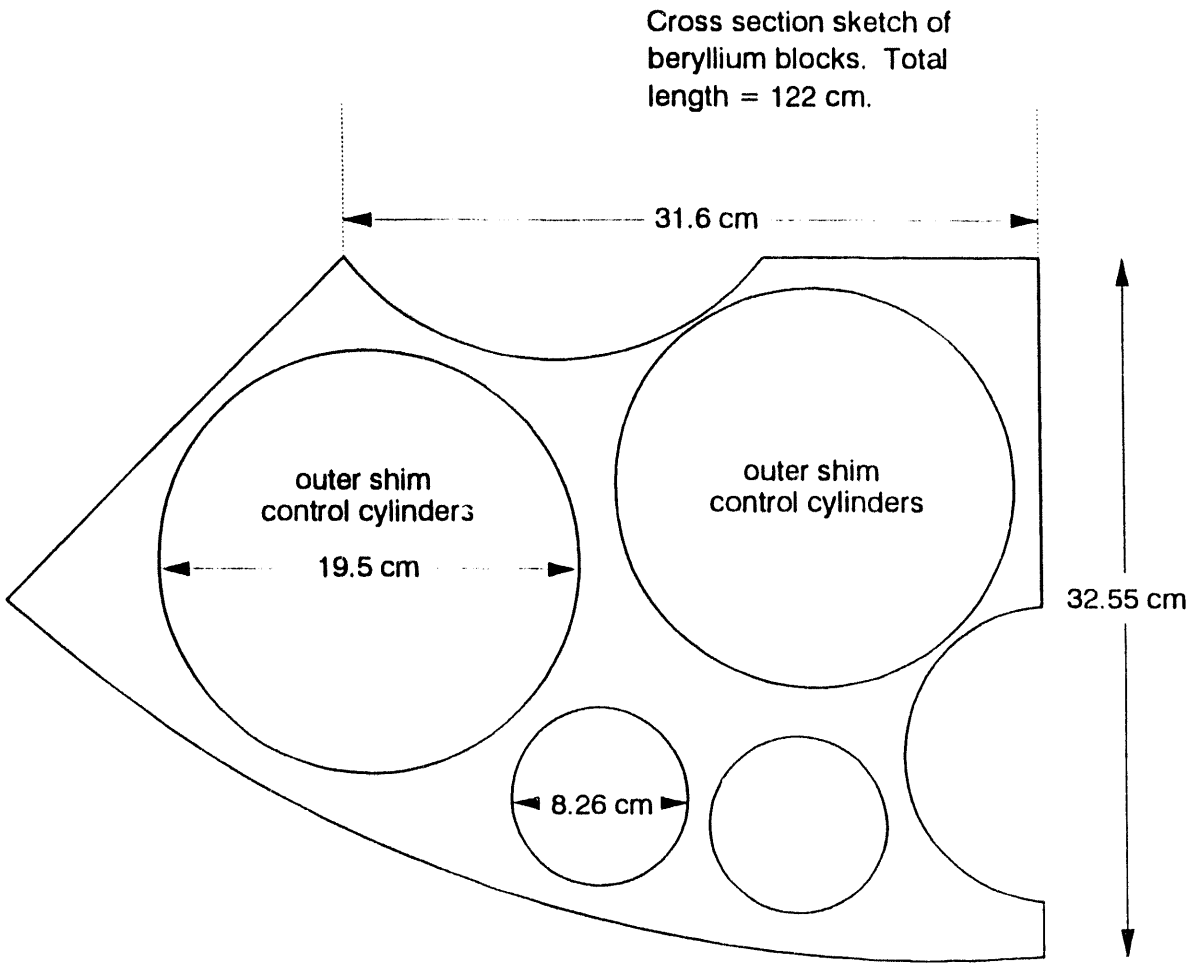

Figure 3-13. Cross section of ATR reflector beryllium blocks.

at least some of the open space surrounding the blocks. One and one-half meters of soil was placed over the top of the last insert.

3.3.1.2.2 Corrosion Release from Beryllium Reflector Blocks. For the purposes of modeling release of tritium from the beryllium blocks, the following assumptions were made concerning the physical representation of the blocks and the activity distribution in the blocks:

1. The blocks represent a flat plate with a surface area of 4.85×10^4 cm^2 and a volume of 4.52×10^4 cm^3

2. The initial activity is distributed uniformly throughout the block at a concentration of 1.08 Ci/cm^3

3. Corrosion may occur over the entire surface area of the block

4. All tritium in the corrosion product is released.

It is apparent from assumption 1 that the effective thickness of the block is less than 1 cm. The large surface area is due to holes drilled in the block to hold the OSCCs, which results in a complex block geometry. Most of the tritium activity in the block is near the fuel-beryllium interface and, therefore, is not distributed evenly across the surface area. Corrosion of portions of the block not close to the fuel beryllium interface results in little release of tritium, while corrosion of the fuel-beryllium interface surface results in larger releases. For simplicity, it was assumed the tritium was distributed evenly throughout the block, present on the entire surface area, and corrosion occurred on all exposed surface areas. Following corrosion, all tritium in the corrosion product was assumed to be released. The corrosion product, beryllium hydroxychloride, is highly insoluble, and it is likely that the tritium may be trapped in the corrosion product.

The corrosion model for beryllium considered two scenarios: wet and dry corrosion. The scenarios were driven primarily by the presence of chloride ions in the pore water. The wet corrosion scenario evaluated the corrosion of beryllium submerged in stagnant pore water that was assumed to be perched in

the soil layer above the soil-basalt interface. The dry corrosion scenario considered the corrosion that occurred while infiltrating water moved through the partially saturated soil containing the blocks. The corrosive behavior of beryllium submerged in aqueous solutions of varying concentrations of salt were investigated in Miller and Boyd (1967). In general, beryllium has a high resistance to corrosion at low temperature and in high purity water with pH values at or slightly below neutral. This observation is verified by experience of beryllium block storage in the ATR canal where the blocks, stored at low temperature and in high purity water, show no detectable corrosion. Beryllium, however, is much less attractive for use in water containing ionic impurities, particularly chloride and sulfate ions.

Miller and Boyd performed experiments where samples of beryllium were immersed in several salt solutions ranging from natural seawater to 3.5% NaCl. In one experiment, pickled beryllium sheets were immersed in natural seawater at 16°C for 60 days, resulting in pitting of 20% of the surface area, maximum pitting depth of 7.62×10^{-3} cm and an overall corrosion rate of 0.165 cm/yr for 30 days. The corrosion rate diminished over time, presumably because of "poisoning" of the reaction by the presence of the corrosion product. The corrosion product is a beryllium hydroxychloride, with the approximate chemical formula of $[Be(H_2O)_4]Cl_2$, and is highly insoluble. Typically, seawater contains about 20,000 mg/L of chloride (Brownlow 1979). Corrosion of beryllium in the presence of sulfate ions was not reported. Measurements of chloride concentration in water collected in lysimeters located in the SDA in 1987 ranged from 5 to 12,500 mg/L, with a geometric mean of 137 mg/L and an arithmetic mean of 1,762 mg/L (Laney et al. 1988) (Figure 3-14). Measurements of chloride concentrations from 1987 to 1989 in Wells W05 and W06 located on either side of the soil vault containing the beryllium blocks ranged from 13 to 11,500 mg/L with an arithmetic mean of 2,653 mg/L (Figure 3-15). Oral communication with the manufacturers of the beryllium used at ATR have indicated the corrosion rate of beryllium in aqueous chloride solutions is roughly proportional to the chloride concentration of the solution.[a] For this analysis, it was assumed that the proportionality was linear. In wet corrosion, it was assumed some fraction of the block inventory was completely

---

a. Oral communication, Terry Thomas, Brush Wellman Inc. Cleveland, Ohio, with Peter Nagata, EG&G Idaho, Inc., December 7, 1993.

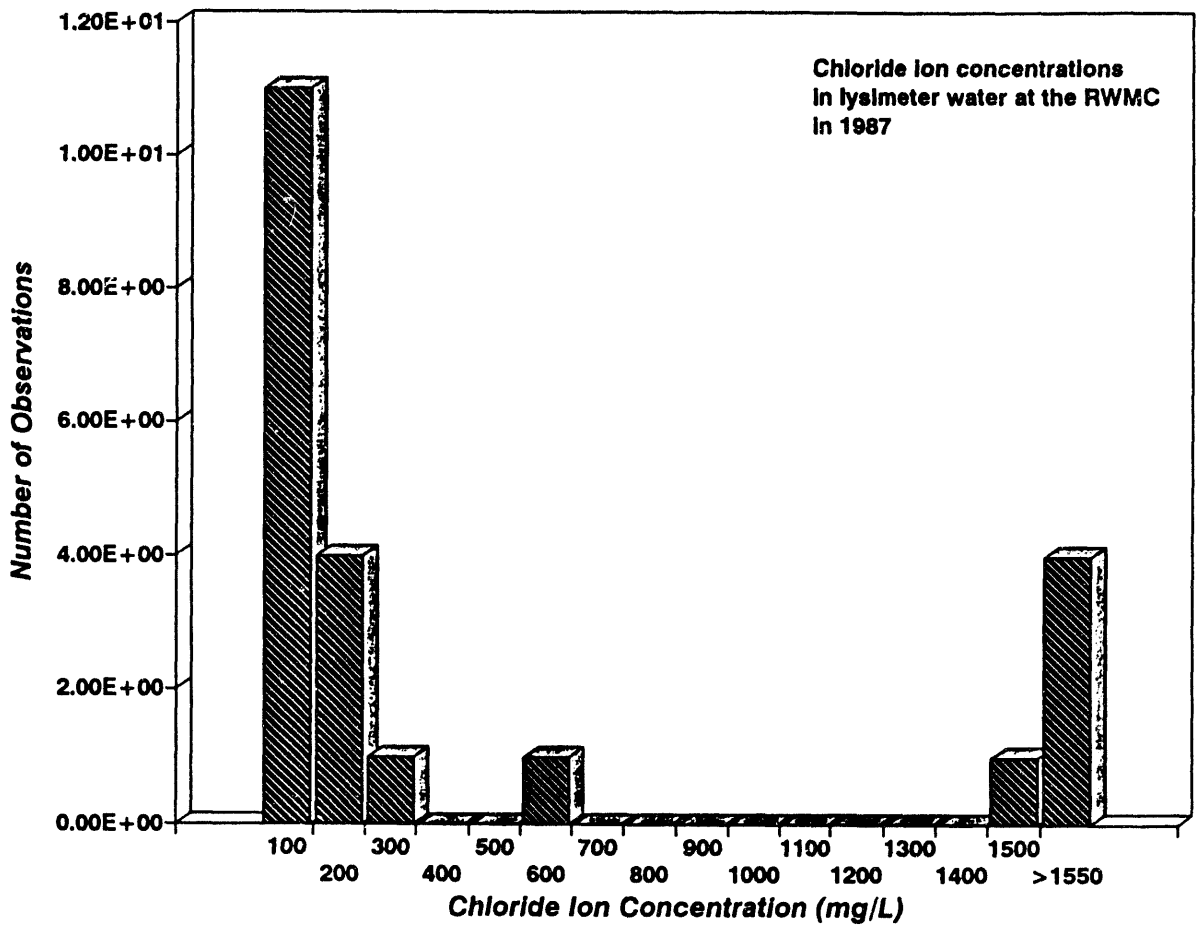

Figure 3-14. Chloride ion concentration in SDA lysimeters (Laney et al. 1988).

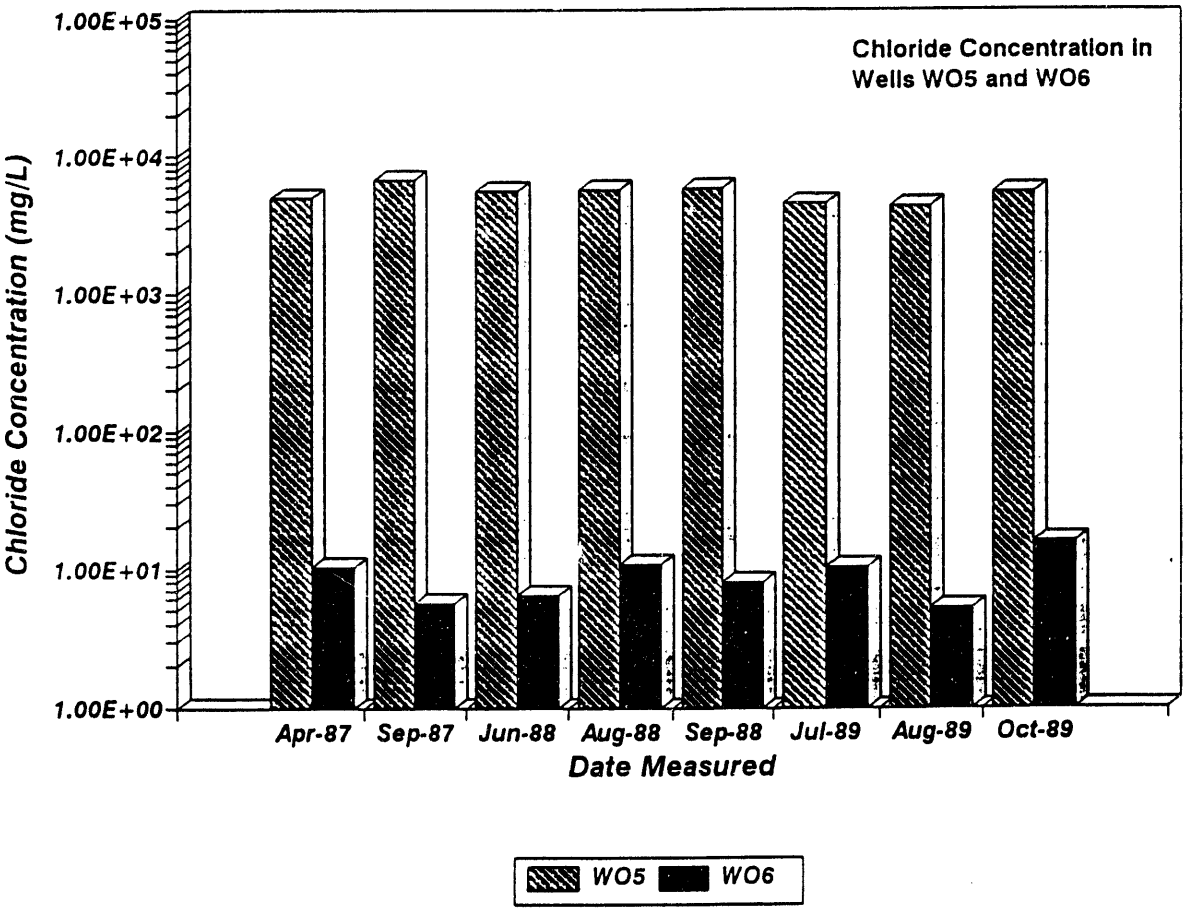

Figure 3-15. Chloride ion concentration in Wells WO5 and WO6 measured from 1987 to 1989.

submerged in pore water containing chloride ions. Corrosion rates for this scenario were obtained from empirical data in Miller and Boyd (1967). For the dry corrosion scenario, it was assumed the soil surrounding the blocks was partially saturated and corrosion was driven primarily by the availability of chloride ion diffusion through pore water to the beryllium surface. The corrosion rate for this scenario was calculated using a model described in Kelmers and Hightower (1987).

During the spring when an infiltration event occurs, perched water has been observed in the surface sediments above the basalt. The thickness of the perching layer is usually from 0.61 to 1.1 m (Hubbell 1993). For the wet corrosion scenario, it was assumed that this perched layer submerges one of the three buried inserts; therefore, two blocks are submerged. The overall corrosion rate is plotted as a function of chloride concentration in Figure 3-16, and a linear regression of the data was performed to estimate the corrosion rate of beryllium in SDA pore water. For the base case analysis, the arithmetic mean of the measured chloride concentration in Wells W05 and W06 was used as the chloride concentration in pore water (2,653 mg/L). Sensitivity cases were run using the geometric mean of all the measurements taken at the RWMC (137 mg/L) and the upper bound limit of 12,500 mg/L. For a pore water concentration of 2,653 mg/L, the corrosion rate was 7.67×10^{-3} cm/yr.

The following assumptions were used to model the corrosion of beryllium during a water perching event:

1. Thickness of the perching layer was 1.22 m above the basalt sediment contact--resulting in two out of the six blocks being completely submerged in water.

2. The chloride content of the perching water was the arithmetic mean of the measured chloride content in wells near the soil vaults. This value was 2,653 mg/L and resulted in a corrosion rate of 7.67×10^{-3} cm/yr.

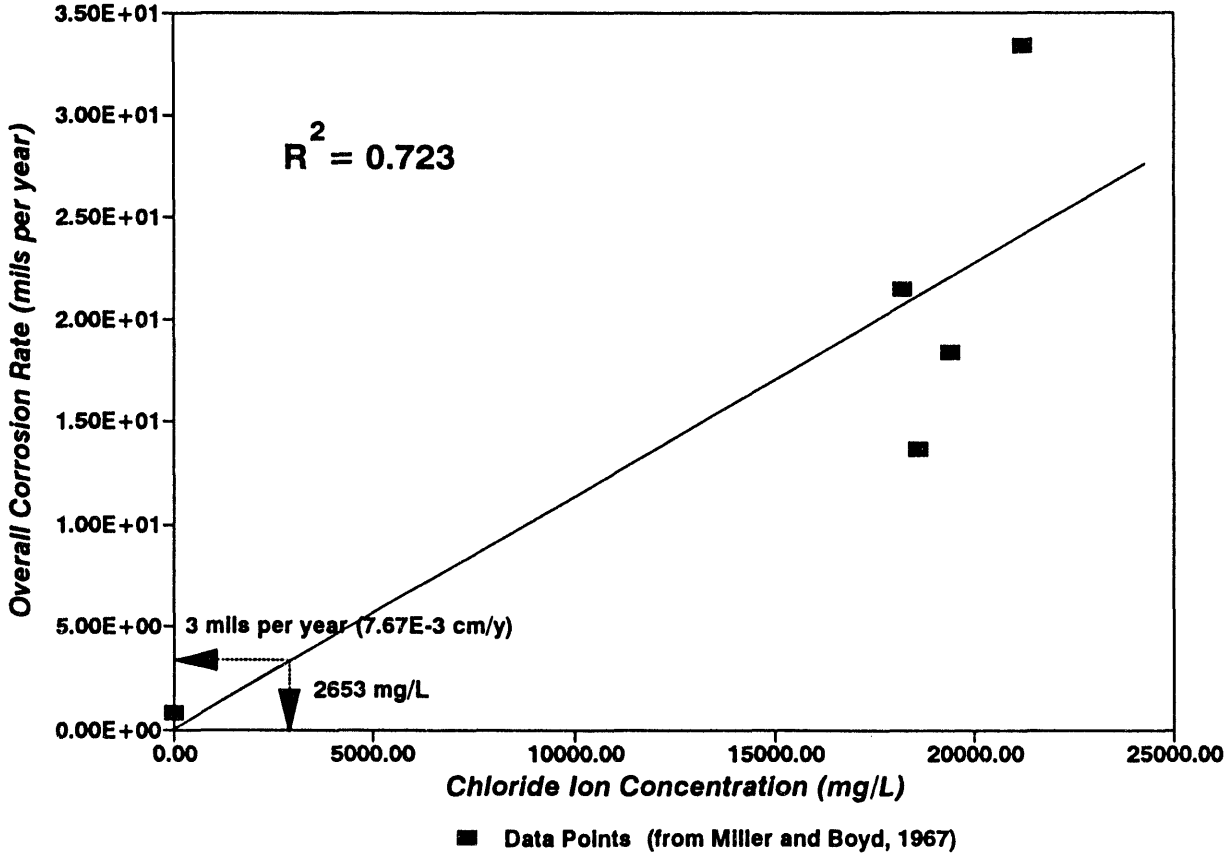

Figure 3-16. Linear regression of corrosion rate as a function of chloride ion (Miller and Boyd 1967).

3. The perching event was assumed to last for 30 days. The effective overall corrosion rate was then 7.67×10^{-3} cm/yr $\times$ 30 d/365 d/yr = 6.3×10^{-4} cm/yr.

4. A sensitivity case was run using the maximum chloride ion concentration measured at the SDA (12,500 mg/L) and the geometric mean of all the measurements (137 mg/L). Effects because of the presence of sulfate ions were not considered.

5. All tritium release was assumed to partition into the liquid water phase and move with the pore water.

The corrosion rates reported in Miller and Boyd are for solutions of NaCl. It has been reported that $MgCl_2$ solutions were sprayed on roads in the RWMC for dust abatement, and it is believed that these solutions are the source of the abnormally high chloride concentrations in the RWMC pore water.[a] It is uncertain whether magnesium or sodium plays an active role in the corrosion process.

For the dry corrosion scenario, it was assumed that the soil surrounding the blocks was partially saturated for the entire year. The corrosion rate was applied to four blocks for an entire year and 0.9 year for the two blocks that undergo wet corrosion. The corrosion rate equation was adapted from equations in Kelmers and Hightower (1987), which assumed the corrosion rate was a function of the availability of oxygen. In this analysis, the corrosion rate was assumed to be a function of the availability of chloride ions because chloride appears to be present in the pore water at the RWMC and is a stronger corrosion agent than oxygen. The calculated corrosion rate based on the availability of oxygen was much less than the corrosion rate based on the availability of chloride. The rate of diffusion of chloride ions from the groundwater to the metal surface was calculated assuming a flat-plate geometry as discussed earlier, with groundwater flowing parallel to the flat-plate and

---

a. Oral communication, Robert Monson, EG&G Idaho, Inc., with Raj Bhatt, EG&G Idaho, Inc., December 15, 1993.

chloride diffusing normal to the water flux. The molar flux of Cl^- has been adapted from Kelmers and Hightower (1987),

$$J = 2\frac{\sqrt{3}}{3}\frac{\epsilon D(C_B - C_I)}{\left(\frac{\epsilon DL}{U}\right)^{1/2}} \qquad (3\text{-}9)$$

where

J = molar flux of Cl^- (g-mol/cm^2 s)

ϵ = volumetric water content in soil (0.33 for 7 cm/yr infiltration)

D = diffusion coefficient of Cl^- in water (1.71×10^{-5} cm^2/s)

C_B = concentration of Cl^- in bulk groundwater (2,653 mg/L equivalent to 7.48×10^{-5} g-mol/cm^2)

C_I = concentration of Cl^- at metal-soil interface (assumed to be 0 g-mol/cm^2)

L = length of block (122 cm)

U = Darcy velocity parallel to reflector (2.22×10^{-7} cm/s).

The corrosion rate of beryllium is given by

$$C_r = \frac{\left(JMW_{Be}\,3.1536\,x10^7\,\frac{s}{y}\right)0.5}{\rho} \qquad (3\text{-}10)$$

where

C_r = corrosion rate of beryllium (cm/yr)

MW_{Be} = molar weight of beryllium (9.001 g/mol)

ρ = density of beryllium (1.85 g/cc).

The factor, 0.5 is included because 2 mole of Cl^- reacts with 1 mole of beryllium. The diffusion coefficient for chloride in water was taken from Learman (1988) and is based on a water temperature of 18°C. The dry season corrosion rate for a chloride concentration of 2,653 mg/L and a net infiltration rate of 7 cm/yr was 6.7×10^{-4} cm/yr. The volumetric water content was based on the volumetric water content used in the source release model for RWMC soils. This assumes the soil completely surrounds and is in contact with the block. Based on a description of the disposal, it is likely that at least some of the blocks may not contact the soil, therefore, making it difficult for Cl^- ions to migrate to the beryllium surface. In addition, the corrosion product may inhibit migration of water to the beryllium surface by clogging the soil pores and reducing the porosity near the soil-beryllium interface. For example, if the porosity is reduced to 0.1, the dry corrosion rate (for 7 cm/yr infiltration) is reduced to 3.7E-4 cm/yr.

The total volume of beryllium corroded by dry corrosion is $C_r \times$ surface area/block $\times$ 4 blocks $\times$ 1 yr + C_r x surface area/block x 2 blocks $\times$ 0.9 yr. For a chloride concentration of 2,653 mg/L, the total volume of beryllium corroded by dry corrosion was 190.2 cm^3/yr. The total volume corroded in 1 year for wet corrosion was 7.67×10^{-3} cm/yr $\times$ 4.85×10^4 cm^2 cm/block $\times$ 2 blocks $\times$ 30 d $\div$ 365 d/yr = 61.1 cm^3/yr. The total volume of beryllium corroded for both wet and dry seasons is 190.2 cm^3/yr + 61.1 cm^3/yr = 251.3 cm^3/yr. The fraction of a beryllium block that corrodes in 1 year is 251.3 cm^3/yr $\div$ 2.712×10^4 cm^3 = 9.27×10^{-4}/yr. This value was used as the rate constant, K_2, in the source release model to describe release from the waste form to the soil. The corrosion rate constants for the three different infiltration rates and three assumed chloride concentrations are presented in Table 3-5.

The approach in Kelmers and Hightower models corrosion under partially saturated soil during infiltration events. Thus, it could be argued that the approach should be used for wet rather than dry season corrosion. However, the Kelmers and Hightower approach makes no allowance for the chloride and

Table 3-5. Corrosion rate constants for beryllium in SDA pore water.

Infiltration rate (cm/yr)	Corrosion rate constant (per yr)		
	Chloride concentration in SDA pore water		
	137 mg/L Cl^-	2,653 mg/L Cl^-	12,500 mg/L Cl^-
4	2.53E-4	7.56E-4	2.72E-3
7	2.62E-4	9.27E-4	3.53E-3
10	2.69E-4	1.06E-3	4.17E-3

sulfate content of some RWMC groundwater samples; therefore, the corrosion rate for beryllium in natural seawater for the wet season was extrapolated. In the dry season, there is little groundwater flow; it is probably slower than the 7 cm/yr Darcy velocity used. Also, the corrosion product poisons the corrosion reaction and to some degree protects the beryllium (Miller and Boyd 1967). Therefore, the release fraction should be smaller than the 9.27×10^{-4} per year calculated.

3.3.1.2.3 Diffusion of Tritium from the Beryllium Blocks. Tritium is produced in the beryllium by the reaction chain:

$$^{9}Be + n \rightarrow {}^{6}He + \alpha$$
$$^{6}He \rightarrow {}^{6}Li + \beta^-$$
$$^{6}Li + n \rightarrow {}^{3}H + \alpha \quad .$$

The first of these reactions has a threshold at 600 keV with a strong resonance (0.105 barn) at 3 MeV. Measurements made on PAEDS samples[a] showed that tritium production at the end of irradiation was approximately 2.2 Ci/g/10^{22} n/cm^2 (E >1 MeV). Considerable helium is produced along with the tritium. Typical values of the He/H-3 ratio are in the range of 17:1. The helium remains finely dispersed as long as the beryllium remains at low

a. Beryllium cylinders nominally 1 cm in diameter and 3 cm long of essentially the same material as the ATR beryllium reflector irradiated to high fluences.

temperature. On heating, or if the irradiations are done at high temperature, the helium clusters coalesce into visible bubbles, eventually connecting to form open porosity (Beeston 1990).

Tritium produced in the beryllium appears to reside in two modes. Rion Causey made acid-solution measurements at Sandia Livermore National Laboratory of tritium inventory in a PAEDS sample (Beeston 1990). He found 32.8 Ci in a 4.7-g sample irradiated to 5×10^{22} n/cm^2 (E >1 MeV) after it had been out of the reactor for 8.2 years. This was within 1% of the predicted value. The unexpected finding in his measurements was that 97.6% of the tritium went through the acid into the air volume above the liquid. Only 2.4% of the tritium went into solution in the acid. This is suggestive that the majority fraction existed in the beryllium as ground-state diatomic molecules, while the 2.4% existed as either $^3H^+$ or $^3H^-$ ions in the beryllium specimen.

An almost identical sample was sent to Dave Baldwin at Battelle Pacific Northwest Laboratory. He performed stepped isothermal anneal tests on disks broken from the sample (Baldwin et al. 1989). Analysis of his data (Longhurst 1990) shows that under thermal desorption, tritium was released again in two modes. About 2% of the tritium came out in stages corresponding to the temperature steps. This was apparently because of thermal decomposition of a tritium-containing compound. It was clearly diffusion-limited in its release with an apparent diffusivity very close to the Jones and Gibson (1967) value.

$$D = 3.0\times10^{-11} \exp\left[\frac{-0.192eV}{kT}\right]\left[\frac{m^2}{s}\right] \quad . \tag{3-11}$$

Further, it had an activation energy for release of 78.8 kJ/mole, strongly suggestive that it was tritium tied up in $Be(O^3H)_2$. Similar behavior was observed more recently by Eberle and coworkers in Germany (Eberle et al. 1993). When Baldwin's samples exceeded 600°C, break-away swelling commenced, and there was a burst release of the remaining tritium. This has been attributed to the unstable growth of helium bubbles resulting in connected pathways to the surface. Tritium apparently came out with trapped helium.

Qualitatively and quantitatively this is in good agreement with Causey's results.

The conclusion from these studies is that about 97.5% of the tritium in ATR-irradiated beryllium is associated with microscopic bubbles and voids caused by neutron displacements and helium. It is estimated that the remaining 2.5% is tied up in a chemical phase, possibly $Be(O^3H)_2$. Based in part on work done at the INEL (Anderl et al. 1992), Causey has inferred a trapping energy of 1.8 eV for tritium tied up in the helium bubbles and vacancies (Causey et al. 1993). Therefore, at low (ambient) temperatures, the helium-trapped tritium is fixed. The release frequency for trapped atoms is 1.46×10^{-19}/s or once in 200 billion years. Helium-trapped tritium would be released only if the beryllium in which it was bound corroded. Thus, for chemically-bound tritium, diffusion is the only independent release mechanism.

Mathematical models have been developed for tritium movement through materials. One of the best is TMAP4 (Longhurst et al. 1992), developed at the INEL. This code may be used to evaluate the tritium release rate from ATR beryllium reflector blocks. An initial data requirement is the state of tritium in the beryllium at the time it is disposed. It has been estimated that the tritium concentration in the beryllium follows an exponential decay away from the fuel-contacting surfaces with a 1/e folding length of 0.0366 m (halving length of 1 in.). An oxide film of 400-Angstrom thickness can also be expected.

Using the measurement data of Causey, the peak concentration at the surface may be assumed to begin at removal from the reactor at 11 Ci/g. Of this, only the 2.5% that is chemically bound is of concern. That corresponds to an atom fraction of 8.5×10^{-5} or a concentration of 1.05×10^{25} H-3/m^3. This chemically-bound tritium may be modelled as being in a 0.8-eV trap (78.8 kJ/mole) and having the solubility

$$S = 1.03 \times 10^{28} \exp\left(\frac{-1\ eV}{kT}\right)\left(\frac{m^{-3}}{Pa^{\frac{1}{2}}}\right) \qquad (3\text{-}12)$$

obtained from Swansiger's data (Swansiger 1986). Diffusivity through nontrapping, high-purity beryllium was measured by Abramov (Abramov et al. 1990) as

$$D = 8.0 \times 10^{-9} \exp\left(\frac{-0.365\ eV}{kT}\right)\left(\frac{m^2}{s}\right) \quad . \tag{3-13}$$

The trap density estimate is based on the known 1.5% BeO content of this material, but that is rather uncertain. Another approach is to consider the measured diffusivity as an effective value, retarded from ideal by the trapping factor, ζ, where

$$\zeta = \frac{\lambda^2 \nu}{\rho D} \exp\left(-\frac{E_t}{kT}\right) \quad . \tag{3-14}$$

where

λ = beryllium lattice constant

ν = Debye frequency (10^{13}/s)

ρ = fraction of lattice sites that are traps (no units)

D = diffusivity (cm^2/s)

E_t = trapping energy (j)

k = Boltzmann's constant (j/°K)

T = temperature (°K).

Then, if Abramov's diffusivity is taken as the ideal nontrapping value, then ρ may be solved as

$$D_{eff} = \frac{D}{1+\frac{1}{\zeta}} \tag{3-15}$$

$$\rho = \lambda^2 \nu \exp\left[-\frac{E_t}{kT}\right]\left[\frac{1}{D_{eff}} - \frac{1}{D}\right] \tag{3-16}$$

which becomes 5.3% at 573 K where Baldwin's measurements were made. The computed value increases and decreases with temperature. The agreement with BeO content is fair.

Solubility of hydrogen isotopes in BeO is given by Macaulay-Newcombe et al. (1992) as being approximately 30 times that in beryllium. Diffusivity of tritium in BeO is given by Fowler et al. (1977) as

$$D = 1.40\times10^{-4}\exp\left[-\frac{2.1\ eV}{T}\right]\left[\frac{m^2}{s}\right] \quad . \tag{3-17}$$

Were it not for radioactive decay, that would be sufficient information to run the TMAP4 code. However, to accommodate decay, it is necessary to use the effective diffusivity value based on the trapping parameter and consider all the tritium as mobile. The diffusivity evident in Baldwin's experiments must be the effective diffusivity. Again, that fits well with the Jones and Gibson value and is consistent with the concept that the traps are chemical and not related to the damage state of the material. Further, it does not require precise determination of trap density and energy.

Two cases were considered. One had a 40-nm oxide film intact. The other had no oxide film. Results are shown in Figures 3-17 to 3-19. Figure 3-17 shows the concentration profile of tritium in the beryllium with the oxide film in place. The slight loss shown at the left-hand edge of the curves represents a small amount of tritium that was absorbed into the oxide film. Permeation of tritium through the oxide film is limited to about 370 tritium molecules/m^2 over the 50 years considered. In other words, it is essentially zero. General inventory reduction is due to radioactive decay of tritium.

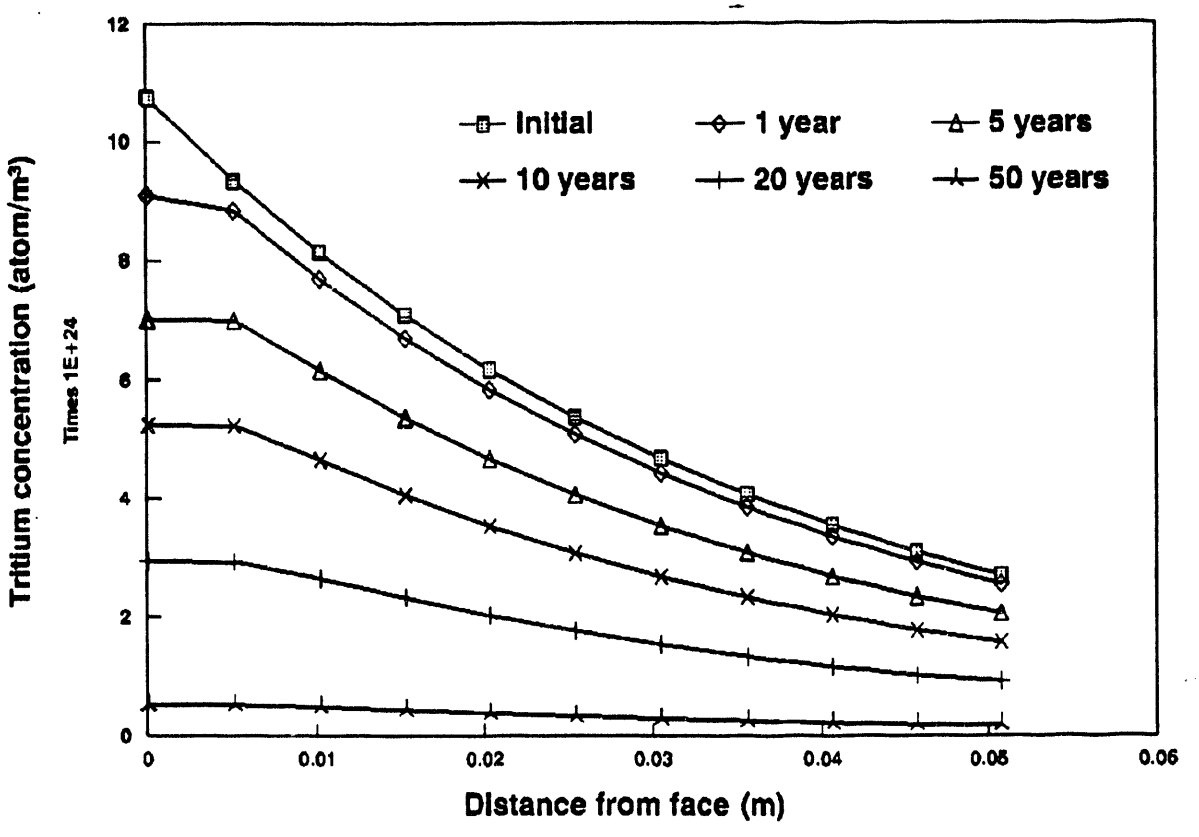

Figure 3-17. Tritium concentration history predicted by TMAP4 in ATR beryllium reflector block with 40-nm oxide film intact.

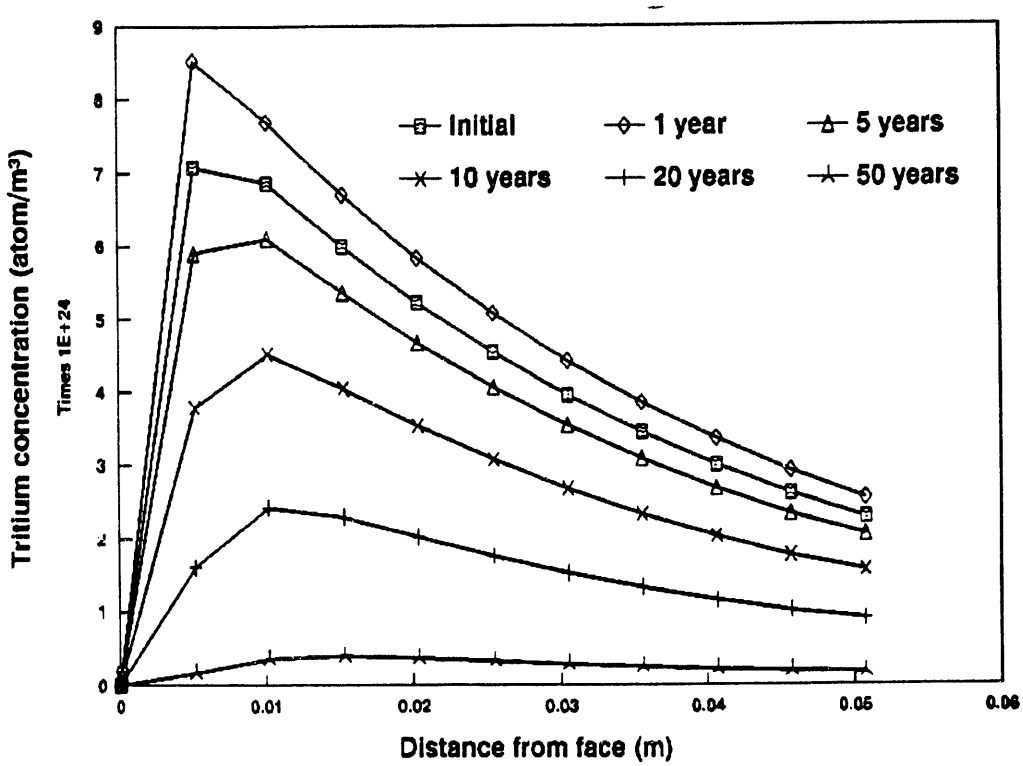

Figure 3-18. Tritium concentration profiles in ATR beryllium reflector with no oxide film in place to inhibit diffusion.

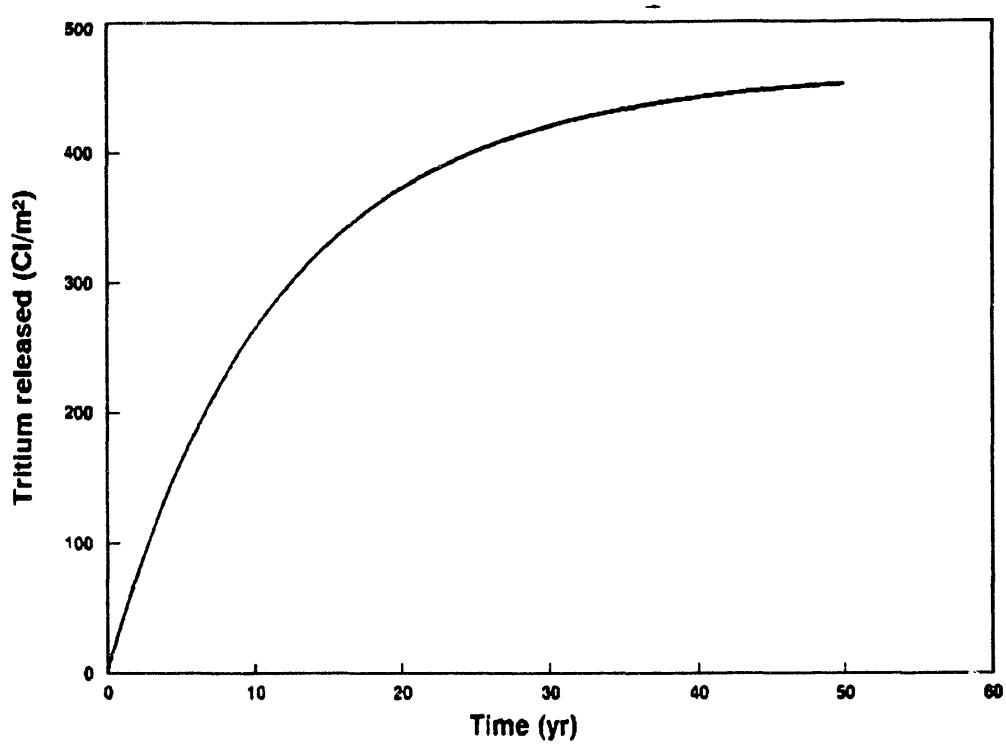

Figure 3-19. Tritium evolution history from ATR beryllium reflector with no oxide film assumed.

For comparison, Figure 3-18 shows the same data for beryllium with no oxide film present. There is a significant diffusion of tritium to the surface and out. Figure 3-19 shows the amount and history of that evolution. This is a simple integration of tritium crossing the surface of the beryllium and does not account for radioactive decay after the tritium is released.

To the extent that the BeO film remains intact, there should be no problem with tritium diffusing from the ATR beryllium reflector blocks. According to Dave Dombrowski,[a] even if corrosion takes place, the oxide film should still remain in place although its thickness may change substantially. It is unlikely that it would get much thinner than about 10 nm, releasing about 1,000 molecules/m^2 (9.7×10^{-17} Ci). Even if the oxide film was not present, the release over the tritium lifetime would be only a few hundred curies. Based on the previous discussion, diffusion of H-3 out of the blocks was considered insignificant and was not included in the analysis. In contrast, release because of corrosion was estimated to be about 500 to 1,200 Ci depending on the assumed chloride concentration. If no oxide film forms (although highly unlikely), then there would be no corrosion and release would be determined by diffusion. Based on the previous discussion, diffusion of tritium out of the blocks was considered insignificant because of the presence of the oxide layer, and it was not included in the analysis.

3.3.1.2.4 Fate of Tritium After Release from the Blocks. Most of the tritium (97.5%) in the blocks is in the form of diatomic hydrogen molecules (HT and T_2) (see discussion in Section 3.3.1.2.3). Tritium, in the form of HT, is oxidized to H_2O in soils relatively rapidly (McFarlane et al. 1979). The oxidation process occurs through the metabolic activity of naturally occurring soil microorganisms. McFarlane measured the oxidation rate of HT in Pancheri silt loam, a soil found in Butte County, Idaho, the county where most of the INEL is located. The measured HT oxidation rate in these soils was 66% per hour, which equates to an effective half-life of T_2 (or HT) of about 1 hour with a mean residence time of 1.5 hours. Other HT oxidation rate measurements in other soils ranged from 12 to 65%. The transient diffusion

---

a. Personal communication, D. Dombrowski, Brush Wellman Corporation, Cleveland, Ohio, with Glen Longhurst, EG&G Idaho, Inc., November 19, 1993.

time of HT in soil can be approximated by L^2/D, where L is the diffusion length and D is the diffusion coefficient. A diffusion coefficient of HT in soil pore air can conservatively be assumed to be 0.032 m^2/day, the approximate value for diffusion of gases in air. The diffusion length of 10 cm was used because most soil microbial activity takes place near the soil surface. Using these parameters, the average diffusion time of HT through the top 10 cm of soil overlying the blocks is 8 hours.

The fraction of HT not converted to HTO can be approximated by

$$f = e^{-f_o \frac{L^2}{d}} \qquad (3\text{-}18)$$

where f_o is the fraction of HT converted per hour.

Using the conversion rate for Pancheri soils of 0.66 per hour, the fraction of HT not converted to HTO was 5.1×10^{-3}. Therefore, little of the tritium will leave the soil as HT, and most of the tritium will be oxidized to HTO. For this model, it was assumed all tritium released as HT was converted to HTO and moved downward with the pore water. This is a conservative assumption for the groundwater pathway because some of the HTO may be reemitted to the atmosphere by evaporation of pore water near the surface and evapotranspiration by plants. This pathway is addressed in the atmospheric scenario.

Release of tritium by partitioning into the water vapor phase and diffusion to the surface was considered a minor pathway. Assuming a temperature of 10°C, 100% relative humidity, and equilibrium between the liquid and vapor phases, the fraction of the total activity of tritium in the pore air to that in the pore water is approximately 1×10^{-5}. If all activity in the vapor phase diffuses to the surface and escapes as HTO, then this amount is only 1×10^{-5} of the calculated release. Therefore, for the groundwater pathway, all tritium released as a gas is assumed to be oxidized to HTO. As discussed previously, evaporation and evapotranspiration may be significant tritium loss mechanisms from the pore water. These pathways were addressed in the atmospheric pathway by conservatively assuming all tritium released into the soil was emitted to the atmosphere, and no mass balance was

performed on the source. In reality, only the tritium lost from the soil pore water by evaporation and evapotranspiration should be considered for the atmospheric pathway.

3.3.1.3 Release from Waste Containers. Waste containers were segregated into two generic types: (1) metal containers including stainless steel 55-gal drums, metal boxes, and bins and (2) all other waste containers including wooden and cardboard boxes and bales. The integrity of wooden boxes and bales can generally be assumed to be poor in comparison to metal containers. After the lifetimes of these containers had expired, radionuclides began releasing from these containers as a first order process. The release rate constant for wooden boxes was 0.03 per year, 0.1 per year for cardboard boxes and bales, and 0.01 per year for metal containers. These release rate constants were estimated through comparing observed concentration of Pu-239,-240 in subpit soil (Humphrey and Tingey 1978) and calibrated model runs using the DOSTOMAN computer code (Case et al. 1990).

Observations made during the Early Waste Retrieval project and Initial Drum Retrieval project in 1976 through 1978 at the RWMC have indicated container lifetimes of around 10 years. During the drum retrieval process, the fraction of drums that had been breached (either by corrosion or other means such as compaction) was estimated. The data on metals drums, plotted over time, were fit to an exponential curve in Walton et al. (1989b), and a drum breaching rate constant was extrapolated. The value, 0.1 per year (10-year average lifetime), was the rate constant used in evaluating the release of organic solvents at the RWMC. This value only accounts for the breach of the drum and not the rate at which radionuclides are released from the drum into the backfilled soil. The data indicate that it is probable that container lifetime is shorter than originally estimated; however, the lifetime represents the drum failure rates of drums disposed between 1966 and 1970. Disposal practices at that time involved random dumping of the drums in a pit or trench, followed by backfilling and compaction using a bulldozer. Disposal practices have significantly improved since this time, and container integrity of more recent waste disposals are expected to be much greater.

Little empirical data exist on the release rates of radionuclides from waste to soil. The previous radiological performance assessment may be

relevant for actinides where movement out of the waste may be limited by the sorptive capacity of plutonium. These release rates may not be appropriate for more mobile nuclides such as H-3 and C-14. Instantaneous release from waste container to soil is both unrealistic and improbable. First, the container must fail so that infiltrating water may move through the waste. Second, water must come in contact with waste having surficial contamination. Third, some fraction of the radionuclide inventory must partition into the pore water; and fourth, the water must move out of the failed waste container and into the surrounding soil. Considering these observations, the following assumptions were made concerning radionuclide release from waste containers:

1. All waste containers, including metal drums, fail to some degree after disposal.

2. Release rate constants from waste containers to soil account for failure of the container and leaching of radionuclides from the container to soil.

3. For waste contained in metal containers, a release rate constant of 0.1 per year was used based on the analysis of the drum retrieval data documented in Walton et al. (1989b).

4. Release of radionuclides from waste in containers other than metal were assumed to occur at a rate 5 times the metal containers (0.5 per year). This releases the entire inventory in the containers over a period of slightly greater than 5 years.

In contrast to the release rate constant of 0.5 per year, the maximum leach rate from the soil compartment was 0.035 per year for the 7 cm/yr infiltration case and a distribution coefficient of zero. The result is a relatively instantaneous release of radionuclides in nonmetal containers to the soil compartment following disposal. Based on this release model, little credit was taken for waste that was not contained in metal containers. The fraction of inventory in metal containers was assumed to remain constant for all future disposals in the RWMC.

3.3.2 Transport in the Unsaturated Zone

As stated previously, water movement in the unsaturated zone underlying the RWMC is not well understood, especially in the fractured basalt. Because of this uncertainty, a simplified plug flow model was used to simulate transport in the unsaturated zone. Advective transport and radioactive decay and ingrowth were considered in the plug flow model; dispersion and diffusion were ignored. In this model, nonsorbing contaminants moved with the vertical velocity of the water calculated using the parameter values described in Section 3.2.5. The amount of radioactive decay and ingrowth that occurred during transit in the unsaturated zone was dependent on the contaminant transit time. The contaminant travel time is given by

$$T_a = \frac{X}{U} R_d \qquad (3\text{-}19)$$

where

X = sedimentary interbed zone thickness (m)

U = unsaturated pore velocity (m/yr)

R_d = retardation coefficient.

The unsaturated pore velocity is given by

$$U = \frac{I}{\theta} \qquad (3\text{-}20)$$

where

I = infiltration rate (m/yr)

θ = volumetric water content in the sedimentary interbeds. (cm^3/cm^3).

The flux at the aquifer-unsaturated zone interface is given by

$$J_u = J_s e^{-\lambda T_a} \quad (3\text{-}21)$$

where

J_u = contaminant flux at the aquifer (Ci/yr)

J_s = contaminant flux at the source-unsaturated interface (Ci/yr).

3.3.3 Transport in the Aquifer

The conceptual model for contaminant transport in the aquifer incorporated the limiting assumptions used in the aquifer flow model. The model is based on an analytic solution to the advection dispersion equation for contaminants in a saturated porous media. These solutions were originally presented in Codell et al. (1982) and implemented in the GWSCREEN code (Rood 1993a). The model contains the following assumptions and limitations:

1. The model uses a cartesian coordinate system (x,y,z) as a frame of reference. The positive x direction is in the direction of flow.

2. The flow is uniform and unidirectional. The model does not account for sources or sinks.

3. The aquifer is modeled as an isotropic, homogeneous porous media of infinite lateral extent and finite thickness. The media in this case is fractured basalt.

4. Molecular diffusion is assumed to be negligible.

5. The source can be represented by a rectangular area of length (L) and width (W) and centered at the origin (0,0,0).

6. The dispersion coefficients remain constant over the domain.

7. Transport is limited to a single species that may decay or degrade as a function of time.

8. The contaminant moves as a dissolved substance. Transport in liquid organic and vapor phases is not considered.

9. Solid and liquid phases are in equilibrium, and concentrations are related by the linear sorption coefficient (K_d).

10. The contaminant is mixed vertically (z direction).

11. Radioactive progeny travel at the same rate as their parent.

Assumption 10 implies that the model is two dimensional ($dC/dz = 0$); therefore, a mixing depth must be assigned. The mixing depth can range from a minimum value up to the effective thickness of the aquifer depending on the distance to the receptor.

Two receptor locations were evaluated in this performance assessment: one at 100 m south of the RWMC facility boundary and one at the nearest INEL Site boundary 5,500 m south of the RWMC. For evaluating compliance with the 25 mrem/yr EDE all pathway dose, the receptor was located at the INEL Site boundary during operations and institutional control (1984 to 2120). During post-institutional control (from 2120 on), the receptor was located 100 m south of the RWMC facility boundary. To evaluate compliance with the National Primary Drinking Water Regulations (40 CFR 141) for community drinking water systems, the receptor was located at the nearest INEL Site boundary. Presently, there are no drinking water wells that serve a community in the vicinity of the nearest Site boundary. The closest community drinking water system is Atomic City, which is about 2,100 m southeast of the RWMC and slightly upgradient. The hypothetical receptor well at the nearest Site boundary was chosen because the conceptual model for aquifer flow can be easily adapted to this location and the estimated concentrations at the well would bound any current or future impacts.

For the RWMC facility boundary scenario (receptor located 100 m south of the RWMC facility boundary), the mixing depth was 12 m; it was based on the average well screen depth for drinking water wells drilled into the Snake River Plain Aquifer (Seitz 1991). Scoping calculations using a three-

dimensional solution to the advection dispersion equation for transient mass fluxes, as reported in Codell et al. (1982), showed approximately 80% of the contaminant mass was in the top 20 m of the aquifer at 100 m downgradient from the RWMC boundary. This simulation was performed using the same transport parameters used in the analysis and a vertical dispersivity value conservatively chosen to be 1 m. Using the 12-m mixing depth for the receptor is a conservative assumption because it is estimated contaminants will be mixed over a greater depth (Codell et al. 1982). For the Site boundary scenario (5,500 m south of the RWMC), contamination was mixed over the effective thickness of the aquifer. This effective thickness was conservatively assumed to be 76 m (Robertson 1974), although more recent data collected in the vicinity of the RWMC (Wylie and Hubbell 1993; Burgess et al. 1993) indicates it may be greater. Scoping calculations using the same three-dimensional solution to the advection dispersion equation showed complete mixing of a contaminant in a 76-m-thick aquifer was obtained at 5,000 m downgradient from the source using a vertical dispersivity value of 1 m.

Dispersivity values used in the analysis were obtained from Arnett et al. (1990) and scaled according to the receptor location. Because dispersivity is scale dependent, smaller values were used for the 100-m receptor. Arnett reports dispersivity values of 90 m (longitudinal) and 40 m (transverse) for an INEL Site boundary receptor using the southern part of the INEL (from the ICPP to the Site boundary, a distance of 12,000 m) as a frame of reference. For the 100-m receptor, these dispensitivity values were reduced by a factor of 10 (9.0 m and 4.0 m). For the INEL site boundary calculations, the dispersivity values were reduced by a factor of 3 (30 and 13.3 m). These reductions in dispersivity were based on the relative differences between the distance of the receptor used by Arnett (from the ICPP to the INEL Site boundary) and the distance to the receptor used in this evaluation (5,500 m). The reduction factor of 3 based on discussions with Arnett, is believed to be conservative and has been used in other risk assessments (DOE-ID 1992).

Calibration studies at the INEL using the groundwater model used in this performance assessment are documented in Codell et al. (1982) and Rood et al. (1989). Tritium plumes from the ICPP injection well and the TRA percolation ponds were modeled. The predicted concentration matched measured data reasonably well considering the simplifications and assumptions of the model

and confirmed that the model could be used to estimate concentrations in real aquifer systems.

Most of the tritium present in the Snake River Plain Aquifer underlying the RWMC originated from upgradient sources at ICPP and TRA percolation ponds. Tritium released from the RWMC would be impossible to distinguish from tritium in the Snake River Plain Aquifer that originated from ICPP or TRA. Evidence of tritium migration from the RWMC would require measuring the perched water or pore water underlying the RWMC. Other radionuclides (Pu-239, U-234, U-238, Ra-226, and Np-237) have not been detected in the Snake River Plain underlying the RWMC. This observation is consistent with the transport model, which predicts contaminant travel times to the aquifer from a few hundred to thousands of years.

The mass balance equation that describes contaminant transport for the stated assumptions is

$$\frac{\partial C}{\partial t} + \frac{U}{R_d}\frac{\partial C}{\partial x} = \frac{D_x}{R_d}\frac{\partial^2 C}{\partial x^2} + \frac{D_y}{R_d}\frac{\partial^2 C}{\partial y^2} - \lambda C \qquad (3\text{-}22)$$

where

C = concentration (g or Ci/m^3)

t = time (yr)

U = groundwater pore velocity (m/yr)

R_d = retardation factor in the aquifer

x = distance from the center of the area source to the receptor parallel to groundwater flow (m)

D_x = dispersion coefficient in the x direction (m^2/yr)

D_y = dispersion coefficient in the y direction (m^2/yr)

y = distance from the center of the area source to the receptor perpendicular to groundwater flow (m)

λ = radioactive decay.

The retardation factor in the aquifer is given by

$$R_d = 1 + K_{da} \frac{\rho_a}{\eta} \quad (3\text{-}23)$$

where

ρ_a = bulk density in the aquifer (g/cm^{-3})

K_{da} = distribution coefficient in the aquifer (mL/g)

η = effective porosity of the aquifer.

The dispersion coefficients (D_x, D_y) are given by

$$D_x = \alpha_L U \quad (3\text{-}24)$$

$$D_y = \alpha_T U \quad (3\text{-}25)$$

where

α_L = longitudinal dispersivity (m)

α_T = transverse dispersivity (m).

The solution to Equation (3-22) for the initial conditions $C = C_o$ at $t = 0$ in the source area and $C = 0$ everywhere else is

$$C = \frac{Q_a}{\eta R_d b}\frac{1}{2L}\left[erf\left(\frac{x+\frac{L}{2}-\frac{Ut}{R_d}}{\sqrt{\frac{4D_x t}{Rd}}}\right) - erf\left(\frac{x-\frac{L}{2}-\frac{Ut}{R_d}}{\sqrt{\frac{4D_x t}{R_d}}}\right)\right] \times \frac{1}{2W}\left[erf\left(\frac{\frac{W}{2}+y}{\sqrt{\frac{4D_y t}{R_d}}}\right) + erf\left(\frac{\frac{W}{2}-y}{\sqrt{\frac{4D_y t}{R_d}}}\right)\right] e^{-\lambda t} \quad (3\text{-}26)$$

where

b = well screen thickness or mixing depth (m)

Q_a = initial total mass in the volume defined by L × W × b

L = length of source parallel to groundwater flow (m)

erf = error function

W = width of source perpendicular to groundwater flow (m).

The terms, L and W are equal to the length and width of the source as defined in Section 3.1.4.1. For an arbitrary release, the concentration may be found by the convolution integral

$$C(t) = \int_0^t C_i(t-\tau)\, F(\tau)\, d\tau \quad (3\text{-}27)$$

where

C(t) = concentration at time t for the arbitrary release (Ci/m^3)

$C_i(t - \tau)$ = concentration at time, $t - \tau$, for an instantaneous release at time $t - \tau = 0$ (Ci/m^3)

$F(\tau)$ = mass flux of the contaminant at time τ (Ci/yr).

The term $F(r)$ is given by the term J_u, in Equation (3-21). Equation (3-27) is solved numerically using a Simpson's rule integration routine.

The GWSCREEN code makes the simplifying assumption that radioactive progeny travel at the same rate as their parent. This assumption greatly simplifies the calculations and has been demonstrated to overestimate progeny concentrations (Codell et al. 1982). The progeny concentration is calculated by multiplying the parent concentration by a factor that relates the progeny activity level relative to the parent (DIF_i/DF_p) and the sorptive properties of the parent to that of the progeny (R_{dp}/R_{di}). The concentration of the i^{th} progeny is given by

$$C_i = C_{parent} \times \frac{DIF_i}{DF_p} \times \frac{R_{d_p}}{R_{d_i}} \qquad (3\text{-}28)$$

where

DIF_i = decay-ingrowth factor of the i^{th} progeny

DF_p = decay factor of the parent

R_{dp} = retardation factor of the parent

R_{di} = retardation factor of the i^{th} progeny.

The decay ingrowth factor for the i^{th} progeny is given by

$$DIF_i = \frac{\lambda_i}{\lambda_1} \prod_{m=1}^{i-1} \lambda_m \left[\sum_{j=1}^{i} \left(\frac{e^{-\lambda_j t}}{\prod_{k \neq j}^{i} (\lambda_k - \lambda_j)} \right) \right] \qquad (3\text{-}29)$$

where

λ_i = decay rate constant for the i^{th} progeny (per yr)

λ_1 = decay rate constant for the parent nuclide (per yr).

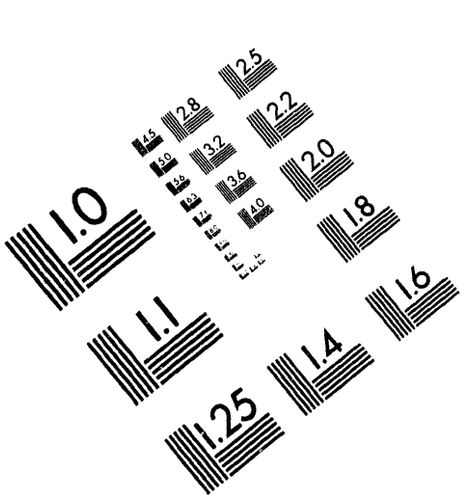

Association for Information and Image Management
1100 Wayne Avenue, Suite 1100
Silver Spring, Maryland 20910
301/587-8202

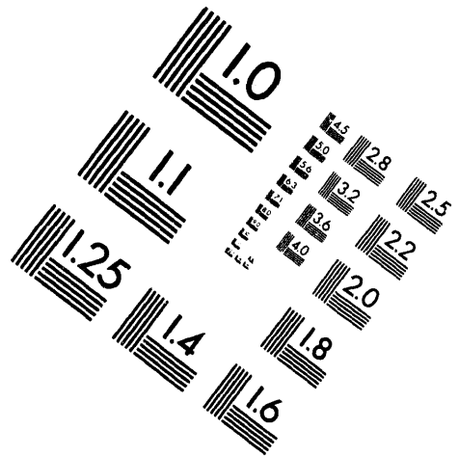

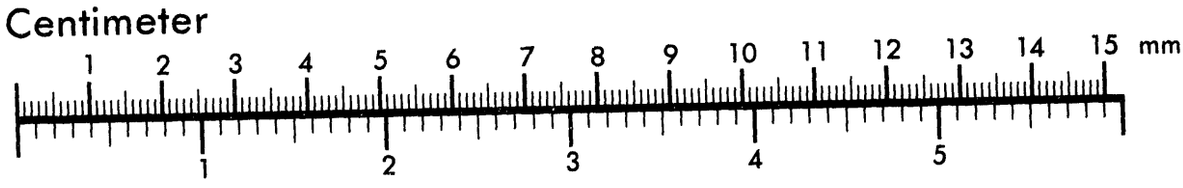

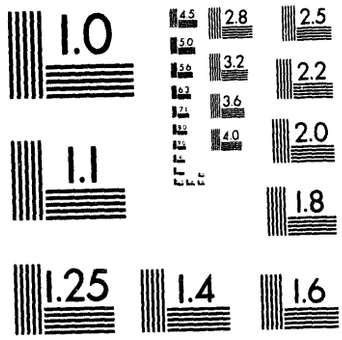

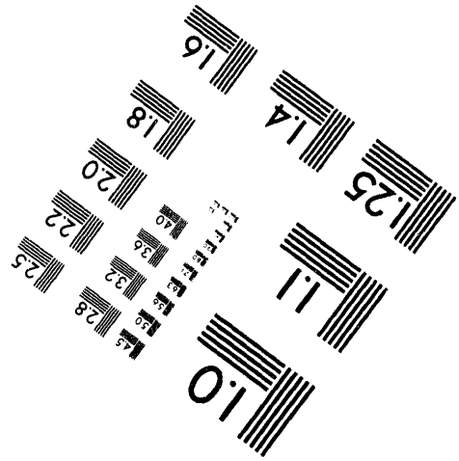

MANUFACTURED TO AIIM STANDARDS
BY APPLIED IMAGE, INC.

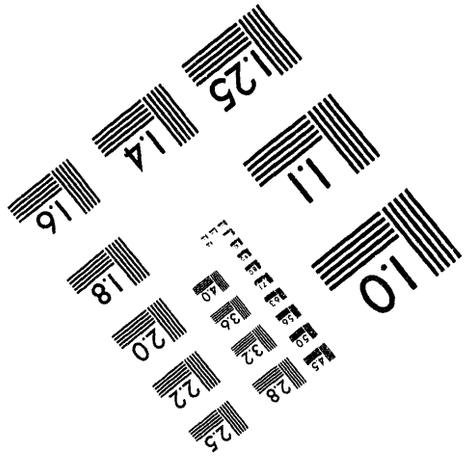

3 of 5

For example, suppose the concentration of Pu-241 in groundwater is 10 pCi/L at 319 years from the time waste disposal began. The concentration of Am-241 is then given by Equation (3-28) where the decay ingrowth factors calculated using Equation (3-29) are 2.13×10^{-7} for Pu-241 and 2.07×10^{-2} for Am-241. Assuming the R_d for Pu-241 is 3,801 and the R_d for Am-241 is 1,331, the concentration of Am-241 is equal to

$$10\ pCi/L \times \frac{2.07 \times 10^{-2}}{2.13 \times 10^{-7}} \times \frac{3801}{1331} = 2.8 \times 10^{6}\ pCi/L \quad .$$

3.3.4 Groundwater Transport Parameters

Tables 3-6 and 3-7 contain a summary of the groundwater transport input parameters used in the analysis for the screened set of radionuclides. Parameter values that were derived as a part of this performance assessment are identified in the table. Because of the sensitivity of model results to the K_d value, a discussion on linear sorption coefficient data (K_d values) is presented in Section 3.3.4.1 and Chapter 2.

3.3.4.1 Discussion on Sorption Coefficients. For the most part, sorption coefficient data used in previous performance assessments were used in this analysis. Where site-specific data existed, they were incorporated into the analysis. A literature review of available sorption coefficient data was performed to evaluate how appropriate these values were for the modeling conditions and to provide some reasonable uncertainty bounds for the uncertainty analysis. The elements of interest in the performance assessment are iodine, strontium, potassium, nickel, technetium, radium, uranium, neptunium, plutonium, thorium, protactinium, lead, actinium, americium, polonium, and cesium. This list does not include the entire inventory, but it does include several of the more important nuclides and nuclides that were not screened from the inventory based on the groundwater pathway. Site-specific adsorption data are only available for strontium, technetium, and cesium from this key list of radionuclides (Del Debbio and Thomas 1989; Schmalz 1972). Distribution coefficients are available for cobalt, chromium, strontium, cesium, cadmium, mercury, and selenium for alluvium and cadmium, mercury, selenium, and strontium for interbed sediments and basalt. Because of the

Table 3-6. Parameters used in the groundwater impact calculations.

Parameter	Value	Reference
Source length parallel to flow	257 m	Section 3.2
Source width perpendicular to flow	122 m	Section 3.2
Source thickness	6.1 m	Section 3.2
Soil density at source	1.5 g cm^{-3}	EG&G Idaho 1984
Aquifer density	1.9 g cm^{-3}	EG&G Idaho 1984
Aquifer porosity	0.10 cm^3 cm^{-3}	Robertson 1974
Pore velocity	560 m/yr	Wood 1989
Well screen thickness	12 m	Seitz 1991[a]
Aquifer thickness	76 m	Robertson 1974[b]
Unsaturated zone thickness	12.5 m	Section 3.2
Infiltration rate	4, 7 and 10 cm/yr	Section 3.2
Source volumetric water content	0.33	Baca et al. 1992
Unsaturated volumetric water content	0.168	Section 3.3[c]
Longitudinal dispersivity	9.0 m	Section 3.3[d]
Transverse dispersivity	4.0 m	Section 3.3[d]
Receptor distance	5,500 m	INEL Site boundary[e]
Receptor distance	100.0 m	RWMC facility boundary[f] downgradient edge of Pits 17-20

a. For receptor 100 m downgraident from the RWMC facility boundary, the 12-m well screen was used as the vertical mixing thicknesses in the aquifer.

b. For the receptor at INEL Site boundary, the 76-m thickness was used because complete vertical mixing occurs at that distance.

c. Value for 7 cm/yr infiltration.

d. Value for receptor at RWMC facility boundary. Values reported in Arnett et al. (1990) were 90 and 40 m and were reduced by a factor of 10 for scale considerations. Values used at INEL Site boundary were reduced by a factor of 3 to 30 and 13 m.

e. Point of compliance for all pathway analysis during operational and institutional control period and for drinking water analysis.

f. Point of compliance for all pathways analysis during post-institutional control period.

Table 3-7. Sorption coefficients used in the groundwater impact calculations for the screened set of radionuclides (mL/g).

Nuclide	Source	Basalt	Reference
H	0	0	Case et al. 1990
Ni	100	100	EG&G Idaho 1984
Tc	0.15	0.15	Baes et al. 1984[a]
C	0	0	Case et al. 1990
I	0.05	0.05	DOE 1987
K	0.55	0.55	Baes et al. 1984[a]
U	1000	100	DOE 1982[c], EG&G Idaho 1984[d]
Ra	50[b]	5	This document[c], EG&G Idaho 1984[d]
Np	50[b]	5	This document[c], EG&G Idaho 1984[d]
Pu	2000	200	DOE 1982[c], EG&G Idaho 1984[d]
Sr	2	2	DOE 1982[c], EG&G Idaho 1984[d]
Th	1000	100	DOE 1982[c], EG&G Idaho 1984[d]

a. The value reported in Baes et al. (1984) was reduced by a factor of 10 to account for the apparent lower sorptive properties of basalt.

b. A value of 50 was selected for this report based on the relative difference between the sorption coefficient values for the other actinides in basalt and sediment.

c. Reference for source K_d value.

d. Reference for basalt K_d value.

lack of site-specific radionuclide sorption information for sediments and basalts at the INEL, K_d values measured for sediments and basalts from other sites were used to calculate retardation factors. Additional information about the geochemistry of the INEL is contained in Chapter 2. The use of nonsite-specific distribution coefficients is not ideal; however, reasonable estimates were made based on other investigations.

3.3.5 Groundwater Screening Methodology

Radionuclide inventories evaluated in this performance assessment were obtained from the RWMIS data base as discussed in Section 2.2.5 and subjected to a screening process for the groundwater pathway. The process involved calculating a screening dose that was then compared to a screening dose criteria. Screening doses were calculated using the GWSCREEN computer code (Rood 1993a) and conservative screening parameter values and model assumptions. The methodology for GWSCREEN is described in Sections 3.3.2 and 3.3.3. For actinides, dose from the ingestion of ingrown radioactive progeny were also accounted for.

Conservative screening model assumptions were as follows:

1. No credit was taken for the rate at which waste was emplaced in the facility. All waste, including current and projected inventory, was put into the facility instantaneously. This results in the highest possible release.

2. No credit was taken for waste containment or sorption reactions in sediment surrounding the waste. This also results in the highest possible release.

3. The upper bound estimate of infiltration (10 cm/yr) was used.

4. Dose was calculated at the time of maximum concentration in groundwater at the downgradient edge of the RWMC. No credit was taken for institutional control or cover emplacement.

5. Dispersivity values were reduced by a factor of 10 from their normal values.

6. Sorption coefficient values for fission/activation products were reduced by a factor of 10 from their nominal values. For actinides, sorption coefficients were held at their nominal value because a lower sorption coefficient for actinides does not always result in high dose because lower transit times result in less progeny ingrowth.

Sorption coefficient data for actinides are listed in Table 3-7. For actinides not reported in this table, sorption coefficients are documented in Rood (1993b). Model assumption 1 above results in a radionuclide leach rate that is given by

$$J = \frac{I}{\theta T} \times Q_o e^{-\left(\frac{I}{\theta T} + \lambda\right)t} \qquad (3\text{-}30)$$

where

J = radionuclide release rate (Ci/yr)

I = infiltration rate (m/yr)

θ = volumetric water content in source (0.34)

T = thickness of waste (6.1 m)

Q_o = entire waste inventory (Ci)

λ = radioactive decay constant (per yr)

t = time (yr).

The unsaturated zone water travel time incorporated the latest understanding of water transport mechanisms in the unsaturated zone and the following conservative assumptions:

1. Water transit time in the basalt is relatively instantaneous and is considered to be zero.

2. Only transport through four sedimentary interbeds is considered.

3. The upper bound infiltration estimate over the Site is 10 cm/yr. This estimate represents a 21.5-year water travel time.

4. Unit gradient conditions exist for three out of the four interbeds. A measured gradient exists for the fourth interbed (C-D).

The unsaturated data are summarized in Table 3-8 and discussed in Section 3.2. The transit time, T_a, through each interbed was calculated by

$$T_a = \frac{T}{\frac{K(\theta)}{\theta}\frac{dH}{dZ}} \qquad (3\text{-}31)$$

where

T = thickness of the interbed (m)

K(θ) = hydraulic conductivity (m/yr)

θ = moisture content in the interbed (m^3/m^3)

dH/dZ = total hydraulic gradient (m/m).

Unit gradient conditions were assumed for Interbeds B-C, D-E, and E-F. Therefore, the hydraulic conductivity was set equal to the upper bound estimate of the net infiltration rate of 0.1 m/yr. For Interbed C-D, a measured hydraulic gradient (McElroy 1990) and representative moisture characteristic curves (Magnuson and McElroy 1993) were incorporated in the calculation. Using the upper bound infiltration estimate and measured hydraulic gradients in the C-D interbed resulted in an unsaturated water travel time of 21.5 years.

Table 3-8. Unsaturated transport data for sedimentary interbeds and 10 cm/yr net infiltration.

Interbed	Thickness (m)	K(θ) (m/yr)	Total hydraulic gradient (m/m)	Moisture content	Travel time (y)
B-C	4	0.1	1.0	0.086[a]	3.4
C-D	5.2	0.1	4.5	0.38[b]	4.4
D-E	1.8	0.1	1.0	0.41[a]	7.5
E-F	1.5	0.1	1.0	0.41[a]	6.2
Total	12.5	---	---	0.172[c]	21.5

a. Based on unit gradient assumption and estimated representative moisture characteristic curves from Magnuson and McElroy (1993).

b. Estimated representative in situ moisture content from Magnuson and McElroy (1993).

c. This value was calculated based on the 21.5-year travel time, 0.1-m/yr infiltration, and 12.5-m thickness

The average moisture content in the interbeds was calculated by

$$\theta_a = \frac{T_w I}{T} \qquad (3\text{-}32)$$

where

T_w = water travel time (yr)

I = net infiltration rate (0.1 m/yr).

Many of the actinides have long decay chains and often the dose contribution from the progeny is higher than the dose given by the parent. For this reason, calculations must consider the ingrowth of radioactive progeny. Because the amount of progeny ingrowth depends on the travel time of the parent radionuclide, the use of lower sorption coefficients in the unsaturated zone and aquifer does not always yield higher doses. For this reason, sorption coefficient values in the unsaturated zone and aquifer for

actinides were held at their nominal values. Sorption coefficients in the source zone, however, were set to zero. Sorption in this region determines the release rate of the nuclide, not the transit time. Therefore, assuming a value of zero results in the highest possible release and is conservative for both actinides and fission activation products. Other transport parameter values are presented in Table 3-9.

Some of the transuranic nuclides were initially screened from the inventory based on the following criteria (Table 3-10):

- Both parent and progeny half-lives were short relative to the contaminant transit times (<10 years).

- The parent half-life was short but the progeny half-life was long, resulting in insignificant activity ingrowth of the progeny. The maximum progeny activity can be estimated by multiplying the parent activity by the ratio of the half-lives. If this activity was less than 1 nCi, then the parent was screened.

- Short-lived progeny of longer-lived parents. Short-lived progeny were included in the longer-lived parent's decay chain. Short-lived progeny do not exist in the environment without the presence of the parent.

- Insignificant inventory in RWMC (<1 nCi in the entire RWMC inventory).

Nuclides screened from the actinide inventory based on the above criteria were usually short half-lived decay products of longer lived actinide parents. The inventory cutoff of 1 nCi was chosen to represent a bounding lower limit inventory where groundwater impacts for any radionuclide would be insignificant. The 1.0 nCi inventory is equivalent to a concentration in the RWMC of about 4×10^{-21} Ci/m^3, which is significantly below activity concentration levels of naturally occurring radionuclides in soils. For fission and activation products and actinides, a screening dose was calculated based on an ingestion rate of 2 L/day for 365 days. Dose conversion factors

Table 3-9. Fixed parameter values used in the actinide screening calculations.

Parameter Description	Value	Reference
Length of source parallel to groundwater flow (m)	2.57E+02	1
Width of source perpendicular to groundwater flow (m)	1.2E+02	1
Thickness of source (m)	6.1E+00	1
Infiltration rate (m/yr)	1.0E-01	2
Volumetric water content in source	3.4E-01	3
Volumetric water content in unsaturated zone	1.7E-01	2
Bulk density at source (g/cm^{-3})	1.5E+00	7
Bulk density in unsaturated zone (interbeds) (g/cm^{-3})	1.5E+00	7
Bulk density of aquifer (g/cm^{-3})	1.9E+00	7
Porosity of aquifer	1.0E-01	1
Dispersivity x direction (m)	9.1E-01	4
Dispersivity y direction (m)	4.0E-01	4
Pore velocity (m/yr)	5.6E+02	6
Well screen thickness (m)	1.2E+01	5
Unsaturated thickness (interbeds) (m)	1.2E+01	2
Distance to receptor along x axis (m)	2.29E+02	2
Distance to receptor along y axis (m)	0.0E+00	2

1. Based on the length, width, and depth of Pits 17 to 20.

2. The distance to the receptor is measured from the center of the source. The source is 257 m long; therefore, the distance to the downgradient edge of the source is 257 ÷ 2 = 129 m.

3. Baca et al. (1992); McElroy and Hubbel (1990).

4. Arnett et al. (1990). Value divided by 100 for conservatism.

5. Seitz (1991).

6. Wood (1989).

7. EG&G Idaho (1984).

Table 3-10. Belowground pit (BGP) and soil vault row (SVR) inventories for actinides that were excluded from the screening calculations for short parent and progeny half lives, (<10 years), short parent half-life and long progeny half-life resulting in insignificant activity of progeny, or insignificant inventory in the RWMC (<1 nCi).

Nuclide	BGP parent (Ci)	SVR parent (Ci)	Total	Nuclide	BGP parent (Ci)	SVR parent (Ci)	Total
U240	5.154E-15	0.000E+00	5.154E-15	AC227	4.434E-01	7.718E-07	4.434E-01
NP240M	5.154E-15	0.000E+00	5.154E-15	TL207	4.440E-01	7.684E-07	4.440E-01
PU244	5.161E-15	0.000E+00	5.161E-15	PO215	4.453E-01	7.706E-07	4.453E-01
AM245	3.558E-14	0.000E+00	3.558E-14	RN219	4.453E-01	7.706E-07	4.453E-01
CM242	3.306E-09	3.521E-13	3.306E-09	PB211	4.453E-01	7.706E-07	4.453E-01
CM248	2.019E-08	0.000E+00	2.019E-08	RA223	4.453E-01	7.706E-07	4.453E-01
CM245	7.280E-07	0.000E+00	7.280E-07	BI211	4.453E-01	7.706E-07	4.453E-01
CM246	8.232E-07	0.000E+00	8.232E-07	PU238	7.991E-01	1.718E-03	8.008E-01
PU236	1.409E-06	0.000E+00	1.409E-06	TH231	1.204E+00	2.636E-03	1.207E+00
TL209	1.446E-06	1.163E-15	1.446E-06	TL208	5.882E+00	2.715E-15	5.882E+00
CM243	1.528E-06	0.000E+00	1.528E-06	PO210	8.583E+00	2.227E-11	8.583E+00
U237	9.702E-06	6.872E-07	1.039E-05	PB210	8.788E+00	2.397E-11	8.788E+00
PO213	6.548E-05	5.268E-14	6.548E-05	BI210	8.793E+00	2.398E-11	8.793E+00
RA225	6.690E-05	5.382E-14	6.690E-05	PO212	1.049E+01	4.842E-15	1.049E+01
AC225	6.692E-05	5.384E-14	6.692E-05	PO214	1.361E+01	1.088E-10	1.361E+01
FR221	6.692E-05	5.384E-14	6.692E-05	PB214	1.361E+01	1.088E-10	1.361E+01
BI213	6.692E-05	5.384E-14	6.692E-05	BI214	1.361E+01	1.088E-10	1.361E+01
AT217	6.692E-05	5.384E-14	6.692E-05	PO218	1.362E+01	1.088E-10	1.362E+01
PB209	6.693E-05	5.384E-14	6.693E-05	RN222	1.362E+01	1.088E-10	1.362E+01
CF250	2.144E-04	0.000E+00	2.144E-04	U232	1.417E+01	0.000E+00	1.417E+01
PO211	1.247E-03	2.158E-09	1.247E-03	TH228	1.630E+01	7.521E-15	1.630E+01
NP239	3.412E-03	0.000E+00	3.412E-03	RA224	1.637E+01	7.558E-15	1.637E+01
CM244	5.590E-03	1.264E-05	5.603E-03	BI212	1.637E+01	7.558E-15	1.637E+01
FR223	6.119E-03	1.065E-08	6.119E-03	PB212	1.637E+01	7.558E-15	1.637E+01
PA233	1.142E-02	5.921E-07	1.142E-02	RN220	1.637E+01	7.558E-15	1.637E+01
PA234	2.773E-02	7.552E-04	2.849E-02	PO216	1.637E+01	7.558E-15	1.637E+01
AC228	3.050E-02	2.934E-15	3.050E-02	PA234M	2.133E+01	5.809E-01	2.191E+01
RA228	3.050E-02	2.934E-15	3.050E-02	TH234	2.133E+01	5.809E-01	2.191E+01
TH227	4.383E-01	7.586E-07	4.383E-01				

were obtained from DOE (1988b). A screening criteria of 0.4 mrem/yr was selected as a cutoff. The value of 0.4 mrem is a factor of 10 less than the limit established for manmade beta-gamma emitting nuclides in community drinking water systems. Regulatory limits on actinides are not strictly based on radiological dose. For community drinking water systems, alpha-emitting radionuclides are limited by a gross activity level of 15 pCi/L excluding Rn-222 and uranium. Uranium isotopes are limited by a maximum concentration limit of 20 μg/L (proposed), and Ra-226-228 isotopes are limited by a maximum concentration limit of 5 pCi/L. Because dose is proportional to concentration, a simplifying screening procedure was employed that only considered the radiological dose of both alpha and beta-gamma emitting nuclides. For additional conservatism, the radiological dose limit of 4 mrem/yr (for community drinking water systems) was divided by 10. Therefore, nuclides with a screening CEDE of <0.4 mrem/yr were eliminated from further consideration.

Radioactivity transfer to food crops was not evaluated in the screening evaluation. In general, the dose from the ingestion of food contaminated by irrigation water is less than through direct ingestion of groundwater. The conservative assumptions and low dose criteria used in the screening process ensured all significant dose-contributing nuclides were included in the detailed analysis.

Screening factor dose for fission and activation products are presented in Table 3-11. Strontium 90, H-3, C-14, I-129, K-40, Ni-59, and Tc-99 all exceeded the 0.4 mrem/yr dose criteria. For the actinides (Table 3-12), U-238 was the largest contributor followed by U-234, U-235, Ra-226, Np-237, Pu-239, Th-232, and Th-230. All these nuclides had CEDE values above the screening level value of 0.4 mrem/yr.

3.4 Pathways and Scenarios

Exposure pathways are the link between contaminated environmental media and the exposure of a receptor. Figure 3-20 summarizes the exposure pathways from LLW disposed of in the RWMC SDA. This diagram does not include processes that recycle radionuclides, such as plant senescence, because these processes

Table 3-11. Fission and activation product screening factors for the RWMC inventory from 1984 to 1993 and forecasted inventory from 1993 to 2020.

Radionulide[a]	Pits (1984-93) (Ci)	Vaults (1984-93) (Ci)	Projected (1993-2020) (Ci/yr)	Projected (1993-2020) (Ci/yr)	Total (Ci)	Half-life (yr)	DCF (rem/μCi)	Kd (mL/g)	Reference[b]	Screening Dose (mrem)
SR-90	1.464E+02	0.000E+00	3.168E+01	8.497E+00	1.23E+03	2.860E+01	1.3E-01	2.0E+00	1&6	1.43E+04
H-3 (BE BLK)	0.000E+00	0.000E+00	0.000E+00	6.133E+04	1.66E+06	1.230E+01	6.3E-05	0.0E+00	5	1.36E+04
SR-90 MFP	5.675E+02	0.000E+00	9.435E+00	0.000E+00	8.22E+02	2.860E+01	1.3E-01	2.0E+00	1&6	9.58E+03
SR-90 UBG	5.085E+01	2.229E+01	2.247E-01	2.229E+01	6.81E+02	2.860E+01	1.3E-01	2.0E+00	1&6	7.93E+03
SR-90 MAP	1.140E+02	0.000E+00	5.036E+00	0.000E+00	2.50E+02	2.860E+01	1.3E-01	2.0E+00	1&6	2.91E+03
H-3	2.972E+03	3.300E+05	6.100E+00	2.391E+00	3.33E+05	1.228E+01	6.3E-05	0.0E+00	5	2.70E+03
NI-59	0.000E+00	1.340E+03	0.000E+00	2.933E+02	9.26E+03	7.500E+04	2.0E-04	1.0E+02	2	1.79E+02
C-14	6.449E-02	9.985E+00	3.968E-03	2.293E+00	7.21E+01	5.730E+03	2.1E-03	0.0E+00	5	6.67E+01
K-40	1.691E-01	0.000E+00	2.156E-02	4.021E-02	1.84E+00	1.277E+09	1.9E-02	5.5E+00	3	1.52E+01
I-129	1.405E-07	5.370E-04	2.855E-03	6.713E-05	7.94E-02	1.570E+07	2.8E-01	5.0E-02	4	9.81E+00
TC-99	2.974E-04	7.253E-03	7.125E-05	4.145E-02	1.13E+00	2.130E+05	1.3E-03	1.5E+00	3	6.46E-01
NI-63	1.158E+04	4.622E+05	9.631E-01	4.422E+04	1.67E+06	1.001E+02	5.4E-04	1.0E+02	2	9.26E-02
NB-94	6.900E-06	3.970E-02	8.625E-07	4.963E-03	1.74E-01	2.030E+04	5.1E-03	3.5E+02	3	2.04E-02
AG-108M	1.000E-03	0.000E+00	0.000E+00	0.000E+00	1.00E-03	1.270E+02	7.5E-03	4.5E+01	3	4.29E-25
IR-192	2.700E-03	0.000E+00	1.394E-03	0.000E+00	4.03E-02	2.022E-01	5.3E-03	0.0E+00	5	6.52E-34
CS-137	9.872E+02	3.084E+03	9.537E+01	3.250E+02	1.54E+04	3.017E+01	5.0E-02	2.0E+01	2	7.32E-35
CS-137 mfp	5.675E+02	0.000E+00	9.435E+00	0.000E+00	8.22E+02	3.017E+01	5.0E-02	2.0E+01	2	3.91E-36
CS-137 ubg	5.085E+01	2.229E+01	2.247E-01	2.229E+01	6.81E+02	3.017E+01	5.0E-02	2.0E+01	2	3.24E-36
Cs-137 map	1.140E+02	0.000E+00	5.036E+00	0.000E+00	2.50E+02	3.017E+01	5.0E-02	2.0E+01	2	1.19E-36
SE-75	4.544E-02	0.000E+00	4.555E-03	2.101E-03	2.25E-01	3.282E-01	8.8E-03	1.0E+00	1	4.45E-39
I-125	1.155E-03	0.000E+00	0.000E+00	0.000E+00	1.16E-03	1.648E-01	3.8E-02	5.0E-02	4	1.26E-43
CO-60	8.254E+03	9.429E+05	2.663E+01	2.338E+05	7.26E+06	5.271E+00	2.6E-02	5.0E+01	6	7.54E-50
CO-60 Be blk	0.000E+00	0.000E+00	0.000E+00	4.763E+03	1.29E+05	5.270E+00	2.6E-02	5.0E+01	6	1.34E-51
FE-55	3.971E+03	1.483E+05	1.107E+01	4.097E+04	1.26E+06	2.700E+00	5.8E-04	2.5E+01	3	5.00E-52
NI-63 Be blk	0.000E+00	0.000E+00	0.000E+00	3.758E+02	1.01E+04	1.000E+02	5.4E-04	1.0E+02	2	8.41E-57
SB-125	5.768E+01	2.831E+03	3.363E+00	8.699E+02	2.65E+04	2.770E+00	5.8E-03	4.5E+01	3	4.83E-93
CR-51	4.522E+03	3.194E+04	5.435E+01	8.317E+03	2.62E+05	7.590E-02	1.3E-04	1.0E+00	6	0.00E-00
S-35	1.302E-04	0.000E+00	0.000E+00	0.000E+00	1.30E-04	2.396E-01	6.5E-04	7.5E+00	3	0.00E-00
NA-22	7.114E-02	0.000E+00	1.824E-02	0.000E+00	5.64E-01	2.602E+00	1.2E-02	1.0E+02	3	0.00E-00
EU-152	6.617E+00	3.900E+00	4.920E-03	0.000E+00	1.06E+01	1.360E+01	6.0E-03	6.5E+02	3	0.00E-00
CD-109	1.317E-02	0.000E+00	1.365E-03	0.000E+00	5.00E-02	1.271E+00	1.2E-02	6.5E+02	3	0.00E-00
AG-110	7.483E-02	0.000E+00	2.973E-03	0.000E+00	1.55E-01	7.791E-07	0.0E+00	4.5E+01	3	0.00E-00
AG-110M	1.944E+00	1.686E-03	4.876E-03	1.543E+00	4.37E+01	6.845E-01	1.1E-01	4.5E+01	3	0.00E-00
BA-133	1.000E-06	0.000E+00	0.000E+00	0.000E+00	1.00E-06	1.050E+01	3.2E-03	6.0E+01	3	0.00E-00
BA-140	2.191E+00	0.000E+00	0.000E+00	4.620E-02	3.44E+00	3.504E-02	8.4E-03	6.0E+01	3	0.00E-00
CA-45	1.015E-03	0.000E+00	1.269E-04	0.000E+00	4.44E-03	4.458E-01	3.0E-03	4.0E+00	3	0.00E-00
CE-141	3.021E+00	0.000E+00	1.930E-01	6.496E-02	9.99E+00	8.904E-02	2.6E-03	1.0E+02	2	0.00E-00
CE-144	2.871E+02	6.362E+02	1.647E+01	2.362E+00	1.43E+03	7.789E-01	2.0E-02	1.0E+02	2	0.00E-00
CO-58	6.320E+01	4.469E+05	2.766E+00	4.746E+04	1.73E+06	1.940E-01	3.5E-03	5.0E+01	6	0.00E-00
CS-134	6.606E+01	2.041E+02	2.922E+00	3.190E+00	4.35E+02	2.062E+00	7.4E-02	2.0E+01	2	0.00E-00
EU-154	5.368E+00	5.850E-01	3.070E-01	7.312E-02	1.62E+01	8.800E+00	9.1E-03	6.5E+02	3	0.00E-00
EU-155	1.601E+00	3.850E-01	3.392E-01	4.812E-02	1.24E+01	4.960E+00	1.3E-03	6.5E+02	3	0.00E-00

Table 3-11. (continued).

Radionulide[a]	Pits (1984-93) (Ci)	Vaults (1984-93) (Ci)	Projected (1993-2020) (Ci/yr)	Projected (1993-2020) (Ci/yr)	Total (Ci)	Half-life (yr)	DCF (rem/μCi)	Kd (mL/g)	Reference[b]	Screening Dose (mrem)
FE-59	4.311E-01	3.660E+03	2.890E-03	2.160E+03	6.20E+04	1.223E-01	6.6E-03	2.5E+01	3	0.00E-00
GD-153	0.000E+00	1.300E+00	0.000E+00	0.000E+00	1.30E+00	6.619E-01	1.1E-03	6.5E+02	3	0.00E-00
HF-175	4.140E-02	2.421E+03	5.175E-03	3.026E+02	1.06E+04	1.161E-01	4.3E-03	1.5E+03	3	0.00E-00
HG-203	1.000E-06	0.000E+00	4.350E-05	4.021E-02	1.09E+00	1.277E-01	1.0E-02	1.0E+01	3&1	0.00E-00
LA-140	2.587E+00	0.000E+00	1.653E-01	5.995E-02	8.67E+00	3.504E-02	7.7E-03	6.5E+02	3	0.00E-00
MN-54	9.976E+01	3.108E+05	7.973E+01	6.818E+04	2.15E+06	8.567E-01	2.7E-03	1.0E+01	2	0.00E-00
NB-95	3.974E+01	3.893E+03	2.096E+00	1.257E+03	3.79E+04	9.606E-02	2.0E-03	3.5E+02	3	0.00E-00
P-32	8.550E-03	0.000E+00	0.000E+00	0.000E+00	8.55E-03	3.915E-02	7.7E-03	3.5E+00	3	0.00E-00
PM-147	6.000E-03	2.390E+00	0.000E+00	2.988E-01	1.05E+01	2.623E+00	9.5E-04	6.5E+02	3	0.00E-00
PR-144	2.411E+02	0.000E+00	1.359E+01	9.857E-02	6.11E+02	3.288E-05	1.1E-04	6.5E+02	3	0.00E-00
RB-86	3.000E-05	0.000E+00	0.000E+00	0.000E+00	3.00E-05	5.112E-02	9.4E-03	6.0E+01	3	0.00E-00
RH-106	1.208E+02	0.000E+00	6.621E+00	2.179E-01	3.05E+02	9.488E-07	0.0E+00	6.0E+01	3	0.00E-00
RU-103	2.501E-01	2.384E-27	2.512E-02	4.205E-02	2.06E+00	1.078E-01	2.7E-03	3.5E+02	3	0.00E-00
RU-106	1.248E+02	2.907E-01	4.210E+04	4.128E-01	1.14E+06	1.009E+00	2.1E-02	3.5E+02	3	0.00E-00
SB-124	6.884E-03	1.800E-01	1.205E-03	4.021E-02	1.31E+00	1.649E-01	9.3E-03	4.5E+01	3	0.00E-00
SC-46	1.047E-01	4.995E+01	1.239E-02	8.313E+01	2.29E+03	2.296E-01	5.6E-03	1.0E+03	3	0.00E-00
SN-113	3.300E-03	2.424E+01	8.324E-03	1.852E+01	5.25E+02	3.153E-01	2.7E-03	2.5E+02	3	0.00E-00
SN-119M	0.000E+00	8.761E+03	0.000E+00	2.505E+03	7.64E+04	8.027E-01	1.2E-03	2.5E+02	3	0.00E-00
SR-89	2.975E+01	3.017E+02	2.694E-01	0.000E+00	3.39E+02	1.385E-01	8.7E-03	2.0E+00	1&6	0.00E-00
SR-92	1.600E-03	0.000E+00	2.000E-04	0.000E+00	7.00E-03	3.094E-04	1.9E-03	2.0E+00	1&6	0.00E-00
TA-182	1.350E-01	1.989E+04	9.562E-04	2.298E+03	8.19E+04	3.144E-01	6.0E-03	6.5E+02	3	0.00E-00
ZN-65	2.586E+01	1.005E+03	6.391E-01	3.984E+02	1.18E+04	6.696E-01	1.4E-02	4.0E+01	3	0.00E-00
ZR-NB-95	5.952E-01	0.000E+00	2.083E+00	6.101E+02	1.65E+04	1.754E-01	3.4E-03	3.0E+03	3	0.00E-00

a. Be Blk = nuclide in beryllium reflector blocks
MFP = mixed fission products
MAP = mixed activation products
UBG = unidentified beta gamma

b. Sorption coefficient values were divided by 10 for screening calculations. These values were used for both sediment and basalt.
1 = Del Debbio and Thomas (1989)
2 = EG&G Idaho (1984) Appendix C, p. 25, Table C-3.
3 = Baes et al. (1984)
4 = DOE (1987) p. C-11
5 = Assumed (these elements are not known to adsorb)
6 = Schmaltz (1972)

Table 3-12. Belowground pit and soil vault row inventories for actinides and the screening level CEDE calculated using GWSCREEN

Nuclide	Pits[a] inventory (Ci)	Vaults[a] inventory (Ci)	Pits[b] forecasted (Ci/yr)	Vaults[b] forecasted (Ci/yr)	Total activity (Ci)	Screening CEDE (mrem)
U238	2.133E+01	5.809E-01	1.960E-01	1.581E-02	2.763E+01	5.8E+03
U234	2.040E-01	1.391E-04	4.747E-04	1.923E-02	7.362E-01	3.9E+02
U235	1.204E+00	2.636E-03	3.474E-03	5.025E-07	1.300E+00	3.4E+02
RA226	1.362E+01	1.088E-10	1.257E-02	0.000E+00	1.396E+01	1.8E+02
NP237	1.142E-02	5.922E-07	2.211E-03	1.513E-08	7.112E-02	4.8E+01
PU239	1.940E+00	1.065E-01	1.034E-02	2.400E-04	2.332E+00	1.7E+01
TH232	3.445E-02	4.825E-15	2.279E-05	0.000E+00	3.507E-02	9.8E+00
TH230	1.809E-02	2.175E-08	0.000E+00	0.000E+00	1.809E-02	3.0E+00
PA231	5.828E-03	1.882E-06	0.000E+00	0.000E+00	5.830E-03	8.0E-02
U233	1.684E-02	4.781E-11	0.000E+00	0.000E+00	1.684E-02	5.4E-02
AM241	1.388E+00	2.802E-03	1.025E-02	2.236E-04	1.674E+00	2.1E-02
U236	4.225E-03	5.213E-06	0.000E+00	1.370E-07	4.234E-03	9.6E-03
PU241	3.955E-01	2.801E-02	2.675E-03	1.620E-03	5.395E-01	6.8E-03
AM243	3.412E-03	0.000E+00	2.550E-05	0.000E+00	4.101E-03	6.2E-03
PU240	3.151E-01	7.482E-03	4.656E-04	6.870E-05	3.370E-01	3.3E-03
PU242	9.098E-04	1.164E-07	6.189E-06	3.125E-09	1.077E-03	1.8E-03
TH229	6.689E-05	5.381E-14	0.000E+00	0.000E+00	6.689E-05	2.2E-05
CF252	1.055E-05	0.000E+00	0.000E+00	0.000E+00	1.055E-05	1.3E-05
CF249	2.498E-04	0.000E+00	0.000E+00	0.000E+00	2.498E-04	1.9E-07
BK249	2.453E-09	0.000E+00	0.000E+00	0.000E+00	2.453E-09	2.7E-13

a. Reported inventory as of 1993 (decay not included).

b. Forecasted inventory from 1993 to 2020.

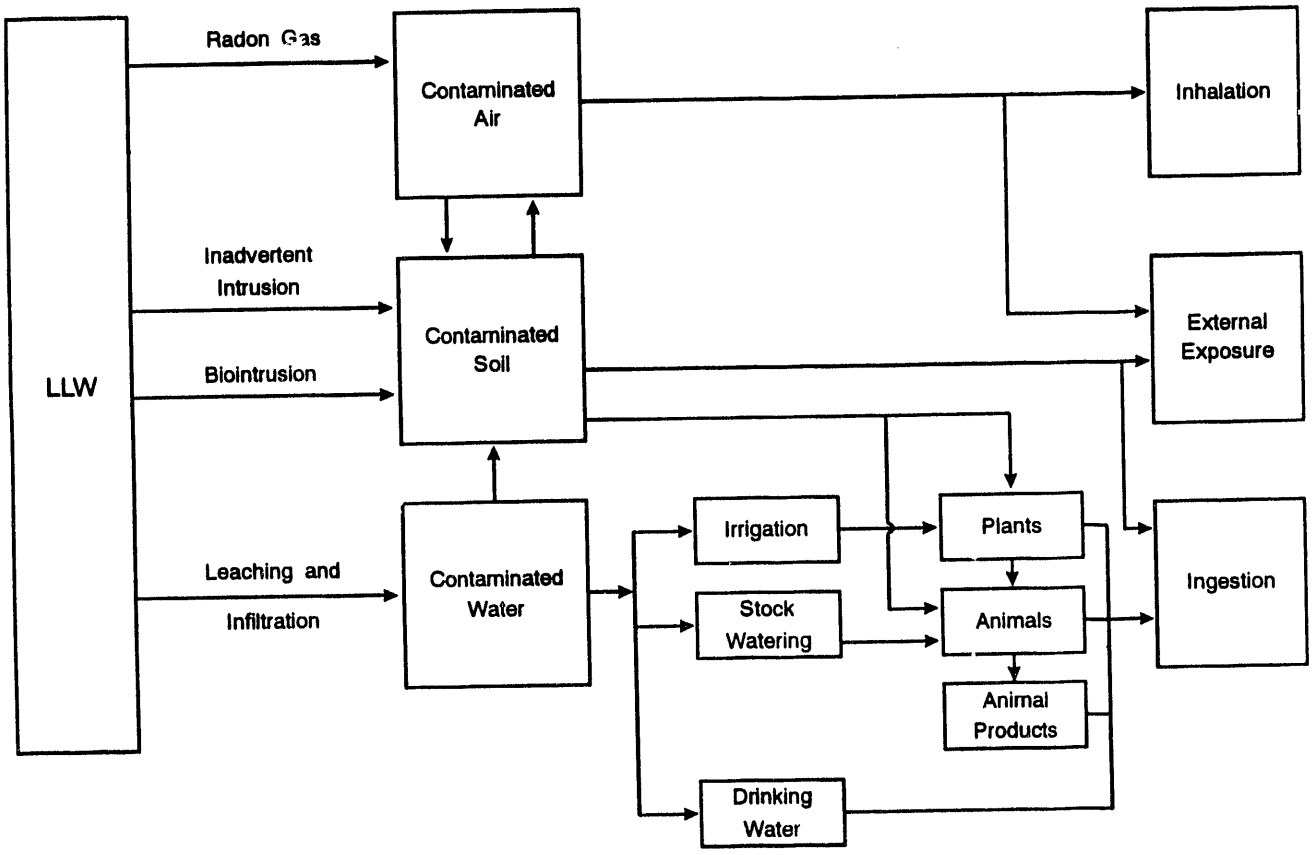

Figure 3-20. Exposure pathways at the RWMC.

tend to dilute the amount of radioactive material available for uptake when compared to direct uptake pathways.

Environmental monitoring has been performed at the RWMC since 1960, and special studies are also periodically conducted. RESL conducts radioecological studies at and around the RWMC. Many of the RESL studies have focused on radionuclide transport via biota. The results of the monitoring and special studies indicate that the greatest potential for the transport of radionuclides to a member of the public is via atmospheric transport of resuspended soil and groundwater transport of radionuclides leached from buried waste. Therefore, this performance assessment focuses on these two routes of exposure for dose assessments for members of the public. For intruders, direct exposure to the waste is assumed, either through excavation or drilling. For excavation and drilling, pathways are evaluated and doses are calculated from ingestion, inhalation, and external exposure to radioactive material.

Two general types of scenarios are evaluated in this performance assessment: (1) doses to members of the public, and (2) doses to inadvertent intruders (see Figure 3-21). Doses to members of the public are evaluated for two subscenarios: atmospheric transport and groundwater transport. To meet the requirements in DOE Order 5820.2A, doses to intruders are also evaluated for two subscenarios: acute exposures and chronic exposures. The receptors for the member of the public dose assessments are located at the INEL Site boundary during operations and institutional control and at 100 m from the RWMC boundary during post-institutional control. The intruder is assumed to reside on the RWMC SDA. The following sections describe the atmospheric, all pathways, intruder, and drinking water scenarios used to evaluate dose impacts.

3.4.1 Atmospheric Scenario

3.4.1.1 Operational and Institutional Control Periods. This section describes the methodology and data used to calculate doses from atmospheric emissions from the RWMC during the operational and institutional control periods. These doses are based on the diffuse emissions dose assessments

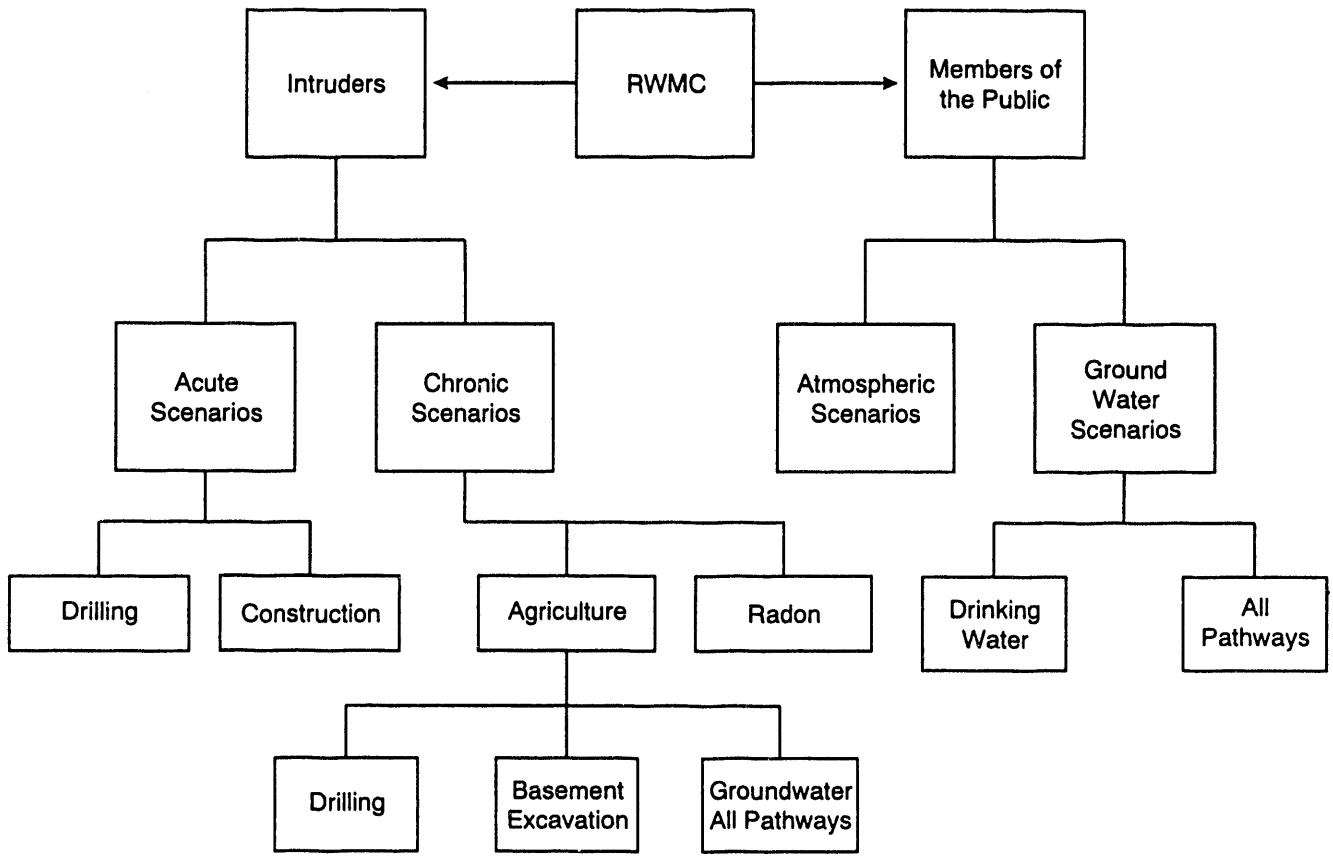

Figure 3-21. Scenarios at the RWMC.

performed for the INEL National Emission Standard for Hazardous Air Pollutants (NESHAP) Annual Report (DOE 1993).

During the operational and institutional control periods, the RWMC will be actively maintained and monitored. Therefore, it is reasonable to postulate that soil contamination levels will not be higher than current levels. In reality, soil contamination will decrease because of environmental remediation activities at the RWMC. DOE (1993) describes the existing soil contamination levels at the RWMC and the areal extent of this contamination. The radionuclide soil concentrations at contaminated areas were estimated based on sampling studies or field survey measurements. The areal extent of each area was also estimated based on field observations and measurements. These data were used to estimate an annual release rate for each radionuclide in units of curies per year. The resuspension rate constant used in this analysis was based on the mass loading model. Appendix B contains additional information on the resuspension rate constant.

As required for NESHAP compliance dose assessments, the receptor location for the operational and institutional control periods was an actual residence located near the INEL Site boundary, 8 km south-southwest of the RWMC (DOE 1993). The atmospheric data, environmental data, and the computer code used in the analyses are also discussed in DOE (1993).

3.4.1.2 Post-Institutional Control Period. This section describes the methodology used to calculate doses from atmospheric emissions of radionuclides from the RWMC SDA after institutional control. The scenario was based on biointrusion contaminating the surface soil at the RWMC SDA. This contaminated surface soil was blown offsite to a member of the public 100 m from the boundary of the RWMC SDA. This hypothetical receptor ate contaminated food, was immersed in contaminated air, breathed contaminated air, and was exposed to contaminated ground surfaces.

The scenario used for this analysis started with the LLW inventory disposed of in the RWMC LLW disposal locations from 1984 to 1993 and was augmented with the forecasted additions for 1994 to 2020 (see Appendix A). A portion of the inventory was brought to the surface through biointrusion and

distributed over the RWMC, forming a large area source of radioactive material that could be resuspended by wind.

The contaminated material was then blown offsite to a hypothetical member of the public located 100 m from the RWMC. The receptor was located in the east-northeast sector, the sector that yielded the largest annual average sector-averaged air concentration at 100 m from the RWMC, using a ground-level release and meteorological data collected from 1987 to 1991 at CFA (Leonard 1992). The sector with the highest air concentration will also yield the highest dose. The sector was determined by calculating air concentrations in all 16 sectors and choosing the sector with the largest value.

For this analysis, the GENII computer code (Version 1.485) (Napier et al. 1988) was used to model the doses resulting from RWMC releases. Although GENII may model both acute and chronic releases to the atmosphere, only the chronic option was exercised in this analysis. The output from GENII is the EDE, which includes the 50-year CEDE from internal exposure through the ingestion and inhalation pathways and the external EDE from ground deposition and air immersion. Napier et al. (1988) completely describes the GENII computer code. The assessments done for operational and institutional control periods (DOE 1993) and GENII use the same pathways.

Inhalation doses were calculated based on exposure to contaminated air for 1 year (8,760 hours). Two inhalation rates were evaluated: 8,030 and 5,840 m^3/yr. ICRP-23 presents 8,030 m^3/yr as the inhalation rate for Reference Man (ICRP 1975). Data presented in Konz et al. (1989) were used to derive an inhalation rate of 5,840 m^3/yr, based on a person spending 11.2 h/day at rest, 11.2 h/day at light activity, 1.4 h/day at moderate activity, and 0.22 h/day at heavy activity. The corresponding inhalation rates for average adults are 0.5, 0.6, 2.1, and 3.9 m^3/h. This yields a time-weighted inhalation rate of 16 m^3/day or 5,840 m^3/yr.

Ground surface doses were calculated assuming 100 years of buildup of radionuclides in the surface soil because of atmospheric deposition. Two shielding factors were evaluated: 0.7 and 0.36. The 0.7 shielding factor is from NRC (1977) and corresponds to the shielding factor used for the maximally

exposed individual. The 0.36 shielding factor was calculated using data presented in Konz et al. (1989), based on a person spending 16.75 h/day at home and indoors and 0.23 h/day at home and outdoors. The corresponding reduction factors for these activities are 0.5 and 1.0. The remaining 7.02 h/day was associated with activities conducted at work and indoors, at work and outdoors, in transit, and activities classified as "other" in Konz et al. (1989). These activities were assigned a reduction factor of 0.0.

Air immersion doses were calculated based on exposure to contaminated air for 1 year, using shielding factors of 0.7 and 0.36, as in the ground surface analyses (see NRC 1977).

Ingestion doses were calculated based on the consumption of contaminated produce, leafy vegetables, milk, and meat. The conceptual model for ingestion doses begins with radionuclides that are deposited on forage, soil, produce, and leafy vegetables. Radionuclides deposited on forage are subsequently transferred through the food chain to meat and milk and then to humans. Radionuclides deposited on produce and leafy vegetables are also consumed by humans. Radionuclides deposited on soil are transferred to forage, produce, and leafy vegetables through the mechanism of root uptake and then transferred to humans through ingestion of contaminated meat, milk, product, and leafy vegetables. The parameters used to calculate food chain doses are contained in Napier et al. (1988). The values for the concentration ratios for forage and crops and the transfer coefficients for milk and meat are contained in Figures B-1 through B-4 of Appendix B. The concentration ratios for forage and crops are in terms of dry weight.

Two diets were evaluated: (1) a diet developed by Rupp (1980) and based on a 1965 U.S Department of Agriculture (USDA) survey and (2) a diet developed by Yang and Nelson (1984, 1986) and based on a 1977 to 1978 USDA survey (see Table 3-13). The Rupp diet was the default diet used in the EPA's NESHAPs Environmental Impact Statement (EPA 1989). The Yang and Nelson diet represents a more realistic diet than the Rupp diet because it is based on a later dietary survey. Dietary fractions representative of rural agricultural areas were used (EPA 1989). Based on the data in EPA (1989), 70% of the receptor's vegetables and produce, 40% of the milk, and 44% of the meat were produced locally.

Table 3-13. Alternative human diets.

Food product	Rupp diet	Yang and Nelson diet
Produce (kg/yr)	176	94
Leafy vegetables (kg/yr)	18	17
Milk (L/yr)	112	89
Meat (kg/yr)	85	55

The dose conversion factors used in this analysis are from the GENII library, which uses the most conservative dose conversion factors contained in DOE (1988b and 1988c).

Two biointrusion mechanisms were examined as potential ways to bring contaminated material to the surface: intrusion by burrowing animals and intrusion by plant roots. Groves and Keller (1983) identified 10 species of small mammals nesting on or near the RWMC. Four species were the most numerous: deer mice (Peromyscus maniculatus), montane voles (Microtus montanus), Ord's kangaroo rats (Dipodomys ordii), and Townsend's ground squirrels (Spermophilus townsendii). Reynolds and Wakkinen (1987) studied the burrow depths of these four species in undisturbed soils and the maximum reported burrow depth for undisturbed soil was 138 cm for a Townsend's ground squirrel. A 1988 study by Reynolds and Laundre examined the burrow depths of the same species in both disturbed and undisturbed soils on the INEL. The maximum burrow depth in disturbed soils documented in Reynolds and Laundre (1988) was 140 cm was for a Townsend's ground squirrel. None of the deer mice burrows extended past 60 cm, none of the montane vole burrows extended past 70 cm, and none of the Ord's kangaroo rat burrows extended past 100 cm.

At maximum erosion, there is 240 cm of cover left over the pits and trenches and 330 cm of cover left over the soil vaults. Based on the site-specific studies in Reynolds and Wakkinen (1987) and Reynolds and Laundre (1988) that report burrow depths are not observed in undisturbed or disturbed soils at the INEL greater than 140 cm deep, intrusion by burrowing small mammals is highly unlikely and was removed from further consideration. The

authors acknowledge that investigators at other sites have observed different results for other species of small mammals (e.g., McKenzie et al. 1982). These other studies were considered in evaluating intrusion by the burrowing small mammal pathway; however, preference was given to the site-specific studies based on the guidance provided in Dodge et al. (1991).

In contrast to burrowing mammals, harvester ants (Pogonomyrmex salinus) burrow deep enough to encounter the waste. For example, Blom et al. (1991) states that harvester ants have been found as deep as 2.7 m in Wyoming and at the Hanford Site. To account for the intrusion of harvester ants into the waste, a model similar to that in Kennedy et al. (1985) was constructed. In contrast to burrowing small mammals, no site-specific data for harvester ant burrow depths exist; therefore, data from Kennedy et al. (1985) were used in the model.

The model was based on harvester ants burrowing into the waste and bringing contaminated material to the surface. The volume of contaminated material that a single harvester ant colony brought to the surface was calculated using the burrow volume and the fraction of the burrow that was deep enough to encounter the waste. Because the waste was at depths greater than 2 m below the surface at maximum erosion, 5% of the burrow volume was estimated to encounter the waste (see Kennedy et al. 1985). An average burrow volume per colony of 0.002 m^3 was also obtained from Kennedy et al. (1985). The resulting volume of contaminated material was multiplied by the radionuclide concentration in the waste to yield the activity that a single harvester ant colony could bring to the surface. This result was multiplied by the average harvester ant colony density and the surface area of the pits and soil vaults to yield the total activity brought to the surface:

$$\begin{aligned} \textit{Activity on the surface } (Ci) = \textit{waste concentration } (Ci/m^3) \times \\ \textit{burrow volume } (m^3/\textit{colony}) \times \textit{fraction of burrow in waste} \times \\ \textit{colony density } (\textit{colonies}/m^2) \times \textit{surface area } (m^2). \end{aligned} \quad (3\text{-}33)$$

Based on data for harvester ant colony densities in big sagebrush (Artemisia tridentata) communities on the INEL (Blom et al. 1991), a density of 35.6 colonies/10,000 m^2 was used. This represents the mean density over five

locations on the INEL. For pits[a] and soil vaults,[b] surface areas of 12,000 and 890 m^2 were calculated, respectively.

The total activity brought to the surface through harvester ant burrowing was then dispersed in the environment and blown to a hypothetical receptor located 100 m from the RWMC. While this is a conservative assumption, it puts an upper bound on the material that a receptor could be exposed to through the atmospheric pathway.

The potential for biointrusion by plant roots was also evaluated. Elevated concentrations of radionuclides in plant species growing on the RWMC have been observed (Arthur 1982). These elevated concentrations were observed in areas where 0.6 to 1.8 m of cover was present over the waste. Reynolds and Fraley (1989) studied root profiles near the RWMC and determined the maximum rooting depth for big sagebrush (Artemisia tridentata) was 225 cm, for green rabbitbrush (Chrysothamnus vicidiflorus) was 190 cm, and for Great Basin wild rye (Leymus cinereus) was 200 cm.

Based on the site-specific data by Reynolds and Fraley (1989), biointrusion by plant roots of pits and soil vaults may be possible. However, biointrusion by plant roots of soil vaults is less likely because of increased cover depth.

To estimate the amount of radioactive material that plant roots could bring to the surface, a model similar to those used in GENII (Napier et al. 1988) and Kennedy et al. (1985) was constructed. First, the dominant plant species in terms of absolute cover were determined. Anderson and Inouye (1988) found that big sagebrush has an absolute cover of 13%, green rabittbush has an absolute cover of 4.3%, and Great Basin wild rye has an absolute cover of 0.013% at the INEL. Russian thistle, another potentially deep rooted species, had an absolute cover of 0.005%. Because big sagebrush is the

---

a. The volume of waste in the pits was 75,600 m^3 and the waste thickness was 6.1 m, which yielded a surface area of 12,000 m^2.

b. The volume of waste in the soil vaults was 2,700 m^3 and the waste thickness was 3.05 m, which yielded a surface area of 890 m^2.

dominant plant species, estimates of biointrusion were based on big sagebrush data.

The aboveground biomass of big sagebrush was then estimated using data from Fraley (1978), which found that big sagebrush had an aboveground biomass of 46 g/m^2 on the INEL Site. Because the waste is at depths greater than 2 m below the surface at maximum erosion, 5% of the plant roots were estimated to encounter the waste (see Kennedy et al. 1985). The activity brought to the surface by plants was estimated by multiplying the radionuclide concentration in the waste by the concentration ratio (CR), the fraction of the roots that can encounter the waste, the biomass, and the area of the pits or soil vaults.

$$\begin{aligned} Activity\ on\ the\ surface\ (Ci) = {} & waste\ concentration\ (Ci/m^3) \times \\ & \frac{1}{density\ (g/m^3)} \times fraction\ of\ roots\ in\ waste \times \\ & CR\left[\frac{Ci/g(plants)}{Ci/g(waste)}\right] \times biomass\ (g/m^2) \times area\ (m^2)\ . \end{aligned} \tag{3-34}$$

Dry weight CRs for pasture from Baes et al. (1984) were used (see Figure B-2). CRs for uptake by cheatgrass and tumbleweed (Russian thistle) of neptunium, plutonium, americium, and curium were also examined and found to be in reasonable agreement (i.e., within an order of magnitude) of the CRs from Baes et al. (1984) (see Price 1972).

The total activity brought to the surface through plant uptake was then dispersed in the environment and blown to a hypothetical receptor 100 m from the RWMC. This implies that the entire big sagebrush aboveground biomass was converted to a dispersible form. While this is a conservative assumption, it puts an upper bound on the material that a receptor could be exposed to through the atmospheric pathway.

Currently, there is no DOE policy on the time of compliance with the performance objectives contained in DOE Order 5820.2A. Therefore, the 10 mrem/yr performance objective in 40 CFR 61 was assumed to apply in perpetuity. For this reason, doses because of harvester ant burrowing and plant uptake were calculated at various points in time after site closure, beginning in 2120 and continuing to 1,000,000 years after site closure. The

year 2120 corresponds to the beginning of the post-institutional period and is the earliest time that biointrusion could occur during the post-institutional period. This is also the time when the maximum fission product and activation product inventory is available for biointrusion because fission and activation products do not contain long-lived decay series with substantial progeny ingrowth. Doses were also calculated at the year 12,000 and 1,000,000 years after site closure. These times were chosen to determine if there were any long-lived actinide decay series that could yield large doses because of progeny ingrowth over long time frames. One million years corresponds to the time when most long-lived decay series have achieved a substantial fraction of secular equilibrium; therefore, it represents a reasonable time to calculate doses.

The fraction of the root or burrow system that contacted the waste did not change as the amount of cover over the waste changed because of erosion. This fraction was held constant over time because the data in Kennedy et al. (1985) do not permit further refinement of the depth profile at depths greater than 2 m. Because the minimum depth to waste at maximum erosion was 2.4 m, the data for the fraction of the root or burrow system at 2 m were applied to all depths greater than 2 m. This approach is conservative because there is undoubtedly a depth-dependent root or burrow profile at depths greater than 2 m that would result in less biointrusion as the depth to the waste increases. However, this approach eliminates the need to consider the erosion rate in the calculations, and maximum dose can be calculated by performing a few representative assessments. In addition, every burrow system or plant over the pits was assumed to contact the waste; this is also a conservative approach.

3.4.1.3 Gaseous Releases of Tritium and Carbon-14. This analysis presents the doses for gaseous release of H-3 and C-14 using release rates based on the hydrological model used to calculate groundwater impacts. Instead of H-3 and C-14 moving downward with water, H-3 and C-14 were assumed to move upward as gases and were transported to receptors downwind of the RWMC. Doses were evaluated for two time periods: (1) the operational and institutional control period, where the receptor was an actual residence located 8,000 m south-southwest from the RWMC at the INEL Site boundary and (2) the post-institutional control period, where the receptor was located

100 m from the RWMC. During each of these periods, the peak release rates for H-3 and C-14 were used.

During the operational and institutional control time period, the peak release rate for C-14 was 0.24 Ci/yr, and the peak release rate for H-3 was 220 Ci/yr. During the post-institutional control period, the peak release rate for C-14 was 0.23 Ci/yr, and the peak release rate for H-3 was 5.3E-3 Ci/yr. The methodology and data used to evaluate H-3 and C-14 doses are the same used for the biointrusion analyses. The H-3 and C-14 dose assessments were performed using the GENII computer code (Napier et al. 1988), which also describes the H-3 and C-14 models.

3.4.2 All Pathways Analysis

The all pathways dose scenario was used to evaluate compliance with the requirement in DOE Order 5820.2A that the annual EDE from all exposure pathways (excluding airborne pathways) received by a member of the public must not exceed 25 mrem from exposure to RWMC effluents. The methodology used to calculate the all pathways dose was based on the methodology presented in NRC (1977) and Peterson (1983). This all pathways scenario assumed that a receptor drank contaminated groundwater, ate leafy vegetables and produce that were irrigated with contaminated groundwater, and consumed milk and meat from animals that consumed contaminated water and pasture grass irrigated with contaminated groundwater. The scenario assumed that groundwater was used for drinking, watering beef and milk cattle, and irrigating crops and pasture. Radionuclide concentrations as a function of time at the receptor well that were calculated using the hydrological transport model described in Section 3.3 were used as input to this model. The receptor was located at the INEL Site boundary during the operational and institutional control period per the guidance in Wood et al. 1992. During this time, the INEL Site boundary is maintained, and access by the public is not allowed. During post-institutional control, the receptor was located 100 m downgradient of the RWMC facility boundary. Table 3-14 contains the parameter values used in the all pathways dose calculation.

Table 3-14. Parameter values used in the all pathway dose calculation.

Parameter	Value	Reference
U_W	258 L/yr	Yang and Nelson (1984)
Q_W (beef cattle)	50 L/day	NRC (1977)
Q_W (milk cattle)	60 L/day	NRC (1977)
Q_F (beef cattle, dry weight)	12 kg/day	NCRP (1984)
Q_F (milk cattle, dry weight)	16 kg/day	NCRP (1984)
U_B	85 kg/yr	Rupp (1980)
U_M	112 L/yr	Rupp (1980)
U_P	176 kg/yr	Rupp (1980)
U_{LV}	18 kg/yr	Rupp (1980)
I	8.47 L/m^2-day	Site specific
k	0.025 mm^{-1}	Peterson (1983)
r/Y_v (leafy veg, wet weight)	0.076 m^2/kg	Calculated from Baes and Orton (1979) and Baes et al. (1984)
r/Y_v (produce, wet weight)	0.032 m^2/kg	Calculated from Baes and Orton (1979) and Baes et al. (1984)
r/Y_v (pasture, dry weight)	2.0 m^2/kg	Calculated from Baes and Orton (1979) and Baes et al. (1984)
P (dry weight)	225 kg/m^2	DOE (1987)
t_i	90 day	Site specific
t_b	365 day	Site specific
f_l	0.25	Site specific
T (leafy veg)	1.0	Ng et al. (1978)
T (produce)	0.1	Ng et al. (1978)
DF (leafy veg)	0.5	Ng et al. (1978)
DF (produce)	1.0	Ng et al. (1978)
FV	0.7	EPA (1989)
FB	0.442	EPA (1989)
FM	0.399	EPA (1989)

The dose from human consumption of drinking water was calculated using

$$D = C_{GW} \times U_W \times DCF \times \frac{10^{-6}\ \mu Ci}{pCi} \times \frac{1{,}000\, mrem}{rem} \qquad (3\text{-}35)$$

where

D = dose (CEDE) from one year's consumption of contaminated media, in this case groundwater (mrem/yr)

C_{GW} = radionuclide concentration in groundwater (pCi/L)

U_W = human consumption rate of water (L/yr)

DCF = ingestion dose conversion factor (rem/μCi).

The dose through water ingestion by beef and milk cattle assumes that cattle drink contaminated water. The receptor is then assumed to drink milk and eat meat from the cattle that drank the contaminated water. Meat and milk were treated separately. The dose was calculated using

Meat:

$$D = C_{GW} \times Q_W \times F_f \times U_B \times DCF \times \frac{10^{-6}\mu Ci}{pCi} \times \frac{1{,}000\, mrem}{rem} \times FB \qquad (3\text{-}36)$$

Milk:

$$D = C_{GW} \times Q_W \times F_m \times U_M \times DCF \times \frac{10^{-6}\mu Ci}{pCi} \times \frac{1{,}000\, mrem}{rem} \times FM \qquad (3\text{-}37)$$

where

Q_W = consumption rate of water by beef or milk cattle (L/day)

F_f = meat transfer coefficient (day/kg)

U_B = human consumption rate of meat (kg/yr)

FB = fraction of beef produced locally (unitless)

F_m = milk transfer coefficient (day/L)

U_M = human consumption rate of milk (L/yr)

FM = fraction of milk produced locally (unitless).

The dose to humans from ingestion of contaminated leafy vegetables and produce was calculated assuming two contamination routes: direct deposition of contaminated irrigation water on plants and deposition of contaminated irrigation water on soil followed by root uptake by plants. Leafy vegetables and produce were treated separately. The dose through direct deposition was calculated using

Leafy Vegetables - Direct Deposition:

$$D = \frac{C_{GW} \times I \times r}{Y_v} \times \frac{1 - e^{-(\lambda_r + kI)\, t_1}}{\lambda_r + kI} \times U_{LV} \times \frac{10^{-6}\,\mu Ci}{pCi} \times DCF \times \times \frac{1{,}000\,mrem}{rem} \times DF \times T \times FV \quad (3\text{-}38)$$

Produce - Direct Deposition:

$$D = \frac{C_{GW} \times I \times r}{Y_v} \times \frac{1 - e^{-(\lambda_r + kI)\, t_1}}{\lambda_r + kI} \times U_P \times \frac{10^{-6}\,\mu Ci}{pCi} \times DCF \times \times \frac{1{,}000\,mrem}{rem} \times DF \times T \times FV \quad (3\text{-}39)$$

where

I = irrigation rate (L/m^2-day)

r = interception fraction (unitless)

Y_v = agricultural yield (kg/m^2, wet weight)

λ_r = radioactive decay constant (per day)

k = washoff constant (mm^{-1})

t_i = irrigation time (day).

U_{LV} = human consumption rate of leafy vegetables (kg/yr)

DF = fraction of activity remaining after preparation and processing (unitless)

T = translocation factor (unitless)

FV = fraction of leafy vegetables and produce produced locally (unitless)

U_P = human consumption rate of produce (kg/yr).

The product kI is also known as the weathering rate constant because of washoff (Peterson 1983). This quantity describes the rate at which material is removed from plant surfaces by water and is analogous to λ_e, the weathering rate constant used in nonirrigation situations. The value of kI was calculated using

$$kI = 0.025 mm^{-1} \times \frac{8.47 L}{m^2\text{-}day} \times \frac{1 m^3}{1{,}000 L} \times \frac{1{,}000 mm}{1 m} = 0.212/day \quad . \qquad (3\text{-}40)$$

The dose from deposition of contaminated irrigation water on soil followed by root uptake by plants and human consumption of plants was calculated using the following equations. Credit was not taken for leaching of radionuclides from the root zone of plants.

Leafy Vegetables - Root Uptake:

$$D = \frac{C_{GW} \times I \times f_I}{P} \times \frac{1 - e^{-\lambda_r t_b}}{\lambda_r} \times CR \times U_{LV} \times \frac{10^{-6}\mu Ci}{pCi} \times \times DCF \times \frac{1{,}000\,mrem}{rem} \times FV \quad (3\text{-}41)$$

Produce - Root Uptake:

$$D = \frac{C_{GW} \times I \times f_I}{P} \times \frac{1 - e^{-\lambda_r t_b}}{\lambda_r} \times CR \times U_P \times \frac{10^{-6}\mu Ci}{pCi} \times \times DCF \times \frac{1{,}000\,mrem}{rem} \times FV \quad (3\text{-}42)$$

where

f_l = fraction of the year that crops are irrigated (unitless)

P = areal density [kg (dry weight soil)/m^2]

CR = concentration ratio [pCi/kg (wet weight plant) ÷ pCi/kg (dry weight soil)]

t_b = build-up time for radionuclides in soil (day).

The dose to humans from ingestion of contaminated animal products was also calculated assuming two contamination routes: direct deposition and root uptake; meat and milk were treated separately. All food (pasture or stored feed) eaten by cattle was assumed to be contaminated. The dose through direct deposition was calculated using

Meat - Direct Deposition:

$$D = \frac{C_{GW} \times I \times r}{Y_v} \times \frac{1 - e^{-(\lambda_r + kI)\, t_i}}{\lambda_r + k\dot{I}} \times Q_F \times F_f \times U_B \times \times \frac{10^{-6}\,\mu Ci}{pCi} \times DCF \times \frac{1{,}000\,mrem}{rem} \times FB \quad (3\text{-}43)$$

Milk - Direct Deposition:

$$D = \frac{C_{GW} \times I \times r}{Y_v} \times \frac{1 - e^{-(\lambda_r + kI)\, t_i}}{\lambda_r + k\dot{I}} \times Q_F \times F_m \times U_M \times \times \frac{10^{-6}\,\mu Ci}{pCi} \times DCF \times \frac{1{,}000\,mrem}{rem} \times FM \quad (3\text{-}44)$$

where

Y_v = agricultural yield (kg/m^2, dry weight)

Q_F = animal consumption rate of pasture and feed [kg (dry)/day].

The dose through deposition on soil followed by root uptake was calculated using the following equations. As with produce and leafy vegetables, credit was not taken for leaching of radionuclides from the root zone of plants.

Meat - Root Uptake:

$$D = \frac{C_{GW} \times I \times f_I}{P} \times \frac{1 - e^{-\lambda_r t_b}}{\lambda_r} \times CR \times Q_F \times F_f \times U_B \times \times \frac{10^{-6}\,\mu Ci}{pCi} \times DCF \times \frac{1{,}000\,mrem}{rem} \times FB \quad (3\text{-}45)$$

Milk - Root Uptake:

$$D = \frac{C_{GW} \times I \times f_I}{P} \times \frac{1 - e^{-\lambda_r t_b}}{\lambda_r} \times CR \times Q_F \times F_m \times U_M \times$$

$$\times \frac{10^{-6}\mu Ci}{pCi} \times DCF \times \frac{1,000 mrem}{rem} \times FM \qquad (3\text{-}46)$$

where

CR = concentration ratio [pCi/kg (dry weight plant) ÷ pCi/kg (dry weight soil)].

Equivalent water intake rates for all pathways were calculated using the above methodology and a spreadsheet. These rates were then input into GWSCREEN to perform all pathway dose calculations.

Secondary and indirect pathways, such as inhalation of contaminated irrigation water, inhalation of contaminated dust, or external exposure from radionuclides deposited on the soil, were omitted from this scenario. These pathways were either not viewed as credible (e.g., a farmer standing under a center pivot irrigator while it was running and inhaling contaminated irrigation water) or would contribute relatively minor amounts when compared to direct pathways such as direct ingestion of contaminated water.

3.4.3 Intruder Scenarios

The following four types of inadvertent intruder scenarios were evaluated in this analysis and are summarized in this section:

1. Acute intruder-drilling
2. Acute intruder-construction
3. Chronic intruder-agriculture
4. Chronic intruder-radon.

The acute intruder-drilling and acute intruder-construction scenarios were used to evaluate compliance with the 500 mrem acute exposure criterion in DOE Order 5820.2A. The chronic intruder-agriculture and chronic intruder-radon scenarios were used to evaluate compliance with the 100 mrem/yr

continuous exposure criterion in DOE Order 5820.2A. These scenarios were based on the scenarios developed and used by the NRC in 10 CFR 61 to evaluate the land disposal of radioactive waste (NRC 1981; NRC 1982; Oztunali and Roles 1986; Kennedy and Peloquin 1988).

The intruder dose assessments used to derive the waste classification limits in 10 CFR 61 were based on contacting waste directly (NRC 1981; NRC 1982) because the intruder dose assessments and performance objective in 10 CFR 61 were designed to prevent direct contact with waste that contains high concentrations of radioactivity. The performance objective in 10 CFR 61 for the general population was designed to complement the intruder performance objective by limiting the releases of radioactivity to the environment. Dose assessments used to demonstrate compliance with this performance objective are dependent on the total activity at a site, not on the concentration. These dose assessments could be used to develop total activity limits for a site, which would complement the waste classification limits that were developed based on activity concentration. The NRC did not find it necessary to incorporate groundwater pathways in the intruder dose assessments, even at arid sites, because of the complementary nature of the general population and intruder performance objectives.

The regulatory position in DOE Order 5820.2A on whether intruder dose assessments are required to include groundwater pathways is not clear. The order states that "committed effective dose equivalents received by individuals who inadvertently may intrude <u>into</u> the facility after loss of active institutional control (100 years) will not exceed. . ." However, the term facility is not defined in such a way that makes it clear whether groundwater pathways are to be included in intruder dose assessments. At the INEL, an intruder who occupied the RWMC SDA would have to use groundwater because there is no reliable source of surface water. At other DOE sites, this may not be the case. In addition, Case and Otis (1988) states that groundwater pathways should be considered in intruder dose assessments. However, DOE Order 5820.2A contains complementary general population and intruder performance objectives that are similar to the performance objectives in 10 CFR 61. Based on NRC precedence and the philosophy of complementary performance objectives, intruder dose assessments would not include groundwater pathways; however, because the regulatory position in DOE Order

5820.2A is unclear, groundwater pathways were included in the intruder dose assessments for this radiological performance assessment. The methodology and data are the same as for the all pathways groundwater dose assessments described in Section 3.4.2. The receptor location was 100 m from the RWMC boundary.

The acute intruder-drilling, acute intruder-construction, chronic intruder-radon, and chronic intruder-agriculture scenarios were evaluated for pits. For the soil vault rows, the acute intruder-drilling, chronic intruder-radon, and chronic intruder-agriculture scenarios were evaluated. The acute intruder-construction scenario was not evaluated for the soil vault rows because a basement excavation would not contact the waste. For the intruder-construction, intruder-agriculture, and intruder-drilling scenarios, the entire inventory in each area was available for intrusion, no depletion because of leaching was assumed. Although leaching will occur over time, this conservative assumption was made for excavation cases; during the drilling cases both the inventory still in the waste and the leached inventory would be contacted during intrusion. Therefore, leaching has no impact on the drilling intruder assessments.

Appendix A contains the inventory used in the intruder assessments. Appendix C provides the radionuclide concentrations in the waste and on the surface for pits and soil vault rows. In all cases, the doses resulting from intrusion include the contributions from the decay and ingrowth of radioactive progeny. Detailed computer runs for intruder analyses are contained in Maheras (1993a). Figure 3-22 summarizes the pathways evaluated for each intruder scenario.

3.4.3.1 Acute Intruder-Drilling Scenario. The acute intruder-drilling scenario assumed that an inadvertent intruder drilled a well into the contents of a soil vault or pit (see Figure 3-23). As in the NRC drilling scenario, the intruder was exposed to contaminated drill cuttings spread over the ground and to contaminated airborne dust. In the NRC drilling scenario, the intruder was exposed to contaminated drill cuttings in a mud pit. Interviews with local well drilling contractors in the Idaho Falls area indicated that drillers spread the cuttings over the ground and do not use mud pits (Seitz 1991); therefore, this site-specific deviation of the NRC drilling scenario

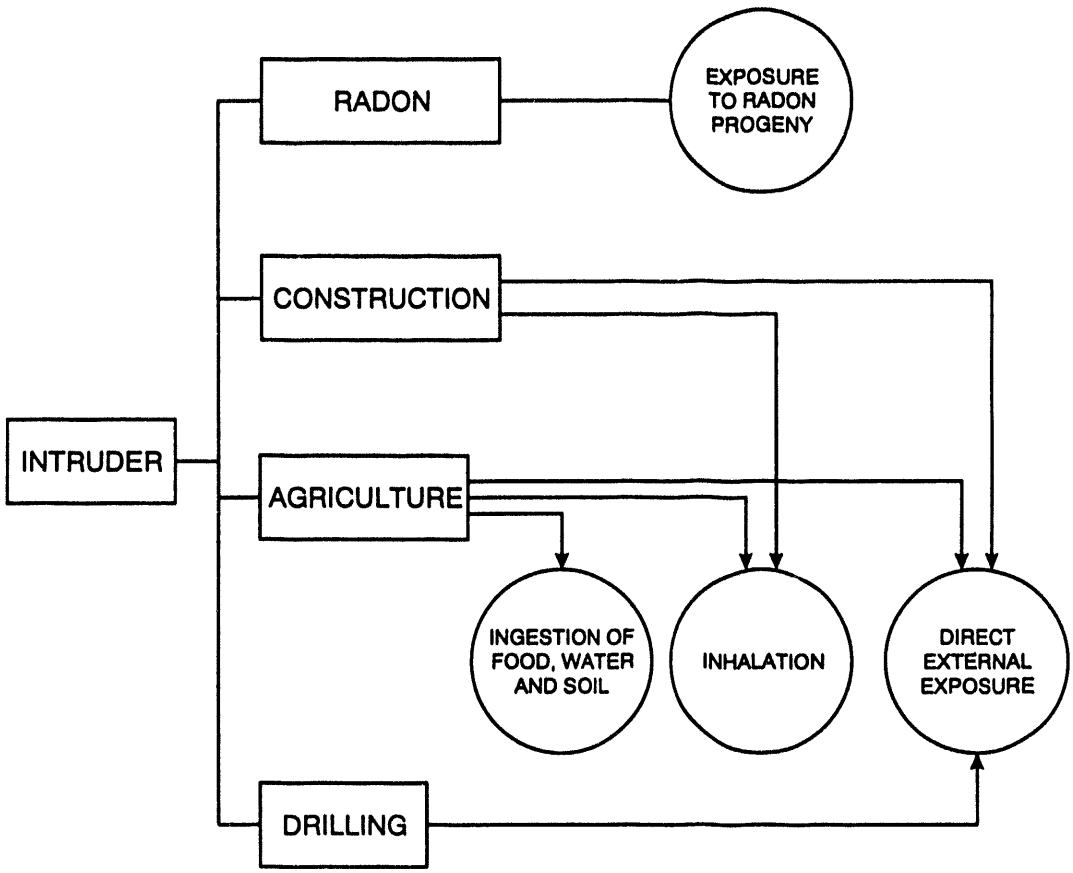

Figure 3-22. RWMC performance assessment intruder pathways.

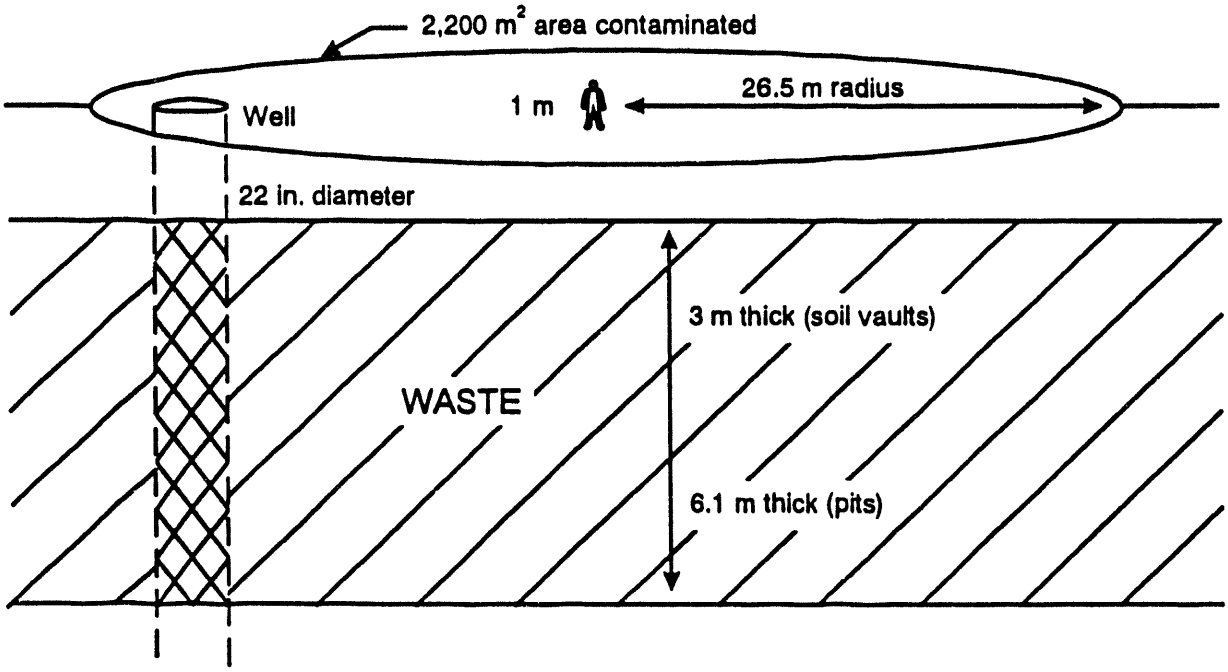

Figure 3-23. Acute intruder-drilling scenario.

was incorporated into the analyses. In addition, spreading the cuttings over the ground yields higher doses than putting the cuttings in a mud pit because of decreased shielding. These cuttings were spread out over a 2,200 m^2 lot (Rogers and Hung 1987). This lot corresponds to about one-half of an acre; lots located outside the city limits of Idaho Falls are typically 1 to 3 acres. Therefore, a 2,200 m^2 lot size is conservative for the local area surrounding Idaho Falls. The intruder was exposed to the contaminated cuttings for 160 hours (Seitz 1991), the time local Idaho Falls well drilling contractors state it would take to drill and develop a 22-in. diameter irrigation well.

Well drilling contractors in the Idaho Falls area reported that two types of wells are typically drilled: small diameter residential wells and large diameter irrigation wells. The small residential wells are typically 6 to 8 in. in diameter, serve a single residence, and also may provide enough water for a family garden and a couple of cows. The large diameter irrigation wells are drilled to serve systems that irrigate hundreds of acres; the wells are located in the middle of farm fields, not near the farmer's residence. Therefore, a farmer would not drill an irrigation well to acquire water for his residence. Large diameter irrigation wells are currently drilled 18-in. in diameter, but drilling contractors thought 22-in. diameter irrigation wells would be drilled in the near future.

Based on the information obtained from Idaho Falls area drilling contractors, an acute drilling exposure could result from drilling either an 8-in. diameter residential well or a 22-in. diameter irrigation well. Because the doses for this scenario are directly proportional to the volume of contaminated cuttings brought to the surface, to provide bounding doses a 22-in. diameter irrigation well was evaluated. The time required to drill and develop a well (160 hours for a large irrigation well and 48 hours for a residential well) also provided bounding doses when an irrigation well was evaluated.

Based on a waste thickness of 6.1 m for pits, the 22-in. well results in 1.5 m^3 of contaminated cuttings being brought to the surface during the acute drilling scenario. Based on a waste thickness of 3 m, for soil vault rows,

the 22-in. well results in 0.75 m^3 of contaminated cuttings being brought to the surface.

Intruder doses were calculated at various points in time after site closure. For pits, these times were 2120 (100 years after site closure), 5020, 12020, and at U-238 equilibrium (approximately 1,000,000 years after site closure). For soil vault rows, these times were 2120, 3020, 12020, and at U-238 equilibrium. Inhalation doses were calculated using the GENII computer code and were based on a dust loading of 1 mg/m^3 (EG&G Idaho 1984), representative of construction activities. The external dose rate was calculated using the MICROSHIELD computer code. The source configuration was modeled as a 26.5-m radius plane, the radius of a circular 2,200 m^2 lot, with a receptor point 1 m above the plane at approximately waist height. The doses include exposure to radioactive progeny. No shielding factors were incorporated into the analyses.

3.4.3.2 Acute Intruder-Construction Scenario. The acute intruder-construction scenario assumes that an inadvertent intruder moves onto the RWMC SDA and excavates a basement in the waste (see Figure 3-24). The intruder is exposed to contaminated dust and contaminated waste in the bottom of the pit. No ingestion doses are postulated for this scenario. This scenario is applicable to pits but not to soil vaults. Soil vaults have extra cover, which precludes intrusion into the waste by digging a basement. Because potatoes are a large cash crop in southeastern Idaho, the potential for an inadvertent intruder to dig a potato cellar was also considered. This scenario was dismissed because potato cellars are relatively shallow, approximately 1 m deep, and the intruder is unable to contact the waste during excavation. Because a basement excavation, which is 3 m deep, contacts the waste, the acute intruder-potato cellar construction scenario is bounded by the acute intruder-basement excavation construction scenario.

Based on an interview with an Idaho Falls construction contractor, the exposure time for this scenario was 64 hours (Sussman 1993). This exposure time includes the time required to excavate the basement, pour the footings, form the basement walls, remove the forms, and backfill and grade the area around the basement. For the inhalation pathway, the dust loading was

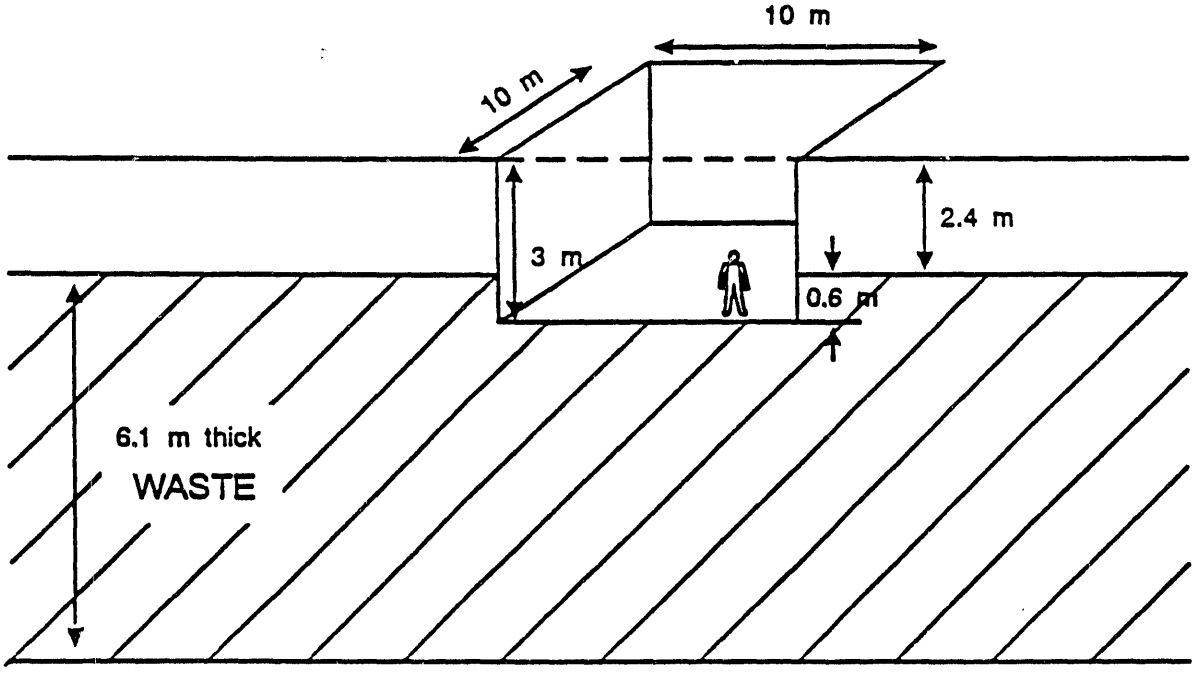

Figure 3-24. Acute intruder-construction scenario.

1 mg/m^3 (EG&G Idaho 1984), representative of construction activities. For the external exposure pathway, the intruder stood directly on the exposed waste. This is conservative because an intruder would spend only a part of the time down inside the excavation. Shielding was not considered except for the self-shielding provided by the waste. The excavation was an 10 x 10-m area and 3-m deep (Rogers and Hung 1987). At the time of maximum erosion (the year 5020), 2.4 m of cover remains over the waste and the 3-m basement protrudes into the waste a distance of 0.6 m. The area of the basement corresponds to 1,100 ft^2, a reasonably-sized home in southeastern Idaho. The sides of the excavation will undoubtedly slope, but because of the small depth that the excavation penetrates the waste (0.6 m or less than 2 ft), sloping sides were not considered. Intruder doses were calculated at various points in time after site closure. Because of cover thickness, intrusion was not possible in 2120. To maximize doses, intrusion was postulated to start in 5020, which corresponds to the time of maximum erosion. Intruder doses were also calculated in 12020 and at U-238 equilibrium (approximately 1,000,000 years after site closure).

GENII was used to model the inhalation pathway, and MICROSHIELD was used to model the external exposure pathway. The source configuration was modeled as a volume source with infinite lateral extent with a receptor point 1 m above the source. In this configuration, the top of the volume source is the floor of the basement. This configuration does not account for the four 0.6-m vertical walls that surround the receptor. An evaluation of the doses from these walls found the doses to be two orders of magnitude less than the doses from the floor of the basement, and the doses from the walls were omitted from further calculations.

3.4.3.3 Chronic Intruder-Agriculture Scenario. The chronic intruder-agriculture scenario assumes that an inadvertent intruder moves onto the RWMC SDA, excavates a basement in the waste, and drills a residential well into the waste disposed of in pits or soil vaults (see Figures 3-25 and 3-26). The waste from the excavation and well is then spread around the site and mixed in the top 0.75 m of soil where crops are grown. The intruder breathes contaminated dust; eats contaminated food stuffs; inadvertently eats soil; is directly exposed to contaminated ground surfaces; and uses contaminated

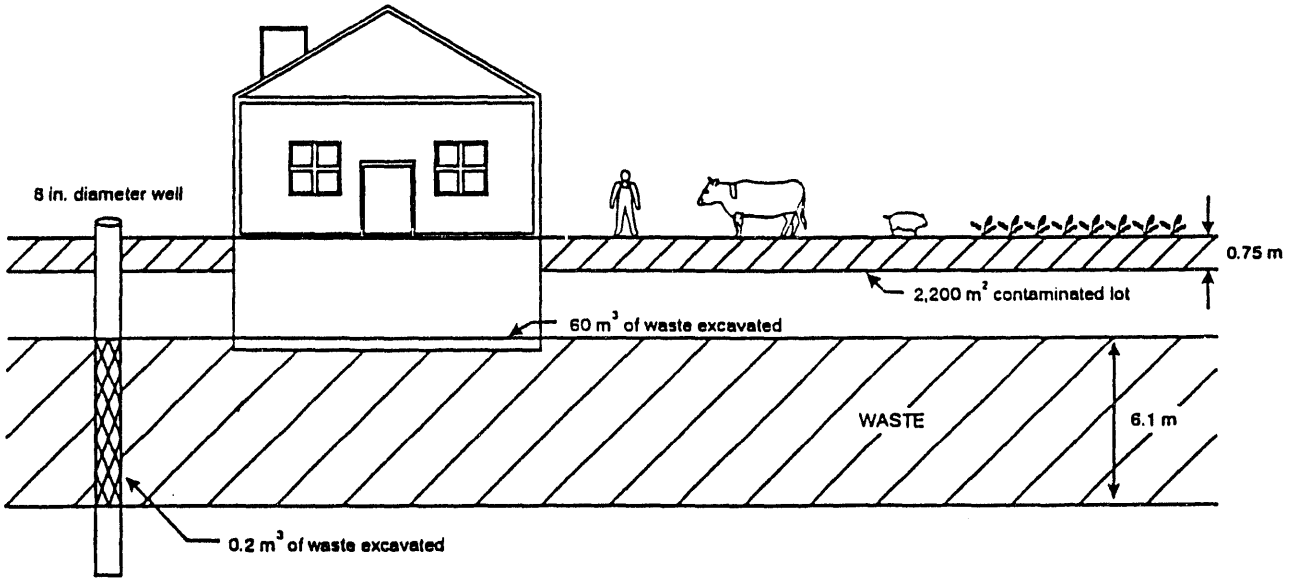

Figure 3-25. Chronic intruder-agriculture scenario for pits.

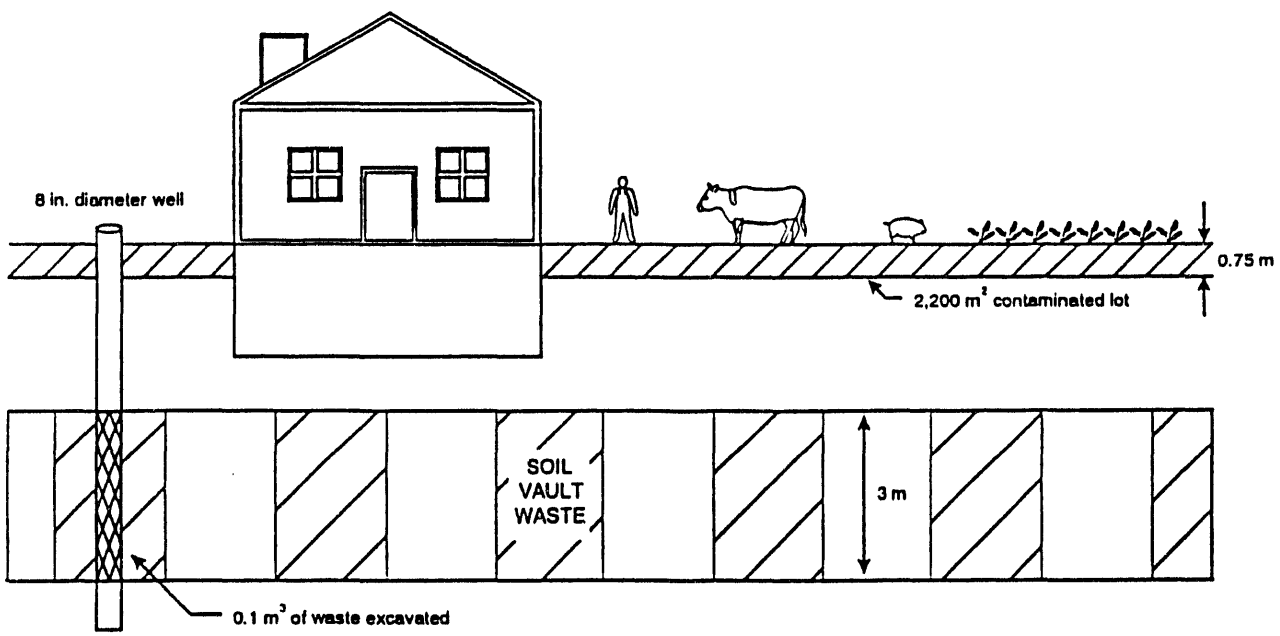

Figure 3-26. Chronic intruder-agriculture scenario for soil vaults.

groundwater for drinking, irrigation, and watering stock. The groundwater pathways and data are described in Section 3.4.2. The direct contact portion of the scenario is described below. The scenario is applicable to pits and soil vault rows.

This scenario evaluates an 8-in. residential well. This type of well serves a single residence and provides enough additional water for a family garden and a couple of cows. As described in the acute intruder-drilling scenario, large diameter irrigation wells are drilled to serve large irrigation systems (hundreds of acres) that are located in the middle of farm fields, not near a farmer's residence. Therefore, in this residence/home garden scenario it is appropriate to evaluate a case where a farmer drills a small diameter residential well near his residence, not a large diameter irrigation well.

As discussed in the acute intruder-construction scenario, the basement excavation was 10 x 10 m in area and 3 m deep (Rogers and Hung 1987). As is the case in the acute intruder-construction scenario, the potential for an inadvertent intruder digging a potato cellar was considered. This scenario was dismissed because potato cellars are relatively shallow, approximately 1 m deep, and the intruder is able to contact more waste during basement excavation, approximately 3 m deep. Therefore, the amount of contaminated material brought to the surface through basement excavation exceeds the amount and bounds the doses calculated from contaminated material brought to the surface during potato cellar construction.

For the pits at minimum cover thickness (maximum waste penetration), 2.4 m of cover is present over the waste, and 60 m^3 of contaminated waste could be brought to the surface[a] through basement excavation. Because an 8-in. diameter residential well is also drilled through the waste, an additional 0.2 m^3 of waste is brought to the surface, for a total of 60.2 m^3 of contaminated material on the surface. At 2120, sufficient cover remains over the pits to preclude intrusion into the waste through basement

---

a. A 3-m excavation depth and a 2.4-m cover thickness results in a 0.6 m penetration of the waste. Based on an area of 10 x 10 m, the volume brought to the surface is 60 m^3 (0.6 x 10 x 10 m).

excavation; however, a well could still penetrate the waste. Based on a 8-in. irrigation well and 6.1-m waste thickness, intrusion at 2120 would bring 0.2 m^3 of contaminated material to the surface.

For the soil vaults, intrusion by basement excavation is precluded by increased cover thickness (greater than 3 m), and the scenario is actually a chronic post-drilling intruder-agriculture scenario. Well drilling was calculated to bring 0.1 m^3 of contaminated material to the surface based on a 3-m waste thickness and an 8-in. diameter residential well.

The exposure time was 1 year (8,760 hours). For the dust inhalation pathway, the intruder spent 24 hours plowing and cultivating (1 mg/m^3 dust loading), 1,200 hours conducting other farm activities (0.07 mg/m^3 dust loading), and 7,536 hours conducting other activities, which result in a dust loading of 0.05 mg/m^3 (EG&G Idaho 1984). This results in a time-weighted average dust loading of 5.53E-8 kg/m^3. The waste was spread out over a 2,200 m^2 lot (Rogers and Hung 1987), and mixed to a depth of 0.75 m. The 2,200-m^2 (0.5-acre) lot is conservative because lots outside of Idaho Falls are typically 1 to 3 acres.

The GENII computer code was used to model the inhalation and food chain doses. Crops were grown onsite in a family garden that contained contaminated soil. Appendix B provides details on parameters used in this analysis, and Napier et al. (1988) provides details on the food chain pathway methodology used in GENII. The contaminated soil was mixed and diluted with uncontaminated excavated soil and surface soil (Rogers et al. 1982). Dietary fractions representative of rural agriculture areas were used (EPA 1989). Based on the data in EPA (1989), 70% of the intruder's vegetables and produce, 40% of the intruder's milk, and 44% of the intruder's meat were assumed to be produced locally. Because 2,200 m^2 is a relatively small lot that cannot fully support beef cattle or milk cows, the consumption rate of contaminated pasture was adjusted to reflect the maximum amount of feed that could be produced on the lot, assuming three cuttings of hay per year and a yield of 0.7 kg/m^2 (wet weight). Stored feed was assumed to be uncontaminated. Based on a total consumption rate of 12 kg/day (dry weight) for beef cattle and 16

kg/day (dry weight) for milk cows and a dry to wet weight conversion factor of 0.2, 9% of the total pasture eaten by the animal was contaminated. The consumption rate for contaminated pasture was 5.4 kg/day (wet weight) for beef cattle and 7.2 kg/day (wet weight) for milk cows.

$$0.7\,kg/m^2\ (wet\ wt.) \times 3\ cuttings\ hay/yr \times 2{,}200 m^2 = 4{,}620\ kg/yr\ (wet\ wt.) \quad (3\text{-}47)$$

$$\frac{12\ kg/d}{0.2} \times 365\ d/yr = 21{,}900\ kg/yr\ (beef\ cattle,\ wet\ wt.) \quad (3\text{-}48)$$

$$\frac{16\ kg/d}{0.2} \times 365\ d/yr = 29{,}200\ kg/yr\ (milk\ cattle,\ wet\ wt.) \quad (3\text{-}49)$$

$$Total = 21{,}900\ kg/yr + 29{,}200\ kg/yr = 51{,}100\ kg/yr\ (wet\ wt.) \quad (3\text{-}50)$$

$$\frac{4{,}620\ kg/yr}{51{,}100\ kg/yr} = 0.090 \quad (3\text{-}51)$$

$$\frac{12\ kg/d}{0.2} \times 0.090 = 5.4\ kg/d\ (beef\ cattle,\ wet\ wt.) \quad (3\text{-}52)$$

$$\frac{16\ kg/d}{0.2} \times 0.090 = 7.2\ kg/d\ (milk\ cattle,\ wet\ wt.) \quad (3\text{-}53)$$

Two sets of human consumption rates were evaluated: (1) a diet developed in Rupp (1980) and based on a 1965 USDA survey and (2) a diet developed in Yang and Nelson (1984, 1986) and based on a 1977-1978 USDA survey. The Rupp diet was the default diet used in the EPA's NESHAPs Environmental Impact Statement (EPA 1989). The Yang and Nelson diet represents a more realistic diet than the Rupp diet because it is based on a later dietary survey (see Table 3-13). As in the atmospheric transport analyses, two inhalation rates were evaluated: 8,030 and 5,840 m^3/yr (see Section 3.4.1). Consumption of contaminated soil by adults was incorporated into the scenario using a consumption rate of 10 mg/day (Konz et al. 1989).

External exposures were calculated using the computer code MICROSHIELD. The intruder was exposed to waste excavated from the basement and spread around a home site (2,200 m^2) to a depth of 0.75 m. The source configuration was modeled as a 26.5-m radius plane and a thickness of 0.75 m. The receptor point was 1 m above the plane (see Figures 3-25 and 3-26).

The excavated waste was diluted and mixed with uncontaminated soil during excavation. The intruder was exposed to the contaminated soil for 8,760 h/yr. Two shielding factors were evaluated: 0.7 and 0.36. The 0.7 shielding factor is from NRC (1977) and corresponds to the shielding factor used for the maximally exposed individual. The 0.36 shielding factor was calculated using data presented in Konz et al. (1989) (See Section 3.4.1).

For pits, intrusion was evaluated at 2120, 5020, 12020, and at U-238 equilibrium (approximately 1,000,000 years after site closure). For soil vault rows, intruder doses were calculated at 2120, 3020, 12020, and at U-238 equilibrium.

3.4.3.4 Chronic Intruder-Radon Scenario. Two scenarios were considered for calculating chronic intruder-radon doses: excavation over pits and excavation over soil vaults. The scenarios were based on an intruder excavating a 10 × 10 × 3-m basement over the waste and constructing a 10 × 10 × 3-m house over the basement. The intruder was exposed to Rn-222 and its short-lived progeny (Po-218, Pb-214, Bi-214, and Po-214) while in the basement and house. The data in Konz et al. (1989) were used to estimate that an individual spent 115 h/week or 68% of their time indoors. This represents the time spent at home and indoors.

The RESRAD computer code (Gilbert et al. 1989), Version 5.03, was used to perform the dose assessments. Site-specific geometry parameters (such as waste layer thickness and cover thickness) were used in the analyses. The data for the properties of the concrete used in the basement foundation were obtained from two instrumented basement structures located at Colorado State University in Fort Collins, Colorado (Gadd 1993).

The Colorado State University structures were constructed and instrumented for research into the transport, entry, and accumulation of radon in residential structures (Ward et al. 1993). The structures were built using standard residential construction techniques and concrete. For example, the concrete was selected from three Fort Collins-area concrete distributors, based on the lowest cost. The concrete aggregate was surveyed to ensure that it did not contain excessive quantities of Ra-226, which would confound soil radon entry measurements.

Although the outside of a foundation is typically water proofed in the Western United States, water proofing was not applied to the basement structure. The walls and floor were constructed slightly thinner than standard because the structural support for a full upper story was not required and to increase the diffusion of radon into the basement from the surrounding soil to minimize radon measurement problems. The basement structures were instrumented to measure indoor-soil pressure differentials; soil gas Rn-222 concentrations; air permeability; soil moisture; and indoor, outdoor, and subslab Rn-222 concentrations (Gadd 1993).

The Colorado State University data (see Table 3-15) were used because they represent residential concrete and construction techniques used in the Western United States, and they were collected under rigorous and known conditions. RESRAD does not model basement and first floor radon exposures separately. Therefore, a total room height of 6 m was used to account for first floor and basement exposures.

Table 3-15 lists the Ra-226 concentrations at the time of maximum dose, taking into account the changing geometry of the scenario because of erosion, radioactive decay and ingrowth, and leaching. For the pits, the peak dose occurred 2,200 years after the site closure, at the time when the floor of the basement just comes into contact with the waste (Figure 3-27). At later times, even though the basement excavation penetrates the waste, the decrease in Ra-226 concentration because of radioactive decay and leaching yields lower doses. At 2,200 years after site closure, almost 100% of the Ra-226 is from disposed Ra-226, not from Ra-226 that ingrew from U-238, U-234, or Th-230.

Table 3-15. Data used in the chronic intruder-radon scenario.

Parameter	Pits	Soil vaults
Basement depth	3 m	3 m
First floor height[a]	3 m	3 m
Total porosity	0.487	0.487
Volumetric water content	0.33	0.33
Soil density	1.5 g/cm^3	1.5 g/cm^3
Ra-226 concentration	3.71 pCi/g	12.7 pCi/g
Waste area	12,400 m^2	15.7 m^2 [b]
Waste thickness	6.1 m	3.05 m
Cover thickness	3 m	3.3 m
Uranium leach rate	7.6E-6/yr[c]	1.5E-5/yr[c]
Thorium leach rate	7.6E-6/yr[c]	1.5E-5/yr[c]
Radium leach rate	1.5E-4/yr[d]	3.1E-4/yr[d]

	Colorado State University value[e]
Diffusion coefficient	2.5E-8 m^2/s
Emanation fraction	0.17
Thickness of building foundation	0.10 m
Density of building foundation	2.1 g/cm^3
Total porosity of building foundation	0.13
Volumetric water content of building foundation	0.13[f]

a. A total room height of 6 m was used.

b. Based on five 2-m diameter soil vaults.

c. Based on a K_d of 1,000 mL/g and an infiltration rate of 0.070 m/yr.

d. Based on a K_d of 50 mL/g and an infiltration rate of 0.070 m/yr.

e. Source: Gadd (1993).

f. Calculated based on 100% saturation of concrete. Because a diffusion coefficient was entered, this parameter is not used by RESRAD.

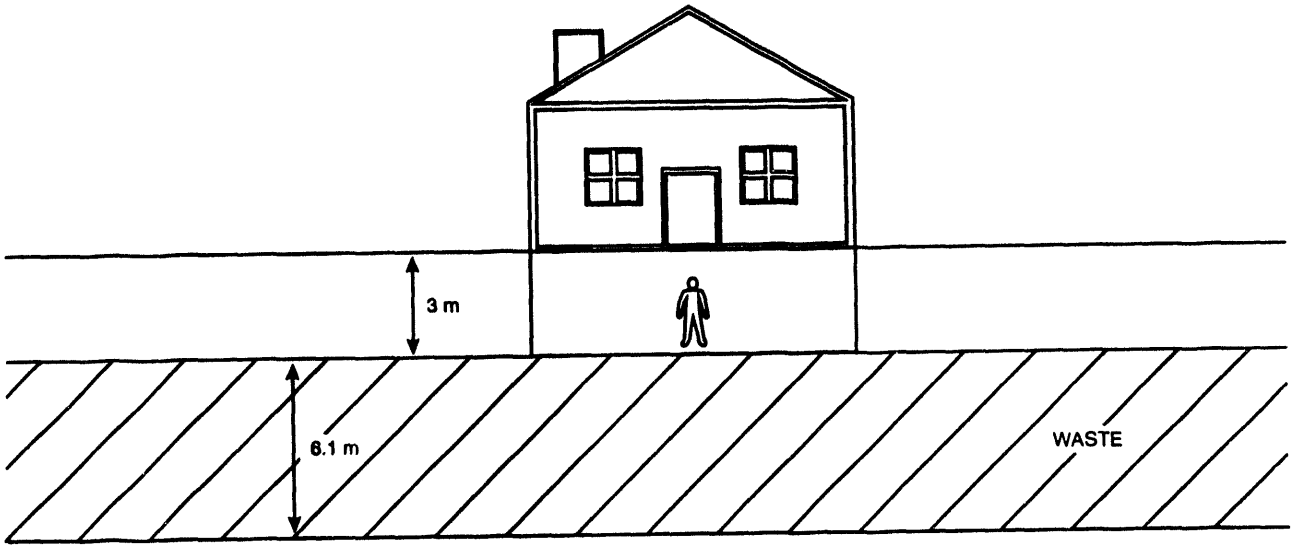

Figure 3-27. Chronic radon scenario for pits.

For soil vaults, the peak dose occurred 53,000 years after site closure because of ingrowth of Ra-226 from U-238. At this time, there was 3.3 m of cover over the waste, and the bottom of the basement and the top of the waste were separated by 0.3 m of soil (Figure 3-28). The analysis was based on excavating a basement over a row of five soil vaults, each with the diameter of 2 m, separated by 0.6 m of clean soil. This is the maximum number of 2-m diameter soil vaults that can fit in the foot print of a 10 × 10-m basement.

3.4.4 Drinking Water

The drinking water pathway scenario was used to evaluate compliance with DOE Order 5820.2A for the requirement that groundwater resources will be protected consistent with Federal, State, and local requirements. For this scenario, compliance with the Federal Primary Drinking Water Regulations (40 CFR 141) was evaluated. These requirements apply strictly to community drinking water systems. The nearest community drinking water system is located at Atomic City, which is about 2,100 m southeast of the RWMC and is slightly upgradient from the RWMC. It is extremely unlikely any radionuclides would migrate to this location because it is upgradient from the site and a significant distance from the plume centerline. For simplicity and conservatism, compliance with 40 CFR 141 was evaluated at the nearest INEL Site boundary in the direction of groundwater flow. This distance is 5,500 m south-southwest from the RWMC. This site was also chosen because, although unlikely, a small town could conceivably be built at this location and derive its water from a well drilled on the Site boundary.

For this scenario, the receptor was assumed to drink 2 L of water per day for 365 days a year. The EDE is limited to 4 mrem/yr for manmade beta-gamma emitting nuclides, 15 pCi/L gross alpha activity, and 5 pCi/L maximum Ra-226,-228 activity concentration. GWSCREEN was used to perform the dose calculations.

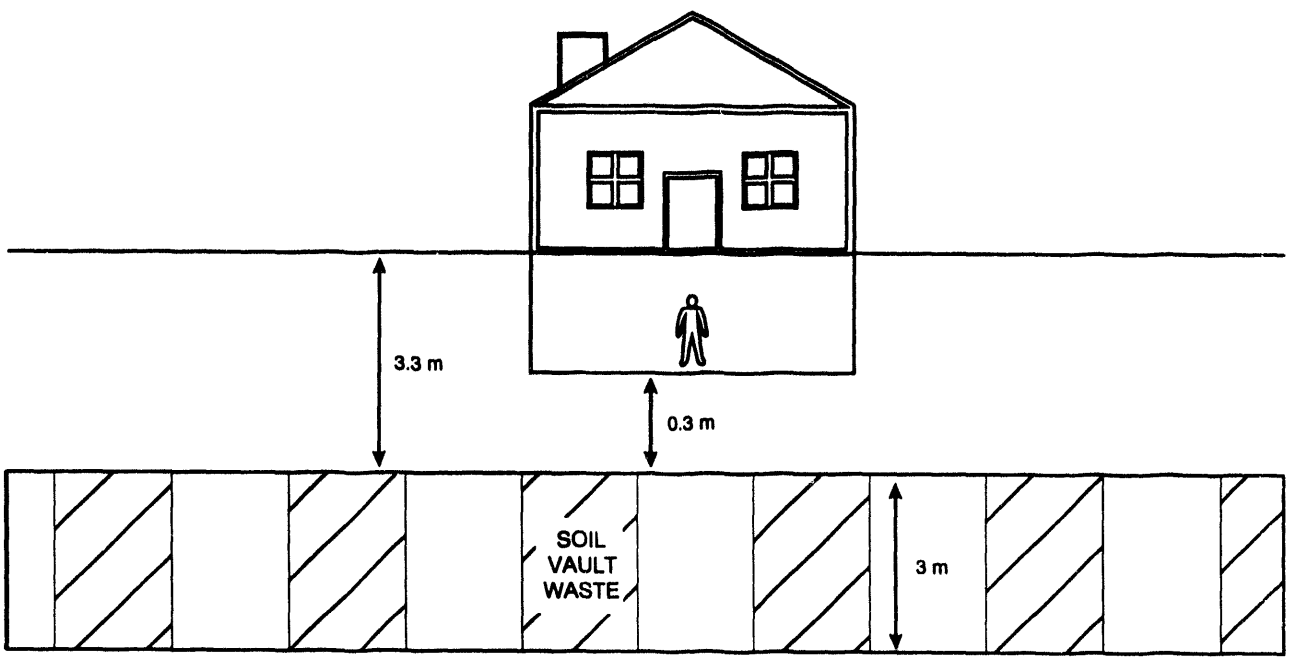

Figure 3-28. Chronic radon scenario for soil vaults.

4. RESULTS OF ANALYSIS

This chapter presents the projected doses for each pathway, sensitivity, and uncertainty related to the doses and an integration and interpretation of the results.

4.1 Projected Doses

Section 4.1 presents projected doses for the atmospheric, all pathways, and intruder analyses. It also presents the drinking water impacts at the INEL Site boundary.

4.1.1 Atmospheric Doses

Based on the dose assessments in the 1992 INEL NESHAP Annual Report (DOE 1993), the emissions from contaminated soil areas at the RWMC yielded a dose of 5.7E-6 mrem/yr during the operational and institutional control periods. Gaseous emissions of H-3 and C-14 during the operational and institutional control periods yielded a dose of 0.0016 mrem/yr. When these doses were combined with the dose from existing monitored and unmonitored emission points at the INEL and existing diffuse sources at other areas of the INEL (DOE 1993), a dose of 0.0031 mrem/yr was calculated (see Table 4-1). This dose was well below the 40 CFR 61 NESHAP standard of 10 mrem/yr.

Post-institutional control doses represent the doses through the ingestion, inhalation, and external exposure pathways. During the post-institutional control period, biointrusion by plant roots and harvester ants was used as the mechanism to move radioactive material to the surface, which was then transported to a receptor via the atmosphere. For both pits and soil vaults, the maximum doses occurred in the year 2120, at the end of institutional control. The doses for pits ranged from 0.026 to 0.039 mrem/yr, and the doses for soil vaults ranged from 0.079 to 0.13 mrem/yr. The dominant dose contributor for the pits was Cs-137, and the dominant dose contributors for the soil vaults were Cs-137 and Ni-63.

Gaseous emissions of H-3 and C-14 during the post-institutional control period yielded a dose of 0.69 mrem/yr. When these doses were combined with

the dose from existing monitored and unmonitored emission points at the INEL and existing diffuse sources at other areas of the INEL (DOE 1993), doses that ranged from 0.80 to 0.86 mrem/yr resulted (see Table 4-1). These doses were well below the 40 CFR 61 NESHAP standard of 10 mrem/yr.

4.1.2 Results of All Pathway Analysis

All pathway doses are presented in this section for the 7 cm/yr infiltration base case with cover for the screened set of fission/activation products and actinides. Two receptor locations were considered: one at 100 m south of the RWMC facility boundary for impacts evaluated during the post-institutional control period and one at the INEL Site boundary 5,500 m south of the RWMC for impacts evaluated during the operational and institutional control period. Graphs are only presented for doses that occur before 10,000 years. Results for time periods after 10,000 years are presented in tables.

Table 4-1. Atmospheric doses.

Time period	EDE (mrem/yr)
Operational and institutional control	
INEL baseline[a]	0.0015
Contaminated soil areas at the RWMC	5.7E-6
Gaseous H-3 and C-14	0.0016
Total	0.0031
Post-institutional control	
INEL baseline[a]	0.0015
Pits	0.026-0.039
Soil vaults	0.079-0.13
Gaseous H-3 and C-14	0.69
Total	0.80-0.86

a. The INEL baseline consists of monitored and unmonitored emission points at the INEL and existing diffuse sources at other areas of the INEL.

All pathway doses for fission/activation products for the base case (7 cm/yr infiltration) were dominated by C-14, H-3, and I-129 during the operational and institutional control period (1984-2120) for the receptor located at the INEL Site boundary (see Figure 4-1). The maximum dose during this period was 0.57 mrem/yr at the INEL Site boundary, which occurred at the year 2060. The dose is below the 25 mrem/yr criteria. After the cover is emplaced in 2020, the source release rate decreases. This reduced release rate results in water containing lower concentrations of radionuclides that are leached from the source. This water undergoes the 30-year travel time in the unsaturated zone and approximately 10-year travel time to the INEL Site boundary and causes the sharp decline in dose at the INEL Site boundary at 2060 (Figure 4-1). The I-129 peak is offset from the H-3 and C-14 peak because it is slightly retarded. Therefore, the peak occurs at a later time. The sensitivity to reduced infiltration associated with the placement of an engineered cover is discussed in section 4.2.

After the institutional control period (any time into the future beyond the year 2120), the maximum dose was 17 mrem at 100 m south of the RWMC facility boundary (Figure 4-2). This dose is below the 25 mrem/yr criteria. Iodine-129, K-40, and C-14 were significant dose contributors during this time period. Tritium doses after institutional control are insignificant because of decay during institutional control. The lag times between the K-40 and C-14 peaks are due to the K-40 retardation and result in slower transit times of K-40. Strontium-90 and Ni-59 doses were insignificant compared to the other fission/activation products. Maximum Sr-90 dose was 3.9×10^{-3} mrem at 589 years, and maximum Ni-59 dose was 4.3×10^{-1} mrem at 33,000 years at 100 m from the RWMC boundary.

All actinide doses for the base case were at time periods greater than 10,000 years (Table 4-2) at 100 m south of the RWMC facility boundary. The greatest dose contributor was U-238 (9.4 mrem) followed by Pu-239. The maximum all pathway dose for all actinides was 12.3 mrem at 1.1×10^{6}--below the 25 mrem/yr criteria. These doses include the doses from radioactive progeny.

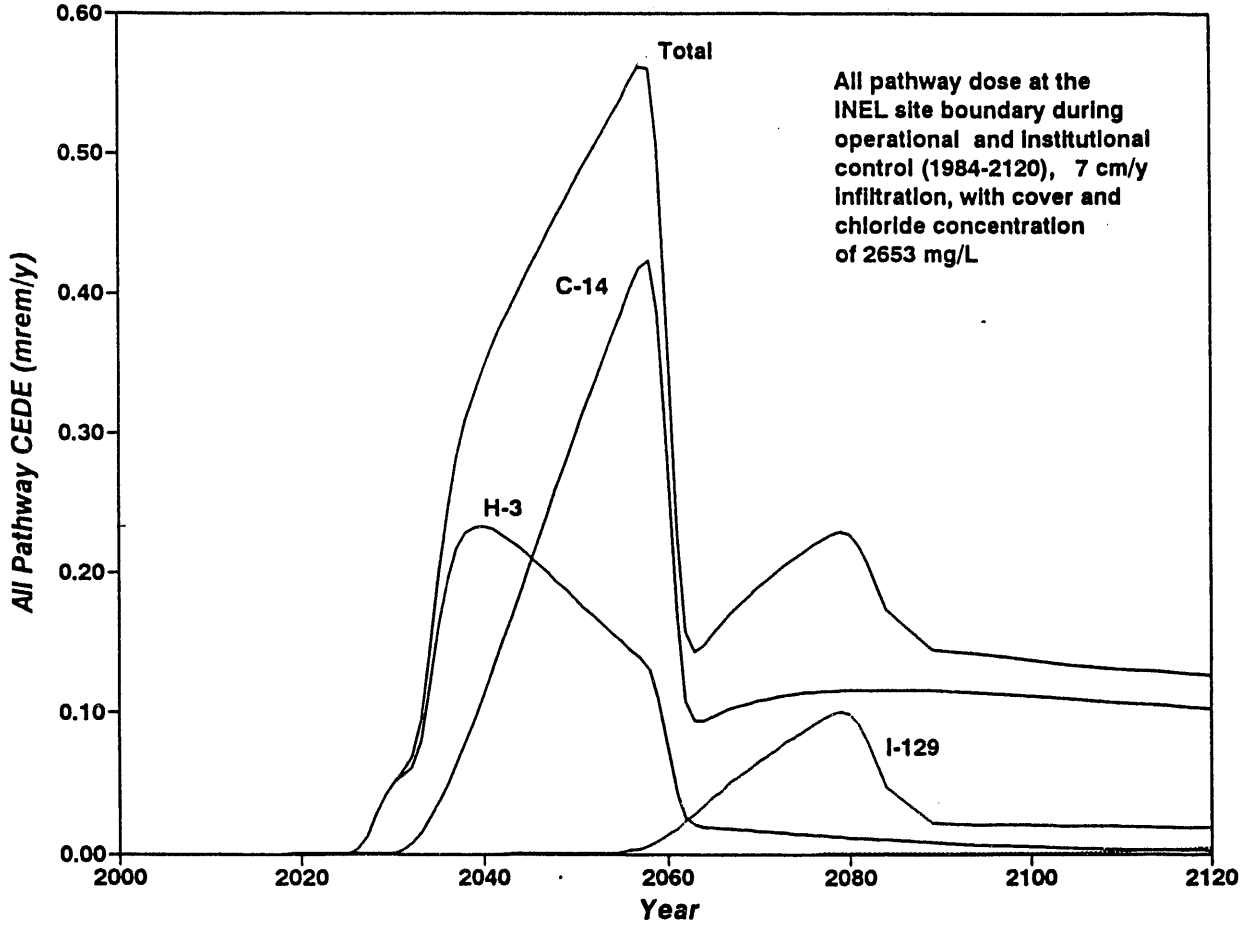

Figure 4-1. All pathway dose for fission and activation products at the INEL Site boundary during operations and institutional control for the base case at 7 cm/yr infiltration and an engineered cover in place at closure.

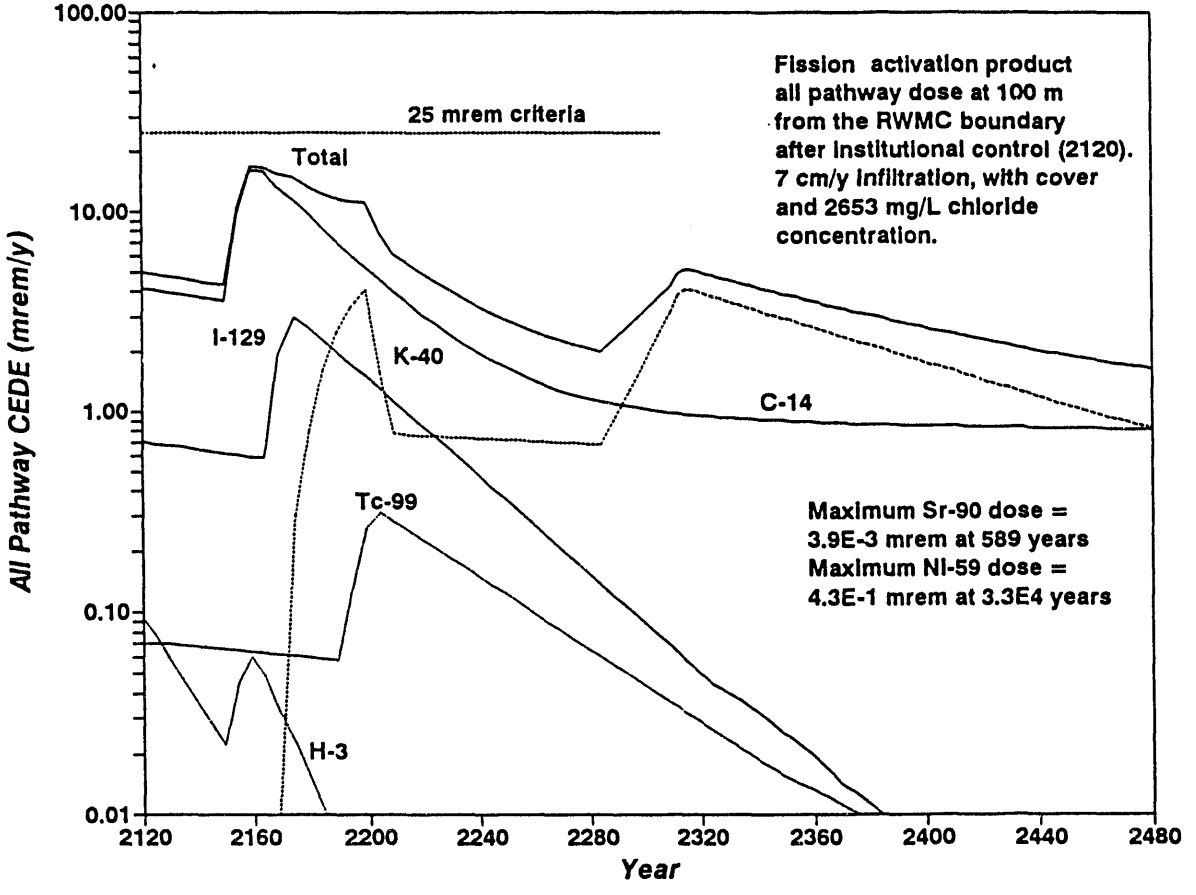

Figure 4-2. All pathway dose for fission and activation products at 100 m from the RWMC facility boundary after institutional control for the base case of 7 cm/yr infiltration and an engineered cover in place at closure.

Table 4-2. All pathway dose for actinides at 100 m from the RWMC facility boundary for the base case of 7 cm/yr infiltration and an engineered cover in place at closure.

Radionuclide	Maximum dose[b] (mrem)	Maximum times (yr)
U-238	9.4	7.2E+05
U-235	0.088	2.7E+05
U-234	0.68	2.7E+05
Pu-239	3.4	1.1E+06
Ra-226	4.8E-3	1.4E+04
Np-237	0.11	1.4E+04
Th-232	7.0E-04	2.7E+05
Th-230	1.2E-05	2.7E+05
Maximum[a]	12.0	1.1E+06

a. The maximum total dose calculated for all radionuclides for all time periods.

b. All doses include radioactive progeny.

4.1.3 Intruder Doses

This section presents doses to inadvertent intruders for acute and chronic exposures.

4.1.3.1 Acute Intruder-Drilling Doses. For the pits, the acute intruder-drilling scenario yielded a peak dose of 8.3 mrem in 2120, the end of institutional control. Inhalation accounted for the majority of the dose; U-232 was the dominant radionuclide. The dominant radionuclide for the external exposure pathway was Cs-137.

For soil vault rows, the acute intruder-drilling scenario yielded a peak dose of 190 mrem in the year 2120, the end of institutional control (see Table 4-3). Inhalation and external exposure accounted for approximately equal portions of the dose. Nickel-63 was the dominant radionuclide for inhalation, and Cs-137 was the dominant radionuclide for external exposures.

Table 4-3. Maximum acute intruder-drilling and acute intruder-construction doses.

Scenario and year	Internal dose (mrem)	External dose (mrem)	Total dose (mrem)
Acute drilling--soil vault rows (2120)	80	110	190
Acute construction--pits (1,000,000 years)	3.0	8.2	11

Doses were below the DOE Order 5820.2A criterion of 500 mrem for an acute exposure for the acute intruder-drilling scenarios associated with the pits and soil vault rows.

4.1.3.2 Acute Intruder-Construction Doses. The acute intruder-construction scenario yielded a peak dose of 11 mrem at 1,000,000 years after site closure, which corresponds to U-238 equilibrium (see Table 4-3). Inhalation accounted for 30% of the dose, and external exposure accounted for 70% of the dose. Uranium-238, U-234 (its long-lived progeny), and Th-230 were the dominant radionuclides. The 11 mrem dose was well below the DOE Order 5820.2A criterion of 500 mrem for an acute exposure.

4.1.3.3 Chronic Intruder-Agriculture Doses. The maximum chronic intruder-agriculture doses for pits resulting from direct contact with the waste occurred at 1,000,000 years after site closure; doses ranged from 15 to 28 mrem/yr (see Table 4-4). When groundwater all pathways doses and radon doses were added to these doses, the doses ranged from 39 to 52 mrem/yr.

The maximum chronic intruder agriculture doses for soil vault rows resulting from direct contact with the waste occurred in 2120; doses ranged from 28 to 53 mrem/yr (see Table 4-4). When groundwater all pathways doses and radon doses were added to these doses, the doses ranged from 50 to 75 mrem/yr.

Actinides (such as U-238) and their progeny dominated the doses for pits, and fission and activation products (such as Sr-90, Cs-137, and Ni-63) dominated the doses for soil vault rows. The intruder doses were below the DOE Order 5820.2A criterion of 100 mrem/yr for a chronic exposure. Appendix C contains additional information about the intruder analyses.

4.1.3.4 Chronic Intruder-Radon Doses. The chronic-intruder radon doses were 12 mrem/yr for pits and 4.5 mrem/yr for soil vaults using the data from the Colorado State University basement structures. For the pits, the peak dose occurred 2,200 years after site closure (year 4320), and almost 100% of the Ra-226 was from disposed Ra-226. For the soil vaults, the peak dose occurred almost 53,000 years after site closure because of ingrowth of Ra-226 from U-238. When the chronic intruder-radon doses were added to the chronic intruder-agriculture doses, the results were 52 mrem/yr for pits and 75 mrem/yr for soil vaults (Table 4-4). These doses were below the DOE Order 5820.2A chronic exposure criterion of 100 mrem/yr. Even though the waste in the pits had a Ra-226 concentration less than one quarter of the Ra-226 concentration in the soil vaults, the pits yielded a higher dose because soil did not separate the basement from the waste, as it did for the soil vaults. In addition, the soil vaults were modeled as five cylinders of limited area (3.14 m^2), which resulted in lower doses.

4.1.4 Drinking Water Impacts at INEL Site Boundary

Drinking water impacts were evaluated at the INEL Site boundary for all time periods. A receptor near the RWMC facility boundary was not evaluated because the drinking water criteria was intended to apply to community drinking water systems, not individual wells. Currently, a community drinking water system does not exist at the INEL Site boundary; the nearest system is at Atomic City. The INEL boundary receptor was chosen to bound any impacts to community drinking water systems downgradient from the INEL. This location was 5,500 m south of the RWMC. The criteria used to measure impacts to drinking water at the INEL Site boundary are stated in Section 3.4. Fission and activation products were measured against the 4 mrem/yr criterion because these nuclides were all manmade beta-gamma emitters. Actinides were

Table 4-4. Maximum chronic intruder doses.

Case	EDE (mrem/yr)
Pits	
8,030 m^3/yr inhalation rate Rupp diet, 0.7 shielding factor	28[a]
5,840 m^3/yr inhalation rate Yang and Nelson diet, 0.36 shielding factor	15[a]
Groundwater all pathways	12
Radon	12
Total	39-52
Soil vault rows	
8,030 m^3/yr inhalation rate Rupp diet, 0.7 shielding factor	53[a]
5,840 m^3/yr inhalation rate Yang and Nelson diet, 0.36 shielding factor	28[a]
Groundwater all pathways	17
Radon	4.5
Total	50-75

a. These doses result from direct contact with the waste from intruder-agriculture scenarios.

evaluated against the 15 pCi/L gross alpha activity criteria and the Ra-226 concentration limit along with the 4 mrem/yr dose limit for beta-gamma emitting radioactive progeny. Dose from the consumption of groundwater at the site boundary (Figure 4-3) for fission and activation products was dominated by C-14, H-3, and I-129. Tritium played a lesser role in the total dose because of decay during transit. The maximum dose at the INEL Site boundary was slightly less than 0.2 mrem at year 2060, and the principle dose contributor was C-14. The two prominent peaks in Figure 4-3 (about year 2060 and 2160) that are separated by a valley are a result of cover emplacement. The first peak is a result of releases that are postulated to occur before emplacement of a cover, and the second peak is a result of releases that are postulated to occur following the loss of institutional control and degradation of the cover. The maximum dose was below the stated criteria of 4 mrem/yr.

Drinking water impacts at the INEL Site boundary for actinides all occurred after 10,000 years as expected (Table 4-5). The maximum gross alpha activity was 0.035 pCi/L at 2.9E5 years, and the maximum alpha activity was dominated by U-238.

4.2 Uncertainty and Sensitivity Analysis

Models[a] are used in many areas of radiological performance assessments to quantify the behavior of complex systems and processes. Typically, the models are deterministic, with a set of parameters used as input and a resulting output value. In reality input parameters are not single values; they exhibit stochastic variability. There is uncertainty in the input data used in a model; therefore, there is uncertainty in the output estimated by the model. This type of uncertainty is known as parameter uncertainty. The objective of a parameter uncertainty analysis is to quantify the uncertainty in the output from a model based on the uncertainty in the input data.

---

a. In this context, the term model refers to the conceptual model of a system or process rather than the term computer code, which refers to a specific computer implementation of a model.

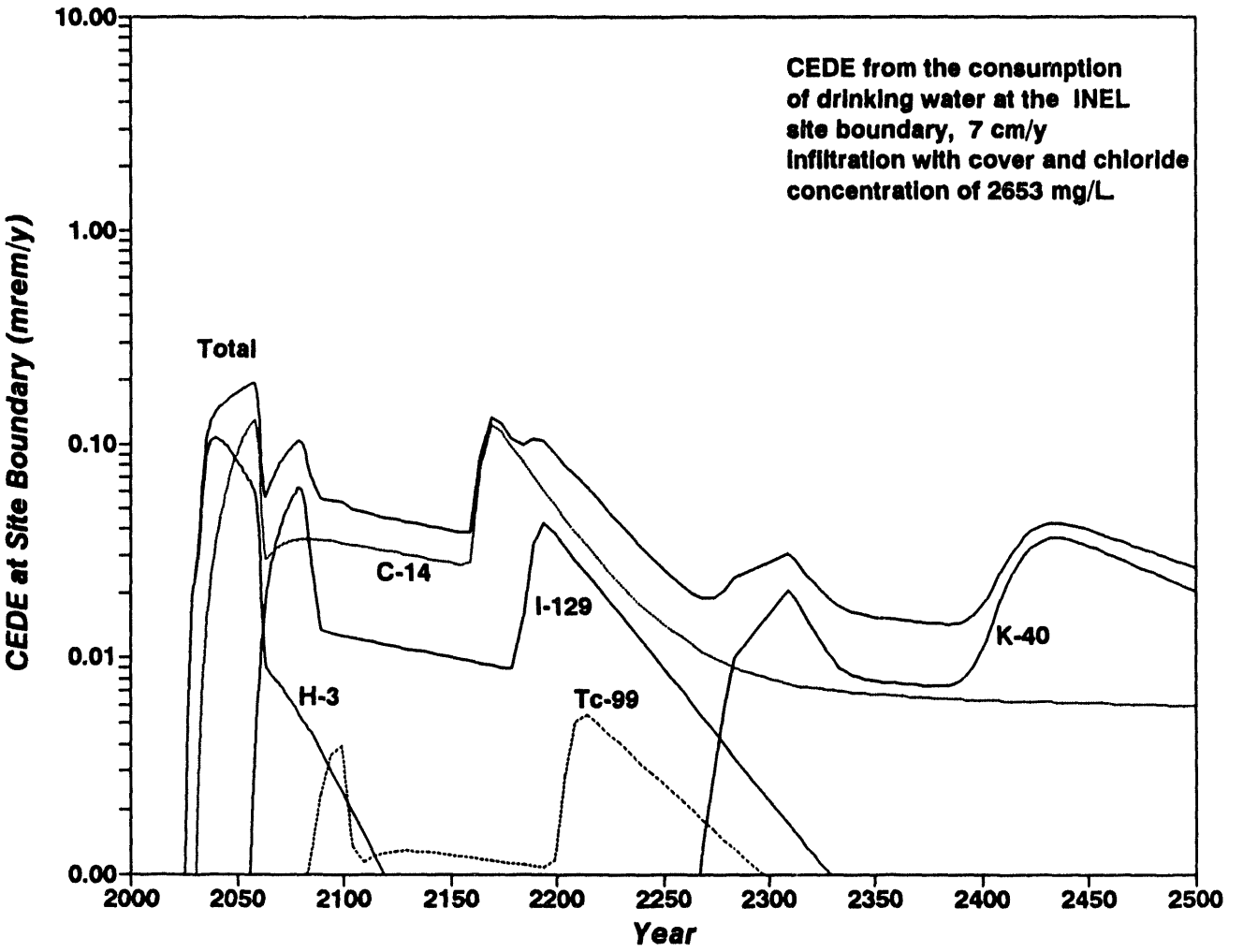

Figure 4-3. Drinking water dose for fission and activation products at the INEL Site boundary for the base case of 7 cm/yr infiltration and an engineered cover in place.

Table 4-5. Groundwater impacts at the site boundary for actinides for the base case of 7 cm/yr infiltration and an engineered cover in place.

Radionuclides	Maximum gross alpha activity concentration (pCi/L)	Maximum Ra-226 concentration (pCi/L)	Maximum beta-gamma CEDE (mrem/yr)	Time of maximum alpha activity (yr)
U-238	0.022	0.11	0.37	2.9E5
U-234	0.0093	.0078	0.025	2.9E5
U-235	0.0042	N/A	0.0016	2.9E5
NP-237	0.0022	N/A	8.3E-7	1.5E4
PU-239	0.0021	N/A	6.0E-4	5.8E5
RA-226	N/A	0.053	1.1E-3	1.5E4
TH-230	1.3E-6	1.2E-6	2.1E-6	2.9E5
TH-232	2.5E-5	N/A	1.1E-5	2.9E5
Maximum[a]	0.035	0.053	0.39	N/A

a. The maximum impacts calculated for all radionuclides for all time periods

There is also uncertainty in formulating the model used to quantify the behavior of the system or process; this is referred to as structural uncertainty. Structural uncertainty results from incomplete knowledge of the system or process and includes the uncertainty in the choice and specification of scenarios. The objective of a structural uncertainty analysis is to quantify the uncertainty in the output data based on the uncertainty in formulating the conceptual model of the system or process. Sensitivity analysis identifies the components of a model that have the most affect on model output.

The approach used in the radiological performance assessment to determine uncertainties relies on the results obtained using the nominal data. These results were used to remove unimportant scenarios, pathways, and radionuclides from further consideration. After they were removed from consideration, a quantitative uncertainty analysis was performed using a variety of techniques, depending on the individual analysis. The techniques used were (1) assigning generic estimates of uncertainty to the results based on similar published analyses, (2) performing simple parameter perturbation analyses, or (3) performing Monte Carlo analyses.

After the uncertainty analyses were performed, sensitivity analyses were used to identify the important contributors to the uncertainty. As with the uncertainty analyses, various techniques were used to estimate sensitivity, such as (1) generic estimates using published sensitivity analyses, (2) simple perturbation analyses, or (3) correlation coefficients calculated from Monte Carlo analyses.

Uncertainty and sensitivity analyses in this radiological performance assessment were divided into four categories: inventory, groundwater, atmospheric, and intruder. Within each one of these categories, dose to receptor was the end point evaluated. Unimportant scenarios, pathways, and radionuclides were removed from further analyses based on the results obtained using the nominal data, allowing the analyses to focus on the important scenarios, pathways, and radionuclides.

4.2.1 Inventory

There are four components to the uncertainty in the radionuclide inventory used in this radiological performance assessment. The first component is the uncertainty in the activity reported to the RWMIS for each radionuclide. The activity is usually determined by sampling and analyses of the waste for radionuclides that are readily measured, by using scaling factors for those radionuclides that are not readily measured, or based on knowledge of facility operations. The uncertainty in the activity for a specific radionuclide will be dependent on a number of factors, such as the decay mode of the radionuclide, the measurement system, the accuracy of scaling factors, and the waste form and container. An added dimension to

measurement system uncertainty is present at the INEL because not all measurement systems or procedures are identical at each INEL facility, and they have changed over time.

At the present time, insufficient data exist to provide a meaningful estimate of uncertainty for the activity reported for individual radionuclides in the RWMIS. Because meaningful uncertainty estimates are not available, the results from a sensitivity analysis would also be highly speculative. For example, insufficient data exist to even establish a range over which the radionuclide inventory might vary. Based on these considerations, sensitivity analysis was not attempted. However, important radionuclides were identified throughout the performance assessment. Radionuclide uncertainty and sensitivity should be examined in future research.

The second component is uncertainty in the identity of the radionuclides reported to the inventory data base. Historically, waste generators have reported readily measured gamma-emitting radionuclides, but they have sometimes neglected to report harder to measure beta-emitting radionuclides. The uncertainty in the identity of radionuclides based on scaling factors or process knowledge is also included in this component of inventory uncertainty. As inventory estimates have become more refined, omissions such as these have become apparent and the inventory has been revised to incorporate previously unreported radionuclides. This process will continue as the performance assessment is revised in the future.

A third component is uncertainty in the radionuclide forecasts. For example, radionuclide forecasts sometimes do not reflect historical data with respect to the radionuclides identified or radionuclide activities. While there may be good reasons for these forecasts, such as the uncertainty in the future mission of the INEL and Decontamination and Decommissioning and Environmental Restoration activities, in some cases they are based on incorrect assumptions or compounded conservative assumptions that do not reflect reality. In the performance assessment, a weighted average of historical and forecast data has been used to minimize this uncertainty. In addition, because of the iterative performance assessment process, this uncertainty will be reduced as time progresses and forecast inventory becomes better defined and as forecast inventory becomes disposal inventory.

A fourth component is the uncertainty in the identity of radioactivity reported to the RWMIS as mixed activation products (MAPs), mixed fission products (MFPs), and unidentified beta-gamma activity. In the performance assessment, unidentified activity accounts for only 0.12% of the activity disposed of in the pits and 0.033% of the activity disposed of in the soil vault rows. All unidentified activity was assigned to be 50% Sr-90 and 50% Cs-137. As an alternative to this assignment, the unidentified activity was assigned to various radionuclides based on historical data for 1984 to 1993. These calculations are discussed in Section 4.2.1.1, and their use in atmospheric, intruder, and groundwater all pathways scenarios is described in Sections 4.2.1.2 and 4.2.1.3. The problem of unidentified activity for future waste has been eliminated because the RWMC waste acceptance criteria does not allow activity to be reported as unidentified.

4.2.1.1 Alternative Inventory Assignment. As an alternative to assigning 50% Sr-90 and 50% Cs-137 to unidentified activity, the historical data for 1984 to 1993 was used to develop a distribution of radionuclides assigned to unidentified activity. This distribution was developed by adding the disposal activity of each radionuclide for 1984 through 1993 to arrive at a total for each radionuclide (see Tables A-1 and A-2). Inventory already identified as MFP, MAP, or unidentified beta-gamma was not included. In addition, H-3 associated with beryllium blocks was not included because MFP, MAP, and unidentified beta-gamma activity is not associated with the blocks.

The radionuclide totals were then normalized by dividing the inventory for each radionuclide by the total activity (summed over all radionuclides). MFP, MAP, unidentified beta-gamma activity, and the H-3 associated with beryllium blocks were also not included in the total activity. The normalized radionuclide distribution was then multiplied by the total unidentified activity to arrive at the radionuclide inventory used in the analyses (see Table 4-6). Radioactive decay was not considered at any point in this process.

4.2.1.2 Scenarios Involving Direct Contact with Waste. As a first step in the uncertainty analysis for scenarios involving direct contact with the waste, the intruder and atmospheric scenarios were examined to identify dominant scenarios, pathways, and radionuclides to limit the scope of the

Table 4-6. Unidentified activity distribution.

Soil vault row unidentified activity distribution		Pit unidentified activity distribution		Soil vault row and pit unidentified activity distribution	
Nuclide	(Ci)	Nuclide	(Ci)	Nuclide	(Ci)
		AC-227	6.894E-03	AC-227	6.894E-03
		AG-108M	4.259E-05	AG-108M	4.259E-05
		AG-110	3.186E-03	AG-110	3.186E-03
AG-110M	4.727E-06	AG-110M	8.151E-02	AG-110M	8.151E-02
AM-241	1.039E-06	AM-241	1.676E-02	AM-241	1.676E-02
		AM-243	7.428E-05	AM-243	7.428E-05
		BA-140	4.258E-02	BA-140	4.258E-02
		BA-133	4.258E-08	BA-133	4.258E-08
		BA-140	5.652E-02	BA-140	5.652E-02
		BE-7	2.803E-05	BE-7	2.803E-05
		BK-249	7.238E-04	BK-249	7.238E-04
		BR-82	4.258E-05	BR-82	4.258E-05
C-14	2.799E-02	C-14	2.746E-03	C-14	3.074E-02
		CA-45	4.322E-05	CA-45	4.322E-05
		CD-109	5.608E-04	CD-109	5.608E-04
		CE-139	1.277E-05	CE-139	1.277E-05
		CE-141	9.883E-02	CE-141	9.883E-02
CE-144	6.572E-01	CE-144	1.207E+01	CE-144	1.273E+01
		CF-249	8.924E-06	CF-249	8.924E-06
		CF-250	4.598E-06	CF-250	4.598E-06
		CF-252	1.936E-05	CF-252	1.936E-05
CM-242	2.935E-14	CM-242	4.221E-09	CM-242	4.221E-09
		CM-243	2.129E-08	CM-243	2.129E-08
CM-244	1.421E-08	CM-244	9.676E-05	CM-244	9.678E-05
		CO-56	3.330E-07	CO-56	3.330E-07
		CO-57	1.995E-03	CO-57	1.995E-03
CO-58	1.070E+03	CO-58	2.635E+00	CO-58	1.073E+03
CO-60	2.288E+03	CO-60	3.503E+02	CO-60	2.638E+03
CR-51	8.412E+01	CR-51	1.734E+02	CR-51	2.575E+02
CS-134	3.351E-01	CS-134	2.807E+00	CS-134	3.142E+00
CS-137	8.150E+00	CS-137	4.202E+01	CS-137	5.017E+01
EU-152	1.093E-02	EU-152	2.817E-01	EU-152	2.927E-01
EU-154	1.640E-03	EU-154	2.285E-01	EU-154	2.302E-01
EU-155	1.079E-03	EU-155	6.815E-02	EU-155	6.923E-02
FE-55	2.623E+02	FE-55	1.691E+02	FE-55	4.314E+02
FE-59	9.292E+00	FE-59	1.836E-02	FE-59	9.310E+00
H-3	5.437E-02	H-3	1.265E+02	H-3	1.266E+02
HF-175	6.786E+00	HF-175	1.763E-03	HF-175	6.788E+00
HF-181	1.077E+01	HF-181	1.996E-01	HF-181	1.097E+01
		HG-203	4.258E-08	HG-203	4.258E-08
		I-125	4.918E-05	I-125	4.918E-05
I-129	1.506E-06	I-129	5.980E-09	I-129	1.512E-06
		I-131	2.929E-03	I-131	2.929E-03
		I-132	4.293E-02	I-132	4.293E-02
		I-133	6.386E-05	I-133	6.386E-05
IR-192	1.822E-03	IR-192	1.150E-04	IR-192	1.937E-03
		K-40	7.201E-03	K-40	7.201E-03
		LA-140	6.904E-02	LA-140	6.904E-02
MN-54	7.480E+02	MN-54	4.246E+00	MN-54	7.523E+02
		MN-56	5.560E-02	MN-56	5.560E-02
		MO-99	1.682E-04	MO-99	1.682E-04
		NA-22	3.029E-03	NA-22	3.029E-03
		NA-24	1.158E-01	NA-24	1.158E-01
NB-94	1.113E-04	NB-94	2.938E-07	NB-94	1.116E-04
NB-95	1.091E+01	NB-95	1.660E+00	NB-95	1.257E+01
NI-63	8.259E+02	NI-63	4.930E+02	NI-63	1.319E+03
NP-237	3.404E-10	NP-237	7.275E-05	NP-237	7.275E-05
		NP-239	4.258E-08	NP-239	4.258E-08
		P-32	3.640E-04	P-32	3.640E-04
		PA-231	2.010E-04	PA-231	2.010E-04
		PB-210	1.320E-06	PB-210	1.320E-06
		PB-212	1.704E-04	PB-212	1.704E-04
PM-147	6.701E-03	PM-147	2.555E-04	PM-147	6.956E-03

Table 4-6. (continued).

Soil vault row unidentified activity distribution		Pit unidentified activity distribution		Soil vault row and pit unidentified activity distribution	
Nuclide	(Ci)	Nuclide	(Ci)	Nuclide	(Ci)
		PR-144	1.027E+01	PR-144	1.027E+01
		PU-236	1.364E-07	PU-236	1.364E-07
PU-238	1.172E-06	PU-238	7.974E-04	PU-238	7.986E-04
PU-239	5.540E-05	PU-239	1.130E-02	PU-239	1.136E-02
		PU-239	5.961E-07	PU-239	5.961E-07
PU-240	4.881E-06	PU-240	1.431E-03	PU-240	1.435E-03
PU-241	3.634E-05	PU-241	3.714E-03	PU-241	3.750E-03
PU-242	6.869E-11	PU-242	1.438E-05	PU-242	1.438E-05
		RA-225	6.386E-08	RA-225	6.386E-08
		RA-226	5.142E-02	RA-226	5.142E-02
		RA-228	4.267E-05	RA-228	4.267E-05
		RB-86	1.277E-06	RB-86	1.277E-06
		RE-188	3.960E-04	RE-188	3.960E-04
		RH-106	5.144E+00	RH-106	5.144E+00
		RN-222	4.262E-05	RN-222	4.262E-05
RU-103	6.684E-30	RU-103	1.065E-02	RU-103	1.065E-02
RU-106	8.150E-04	RU-106	5.312E+00	RU-106	5.313E+00
		S-35	5.543E-06	S-35	5.543E-06
SB-124	5.047E-04	SB-124	2.931E-04	SB-124	7.977E-04
SB-125	7.937E+00	SB-125	2.456E+00	SB-125	1.039E+01
SC-46	1.400E-01	SC-46	4.458E-03	SC-46	1.445E-01
		SE-75	1.935E-03	SE-75	1.935E-03
SN-113	6.795E-02	SN-113	1.405E-04	SN-113	6.809E-02
SR-85	8.184E-04	SR-85	4.136E-06	SR-85	8.225E-04
		SR-89	1.267E+00	SR-89	1.267E+00
SR-90	3.990E-01	SR-90	6.232E+00	SR-90	6.631E+00
		SR-91	1.873E-04	SR-91	1.873E-04
		SR-92	6.812E-05	SR-92	6.812E-05
TA-182	5.560E+01	TA-182	5.746E-03	TA-182	5.561E+01
TC-99	2.033E-05	TC-99	1.267E-05	TC-99	3.300E-05
		TE-129	6.957E-04	TE-129	6.957E-04
		TE-132	1.277E-05	TE-132	1.277E-05
		TH-228	4.411E-01	TH-228	4.411E-01
		TH-229	9.065E-08	TH-229	9.065E-08
		TH-230	2.550E-06	TH-230	2.550E-06
		TH-232	4.092E-04	TH-232	4.092E-04
		TH-234	2.018E-07	TH-234	2.018E-07
		U-232	9.445E-02	U-232	9.445E-02
		U-233	1.268E-04	U-233	1.268E-04
U-234	6.325E-08	U-234	6.253E-04	U-234	6.254E-04
U-235	1.069E-06	U-235	2.366E-03	U-235	2.367E-03
U-236	3.073E-09	U-236	8.554E-06	U-236	8.557E-06
U-238	3.448E-04	U-238	9.186E-02	U-238	9.220E-02
		V-48	1.065E-03	V-48	1.065E-03
		Y-88	1.277E-04	Y-88	1.277E-04
Y-90	1.192E-04	Y-90	5.249E+00	Y-90	5.249E+00
Y-91M	2.614E-24	Y-91M	2.802E-02	Y-91M	2.802E-02
		Y-93	4.713E-03	Y-93	4.713E-03
ZN-65	2.818E+00	ZN-65	1.101E+00	ZN-65	3.919E+00
ZR-95	5.960E+00	ZR-95	2.801E+00	ZR-95	8.760E+00
W-185	1.533E+01			W-185	1.533E+01
W-187	2.566E+00			W-187	2.566E+00
SN-117M	3.344E-01			SN-117M	3.344E-01
SN-119M	2.456E+01			SN-119M	2.456E+01
SN-121M	3.364E-05			SN-121M	3.364E-05
TE-125M	1.169E-01			TE-125M	1.169E-01
NI-59	3.757E+00			NI-59	3.757E+00
GD-153	3.645E-03			GD-153	3.645E-03
TOTAL	5.446E+03	TOTAL	1.420E+03	TOTAL	6.865E+03

uncertainty analysis. Based on the results obtained using nominal parameter values, the atmospheric scenario yielded a dose that was 8.6% of the 10 mrem dose limit. The intruder scenarios related to direct contact with waste yielded doses that were up to 53% of the 100-mrem dose limit. The intruder scenarios were identified as the dominant scenarios, and the atmospheric scenario was not considered further in the inventory uncertainty analysis. The groundwater all pathways analyses are evaluated in the following section.

Within the intruder scenarios, the soil vaults consistently yielded higher doses than the pits. Using nominal parameter values, the soil vaults yielded doses (190 mrem) that were 38% of the 500-mrem dose limit for the acute scenarios, and the pits yielded doses (11 mrem) that were 2.2% of the dose limit. For the chronic scenarios, soil vaults yielded doses (53 mrem) that were 53% of the 100-mrem dose limit, and pits yielded doses (28 mrem) that were 28% of the dose limit. The maximum doses for pits were calculated approximately 1,000,000 years after site closure without incorporating leaching of radionuclides from the waste. If leaching were incorporated, the doses from the pits would be reduced substantially. The maximum doses for soil vaults occurred at the end of institutional control, so leaching would have little effect on the doses. Based on these results, the soil vault scenarios were the dominant contributor to dose for the intruders, and the pits were not considered further in the inventory uncertainty analysis.

Intruder doses were recalculated using the soil vault unidentified activity distribution developed in the previous section (see Table 4-6) for the acute intruder-drilling scenario and the chronic intruder-agriculture scenario (see Table 4-7). As shown in Table 4-7, the dose for the acute intruder-drilling scenario did not change, the dose for the chronic intruder-agriculture scenario decreased slightly, and the assignment of unidentified activity is not critical for the intruder analyses in this performance assessment.

4.2.1.3 Groundwater All Pathways Scenario. Using the alternative inventory for unidentified activity that was developed in Section 4.2.1.1 (see Table 4-6), the groundwater all pathways dose assessment was performed using nominal hydrologic data. The peak dose at 100 m south of the RWMC facility

Table 4-7. Nominal and alternative intruder doses for soil vaults.

Scenario	Nominal EDE	Alternative EDE
Acute intruder-drilling	190 mrem[a]	190 mrem[b]
Chronic intruder-agriculture	53 mrem/yr[a]	49 mrem/yr[b]

a. Calculated based on conversion of unidentified activity to 50% Cs-137 and 50% Sr-90.

b. Calculated based on conversion of unidentified activity to the soil vault activity distribution on Table 4-6.

boundary during the post-institutional control period was 17 mrem/yr using the 50% Cs-137 and 50% Sr-90 unidentified activity assignment. Using the alternative inventory assignment, the peak dose at the RWMC facility boundary (100 m) during the post-institutional control period was also 17 mrem/yr.

The peak dose at the INEL Site boundary 5,500 m south of the RWMC during the operational and institutional control periods was 0.57 mrem/yr using the 50% Sr-90 and 50% Cs-137 inventory assignment. Using the alternative inventory assignment, the peak dose at the INEL Site boundary (5,500 m) was also 0.57 mrem/yr.

Based on the analyses, the uncertainty in the assignment of unidentified activity is not an important component of the uncertainty in the inventory used in the performance assessment.

4.2.2 Groundwater Pathway

This section addresses the sensitivity of the projected doses to variation in individual parameter values and assumptions used in the groundwater pathway model. It also evaluates the overall range of uncertainty in the projected doses. Because of limited data availability, distributions of parameter values were not established; therefore, the uncertainty analysis

did not attempt to define a distribution of projected doses. Rather, a range of projected doses are presented that represent the most favorable and least favorable cases. No confidence level is attached to either of these values. The range establishes the upper and lower bound on the projected doses.

The uncertainty and sensitivity analyses used in this radiological performance assessment employed the simple perturbation approach. In a simple perturbation analysis, the value of one parameter is varied over its range of values, while the other parameters are held constant. In this performance assessment analysis, only the endpoints of the range were evaluated. Parameters held constant were held at their nominal value. This technique is suggested as a first step in performing more rigorous uncertainty and sensitivity analyses (Seitz et al. 1991) and was appropriate for the groundwater transport model used in this performance assessment. Sophisticated uncertainty and sensitivity analysis techniques were not used for the groundwater transport model because of the numerous simplifications employed in the model and the difficulty in obtaining defensible statistical data needed to quantify parameter distributions.

The output variable used in the sensitivity and uncertainty analysis was the all pathway dose at the INEL Site boundary 5,500 m south of the RWMC and the all pathway dose 100 m south of the RWMC facility boundary. Drinking water dose was not evaluated as an output variable because drinking water doses can be estimated from all pathway doses. All pathway doses were generally a factor of three greater than drinking water doses for the same concentrations of radionuclides in groundwater. Uncertainty was quantified as the observed range in doses. Sensitivity was quantified as the percent change in doses and the percent change in doses divided by the percent change in input.

Six cases were evaluated (Table 4-8). Case 1 evaluated the effect of assigning the infiltration rate as either the upper or lower bound of the estimated infiltration range. Case 2 evaluated the effect of not installing an engineered cover for the base case[a] of 7 cm/yr infiltration. Case 3 evaluated the effect of different sorption coefficient values used in

a. The base case is defined as the analyses performed using nominal parameter values.

Table 4-8. Description of the six uncertainty and sensitivity analysis cases for the groundwater pathway.

Case	Description	Receptor location	Radionuclides evaluated
1	Evaluate dose impacts assuming infiltration of 4 and 10 cm/yr with an engineered cover in place for the all pathway analysis	RWMC boundary[a] after institutional control	All fission and activation products. Actinides evaluated only for the 10 cm/yr case.
2	Evaluate the impact of not installing an engineered cover over the waste	RWMC boundary[a] and INEL Site boundary for all time periods	All fission and activation products.
3	Evaluate the effect of reducing the sorption coefficients for nuclides that sorb in the all pathways analysis	RWMC boundary[a]	Ra-226, Np-237, U-238, and Pu-239
4	Evaluate the effect of the chloride content in the RWMC pore water on the release of H-3 from beryllium reflector blocks	INEL Site boundary during institutional control	H-3
5	Evaluate the impact of a flood of magnitudes 3, 5, and 10 times the base case infiltration rate after loss of institutional control and degradation of the cover	RWMC boundary[a]	C-14, I-129
6	Evaluate impact of D-E and E-F interbeds being absent	INEL Site boundary	C-14, I-129, Sr-90

a. Refers to the receptor location 100 m south of the RWMC facility boundary.

the base case analysis for nuclides subjected to sorption processes. Case 4 evaluated the effect of the chloride concentration in RWMC soil pore water on tritium releases. Case 5 evaluated possible impacts resulting from a flood at the RWMC after the period of institutional control and after the cover was assumed to degrade. Case 6 evaluated the impact of the lower two interbeds, D-E and E-F, not being present underneath the LLW pits.

The cases were evaluated at different receptor locations: 100 m from RWMC boundary, at the INEL Site boundary, or at both locations. The receptor location was determined by how the varied parameter or assumption impacted the dose at each location. For example, if the arrival time of a contaminant at the aquifer was beyond the year 2120, then the impacts were evaluated only at a receptor located 100 m south of the RWMC because the receptor at the INEL Site boundary is not considered after this time. A summary of the results of the uncertainty and sensitivity analyses is presented in Table 4-9.

To establish the overall uncertainty and sensitivity, the least favorable and most favorable parameter values were used to calculate the doses at 100 m south of the RWMC facility boundary and at the INEL Site boundary. Parameters varied in the overall uncertainty and sensitivity analysis included the parameters used in the groundwater pathway analyses. In addition, the alternative radionuclide inventory for unidentified activity described in Section 4.2.1.1 and lateral and transverse dispersivities in the aquifer different from the base case were used in the analysis. A summary of the results from these overall uncertainty cases are reported in Table 4-9. The remainder of this section discusses the six uncertainty and sensitivity cases and the overall uncertainty and sensitivity case.

4.2.2.1 Infiltration Rate. In general, the rate of moisture infiltration into the subsurface controls contaminant transport in the unsaturated zone. The actual amount of infiltration into the SDA in an average year is unknown, but it was estimated to range from 4 to 10 cm/yr (see Section 3.2 for a discussion of this estimate). The nominal value of 7 cm/yr was used as the basis for the flow and transport dose calculations. The resulting net water travel time down through the unsaturated zone is 30 years. This section presents the uncertainty and sensitivity of the estimated all pathway dose to the upper and lower bounds of infiltration.

Table 4-9. Summary of uncertainty and sensitivity cases evaluated for the groundwater pathway.

Case[a]	Base case dose (mrem)	Maximum dose (mrem)	Percent change in dose	Δ output divided by Δ input
RWMC receptor	17	--	--	--
INEL receptor	0.57	--	--	--
1. Infiltration (7 cm/yr base case)				
4 cm/yr	17	13	-24	55
10 cm/yr	17	23	35	82
2. Engineered cover (cover emplaced for base case)				
No cover, RWMC	17	7	-59	--[b]
No cover, INEL	0.57	0.7	23	--[b]
3. Sorption coefficients RWMC	17	17	0	0
4. Chloride concentration (base case 2,653 mg/L)				
137 mg/L at INEL	0.57	0.47	-18	18
12,500 mg/L at INEL	0.57	0.9	58	16
5. Flooding (base case no flooding)				
20 cm, RWMC	17	17	0	--[b]
35 cm, RWMC	17	17	0	--[b]
70 cm, RWMC	17	28	65	--[b]
6. Interbeds (Thickness = 12.5 m)				
9.2 m thick interbed, INEL	0.57	1	75	286
7. Overall uncertainty and sensitivity				
Upper bounds, RWMC	17	29	71	--[c]
Lower bounds, RWMC	17	9.5	-44	--[c]
Upper bounds, INEL	0.57	9.1	1,500	--[c]
Lower bounds, INEL	0.57	0.2	-65	--[c]

a. INEL = receptor at INEL Site boundary.
RWMC = receptor 100 m south of RWMC facility boundary.
b. Change in input cannot be quantified.
c. Not applicable.

Tables 4-10 and 4-11 show the corresponding velocities and travel times across each interbed for the cases of 4 and 10 cm/yr infiltration, respectively. The hydrologic conceptual model in each case is the same as the base case discussed earlier. The net water travel time down through the unsaturated zone is either 50 or 21 years, indicating the importance of the assigned infiltration rate for short-lived nuclides. These net water travel times were implemented in GWSCREEN simulations by using effective water contents of 0.161 and 0.172 for 4 and 10 cm/yr, respectively. This was the same methodology used in the base case analysis for 7 cm/yr infiltration. The receptor location was chosen to be 100 m south of the RWMC facility boundary because for fission and activation products, doses for that location after institutional control were closer to the 25 mrem all pathway limit. In addition, all pathway doses for actinides are only evaluated at 100 m south of the RWMC boundary because all doses occur after the period of institutional control (2120). Actinide doses were only evaluated for the 10 cm/yr case because all doses for the 7 cm/yr base cases were at time periods greater than 10,000 years.

Release rates of radionuclides from waste to soil were not changed except for tritium in beryllium blocks, where its release rate is a function of the Darcy velocity in soil (see Section 3.3.1.3). Leach rates from soil to the unsaturated zone were changed according to the assigned infiltration rate.

Variation in the infiltration rate on the all pathway scenario (Figure 4-4) results in a range of estimated doses from 13 to 23 mrem/yr for fission and activation products, which represents a 35% increase from the base case for an infiltration rate of 10 cm/yr and a decrease of 24% from the base case for an infiltration rate of 4 cm/yr. All actinide doses, with the exception of Ra-226 and Np-237, occurred after 10,000 years for the 10 cm/yr infiltration case (Table 4-12) and were below the 25 mrem/yr criteria. Note that the U-238 dose is less for the 10 cm/yr case (5.9 mrem/yr) than for the dose calculated in the 7 cm/yr case (6.5 mrem/yr) (Table 4-2). The higher dose in the 7 cm/yr infiltration case was a result of greater ingrowth of Ra-226 because of the longer transit time to the receptor.

Table 4-10. Interbed hydrologic parameters, estimated velocities, and water travel times for 4 cm/yr infiltration.

Interbed	Thickness[a] (m)	$K(\theta_v)$ (m/yr)	θ_v (cm^3/cm^3)	$\frac{\partial H}{\partial z}$ (m/m)	Velocity (m/yr)	Travel time (yr)
B-C	4.0	0.04[b]	0.076[d]	1[f]	0.53	7.5
C-D	5.2	0.04[c]	0.38[e]	4.5[g]	0.47	10.9
D-E	1.8	0.04[b]	0.38[d]	1[f]	0.10	17.5
E-F	1.5	0.04[b]	0.38[d]	1[f]	0.10	14.5
Total	12.5	–	–	–	–	50.4

a. Average thicknesses from Anderson and Lewis (1989).

b. Assigned lower end of 4 to 10 cm/yr range.

c. Lower value of estimated unsaturated conductivities at in situ moisture content from representative moisture characteristic curves from Magnuson and McElroy (1993).

d. Based on unit-gradient assumption, assigned infiltration rate, and estimated representative moisture characteristic curves from Magnuson and McElroy (1993).

e. Estimated representative in situ moisture content value, Magnuson and McElroy (1993)

f. Assumed.

g. Measured value in Well TW1, McElroy (1990).

Table 4-11. Interbed hydrologic parameters, estimated velocities, and water travel times for 10 cm/yr infiltration.

Interbed	Thickness[a] (m)	$K(\theta_v)$ (m/yr)	θ_v (cm^3/cm^3)	$\frac{\partial H}{\partial z}$ (m/m)	Velocity (m/yr)	Travel time (yr)
B-C	4.0	0.10[b]	0.086[d]	1[f]	1.17	3.4
C-D	5.2	0.10[c]	0.38[e]	4.5[g]	1.18	4.4
D-E	1.8	0.10[b]	0.41[d]	1[f]	0.24	7.5
E-F	1.5	0.10[b]	0.41[d]	1[f]	0.24	6.2
Total	12.5	---	---	---	---	21.5

a. Average thicknesses from Anderson and Lewis (1989).

b. Assigned upper end of 4 to 10 cm/yr range.

c. Upper value of estimated unsaturated conductivities at in situ moisture content from representative moisture characteristic curves from Magnuson and McElroy (1993).

d. Based on unit-gradient assumption, assigned infiltration rate, and estimated representative moisture characteristic curves from Magnuson and McElroy (1993).

e. Estimated representative in situ moisture content value, Magnuson and McElroy (1993).

f. Assumed.

g. Measured value in Well TW1, McElroy (1990).

Table 4-12. All pathway actinide doses 100 m from the RWMC facility boundary for the 10 cm/yr infiltration case.

Radionuclide	Maximum dose (mrem/yr)	Maximum time (yr)
U-238	5.9	1.9E+05
U-235	0.12	1.9E+05
U-234	1.0	1.9E+05
Pu-239	1.7E-05	3.8E+05
Ra-226	0.062	9.7E+03
Np-237	0.15	9.7E+03
Th-232	1.0E-03	1.9E+05
Th-230	3.5E-05	1.9E+05
Maximum[a]	7.0	1.9E+05

a. The maximum total dose calculated for all radionuclides for all time periods.

4.2.2.2 Placement of the Engineered Cover During Institutional Control. The performance assessment assumed that the engineered cover reduced net infiltration from 7 to 1 cm/yr during institutional control. The uncertainty and sensitivity associated with not installing an engineered cover over the facility after closure was evaluated for the all pathway scenario for fission and activation products (Figure 4-5) for receptor locations at the INEL Site boundary and 100 m from the RWMC facility boundary. Both of these locations were evaluated because emplacement of the cover impacts the dose at both locations. The maximum dose after institutional control at the RWMC boundary (7 mrem/yr) was less than the dose with the cover because most nuclides that leach the fastest (C-14, H-3, and I-129) already reached the groundwater, and the plume passed during the period of institutional control. This change represented a decrease of 59%. The maximum dose at the INEL Site boundary during institutional control was 0.7 mrem/yr, which is an increase of about 23% from the base case of 0.57 mrem/yr.

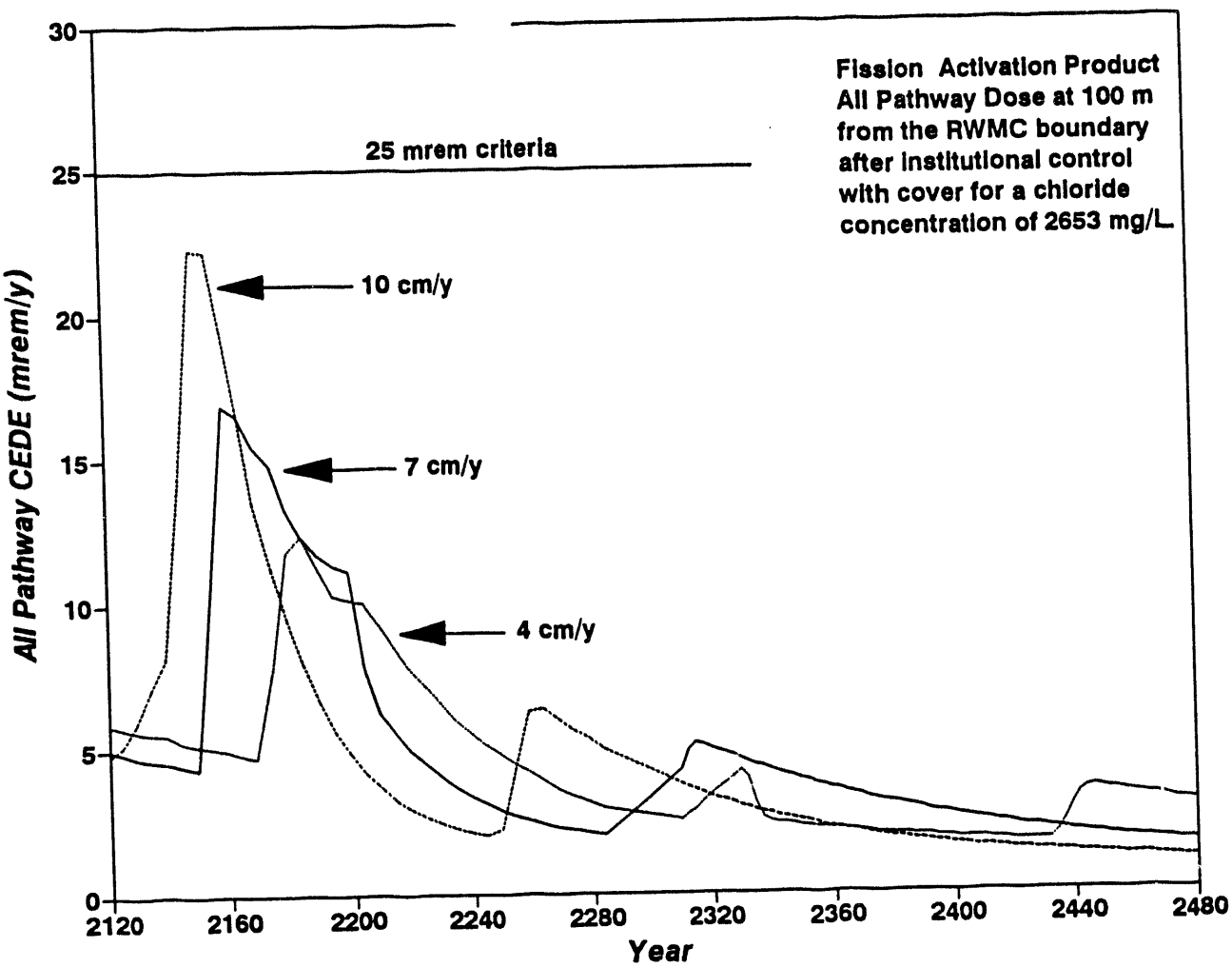

Figure 4-4. Fission and activation product all pathway doses at 100 m from the RWMC facility boundary for the base case of 7 cm/yr infiltration and sensitivity cases of 4 and 10 cm/yr.

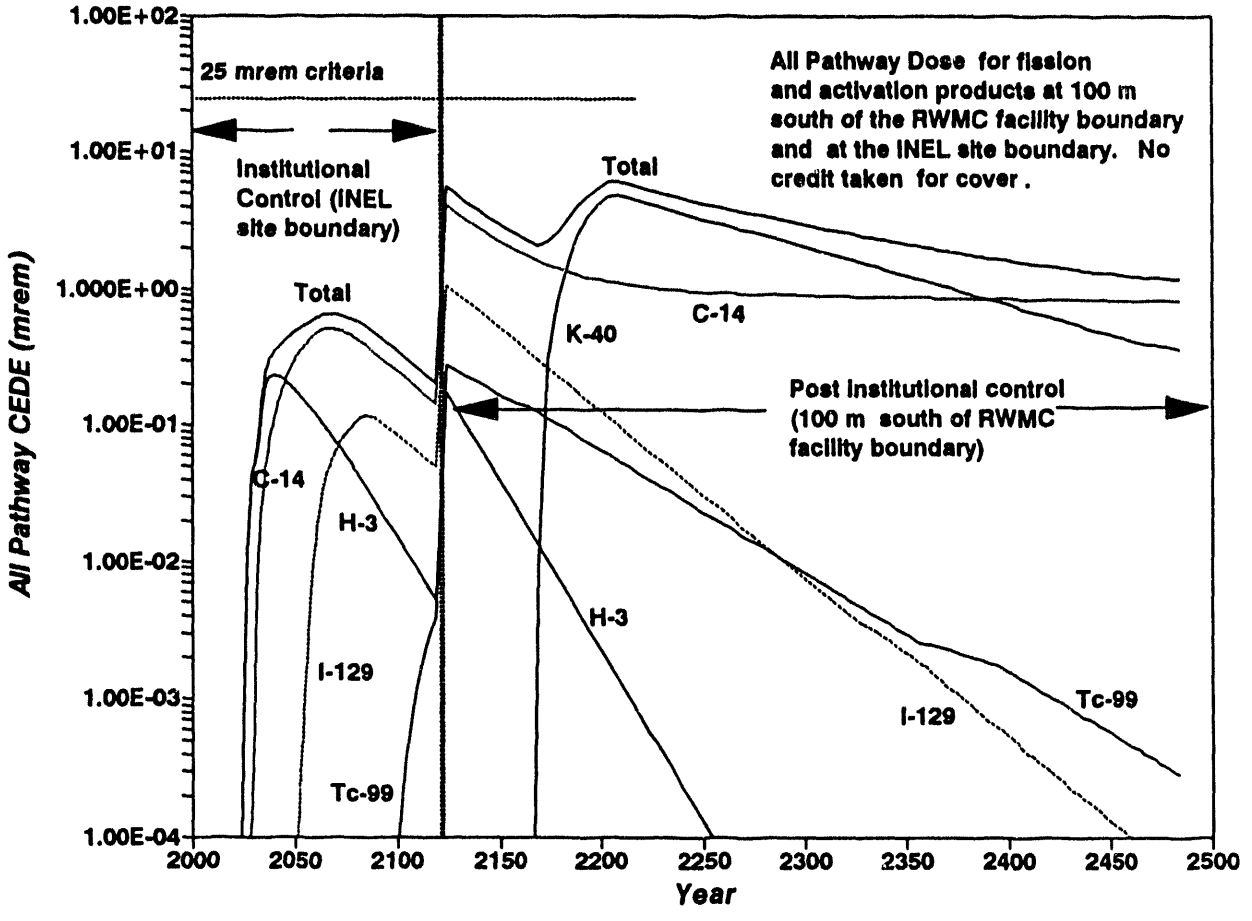

Figure 4-5. Fission and activation product all pathway doses at the INEL Site boundary and 100 m from the RWMC facility boundary for the base case of 7 cm/yr infiltration--no credit for engineered cover.

4.2.2.3 Sorption Coefficients. Sorption coefficients are the parameter with the greatest range of possible values (see discussion in Section 3.3.4). A range of several orders of magnitude is not uncommon. Sorption retards movement of dissolved substances in the groundwater and increases the travel time of the contaminant plume to the receptor. Some of the more highly sorbed elements are the actinides, as reflected in the sorption coefficients used in this performance assessment. The relatively high sorptive capacity of the actinides results in unsaturated travel times exceeding 10,000 years for the base case. Most of the fission and activation products, with the exception of Ni-59, have low sorption coefficients or do not possess any sorptive properties. For this reason, only selected actinides were addressed for the uncertainty and sensitivity analyses of the sorption coefficients. In this analysis, the uncertainty and sensitivity of the model to changes in the sorption coefficient was not evaluated; rather, the uncertainty and sensitivity of the model to sorption coefficients derived from other sources was evaluated. The receptor for this analysis was located 100 m south of the RWMC boundary because all actinide travel times exceeded the institutional control period.

Section 3.3.4 presents ranges of K_d values obtained from the literature and K_d values used in this performance assessment. For the uncertainty and sensitivity analysis, two cases were run. In the first case (Table 4-13), minimum K_d values for sediment and basalt tabulated in the Sheppard and Thibault (1990) and the NEA data base (Ticknor and Ruegger 1989) were used in the groundwater transport model. In the second case, K_d values listed in the methodology for assessing low probability hazard sites at the INEL (DOE 1992) were employed. In the latter case, the K_d values have the concurrence of the State of Idaho and the EPA, and both agencies consider the values to be conservative estimates of sorption coefficients. In most cases, the minimum K_d value reported was lower than the K_d value used in the base case; however, there were some exceptions such as the radium K_d from DOE (1992) and the uranium basalt K_d from the NEA data base.

For case 1 (Figure 4-6), the maximum all pathway dose at 100 m from the RWMC boundary was slightly less than 5 mrem/yr, and it occurred at 330 years

Table 4-13. Actinide sorption coefficient values derived from other sources and used in the uncertainty and sensitivity analysis.

	Case 1[a]		Case 2[b]
Radionuclide	K_d Backfill soil and interbeds (mL/g)	K_d Basalt (mL/g)	K_d (mL/g) basalt, backfill soil and interbeds
U-238	0.03	731	6
U-234	0.03	731	6
Ra-226	10[c]	1080	500
Np-237	.5	1.3	no value reported
Pu-239	27	35	22

a. Basalt K_d values from the NEA data base (Ticknor and Ruegger 1989). Backfill soil and interbed K_d values used the minimum sand value reported in Sheppard and Thibault (1990).

b. All K_d values from DOE (1992).

c. No minimum value reported, a value of 10 mL/g was assumed.

from 1984 (year 2314). The maximum dose was from Np-237. The total dose, including fission product dose at the year 2314 (time of maximum Np-237 dose), was about 10 mrem/yr, which is below the 25 mrem/yr criteria. At the time of the first Np-237 peak, the maximum fission product dose was 12 mrem/yr at year 2189, and the maximum Np-237 dose was 4.4 mrem/yr. Therefore, the total dose of 17 mrem/yr is less than the 25 mrem/yr criteria, which is the same dose obtained using the nominal data. For case 2 (Figure 4-7), the maximum all pathway dose was slightly less than 8 mrem/yr, and it occurred around 2,000 years from 1984. These impacts would not overlap fission product impacts; therefore, the doses are not additive. The maximum dose contributor was from U-238 (7.2 mrem/yr), and the total dose was below the 25 mrem/yr criteria. This represents a 53% decrease.

4.2.2.4 Chloride Concentrations. As discussed in Section 3.3.1.3, the corrosion of beryllium (and the resulting release of tritium from the beryllium) is dependent on the chloride ion concentration in the pore water. For the base case, the chloride ion concentration was assumed to be the

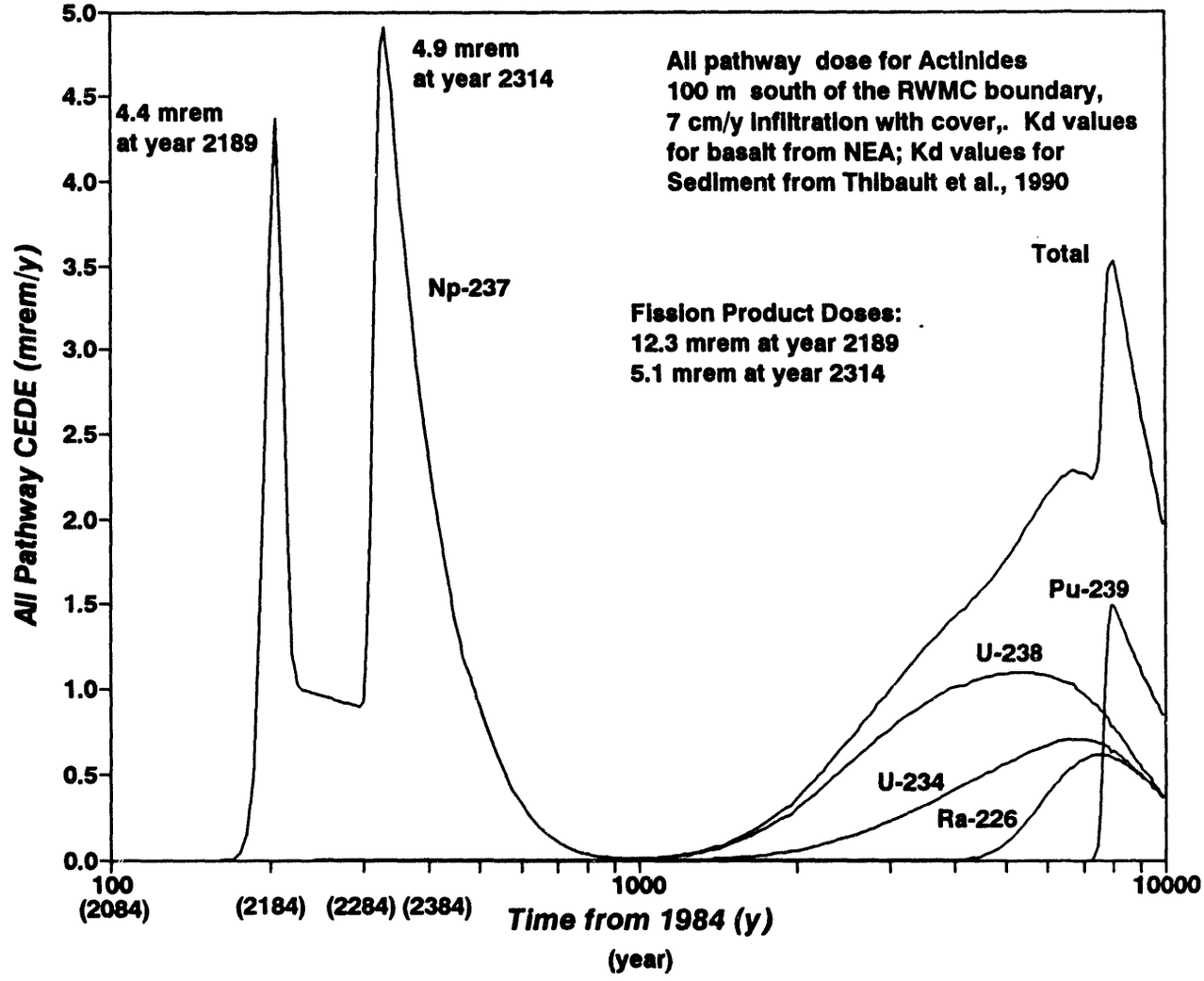

Figure 4-6. All pathway dose at 100 m from the RWMC boundary for selected actinides using K_d values from Sheppard and Thibault (1990) and the NEA data base.

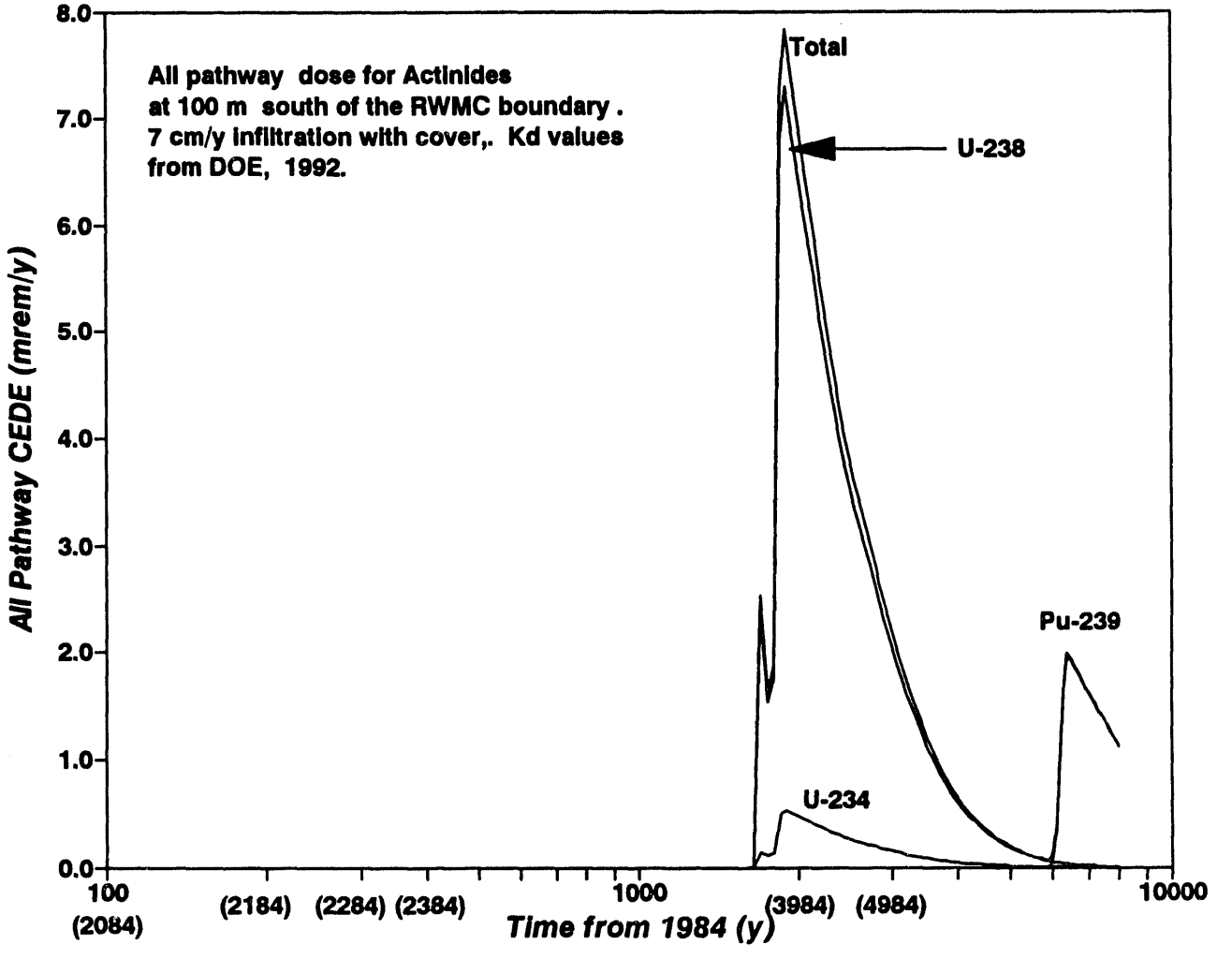

Figure 4-7. All pathway dose at 100 m from the RWMC boundary for selected actinides using K_d values from DOE (1992).

arithmetic mean (2,653 mg/L) of the chloride concentration in the two wells nearest the soil vault containing the beryllium blocks. The uncertainty and sensitivity cases looked at the geometric mean of the measured chloride concentrations found in all lysimeters at the SDA (137 mg/L) and the maximum chloride ion concentration measured at the SDA (12,500 mg/L). All other base case parameters remained the same. This change only affects the tritium results; however, cumulative effects were also computed. The receptor was selected to be at the INEL Site boundary because impacts were only apparent during operations and institutional control (1984 to 2120). After institutional control, most of the tritium had decayed; therefore, impacts were not significant at any receptor location (see Figure 4-8). The maximum all pathway dose (for all nuclides) during institutional control at the INEL Site boundary ranged from 0.9 mrem/yr for the 12,500 mg/L Cl^- concentration to 0.47 mrem/yr for a Cl^- concentration of 137 mg/L. This represents an increase in dose of 58% for the 12,500 mg/L Cl^- concentration and a decrease in dose of 18% for the 137 mg/L Cl^- concentration. The maximum tritium dose for a chloride concentration of 12,500 mg/L was 0.68 mrem/yr, which is about a 200% increase over the base case tritium dose of 0.23 mrem/yr.

4.2.2.5 Flooding. This scenario evaluated flooding in terms of the impacts on release rate from the source and travel time to the aquifer. It was not intended to be a detailed analysis of the hydrologic consequences of a flood or evaluate the short-term impacts to flow in the aquifer from a flood. The flooding event was assumed to occur at 2125, after the institutional control period ended and after the engineered barrier was assumed to degrade. Flooding was not considered before this time because dikes and general maintenance of the facility prevent flooding. Based on these constraining assumptions, the chosen flood time resulted in the maximum increase in resulting doses for the groundwater pathway for receptors at 100 m from the RWMC facility boundary.

4.2.2.5.1 Hydrologic and Transport Model--There are currently no estimates of the expected frequency of floods for the local basin or of the amount of water that may be available for infiltration as a result of

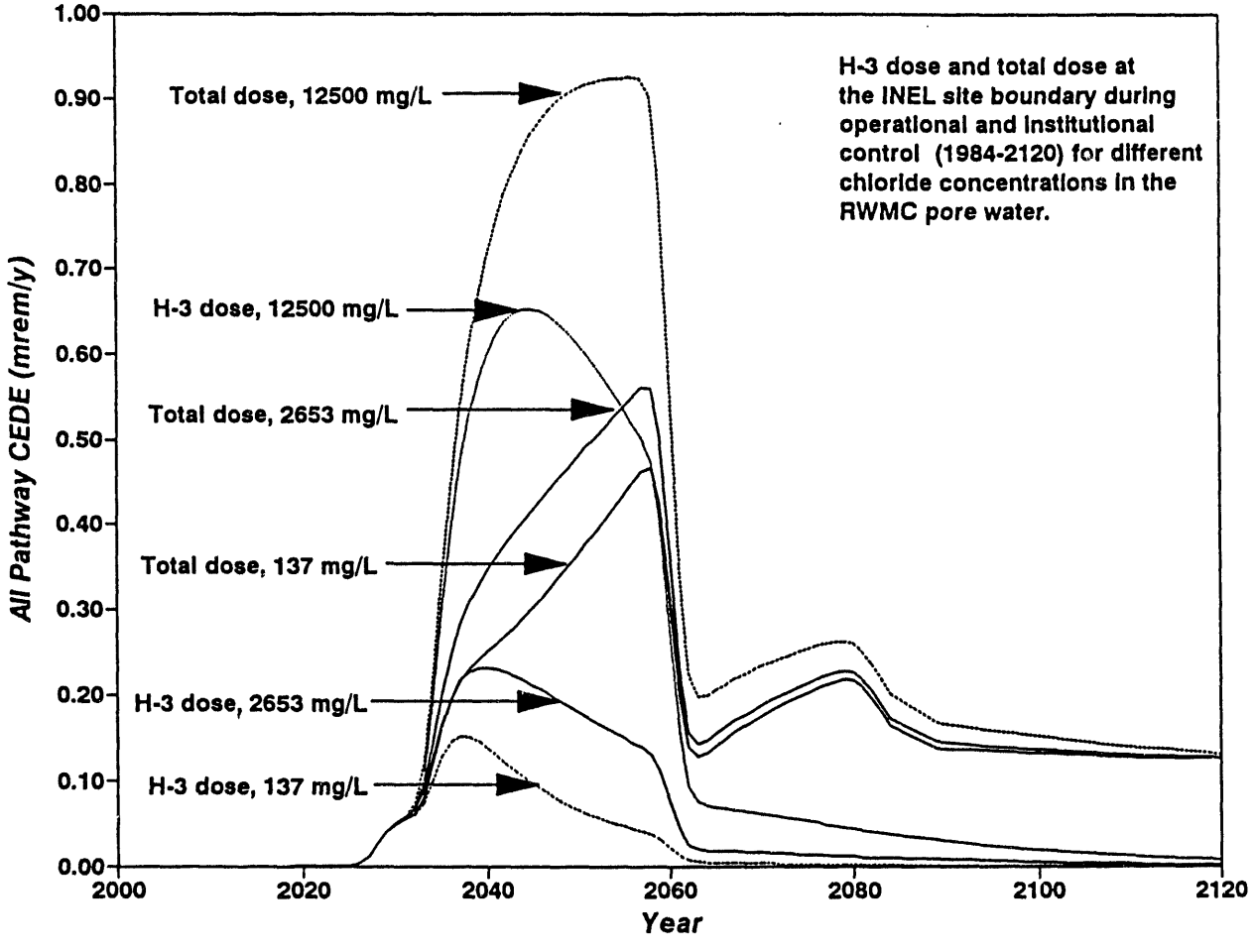

Figure 4-8. Tritium dose and total dose at the INEL Site boundary during operations and institutional control for 7 cm/yr infiltration and different Cl^- concentrations.

flooding. This is an area for future study as addressed in Section 5.2. For purposes of evaluation, three different magnitude floods were assumed. The magnitudes were roughly factors of 3, 5, and 10 times the annual infiltration of 7 cm. Although a flood would occur in a matter of hours, the time required for the water to infiltrate into the subsurface would be longer. For purposes of this sensitivity analysis, the additional flood water was allowed to infiltrate over a period of 0.1 years.

A transient analysis of water movement in the unsaturated zone is beyond the capability of the GWSCREEN model, which can only consider water movement in the unsaturated zone that has a constant velocity. The transient nature of water movement under flooding conditions required use of a numerical simulation code that solved the governing equation for unsaturated flow under conditions of varying water infiltration rates. Additionally, the code had to solve the transport equations for this time-varying flow field with a time-varying mass loading rate. The PORFLOW code, Version 2.5 (Runchal and Sagar 1993) was used for the flooding simulations because it had these capabilities. The GWSCREEN code was still used for the aquifer flow portion of the groundwater pathway in this flooding analysis. The additional water added to the aquifer because of flooding was not accounted for; instead, the nuclide flux through the base of the lowest interbed was used as input to the GWSCREEN code for the aquifer flow portion of the groundwater pathway.

The hydrologic conceptual model for the unsaturated zone was the same as that in the base case evaluation. The fractured basalts were still assumed to have negligible water travel times and were not included. The four sedimentary interbeds were the only material through which water flow was considered. In the PORFLOW simulation, the four interbeds were stacked together so they were in direct contact with each other. Figure 4-9 shows the interbeds in relation to the PORFLOW simulation coordinates. The hydrologic properties assigned to each interbed were the same as in Tables 3-2 and 3-3.

Implementing this same hydrologic conceptual model into the PORFLOW code required some deviations from the GWSCREEN representation of the unsaturated zone. The increased water velocity across the C-D interbed from the base case hydrologic conceptual model could not be included. While an additional source of water could have been added immediately above and extracted below the

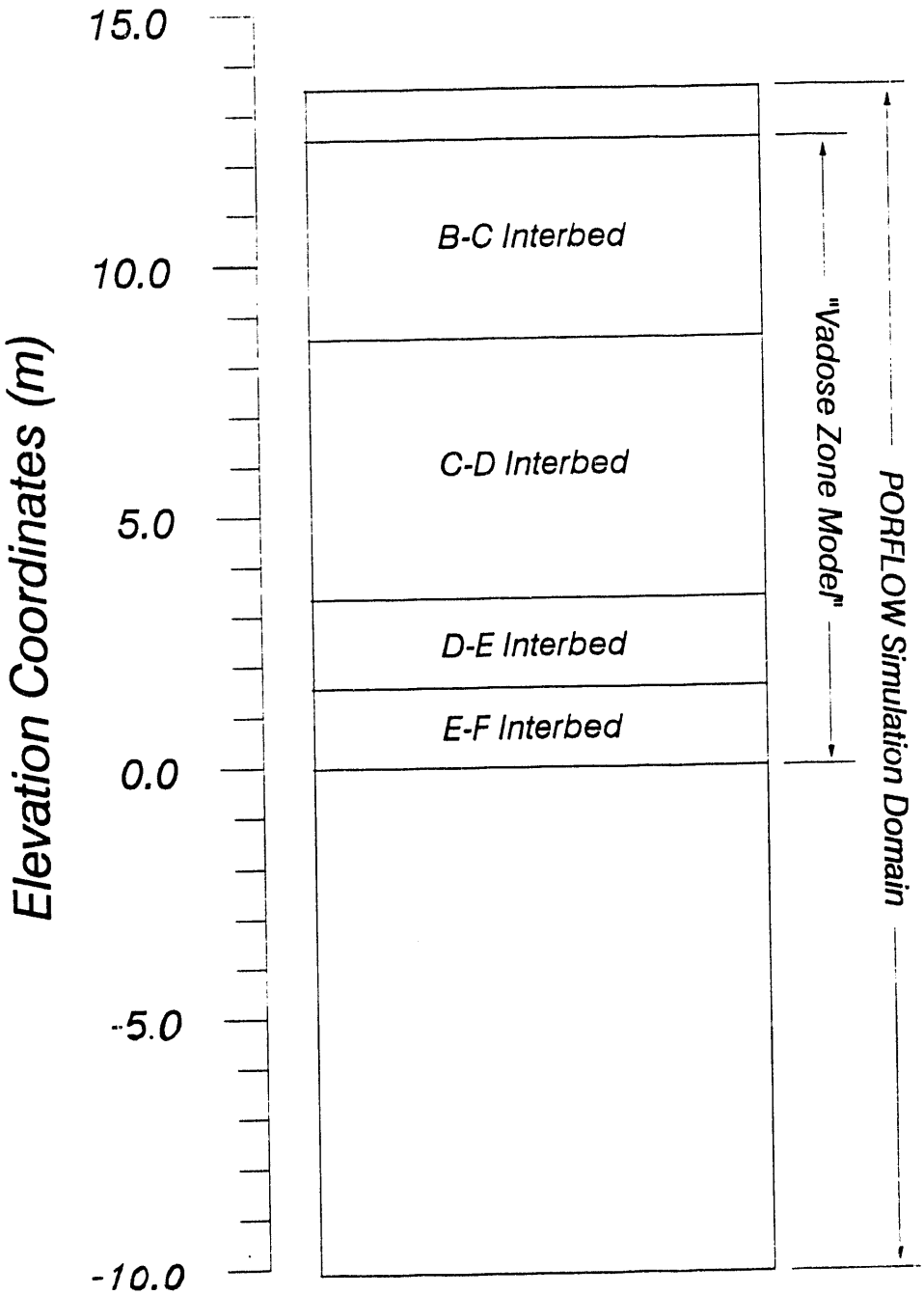

Figure 4-9. PORFLOW simulation domain showing sedimentary interbeds stacked together.

C-D interbed, it would have resulted in an incorrect loss of nuclide mass. As a result, using the same constant background infiltration of 7 cm/yr would have resulted in a longer travel time than the base case simulated with GWSCREEN. The purpose of this scenario was to evaluate the impacts of flooding in terms of mass release rates and shorter travel times--not to hydrologically mass balance the system. Therefore, the travel time was matched by increasing the background water flux assigned at the upper boundary to 13 cm/yr. This resulted in a water travel time through the PORFLOW unsaturated zone model of 30 years. Any additional water from flood events was added to this background infiltration.

The only change to the source term model from the base case was in the net infiltration rate as a function of time. The base case data were used from 1984 to 2125. At 2125, a short water pulse lasting 0.1 year occurred. This pulse corresponded to 3, 5, and 10 times the base case annual infiltration of 7 cm. After that time, the water flux rate was returned to the original base case infiltration rate of 7 cm/yr. The additional water resulted in higher leach rates from soil to the unsaturated zone. Changes to the release rate from waste to soil because of flooding were not considered. The time period selected for the flood (after institutional control) was chosen because radionuclide inventories in the soil would be near their maximum, resulting in the highest potential release. Equilibrium partitioning was still assumed during the periods of flooding. This assumption is conservative because under conditions of rapid water movement, equilibrium between the solid and liquid phases may not be reached, which would result in a lower mass flux rate from the source. Only two nuclides were selected for this analysis: C-14 and I-129. Tritium was not included because at the time of the flood, most of the tritium had already decayed. Actinides were not considered because their transit times for the base case were significantly longer than 10,000 years, and their high partition coefficients would still prevent migration in the dissolved phase. Iodine-129 and C-14 were the two largest dose contributors after loss of institutional control, and they were also very mobile (low sorptive capacity).

There was a slight offset in the PORFLOW simulation for the locations where the boundary conditions for water were assigned and where the nuclide mass was input into the system to avoid mass balance difficulties with the

upper boundary condition for transport. The PORFLOW simulation domain was extended upward 1 m from the top of the B-C interbed. The effect of this slight offset can be seen in Figure 4-10, which shows the water flux at the top of the B-C interbed superimposed on the C-14 mass loading at the top of the B-C interbed. The wetting front from the flood travels rapidly through this 1-m offset, as can be seen by the overlap of the water flux and the nuclide source loading.

The simulation domain was similarly extended below the bottom of the E-F interbed to prevent interference from boundary condition problems. The simulation domain below the E-F interbed was considered to have the same hydrologic properties as the E-F interbed. At the lower boundary, a constant downward 13 cm/yr water flux was assigned. A zero nuclide concentration was assigned for the bottom boundary, which meant that any nuclide reaching this depth could diffuse out the bottom of the simulation domain.

As in the base case, no dispersion in the unsaturated zone was assumed. However, molecular diffusion was included to ease the numerical solution and prevent nuclide mass balance problems. Because this was an advective dominated transport problem, the addition of molecular diffusion had only a small effect on the transport results. The assigned value was 1.0×10^{-5} cm^2/s, a commonly reported value for diffusion of nuclides in free water. This diffusion coefficient was not reduced by any tortuosity factor because diffusion was a minor component of transport.

The flux of nuclide across the 0.0-m elevation, internal to the simulation domain, was the interface between the unsaturated zone and aquifer portions of the groundwater pathway. This nuclide flux was then input into GWSCREEN, which was parameterized in exactly the same way for the aquifer as it was for the base case analysis.

To demonstrate the appropriateness of the PORFLOW simulation results to the GWSCREEN conceptual model, the base case of no flooding was also simulated. Figures 4-11 and 4-12 show the nuclide loading into the PORFLOW

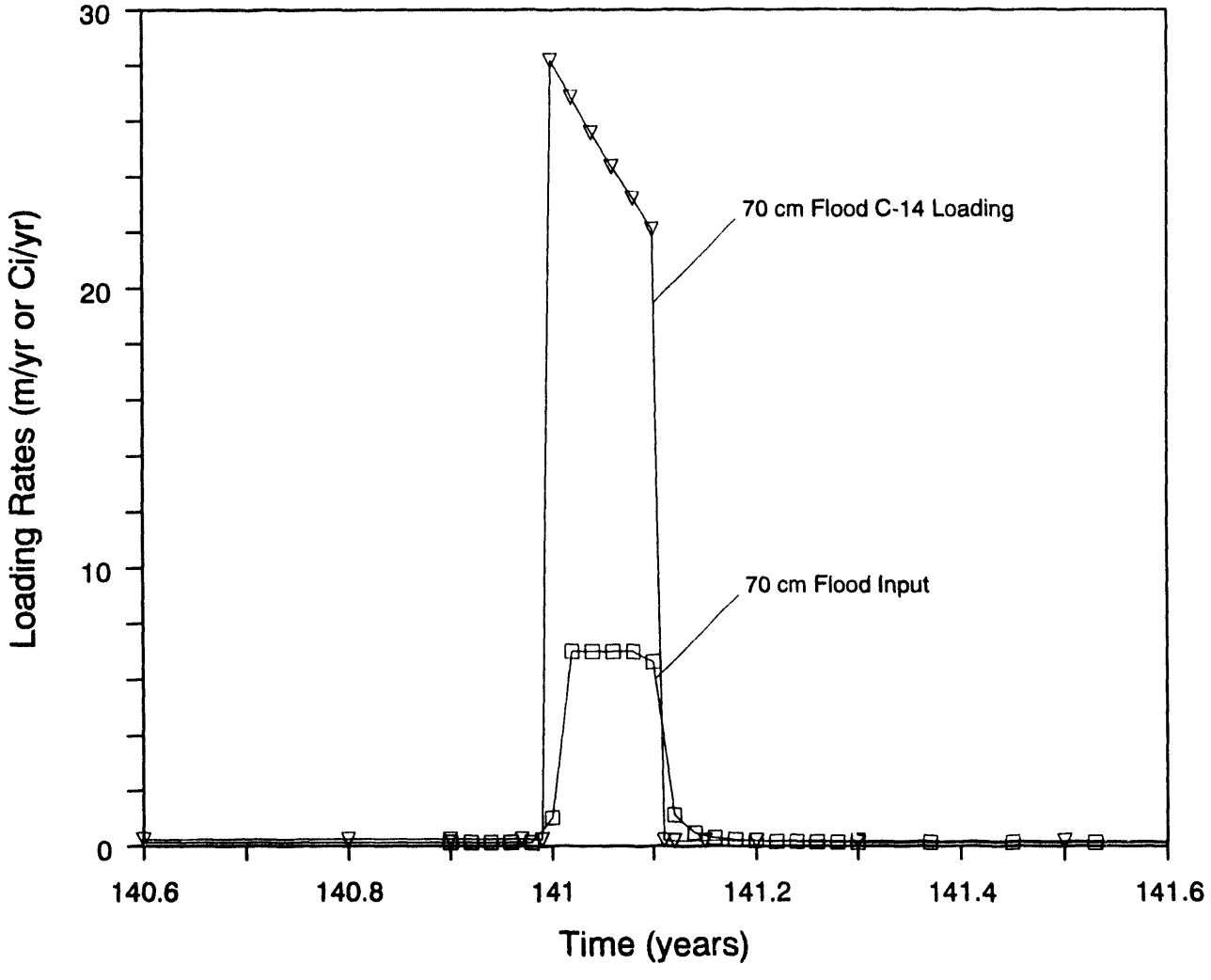

Figure 4-10. Water flux and C-14 loading at 12.5 m (top of B-C interbed) as a result of a 70-cm flood event.

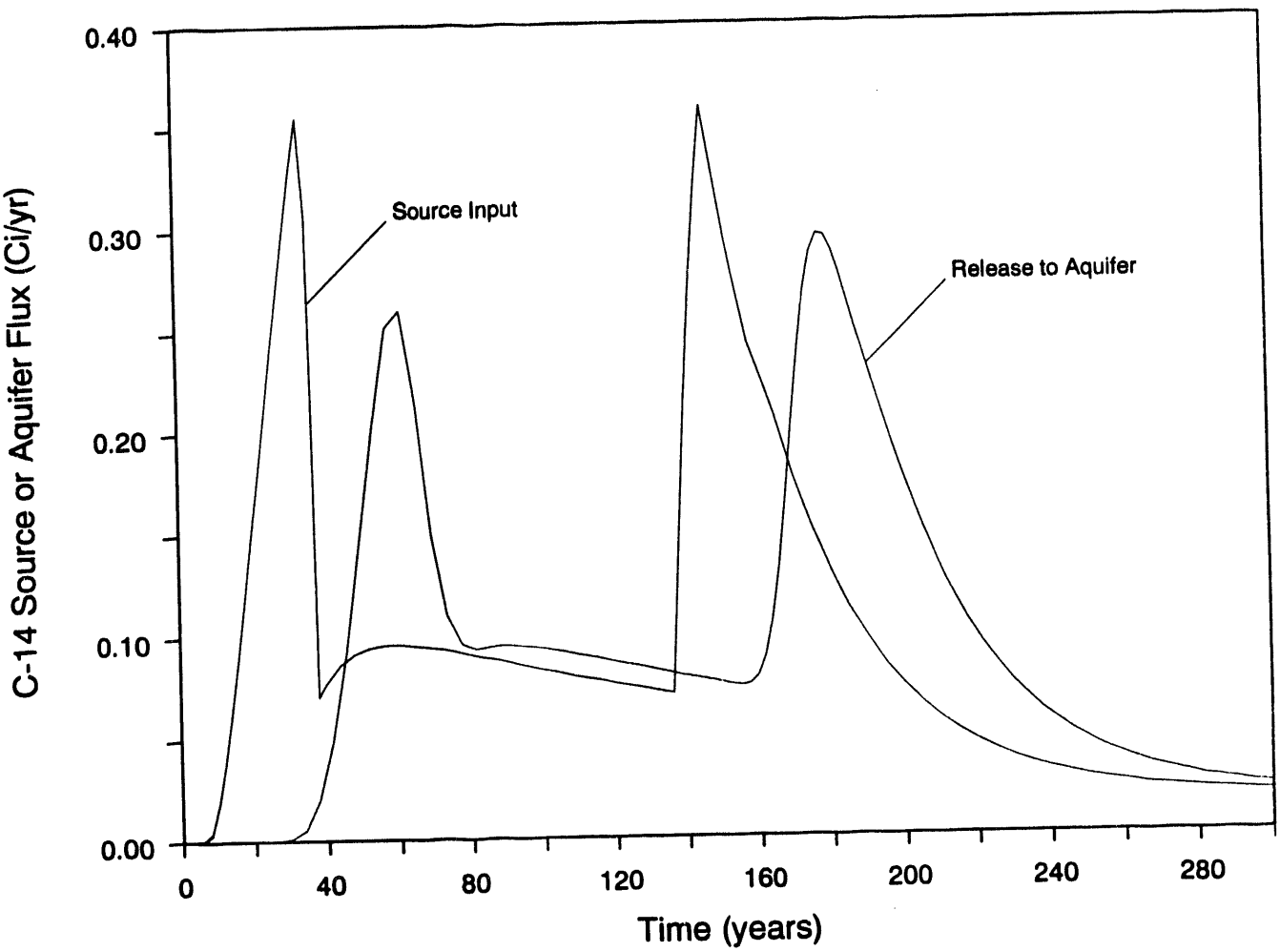

Figure 4-11. Carbon-14 source loading and flux to the aquifer for no flooding simulated with PORFLOW.

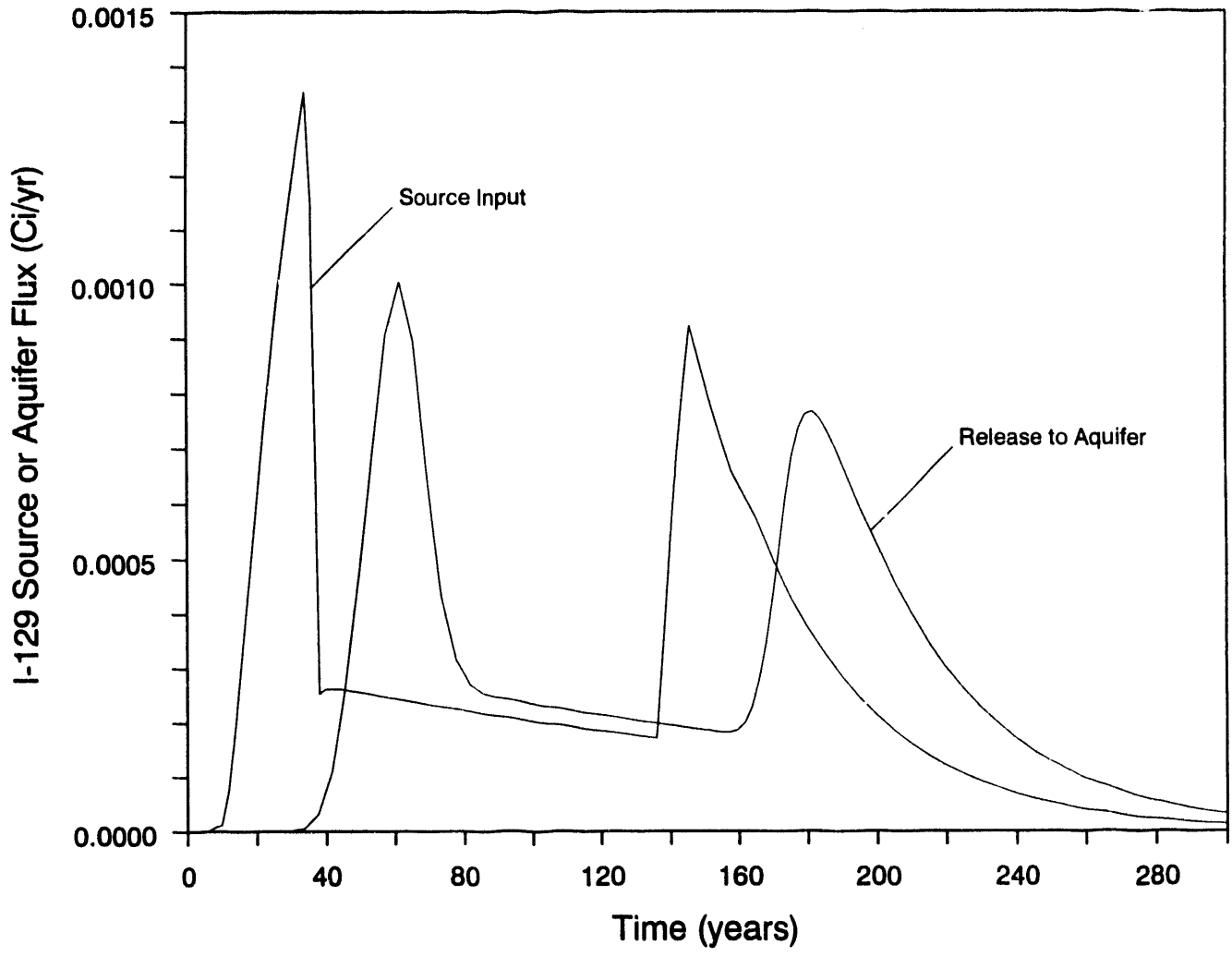

Figure 4-12. Iodine-129 source loading and flux to the aquifer for no flooding simulated with PORFLOW.

simulation and the nuclide flux across the bottom of the E-F interbed at 0.0 m for C-14 and I-129, respectively, for the base case or nonflooding simulation. If the PORFLOW simulation for unsaturated zone transport exactly matched the GWSCREEN plug-flow simulations, the two curves would be exactly the same with an offset equivalent to the nuclide travel time through the unsaturated zone. For nonsorbing C-14, the time-offset in Figure 4-11 is 30 years initially, and it only grows slightly to 32 years for the second peak. The magnitudes of the peaks in the flux to the aquifer are dampened slightly as a result of including molecular diffusion in the unsaturated zone. The I-129 travel time is faster than the base case in part because the moisture content varies vertically in the PORFLOW simulation and is different from the effective moisture content assigned in the base case evaluation with GWSCREEN.

4.2.2.5.2 Hydrologic Results--Figure 4-13 shows the water fluxes through the top of the unsaturated zone model at 12.5 m and through the 0.0 m elevation, which corresponded to the base of the E-F interbed. The wetting fronts move rapidly through the combined interbeds with the first arrival for the 70-cm flood occurring approximately 0.3 years after the flood. Part of this fast flooding front movement is related to the wetter preflood conditions resulting from the 13-cm/yr flux. This causes the unsaturated hydraulic conductivities to be higher than they would be under the case of 7-cm/yr infiltration. For all three magnitude floods, the additional water present because of flooding is removed from the unsaturated zone domain after 4 years.

4.2.2.5.3 Dose Results--The maximum all pathway dose of 28 mrem/yr was greater than 25 mrem/yr for C-14 and I-129 (Figure 4-14). When the flooding occurs, not all nuclides move exactly with the wetting front. Dilution of the nuclide front occurs because of mixing with water of a lower concentration ahead of the wetting front. The first sharp peak is the result of the higher water flux through the 0-m elevation in the simulation domain. At this depth, the nuclide concentration is the same as it was in the base case. The nuclide flux to the aquifer (linearly related to the CEDE) is the product of this nuclide concentration (same as the base case) and the higher water flux. The second peak is due to increased infiltration resulting from degradation of the cover. Changes in the second peak are due to redistribution of contaminant mass during the flooding event. The time lag between the end of the flood event spike and the rise of dose because of cover

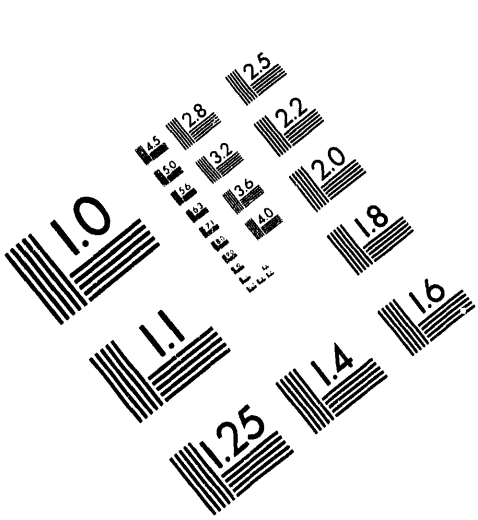

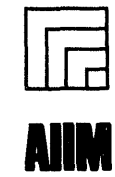

Association for Information and Image Management
1100 Wayne Avenue, Suite 1100
Silver Spring, Maryland 20910
301/587-8202

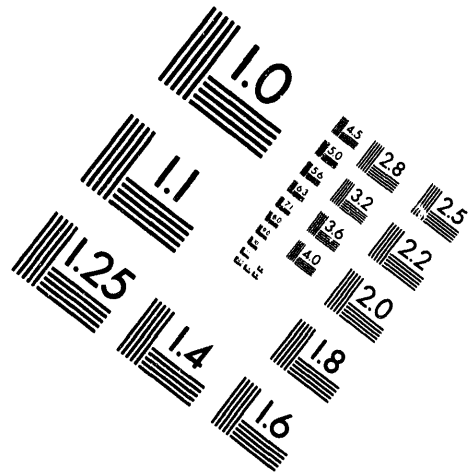

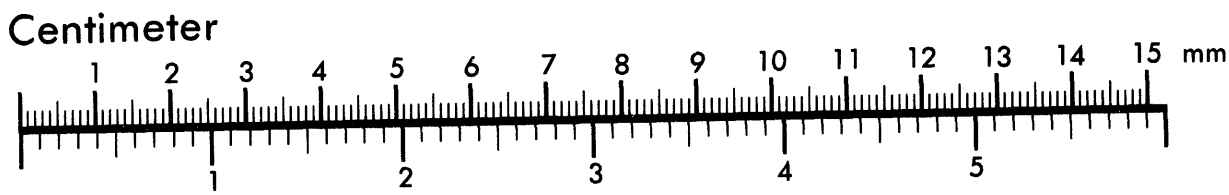

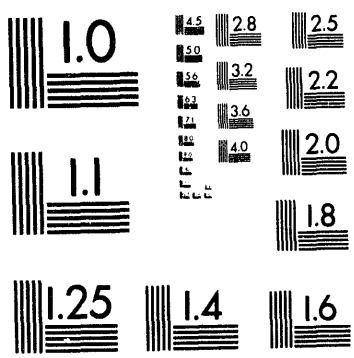

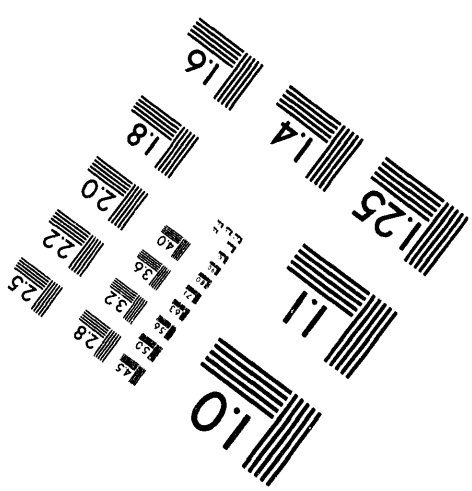

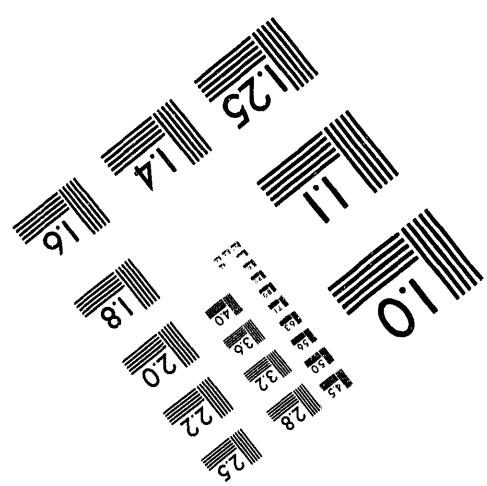

4 of 5

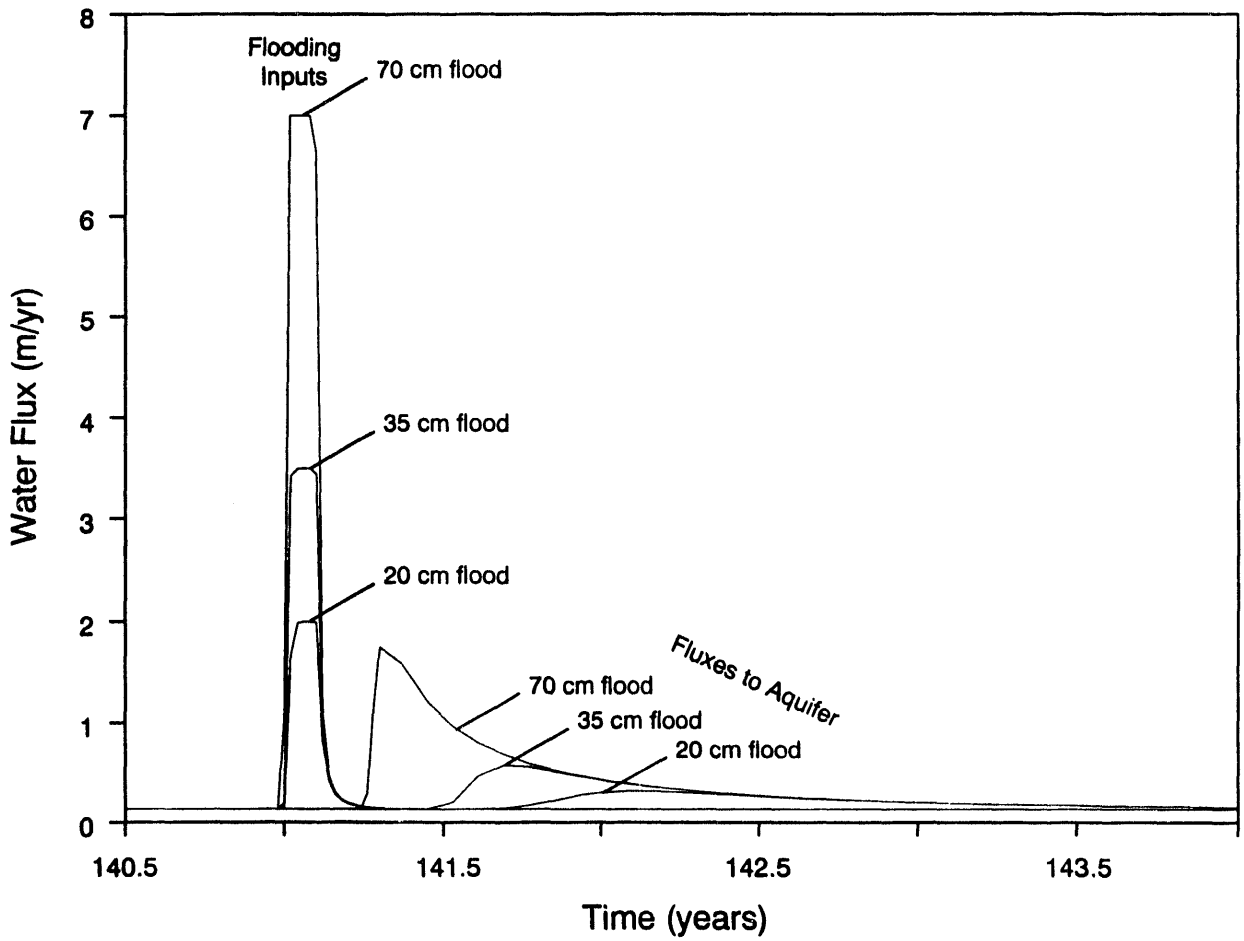

Figure 4-13. Flooding inputs and water flux at 0.0 m elevation (bottom of E-F interbed) for 20-,35-, and 70-cm flood events.

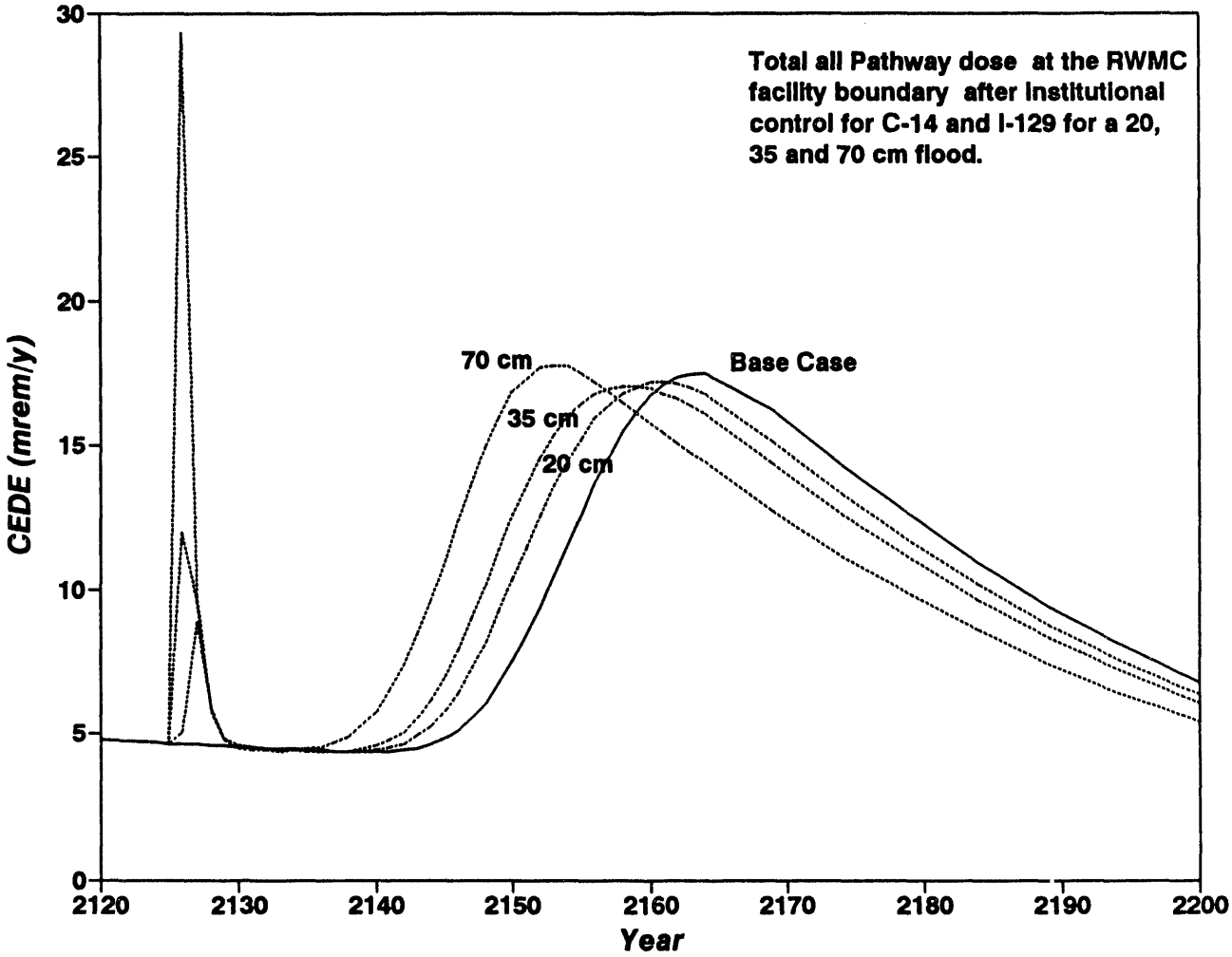

Figure 4-14. Total all pathway dose for C-14 and I-129 resulting from floods of 20, 35 and 70 cm.

degradation is smaller for the larger flood events. This is because in the larger flood events, more contaminant mass is moved down the unsaturated zone, resulting in shorter transit times in the aquifer when infiltration increases because of cover degradation.

4.2.2.6 Absence of Lower Interbeds. The hydrologic conceptual model used in the base case assumed the presence of two lower interbeds (D-E and E-F), which are responsible for 19 years of the 30-year water travel time through the unsaturated zone. These interbeds are assumed to be present because they occur in wells drilled outside the SDA. However, there are no wells drilled to the aquifer inside the SDA to confirm their presence. This case tested the sensitivity of the all pathway doses to the absence of the two lower interbeds. The receptor location selected for this analysis was at the INEL Site boundary. Shortening the travel time in the unsaturated zone only impacts H-3 and Sr-90, nuclides with short half-lives relative to the contaminant transit time. Considering H-3 and Sr-90, only tritium was important because the contaminant transit time for Sr-90, even with the shortened travel time, was still significantly greater than the Sr-90 half-life. Tritium was not important after institutional control; therefore, only the receptor at the INEL Site boundary during operations and institutional control was important.

This case was implemented in GWSCREEN by reducing the combined thickness of interbeds in the unsaturated zone from 12.5 to 9.2 m. From Table 3-3, the travel time through just the B-C and C-D interbeds was 11 years. With the base case infiltration of 7 cm/yr, an effective water content of 0.084 was used to match this water travel time through the unsaturated zone. The overall impact of this case was to reduce the travel time in the unsaturated zone. Because dispersion was not considered in the unsaturated zone, the only impact this change had on the results was for nuclides with half-lives that were in the same order of magnitude as the travel time.

The estimated doses resulting from the simulation without the two lower interbeds are shown in Figure 4-15. The primary effect was to increase the tritium dose. Maximum tritium dose occurred during institutional control at the INEL Site boundary, and it increased from 0.23 to about 0.7 mrem/yr. The maximum total dose increased 75%, from 0.57 to 1.0 mrem/yr. The C-14, I-129,

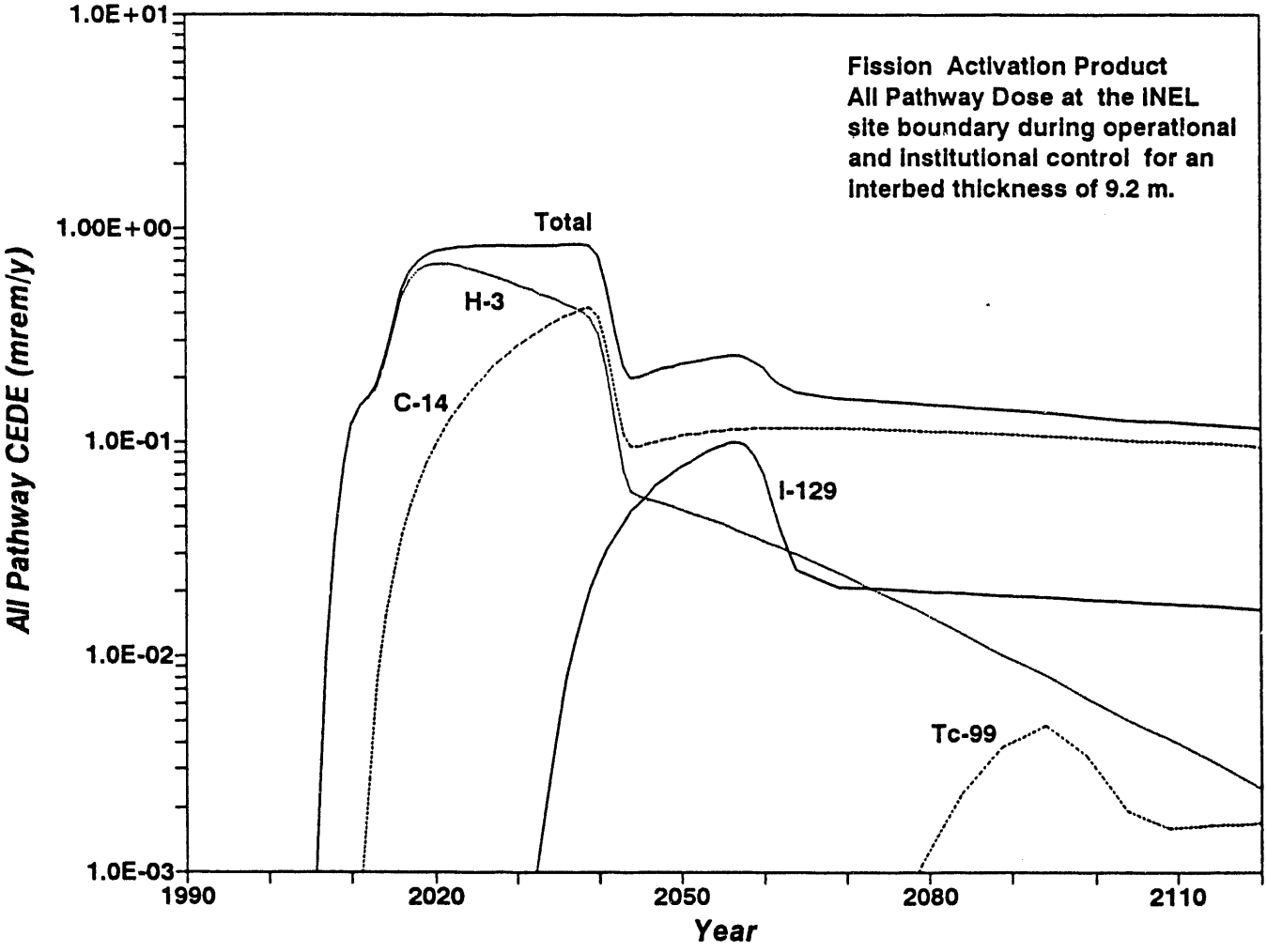

Figure 4-15. Estimated all pathway dose for fission and activation products at the INEL Site boundary during operations and institutional control using an interbed thickness of 9.2 m.

and K-40 doses did not change appreciably because little decay occurred during transit for either the 12.5- or 9-m sedimentary interbed thickness. Strontium-90 dose was insignificant.

4.2.2.7 Overall Uncertainty and Sensitivity. This analysis calculated the impacts using most favorable and least favorable parameters and presented the results as a range of doses. The analysis was limited to only the primary dose contributors, which were C-14, H-3, I-129, and Np-237. For all nuclides, a 10 cm/yr infiltration rate was assumed for the least favorable case, and a 4 cm/yr infiltration rate was assumed for the most favorable case. Both scenarios assumed a cover to be emplaced and evaluated the receptor at 100 m downgradient from the RWMC facility boundary for post-institutional control exposures and at the INEL Site boundary for exposures that occurred during operational and institutional control.

The least favorable case scenario assumed a chloride concentration of 12,500 mg/L and a mean corrosion time of activated core components of 1,840 years, an unsaturated zone thickness of 9.2 m, and dispersivity values that were a factor of 2 less than the nominal values. In addition, Np-237 was assumed to have the low K_d value reported in Sheppard and Thibault (1990), resulting in a contaminant travel time of less than 10,000 years. The tritium inventory in beryllium blocks was increased by a factor of 2 based on the accuracy of the inventory estimate reported by T. A. Tomberlin.[a] The corresponding leach rate constant for C-14 in activated core components was 5.4E-4 per year, and a leach rate constant for H-3 in beryllium was 5.01E-3 per year. The unsaturated zone water travel time was 7.8 years (based on 9.2-m interbed thickness and 0.1-m/yr infiltration).

The most favorable scenario assumed a chloride concentration of 137 mg/L, a mean corrosion time of activated core components of 3,350 years, and dispersivity values that were a factor of 2 higher than the nominal values. The Np-237 sorption coefficient was set equal to its nominal value, and the tritium inventory was reduced by a factor of 2 based on the accuracy of the inventory estimate by T. A. Tomberlin.[a] Using these assumptions

a. Personal communication, T. A. Tomberlin, EG&G Idaho, Inc., with D. E. Sheldon, EG&G Idaho, Inc., December 22, 1986.

resulted in a leaching rate constant for C-14 in activated core components of 2.99E-4 per year and a leaching rate constant for H-3 in beryllium of 3.91E-5 per year.

The range of all pathway doses during operations and institutional control at the INEL Site boundary was 0.2 to 9.1 mrem/yr, with the base case estimated to be 0.57 mrem/yr. The range of all pathway doses (Figure 4-16) after institutional control at 100 m downgradient from the RWMC facility boundary was from 9.5 to 29 mrem/yr, with the base case estimated to be 17 mrem/yr.

4.2.3 Atmospheric Pathway

4.2.3.1 Uncertainty. The uncertainty in the atmospheric pathway analyses can be divided into the uncertainty in the

- Radionuclide dose conversion factors
- Gaussian plume atmospheric dispersion model
- Terrestrial transport models (including environmental transport and human consumption)
- Biointrusion models.

The uncertainty in the radionuclide dose conversion factors is the subject of considerable research and is beyond the scope of these analyses. However, the analyses for this performance assessment used the most conservative combinations of inhalation and ingestion dose conversion factors in DOE (1988b) as implemented in GENII.

Because of the multiplicative chain structure of most radiological assessment models, the results from radiological assessment models are usually distributed lognormally (Hoffman and Gardner 1983), where the mean and variance of the ln-transformed data are denoted μ and σ^2, respectively. The

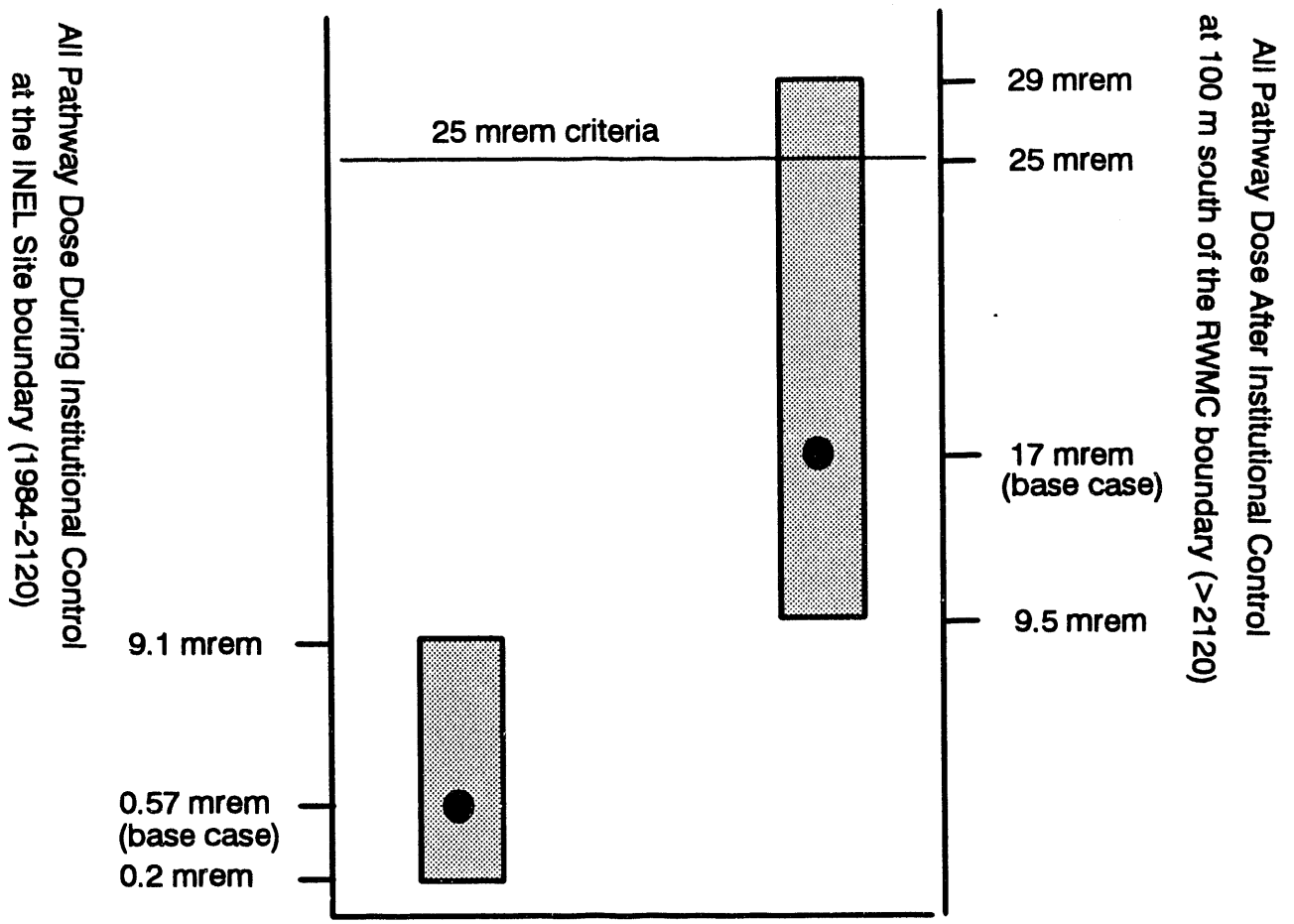

Figure 4-16. Range of calculated all pathway doses.

geometric standard deviation, s_g, is calculated using the formula $s_g = e^{\sigma}$; it is a measure of the variability in the nontransformed data.

Generic discussions of uncertainty and generic estimates of uncertainty are provided for the Gaussian plume atmospheric dispersion model and the terrestrial transport models. A simple Monte Carlo analysis was performed to evaluate uncertainty for the biointrusion model. The uncertainty in the inventory was assessed in Section 4.2.1 and will not be repeated in this section. The analyses were limited to soil vaults because the analyses performed using nominal parameter values showed that the soil vaults contributed over three times as much dose as the pits (see Table B-3 in Appendix B). In addition, the analyses were limited to critical radionuclides identified in the analyses performed using nominal parameter values. Based on the results of the soil vault analyses, Cs-137, Sr-90, and Ni-63 contribute between 95 and 99% of the dose; therefore, these radionuclides were incorporated into the uncertainty analysis.

4.2.3.1.1 Uncertainty in the Gaussian Plume Atmospheric Dispersion Model--Based on data presented in Miller and Hively (1987), the geometric standard deviation of the ratio of the predicted-to-observed air concentrations associated with the Gaussian plume atmospheric dispersion model ranges from 1.5 to 2.2 ($0.16 \leq \sigma^2 \leq 0.64$). This range is applicable to annual average conditions with relatively flat terrain, found at the INEL, for distances up to 150 km from the release point. When the geometric standard deviation of 2.2 ($\sigma^2 = 0.64$) is applied to the atmospheric dispersion factor (χ/Q) calculated for the receptor located 100 m from the RWMC, a 95% confidence interval can be constructed based on a nominal dose of 0.86 mrem/yr. This confidence interval was calculated to be 0.18 to 4.0 mrem/yr for the soil vault doses in the year 2120.

4.2.3.1.2 Uncertainty in the Terrestrial Transport Models--Uncertainty analyses performed for terrestrial transport models exhibit greater variability than annual average predictions from the Gaussian plume model. For example, Shaeffer and Hoffman (1979) obtained a geometric standard deviation of 2.1 for I-131 transport in the pasture-cow-milk pathway, Schwarz and Hoffman (1980) present a geometric standard deviation of 1.9 for I-131

transport in the pasture-cow-milk pathway, and O'Neill et al. (1981) obtained a geometric standard deviation of 2.0 for I-131 transport in the pasture-cow-milk pathway. Hoffman and Gardner (1983) reports a geometric standard deviation that ranged from 3.1 to 4.3 for Sr-90 in the leafy vegetable, produce, meat, and milk pathways. For the combined ingestion pathways, a geometric standard deviation of 2.4 was estimated.

Maheras (1988) obtained geometric standard deviations that ranged from 1.1 to 2.3, depending on the radionuclide and pathway under consideration. The inhalation and immersion pathways showed less variability, with geometric standard deviations that ranged from 1.1 to 1.4. The ingestion pathway showed slightly more variability, with geometric standard deviations that ranged from 1.9 to 2.3.

Hoffman et al. (1982) examined terrestrial ingestion pathways and presented geometric standard deviations that ranged from 2.2 to 4.2, depending on the radionuclide and the specific ingestion pathway (leafy vegetables, produce, meat, or milk) under consideration.

Otis (1983) calculated geometric standard deviations for time-integrated radionuclide concentrations in food that ranged from 1.4 to 2.0, depending on the radionuclide and food stuff under consideration. When uncertainties in human dietary habits were incorporated, the geometric standard deviation increased to 2.4 (Otis et al. 1985).

Breshears (1987) estimated geometric standard deviations that ranged from 1.3 to 2.4 for radionuclide concentrations in milk, depending on the radionuclide. Breshears et al. (1989) estimated geometric standard deviations for time-integrated radionuclide across all foods as a function of physical half-life. Ranges were obtained for radionuclides with physical half-lives less than 30 days (1.7 to 2.7), 30 to 500 days (1.8 to 2.3), and greater than 500 days (1.9 to 2.1).

Based on past uncertainty analyses for terrestrial transport models, 2.0 (σ^2 = 0.48) is a reasonable generic estimate of the uncertainty in terrestrial transport models using the geometric standard deviation to

quantify the uncertainty. If this geometric standard deviation is applied to the terrestrial transport results (0.86 mrem/yr), a 95% confidence interval of 0.22 to 3.3 mrem/yr can be constructed for the soil vault doses in the year 2120.

4.2.3.1.3 Uncertainty in the Biointrusion Model--In contrast to the Gaussian plume and terrestrial transport models, relatively few uncertainty analyses have been performed for biointrusion models. McKenzie et al. (1986) documents a perturbation analysis of a biointrusion model that was similar to the model used in this analysis. However, the model analyzed in McKenzie et al. incorporated burrowing rodents and perturbed parameter values over a relatively small range. Because of these differences, a simple Monte Carlo analysis was performed using the biointrusion model to yield estimates of uncertainty. This analysis did not include gaseous releases of tritium and C-14.

The goal of the uncertainty analysis was to quantify the uncertainty in the activity brought to the surface through biointrusion by plant roots and harvester ants. Therefore, the uncertainty in the inventory was not considered, and the inventory was held constant in the analyses.

Five parameters were varied in the uncertainty analysis:

1. The volume of contaminated soil brought to the surface by a single harvester ant colony

2. The colony density of harvester ants

3. The fraction of plant roots that contact the waste

4. The aboveground biomass

5. The soil to plant concentration ratio.

The volume of contaminated soil brought to the surface by a harvester ant colony is the product of the burrow volume and the fraction of the burrow volume that contacts the waste. These parameters have nominal values of

0.002 m^3 and 0.050, respectively. Therefore, the nominal value for the volume of contaminated soil brought to the surface was 0.00010 m^3. No statistical data were available for this parameter. However, the biointrusion model assumed that all harvester ant burrows contacted the waste. This is highly unlikely; therefore, the volume was decreased by an order of magnitude, increased by 50% (to account for deeper burrowing ants), and assigned a triangular distribution in the uncertainty analysis (see Table 4-14).

Based on the data in Blom et al. (1991), the maximum colony density for harvester ants in sagebrush communities was 114.0 colonies/ha, the mean density was 35.6 colonies/ha, and the minimum colony density was 4.0 colonies/ha. In the uncertainty analysis, these data were used as the minimum, mode, and maximum of a triangular distribution (see Table 4-14).

Statistical data were not available for the fraction of roots that contact the waste. As with the volume of contaminated soil brought to the surface, the biointrusion model assumed that all plant roots contact the waste. This is highly unlikely; therefore, this parameter was decreased by an order of magnitude, increased by 10% (to account for deeper penetrating

Table 4-14. Statistical data used in biointrusion analysis.

Parameter	Nominal value	Statistical distribution
Volume of contaminated soil brought to the surface by a single ant colony	0.00010 m^3	~TRIA(10^{-5}, 10^{-4}, 0.00015)
Colony density	35.6 colonies/ha	~TRIA(4.0, 35.6, 114.0)
Fraction of plant roots that contact the waste	0.050	~TRIA(0.0050, 0.050, 0.055)
Aboveground biomass	46 g/m^2	~UNIF(22.0, 46.0)
Concentration ratios		
Cs-137	0.080	~LN(0.041, 3.5)
Sr-90	2.5	~LN(1.8, 3.8)
Ni-63	0.060	~LN(0.034, 3.2)

plants), and assigned a triangular distribution in the uncertainty analysis (see Table 4-14).

In Fraley (1978), the maximum aboveground biomass observed in the control areas was 46 g/m^2 and the minimum was 22 g/m^2. In the uncertainty analysis, these data were used as the maximum and minimum of a uniform distribution (see Table 4-14).

Statistical data for the Cs-137, Sr-90, and Ni-63 concentration ratios were taken from Ng et al. (1982). Cesium-137 was assigned a lognormal distribution with a geometric mean of 0.041 and a geometric standard deviation of 3.5, Sr-90 was assigned a lognormal distribution with a geometric mean of 1.8 and a geometric standard deviation of 3.8, and Ni-63 was assigned a lognormal distribution with a geometric mean of 0.034 and a geometric standard deviation of 3.2 (see Table 4-14).

The results of the biointrusion uncertainty analysis are contained in Table 4-15, which contains the nominal results and the statistical results based on 5,000 Monte Carlo replications. The geometric means of the activity brought to the surface through biointrusion were slightly less than the

Table 4-15. Biointrusion uncertainty analysis results.

Radionuclide	Nominal results (Ci)	Statistical results (Ci)	95% confidence interval (mrem/yr)
Cs-137	1.4E-4	1.3E-4[a], 1.9[b]	1.9E-2 - 2.4E-1[c]
Sr-90	1.8E-4	8.9E-5[a], 2.9[b]	1.1E-3 - 7.2E-2[d]
Ni-63	9.1E-2	8.6E-2[a], 1.9[b]	1.0E-2 - 1.3E-1[e]

a. Geometric mean.

b. Geometric standard deviation.

c. Mean dose of 0.068 mrem/yr.

d. Mean dose of 0.0089 mrem/yr.

e. Mean dose of 0.036 mrem/yr.

nominal values. Cesium-137 and Ni-63 yielded geometric standard deviations of 1.9, Sr-90 yielded a geometric standard deviation of 2.9. If these geometric standard deviations are applied to the biointrusion results, 95% confidence intervals can be constructed for the soil vault doses in the year 2120 (see Table 4-15). These confidence intervals indicate that there is approximately a one order of magnitude range in the doses based on the uncertainty in the biointrusion model.

4.2.3.2 Sensitivity. As with the uncertainty analysis, sensitivity was evaluated generically for the Gaussian plume atmospheric dispersion model and the terrestrial transport models. A simple perturbation analysis was used to evaluate the sensitivity of the biointrusion model.

4.2.3.2.1 Sensitivity of the Gaussian Plume Atmospheric Dispersion and Terrestrial Transport Models--Horwedel et al. (1989) presents a sensitivity analysis of the AIRDOS-EPA computer code, which is similar in form and function to the GENII computer code. For example, the GENII computer code has been used to verify and validate the results from the AIRDOS-EPA computer code in the INEL NESHAP Annual Report to show that AIRDOS-EPA results meet the requirements of NQA-1 (see Miller and Maheras 1991; DOE 1992, 1993). The sensitivity analysis was performed using local sensitivity techniques and measures.

The sensitivity analysis conducted by Horwedel et al. identified parameters related to the atmospheric dispersion data and food chain transport as being sensitive. Specifically, the reciprocal averaged windspeeds and the frequencies of stability classes were identified as sensitive parameters in the atmospheric dispersion model. In the terrestrial transport model, parameters related to the direct deposition of radioactive material on to plants were found to be sensitive. These were parameters such as the deposition velocity, the weathering rate constant, the agricultural productivity, and the interception fraction. Parameters related to the root uptake of radioactive material were found to be less sensitive. These were parameters such as the areal density of soil and the concentration ratio.

4.2.3.2.2 Sensitivity of the Biointrusion Model--Because the biointrusion model has a relatively simple structure as implemented in the

uncertainty analysis (a linear combination of five parameters), a perturbation analysis was used to evaluate sensitivity. The structure of the biointrusion model consists of two components: (1) a linear combination of two parameters that describe the activity brought to the surface by harvester ants and (2) a linear combination of three parameters that describe the activity brought to the surface by plant roots.

With parameter values set at nominal values (see Table 4-14), the harvester ant component of the biointrusion model brought more activity to the surface than the plant root component of the biointrusion model when the concentration ratio (CR) was less than 0.23. This is important because there are relatively few radionuclides with CRs greater than 0.23 (see Figure B-2 in Appendix B). For example, none of the actinides or lanthanides have CRs greater than 0.23. The only significant radionuclides present in the RWMC SDA whose transport to the surface will be controlled by root uptake are Sr-90 (CR = 2.5) and Tc-99 (CR = 9.5).

Based on the statistical data for the Cs-137 and Ni-63 CRs presented in Table 4-14, the CRs for these radionuclides would have to increase by 1.4 and 1.6 geometric standard deviations for their CRs to exceed 0.23. The CR for Sr-90 would have to decrease by 1.5 geometric standard deviations to be reduced to 0.23.

When perturbation analyses were conducted for Cs-137 and Ni-63 (radionuclides with CRs less than 0.23), perturbation by 10% of either the volume of the soil brought to the surface by a single harvester ant colony or the colony density resulted in increasing the activity on the surface by 7.3% for Cs-137 and 8.0% for Ni-63. When perturbation analyses were conducted for Sr-90 (CR = 2.5), perturbation by 10% of either the volume of the soil brought to the surface by a single harvester ant colony or the colony density resulted in increasing the activity on the surface by less than 1%.

The same pattern was observed when the fraction of plant roots that contact the waste or the aboveground biomass were perturbed by 10%. For Cs-137 and Ni-63 (radionuclides with CRs less than 0.23), the activity on the surface increased by 2.5 and 2.0%, respectively. However, for Sr-90 (CR = 2.5), the activity increased by 9.1%.

Based on these analyses, parameters related to harvester ant intrusion are the most sensitive for almost all radionuclides because most radionuclides have CRs less than 0.23. However, for a few radionuclides, such as Sr-90 and Tc-99 with CRs greater than 0.23, parameters related to plant root uptake are the most sensitive.

4.2.4 Intruder Analyses

This section describes the uncertainty and sensitivity analyses regarding intruder dose assessments for direct contact with waste.

4.2.4.1 Uncertainty. In the context of the intruder dose assessments, structural uncertainty was defined as the uncertainty in the structure of the scenario. Structural uncertainty in the intruder dose assessments was evaluated using a wide range of alternative intruder scenarios. For example, two separate acute scenarios (intruder-drilling and intruder-construction) were used to evaluate structural uncertainty in the acute exposure scenarios. To evaluate structural uncertainty in the chronic exposure scenarios, two variations of the chronic intruder-agriculture scenario were developed using different shielding factors, dietary regimes, and inhalation rates. In addition, site-specific variations of the intruder scenarios were evaluated, such as spreading out drill cuttings on a flat plane instead of using a mud pit.

Intruder dose assessments include parameter uncertainty in radionuclide dose conversion factors and human intrusion and terrestrial transport models.

As with the atmospheric pathway, the uncertainty in the radionuclide dose conversion factors is the subject of considerable research and is beyond the scope of these analyses. However, the intruder analyses for this performance assessment used the most conservative combinations of inhalation and ingestion dose conversion factors as implemented in GENII.

Throughout the intruder analyses, soil vaults yielded higher doses than pits. For example, the doses because of direct contact with waste through the chronic intruder-agriculture scenario for soil vaults ranged from 28 to 53 mrem/yr, while the doses for pits because of direct contact with waste

ranged from 15 to 28 mrem/yr. In the acute scenarios, the scenario with the largest dose for soil vaults (intruder-drilling) resulted in a dose of 190 mrem, while the scenario with the largest dose for pits (intruder-construction) resulted in a dose of 11 mrem.

Using the 100-mrem/yr chronic exposure criterion as a reference point, the doses through the chronic intruder-agriculture scenario were below the criterion by a factor of 1.9 for soil vaults and 3.6 for pits. The maximum doses for pits were calculated approximately 1,000,000 years after site closure without incorporating leaching of radionuclides from the waste. If leaching were incorporated, the doses from the pits would be reduced substantially. The maximum doses for soil vaults occurred at the end of institutional control, so leaching would have little effect on the doses. Using the 500-mrem acute exposure criterion as a reference point, the acute doses were below the reference point by a factor of 2.6 for soil vaults and a factor of 45 for pits. Based on these results, soil vault performance is more important than pit performance relative to the chronic exposure criterion, and the chronic exposure criterion is more important than the acute exposure criterion. Therefore, the uncertainty analysis was limited to the chronic intruder-agriculture scenario for soil vaults.

Within the soil vault chronic intruder-agriculture scenario, the external exposure pathway was the dominant pathway, contributing over 70% of the dose. Cesium-137 was the critical radionuclide, contributing 98% of the dose through the external exposure pathway. Therefore, the uncertainty analysis was further refined to examine only Cs-137 doses through the external exposure pathway. The uncertainty in inventory was not examined because it was previously shown to be unimportant for intruders (see Section 4.2.1.2).

A simple Monte Carlo analysis of the external Cs-137 doses through the chronic intruder-agriculture scenario was performed to assess uncertainty. Four parameters were varied in the uncertainty analysis:

1. Volume of contaminated soil brought to the surface

2. Mixing volume of contaminated soil on the surface

3. Exposure time

4. Shielding factor.

The volume of contaminated soil brought to the surface was the product of the area of the well[a] and the thickness of the waste. These parameters had nominal values of 0.0324 m^{2b} and 3.05 m, respectively. The nominal value for the volume of contaminated soil brought to the surface was 0.0989 m^3. No statistical data were available for this parameter. Instead, the volume was increased and decreased by 50% and assigned a triangular distribution in the uncertainty analysis (see Table 4-16).

The mixing volume of contaminated soil on the surface was the product of the lot size and the mixing depth. These parameters had nominal values of 2,200 m^2 and 0.75 m, respectively. The nominal value for the mixing volume of contaminated soil on the surface was 1,650 m^3. No statistical data were available for this parameter. Instead, the mixing volume was increased and decreased by 50% and assigned a triangular distribution in the uncertainty analysis (see Table 4-16).

Table 4-16. Stochastic data used in intruder analyses.

Parameter	Nominal value	Statistical distribution
Volume of contaminated soil brought to the surface	0.0989 m^3	-TRIA(0.0495, 0.0989, 0.148)
Mixing volume of contaminated soil on the surface	1,650 m^3	-TRIA(825, 1650, 2475)
Exposure time	8,760 h/yr	-LN(540,1.72)
Shielding factor	0.36 and 0.70	-UNIF(0.36, 0.70)

a. In the chronic intruder-agriculture scenario for soil vaults, intrusion by basement excavation is precluded by the depth to the waste, and only intrusion by drilling is possible.

b. Based on a well diameter of 8 in.

The nominal value of the exposure time was 8,760 h/yr, the maximum value possible. For the uncertainty analysis, the exposure time was assigned a lognormal distribution with a geometric mean of 540 and a geometric standard deviation of 1.72 (Farris 1988) (see Table 4-16).

The nominal values for the shielding factor were 0.36 and 0.70. For the uncertainty analysis, these values were used as the minimum and maximum of a uniform distribution (see Table 4-16).

Using the nominal values for parameters, a dose of 39 mrem/yr resulted for Cs-137 doses through external exposures. The uncertainty analysis yielded a geometric mean of 1.9 mrem/yr and a geometric standard deviation of 1.9 using 5,000 Monte Carlo replications. Based on these results, a 95% confidence interval of 0.54 to 6.7 mrem/yr was constructed. The nominal dose of 39 mrem/yr was above the upper bound of the 95% confidence interval, which illustrates the conservative nature of the nominal data, and both doses were well below the chronic exposure criterion of 100 mrem/yr.

4.2.4.2 Sensitivity. Because the intrusion model for external exposures to Cs-137 in the chronic intruder-agriculture scenario had such a simple structure (a linear combination of five parameters with one quotient), a simple sensitivity analysis was done using the results of the Monte Carlo uncertainty analysis. The rank correlation coefficient (ρ) was used to measure sensitivity. The exposure time was found to be the most sensitive parameter (ρ = 0.82). The volume of contaminated soil brought to the surface, the mixing volume of contaminated soil on the surface, and the shielding factor all exhibited small but similar sensitivities (ρ = 0.32, -0.31, and 0.29 respectively).

4.3 Integration and Interpretation

The results presented in Section 4.1 can be interpreted by comparing the calculated doses to dose limits (see Table 4-17). These results indicate that the RWMC will meet the performance objectives of DOE Order 5820.2A. The results are based on assumptions, simplifications, and scenarios that, in most cases, erred on the side of conservatism. Therefore, the results are more likely to overestimate rather than underestimate doses.

Table 4-17. Regulatory requirements and performance assessment results.

Regulatory requirement	Limit	RWMC performance
Protection of the public Air (40 CFR 61)	10 mrem/yr	0.86 mrem/yr
Protection of the public All pathways but air (DOE Order 5820.2A)	25 mrem/yr	0.57 mrem/yr during operational and institutional control 17 mrem/yr during post-institutional control
Inadvertent intrusion Chronic (DOE Order 5820.2A)	100 mrem/yr	Soil vaults 53 mrem/yr direct contact 17 mrem/yr groundwater all pathways 4.5 mrem/yr radon 75 mrem/yr total Pits 28 mrem/yr direct contact 12 mrem/yr groundwater all pathways 12 mrem/yr radon 52 mrem/yr total
Inadvertent intrusion Acute (DOE Order 5820.2A)	500 mrem	190 mrem (soil vaults) 11 mrem (pits)
Public Drinking Water (40 CFR 141)	4 mrem/yr	0.2 mrem/yr
	15 pCi/L (adjusted alpha)	0.035 pCi/L

However, the results presented in Section 4.1 incorporate a significant degree of uncertainty, which is discussed in Section 4.2. In addition, limited data exist for use in the uncertainty analysis, and realistic and definitive uncertainty analyses cannot be performed. In this section, the results are interpreted to provide reasonable assurance that the objectives of DOE Order 5820.2A are met.

4.3.1 Groundwater Pathway

For offsite members of the public, groundwater was demonstrated to be the primary pathway of concern. During the operational and institutional control periods, the dose was estimated to be 0.57 mrem/yr, with H-3, C-14, I-129, and K-40 being the radionuclides of concern. After institutional control, the dose was estimated to be 17 mrem/yr, with C-14 being the radionuclide of concern. Actinides (7.3 mrem/yr) were not significant dose contributors when compared to C-14. At the INEL Site boundary, the range of estimated doses through the groundwater pathway was 0.? to 9.1 mrem/yr. At the RWMC boundary, the range of estimated doses was 9.5 to 29 mrem/yr (see Section 4.2.2.7).

These dose assessments were performed using a drinking water consumption rate of 258 L/yr from Yang and Nelson (1984, 1986). If the drinking water rate consumption rate of 93 L/yr from Rupp (1980) were used, doses would decrease appreciably. The 100-m RWMC bounding receptor location, although required by performance assessment guidance (Dodge et al. 1991), is not consistent with existing land use patterns around the INEL. Existing land use patterns in Southeast Idaho indicate that the area near the RWMC would most likely be used for grazing after the end of institutional control, not for farming. The area near the RWMC is not presently suited for extensive agriculture. Areas to the east and northeast of the INEL are cultivated, but areas near the INEL boundary to the south of the RWMC are not cultivated.

The drilling of a well through over 100 m of basalt near the RWMC implies a high degree of technology. It is probable that if members of the public possessed this technology, then they would also possess the knowledge of the RWMC and the potential for contamination and would either choose to live and farm elsewhere or adequately treat their water.

As discussed in Section 4.2.2, there is substantial uncertainty in the data used in the groundwater flow and transport calculations; consequently, a simple conceptual model was used. Based on a simple perturbation analysis, groundwater concentrations derived from nominal estimates, as opposed to least favorable or most favorable estimates, were used. The range of groundwater concentrations and doses was moderate, which indicates the need for continued hydrological research at the RWMC. Key areas that need to be examined and incorporated in the radiological performance assessment include unsaturated flow and transport, especially those parameters related to the unsaturated zone groundwater travel time; seasonal variation in water infiltration; flooding within the local basin; and geochemical interactions between waste, soil, basalt, and radionuclides. These data will also be used to refine the conceptual model for groundwater flow and transport at the RWMC to provide more realistic estimates and refine the uncertainty in the estimates.

The impact of future climatic changes was not addressed in this performance assessment. There is substantial uncertainty in any dose assessment carried out for time periods far in the future. Changes in climatic conditions and natural phenomena could have significant impacts on the performance of the facility. For example, an earthquake could crack open the RWMC, or a volcano could result in a lava flow that might cause combustible waste to burn. Both these scenarios could increase doses to members of the public and intruders. A lava flow could also create an extremely effective intruder barrier, reducing doses.

The failure of the Mackay Dam was examined for flooding potential. A detailed flood-routing analysis of a hypothetical failure of Mackay Dam resulting from hydrologic and seismic failures showed the RWMC would not be affected by this severe flooding (Koslow and Van Haaften 1986). The RWMC is disconnected from the Big Lost River by a lava ridge that is a hydraulic barrier. This study concluded that the diversion dam would give way before significant flow occurred to the spreading areas. As a result, there is little danger of flooding from the Big Lost River affecting the RWMC.

Based on the best data collected to date and current analyses, the RWMC should comply with the performance objectives in DOE Order 5820.2A. However, an iterative data collection and analysis process for the performance

assessment will help to provide reasonable assurance that the performance objectives are met.

4.3.2 Atmospheric Pathway

The atmospheric pathway proved to be a relatively minor contributor to dose at the RWMC using conservative assumptions. Although biointrusion by plant roots and harvest ants could possibly occur, the assessment assumed that every plant's roots and every harvester ant burrow enter the waste. In addition, site-specific rooting depths were found to just barely contact the waste. Based on site-specific studies of burrow depths, intrusion by burrowing small mammals was found not to be a problem. In addition, the material brought to the surface by plants and harvester ants was assumed to be instantaneously available for atmospheric transport. Given these considerations and the highly unlikely event that a receptor moves to within 100 m of the RWMC SDA, the RWMC should meet the dose objectives in DOE Order 5820.2A.

4.3.3 Inadvertent Intruders

The results of the inadvertent intruder analyses provide reasonable assurance that the performance objectives in DOE Order 5820.2A will be met for both the chronic and acute scenarios. A wide range of intruder scenarios were evaluated, with site-specific attributes incorporated into the scenarios. The most critical of these was the use of a 22-in. irrigation well, rather than the 4-in. well used in 10 CFR 61. Also, two sets of analyses were performed: one with conservative parameter values and the other with more realistic parameter values. Intruder calculations were performed at various points in time, providing further evidence that the dose objectives will be met.

Leaching was not incorporated into the intruder dose assessments involving direct contact with waste. This will have little impact on the doses from soil vaults because peak soil vault doses occur in 2120 and little leaching can occur over this relatively short time period. However, for pits this is an extremely conservative assumption. The peak doses for pits occurred 1,000,000 years after site closure. If leaching is incorporated, the doses at 1,000,000 years would be reduced from 52 to 24 mrem/yr.

Radon doses to intruders were well below the dose objectives in DOE Order 5820.2A even when added to the results of the chronic intruder-agriculture scenario (the bounding scenario). These results were obtained using realistic data collected from instrumented basement structures, as opposed to conservative default values.

Soil vaults yielded the maximum intruder doses. This was because of the presence of large quantities of Cs-137. The maximum intruder doses occurred in 2120, at the end of institutional control. If an intruder barrier that lasts until 2220 were to be incorporated into the design of an engineered barrier at the RWMC, the doses would be reduced substantially. Because most intruder barriers are designed to last between 300 and 1,000 years, this goal appears to be feasible and provides additional assurance that the requirements of DOE Order 5820.2A would be met.

5. PERFORMANCE EVALUATION

The environmental monitoring program at the INEL is the primary mechanism that will be used to determine RWMC compliance with applicable performance objectives. Results of the environmental monitoring program are analyzed for potential problems so corrective actions to waste disposal methods at the RWMC can be taken if needed.

In addition, based on the results and analyses for the radiological performance assessment, data needs have been identified for consideration in planning future studies and enhancements to the monitoring program. These studies are directed at improving confidence in the assumptions and results of the radiological performance assessment. Because the radiological performance assessment will be updated periodically, future revisions will benefit from these studies and enhancements.

Section 5.1 discusses the environmental monitoring programs already established at the RWMC, and Section 5.2 discusses monitoring enhancements and studies that should be considered for addition to the monitoring program.

5.1 Environmental Monitoring Program

Four organizations have environmental monitoring responsibilities at and adjacent to the RWMC: (1) DOE-RESL, (2) USGS, (3) EG&G Idaho, and (4) Idaho State University (ISU). DOE-RESL performs routine monitoring outside of the RWMC, around other operational facilities on the INEL, at the INEL boundaries, and at distant locations off the INEL. DOE-RESL routinely monitors air, animal tissues, food stuffs, soil, direct radiation, offsite community drinking water, production wells on the INEL, surface water samples from the Snake River, and a few surface springs in the Twin Falls, Idaho, area. Offsite and onsite drinking water samples are split with the ISU Environmental Monitoring Program for their independent surveillance program. In addition, the State of Idaho's INEL Oversight Program conducts independent air and water monitoring programs offsite of the INEL and evaluates the monitoring programs at the INEL.

The USGS extensively monitors the Snake River Plain Aquifer and perched water bodies above it on the INEL and at a few locations beyond the southern and western INEL boundaries. The USGS also maintains more than 90 aquifer observation wells on or near the INEL, and more than 170 wells and auger holes are available for sampling perched water bodies. As with the RESL environmental monitoring program, some water samples are split with the ISU Environmental Monitoring Program.

The EG&G Idaho Environmental Monitoring's Radiological Environmental Surveillance Program (RESP) conducts a comprehensive radiological monitoring program at the RWMC and other waste management facilities (Wilhelmsen and Wright 1992; Wilhelmsen et al. 1993). This program includes routine and special studies of radioactive materials in air, water, soil, and biota (vegetation and small mammals), as well as monitoring direct radiation.

The primary purposes of monitoring are to evaluate environmental conditions, provide and interpret data, ensure compliance with applicable regulations or standards, and ensure protection of human health and the environment.

5.1.1 Ambient Air

The specific objectives of ambient air monitoring are to determine concentrations of airborne radionuclides in the vicinity of EG&G Idaho waste management facilities, report comparisons of measured concentrations to reference levels based on derived concentration guides (DCGs) for the public given in DOE Order 5400.5, and determine long-term trends (DOE 1990).

Airborne transport is the most likely pathway for radionuclide migration from the active RWMC facilities. Consequently, more extensive air monitoring is conducted at these facilities to detect airborne transport of radionuclides. Airborne materials from the RWMC are predominantly fugitive dusts with small amounts of adsorbed radionuclides. Fugitive dusts at the RWMC are monitored at the perimeter of the facility.

Air filters are collected and analyzed semimonthly for gross alpha and gross beta activity, and monthly composites at each location are analyzed

quantitatively for gamma-emitting nuclides. All filters from the RWMC are also composited quarterly and analyzed for specific alpha- and beta-emitting nuclides. Samples are compared to data supplied by RESL and RESP from air sampling locations onsite and offsite.

The primary purpose of gross alpha analysis is to detect significant changes in concentration of airborne alpha activity at the RWMC. The gross alpha results are also used as a criterion to screen samples for immediate radiochemical analyses for specific alpha-emitters.

Results of gross beta analyses are evaluated to determine if there are significant increases in the sample radioactivity that may require more immediate and/or more in-depth analysis by gamma spectroscopy or radiochemistry. Gross beta analysis is used as a quick and inexpensive screening tool. These results are also used to indicate trends in environmental radioactivity.

EG&G Idaho has measured gross beta activity since 1979. The quarterly averages of RWMC gross beta activity show a rise from late 1980 through 1981 and another rise in 1986. The beta activity rise from late 1980 through 1981 is attributed to the fallout from an October 1980 atmospheric nuclear detonation by the People's Republic of China. The rise in beta activity in 1986 is attributed to fallout from the April 1986 Chernobyl accident in the former Soviet Union. Gross beta data from the RWMC at SDA and SWEPP historically follow a seasonal trend that usually increase during the latter part of the year. Data from 1992 followed this trend.

All gross beta activities of airborne particulate material measured in 1992 at the RWMC were below DOE DCGs for airborne release to a public area. There were no statistically significant differences between gross beta concentrations of airborne particulates measured at the RWMC and those measured at the control location, and the concentrations were consistent with historical values. No gamma-emitting nuclides resulting from operational activities were detected at levels above background in airborne particulates at the RWMC.

Plutonium-239,-240 and Am-241 concentrations have been measured at all RWMC locations at levels below the DOE DCGs since the first quarter of 1986. These radionuclides are usually detected annually.

During the first and third quarters of 1992, Am-241 was detected in composite air samples from SDA locations 2 and 4 (see Figure 5-1). These detections indicate relatively low levels of airborne activity, with the maximum concentration of 9.4 ± 1.7 E-18 μCi/cc. This concentration corresponds to 0.05% of the DCG for airborne releases of Am-241 to the public. These concentrations are mostly from resuspended soil around the previously flooded areas, and they are below concentrations detected in previous years.

During the second quarter, two low-level detections of Pu-239,-240 were noted at SDA locations 2 and 6 with the maximum concentration of 9.6 ± 1.6 E-18 μCi/cc. This concentration corresponds to 0.03% of the DCG for airborne releases to the public. This concentration was also noted in previous samples collected at the SDA and around the previously flooded areas. These two detections were the only detections of Pu-239,-240 noted during 1992. No specific alpha- and beta-emitting radionuclides were detected during the fourth quarter.

5.1.2 Surface Soil

RESP is responsible for routine soil monitoring at the RWMC. A preliminary assessment of surface soils was conducted at all EG&G Idaho facilities in 1990, and periodic soil monitoring outside the RWMC is conducted by RESL. The purposes of soil sampling and analysis are to determine if RWMC operations contribute to soil contamination and to determine long-term trends. Surface soils at the RWMC demonstrate radionuclide levels slightly above background because of waste handling, past flooding of open pits, and biotic transport from buried waste.

Measured concentrations of Pu-239,-240 and Am-241 from past flooding in surface soils in and outside the northeast corner of the SDA are of particular concern. Wind, water, and biota can transport contaminated solid particulates onsite and offsite. Soil samples were collected at the SDA and TSA areas. No

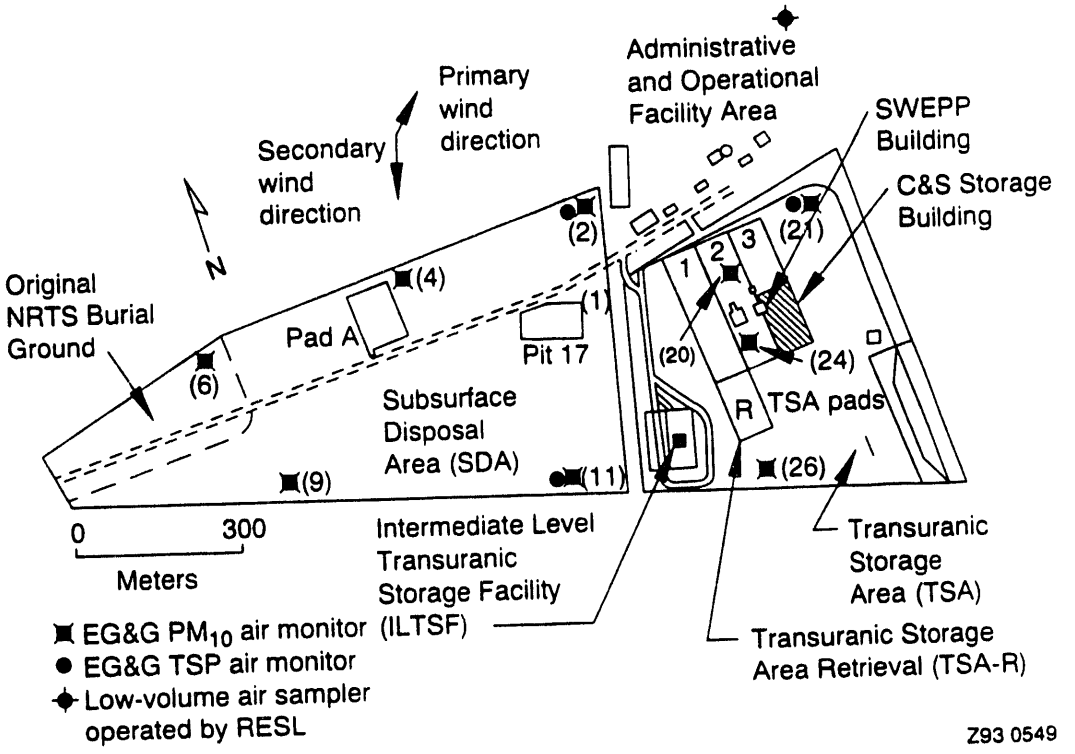

Figure 5-1. RWMC air monitoring locations after July 2, 1992.

gamma-emitting nuclides that can be attributed to waste management operations were detected. Baseline samples were collected within the SWEPP area during 1992. Cesium-137 was the only gamma-emitting radionuclide detected in the soils. The maximum Cs-137 concentration in soil was 1.20 ± 0.04 pCi/g; the sample was collected from a location northeast of the SWEPP building. This concentration is consistent with Cs-137 levels found in undisturbed areas in and around the INEL. Concentrations at this level are attributed to fallout--not a result of INEL operations. The mean Cs-137 concentration for all locations at SWEPP was less than the mean concentration found at the control location.

Selected soil samples were also submitted for specific alpha- and beta-emitting radionuclide analysis during 1991. Strontium-90, Pu-239,-240, and Am-241 were detected in all major areas of the RWMC (see Figure 5-2). The maximum concentration, which was for Am-241 at the TSA, was 1.0E + 0.1E-6 μCi/g, which is less than the environmental concentration guideline of 4.0E-5 μCi/g. Plutonium-239,-240 and Am-241 concentrations have generally decreased because of recontouring efforts with the exception of Pad A and TSA, which have not been recontoured. Concentrations of Pu-238 are consistent with historical concentrations at both the RWMC and distant community locations. The concentrations are considerably less than environmental concentration guidelines (DOE Order 5400.5) that are calculated to correspond to a 50-year dose commitment of 100 mrem/yr to a homesteader beginning in the first year after release of a facility. The concentration guidelines assume uniform contamination of an area adequate for subsistence farming.

5.1.3 Biota

Biota can affect the integrity of buried contaminated waste by penetrating the soil and allowing water to reach the waste or by transporting radionuclides to the surface. Therefore, routine sampling of small mammals and vegetation is also conducted by RESP to detect potential biological radionuclide transport. In addition, the specific objectives of biotic monitoring are to identify biotic conditions that may compromise waste confinement and determine long-term trends.

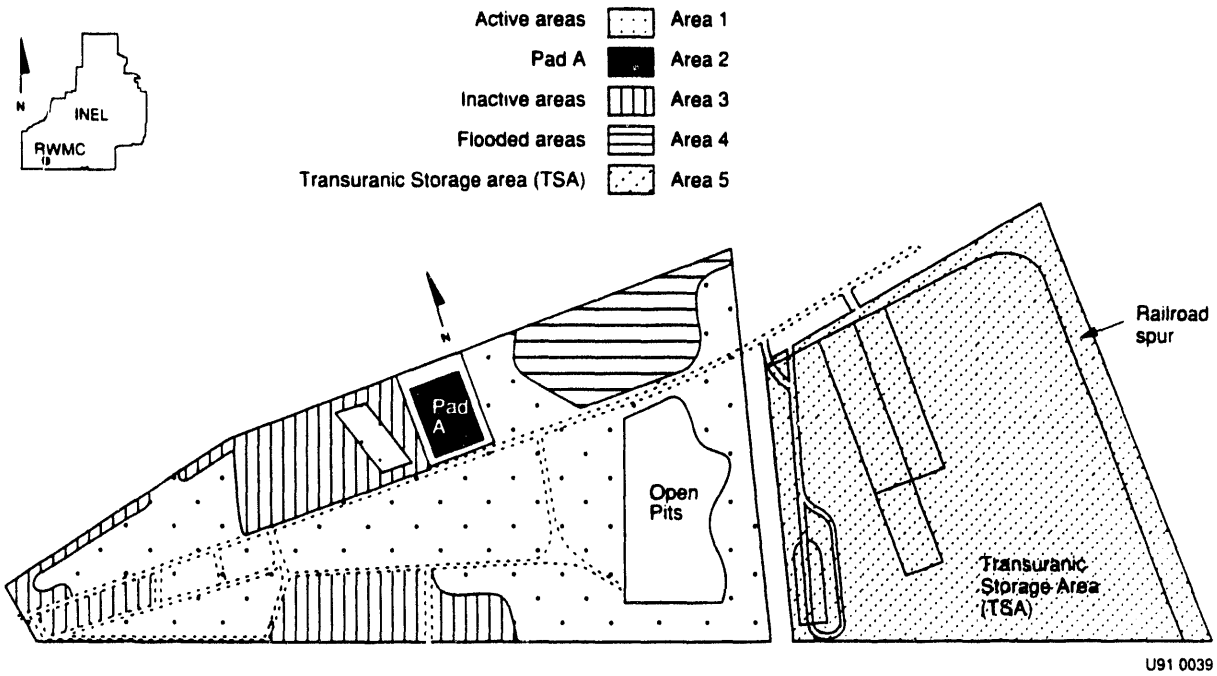

Figure 5-2. Five major areas of the RWMC used for vegetation, mammal, and soil collection.

Vegetation sampling in the even numbered years includes collecting Russian thistle; in the odd numbered years, crested wheatgrass and sagebrush or rabbitbrush are collected. Crested wheatgrass was collected in 1991 and Russian thistle was collected in 1992 from the five major areas of the RWMC. Control samples were collected near Frenchman's Cabin, located approximately 11 km south of the SDA at the base of the Big Southern Butte. No gamma-emitting nuclides were detected in any of the samples from the five major areas or in the control samples.

Selected crested wheatgrass samples, one from each of the five major areas, submitted for specific alpha- and beta-emitting nuclides contained a detectable concentrations of Am-241 that slightly exceeded the levels found in the control sample. Selected Russian thistle samples submitted for specific alpha- and beta-emitting radionuclides contained detectable concentrations of Sr-90 and Am-241 that slightly exceeded the levels found in the control sample. These detections were less than those reported in previous years from crested wheatgrass and Russian thistle samples collected at the RWMC. These concentrations were also within the range of results reported by DOE-RESL (Arthur 1982).

Small mammal sampling in the even years includes collecting ground squirrels; in the odd years, deer mice are collected. During 1991, deer mice samples were collected, prepared, and submitted for gamma spectroscopy and specific radiochemical analysis. Each composite sample consisted of 10 deer mice. Eighteen composite samples of deer mice were collected during 1991. Three samples were collected within each of the five major areas of the RWMC and three samples from the control area near Frenchman's Cabin. All 18 samples were analyzed for gamma-emitting nuclides. Cobalt-60 and Cs-137 were the only positive gamma-emitting nuclides detected at the 3-sigma confidence level. Both positive detections were collected from the previously flooded area in closer proximity to the active pit than in previous years. The maximum concentration of the Cs-137 was 7.32 ± 0.23 pCi/g, and the maximum concentration of Co-60 was 1.84 ± 0.18 pCi/g. These concentrations are consistent with concentrations found in previous years in samples collected in close proximity to the active pit area (Pit 17-20).

During 1992, ground squirrels were scheduled to be collected at the RWMC. However, the recontouring effort of recent years has diminished the ground squirrel population. The results of an investigation showed that a representative sample of ground squirrels would not be available for analysis during 1992; therefore, samples were not collected.

In addition to small mammal samples, excavated soil from mammal burrows is collected at the RWMC. Samples of soil excavated by burrowing animals were scheduled to be collected during 1992 at the RWMC from each of the five major areas. Samples were not collected because of recontouring activities and the diminishing population of small mammals at the facility.

5.1.4 Water

5.1.4.1 Surface Water. The specific objectives of surface water monitoring are to determine the concentrations of radionuclides in any surface water leaving the RWMC, report comparisons of measured concentrations against reference levels based on DCGs for the public given in DOE Order 5400.5 (DOE 1990), and determine long-term trends.

Surface water runoff occurs at the SDA only during periods of snowmelt or heavy precipitation. At these times, water is pumped out of the SDA into a drainage canal. Water also runs off the asphalt pads around TSA and into drainage culverts and the drainage canal, which direct the flow outside the RWMC. The canal also carries outside runoff that has been diverted around the RWMC. Ponding of runoff in a few low areas may increase subsurface saturation, enhancing subsurface migration.

Water samples are collected during each quarter rainfall or snowmelt produce runoff water. These samples are analyzed for gamma-emitting nuclides and specific alpha- and beta-emitting nuclides. During 1991, Cs-137 was detected in the particulate fraction, which is comparable to activity of fallout normally distributed in surface soils at the INEL. No other gamma-emitting nuclides were detected at ambient concentrations during 1991.

During 1992, surface water runoff samples were only collected during the first and second quarters because of the availability of runoff waters.

Gamma-emitting radionuclides were not detected at above ambient concentrations during 1992.

Water runoff samples were also submitted and analyzed for specific alpha- and beta-emitting radionuclides. Americium-241 was detected at the TSA location 4 (in the northeast section of TSA). This concentration was 1.2 ± 0.2E-10 μCi/mL and represents 0.04% of the DCG in water. Comparable concentrations of Am-241 have been noted at the RWMC in the past. These concentrations are near the detection limits and are comparable to concentrations noted at distant community locations.

Generally, most concentrations of radionuclides detected in surface water at the RWMC were at or near environmental levels. Each detection found above background level was at only a small fraction of the applicable DCGs.

5.1.4.2 Drinking Water. The EG&G Idaho drinking water monitoring program was centralized in FY 1988 to monitor EG&G Idaho facilities at the INEL to ensure compliance with applicable drinking water standards. This program monitors all drinking water at EG&G Idaho-operated facilities located at the INEL (Andersen and Peterson-Wright 1993).

Currently, the drinking water program monitors 17 wells and 11 distribution systems on a routine schedule at the INEL, including the RWMC well distribution system. Monthly or quarterly drinking water samples are collected from all water systems and are analyzed for the following: (a) radiological contamination, (b) volatile organic compounds, (c) coliform bacteria, and (d) other chemical parameters. In addition, semiannual monitoring was initiated in 1992 for lead and copper levels according to EPA's requirements (40 CFR 141.80 to 141.91). Maximum contaminant levels are levels established for primary drinking water standards by EPA standards. No parameters were exceeded for the RWMC drinking water system.

5.1.4.3 Subsurface Water. The USGS monitors groundwater in the Snake River Plain Aquifer, approximately 177 m beneath the RWMC. This monitoring helps determine whether radionuclides and hazardous constituents have migrated from the waste to the groundwater below the RWMC. Water samples are collected

quarterly from eight aquifer wells and one perched water well located in and adjacent to the RWMC SDA. These samples are analyzed for radioactivity as well as nonradiological parameters.

Each quarter the USGS measures specific conductance, pH, temperature, and chloride as well as H-3 and Sr-90. During 1992, samples from all eight wells were analyzed for gamma-emitting radionuclides (Co-60 and Cs-137) and transuranics (Pu-238, Pu-239,-240, and Am-241). In addition, the RWMC Production Well (which is used for drinking water) is sampled monthly for purgeable/organic compounds while all other wells, except Well 92, are sampled quarterly.

Since operations began in the 1950s, wastewater disposal at the INEL has increased the specific conductance of groundwater in the Snake River Plain Aquifer in the vicinity of INEL facilities. The background-specific conductance of water from the Snake River Plain Aquifer at the INEL generally ranged from 178 to 860 μS/cm (Orr and Cecil 1991). This range was compared to the specific conductance measurements of water samples collected from wells at the RWMC in 1992. These specific conductance measurements are comparable to those made in previous years.

During October 1992, analyses for sodium were performed. Water from some of the RWMC monitoring wells contained sodium concentrations higher than the background level of 10 mg/L (10 ppm). Sodium concentrations have fluctuated in water from these wells. One possible cause for these fluctuations is the method used to construct the wells. During construction, the wells were pressure-cemented to prevent water from cascading from perched zones down to the Snake River Plain Aquifer. The cement could contribute to higher sodium concentrations.

The chloride concentration was also above background levels, but it was well below the chloride secondary maximum contaminant level. These concentrations may be from the same process described for sodium. Both the chloride and sodium concentrations are comparable to previous concentrations of past years at these well locations.

The results of the gamma spectrometry analysis performed on well samples taken in 1992 showed no positive detection of any gamma-emitting radionuclide.

Tritium was detected in Wells 87 and 90 and in the RWMC Production Well. No other radionuclides were detected in the wells in any quarter. The average concentrations of H-3 in Wells 87 and 90 and in the RWMC Production Well were 1.0, 1.4, and 1.5 pCi/mL, respectively. These concentrations are well below the DCGs for the public (<0.1% of the DCGs). The source of H-3 is attributed to past disposal of wastewater from operations at ICPP and TRA as reported in Orr and Cecil (1991).

5.2 Enhancements to Environmental Monitoring and Data Needs

Based on the results and analyses for the RWMC LLW radiological performance assessment, data needs have been identified for consideration in planning future studies and enhancements to the monitoring program. These studies are directed at improving confidence in the assumptions and results of the RWMC LLW radiological performance assessment. Because the radiological performance assessment will be updated periodically, future iterations will benefit from these studies.

The majority of the identified data needs are related to water movement or chemical processes occurring within the unsaturated zone. Some of the data needs identified in the following discussions are currently being or are planned to be addressed. These ongoing activities are identified where appropriate. A level of priority, high or medium, is also assigned based on technical judgment for the potential impact to future iterations of this radiological performance assessment.

5.2.1 Infiltration

As has been discussed, water infiltration is the driving force for all subsequent radionuclide movement considered in this performance assessment. The infiltration estimates used in this radiological performance assessment are of necessity, simplistic. In the base case evaluation, transient pulses are assumed to be dampened out at depth so they can be considered constant.

The infiltration estimates are based upon sparse field information, primarily from five core samples from depth that were hydrologically characterized. Information on infiltration inside the SDA at the surface is limited to two neutron access tubes that yield widely disparate results. From just these two locations, it is obvious that the amount of infiltration can vary widely across the SDA.

A study of the amount, timing, and spatial distribution of infiltration inside the SDA needs to be conducted. An ongoing field project has recently expanded the number of neutron monitoring locations from 2 to 17, with an emphasis on the region near the active LLW disposal pit. Monitoring results from this project will be analyzed to further define the amount of infiltration occurring within the SDA. Water equivalents in the winter snowpack will also be collected as part of this project to corroborate the infiltration measurements. An important aspect of this project will be at least two monitoring locations in the fill placed over waste in Pit 17. Monitoring at these two locations will provide a direct measurement of water infiltration and will limit the need to interpolate or estimate infiltration into the emplaced waste from other locations around the SDA.

The potential impacts to the radiological performance assessment of infiltration are difficult to predict. The net infiltration estimates used in this radiological performance assessments are reasonable; they range from 10% to almost 50% of annual precipitation. The main benefit from an infiltration study will be a validation of the infiltration estimates. As such, in terms of potential impact to the performance assessment, the field infiltration project should be a high priority.

5.2.2 Water Movement in Fractured Basalts

An adequate description of the movement of water and radionuclides down through the fractured basalts, which comprise the majority of the unsaturated zone beneath the SDA, is not available. As a result, the movement of water in this region was conservatively considered to be instantaneous. The lack of information related to water movement in the basalts was pointed out by the DOE Peer Review Panel after their review of the preliminary performance assessment (Case et al. 1990). The deficiency was also previously pointed out

by a external peer review of the Subsurface Investigation Program (EG&G Idaho 1988). This persistent data gap is partially the result of past subsurface investigations determining radionuclide migration from waste as their first priority. Characterization of hydrologic behavior was always a lower priority in planning and budgeting. The other cause of the data gap is the technical difficulty in determining the relative contributions of the fractures and the basalt matrix in controlling flow.

Three studies are recommended to improve the description of water movement through the unsaturated fractured basalts: two large field-scale studies and a smaller-scale study.

The first field-scale study is the ongoing perched water monitoring study that is attempting to improve the understanding of water movement in the fractured basalts. Preliminary results from this study have been used in this radiological performance assessment as a basis for assuming rapid water movement in the basalts. However, no conclusive results from the study are available to provide an adequate description of flow in the fractured basalts. This perched water level monitoring study needs to be continued over a longer period of time and expanded to make conclusive statements about rates of water movement. The expansion should consist of either more monitoring locations for perched water or reactivation or further expansion of moisture monitoring instrumentation already present in the sedimentary interbeds at depth.

The perched water monitoring study is limited because only six observation wells have been completed. In addition, some of these monitoring wells are constructed so water can enter the borehole at depth and cascade down to where the wells are completed. It needs to be determined whether these monitoring wells are resulting in short-circuit water pathways. If these pathways exist, well construction needs to be modified to prevent preferential movement so the perched water measurements reflect the natural system. The potential benefits from this perched water study in improving the understanding of water movement and water travel times down through the basalts makes this a high priority.

The second field-scale study is a funded study that will conduct a large-scale infiltration test approximately 1.6 km to the south of the SDA. This

test will yield information on the large-scale hydrologic and transport properties of the basalts under flooding and subsequent drain-out conditions. An artificial circular flooding basin (26,000 m^2) has been constructed, and unsaturated zone monitoring instrumentation has been installed. The infiltration test, including short-lived radioactive tracers, is scheduled to be conducted during the summer of 1994.

The technical problems associated with characterizing unsaturated fracture flow are being researched, primarily associated with the high-level waste repository. As recommended in EG&G Idaho (1988), a third study is proposed to investigate the mechanism by which water enters into the fractured basalts from the overlying surficial sediments. This study would use an existing exposed face of the active waste disposal pit and intensely monitor water and/or tracer movement using horizontal wells drilled into the face. The monitoring would be conducted under two flow regimes: background infiltration and supplemental precipitation. This monitoring coupled with geophysical characterization of fracture locations could significantly improve the understanding of fracture flow mechanisms beneath the SDA. The study is currently unfunded. Technical problems associated with monitoring water movement in the basalts limit the priority of this study to medium.

Together, these three studies would significantly improve understanding of water movement, including the dimensionality of water movement. The conceptual model simulated in this report consists of one-dimensional downward movement of water. These studies would yield insight as to the appropriateness of that assumption.

5.2.3 Simulation of Unsaturated Flow and Transport

The two previous sections detailed studies either proposed or being conducted to improve the understanding of water movement in the unsaturated zone beneath the SDA. This new understanding can be used in an improved conceptual model of water movement and implemented in numerical simulation codes to make long-term predications of flow and transport. Depending on the mechanisms that control flow, existing commonly-used simulation approaches (Baca et al. 1992; Magnuson and Sondrup 1992) may be applicable. If non-

Darcian flow is a dominant process, numerical solution techniques from other disciplines, such as computational fluid dynamics, may need to be incorporated into the simulations.

Additionally, if flow is found to be infrequent but rapid, equilibrium assumptions regarding the partitioning of radionuclides between solid and dissolved phases used in this radiological performance assessment may be inappropriate. Instead, simulation approaches using reactive (kinetic) transport models would be incorporated.

Further simulation studies of water movement should be conducted in parallel or shortly after the field investigations. The simulation studies of water movement in the unsaturated zone have an equally high priority to the field studies because an accurate description of water behavior in the unsaturated zone will not benefit the performance assessment unless it can be implemented into a flow and transport simulation.

5.2.4 Water Movement in the Snake River Plain Aquifer

A simple, quasi-analytical, two-dimensional flow and transport model was used for simulating water flow in the aquifer. More complex numerical simulation codes are available and are being used for other projects at the INEL. For example, the MAGNUM-3D code (Estey et al. 1985) is being used to simulate the entire Snake River Plain Aquifer underneath the INEL for a Site-wide environmental impact study. The well-known USGS code, MODFLOW (McDonald and Harbaugh 1988), is being used for the WAG-10 regional groundwater modeling study. Additionally, the FLASH (Baca and Magnuson 1992) simulation code was recently used to simulate a portion of the Snake River Plain Aquifer for the ongoing Test Area North Remedial Investigation/Feasibility Study. These codes should be considered for use in further evaluations of groundwater transport beneath the RWMC as data become available to justify code use. This study is assigned a medium priority.

In conjunction with the infiltration test mentioned previously, a large-scale aquifer pump/stress test will be conducted south of the SDA that will provide some of the necessary data. The pumping test will yield valuable information on the effective depth of the aquifer in the vicinity of the RWMC,

a large-scale measurement of transmissivity, and an indication of the degree of anisotropy within the aquifer.

5.2.5 Future Flooding Impacts

The dose results in the uncertainty section indicate that future flooding could significantly increase radionuclide flux to the aquifer and the related dose at the hypothetical receptor location for mobile radionuclides. Several assumptions related to flooding were used in this radiological performance assessment. For the base case, no flooding was assumed to occur. In the uncertainty section, the sensitivity of predicted doses to flooding events was included but with the provision that no flooding occurred during the period of institutional control.

The SDA is in a topographic low within the local drainage basin. Flooding from snowmelt within this local basin has resulted in flood water entering the SDA on three occasions during historical operations at the SDA. Flood control measures implemented since the last flooding event in 1982 are believed to be capable of preventing additional flooding in the future. This assumption needs to be validated by an in-depth flooding analysis of the local basin. A two-dimensional floodplain model has been developed at the INEL to predict overland flow. The model solves a class of nonlinear equations called the shallow water equations. It is uniquely capable of simulating flood wave propagation over a dry surface.

A study should be conducted with this two-dimensional floodplain model to evaluate the potential for over-topping the existing dikes surrounding the SDA because of rapid snowmelt events. This study could be used to determine the validity of the assumption of no flooding in the future. This flooding study should address the variability of snowpack thicknesses in the local basin. Determining this variability would further require a field study of snowpack thicknesses in the local basin during one or more years when a snowpack develops.

If over-topping is predicted, it will likely spur further corrective actions such as further elevating the exterior dikes around the SDA. The

effect on additional snow accumulation and resulting increased infiltration from further elevating the dikes would also have to be considered.

Nevertheless, two key results of this flooding study using the existing dikes would be estimates of expected recurrence interval for flooding inside the SDA and the amount of flood water available for infiltration into the sediments overlying the LLW pits. This study could also consider the effect on surface flows of any closure cover emplaced over the LLW pits.

Because of the importance of the assumption of no flooding and the fact that the simulation tool is already developed, this flooding potential study is given a high priority in terms of the potential impacts to the radiological performance assessment. This flooding potential study is currently not planned or funded.

5.2.6 Engineered Barrier/Closure Cover Studies

This performance assessment assumed a closure cover that was effective in reducing net infiltration from 7 to 1 cm/yr. The graphical results for dose as a function of time indicate the importance of this reduced infiltration assumption. While it is reasonable to use a reduced infiltration rate, the basis for assigning the rate should be improved. The current basis is a simulation study (Magnuson 1993) that predicts water movement in two proposed designs using (a) best estimates for hydrologic properties of materials that will be used in the barriers, (b) estimates for expected transpiration based upon limited studies related to crested wheatgrass, and (c) site-specific meteorological data. While the results of this simulation study indicate how the barriers are likely to perform, field validation of the barrier performance has not been conducted.

A study has been initiated to construct small-scale (3 x 3 x 3 m) field plots of the two barrier designs. The field study at the INEL will be completed to provide field-based site-specific performance information for future iterations of this performance assessment. While the movement of water within sediments (classical Darcian flow) is undoubtedly the same in most locations, there are sufficient differences between weather patterns at the INEL and other DOE sites; therefore, the transferability of results from other

barrier studies is questionable. While the results from this field study would be useful in estimating barrier performance on a larger scale, the study alone will not suffice for a final closure design. Inherent problems associated with scaling-up the results from the 3 × 3 × 3-m experimental plots to field scale would require performing an engineering study.

The high potential impact of the results from the engineered barrier study, either in increasing or decreasing the estimated doses, makes the engineered barrier study a high priority. The capillary barrier simulation (Magnuson 1993) indicated a potential for preventing any water from infiltrating to depth and contacting the emplaced waste. If this is the case, the estimated doses are overpredicted during the period of institutional control.

5.2.7 Distribution Coefficients

Knowledge of the contaminant retardation during transport is key to understanding the movement of contaminants at the RWMC. Currently, there is limited information on the mobility of contaminants in the subsurface environment at the INEL. Site-specific distribution coefficients (K_ds) that are typically used in numerical transport simulation are lacking. However, the Basalt Waste Isolation Project at Hanford, Washington, conducted a great deal of work on radionuclide adsorption onto basalts. These data could be used to develop reasonable estimates of the K_ds for basalt at the INEL. Compiling and evaluating these data could provide a consistent set of reasonable K_d values for future transport studies. Also, these values could be used to compare results of future experiments conducted on INEL Site materials. This unfunded study is given a medium priority.

5.2.8 Soil Water Chemistry

Environmental parameters such as pH and Eh must be defined for soil waters to estimate the source term chemistry for the RWMC. A great deal of soil water chemistry data has been collected from the subsurface at the RWMC. These data could potentially be useful in evaluating the migration of radionuclides in the surface. However, a significant question remains to be

answered about the validity of the collected data. The samples were collected using suction lysimeters with a silica flour packing to ensure good hydraulic connectivity between sediments and the lysimeter. The sample analyses indicate that the water collected is saturated with silica. It is unclear if this means that silica is naturally at saturation with a potential to form colloids or if the saturation is related to the use of silica flour as a packing material. Because the lysimeters were also used as monitors for radionuclides, it would also be interesting to determine if the silica flour could act as an adsorbent. This could result in underestimating radionuclides in the soil pore water. Some simple experiments could be conducted to evaluate the impact of silica flour on the chemistry of the pore water. This would increase the understanding of the potential for radionuclide movement in the subsurface. The priority for the soil water chemistry experiments is medium.

5.2.9 Active Waste Monitoring

Knowledge of actual contaminant migration from waste emplaced in the LLW pits is vital to predicting further contaminant movement down through the unsaturated zone. A program needs to be initiated to install instrumentation for monitoring leachate concentrations in and beneath the active LLW pit. This program has been previously proposed in Hubbell (1990b).

The technology necessary for this monitoring is well established and has been used at other LLW sites, including the Radioactive Waste Management Site on the Nevada Test Site. The proposed program consists primarily of installing soil-suction lysimeters to extract soil water for chemical analysis. There is also a necessary water flux monitoring component proposed in the program because knowledge of concentration alone does not allow prediction of whether the contaminant is moving. This water monitoring would be accomplished with neutron access tubes installed at the time of waste emplacement. These tubes would extend from eventual land surface, including any cover added over the waste to below the wastes. Additionally, instrumentation to measure matric potentials would be required to determine the direction of the hydraulic gradient. After the instrumentation is installed, regular monitoring would provide a reasonably accurate description of both contaminant and water movement within and below the emplaced wastes.

The other benefit of an active waste monitoring program is to provide early detection of contaminant migration that is originating strictly from the waste emplaced in the LLW pit. If significant contaminant movement is observed, it would be detected early enough to allow corrective actions to either mitigate, reduce, or eliminate the contaminant movement. Because the source release is a major component of doses estimated in this radiological performance assessment, this study is given a high priority.

5.2.10 Tritium Monitoring

Predicted releases of tritium from beryllium reflector blocks disposed of in soil vaults are a significant contributor to doses calculated at the INEL Site boundary. The effect of uncertain chloride concentrations in soil around the disposed blocks was shown in the uncertainty section to approximately triple the estimated doses. The predicted concentrations of tritium at the receptor location are a result of conservative assumptions used to simulate the release of tritium from the beryllium reflector blocks. This estimated tritium release has not been validated through a field monitoring program.

Because of the large tritium inventory and the mobility of tritium after it is released, a study has been initiated to improve confidence in the predicted release of tritium from the beryllium blocks. In brief, the study consists of sampling subsurface air in proximity to the soil vault(s) containing the beryllium blocks, condensing water vapor from the air samples, and analyzing it for tritium. The tritium in air concentrations measured in the vicinity of the beryllium blocks can be used to determine the reasonableness of the assumed release from those blocks. This study also uses neutron monitoring to provide a better estimate of soil moisture conditions in the vicinity of the soil vault. Soil suction lysimeters are used to provide an additional check on tritium and chloride concentrations in the immediate vicinity of the soil vault. Because of the possible high impact on the performance assessment, this study is given a high priority.

5.2.11 Inventory

As discussed in Section 4.2.1, no estimates of uncertainty are available for the radionuclide inventory used in this performance assessment. Historical inventory analyses will continue to be performed and the results factored into the performance assessment, but these analyses do not completely address the issue of the uncertainty in the radionuclide inventory reported to the inventory data base.

To address this issue, it is recommended that studies be conducted to estimate radionuclide inventory uncertainty. Potential studies should estimate the uncertainty in (a) radionuclide measurements and (b) scaling factors. These types of studies should be done on a content code basis and would involve sampling waste packages to verify measurements and scaling factors. After uncertainty estimates are developed, sensitivity analyses should be conducted.

As a preliminary step in this analysis, it is recommended that important content codes and waste generators be identified using the results of the performance assessment. This would have to be done from the perspective of scenarios dependent on waste concentration (e.g., intruders) and scenarios dependent on total activity (e.g., groundwater).

After the uncertainties are established, changes to the waste acceptance criteria may have to be made to ensure that this information is kept current because measurement systems and waste streams could change. The priority for the inventory studies is medium.

6. PERFORMANCE ASSESSMENT PREPARERS

The information in the RWMC LLW radiological performance assessment was provided by many people at the INEL; however, five people were the primary preparers of the performance assessment. The following briefly describes their contributions, expertise, and experience.

Rajiv N. Bhatt received a B.S. degree in mechanical engineering from M.S. University of Baroda, India, in 1978. Before joining EG&G Idaho in 1990, he worked for 12 years in design and construction of commercial nuclear power plants. He was instrumental in establishing the LLW inventory used in the performance assessment. He also played a key role in finalizing the hydrological conceptual model, defining the tritium inventory in beryllium blocks and near-field release rates of radioactivity (tritium) from beryllium blocks through diffusion and/or corrosion.

Steven J. Maheras served as the technical lead for the RWMC LLW radiological performance assessment. Maheras received Ph.D. and M.S. degrees in health physics from Colorado State University in Fort Collins, Colorado, in 1988 and 1985 and a B.A. degree in zoology from the University of New Hampshire in 1982. He has 10 years of experience in multimedia contaminant transport modeling and exposure assessment for radionuclides and is a Certified Health Physicist. For the past 5 years, Maheras has worked primarily on radiological assessments for atmosphere releases of radionuclides and performance assessments for buried waste. Maheras served as the INEL member on the U.S. Department of Energy Headquarters Performance Assessment Peer Review Panel from 1990 to 1993. He conducted biointrusion, atmospheric, and inadvertent intruder analyses as described in Chapters 3 and 4 of this performance assessment. He also performed a comprehensive evaluation of the inventory and developed time dependent inventory models and forecasts as described in Chapter 2 that were used in the performance assessment.

Swen O. Magnuson received an M.S. degree in hydrology from the New Mexico Institute of Mining and Technology in Socorro, New Mexico, in 1988. Since that time, he has worked at EG&G Idaho as a unsaturated zone modeler and has developed expertise in the synthesis of hydrological conceptual models based on field information. By understanding the implications of field

measurements of water contents and matric potentionals, he integrated the data and results of hydrologic studies performed at the INEL into the hydrological description in Chapter 2. He developed the hydrologic conceptual model described in Chapter 3 used in this radiological performance assessment and collaborated on the hydrologic transport analyses described in Chapters 3 and 4. He also performed flooding simulations for the uncertainty analysis in Chapter 4. Magnuson has made similar contributions to performance assessments at the Nevada Test Site and the Savannah River Technology Center.

Arthur S. Rood received an M.S. degree in health physics from Colorado State University in Fort Collins, Colorado, in 1987 and a B.S. degree in geology from Mesa State College in Grand Junction, Colorado, in 1982. He has 10 years of experience in the nuclear-related industry, which includes uranium exploration and mining, analytical measurements of uranium mill by-products, and multimedia contaminant transport modeling and exposure assessment for radionuclide releases. For the past 5 years, Rood has worked primarily on the development of groundwater screening methodology and codes, food chain transport models, and contaminant transport modeling in support of environmental restoration activities and performance assessment at the INEL. Rood developed the hydrologic transport conceptual model described in Chapter 3, and he was a key contributor to the determination of the release mechanism of tritium in beryllium blocks. Rood collaborated on the hydrologic flow conceptual model described in Chapter 3. He also performed hydrologic transport analyses described in Chapters 3 and 4 and conducted hydrologic uncertainty analyses for Chapter 4.

Mary E. Sussman received a B.S. degree in Mathematics in 1976 from Clemson University, Clemson, South Carolina. Sussman is the project manager for the RWMC LLW radiological performance assessment and has overall responsibility for the document. Sussman was responsible for production of the June 1990 draft performance assessment document, which received a preliminary review by the Performance Assessment Peer Review Panel. She performed project oversight and technical support for revisions to the performance assessment document and conducted internal and external reviews of the 1993 draft document and the associated comment resolution for finalization of the performance assessment document. Sussman manages several projects in the Environmental Restoration and Waste Management Department and has worked

in low-level radioactive waste management for 4 years. Sussman has worked for EG&G Idaho for over 13 years and has held several positions in the Company.

7. REFERENCES

Abramov, E. et. al., 1990, "Deuterium Permeation and Diffusion in High Purity Beryllium," Journal of Nuclear Materials, 175, p. 90.

American Ornithologist's Union, 1983, Checklist of North American Birds, Lawrence, Kansas: Allen Press.

Anderl, R. A. et al., 1992, "Hydrogen Transport of Beryllium," Journal of Nuclear Materials, 196-198, pp. 986-991.

Andersen, B. D. and L. J. Peterson-Wright, 1993, Drinking Water Program 1992 Annual Report, EGG-2678(92), August.

Anderson, J. E. and R. Inouye, 1988, Long-term Dynamics of Vegetation on a Sagebrush Steppe of Southeastern Idaho, Department of Biological Services, Idaho State University.

Anderson, S. R., 1991, Stratigraphy of the Unsaturated Zone and Uppermost Part of the Snake River Plain Aquifer at the Idaho Chemical Processing Plant and Test Reactor Area, Idaho National Engineering Laboratory, Idaho, U.S. Geological Survey Water-Resources Investigations Report 91-4010, DOE/ID-22095.

Anderson, M. E., 1993, "Projected Radionuclide Inventories to be Delivered to the RWMC," EDF RWMC-682, Science Applications International Corporation, October 20.

Anderson, S. R. and B. D. Lewis, 1989, Stratigraphy of the Unsaturated Zone at the Radioactive Waste Management Complex, Idaho National Engineering Laboratory, U.S. Geological Survey Water-Resources Investigations Report 89-4065, DOE/ID-22080, May.

Arnett, R. C., R. C. Martineau, M. J. Lehto, 1990, Preliminary Numerical Model of Radionuclide Transport in the Snake River Plain Aquifer Near the Idaho National Engineering Laboratory, EGG-WM-8820.

Arthur, W. J., 1982, "Radionuclide Concentrations in Vegetation at a Solid Radioactive Waste Disposal Area in Southeastern Idaho," Journal of Environmental Quality, 11, 3, pp. 394-399.

Arthur, W. J. and O. D. Markham, 1978, "Ecological Studies at the Idaho National Engineering Laboratory Radioactive Waste Management Complex," Ecological Studies on the Idaho National Engineering Laboratory Site, 1978 Progress Report, IDO-12087.

Arthur, W. J. and O. D. Markham, 1982, "Radionuclide Export and Elimination by Coyotes at Two Radioactive Waste Disposal Areas in Southeastern Idaho," Health Physics, 43, 4, pp. 493-500.

Arthur, W. J., J. C. Grant, O. D. Markham, 1983, "Importance of Biota in Radionuclide Transport at the SL-1 Radioactive Waste Disposal Area," Idaho National Engineering Laboratory Radioecology and Ecology Programs, 1983 Progress Report, DOE/ID-12098.

Arthur, W. J. et al., 1986, "Radiation Doses to Small Mammals Inhabiting a Solid Radioactive Waste Disposal Area," Journal of Applied Ecology, 23, pp. 13-26.

Baca, R. G. and S. O. Magnuson, 1992, FLASH—A Finite Element Computer Code for Variably Saturated Flow, EGG-GEO-10274, May.

Baca, R. G. et al., 1992, A Modeling Study of Water Flow in the Vadose Zone Beneath the Radioactive Waste Management Complex, EGG-GEO-10068.

Baes, C. F. III and T. H. Orton, 1979, "Productivity of Agricultural Crops and Forage, Y_v, in A Statistical Analysis of Selected Parameters for Predicting Food Chain Transport and Internal Dose of Radionuclides, NUREG/CR-1004, November.

Baes C. F., III and R. D. Sharp, 1983, "A Proposal for Estimation of Soil Leaching and Leaching Constants for Use in Assessment Models," Journal of Environmental Quality, 12, pp. 17-28.

Baes, C. F. et al., 1984, A Review and Analysis of Parameters for Assessing Transport of Environmentally Released Radionuclides through Agriculture, ORNL-5786.

Baldwin, D. A., O. D. Slagle, D. S. Gelles, 1989, Tritium Release from Irradiate Beryllium at Elevated Temperatures, Pacific Northwest Laboratory, PNL-SA-16998, November.

Barnard, C. J., 1992, Verification and Updating of the Radioactive Waste Management Information System for the Inactive TRU and non-TRU Pits and Trenches at the Radioactive Waste Management Complex Subsurface Disposal Area, EGG-ER-10519, Revision 0, November.

Barraclough, J. T. et al., 1967, Hydrology of the National Reactor Testing Station, Idaho, 1966, U.S. Geological Survey Open-File Report, IDO-22049.

Barraclough, J. T. et al., 1976, Hydrology of the Solid Waste Burial Ground as Related to the Potential Migration of Radionuclides, U.S. Geological Survey Open-File Report 76-471, IDO-22056, August.

Beeston, J. M. et al., 1990, Gas Retention in Irradiated Beryllium, EGG-FSP-9125, June.

Bennett, C. M., 1986, Capacity of the Diversion Channel Below the Flood-Control Dam on the Big Lost River at the Idaho National Engineering Laboratory, U.S. Geological Survey Water-Resources Investigations Report 86-4204.

Bischoff, J. R. and R. J. Hudson, 1979, Early Waste Retrieval Final Report, TREE-1321.

Bishop, C. W., 1991, "Hydraulic Properties of Vesicular Basalt," Master's thesis, University of Arizona, Tucson, Arizona.

Blackwell, D. D., 1989, "Regional Implications of Heat Flow of the Snake River Plain, Northwestern United States," Tectonophysics, 164, pp. 323-343.

Blom, P. E., W. H. Clark, J. B. Johnson, 1991, "Colony Densities of the Seed Harvesting Ant Pogonomyrmex salinus in Seven Plant Communities on the Idaho National Engineering Laboratory", Journal of the Idaho Academy of Science, 27, 1, pp. 28-36.

Breshears, D. D., 1987, "Uncertainty and Sensitivity Analyses of Simulated Concentrations of Radionuclides in Milk", M.S. Thesis, Colorado State University, Fort Collins, Colorado.

Breshears, D. D. et al., 1989, "Uncertainty in Predictions of Fallout Radionuclides in Foods and of Subsequent Ingestion", Health Physics, 57, 6, pp. 943-953.

Brownlow, A. H., 1979, Geochemistry, Englewood Cliffs NJ: Prentice Hall Inc.

Burgess, J. D., B. D. Higgs, T. R. Wood, 1993, WAG 7 Groundwater Pathway Draft Track 2 Summary Report, Revision 0, EGG-ER-10731.

Case, M. J. and M. D. Otis, 1988, Guidelines for Radiological Performance Assessment of DOE Low-Level Radioactive Waste Disposal Sites, DOE/LLW-62T, July.

Case, M. J. et al., 1990, Radioactive Waste Management Complex Performance Assessment, EGG-WM-8773.

Causey, R. A. et al., 1993, "Tritium Recycling, Permeation, and Inventory in Beryllium," Sixth International Conference on Fusion Reactor Materials, Stresa, Italy, September 27 - October 1, 1993.

Cecil, L. D. et al., 1992, "Water Infiltration Rates in the Unsaturated Zone at the Idaho National Engineering Laboratory Estimated from Chlorine-36 and Tritium Profiles, and Neutron Logging," in Proceedings of the 7th International Symposium on Water-Rock Interaction-WRI-7, Y. K. Kharaka and A. S. Meest (eds.), Park City, Utah, July 13-18.

CFR (Code of Federal Regulations), 1992, "National Emission Standards for Hazardous Air Pollutants (Clean Air Act)," 40 CFR 61, U.S. Environmental Protection Agency, Office of the Federal Register.

Champion, D. E., M. A. Lanphere, M. A. Kuntz, 1988, "Evidence for a New Geomagnetic Reversal From Lava Flows in Idaho: Discussion of Short Polarity Reversals in the Brunhes and Late Matuyama Polarity Chorns," Journal of Geophysical Research, 83, pp. 11,667-11,680.

Cholewa, A. F. and D. M. Henderson, 1984, "A Survey and Assessment of the Rare Vascular Plants of the Idaho National Engineering Laboratory," Great Basin Naturalist, 44, pp. 140-144.

Clawson, K. L., G. E. Start, N. R. Ricks, 1989, Climatography of the Idaho National Engineering Laboratory, NOAA Environmental Research Laboratories, DOE/ID-12118.

Codell, R. B., K. T. Key, G. Whelan, 1982, A Collection of Mathematical Models for Dispersion in Surface Water and Groundwater, NUREG-0868.

Coughtrey, P. J., D. Jackson, M. C. Thorne, 1985, Radionuclides Distribution and Transport in Terrestrial and Aquatic Ecosystems. A Compendium of Data, A. A. Balkema.

Culbertson-Arendts, K. H., 1993, "RWMIS LLW Inventory for RWMC LLW Radiological Performance Assessment," EDF RWMC-528, Rev. 1., EG&G Idaho, Inc., November.

Daniels W. R. et al., 1982, Summary Report on the Geochemistry of Yucca Mountain and Environs, Los Alamos National Laboratory, LA-9328-MS.

Dechert, T. V., P. A. McDaniel, A. L. Falen, 1993, Aggregational and Erosional History of the Radioactive Waste Management Complex at the Idaho National Engineering Laboratory, Draft, EGG-WM-11049, July.

Del Debbio, J. A. and T. R. Thomas, 1989, Transport Properties of Radionuclides and Hazardous Chemical Species in Soils at the Idaho Chemical Processing Plant, WINCO-1068.

Dodge, R. L. et al., 1991, Performance Assessment Review Guide for DOE Low-Level Radioactive Waste Disposal Facilities, Idaho National Engineering Laboratory, EG&G Idaho, DOE/LLW-93, October.

DOE (U.S. Department of Energy), 1982, Environmental and Other Evaluations of Alternatives for Long-Term Management of Defense Transuranic Waste at the Idaho National Engineering Laboratory, IDO-10103.

DOE, 1987, Environmental Assessment: Fuel Processing and Restoration at the Idaho National Engineering Laboratory, DOE/EA-0306.

DOE, 1988a, "Radioactive Waste Management," Order 5820.2A, September 26.

DOE, 1988b, Internal Dose Conversion Factors for Calculation of Dose to the Public, DOE/EH-0071.

DOE, 1988c, External Dose-Rate Conversion Factors for Calculation of Dose to the Public, DOE/EH-0070.

DOE, 1990, "Radiation Protection of the Public and the Environment," DOE Order 5400.5, June.

DOE, 1991, Draft EIS for the Siting, Construction, and Operation of New Production Reactor Capacity, DOE/EIS-0144D, April.

DOE, 1992, 1991 INEL National Emission Standard for Hazardous Air Pollutants Annual Report (1990/1991 Supplement), DOE/ID-10342(91S).

DOE, 1993, 1992 INEL National Emission Standard for Hazardous Air Pollutants Annual Report, DOE/ID-10342(92).

DOE, 1994, INEL Reusable Property, Recyclable Materials, and Waste Acceptance Criteria, DOE/ID-10381, February.

DOE-ID (U.S. Department of Energy Idaho Operations Office), 1992, Track 1 Sites: Guidance for Assessing Low Probability Hazard Sites at the INEL, Revision 1, DOE/ID-10340(92), July.

Eberle, T. B., L. Dorr, H. Werle, 1993, "Long-time Release from Irradiated Beryllium (SEBELIUS Irradiation)," Workshop on Beryllium for Fusion Applications, Karlsruhe, Germany, October 4-5, 1993.

EG&G Idaho, 1984, Environmental and Other Evaluations of Low-Level Waste at the Radioactive Waste Management Complex, EGG-WM-6523.

EG&G Idaho, 1988, Radioactive Waste Management Complex (RWMC) Subsurface Investigations Program Peer Review Report, EGG-BEG-8071, April.

EPA (U.S. Environmental Protection Agency), 1989, Risk Assessments Methodology, Environmental Impact Statement, NESHAPs for Radionuclides, Background Information Document - Volume 1, EPA/520/1-89-005.

Estey, S. A., R. C. Arnett, D. R. Aichele, 1985, Users Guide for MAGNUM-3D: A Three-Dimensional Groundwater Flow Numerical Model, RHO-BW-ST-67P, Rockwell Hanford Company.

Evenson, L., 1981, Systematic Effects of Radiation Exposure on Rodents Inhabiting Liquid and Solid Radioactive Waste Disposal Areas, M.S. thesis, University of Idaho, Moscow, Idaho.

Farris, W. T., 1988, Probabilistically Derived Concentration Limits for Near-Surface Disposal of Radioactive Waste, M.S. thesis, University of Washington, Seattle, Washington.

Forman, S. L. et al., 1993, "Stratigraphic and Chronologic Constraints on Late Pleistocene Loess Deposition on the Eastern Snake River Plain, Idaho," Quaternary Research.

Fowler J. D. et al., 1977, "Tritium Diffusion in Al_2O_3 and BeO," Journal of the American Ceramic Society, 60, 304, pp. 155-161.

Fraley, L., Jr., 1978, "Revegetation Following a 1974 Fire at the Idaho National Engineering Laboratory," in Ecological Studies on the Idaho National Engineering Laboratory Site 1978 Progress Report, O. D. Markham (ed.), IDO-12087, pp. 194-199.

Gadd, M, S., 1993, The Origins and Pathways of ^{222}Rn Entering into Basement Structures, Ph.D. Dissertation, Colorado State University, Fort Collins, Colorado.

Garabedian, S. P., 1989, Hydrology and Digital Simulation of the Regional Aquifer System, Eastern Snake River Plain, Idaho, U.S. Geological Survey Open-File Report 87-237.

Gilbert, T. L. et al., 1989, A Manual for Implementing Residual Radioactive Material Guidelines, ANL/ES-160, DOE/CH/8901, June.

Glover, P. A. et al., 1976, "Plutonium and Americium Behavior in the Soil/Water Environment, I. Sorption of Plutonium and Americium by Soils," in Proceedings of an Actinide-Sediment Reactions Working Meeting at Seattle, Washington, on February 10-11, 1976, BNWL-2117.

Gorman, V. W. and R. C. Guenzler, 1983, The 1983 Borah Peak Earthquake and INEL Structural Performance, EGG-EA-6501.

Groves, C. R., 1978, "Home Range and Local Movement of Small Mammals on the Radioactive Waste Management Complex, Idaho National Engineering Laboratory Site," Ecological Studies on the Idaho National Engineering Laboratory Site, 1978 Progress Report, IDO-12087.

Groves, C. R. and B. L. Keller, 1983, "Ecological Characteristics of Small Mammals on a Radioactive Waste Disposal Area in Southeastern Idaho," The American Midland Naturalist, 109, 2, pp. 253-265.

Hackett, W. R. and R. P. Smith, 1992, Quaternary Volcanism, Tectonics, and Sedimentation in the INEL Area, Utah Geological Survey Miscellaneous Publication 92-3, p. 1-18.

Hackett, W. R. et al., 1993, Geologic Processes in the RWMC Area, Idaho National Engineering Laboratory: Implications for Long-Term Stability and Performance Assessment of the RWMC, EG&G Idaho, informal report (should be finalized in November 1993).

Harniss, R. O. and N. E. West, 1973, "Vegetation Patterns of the National Reactor Testing Station, Southeastern Idaho," Northwest Science, 47, pp. 30-43.

Hitchcock, C. L. and A. Cronquist, 1974, Flora of the Pacific Northwest, Seattle, WA: University of Washington Press.

Hoff, D. L. et al., 1990, The Idaho National Engineering Laboratory Site Environmental Report for Calendar Year 1989, DOE/ID-12082(89).

Hoff, D. L. et al., 1991, The Idaho National Engineering Laboratory Site Environmental Report for Calendar Year 1990, DOE/ID-12082(90).

Hoffman, F. O. and R. H. Gardner, 1983, "Evaluation of Uncertainties in Radiological Assessment Models", Chapter 11 in Radiological Assessment - A Textbook on Environmental Dose Analysis, J. E. Till and H. R. Meyer (eds.), NUREG/CR-3332.

Hoffman, F. O., R. H. Gardner, K. F. Eckerman, 1982, Variability in Dose Estimates Associated with the Food Chain Transport and Ingestion of Selected Radionuclides, NUREG/CR-2612, ORNL/TM-8099.

Horwedel, J. E., R. J. Raridon, R. Q. Wright, 1989, Sensitivity Analysis of AIRDOS-EPA Using ADGEN with Matrix Reduction Algorithms, ORNL/TM-11373.

Hubbell, J. M., 1990a, Perched Ground Water at the Radioactive Waste Management Complex of the Idaho National Engineering Laboratory, EGG-ER-8779, October.

Hubbell, J. M., 1990b, Active Waste Disposal Monitoring at the Radioactive Waste Management Complex, Idaho National Engineering Laboratory, EGG-WM-9276, October.

Hubbell, J. M., 1992, "Perched Water at the Radioactive Waste Management Complex," EDF VVED-ER-098, EG&G Idaho, Inc., December.

Hubbell, J. M., 1993, "Perched Ground Water Monitoring in the Subsurface Disposal Area of the Radioactive Waste Management Complex, FY-1993," EDF ER&WM-EDF-002293, EG&G Idaho, Inc., November.

Hull, L. C., 1989, Conceptual Model and Description of the Affected Environment for the TRA Warm Waste Pond (Waste Management Unit TRA-03), EGG-ER-8644, October.

Humphrey P. A., E. M. Wilkins, D. M. Morgan, 1953, Atmospheric Dust at the National Reactor Testing Station, Final Report, U.S. Department of Commerce, Weather Bureau Office, Idaho Falls, Idaho.

Humphrey, T. G. and F. H. Tingey, 1978, The Subsurface Migration of Radionuclides at the Radioactive Waste Management Complex: 1976-1977, TREE-1171.

ICRP (International Commission on Radiological Protection), 1975, International Commission on Radiological Protection, Task Group Report on Reference Man, ICRP Publication 23, Pergamon Press, NY.

Irving, J. S., 1993, Environmental Resource Document for the Idaho National Engineering Laboratory, EGG-WMO-10279, July.

Jackson, S. M., 1985, Acceleration Data from the 1983 Borah Peak, Idaho, Earthquake Recorded at the Idaho National Engineering Laboratory," in R. S. Stein et al. (eds.), Workshop XXVIII on the Borah Peak Idaho, Earthquake, USGS Open-File Report 85-290, pp. 385-400.

Jackson, S. M. et al., 1993, "Contemporary Seismicity in the Eastern Snake River Plan, Idaho, Based on Microearthquake Monitoring," Bulletin of the Seismological Society of America, 83, pp. 680-695.

Jeppson, R. J. and K. E. Holte, 1978, "Flora of the Idaho National Engineering Laboratory Site," Ecological Studies on the Idaho National Engineering Laboratory Site, 1978 Progress Report, IDO-12087.

Jones, P. M. S. and R. Gibson, 1967, "Hydrogen in Beryllium," Journal of Nuclear Materials, 21, pp. 353-354.

Jones, J. K., Jr., B. C. Carter, H. H. Genoways, 1979, Revised Checklist of North American Mammals North of Mexico, 1979, Occasional Papers Museum Texas Tech University, No.-62, Lubbock, Texas.

Keller, B. L., 1978, "Dispersal and Density of Small Mammals on the Radioactive Waste Management Complex, Idaho National Engineering Laboratory Site," Ecological Studies on the Idaho National Engineering Laboratory Site, 1978 Progress Report, IDO-12087.

Kelmers, A. D. and J. R. Hightower, 1987, Calculation of the Inventory and Near-Field Release Rates of Radioactivity from Neutron-Activated Metal Parts Discharged from the High Flux Isotope Reactor and Emplaced in Solid Waste Storage Area 6 at Oak Ridge National Laboratory, ORNL/TM-10233, May.

Kennedy, W. E., Jr., L. L. Cadwell, D. W. McKenzie, 1985, "Biotic Transport of Radionuclides from a Low-Level Radioactive Waste Site," Health Physics, 49, 1, pp. 11-24.

Kennedy, W. E., Jr. and R. A. Peloquin, 1988, Intruder Scenarios for Site-Specific Low-Level Radioactive Waste Classification, DOE/LLW-71T.

Knutson, C. F. et al., 1992, 3D RWMC Vadose Zone Modeling (Including FY-89 to FY-90 Basalt Characterization Results), EGG-ERD-10246, May.

Konz, J. J. et al., 1989, Exposure Factors Handbook, EPA/600/8-89/043.

Koslow, K. N. and D. H. Van Haaften, 1986, Flood Routing Analysis for a Failure of Mackay Dam, EGG-EP-7184, June.

Kuntz, M. A. et al., 1990, Revised Geologic Map of the INEL and Adjoining Areas, Eastern Idaho, U.S. Geological Survey Open-File Report 90-333.

Kuntz, M. A., H. R. Covington, L. J. Schorr, 1992, "An overview of basaltic volcanism on the ESRP" in P. K. Link, M. A. Kuntz, L. Platt (eds.), Regional Geology of Eastern Idaho and Western Wyoming, Geological Society of America Memoir 179, pp. 227-268.

Lamke, R. D., 1969, Stage Discharge Relations on Big Lost River Within National Reactor Testing Station, Idaho, U.S. Geological Survey Open-File Report, IDO-22050.

Laney, P. T. et al., 1988, Annual Progress Report: FY-1987--Subsurface Investigations Program at the Radioactive Waste Management Complex of the Idaho National Engineering Laboratory, DOE/ID-10183.

Learman, A. 1988, "Geochemical Processes Water and Sediment Environments" Malabar, Florida: Robert E. Krieger Publishing Company.

Leonard, P. R., 1992, "Radon Doses to Inadvertent Intruders into the Pits and Trenches and the Soil Vaults 100 years and 3,000 Years After Closure," EDF RWMC-589, EG&G Idaho.

Longhurst, G. R., 1990, Tritium Behavior in ITER Beryllium, EGG-FSP-9304, October.

Longhurst, G. R. et al., 1992, TMAP4 User's Manual, EGG-FSP-10315, June 12.

McBride, R. et al., 1978, Vegetation Types and Surface Soils of the Idaho National Engineering Laboratory Site, IDO-12084.

McDonald, M. G. and A. W. Harbaugh, 1988, A Modular Three-Dimensional Finite-Difference Groundwater Flow Model, USGS Survey Techniques of Water-Resources Investigations, Book 6, Chapter A1.

McElroy, D. L., 1990, Vadose Zone Monitoring at the Radioactive Waste Management Complex at the Idaho National Engineering Laboratory 1985-1989, EGG-WM-9299.

McElroy, D. L., 1993, Soil Moisture Monitoring Results at the Radioactive Waste Management Complex of the Idaho National Engineering Laboratory, FY-1993, EGG-WM-11066, November.

McElroy, D. L. and J. M. Hubbel, 1990, Hydrologic and Physical Properties of Sediments at the Radioactive Waste Management Complex, EGG-BG-9147, September.

McElroy, D. L. et al., 1992, RWMC SDA Engineered Barrier Test Plan (Draft), EGG-WMO-10284, June.

McFarlane, J. C., R. D. Rogers, D. V. Bradley, Jr., 1979, "Tritium Oxidation in Surface Soils. A Survey of Soils Near Five Nuclear Reprocessing Plants," Environmental Science and Technology, 13, 5, pp. 607-608.

McKenzie et al. 1982, Relevance of Biotic Pathways to the Long-Term Regulation of Nuclear Waste Disposal, Topical Report on Reference Western Arid Low-Level Sites, NUREG/CR-2675, Volume 2.

McKenzie, D. H. et al., 1986, Relevance of Biotic Pathways to the Long-Term Regulation of Nuclear Waste Disposal, Phase II Final Report, Volume 6, NUREG/CR-2675.

McKinley, K. B. and J. D. McKinney, 1978, Early Waste Retrieval Interim Report, TREE-1266.

Macaulay-Newcombe, R. G., D. A. Thompson, W. W. Smeltzer, 1992, "Thermal Absorption and Desorption of Deuterium in Beryllium and Beryllium Oxide," Journal of Nuclear Materials, 191-194, pp. 263-267.

Magnuson, S. O., 1993, A Simulation Study of Moisture Movement in Proposed Barriers for the Subsurface Disposal Area, INEL, EGG-WM-10947, September.

Magnuson, S. O. and D. L. McElroy, 1993, "Estimation of Infiltration From In Situ Moisture Contents and Representative Moisture Characteristic Curves for the 30', 110', and 240' Interbeds," EDF RWM-93-001.1, EG&G Idaho, August 18.

Maheras, S. J., 1988, "Methods for Probabilistic Radiological Dose Assessment at a High-Level Radioactive Waste Repository", Ph.D. Dissertation, Colorado State University, Fort Collins, Colorado.

Maheras, S. J., 1993, "Revised Doses to Inadvertent Intruders for the RWMC Radiological Performance Assessment," EDF RWMC-622, Rev. 1, Science Applications International Corporation.

Maheras, S. J. and A. S. Rood, 1991a, "Summary Report: Waste Concentration Limits for RWMC," EDF RWMC-484, EG&G Idaho, Inc., August.

Maheras, S. J. and A. S. Rood, 1991b, "Detail Report: Waste Concentration Limits for RWMC," EDF RWMC-485, EG&G Idaho, Inc., August.

Malde, H. E., 1991, "Quaternary Geology and Structural History of the Snake River Plain, Idaho, and Oregon," in Quaternary Nonglacial Geology; Conterminous United States: Boulder, Colorado, The Geology of North American, R. B. Morrison (ed.), Geological Society of America, Vol. K-2, pp. 251-281.

Mann, L. J., 1986, Hydraulic Properties of Rock Units and Chemical Quality Water for INEL-1--A 10,365-foot Deep Test Hole Drilled at the Idaho National Engineering Laboratory, Idaho, U.S. Geological Survey Water-Resources Report 86-4020, IDO-22070.

Markham, O. D., 1987, Summaries of the Idaho National Engineering Laboratory Radioecology and Ecology Programs Research Projects, DOE/ID-12111.

Martin, K. L. et al., 1992, Preliminary Assessment of Surface Soils at Active EG&G Idaho Facilities Data Document, EGG-ESQ-9225, Revision 1, May.

Martineau, R. C. et al., 1990, Hydrologic Modeling Study of Potential Flooding at the Subsurface Disposal Area from a Hypothetical Breach of Dike 2 at the Idaho National Engineering Laboratory, EGG-WM-9502.

Miller, P. D. and W. K. Boyd, 1967, "Corrosion of Beryllium," Defence Metals Information Center, DMIC 242, December 11.

Miller, C. W. and L. M. Hively, 1987, "A Review of Validation Studies for the Gaussian Plume Atmospheric Dispersion Model", Nuclear Safety, 28, 4, pp. 522-531.

Miller, G. V. and S. J. Maheras, 1991, Software Verification and Validation Plan for CAP-88 Codes, EGG-CATT-9975, December.

Miller, S. J., 1992, INEL Draft Management Plan for Cultural Resources, DOE/ID-10361.

Miller, S. M., J. E. Hammel, L. F. Hall, 1990, Characterization of Soil Cover and Estimation of Water Infiltration at Central Facilities Area II, Idaho National Engineering Laboratory, Research Technical Completion Report, Idaho Water Resources Institute, University of Idaho, June.

Mosely R. and C. Groves, 1990, "Rare, Threatened, and Endangered Plants and Animals of Idaho," Natural Heritage Section, Nongame and Endangered Wildlife Program, Idaho Department of Fish and Game.

Mundorff, M. J. et al., 1964, Ground Water Irrigation in the Snake River Basin in Idaho, U.S. Geological Survey Water Supply Paper 1954.

Napier, B. A. et al., 1988, GENII - The Hanford Environmental Radiation Dosimetry Software System, Volumes 1-3, PNL-6584, December.

NCRP (National Council on Radiation Protection and Measurements), 1984, Radiological Assessment: Predicting the Transport, Bioaccumulation, and Uptake by Man of Radionuclides Released to the Environment, NCRP Report No. 76, March.

Ng, Y. C., C. S. Colsher, S. E. Thompson, 1982, Soil-to-Plant Concentration Factors for Radiological Assessments, NUREG/CR-2975.

Ng, Y. C. et al., 1978, Methodology for Assessing Dose Commitment to Individuals and to the Population from Ingestion of Terrestrial Foods Contaminated by Emissions from a Nuclear Fuel Reprocessing Plant at the Savannah River Plant, UCID-17743, Lawrence Livermore Laboratory, March.

NRC (U.S. Nuclear Regulatory Commission), 1977, Regulatory Guide 1.109 Calculation of Annual Doses to Man From Routine Releases of Reactor Effluents for the Purpose of Evaluating Compliance With 10 CFR Part 50 Appendix I, Revision 1.

NRC, 1981, Draft Environmental Impact Statement on 10 CFR Part 61 "Licensing Requirements for Land Disposal of Radioactive Waste", NUREG-0782, Volumes 1-4.

NRC, 1982, Final Environmental Impact Statement on 10 CFR Part 61 "Licensing Requirements for Land Disposal of Radioactive Waste", NUREG-0945, Volumes 1-3.

Nussbaum, R. A., E. D. Brodie, Jr., R. M. Storm, 1983, Amphibians and Reptiles of the Pacific Northwest, Moscow, Idaho: University Press of Idaho.

O'Neill, R. V. et al., 1981, "Parameter Uncertainty and Estimated Radiological Dose to Man from Atmospheric ^{131}I Releases: A Monte Carlo Approach", Health Physics, 40, 5, pp. 760-764.

Orr, B. R. and L. D. Cecil, 1991, Hydrologic Conditions and Distribution of Selected Chemical Constituents in Water, Snake River Plain Aquifer, Idaho National Engineering Laboratory, Idaho, 1986 to 1988, U.S. Geological Survey Water-Resources Investigations Report 91-4047, DOE/ID-22096, March.

Otis, M. D., 1983, "Sensitivity and Uncertainty Analysis of the PATHWAY Radionuclide Transport Model", Ph.D. Dissertation, Colorado State University, Fort Collins, Colorado.

Otis, M. D., T. B. Kirchner, F. W. Whicker, 1985, "Uncertainty Estimates for Radionuclide Ingestion in Utah Following Atmospheric Atomic Weapons Tests", in Environmental Radiation '85: Proceedings of the Eighteenth Midyear Topical Symposium of the Health Physics Society, January 6-10, Colorado Springs, Colorado, pp. 79-83.

Overton, C. K. et al., 1976, "Big Lost River Fisheries," Summaries of the Idaho National Engineering Laboratory Site Ecological Information Meeting, July 10-11, 1975, U.S. Energy Research and Development Administration, Idaho Operations Office, pp. 42-43.

Oztunali, O. I. and G. W. Roles, 1986, Update of Part 61 Impacts Analysis Methodology, NUREG/CR-4370, Volumes 1 and 2.

Paarmann, M. L., Reubelman, K. L., P. B. Swain, 1991, Radioactive Waste Management Complex Investigations Report, EGG-WM-9707, December.

Pelton, J. R., R. J. Vincent, N. J. Anderson, 1990, "Microearthquakes in the Middle Butte/East Butte Area, Eastern Snake River Plain Idaho," Bulletin of the Seismological Society of America, 80, 1, pp. 209-212.

Peterson, H. T. Jr., 1983, "Terrestrial and Aquatic Food Chain Pathways", in Radiological Assessment - A Textbook on Environmental Dose Analysis, J.E. Till and H.R. Meyer (eds.), NUREG/CR-3332.

Pierce, K. L. and L. A. Morgan, 1992, "The track of the Yellowstone hot spot: Volcanism, faulting, and uplift," in P. K. Link, M. A. Kuntz, L. Platt (eds.), Regional Geology of Eastern Idaho and Western Wyoming, Geological Society of America Memoir 179.

Pittman, J. R., R. G. Jensen, P. R. Fisher, 1988, Hydrologic Conditions at the Idaho National Engineering Laboratory, 1982 to 1985, U.S. Geological Survey Water-Resources Investigations Report 89-4008, DOE/ID-22078, December.

Plansky, L. E. and S. A. Hoiland, 1992, Analysis of the Low-Level Waste Radionuclide Inventory for the Radioactive Waste Management Complex Performance Assessment, EGG-WM-9857, Revision 1, June.

Poreda, R. J. and T. E. Cerling, 1992, "Cosmogenic Neon in Recent Lavas from the Western United States," Geophysical Research Letters, 19, pp. 1863-1866.

Press, W. H. et al. 1992, Numerical Recipes in Fortran, The Art of Scientific Computing, Second Edition, Cambridge University Press.

Price, K. R., 1972, Uptake of Np-237, Pu-239, Am-241, and Cm-244 from Soil by Tumbleweed and Cheatgrass, BNWL-1688.

Rathburn, S. L., 1991, Quaternary Channel Changes and Paleoflooding Along the Big Lost River Idaho National Engineering Laboratory, EGG-WM-9909, January.

Reynolds, T. M. and W. L. Wakkinen, 1987, "Characteristics of the Burrows of Four Species of Rodents in Undisturbed Soils in Southeastern Idaho," The American Midland Naturalist, 118, 2, pp. 245-250.

Reynolds, T. D. and J. W. Laundre, 1988, "Vertical Distribution of Soil Removed by Four Species of Burrowing Rodents in Disturbed and Undisturbed Soils," Health Physics, 54, 4.

Reynolds, T. D. and L. Fraley, Jr., 1989, "Root Profiles of Some Native and Exotic Plant Species in Southeastern Idaho, Environmental and Experimental Botany, 29, pp. 241-248.

Reynolds, T. D. et al., 1986, "Vertebrate Fauna of the Idaho National Environmental Research Park," Great-Basin Naturalist, 46, pp. 513-527.

Rightmire, C. T. and B. D. Lewis, 1987, Hydrogeology and Geochemistry of the Unsaturated Zone, Radioactive Waste Management Complex, Idaho National Engineering Laboratory, Idaho, U.S. Geological Survey Water-Resources Investigations Report 87-4198, DOE/ID-22073.

Ringe, B. L., 1992, Archaeological Test Excavation of 10-BT-1230, EGG-CS-10268.

Robertson, J. B., 1974, Digital Modeling of Radioactive and Chemical Waste Transport in the Snake River Plain Aquifer at the National Reactor Testing Station, Idaho, U.S. Geological Survey Open File Report, IDO-22054.

Robertson, J. B. et al., 1974, The Influence of Liquid Waste Disposal on the Geochemistry of Water at the National Reactor Testing Station, Idaho, 1952-1970, IDO-22053.

Rogers, V. C. and C. Hung, 1987, PATHRAE-EPA: A Low-Level Radioactive Waste Environmental Transport and Risk Assessment Code, Methodology and Users Manual, EPA 520/1-87-028.

Rogers, V. C., M. W. Grant, A. A. Sutherland, 1982, Low-Level Waste Disposal Site Performance Assessment With the RQ/PQ Methodology, EPRI-NP-2665.

Rood, A. S., R. C. Arnett, J. T. Barraclough, 1989, Contaminant Transport in the Snake River Plain Aquifer: Phase I, Part 1: Simple Analytical Models of Individual Plumes, EGG-ER-8623.

Rood, A. S., 1993a, GWSCREEN: A Semi-Analytical Model for Assessment of the Groundwater Pathway from Surface or Buried Contamination: Version 2.0 Theory and User's Manual, EGG-GEO-10797, June.

Rood, A. S., 1993b, "Groundwater Pathway Screening for the RWMC Inventory from 1984-1993 and Forecasted Inventory to 2020," EDF RWM-93-001.2, Rev. 1, EG&G Idaho, November 15.

Runchal, A. K. and B. Sagar, 1993, PORFLOW: A Model for Fluid Flow, Heat and Mass Transport in Multifluid, Multiphase Fractured or Porous Media, User's Manual, Version 2.50, Analytic & Computational Research, Inc., Bel Air, California, July 6.

Rupp, E. M., 1980, "Age-Dependent Values of Dietary Intake for Assessing Human Exposures to Environmental Pollutants," Health Physics, 39, pp. 151-163.

Sagendorf, J., 1991, Meteorological Information for RWMC Flood Potential Studies, NOAA, Environmental Research Laboratories, Air Resources Laboratory Field Research Division, Idaho Falls, Idaho.

Schmalz, B. L., 1972, Radionuclide Distribution in Soil Mantle of the Lithosphere as a Consequence of Waste Disposal at the National Reactor Testing Station, IDO-10049.

Schwarz, G. and F. O. Hoffman, 1980, "Imprecision of Dose Predictions for Radionuclides Released to the Environment: An Application of a Monte Carlo Simulation Technique", Environment International, 4, pp. 289-297.

Scott, W. E., 1982, "Surficial geologic map the Eastern Snake River Plain and adjacent areas, 111 to 115 degrees west, Idaho and Wyoming," USGS Miscellaneous Investigations Series Map I-1372, 2 sheets, 1:250,000.

Seitz, R. R., 1991, "Well Parameters for Intruder Drilling Scenario at RWMC," SEM-RWMC-91-002, EG&G Idaho, August.

Seitz, R. R. et al., 1991, Sample Application of Sensitivity/Uncertainty Analysis Techniques to a Groundwater Transport Problem, DOE/LLW-108.

Shaeffer, D. L. and F. O. Hoffman, 1979, "Uncertainties in Radiological Assessments--A Statistical Analysis of Radioiodine Transport Via the Pasture-Cow-Milk Pathway", Nuclear Technology, 45, pp. 99-106.

Sheppard, M. I. and D. H. Thibault, 1990, "Default Soil Solid/Liquid Partition Coefficients, Kds, for Four Major Soil Types: A Compendium," Health Physics, 59, pp. 471-482.

Simpson, J. C. and R. L. Wallace, 1978, Fishes of Idaho, Moscow, Idaho: University Press of Idaho.

Sussman, M. E., 1993, "Parameters for Basement Construction for Intruder Scenarios at RWMC," EDF RWMC-603, EG&G Idaho, March 23.

Swansiger, W. A., 1986, "Tritium Solubility in High-Purity Beryllium," Summary Abstract, Journal of Vacuum Science and Technology, A 4, p. 1216.

Ticknor, K. V. and B. Ruegger, 1989, A Guide to the NEA's Sorption Data Base, Version 2.0, September.

Tkachyk, J. W., P. D. Ritter, R. N. Wilhelmsen, 1988, Annual Report-1987 Environmental Surveillance for the EG&G Idaho Radioactive Waste Management Areas at the Idaho National Engineering Laboratory, EGG-2550, August.

Tullis, J. A., 1993, "Quaternary Stratigraphy and Soil Development at the Radioactive Waste Management Complex and Adjacent Areas, Idaho National Engineering Laboratory, Idaho," EDF EGG-EELS-003, EG&G Idaho, March 2.

Tullis, J. A. and K. N. Koslow, 1983, Characterization of Big Lost River Floods with Recurrence Intervals Greater than 25 Years, RE-PB-83-044, EG&G Idaho.

van Genuchten, M. T., 1980, "A Closed-Form Equation for Predicting the Hydraulic Conductivity of Unsaturated Soils," Soil Science Society of America Journal, 44, pp. 892-898.

Walton, J. C., R. G. Baca, T. L. Rasmussen, 1989a, "Flow and Transport of Radionuclides in Unsaturated Fractured Basalt, Waste Management '89, University of Arizona, pp. 775-780.

Walton, J. C. et al., 1989b, "Model for Estimation of Chlorinated Solvent Release from Waste Disposal Sites," Journal of Hazardous Materials, 21, pp. 15-34.

Ward, D. C., T. B. Borak, M. S. Gadd, 1993, "Characterization of ^{222}Rn Entry into a Basement Structure Surrounded by Low-Permeability Soil," Health Physics, 65, 1, July.

Wilhelmsen, R. N. and K. C. Wright, 1992, Annual Report-1991 Environmental Surveillance for EG&G Idaho Waste Management Facilities at the Idaho National Engineering Laboratory, EGG-2679(91), August.

Wilhelmsen, R. N., K. C. Wright, D. W. McBride, 1993, Annual Report-1992 Environmental Surveillance for EG&G Idaho Waste Management Facilities at the Idaho National Engineering Laboratory, EGG-2679(92), August.

Wood, T. R., 1989, Preliminary Assessment of the Hydrogeology at the Radioactive Waste Management Complex, Idaho National Engineering Laboratory, EGG-WM-8694, December.

Wood, D. E. et al., 1992, Performance Assessment Task Team Draft Progress Report, DOE/LLW-157, Rev. 0.

Wylie, A. H. and J. M. Hubbell, 1993, "Aquifer testing of wells M1S, M3S, M4D, M6S, M7S, and M10S at the Radioactive Waste Management Complex," EDF ER-WAG7-26, EG&G Idaho, Inc.

Yang, Y. Y. and C. B. Nelson, 1984, An Estimation of the Daily Average Food Intake by Age and Sex for Use in Assessing the Radionuclide Intake of Individuals in the General Population, EPA 520/1-84-021.

Yang, Y. Y. and C. B. Nelson, 1986, "An Estimation of Daily Food Usage factors for Assessing Radionuclide Intakes in the U.S. Population", Health Physics, 50, 2, pp. 245-257.

Zelus, P., J. Tokle, R. Kushwaha, 1991, Socioeconomic Impacts of the Idaho National Engineering Laboratory, Idaho State University, Pocatello, Idaho, December.

APPENDIX A

WASTE INVENTORY

APPENDIX A
WASTE INVENTORY

The RWMC radiological performance assessment evaluates LLW disposed of in the SDA from 1984 through 1993. In addition, it evaluates projected LLW that will be disposed of in the SDA from 1994 through 2020. The LLW disposed of in the SDA from 1984 through 1993 is buried in Pits 17 through 20 and Soil Vault Rows 14 through 20. No trench burial occurred during this time period; the last open trench, Trench 55, closed in 1982. The inventory data used in the radiological performance assessment was generated from the RWMIS data base, which is the official reporting source for INEL waste information.

Although DOE Order 5820.2A applies only to LLW disposed of after September 26, 1988, LLW disposed of before this date was included in the radiological performance assessment. The environmental restoration program at the INEL will assess wastes buried in the SDA from 1952 through 1983 in accordance with the National Contingency Plan under CERCLA. The year 1983 was selected as the cutoff date for the waste to be assessed under CERCLA based on the following rationale. High-efficiency particulate air filters from the Waste Calcining Facility, located at the Idaho Chemical Processing Plant, containing the hazardous materials mercury and cadmium were disposed of in the SDA as late as June 1983. Therefore, the trenches, pits, and soil vaults rows that were open before June 1983 could potentially contain mixed waste, which falls under the domain of the Environmental Restoration Program and will be assessed under CERCLA.

In terms of disposal locations, this includes waste buried in Trenches 1 through 58, Soil Vault Rows 1 through 13, and Pits 1 through 16. Because it is impractical to remediate only part of pit or soil vault row, all wastes buried in Pit 16 and Soil Vault Row 13 will be assessed under CERCLA even though Pit 16 closed on October 15, 1984, and Soil Vault Row 13 closed on December 21, 1984. Soil Vault Row 14 and Pit 17 opened on October 16, 1984, and May 5, 1984, respectively. Therefore, they should contain only LLW, not the mixed waste described previously and are a logical point to begin the radiological performance assessment. Using this date will ensure that all waste is accounted for either in the radiological performance assessment

performed under DOE Order 5820.2A or in the baseline risk assessments performed under CERCLA.

A-1 WASTE INVENTORY

Knowledge of the radionuclide inventory in the disposed waste is essential to the performance assessment. Operations at the INEL that produce LLW include research and development programs associated with reactor designs at Argonne National Laboratory-West facilities, fuel processing activities at the Idaho Chemical Processing Plant, reactor development and training facilities at the Naval Reactor Facilities, a production facility for the Army at Test Area North, and development, testing, and analysis of materials and fuels used in nuclear reactor applications at the Test Reactor Area. It is expected that decontamination and decommissioning operations and environmental restoration actions will become a major generator of LLW in the future.

During the time period evaluated in the radiological performance assessment, 1984 through 2020, unidentified activity accounts for only 0.12% of the activity disposed of in the pits and 0.033% of the activity disposed of in the soil vault rows. For the purposes of analysis, unidentified activity (denoted mixed activation products, mixed fission products, and unidentified beta-gamma in the RWMIS data base) was assumed to be 50% Sr-90 and 50% Cs-137. The use of other radionulcides for unidentified activity was evaluated in the uncertainty analysis. The inventory reported in the RWMIS data base is contained in Tables A-1 (pits) and A-2 (soil vault rows) for the years 1984 through 1993.

A-1.1 Radionuclide Forecasts

The RWMC LLW radiological performance assessment assumes that waste is disposed of in the SDA until the year 2020, an additional 27 years of inventory that must be forecast. Two methods are commonly used to forecast inventory. In the first method, generator forecasts are combined to yield an annual inventory to be disposed of in the future. In the second method, the past several years of historical disposal data are used to arrive at an annual inventory to be disposed of in the future. Both methods have their drawbacks. For example, waste generators may not report all radionuclides of importance

Table A-1. Radioactivity (Ci) disposed of in pits by year (1984 to 1993) and radionuclide as reported to RWMIS.[a,b,c]

Radionuclide	1984	1985	1986	1987	1988	1989	1990	1991	1992	1993	TOTAL
AC-227			1.593E-02	1.460E-01							1.619E-01
AG-108M				1.000E-03						3.939E-07	1.000E-03
AG-110			1.314E-06	5.104E-02	2.370E-02	8.000E-05		2.640E-06			7.483E-02
AG-110M			1.259E-06	1.913E+00			1.420E-03			6.571E-06	1.914E+00
AM-241	6.045E-06	1.091E-01	6.075E-02	1.269E-01	3.501E-03	7.104E-02	7.680E-05	3.258E-06	7.300E-03	1.501E-02	3.937E-01
AM-243	9.250E-07	1.297E-03	2.242E-04	1.850E-05	2.040E-04						1.745E-03
BA-LA-140		1.000E+00									1.000E+00
BA-133		1.000E-06									1.000E-06
BA-137M							1.298E-01	2.476E-03	1.100E-05	2.700E-02	1.593E-01
BA-140	2.204E-01	7.800E-02					8.357E-02	6.060E-02	8.813E-01	3.600E-03	1.327E+00
BE-7			6.584E-04								6.584E-04
BK-249		1.700E-02	2.366E-08								1.700E-02
BR-82								1.000E-03			1.000E-03
C-14	2.434E-04	5.000E-07	1.085E-03	7.623E-03	1.211E-02		1.400E-06	4.355E-03	8.722E-03	3.035E-02	6.449E-02
CA-45					1.015E-03						1.015E-03
CD-109	1.120E-03		5.862E-04	5.483E-04	1.700E-05			1.090E-02			1.317E-02
CE-139									3.000E-04		3.000E-04
CE-141	3.380E-01	3.800E-01		2.400E-02			2.244E-01	1.706E-01	1.149E+00	3.520E-02	2.321E+00
CE-144	5.521E+01	2.002E+01	4.639E+01	4.082E+01	3.672E+01	3.113E+01	4.451E+01	5.491E+00	2.608E+00	5.797E-01	2.835E+02
CF-249		2.055E-04	4.091E-06	8.180E-10							2.096E-04
CF-250			1.080E-04								1.080E-04
CF-252	9.945E-11	4.296E-04	2.505E-05								4.547E-04
CM-242							9.834E-08			8.000E-10	9.914E-08
CM-243			5.000E-07								5.000E-07
CM-244		9.991E-08				2.250E-03	2.780E-06			1.977E-05	2.273E-03
CO-56			7.822E-06								7.822E-06
CO-57			2.750E-05	3.605E-05			1.529E-02	5.108E-03	2.617E-02	2.270E-04	4.685E-02
CO-58	4.778E-01	2.175E-01	1.284E+01	2.569E+01	8.340E-01	8.532E-01	1.641E+00	1.674E+01	1.581E+00	1.015E+00	6.189E+01
CO-60	7.834E+03	3.809E+01	1.600E+02	9.937E+01	6.443E+00	1.967E+01	9.456E+00	3.819E+01	1.407E+01	7.208E+00	8.227E+03
CR-51	2.829E+02	2.019E+03	1.028E+03	2.619E+02	1.346E+02	7.137E+01	5.326E+01	1.190E+02	5.649E+01	4.583E+01	4.072E+03
CS-134	2.722E-01	5.130E+01	1.506E-02	7.075E-01	3.100E-03	5.323E+00	7.171E-02	1.723E+00	6.400E+00	1.058E-01	6.592E+01
CS-137	2.801E+01	3.609E+02	2.097E+01	6.065E+01	1.788E+01	7.938E+01	2.581E+01	5.485E+01	3.369E+02	1.663E+00	9.870E+02
EU-152	1.000E-05	1.175E-03	1.000E-01	6.486E+00	1.000E-05		1.806E-03	1.553E-02	1.202E-02	5.255E-04	6.617E+00
EU-154		2.570E-01	1.200E-05	4.578E+00			1.872E-03	4.455E-01	6.742E-02	1.805E-02	5.368E+00

Table A-1. (continued).

Radionuclide	1984	1985	1986	1987	1988	1989	1990	1991	1992	1993	TOTAL
EU-155				9.684E-01		3.677E-01	6.429E-03	1.104E-01	1.477E-01	4.995E-05	1.601E+00
FE-55	3.830E+03				1.700E-01	1.837E+01	2.044E+00	6.327E+01	2.233E+00	5.532E+01	3.971E+03
FE-59	1.001E-02	3.511E-01	5.039E-02				5.944E-03	8.285E-03	5.363E-03	5.000E-05	4.311E-01
H-3	2.236E+00	2.097E+01	1.100E+02	8.252E+02	4.713E+01		8.934E-03	2.820E-02	2.676E-02	1.966E+03	2.972E+03
HF-175								4.090E-02	5.000E-04		4.140E-02
HF-181		2.832E-01		2.741E+00	7.570E-02	1.473E-01	3.395E-01	1.410E-01	9.267E-01	3.480E-02	4.689E+00
HG-203			1.000E-06								1.000E-06
I-125				1.155E-03							1.155E-03
I-129							2.400E-10	1.303E-09	1.731E-08	1.216E-07	1.405E-07
I-131								5.680E-02	5.600E-03	6.400E-03	6.880E-02
I-132								4.460E-02	9.636E-01		1.008E+00
I-133									1.500E-03		1.500E-03
IR-192									8.000E-04	1.900E-03	2.700E-03
K-40		1.000E-06	2.132E-05			1.500E-01	1.446E-03	1.763E-02	3.000E-05		1.691E-01
LA-140	2.204E-01	8.460E-02					1.004E-01	7.758E-02	1.135E+00	3.600E-03	1.622E+00
MAP	2.411E+01	5.837E+01	2.756E+01	3.676E+01	5.376E+01	1.961E+01	5.450E+00	1.760E+00			2.274E+02
MFP	2.537E+02	1.962E+02	1.144E+02	4.148E+02	9.803E+01	4.390E+01	7.174E+00	1.846E+00			1.130E+03
MN-54	6.325E+01	3.795E+00	1.221E+01	9.680E+00	3.190E-01	5.074E+00	7.126E-01	3.653E+00	6.726E-01	3.626E-01	9.973E+01
MN-56									1.306E+00		1.306E+00
MO-99									3.950E-03		3.950E-03
NA-22	2.001E-02	5.000E-05	3.339E-04	3.814E-05			7.093E-04	5.000E-02			7.114E-02
NA-24			2.200E+00						5.195E-01		2.719E+00
NB-94							6.900E-06				6.900E-06
NB-95	8.534E+00	3.541E+00	5.825E+00	4.188E+00	5.479E+00	3.308E+00	6.926E+00	8.420E-01	1.916E-01	1.533E-01	3.899E+01
NI-63	1.141E+04			2.002E-03	5.400E-02	1.050E+00	1.963E+00	1.747E+00	4.339E-01	1.631E+02	1.158E+04
NP-237	1.346E-05	5.133E-04	7.578E-04	3.751E-04	4.900E-05						1.709E-03
NP-239		1.000E-06									1.000E-06
P-32	1.000E-03	7.500E-03	5.000E-05								8.550E-03
PA-231	4.720E-03										4.720E-03
PB-210	2.000E-05		1.000E-06	1.000E-05							3.100E-05
PB-212		4.000E-03	3.000E-06								4.003E-03
PM-147	6.000E-03										6.000E-03
PR-144	5.423E+01	1.914E+01	3.988E+01	2.656E+01	3.302E+01	2.018E+01	4.264E+01	4.747E+00	4.799E-01	2.537E-01	2.411E+02
PU-236		1.012E-07	1.141E-06	1.961E-06							3.203E-06

Table A-1. (continued).

Radionuclide	1984	1985	1986	1987	1988	1989	1990	1991	1992	1993	TOTAL
PU-238	1.740E-02	1.796E-05	1.358E-05	3.913E-04	2.114E-04	8.482E-10	1.965E-04		8.600E-08	4.976E-04	1.873E-02
PU-239	5.510E-02	6.910E-02	6.834E-02	2.821E-02	1.760E-02	2.337E-02	1.983E-03	1.426E-03	2.838E-04	9.504E-05	2.655E-01
PU-239-240	1.400E-05										1.400E-05
PU-240	2.041E-02	5.730E-03	9.725E-04	4.859E-03	1.567E-03	4.147E-05	1.598E-05	1.384E-06	3.111E-06		3.360E-02
PU-241			1.550E-04	6.581E-02	2.127E-02	2.403E-08					8.724E-02
PU-242	9.922E-07	2.104E-04	5.953E-05	2.588E-05	4.087E-05	1.697E-09					3.377E-04
RA-225			1.500E-06								1.500E-06
RA-226	1.426E-04	7.718E-02	1.023E+00	6.998E-03	1.005E-01						1.208E+00
RA-228	1.000E-03		2.000E-06	1.000E-07							1.002E-03
RB-86			3.000E-05								3.000E-05
RE-188									9.300E-03		9.300E-03
RH-106	2.753E+01	9.713E+00	1.841E+01	1.348E+01	1.765E+01	1.024E+01	2.114E+01	2.446E+00	2.112E-01		1.208E+02
RN-222	1.000E-06	1.000E-03									1.001E-03
RU-103			4.395E-02				1.015E-01	1.890E-02	8.022E-02	5.600E-03	2.501E-01
RU-106	2.753E+01	9.851E+00	1.841E+01	1.348E+01	1.765E+01	1.411E+01	2.115E+01	2.369E+00	2.198E-01	4.125E-04	1.248E+02
S-35			1.202E-04	1.000E-05							1.302E-04
SB-124			3.848E-06				6.800E-04	5.400E-03	3.000E-04	5.000E-04	6.884E-03
SB-125	1.211E+01	4.274E+00	8.102E+00	8.256E+00	7.764E+00	4.844E+00	9.318E+00	1.040E+00	1.965E+00	5.329E-04	5.768E+01
SC-46			8.030E-06				2.870E-02	2.990E-02	4.050E-02	5.600E-03	1.047E-01
SE-75							1.014E-02	2.000E-02	6.300E-03	9.000E-03	4.544E-02
SN-113							3.300E-03				3.300E-03
SR-85									9.714E-05		9.714E-05
SR-89			2.680E+01				4.769E-01	9.000E-04	1.675E+00	8.015E-01	2.975E+01
SR-90	2.753E+01	9.713E+00	3.054E+01	1.600E+01	1.780E+01	1.109E+01	2.130E+01	2.749E+00	9.962E-01	8.664E+00	1.464E+02
SR-91									4.400E-03		4.400E-03
SR-92							1.600E-03				1.600E-03
TA-182		5.000E-04	1.268E-01				6.050E-03	1.600E-03			1.350E-01
TC-99			3.970E-05	1.110E-05	1.000E-06			2.104E-04	4.721E-06	3.056E-05	2.974E-04
TE-129			1.634E-02								1.634E-02
TE-132									3.000E-04		3.000E-04
TH-228		1.003E-03	1.473E-02	8.230E+00	1.000E-05					2.115E+00	1.036E+01
TH-229			2.129E-06								2.129E-06
TH-230			2.003E-05	8.788E-06						3.108E-05	5.989E-05
TH-232	3.581E-03	2.708E-03	2.048E-04	2.916E-03	1.824E-04					1.973E-05	9.612E-03

Table A-1. (continued).

Radionuclide	1984	1985	1986	1987	1988	1989	1990	1991	1992	1993	TOTAL
TH-234	1.308E-07		2.000E-06			6.400E-07	1.600E-06			3.682E-07	4.739E-06
U-232			2.090E-04	2.090E-04	2.218E+00						2.218E+00
U-233	1.360E-05	1.820E-03	4.025E-04	7.415E-04							2.977E-03
U-234	1.302E-02		2.931E-05	3.405E-04	3.630E-04		7.538E-04			1.800E-04	1.469E-02
U-235	9.435E-03	8.518E-04	5.973E-03	1.367E-02	1.767E-02	5.204E-03	1.703E-03	2.624E-04	7.916E-04	1.526E-06	5.556E-02
U-236	2.009E-04	4.167E-16									2.009E-04
U-238	2.057E-01	2.000E-01	3.266E-02	1.537E-01	7.785E-01	2.941E-01	2.369E-01	2.472E-01	6.042E-03	2.659E-03	2.157E+00
UN-ID-B+G	1.742E+01	2.501E+01	8.717E+00	7.511E+00	3.595E+00						6.225E+01
V-48	2.501E-02										2.501E-02
Y-88							3.000E-03				3.000E-03
Y-90	2.753E+01	9.713E+00	1.841E+01	1.600E+01	1.765E+01	1.024E+01	2.114E+01	2.390E+00	2.113E-01	6.300E-03	1.233E+02
Y-91M			6.582E-01								6.582E-01
Y-93									1.107E-01		1.107E-01
ZN-65	4.760E-01	3.264E-01	3.156E-05	1.948E+01	2.493E-01	3.250E-01	1.232E+00	2.167E+00	1.129E+00	4.733E-01	2.586E+01
ZR-NB-95				5.952E-01							5.952E-01
ZR-95	8.533E+00	3.283E+00	3.304E+01	4.184E+00	5.472E+00	3.185E+00	6.886E+00	8.387E-01	2.678E-01	8.787E-02	6.578E+01
TOTAL	2.400E+04	2.867E+03	1.744E+03	1.931E+03	5.256E+02	3.743E+02	3.056E+02	3.295E+02	4.362E+02	2.254E+03	3.476E+04

a. For modeling analysis, mixed activation product (MAP), mixed fission produce (MFP), and unidentified beta-gamma (UN-ID-B+G) were converted to 50% Sr-90 and 50% Cs-137.

b. These values are printed in the default format used by the RWMIS data base, which includes four significant figures.

c. The data for 1984 include data only for Pit 17.

Table A-2. Radioactivity (Ci) disposed of in soil vault rows by year (1984 to 1993) and radionuclide as reported to RWMIS.[a,b,c]

Radionuclide	1984	1985	1986	1987	1988	1989	1990	1991	1992	1993	TOTAL
AG-110M							1.686E-03				1.686E-03
AM-241							3.707E-04				3.707E-04
BA-137M								4.330E+00			4.330E+00
C-14							2.782E+00	4.789E+00	1.231E+00	1.183E+00	9.985E+00
CE-144	7.000E+00	6.149E+01	1.390E+02	9.100E+00	6.000E+00	6.000E+00	1.599E-04		5.836E+00		2.344E+02
CM-242							1.047E-11				1.047E-11
CM-244							5.068E-06				5.068E-06
CO-58		6.076E+04	2.404E+04	9.791E+04	7.580E+04	7.478E+04	2.493E+04	1.592E+04	3.215E+03	4.471E+03	3.818E+05
CO-60	1.100E+02	6.900E+04	2.537E+04	4.681E+04	1.638E+04	3.693E+05	9.888E+04	7.619E+04	9.370E+04	2.042E+04	8.162E+05
CR-51		2.574E+03	6.591E+02	4.007E+03	2.244E+03	3.027E+03	9.855E+03	5.360E+03	5.643E+02	1.712E+03	3.000E+04
CS-134	1.500E+01	3.359E+01	3.305E+01	1.362E+01	1.200E+00	1.200E+00	2.110E+01		7.672E-01		1.195E+02
CS-137	5.000E+01	1.067E+02	1.062E+02	4.928E+01	2.400E+00	2.400E+00	2.567E+03	4.841E+00	1.824E+01	4.680E-02	2.907E+03
EU-152				3.900E+00							3.900E+00
EU-154									5.850E-01		5.850E-01
EU-155									3.850E-01		3.850E-01
FE-55		2.268E+04	5.747E+03	4.743E+03	1.077E+03	1.944E+04	1.188E+04	1.318E+04	7.628E+03	7.181E+03	9.356E+04
FE-59		4.470E+02	1.190E+02	6.141E+02	3.380E+02	5.260E+02	6.371E+02	2.978E+02	2.280E+02	1.073E+02	3.314E+03
GD-153				1.300E+00							1.300E+00
H-3							9.549E-01	1.812E+01	6.902E-05	2.930E+05	2.950E+05
HF-175								2.060E+03	3.604E+02		2.421E+03
HF-181								3.240E+03	6.014E+02		3.842E+03
I-129							5.370E-04				5.370E-04
IR-192				6.500E-01							6.500E-01
MAP		2.857E+00		2.688E+03							2.691E+03
MFP		1.429E+01	1.000E+01	2.688E+03							2.712E+03
MN-54		4.315E+04	1.845E+04	7.115E+04	4.974E+04	4.850E+04	1.802E+04	8.499E+03	7.213E+03	2.080E+03	2.668E+05
NB-94								3.803E-02	1.674E-03	9.000E-07	3.970E-02
NB-95		1.157E+01					1.057E+03	1.360E+03	1.067E+03	3.944E+02	3.890E+03
NI-59						4.752E+02	2.589E+02	2.557E+02	1.717E+02	1.786E+02	1.340E+03
NI-63		6.945E+04	1.760E+04	1.453E+04	3.297E+03	7.363E+04	3.470E+04	3.406E+04	2.271E+04	2.461E+04	2.946E+05
NP-237							1.214E-07				1.214E-07
PM-147									2.390E+00		2.390E+00
PU-238							4.182E-04				4.182E-04
PU-239		3.283E-03	1.428E-02	2.736E-04	3.787E-04	4.289E-04	1.052E-03	4.419E-06	5.639E-05	3.614E-06	1.976E-02
PU-240		9.589E-04	2.265E-04	5.866E-06	4.947E-06	1.278E-04	2.573E-04	2.819E-07	1.592E-04	6.810E-08	1.741E-03

Table A-2. (continued).

Radionuclide	1984	1985	1986	1987	1988	1989	1990	1991	1992	1993	TOTAL
PU-241							1.296E-02				1.296E-02
PU-242							2.450E-08				2.450E-08
RU-103							2.384E-27				2.384E-27
RU-106							2.907E-01				2.907E-01
SB-124				1.800E-01							1.800E-01
SB-125							7.703E+02	9.904E+02	5.850E+02	4.852E+02	2.831E+03
SC-46								4.995E+01			4.995E+01
SN-113								1.997E+01	4.266E+00		2.424E+01
SN-117M								1.120E+02	7.280E+00		1.193E+02
SN-119M							2.815E+03	2.707E+03	1.883E+03	1.356E+03	8.761E+03
SN-121M										1.200E-02	1.200E-02
SR-85									2.919E-01		2.919E-01
SR-90		1.840E+01	5.440E+01	2.400E+00	2.400E+00	2.400E+00	6.227E+01	4.250E-02	1.310E-02	3.472E-03	1.423E+02
TA-182		2.080E+02	9.784E+02	2.680E+02	3.383E+02	3.000E-01		1.598E+04	2.059E+03		1.983E+04
TC-99							5.916E-03	5.486E-04	3.750E-04	4.135E-04	7.253E-03
TE-125M								1.000E+00	4.069E+01		4.169E+01
U-234							2.256E-05				2.256E-05
U-235	1.070E-04	1.010E-04	1.135E-04	5.560E-05	5.334E-07		3.487E-06		1.045E-10		3.811E-04
U-236							1.096E-06				1.096E-06
U-238		1.212E-03	1.019E-03	1.155E-01	5.259E-03		8.288E-06		9.020E-12		1.230E-01
UN-ID-B+G	1.290E+01	1.936E+01	4.350E+00	5.900E+00							4.251E+01
W-185								4.676E+03	7.930E+02		5.469E+03
W-187								9.152E+02			9.152E+02
Y-90								4.250E-02			4.250E-02
Y-91M							9.324E-22				9.324E-22
ZN-65								7.612E+02	1.621E+02	8.200E+01	1.005E+03
ZR-95	5.000E+00	2.826E+01	2.452E+01	1.400E+01			7.753E+02	5.706E+02	4.946E+02	2.134E+02	2.126E+03
TOTAL	1.999E+02	2.686E+05	9.334E+04	2.455E+05	1.492E+05	5.897E+05	2.072E+05	1.872E+05	1.435E+05	3.933E+05	2.278E+06

a. For modeling analysis, MAP, MFP, and UN-ID-B+G were converted to 50% Sr-90 and 50% Cs-137.

b. These values are printed in the default format used by the RWMIS data base, which includes four significant figures.

c. The data for 1984 does not include data for Soil Vault Row 13.

in a radiological performance assessment. Past operations may also not be representative of future operations, especially when considering the changing role of DOE and the changing mission of the INEL.

To address this uncertainty in projecting future LLW inventories, a combination of the two methods was used to forecast inventory to be disposed of from 1994 through 2020. First, an annual disposal rate based on the past 5 years of historical data was calculated. Second, an annual disposal rate based on 3 years of generator forecast data was calculated. The annual disposal rate calculated from 5 years of historical data was weighted by 5/8, and the annual disposal rate calculated from 3 years of generator forecast data was weighted by 3/8. These two quantities were then added to arrive at an 8-year weighted average annual disposal rate.

$$8\ \textit{year weighted average} = \frac{5}{8}\left[5\ \textit{year historical average}\right] + \frac{3}{8}\left[3\ \text{year generator average}\right] \quad \text{(A-1)}$$

Five years (1989 to 1993, inclusive) was chosen for the historical data average because radionuclide reporting requirements are more comprehensive for this time period than for earlier time periods. In addition, the past 5 years of data should more accurately reflect future operations than data collected 10 or 15 years ago. Three years (1994 to 1996, inclusive) was chosen for generator forecast data because waste generators are able to forecast 1 to 3 years with reasonable accuracy. Table A-3 contains the 8-year weighted average forecast data for pits and soil vault rows.

A-1.2 Decay and Ingrowth of Inventory

The ORIGEN2 computer code was used to decay and ingrow the inventory in Tables A-1 and A-2 and forecast data contained in Table A-3. The decay and ingrowth was done on a time dependent basis. For example, the inventory for pits in 1984 was decayed and ingrown for 1 year and added to the inventory disposed of in 1985. This sum was decayed and ingrown for 1 year and then added to the inventory disposed of in 1986. This process was continued until

Table A-3. Annual projection from 8-year weighted average forecast data (Ci) for pits and soil vault rows.[a]

Radionuclide	Pits	Soil vault rows
H 3	6.100E+00	2.390E+00
C 14	3.968E-03	2.293E+00
NA 22	1.824E-02	0.000E+00
NA 24	6.494E-02	0.000E+00
K 40	2.156E-02	4.021E-02
SC 46	1.239E-02	8.313E+01
CR 51	5.435E+01	8.317E+03
CA 45	1.269E-04	0.000E+00
MN 54	7.973E+01	6.818E+04
FE 55	1.107E+01	4.097E+04
FE 59	2.890E-03	2.160E+03
CO 58	2.766E+00	4.746E+04
MN 56	1.632E-01	0.000E+00
CO 60	2.663E+01	2.386E+05
NI 59	0.000E+00	2.933E+02
NI 63	9.631E-01	4.460E+04
ZN 65	6.391E-01	3.984E+02
SE 75	4.555E-03	2.101E-03
SR 85	1.214E-05	3.649E-02
SR 90	4.638E+01	8.497E+00
Y 90	3.131E+01	3.445E-02
BR 82	1.250E-04	0.000E+00
ZR 95	2.083E+00	6.101E+02
NB 94	8.625E-07	4.963E-03
SR 89	2.694E-01	0.000E+00
NB 95	2.096E+00	1.257E+03
TC 99	7.125E-05	4.145E-02
SR 91	5.500E-04	0.000E+00
RU 103	2.512E-02	4.205E-02
RU 106	4.210E+04	4.128E-01
Y 93	1.384E-02	0.000E+00
RH 106	6.621E+00	2.179E-01
AG 110M	4.876E-03	1.543E+00
SN 113	8.324E-03	1.852E+01
SN 117M	4.280E-03	1.491E+01
MO 99	4.938E-04	0.000E+00

Table A-3. (continued).

Radionuclide	Pits	Soil vault rows
SN 119M	0.000E+00	2.505E+03
SB 124	1.205E-03	4.021E-02
SB 125	3.363E+00	8.699E+02
TE 125M	0.000E+00	2.070E+01
I 129	2.855E-03	6.713E-05
AG 110	2.973E-03	0.000E+00
CS 134	2.922E+00	3.190E+00
CS 137	1.101E+02	3.250E+02
CD 109	1.365E-03	0.000E+00
IN 113M	6.710E-03	0.000E+00
BA 140	0.000E+00	4.620E-02
LA 140	1.653E-01	5.995E-02
CE 141	1.930E-01	6.496E-02
CE 144	1.647E+01	2.362E+00
PR 144	1.359E+01	9.857E-02
PM 147	0.000E+00	2.988E-01
I 131	1.088E-02	0.000E+00
I 132	1.260E-01	0.000E+00
EU 154	3.070E-01	7.312E-02
EU 155	3.392E-01	4.812E-02
HF 175	5.175E-03	3.026E+02
HF 181	2.042E-01	4.803E+02
BA 137M	5.234E-01	1.104E+00
TA 182	9.562E-04	2.298E+03
BA 140	1.292E-01	0.000E+00
W 185	0.000E+00	6.836E+02
W 187	0.000E+00	1.144E+02
CE 139	3.750E-05	0.000E+00
HG 203	4.350E-05	4.021E-02
TH 234	3.653E-05	1.515E-02
PA 234M	3.625E-05	1.515E-02
U 234	4.747E-04	1.923E-02
U 235	3.474E-03	5.025E-07
U 236	0.000E+00	1.370E-07
U 238	1.960E-01	1.581E-02
EU 152	4.920E-03	0.000E+00

Table A-3. (continued).

Radionuclide	Pits	Soil vault rows
NP 237	2.211E-03	1.513E-08
PU 238	8.779E-05	1.462E-02
PU 239	1.[illegible]E-02	2.400E-04
PU 240	4.656E-04	6.870E-05
PU 241	2.675E-03	1.620E-03
PU 242	6.189E-06	3.125E-09
RE 188	1.163E-03	0.000E+00
IR 192	1.394E-03	0.000E+00
AU 198	1.958E-03	0.000E+00
AM 241	1.025E-02	2.236E-04
RA 226	1.257E-02	0.000E+00
CM 244	2.816E-04	6.335E-07
TH 228	1.250E-06	0.000E+00
TH 232	2.279E-05	0.000E+00
U 232	2.772E-01	0.000E+00
AM 243	2.550E-05	0.000E+00
CM 242	1.225E-08	0.000E+00
SR 92	2.000E-04	0.000E+00
TE 132	4.695E-04	0.000E+00
I 133	1.875E-04	0.000E+00
TOTAL	4.252E+04	5.219E+05

a. These values are printed in the default format used by the RWMIS data base, which includes four significant figures.

the year 2020, using actual data for 1984 through 1993 and forecast data for 1994 through 2020. After 2020, there were no more inventory additions because the SDA was assumed to be closed. The inventory in 2020 was decayed and ingrown for 10,000 years after SDA disposal ends, the year 12,020. Tables A-4 and A-5 contain the results of these calculations at various points in time.

Abbott (1992) contains a detailed explanation of the derivation and format of the ORIGEN2 input files. Maheras (1993) contains the detailed ORIGEN2 batch files, input data, input code, and output for the decay and ingrowth of the pit and soil vault inventory.

Table A-4. Decay and ingrown inventory (Ci) for 10,000 years after disposal for pits.[a]

Radio-nuclide	1993	2020	2120	2220	2320	2520	3020	5020	7020	12020
H 3	2.534E+03	6.391E+02	2.333E+00	8.508E-03	3.103E-05	4.134E-10	2.678E-22	0.000E+00	0.000E+00	0.000E+00
C 14	6.447E-02	1.712E-01	1.692E-01	1.671E-01	1.651E-01	1.612E-01	1.517E-01	1.191E-01	9.350E-02	5.106E-02
NA 22	2.417E-02	5.973E-02	1.609E-13	4.335E-25	1.168E-36	0.000E+00	0.000E+00	0.000E+00	0.000E+00	0.000E+00
S 35	3.009E-14	8.578E-20	0.000E+00	0.000E+00	0.000E+00	0.000E+00	0.000E+00	0.000E+00	0.000E+00	0.000E+00
K 40	1.691E-01	7.513E-01	7.513E-01	7.513E-01	7.513E-01	7.513E-01	7.513E-01	7.513E-01	7.513E-01	7.512E-01
CA 45	9.084E-08	3.404E-05	0.000E+00	0.000E+00	0.000E+00	0.000E+00	0.000E+00	0.000E+00	0.000E+00	0.000E+00
SC 46	3.728E-04	6.348E-04	0.000E+00	0.000E+00	0.000E+00	0.000E+00	0.000E+00	0.000E+00	0.000E+00	0.000E+00
CR 51	4.932E-03	5.849E-03	0.000E+00	0.000E+00	0.000E+00	0.000E+00	0.000E+00	0.000E+00	0.000E+00	0.000E+00
MN 54	8.083E-01	6.388E+01	4.178E-34	0.000E+00	0.000E+00	0.000E+00	0.000E+00	0.000E+00	0.000E+00	0.000E+00
FE 55	3.440E+02	3.646E+01	9.634E-11	2.545E-22	6.724E-34	0.000E+00	0.000E+00	0.000E+00	0.000E+00	0.000E+00
FE 59	2.501E-07	1.045E-05	0.000E+00	0.000E+00	0.000E+00	0.000E+00	0.000E+00	0.000E+00	0.000E+00	0.000E+00
CO 58	2.998E-02	7.955E-02	0.000E+00	0.000E+00	0.000E+00	0.000E+00	0.000E+00	0.000E+00	0.000E+00	0.000E+00
CO 60	2.271E+03	2.492E+02	4.801E-04	9.310E-10	1.805E-15	6.786E-27	0.000E+00	0.000E+00	0.000E+00	0.000E+00
NI 63	1.075E+04	8.794E+03	4.140E+03	1.949E+03	9.174E+02	2.033E+02	4.700E+00	1.343E-06	3.836E-13	1.673E-29
ZN 65	4.407E-01	3.504E-01	0.000E+00	0.000E+00	0.000E+00	0.000E+00	0.000E+00	0.000E+00	0.000E+00	0.000E+00
SE 75	1.217E-03	6.260E-04	0.000E+00	0.000E+00	0.000E+00	0.000E+00	0.000E+00	0.000E+00	0.000E+00	0.000E+00
SR 85	3.943E-08	2.496E-07	0.000E+00	0.000E+00	0.000E+00	0.000E+00	0.000E+00	0.000E+00	0.000E+00	0.000E+00
SR 89	5.402E-03	1.803E-03	0.000E+00	0.000E+00	0.000E+00	0.000E+00	0.000E+00	0.000E+00	0.000E+00	0.000E+00
SR 90	7.137E+02	1.288E+03	1.192E+02	1.103E+01	1.021E+00	8.737E-03	5.927E-08	1.255E-28	0.000E+00	0.000E+00
Y 90	7.139E+02	1.288E+03	1.192E+02	1.103E+01	1.021E+00	8.740E-03	5.928E-08	1.255E-28	0.000E+00	0.000E+00
Y 91	2.195E-09	2.105E-08	0.000E+00	0.000E+00	0.000E+00	0.000E+00	0.000E+00	0.000E+00	0.000E+00	0.000E+00
ZR 93	8.337E-11	3.648E-10	3.648E-10	3.648E-10	3.647E-10	3.647E-10	3.646E-10	3.643E-10	3.640E-10	3.631E-10
ZR 95	1.785E-03	4.061E-02	0.000E+00	0.000E+00	0.000E+00	0.000E+00	0.000E+00	0.000E+00	0.000E+00	0.000E+00
NB 93M	7.675E-12	1.869E-10	3.456E-10	3.465E-10	3.465E-10	3.465E-10	3.464E-10	3.461E-10	3.458E-10	3.450E-10
NB 94	6.899E-06	3.017E-05	3.007E-05	2.996E-05	2.986E-05	2.966E-05	2.916E-05	2.723E-05	2.543E-05	2.144E-05
NB 95	3.930E-03	8.823E-02	0.000E+00	0.000E+00	0.000E+00	0.000E+00	0.000E+00	0.000E+00	0.000E+00	0.000E+00
NB 95M	1.324E-05	3.012E-04	0.000E+00	0.000E+00	0.000E+00	0.000E+00	0.000E+00	0.000E+00	0.000E+00	0.000E+00
TC 99	2.975E-04	2.221E-03	2.220E-03	2.220E-03	2.219E-03	2.218E-03	2.214E-03	2.200E-03	2.185E-03	2.150E-03
RU103	9.098E-06	3.997E-05	0.000E+00	0.000E+00	0.000E+00	0.000E+00	0.000E+00	0.000E+00	0.000E+00	0.000E+00
RU106	2.680E+00	4.257E+04	5.793E-26	0.000E+00	0.000E+00	0.000E+00	0.000E+00	0.000E+00	0.000E+00	0.000E+00
RH106	2.680E+00	4.257E+04	5.793E-26	0.000E+00	0.000E+00	0.000E+00	0.000E+00	0.000E+00	0.000E+00	0.000E+00
AG108	8.570E-05	7.396E-05	4.285E-05	2.483E-05	1.439E-05	4.829E-06	3.153E-07	5.734E-12	1.042E-16	1.469E-28
AG108M	9.629E-04	8.310E-04	4.815E-04	2.790E-04	1.616E-04	5.426E-05	3.543E-06	6.441E-11	1.171E-15	1.650E-27
AG109M	2.146E-03	1.881E-03	3.785E-27	0.000E+00	0.000E+00	0.000E+00	0.000E+00	0.000E+00	0.000E+00	0.000E+00

Table A-4. (continued).

Radio-nuclide	1993	2020	2120	2220	2320	2520	3020	5020	7020	12020
AG110	2.152E-05	3.697E-05	0.000E+00	0.000E+00	0.000E+00	0.000E+00	0.000E+00	0.000E+00	0.000E+00	0.000E+00
AG110M	1.618E-03	2.779E-03	0.000E+00	0.000E+00	0.000E+00	0.000E+00	0.000E+00	0.000E+00	0.000E+00	0.000E+00
CD109	2.146E-03	1.881E-03	3.785E-27	0.000E+00	0.000E+00	0.000E+00	0.000E+00	0.000E+00	0.000E+00	0.000E+00
IN113M	4.987E-07	1.038E-03	0.000E+00	0.000E+00	0.000E+00	0.000E+00	0.000E+00	0.000E+00	0.000E+00	0.000E+00
SN113	4.984E-07	1.038E-03	0.000E+00	0.000E+00	0.000E+00	0.000E+00	0.000E+00	0.000E+00	0.000E+00	0.000E+00
SN117M	0.000E+00	6.032E-11	0.000E+00	0.000E+00	0.000E+00	0.000E+00	0.000E+00	0.000E+00	0.000E+00	0.000E+00
SB124	7.540E-06	1.824E-05	0.000E+00	0.000E+00	0.000E+00	0.000E+00	0.000E+00	0.000E+00	0.000E+00	0.000E+00
SB125	1.219E+01	1.183E+01	1.603E-10	2.171E-21	2.942E-32	0.000E+00	0.000E+00	0.000E+00	0.000E+00	0.000E+00
TE125M	2.974E+00	2.875E+00	3.910E-11	5.298E-22	7.179E-33	0.000E+00	0.000E+00	0.000E+00	0.000E+00	0.000E+00
I129	1.405E-07	7.709E-02	7.709E-02	7.709E-02	7.709E-02	7.709E-02	7.708E-02	7.708E-02	7.707E-02	7.705E-02
XE131M	8.473E-14	1.448E-13	0.000E+00	0.000E+00	0.000E+00	0.000E+00	0.000E+00	0.000E+00	0.000E+00	0.000E+00
CS134	7.549E+00	7.313E+00	1.840E-14	4.628E-29	0.000E+00	0.000E+00	0.000E+00	0.000E+00	0.000E+00	0.000E+00
CS137	1.461E+03	2.968E+03	2.945E+02	2.921E+01	2.898E+00	2.852E-02	2.741E-07	2.337E-27	0.000E+00	0.000E+00
BA133	5.594E-07	9.792E-08	1.541E-10	2.424E-13	3.804E-16	9.420E-22	9.087E-36	0.000E+00	0.000E+00	0.000E+00
BA137M	1.382E+03	2.808E+03	2.786E+02	2.763E+01	2.741E+00	2.698E-02	2.593E-07	2.210E-27	0.000E+00	0.000E+00
BA140	9.106E-12	3.265E-10	0.000E+00	0.000E+00	0.000E+00	0.000E+00	0.000E+00	0.000E+00	0.000E+00	0.000E+00
LA140	1.048E-11	3.757E-10	0.000E+00	0.000E+00	0.000E+00	0.000E+00	0.000E+00	0.000E+00	0.000E+00	0.000E+00
CE139	7.571E-06	7.083E-06	0.000E+00	0.000E+00	0.000E+00	0.000E+00	0.000E+00	0.000E+00	0.000E+00	0.000E+00
CE141	1.481E-05	8.014E-05	0.000E+00	0.000E+00	0.000E+00	0.000E+00	0.000E+00	0.000E+00	0.000E+00	0.000E+00
CE144	2.989E+00	1.146E+01	2.383E-38	0.000E+00	0.000E+00	0.000E+00	0.000E+00	0.000E+00	0.000E+00	0.000E+00
PR144	2.953E+00	1.133E+01	0.000E+00	0.000E+00	0.000E+00	0.000E+00	0.000E+00	0.000E+00	0.000E+00	0.000E+00
ND144	1.028E-13	2.626E-13	2.668E-13	2.668E-13	2.668E-13	2.668E-13	2.668E-13	2.668E-13	2.668E-13	2.668E-13
PM147	4.273E-04	3.408E-07	1.143E-18	3.832E-30	0.000E+00	0.000E+00	0.000E+00	0.000E+00	0.000E+00	0.000E+00
SM147	1.366E-13	1.471E-13	1.471E-13	1.471E-13	1.471E-13	1.471E-13	1.471E-13	1.471E-13	1.471E-13	1.471E-13
EU152	4.633E+00	1.241E+00	7.590E-03	4.644E-05	2.841E-07	1.063E-11	9.117E-23	0.000E+00	0.000E+00	0.000E+00
EU154	3.154E+00	3.601E+00	1.138E-03	3.596E-07	1.136E-10	1.135E-17	3.577E-35	0.000E+00	0.000E+00	0.000E+00
EU155	7.348E-01	2.226E+00	1.894E-06	1.612E-12	1.371E-18	9.926E-31	0.000E+00	0.000E+00	0.000E+00	0.000E+00
GD152	6.960E-14	1.933E-13	2.366E-13	2.368E-13	2.368E-13	2.368E-13	2.368E-13	2.368E-13	2.368E-13	2.368E-13
HF175	1.154E-06	1.429E-04	0.000E+00	0.000E+00	0.000E+00	0.000E+00	0.000E+00	0.000E+00	0.000E+00	0.000E+00
HF181	9.477E-05	5.220E-04	0.000E+00	0.000E+00	0.000E+00	0.000E+00	0.000E+00	0.000E+00	0.000E+00	0.000E+00
TA182	3.076E-06	1.189E-04	0.000E+00	0.000E+00	0.000E+00	0.000E+00	0.000E+00	0.000E+00	0.000E+00	0.000E+00
IR192	6.298E-05	4.712E-05	0.000E+00	0.000E+00	0.000E+00	0.000E+00	0.000E+00	0.000E+00	0.000E+00	0.000E+00
HG203	0.000E+00	1.906E-07	0.000E+00	0.000E+00	0.000E+00	0.000E+00	0.000E+00	0.000E+00	0.000E+00	0.000E+00
TL207	1.306E-01	5.804E-02	7.190E-03	5.377E-03	5.593E-03	6.194E-03	7.794E-03	1.364E-02	1.925E-02	3.227E-02

Table A-4. (continued).

Radio-nuclide	1993	2020	2120	2220	2320	2520	3020	5020	7020	12020
TL208	1.452E+00	2.798E+00	1.156E+00	4.435E-01	1.716E-01	2.816E-02	3.873E-03	3.675E-03	3.675E-03	3.675E-03
TL209	9.684E-08	2.606E-07	8.659E-07	1.471E-06	2.075E-06	3.283E-06	6.293E-06	1.822E-05	2.996E-05	5.865E-05
PB209	4.483E-06	1.206E-05	4.009E-05	6.809E-05	9.608E-05	1.520E-04	2.913E-04	8.433E-04	1.387E-03	2.715E-03
PB210	2.615E-01	9.043E-01	1.453E+00	1.418E+00	1.359E+00	1.246E+00	9.899E-01	4.168E-01	1.768E-01	2.787E-02
PB211	1.310E-01	5.821E-02	7.210E-03	5.392E-03	5.608E-03	6.211E-03	7.815E-03	1.368E-02	1.930E-02	3.236E-02
PB212	4.040E+00	7.788E+00	3.216E+00	1.234E+00	4.777E-01	7.838E-02	1.078E-02	1.023E-02	1.023E-02	1.023E-02
PB214	1.204E+00	1.527E+00	1.462E+00	1.400E+00	1.341E+00	1.229E+00	9.901E-01	4.169E-01	1.768E-01	2.788E-02
BI210	2.617E-01	9.049E-01	1.454E+00	1.418E+00	1.359E+00	1.246E+00	9.899E-01	4.168E-01	1.768E-01	2.787E-02
BI211	1.310E-01	5.821E-02	7.210E-03	5.392E-03	5.608E-03	6.211E-03	7.815E-03	1.368E-02	1.930E-02	3.236E-02
BI212	4.040E+00	7.788E+00	3.216E+00	1.234E+00	4.777E-01	7.838E-02	1.078E-02	1.023E-02	1.023E-02	1.023E-02
BI213	4.483E-06	1.206E-05	4.009E-05	6.809E-05	9.608E-05	1.520E-04	2.913E-04	8.433E-04	1.387E-03	2.715E-03
BI214	1.204E+00	1.527E+00	1.462E+00	1.400E+00	1.341E+00	1.229E+00	9.901E-01	4.169E-01	1.768E-01	2.788E-02
PO210	2.418E-01	8.811E-01	1.454E+00	1.418E+00	1.359E+00	1.246E+00	9.899E-01	4.168E-01	1.768E-01	2.787E-02
PO211	3.668E-04	1.630E-04	2.019E-05	1.510E-05	1.570E-05	1.739E-05	2.188E-05	3.831E-05	5.405E-05	9.062E-05
PO212	2.589E+00	4.990E+00	2.061E+00	7.909E-01	3.061E-01	5.022E-02	6.907E-03	6.553E-03	6.553E-03	6.553E-03
PO213	4.386E-06	1.180E-05	3.922E-05	6.662E-05	9.400E-05	1.487E-04	2.850E-04	8.251E-04	1.357E-03	2.656E-03
PO214	1.203E+00	1.526E+00	1.462E+00	1.400E+00	1.340E+00	1.229E+00	9.899E-01	4.168E-01	1.768E-01	2.787E-02
PO215	1.310E-01	5.821E-02	7.210E-03	5.392E-03	5.608E-03	6.211E-03	7.815E-03	1.368E-02	1.930E-02	3.236E-02
PO216	4.040E+00	7.788E+00	3.216E+00	1.234E+00	4.777E-01	7.838E-02	1.078E-02	1.023E-02	1.023E-02	1.023E-02
PO218	1.204E+00	1.527E+00	1.462E+00	1.400E+00	1.341E+00	1.230E+00	9.903E-01	4.169E-01	1.769E-01	2.788E-02
AT217	4.483E-06	1.206E-05	4.009E-05	6.809E-05	9.608E-05	1.520E-04	2.913E-04	8.433E-04	1.387E-03	2.715E-03
RN219	1.310E-01	5.821E-02	7.210E-03	5.392E-03	5.608E-03	6.211E-03	7.815E-03	1.368E-02	1.930E-02	3.236E-02
RN220	4.040E+00	7.788E+00	3.216E+00	1.234E+00	4.777E-01	7.838E-02	1.078E-02	1.023E-02	1.023E-02	1.023E-02
RN222	1.204E+00	1.527E+00	1.462E+00	1.400E+00	1.341E+00	1.230E+00	9.903E-01	4.169E-01	1.769E-01	2.788E-02
FR221	4.483E-06	1.206E-05	4.009E-05	6.809E-05	9.608E-05	1.520E-04	2.913E-04	8.433E-04	1.387E-03	2.715E-03
FR223	1.800E-03	8.001E-04	9.940E-05	7.440E-05	7.739E-05	8.571E-05	1.079E-04	1.888E-04	2.664E-04	4.466E-04
RA223	1.310E-01	5.821E-02	7.210E-03	5.392E-03	5.608E-03	6.211E-03	7.815E-03	1.368E-02	1.930E-02	3.236E-02
RA224	4.040E+00	7.788E+00	3.216E+00	1.234E+00	4.777E-01	7.838E-02	1.078E-02	1.023E-02	1.023E-02	1.023E-02
RA225	4.481E-06	1.206E-05	4.009E-05	6.809E-05	9.608E-05	1.520E-04	2.913E-04	8.433E-04	1.387E-03	2.715E-03
RA226	1.204E+00	1.527E+00	1.462E+00	1.400E+00	1.341E+00	1.230E+00	9.902E-01	4.169E-01	1.769E-01	2.788E-02
RA228	6.009E-03	9.810E-03	1.023E-02	1.023E-02	1.023E-02	1.023E-02	1.023E-02	1.023E-02	1.023E-02	1.023E-02
AC225	4.483E-06	1.206E-05	4.009E-05	6.809E-05	9.608E-05	1.520E-04	2.913E-04	8.433E-04	1.387E-03	2.715E-03
AC227	1.305E-01	5.798E-02	7.203E-03	5.391E-03	5.608E-03	6.211E-03	7.815E-03	1.368E-02	1.930E-02	3.236E-02
AC228	6.010E-03	9.811E-03	1.023E-02	1.023E-02	1.023E-02	1.023E-02	1.023E-02	1.023E-02	1.023E-02	1.023E-02

Table A-4. (continued).

Radio-nuclide	1993	2020	2120	2220	2320	2520	3020	5020	7020	12020
TH227	1.290E-01	5.730E-02	7.111E-03	5.317E-03	5.531E-03	6.125E-03	7.708E-03	1.349E-02	1.904E-02	3.192E-02
TH228	4.021E+00	7.754E+00	3.216E+00	1.234E+00	4.777E-01	7.838E-02	1.078E-02	1.023E-02	1.023E-02	1.023E-02
TH229	4.481E-06	1.206E-05	4.009E-05	6.809E-05	9.608E-05	1.520E-04	2.913E-04	8.433E-04	1.387E-03	2.715E-03
TH230	6.114E-05	6.636E-05	9.236E-05	1.202E-04	1.500E-04	2.151E-04	4.103E-04	1.651E-03	3.613E-03	1.157E-02
TH231	5.556E-02	1.494E-01	1.494E-01	1.494E-01	1.494E-01	1.494E-01	1.494E-01	1.494E-01	1.494E-01	1.494E-01
TH232	9.612E-03	1.023E-02	1.023E-02	1.023E-02	1.023E-02	1.023E-02	1.023E-02	1.023E-02	1.023E-02	1.023E-02
TH234	2.157E+00	7.449E+00	7.449E+00	7.449E+00	7.449E+00	7.449E+00	7.449E+00	7.449E+00	7.449E+00	7.449E+00
PA231	4.727E-03	4.785E-03	5.090E-03	5.395E-03	5.700E-03	6.306E-03	7.811E-03	1.368E-02	1.930E-02	3.235E-02
PA233	1.710E-03	6.141E-02	6.143E-02	6.144E-02	6.146E-02	6.147E-02	6.150E-02	6.148E-02	6.144E-02	6.134E-02
PA234M	2.157E+00	7.449E+00	7.449E+00	7.449E+00	7.449E+00	7.449E+00	7.449E+00	7.449E+00	7.449E+00	7.449E+00
PA234	2.805E-03	9.684E-03	9.684E-03	9.684E-03	9.684E-03	9.684E-03	9.684E-03	9.684E-03	9.684E-03	9.684E-03
U232	2.094E+00	8.174E+00	3.121E+00	1.192E+00	4.550E-01	6.634E-02	5.385E-04	2.337E-12	1.014E-20	1.392E-41
U233	2.978E-03	2.981E-03	3.007E-03	3.032E-03	3.058E-03	3.109E-03	3.236E-03	3.744E-03	4.246E-03	5.482E-03
U234	1.472E-02	2.791E-02	3.002E-02	3.212E-02	3.423E-02	3.843E-02	4.893E-02	9.077E-02	1.324E-01	2.354E-01
U235	5.556E-02	1.494E-01	1.494E-01	1.494E-01	1.494E-01	1.494E-01	1.494E-01	1.494E-01	1.494E-01	1.494E-01
U236	2.009E-04	2.009E-04	2.011E-04	2.012E-04	2.013E-04	2.016E-04	2.022E-04	2.044E-04	2.062E-04	2.093E-04
U237	1.546E-06	1.389E-06	1.133E-08	1.788E-10	1.171E-10	1.624E-10	2.101E-10	2.071E-10	1.765E-10	1.174E-10
U238	2.157E+00	7.449E+00	7.449E+00	7.449E+00	7.449E+00	7.449E+00	7.449E+00	7.449E+00	7.449E+00	7.449E+00
U240	1.450E-16	8.469E-16	3.482E-15	6.116E-15	8.750E-15	1.402E-14	2.717E-14	7.966E-14	1.319E-13	2.617E-13
NP237	1.710E-03	6.141E-02	6.143E-02	6.144E-02	6.146E-02	6.147E-02	6.150E-02	6.148E-02	6.144E-02	6.134E-02
NP239	1.743E-03	2.426E-03	2.404E-03	2.381E-03	2.359E-03	2.315E-03	2.209E-03	1.831E-03	1.517E-03	9.486E-04
NP240M	1.450E-16	8.469E-16	3.482E-15	6.116E-15	8.750E-15	1.402E-14	2.717E-14	7.966E-14	1.319E-13	2.617E-13
PU236	5.321E-07	7.500E-10	2.071E-20	5.720E-31	0.000E+00	0.000E+00	0.000E+00	0.000E+00	0.000E+00	0.000E+00
PU238	1.736E-02	1.615E-02	7.332E-03	3.328E-03	1.510E-03	3.111E-04	5.992E-06	8.242E-13	1.134E-19	7.956E-37
PU239	2.655E-01	5.443E-01	5.428E-01	5.412E-01	5.397E-01	5.366E-01	5.289E-01	4.994E-01	4.716E-01	4.085E-01
PU240	3.357E-02	4.604E-02	4.557E-02	4.509E-02	4.461E-02	4.367E-02	4.142E-02	3.350E-02	2.710E-02	1.595E-02
PU241	6.302E-02	5.664E-02	4.618E-04	7.292E-06	4.778E-06	6.630E-06	8.577E-06	8.452E-06	7.202E-06	4.791E-06
PU242	3.377E-04	5.048E-04	5.047E-04	5.046E-04	5.045E-04	5.043E-04	5.039E-04	5.020E-04	5.003E-04	4.958E-04
PU244	1.452E-16	8.480E-16	3.486E-15	6.124E-15	8.761E-15	1.403E-14	2.721E-14	7.976E-14	1.321E-13	2.620E-13
AM241	3.901E-01	6.468E-01	5.526E-01	4.707E-01	4.010E-01	2.909E-01	1.305E-01	5.289E-03	2.212E-04	4.864E-06
AM243	1.743E-03	2.426E-03	2.404E-03	2.381E-03	2.359E-03	2.315E-03	2.209E-03	1.831E-03	1.517E-03	9.486E-04
AM245	1.994E-10	1.055E-19	0.000E+00	0.000E+00	0.000E+00	0.000E+00	0.000E+00	0.000E+00	0.000E+00	0.000E+00
CM242	3.681E-10	3.295E-09	0.000E+00	0.000E+00	0.000E+00	0.000E+00	0.000E+00	0.000E+00	0.000E+00	0.000E+00
CM243	4.116E-07	2.134E-07	1.875E-08	1.647E-09	1.447E-10	1.117E-12	5.847E-18	4.379E-39	0.000E+00	0.000E+00

Table A-4. (continued).

Radio-nuclide	1993	2020	2120	2220	2320	2520	3020	5020	7020	12020
CM244	1.880E-03	5.318E-03	1.157E-04	2.519E-06	5.483E-08	2.597E-11	1.268E-19	0.000E+00	0.000E+00	0.000E+00
CM245	1.787E-07	7.090E-07	2.434E-06	3.834E-06	4.969E-06	6.621E-06	8.567E-06	8.438E-06	7.190E-06	4.783E-06
CM246	1.030E-07	2.598E-07	2.931E-07	2.891E-07	2.849E-07	2.766E-07	2.571E-07	1.918E-07	1.431E-07	6.878E-08
CM248	3.101E-09	3.428E-09	3.427E-09	3.426E-09	3.426E-09	3.424E-09	3.421E-09	3.407E-09	3.393E-09	3.358E-09
BK249	1.375E-05	7.275E-15	0.000E+00	0.000E+00	0.000E+00	0.000E+00	0.000E+00	0.000E+00	0.000E+00	0.000E+00
CF249	2.477E-04	2.349E-04	1.927E-04	1.581E-04	1.298E-04	8.737E-05	3.250E-05	6.223E-07	1.192E-08	6.047E-13
CF250	7.068E-05	1.690E-05	8.446E-08	4.219E-10	2.108E-12	5.263E-17	1.639E-28	0.000E+00	0.000E+00	0.000E+00
CF252	4.343E-05	3.604E-08	1.398E-19	5.426E-31	0.000E+00	0.000E+00	0.000E+00	0.000E+00	0.000E+00	0.000E+00
Y 91	4.589E-19	6.174E-20	0.000E+00	0.000E+00	0.000E+00	0.000E+00	0.000E+00	0.000E+00	0.000E+00	0.000E+00
TE132	0.000E+00	5.618E-38	0.000E+00	0.000E+00	0.000E+00	0.000E+00	0.000E+00	0.000E+00	0.000E+00	0.000E+00
XE133	0.000E+00	4.138E-26	0.000E+00	0.000E+00	0.000E+00	0.000E+00	0.000E+00	0.000E+00	0.000E+00	0.000E+00
TOTAL	2.026E+04	1.034E+05	5.017E+03	2.075E+03	9.659E+02	2.399E+02	3.831E+01	2.835E+01	2.623E+01	2.501E+01

a. These values are printed in the default format used by the ORIGEN2 computer code, which includes four significant figures.

Table A-5. Decayed and ingrown inventory (Ci) for 10,000 years after disposal for soil vault rows.[a]

Radio-nuclide	1993	2020	2120	2220	2320	2520	3020	5020	7020	12020
H 3	2.950E+05	6.424E+04	2.264E+02	7.981E-01	2.813E-02	3.495E-08	1.902E-20	0.000E+00	0.000E+00	0.000E+00
C 14	9.981E+00	7.175E+01	7.089E+01	7.004E+01	6.920E+01	6.754E+01	6.358E+01	4.991E+01	3.919E+01	2.140E+01
K 40	0.000E+00	1.086E+00	1.086E+00	1.086E+00	1.086E+00	1.086E+00	1.086E+00	1.086E+00	1.086E+00	1.086E+00
SC 46	5.783E-03	4.259E+00	0.000E+00	0.000E+00	0.000E+00	0.000E+00	0.000E+00	0.000E+00	0.000E+00	0.000E+00
CR 51	1.842E-01	8.951E-01	0.000E+00	0.000E+00	0.000E+00	0.000E+00	0.000E+00	0.000E+00	0.000E+00	0.000E+00
MN 54	5.338E+03	5.462E+04	3.573E-31	0.000E+00	0.000E+00	0.000E+00	0.000E+00	0.000E+00	0.000E+00	0.000E+00
FE 55	2.881E+04	1.340E+05	3.541E-07	9.355E-19	2.471E-30	0.000E+00	0.000E+00	0.000E+00	0.000E+00	0.000E+00
FE 59	3.896E-01	7.810E+00	0.000E+00	0.000E+00	0.000E+00	0.000E+00	0.000E+00	0.000E+00	0.000E+00	0.000E+00
CO 58	1.279E+02	1.365E+03	0.000E+00	0.000E+00	0.000E+00	0.000E+00	0.000E+00	0.000E+00	0.000E+00	0.000E+00
CO 60	4.471E+05	1.661E+06	3.210E+00	6.223E-06	1.207E-11	4.536E-23	0.000E+00	0.000E+00	0.000E+00	0.000E+00
NI 59	1.340E+03	9.258E+03	9.250E+03	9.242E+03	9.234E+03	9.218E+03	9.178E+03	9.020E+03	8.865E+03	8.490E+03
NI 63	2.831E+05	1.316E+06	6.197E+05	2.917E+05	1.373E+05	3.043E+04	7.036E+02	2.010E-04	5.742E-11	2.505E-27
ZN 65	8.316E+01	2.184E+02	0.000E+00	0.000E+00	0.000E+00	0.000E+00	0.000E+00	0.000E+00	0.000E+00	0.000E+00
SE 75	0.000E+00	2.887E-04	0.000E+00	0.000E+00	0.000E+00	0.000E+00	0.000E+00	0.000E+00	0.000E+00	0.000E+00
SR 85	1.185E-04	7.503E-04	0.000E+00	0.000E+00	0.000E+00	0.000E+00	0.000E+00	0.000E+00	0.000E+00	0.000E+00
SR 90	2.426E+03	1.443E+03	1.336E+02	1.236E+01	1.143E+00	9.790E-03	6.641E-08	1.406E-28	0.000E+00	0.000E+00
Y 90	2.427E+03	1.444E+03	1.336E+02	1.236E+01	1.144E+00	9.793E-03	6.643E-08	1.407E-28	0.000E+00	0.000E+00
ZR 95	4.265E+00	1.189E+01	0.000E+00	0.000E+00	0.000E+00	0.000E+00	0.000E+00	0.000E+00	0.000E+00	0.000E+00
NB 94	3.970E-02	1.736E-01	1.730E-01	1.724E-01	1.718E-01	1.707E-01	1.678E-01	1.567E-01	1.464E-01	1.234E-01
NB 95	9.407E+00	2.632E+01	0.000E+00	0.000E+00	0.000E+00	0.000E+00	0.000E+00	0.000E+00	0.000E+00	0.000E+00
NB 95M	3.164E-02	3.823E-02	0.000E+00	0.000E+00	0.000E+00	0.000E+00	0.000E+00	0.000E+00	0.000E+00	0.000E+00
TC 99	7.253E-03	1.126E+00	1.126E+00	1.126E+00	1.125E+00	1.125E+00	1.123E+00	1.115E+00	1.108E+00	1.090E+00
RU103	0.000E+00	6.690E-05	0.000E+00	0.000E+00	0.000E+00	0.000E+00	0.000E+00	0.000E+00	0.000E+00	0.000E+00
RU106	1.857E-02	4.174E-01	5.704E-31	0.000E+00	0.000E+00	0.000E+00	0.000E+00	0.000E+00	0.000E+00	0.000E+00
RH106	1.857E-02	4.174E-01	5.702E-31	0.000E+00	0.000E+00	0.000E+00	0.000E+00	0.000E+00	0.000E+00	0.000E+00
AG110	3.897E-07	1.170E-02	0.000E+00	0.000E+00	0.000E+00	0.000E+00	0.000E+00	0.000E+00	0.000E+00	0.000E+00
AG110M	2.930E-05	8.796E-01	0.000E+00	0.000E+00	0.000E+00	0.000E+00	0.000E+00	0.000E+00	0.000E+00	0.000E+00
IN113M	7.968E-02	2.310E+00	0.000E+00	0.000E+00	0.000E+00	0.000E+00	0.000E+00	0.000E+00	0.000E+00	0.000E+00
SN113	7.963E-02	2.309E+00	0.000E+00	0.000E+00	0.000E+00	0.000E+00	0.000E+00	0.000E+00	0.000E+00	0.000E+00
SN117M	1.445E-15	2.101E-07	0.000E+00	0.000E+00	0.000E+00	0.000E+00	0.000E+00	0.000E+00	0.000E+00	0.000E+00
SN119M	8.881E+02	1.384E+03	0.000E+00	0.000E+00	0.000E+00	0.000E+00	0.000E+00	0.000E+00	0.000E+00	0.000E+00
SN121M	1.183E-02	8.138E-03	2.033E-03	5.078E-04	1.269E-04	7.916E-06	7.701E-09	6.897E-21	6.176E-33	0.000E+00
SB124	2.948E-14	6.086E-04	0.000E+00	0.000E+00	0.000E+00	0.000E+00	0.000E+00	0.000E+00	0.000E+00	0.000E+00
SB125	1.483E+03	3.058E+03	4.143E-08	5.613E-19	7.606E-30	0.000E+00	0.000E+00	0.000E+00	0.000E+00	0.000E+00

Table A-5. (continued).

Radio-nuclide	1993	2020	2120	2220	2320	2520	3020	5020	7020	12020
TE125M	3.603E+02	7.435E+02	1.011E-08	1.370E-19	1.856E-30	0.000E+00	0.000E+00	0.000E+00	0.000E+00	0.000E+00
I129	5.370E-04	2.349E-03	2.349E-03	2.349E-03	2.349E-03	2.349E-03	2.349E-03	2.349E-03	2.349E-03	2.348E-03
CS134	1.196E+01	7.984E+00	2.009E-14	5.053E-29	0.000E+00	0.000E+00	0.000E+00	0.000E+00	0.000E+00	0.000E+00
CS137	4.938E+03	9.099E+03	9.027E+02	8.955E+01	8.884E+00	8.743E-02	8.402E-07	7.163E-27	0.000E+00	0.000E+00
BA137M	4.671E+03	8.608E+03	8.540E+02	8.472E+01	8.405E+00	8.272E-02	7.948E-07	6.776E-27	0.000E+00	0.000E+00
BA140	0.000E+00	1.167E-10	0.000E+00	0.000E+00	0.000E+00	0.000E+00	0.000E+00	0.000E+00	0.000E+00	0.000E+00
LA140	0.000E+00	1.343E-10	0.000E+00	0.000E+00	0.000E+00	0.000E+00	0.000E+00	0.000E+00	0.000E+00	0.000E+00
CE141	0.000E+00	2.697E-05	0.000E+00	0.000E+00	0.000E+00	0.000E+00	0.000E+00	0.000E+00	0.000E+00	0.000E+00
CE144	1.232E+00	1.644E+00	3.220E-39	0.000E+00	0.000E+00	0.000E+00	0.000E+00	0.000E+00	0.000E+00	0.000E+00
PR144	1.218E+00	1.624E+00	0.000E+00	0.000E+00	0.000E+00	0.000E+00	0.000E+00	0.000E+00	0.000E+00	0.000E+00
ND144	8.544E-14	1.087E-13	1.093E-13	1.093E-13	1.093E-13	1.093E-13	1.093E-13	1.093E-13	1.093E-13	1.093E-13
PM147	1.409E+00	9.884E-01	3.314E-12	1.111E-23	3.726E-35	0.000E+00	0.000E+00	0.000E+00	0.000E+00	0.000E+00
SM147	2.405E-11	2.321E-10	2.564E-10	2.564E-10	2.564E-10	2.564E-10	2.564E-10	2.564E-10	2.564E-10	2.564E-10
EU152	2.730E+00	6.895E-01	4.218E-03	2.581E-05	1.579E-07	5.910E-12	5.067E-23	0.000E+00	0.000E+00	0.000E+00
EU154	4.979E-01	8.288E-01	2.619E-04	8.277E-08	2.616E-11	2.612E-18	8.233E-36	0.000E+00	0.000E+00	0.000E+00
EU155	2.911E-01	3.201E-01	2.723E-07	2.317E-13	1.972E-19	1.427E-31	0.000E+00	0.000E+00	0.000E+00	0.000E+00
GD152	4.106E-14	1.126E-13	1.367E-13	1.368E-13	1.368E-13	1.368E-13	1.368E-13	1.368E-13	1.368E-13	1.368E-13
GD153	8.585E-04	4.647E-16	0.000E+00	0.000E+00	0.000E+00	0.000E+00	0.000E+00	0.000E+00	0.000E+00	0.000E+00
HF175	3.002E-01	8.355E+00	0.000E+00	0.000E+00	0.000E+00	0.000E+00	0.000E+00	0.000E+00	0.000E+00	0.000E+00
HF181	3.965E-03	1.228E+00	0.000E+00	0.000E+00	0.000E+00	0.000E+00	0.000E+00	0.000E+00	0.000E+00	0.000E+00
TA182	4.685E+01	2.859E+02	0.000E+00	0.000E+00	0.000E+00	0.000E+00	0.000E+00	0.000E+00	0.000E+00	0.000E+00
W185	1.125E+00	2.432E+01	0.000E+00	0.000E+00	0.000E+00	0.000E+00	0.000E+00	0.000E+00	0.000E+00	0.000E+00
W187	0.000E+00	0.000E+00	0.000E+00	0.000E+00	0.000E+00	0.000E+00	0.000E+00	0.000E+00	0.000E+00	0.000E+00
RE187	4.991E-11	2.183E-10	2.183E-10	2.183E-10	2.183E-10	2.183E-10	2.183E-10	2.183E-10	2.183E-10	2.183E-10
IR192	2.597E-11	0.000E+00	0.000E+00	0.000E+00	0.000E+00	0.000E+00	0.000E+00	0.000E+00	0.000E+00	0.000E+00
HG203	0.000E+00	1.762E-04	0.000E+00	0.000E+00	0.000E+00	0.000E+00	0.000E+00	0.000E+00	0.000E+00	0.000E+00
TL207	8.844E-09	1.174E-07	8.682E-07	1.695E-06	2.523E-06	4.174E-06	8.530E-06	2.449E-05	3.979E-05	7.533E-05
TL208	5.047E-18	7.549E-16	9.210E-15	1.857E-14	2.712E-14	4.427E-14	8.747E-14	2.643E-13	4.465E-13	9.198E-13
TL209	8.228E-18	1.002E-15	3.848E-14	1.466E-13	3.432E-13	1.059E-12	5.174E-12	6.130E-11	1.777E-10	6.682E-10
PB209	3.809E-16	4.637E-14	1.781E-12	6.787E-12	1.589E-11	4.901E-11	2.396E-10	2.838E-09	8.227E-09	3.094E-08
PB210	3.194E-14	4.705E-08	7.710E-06	3.361E-05	7.813E-05	2.200E-04	9.010E-04	6.161E-03	1.364E-02	3.485E-02
PB211	8.869E-09	1.178E-07	8.707E-07	1.699E-06	2.530E-06	4.186E-06	8.554E-06	2.456E-05	3.990E-05	7.554E-05
PB212	1.405E-17	2.101E-15	2.563E-14	5.167E-14	7.547E-14	1.232E-13	2.434E-13	7.355E-13	1.243E-12	2.560E-12
PB214	7.779E-13	2.591E-07	1.300E-05	4.499E-05	9.541E-05	2.484E-04	9.012E-04	6.162E-03	1.364E-02	3.486E-02

Table A-5. (continued).

Radio-nuclide	1993	2020	2120	2220	2320	2520	3020	5020	7020	12020
BI210	3.195E-14	4.707E-08	7.711E-06	3.361E-05	7.814E-05	2.200E-04	9.010E-04	6.161E-03	1.364E-02	3.485E-02
BI211	8.869E-09	1.178E-07	8.707E-07	1.699E-06	2.530E-06	4.186E-06	8.554E-06	2.456E-05	3.990E-05	7.554E-05
BI212	1.405E-17	2.101E-15	2.563E-14	5.167E-14	7.547E-14	1.232E-13	2.434E-13	7.355E-13	1.243E-12	2.560E-12
BI213	3.809E-16	4.637E-14	1.781E-12	6.787E-12	1.589E-11	4.901E-11	2.396E-10	2.838E-09	8.227E-09	3.094E-08
BI214	7.779E-13	2.591E-07	1.300E-05	4.499E-05	9.541E-05	2.484E-04	9.012E-04	6.162E-03	1.364E-02	3.486E-02
PO210	2.188E-14	4.302E-08	7.711E-06	3.361E-05	7.814E-05	2.200E-04	9.010E-04	6.161E-03	1.364E-02	3.485E-02
PO211	2.483E-11	3.298E-10	2.438E-09	4.758E-09	7.084E-09	1.172E-08	2.395E-08	6.877E-08	1.117E-07	2.115E-07
PO212	8.999E-18	1.346E-15	1.642E-14	3.311E-14	4.835E-14	7.894E-14	1.560E-13	4.712E-13	7.963E-13	1.640E-12
PO213	3.727E-16	4.537E-14	1.743E-12	6.641E-12	1.554E-11	4.795E-11	2.344E-10	2.777E-09	8.049E-09	3.027E-08
PO214	7.777E-13	2.590E-07	1.299E-05	4.498E-05	9.539E-05	2.483E-04	9.010E-04	6.161E-03	1.364E-02	3.485E-02
PO215	8.869E-09	1.178E-07	8.707E-07	1.699E-06	2.530E-06	4.186E-06	8.554E-06	2.456E-05	3.990E-05	7.554E-05
PO216	1.405E-17	2.101E-15	2.563E-14	5.167E-14	7.547E-14	1.232E-13	2.434E-13	7.355E-13	1.243E-12	2.560E-12
PO218	7.780E-13	2.591E-07	1.300E-05	4.500E-05	9.543E-05	2.484E-04	9.014E-04	6.164E-03	1.365E-02	3.487E-02
AT217	3.809E-16	4.637E-14	1.781E-12	6.787E-12	1.589E-11	4.901E-11	2.396E-10	2.838E-09	8.227E-09	3.094E-08
RN219	8.869E-09	1.178E-07	8.707E-07	1.699E-06	2.530E-06	4.186E-06	8.554E-06	2.456E-05	3.990E-05	7.554E-05
RN220	1.405E-17	2.101E-15	2.563E-14	5.167E-14	7.547E-14	1.232E-13	2.434E-13	7.355E-13	1.243E-12	2.560E-12
RN222	7.780E-13	2.591E-07	1.300E-05	4.500E-05	9.543E-05	2.484E-04	9.014E-04	6.164E-03	1.365E-02	3.487E-02
FR221	3.809E-16	4.637E-14	1.781E-12	6.787E-12	1.589E-11	4.901E-11	2.396E-10	2.838E-09	8.227E-09	3.094E-08
FR223	1.242E-10	1.628E-09	1.201E-08	2.345E-08	3.491E-08	5.776E-08	1.180E-07	3.389E-07	5.507E-07	1.042E-06
RA223	8.869E-09	1.178E-07	8.707E-07	1.699E-06	2.530E-06	4.186E-06	8.554E-06	2.456E-05	3.990E-05	7.554E-05
RA224	1.405E-17	2.101E-15	2.563E-14	5.167E-14	7.547E-14	1.232E-13	2.434E-13	7.355E-13	1.243E-12	2.560E-12
RA225	3.808E-16	4.635E-14	1.781E-12	6.787E-12	1.589E-11	4.901E-11	2.396E-10	2.838E-09	8.227E-09	3.094E-08
RA226	7.780E-13	2.591E-07	1.300E-05	4.500E-05	9.543E-05	2.484E-04	9.014E-04	6.164E-03	1.365E-02	3.487E-02
RA228	3.919E-17	2.529E-15	2.563E-14	5.167E-14	7.547E-14	1.232E-13	2.434E-13	7.355E-13	1.243E-12	2.560E-12
AC225	3.809E-16	4.637E-14	1.781E-12	6.787E-12	1.589E-11	4.901E-11	2.396E-10	2.838E-09	8.227E-09	3.094E-08
AC227	8.997E-09	1.180E-07	8.705E-07	1.699E-06	2.530E-06	4.186E-06	8.554E-06	2.456E-05	3.990E-05	7.554E-05
AC228	3.919E-17	2.530E-15	2.563E-14	5.167E-14	7.547E-14	1.232E-13	2.434E-13	7.355E-13	1.243E-12	2.560E-12
TH227	8.731E-09	1.159E-07	8.587E-07	1.676E-06	2.495E-06	4.128E-06	8.436E-06	2.422E-05	3.935E-05	7.450E-05
TH228	1.400E-17	2.092E-15	2.563E-14	5.167E-14	7.547E-14	1.232E-13	2.434E-13	7.355E-13	1.243E-12	2.560E-12
TH229	3.808E-16	4.634E-14	1.781E-12	6.787E-12	1.589E-11	4.901E-11	2.396E-10	2.838E-09	8.227E-09	3.094E-08
TH230	8.870E-10	6.544E-05	5.326E-04	9.994E-04	1.466E-03	2.398E-03	4.719E-03	1.391E-02	2.293E-02	4.481E-02
TH231	3.811E-04	3.947E-04	3.947E-04	3.947E-04	3.947E-04	3.947E-04	3.947E-04	3.948E-04	3.948E-04	3.949E-04
TH232	2.164E-16	4.233E-15	2.793E-14	5.167E-14	7.547E-14	1.232E-13	2.434E-13	7.355E-13	1.243E-12	2.560E-12
TH234	1.230E-01	5.499E-01	5.499E-01	5.499E-01	5.499E-01	5.499E-01	5.499E-01	5.499E-01	5.499E-01	5.499E-01

Table A-5. (continued).

Radio-nuclide	1993	2020	2120	2220	2320	2520	3020	5020	7020	12020
PA231	7.051E-08	2.949E-07	1.129E-06	1.960E-06	2.790E-06	4.445E-06	8.551E-06	2.455E-05	3.989E-05	7.552E-05
PA233	1.219E-07	5.645E-07	8.026E-07	1.010E-06	1.187E-06	1.467E-06	1.874E-06	2.191E-06	2.202E-06	2.199E-06
PA234M	1.230E-01	5.499E-01	5.499E-01	5.499E-01	5.499E-01	5.499E-01	5.499E-01	5.499E-01	5.499E-01	5.499E-01
PA234	1.599E-04	7.148E-04	7.148E-04	7.148E-04	7.148E-04	7.148E-04	7.148E-04	7.148E-04	7.148E-04	7.148E-04
U233	2.071E-12	4.271E-11	3.427E-10	7.400E-10	1.221E-09	2.387E-09	6.089E-09	2.437E-08	4.331E-08	8.997E-08
U234	2.497E-05	5.193E-01	5.193E-01	5.194E-01	5.194E-01	5.194E-01	5.195E-01	5.196E-01	5.198E-01	5.202E-01
U235	3.811E-04	3.947E-04	3.947E-04	3.947E-04	3.947E-04	3.947E-04	3.947E-04	3.948E-04	3.948E-04	3.949E-04
U236	1.096E-06	4.798E-06	4.808E-06	4.819E-06	4.829E-06	4.849E-06	4.898E-06	5.070E-06	5.209E-06	5.451E-06
U237	2.622E-07	6.577E-07	5.338E-09	4.333E-11	3.517E-13	2.317E-17	8.162E-28	0.000E+00	0.000E+00	0.000E+00
U238	1.230E-01	5.499E-01	5.499E-01	5.499E-01	5.499E-01	5.499E-01	5.499E-01	5.499E-01	5.499E-01	5.499E-01
NP237	1.219E-07	5.647E-07	8.026E-07	1.010E-06	1.187E-06	1.467E-06	1.874E-06	2.191E-06	2.202E-06	2.199E-06
PU238	4.052E-04	3.544E-01	1.609E-01	7.300E-02	3.313E-02	6.825E-03	1.314E-04	1.808E-11	2.487E-18	1.745E-35
PU239	1.976E-02	2.622E-02	2.614E-02	2.607E-02	2.599E-02	2.584E-02	2.547E-02	2.405E-02	2.270E-02	1.966E-02
PU240	1.740E-03	3.587E-03	3.549E-03	3.511E-03	3.474E-03	3.402E-03	3.226E-03	2.609E-03	2.111E-03	1.242E-03
PU241	1.069E-02	2.681E-02	2.176E-04	1.766E-06	1.434E-08	9.444E-13	3.327E-23	0.000E+00	0.000E+00	0.000E+00
PU242	2.450E-08	1.089E-07	1.089E-07	1.088E-07	1.088E-07	1.088E-07	1.087E-07	1.083E-07	1.079E-07	1.069E-07
AM241	4.437E-04	7.231E-03	6.939E-03	5.918E-03	5.041E-03	3.658E-03	1.640E-03	6.638E-05	2.686E-06	8.847E-10
CM242	2.113E-14	3.852E-20	0.000E+00	0.000E+00	0.000E+00	0.000E+00	0.000E+00	0.000E+00	0.000E+00	0.000E+00
CM244	4.349E-06	1.201E-05	2.613E-07	5.688E-09	1.238E-10	5.864E-14	2.863E-22	0.000E+00	0.000E+00	0.000E+00
TOTAL	1.078E+06	3.267E+06	6.313E+05	3.012E+05	1.467E+05	3.972E+04	9.950E+03	9.075E+03	8.909E+03	8.516E+03

a. These values are printed in the default format used by the ORIGEN2 computer code, which includes four significant figures.

A-2 VOLUMES AND CONTAINERS

Table A-6 contains the annual and total volume of LLW that was disposed of in the SDA for 1984 through 1993 for pits and soil vault rows. Based on the total volume of LLW disposed of in the pits from 1984 through 1993, 20,000 m^3, an annual average disposal rate of 2,000 m^3 was calculated for pits. Based on the total volume of LLW disposed of in the soil vault rows from 1984 through 1993, 730 m^3, an average annual disposal rate of 73 m^3 was calculated for the soil vault rows. The total volume of LLW was calculated to be 75,600 m^3 in the pits and 2,700 m^3 in the soil vault rows based on 27 additional years of disposal (1994 through 2020).

LLW is disposed of in a wide variety of containers. From 1984 to 1993, of the 16,334 containers disposed of in pits, bales are the largest number (8,302), followed by wooden boxes (5,038), and metal barrels (1,576). For the same time period, of the 450 containers disposed of in soil vault rows, inserts are the largest number (419). These are not high-integrity containers; therefore, no credit was taken for them in the radiological performance assessment.

Table A-6. Volumes of LLW disposed of in pits and soil vault rows for 1984 through 1993.[a]

Year	Volume in pits (m^3)	Volume in soil vault rows (m^3)
1984	3.817E+03	8.859E+01
1985	3.028E+03	1.124E+02
1986	3.377E+03	6.047E+01
1987	2.856E+03	1.025E+02
1988	1.995E+03	5.018E+01
1989	1.280E+03	8.395E+01
1990	1.696E+03	6.602E+01
1991	1.175E+03	9.694E+01
1992	8.088E+02	3.531E+01
1993	4.012E+02	3.242E+01
Total	2.043E+04	7.287E+02

a. These values are printed in the default format used by the RWMIS data base, which includes four significant figures.

A-3 REFERENCES

Abbott, M. L., 1992, "ORIGEN2 Runs on RWMIS Inventory for RWMC Performance Assessment," EDF SEM-RWMC-91.002.1, EG&G Idaho.

Culbertson-Arendts, K. H., 1993, "RWMIS LLW Inventory for RWMC LLW Radiological Performance Assessment," EDF RWMC-528, Rev. 1., EG&G Idaho, Inc., November.

Maheras, S. J., 1993, "Revised 1984 through 2020 Low-Level Waste Inventory for the RWMC Radiological Performance Assessment," EDF RWMC-613, Rev. 1, Science Applications International Corporation.

APPENDIX B

ATMOSPHERIC PATHWAY ANALYSIS

APPENDIX B
ATMOSPHERIC PATHWAY ANALYSIS

B-1 REGULATORY REQUIREMENTS

The regulatory requirement for the atmospheric pathway analysis is contained in DOE Order 5820.2A §III.3.a(2) (DOE 1988a), which states that "releases to the atmosphere shall meet the requirements of 40 CFR 61." Based on 40 CFR 61, Subpart H, "National Emission Standards for Emissions of Radionuclides Other Than Radon From Department of Energy Facilities" (CFR 1992), a limit of 10 mrem/yr was considered to apply. Requirements in 40 CFR 61, Subpart H, apply to monitored, unmonitored, and diffuse emissions.

At the present time, there is no DOE policy on the time of compliance with the performance objectives contained in DOE Order 5820.2A. Therefore, the 10 mrem/yr performance objective in 40 CFR 61 was assumed to apply in perpetuity. In addition, it is not clear whether the performance objective contained in 40 CFR 61 as implemented in DOE Order 5820.2A applies to just the LLW disposal facility or to the entire INEL. The EPA approach to 40 CFR 61 compliance considers the entire INEL in the 10 mrem/yr compliance determination. However, in "Clarification of Requirements of DOE Order 5820.2A",[a] it is specifically stated that "the performance objectives are intended to apply to each LLW facility on a reservation rather than to the reservation as a whole." Because of these seemingly contradictory regulatory positions, it was decided to evaluate atmospheric emissions on a single facility basis and on an INEL-wide basis, using the present levels of INEL emissions as a baseline. No attempt was made to derive emission estimates for new facilities that may be built or for projects that may take place in the future.

---

a. Letter from Thomas B. Hindman to Distribution, February 28, 1989, and Letter from Thomas B. Hindman to P. Saxman et al., March 28, 1989. These letters are contained in Dodge et al. (1991).

B-2 OPERATIONAL AND INSTITUTIONAL CONTROL PERIODS

B-2.1 Methodology and Data

This section describes the methodology and data used to calculate doses from atmospheric emissions from the RWMC during the operational and institutional control periods. These doses are based on the diffuse emissions dose assessments performed for the INEL National Emission Standard for Hazardous Air Pollutants (NESHAP) Annual Report (DOE 1993).

During the operational and institutional control periods, the RWMC will be actively maintained and monitored. Therefore, it is reasonable to postulate that soil contamination levels will not be higher than current levels; in reality, soil contamination will decrease because of environmental remediation activities at the RWMC. DOE (1993) describes the existing soil contamination levels at the RWMC and the areal extent of this contamination. The radionuclide soil concentrations at contaminated areas were estimated based on sampling studies or field survey measurements. The areal extent of each area was also estimated based on field observations and measurements. These data were used to estimate an annual release rate for each radionuclide in units of curies per year.

Data provided as activity per unit mass were converted to release rate by using a resuspension rate constant of 3.2E-5/yr (10^{-12}/s), a soil density of 2 g/cm^3, and a resuspendable soil depth of 1 cm:

$$I\,(Ci/yr) = C_r\left(\frac{Ci}{g}\right) \times \rho\left(\frac{g}{cm^3}\right) \times d\,(cm) \times A\,(m^2) \times S\,(yr^{-1}) \times \frac{10^4\,cm^2}{m^2} \qquad (B\text{-}1)$$

where

I = annual release rate (Ci/yr)

C_r = radionuclide concentration (Ci/g)

ρ = soil density (g/cm^3)

d = depth of contamination (cm)

A = area of diffuse source (m^2)

S = resuspension rate constant (per yr).

Data provided as activity per unit area were converted to release rate by using a resuspension rate constant of 3.2E-5/yr (10^{-12}/s) and assuming that the entire soil inventory was present in the resuspendable soil layer:

$$I\,(Ci/yr) = C_r\left(\frac{Ci}{m^2}\right) \times A\,(m^2) \times S\,(yr^{-1}) \qquad \text{(B-2)}$$

where

C_r = radionuclide areal concentration (Ci/m^2).

Resuspension rate constants have been the subject of considerable research, which indicates they are extraordinarily variable. The resuspension rate constant used in this analysis was based on the mass loading model. This treatment of resuspension states that the rate of change of material on the ground is given by (Peterson 1983):

$$\frac{dC_A}{dt} = v_d \times \chi - S \times C_A \qquad \text{(B-3)}$$

where

C_A = areal concentration of the material on the ground (per m^2)

v_d = deposition velocity (m/s)

χ = atmospheric concentration of the material (per m^3)

S = resuspension rate constant (per s).

At equilibrium, $dC_A/dt = 0$, $v_d \chi = S\ C_A$, and

$$S = \frac{\chi \times v_d}{C_A} \quad . \tag{B-4}$$

The atmospheric concentration of particulate material on the INEL has been determined by measurements conducted during 1983 to 1990 (Hoff et al. 1984, 1985, 1986, 1987; Chew and Mitchell 1988; Hoff et al. 1989, 1990, 1991). These data show that the average particulate air concentration on the INEL is 25.4 $\mu g/m^3$. Using an areal density of 20,000 g/m^2 (for a 1 cm depth and a density of 2 g/cm^3) and a deposition velocity of 0.002 m/s (DOE 1993), a resuspension rate constant of 10^{-12}/s can be calculated:

$$S = \frac{25.4E\text{-}6\ g/m^3 \times 0.002 m/s}{20{,}000 g/m^2} \approx 10^{-12} s^{-1} \approx 3.2E\text{-}5 yr^{-1} \quad . \tag{B-5}$$

The receptor location for the operational and institutional control periods was located near the INEL site boundary, 8 km south-southwest of the RWMC (DOE 1993). The atmospheric data, environmental data, and the computer code used in the analyses are also discussed in DOE (1993).

B-2.2 Results

Based on the dose assessments in the 1992 INEL NESHAP Annual Report (DOE 1993), the contaminated soil areas at the RWMC yielded a dose of 5.7E-6 mrem/yr. This dose was well below the 40 CFR 61 NESHAP standard of 10 mrem/yr. When this dose was combined with the dose from existing monitored and unmonitored emission points at the INEL and existing diffuse sources at other areas of the INEL (DOE 1993), a dose of 1.5E-3 mrem/yr was calculated. This dose was also well below the NESHAP standard of 10 mrem/yr.

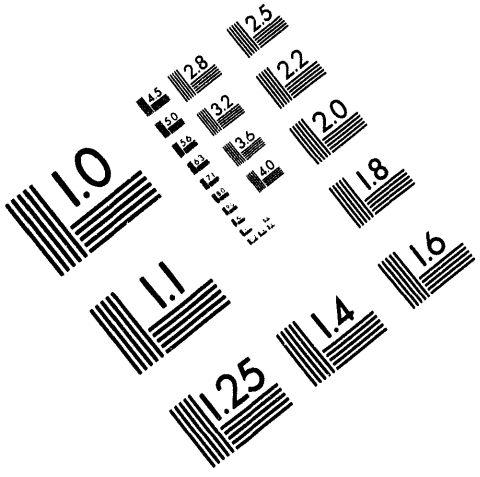

Association for Information and Image Management

1100 Wayne Avenue, Suite 1100
Silver Spring, Maryland 20910

301/587-8202

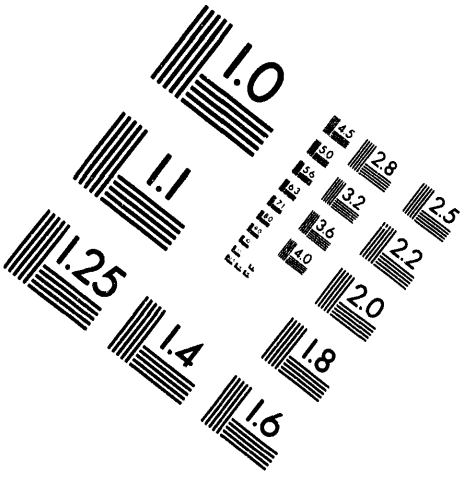

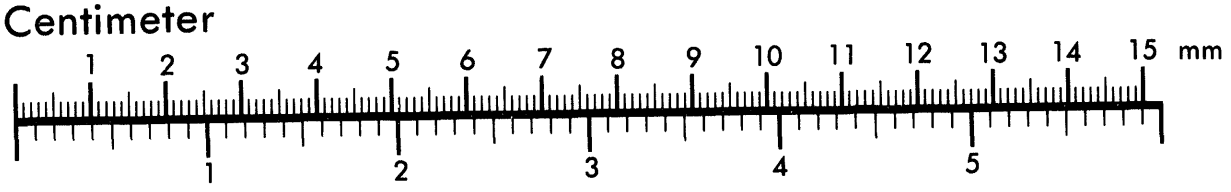

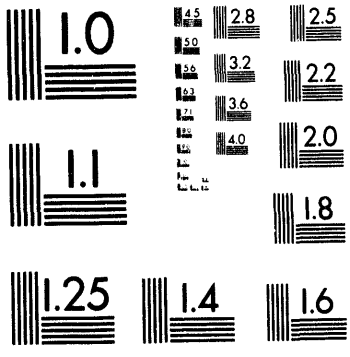

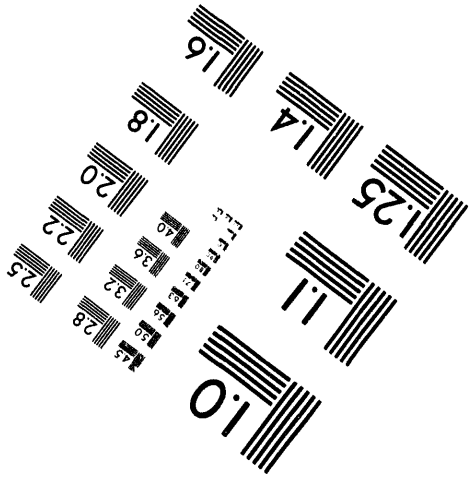

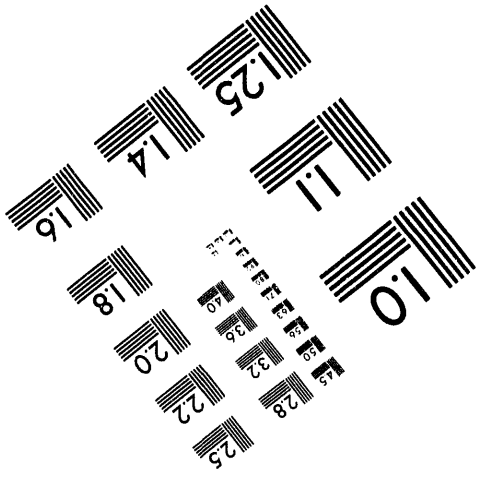

MANUFACTURED TO AIIM STANDARDS
BY APPLIED IMAGE, INC.

5 of 5

B-3 POST-INSTITUTIONAL CONTROL PERIOD

B-3.1 Methodology and Data

This section describes the methodology used to calculate doses from atmospheric emissions of radionuclides from the RWMC SDA. The scenario is based on biointrusion contaminating the surface soil at the RWMC SDA. This contaminated surface soil was then blown offsite to a member of the public 100 m from the RWMC SDA boundary. This hypothetical receptor ate contaminated food, was immersed in contaminated air, breathed contaminated air, and was exposed to contaminated ground surfaces.

The scenario used for this analysis started with the inventory disposed of in the RWMC LLW disposal locations from 1984 to 1993 and was augmented with the forecasted additions for 1994 to 2020 (see Appendix A). A portion of the inventory was then brought to the surface through biointrusion and distributed over the RWMC, forming a large area source of radioactive material that could be resuspended by wind.

The contaminated material was then blown offsite to a hypothetical member of the public located 100 m[a] from the RWMC. The receptor was located in the east-northeast sector, the sector that yielded the largest annual average sector-averaged air concentration at 100 m from the RWMC, using a ground-level release and meteorological data collected from 1987 to 1991 at the Central Facilities Area (CFA) (Leonard 1992). The meteorological data contained in Leonard (1992) consist of the joint frequency of stability class, windspeed class, and wind direction and incorporate data for periods of time when there were calms or inversions.

For this analysis, the GENII computer code (Version 1.485) was used to model the doses resulting from RWMC releases (Napier et al. 1988). GENII meets the requirements of NQA-1 Basic Requirement 3 (Design Control) and Supplementary Requirement 3S-1 (Supplementary Requirements for Design Control), which include extensive requirements for the verification and

---

a. The distance of 100 m is based on the recommendation made by the Performance Assessment Task Team contained in Wood et al. (1992).

validation of computer codes (ASME 1989). Although GENII can model both acute and chronic releases to the atmosphere, only the chronic option was exercised in this analysis. The output from GENII is the effective dose equivalent (EDE), which includes the 50-year committed EDE (CEDE) from internal exposure through the ingestion and inhalation pathways and the external EDE from ground deposition and air immersion. Napier et al. (1988) contains a complete description of the GENII computer code.

Inhalation doses were calculated based on exposure to contaminated air for 1 year (8,760 hours). Two inhalation rates were evaluated and described in Section 3.4.1.2: 8,030 and 5,840 m^3/yr.

Ground surface doses were calculated based on 100 years of buildup of radionuclides in the surface soil because of atmospheric deposition. Two shielding factors were evaluated and described in Section 3.4.1.2: 0.7 and 0.36.

Air immersion doses were calculated based on exposure to contaminated air for 1 year (8,760 hours), using shielding factors of 0.7 and 0.36, as in the ground surface analyses.

Ingestion doses were calculated based on the consumption of contaminated produce, leafy vegetables, milk, and meat. The conceptual model for ingestion doses first assumes that radionuclides are deposited on forage, soil, produce, and leafy vegetables. Radionuclides deposited on forage are subsequently transferred through the food chain to meat and milk and then to humans. Radionuclides deposited on produce and leafy vegetables are also consumed by humans. Radionuclides deposited on soil are transferred to forage, produce, and leafy vegetables through the mechanism of root uptake and then transferred to humans through ingestion of contaminated meat, milk, produce, and leafy vegetables. The parameters used to calculate food chain doses are contained in Napier et al. (1988). The values for the concentration ratios for forage and crops and the transfer coefficients for milk and meat are contained in Figures B-1 through B-4. The concentration ratios for forage and crops are in terms of dry weight.

Two diets were evaluated: (a) a diet developed by Rupp (1980) and based on a 1965 U.S Department of Agriculture (USDA) survey and (b) a diet developed by Yang and Nelson (1984, 1986) and based on a 1977 to 1978 USDA survey (see Table B-1). The Rupp diet was the default diet used in the EPA's NESHAP Environmental Impact Statement (EPA 1989). The Yang and Nelson diet represents a more realistic diet than the Rupp diet because it is based on a later dietary survey. Dietary fractions representative of rural agricultural areas were used (EPA 1989). Based on the data in EPA (1989), 70% of the receptor's vegetables and produce, 40% of the milk, and 44% of the meat were produced locally.

The dose conversion factors used in this analysis are from the GENII library that uses the most conservative dose conversion factors contained in DOE (1988b) and DOE (1988c).

Two biointrusion mechanisms were examined as potential ways to bring contaminated material to the surface: intrusion by burrowing animals and intrusion by plant roots. Groves and Keller (1983) identified 10 species of small mammals nesting on or near the RWMC. Four species accounted for about 95% of the small mammals inhabiting the SDA: (1) deer mice (Peromyscus maniculatus), 58%, (2) montane voles (Microtus montanus), 18%, (3) Ord's kangaroo rats (Dipodomys ordii), 12%, and (4) Townsend's ground squirrels (Spermophilus townsendii), 5%.

Based on the site-specific studies in Reynolds and Wakkinen (1987) and Reynolds and Laundre (1988), described in Section 3.6.1.2, that report burrow depths are not observed in undisturbed or disturbed soils at the INEL greater than 140 cm deep, intrusion by burrowing small mammals is highly unlikely and was removed from further consideration. The authors acknowledge that investigators at other sites have observed different results for other species of small mammals (e.g., McKenzie et al. 1982). These other studies were considered in evaluating the intrusion by the burrowing small mammal pathway; therefore, preference was given to the site-specific studies based on the guidance provided in Dodge et al. (1991).

Table B-1. Alternative human diets.

Food product	Rupp diet	Yang and Nelson diet
Produce (kg/yr)	176	94
Leafy vegetables (kg/yr)	18	17
Milk (L/yr)	112	89
Meat (kg/yr)	85	55

In contrast to burrowing mammals, harvester ants (Pogonomyrmex salinus) burrow deep enough to encounter the waste. For example, Blom et al. (1991) states that harvester ants have been found as deep as 2.7 m in Wyoming and at the Hanford Site. To account for the intrusion of harvester ants into the waste, a model similar to that in Kennedy et al. (1985) was constructed.

The model was based on harvester ants burrowing into the waste and bringing contaminated material to the surface and is discussed in Section 3.4.1.2.

The total activity brought to the surface through harvester ant burrowing was then dispersed in the environment and blown to a hypothetical receptor located 100 m from the RWMC. While this is a conservative assumption, it puts an upper bound on the material that a receptor could be exposed to through the atmospheric pathway. The potential for biointrusion by plant roots was also evaluated.

Based on the site-specific data by Reynolds and Fraley (1989), as discussed in Section 3.4.1.2, biointrusion by plant roots of pits and soil vaults may be possible. However, biointrusion by plant roots of soil vaults is less likely because of increased cover depth.

To estimate the amount of radioactive material that plant roots could bring to the surface, a model similar to those in GENII (Napier et al. 1988)

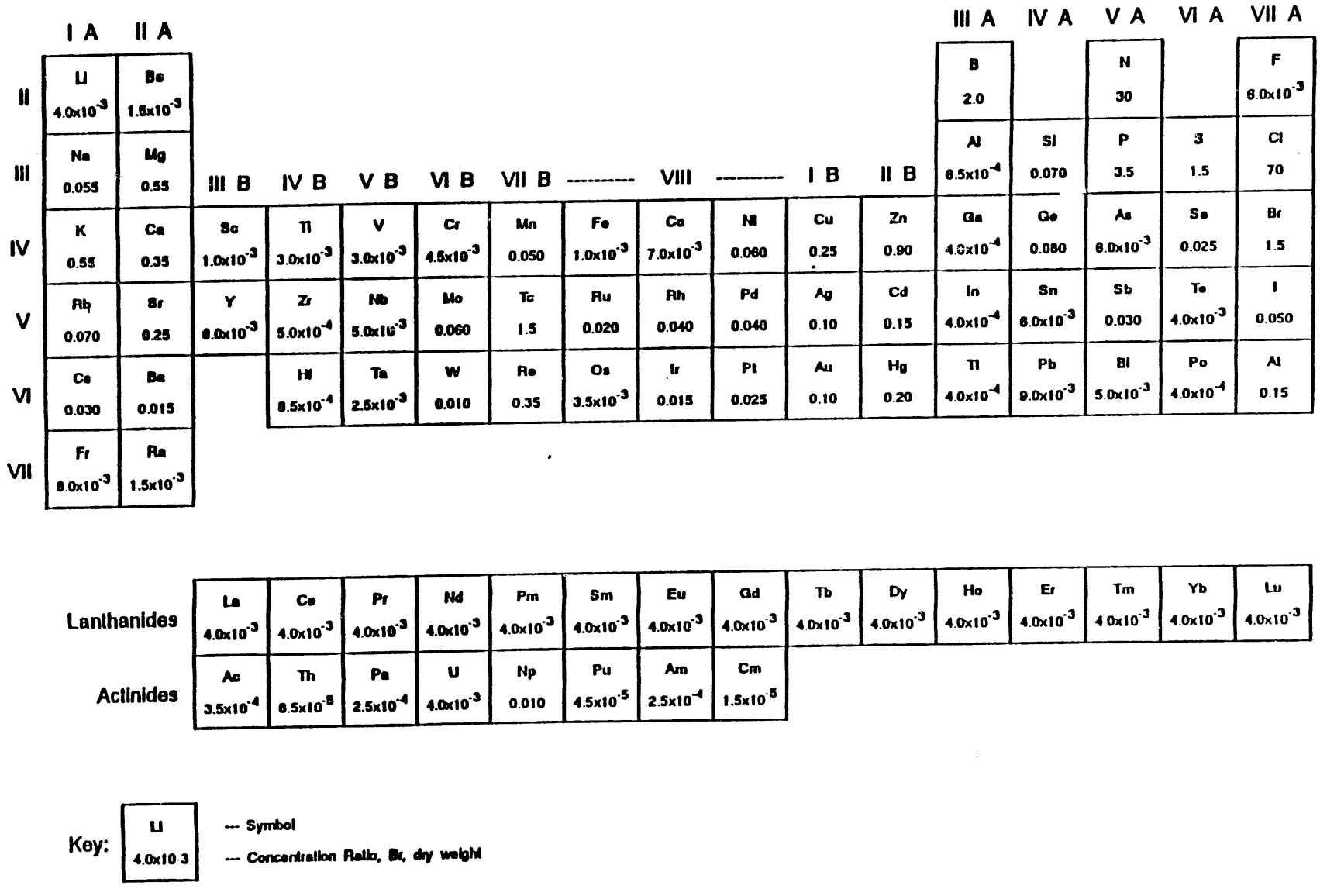

Figure B-1. Concentration ratios for crops (from Baes et al. 1984).

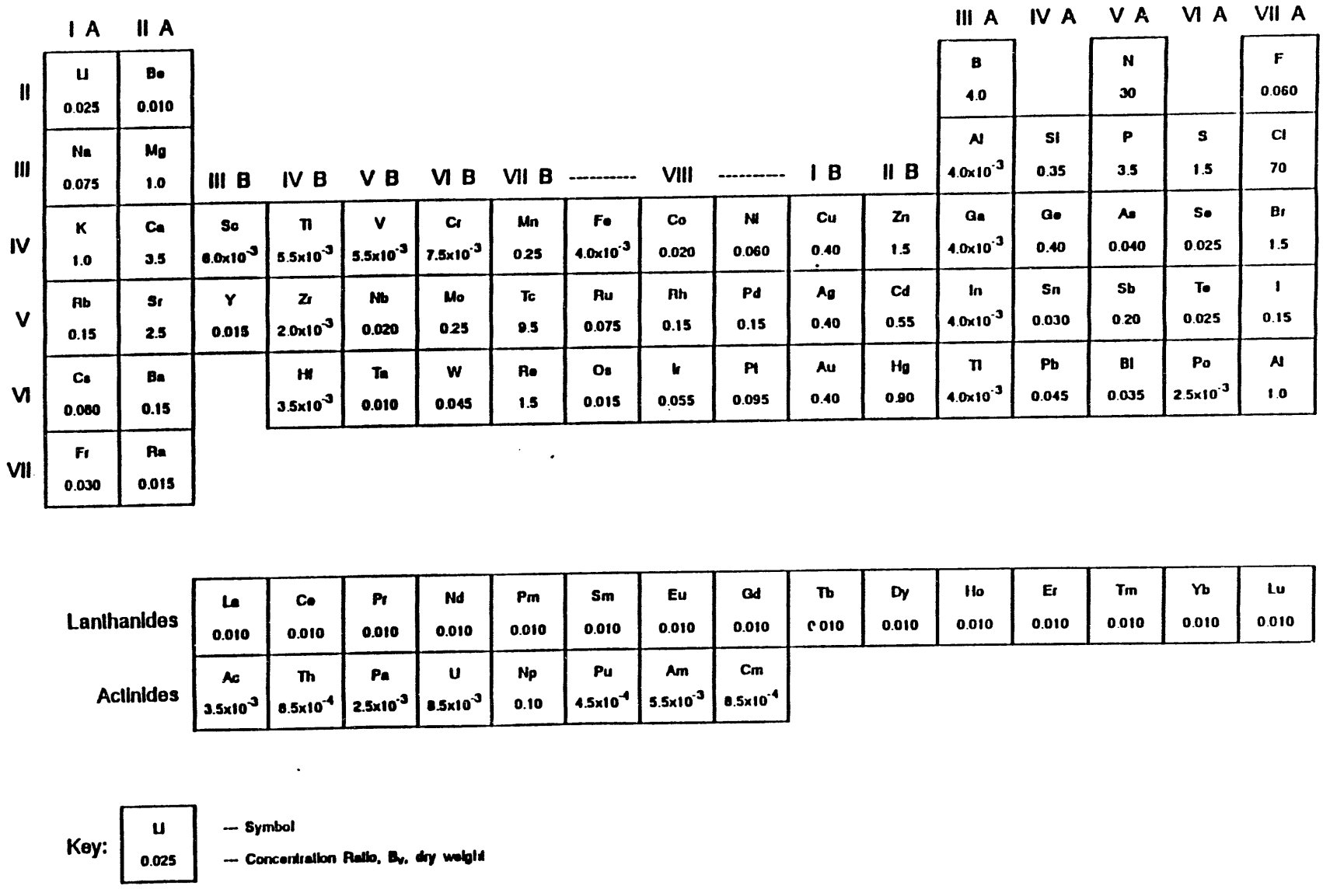

Figure B-2. Concentration ratios for forage (from Baes et al. 1984).

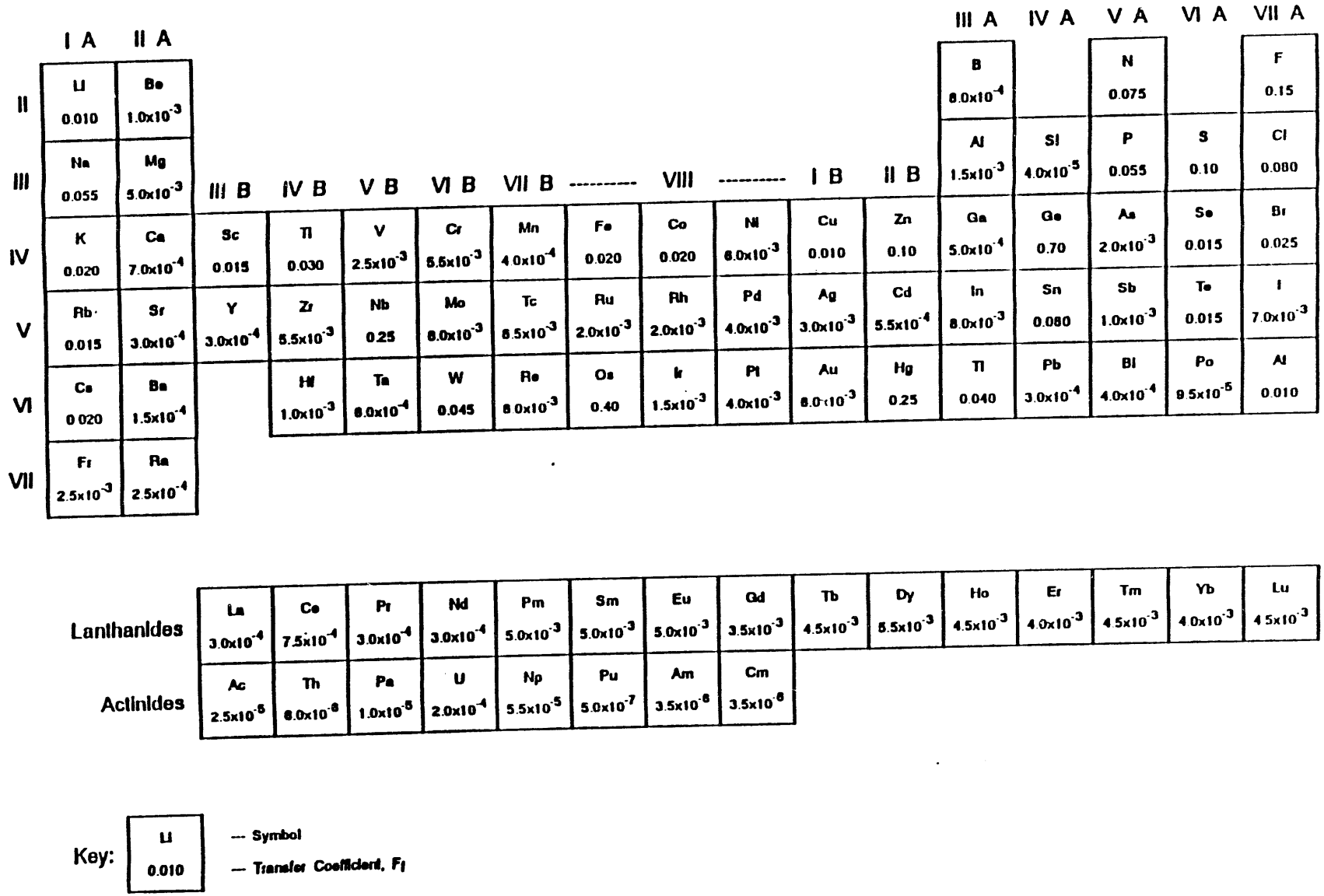

Figure B-3. Transfer coefficients for meat (from Baes et al. 1984).

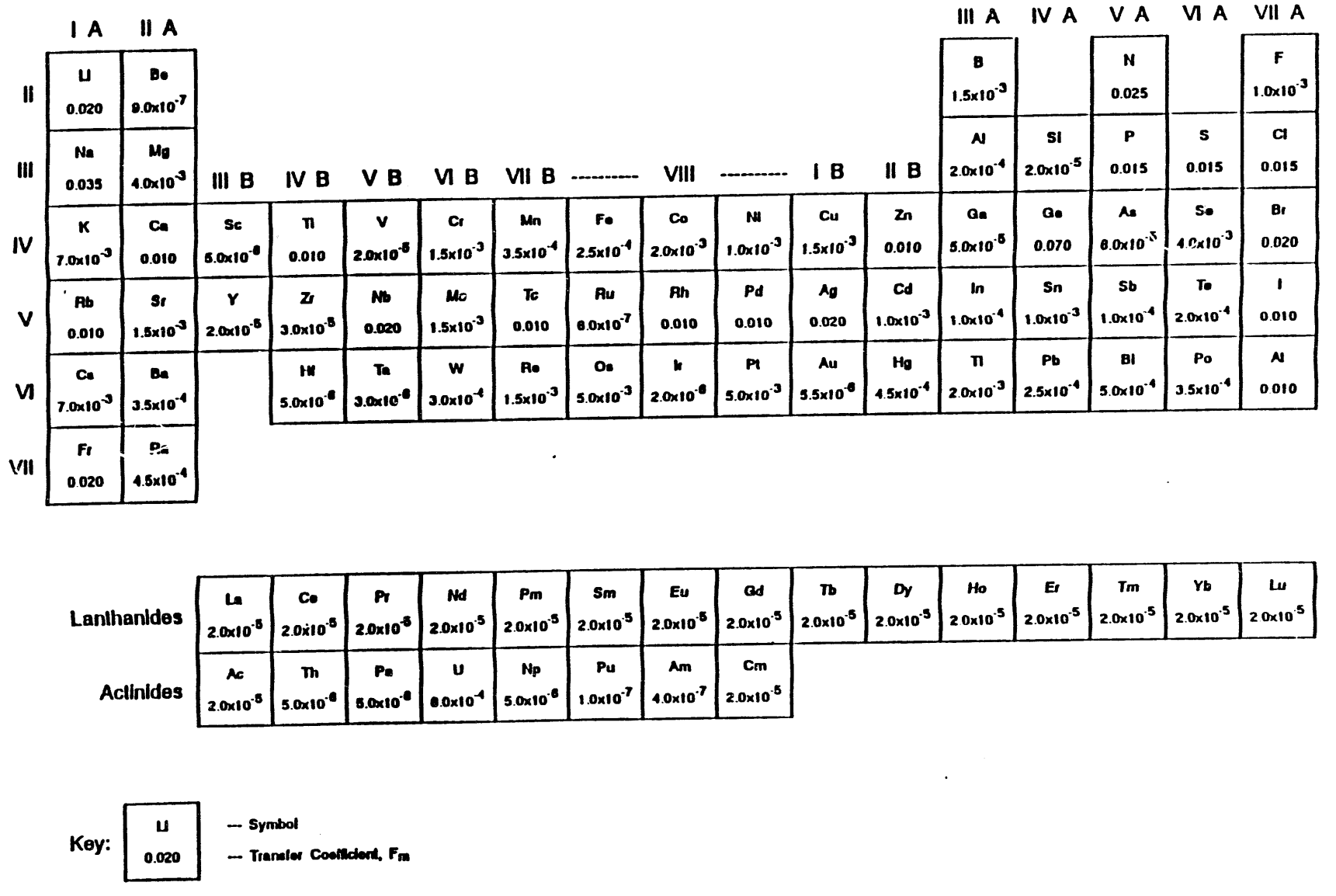

Figure B-4. Transfer coefficients for milk (from Baes et al. 1984).

and Kennedy et al. (1985) was constructed. This model is described in Section 3.4.1.2.

The total activity brought to the surface through plant uptake was then dispersed in the environment and blown to a hypothetical receptor 100 m from the RWMC. This implies that the entire big sagebrush aboveground biomass was converted to a dispersible form. While this is a conservative assumption, it puts an upper bound on the material that a receptor could be exposed to through the atmospheric pathway.

Doses because of harvester ant burrowing and plant uptake were calculated at various points in time after site closure, beginning in 2120 and continuing to 1,000,000 years after site closure. The year 2120 corresponds to the beginning of the post-institutional period and is the earliest time that biointrusion could occur during the post-institutional period. This is also the time when the maximum fission product and activation product inventory is available for biointrusion because fission and activation products do not contain long-lived decay series with substantial progeny ingrowth. Doses were also calculated at the year 12,000 and 1,000,000 years after site closure. These times were chosen to determine if there were any long-lived actinide decay series that could yield large doses because of progeny ingrowth over long time frames. One million years corresponds to the time when most long-lived decay series have achieved a substantial fraction of secular equilibrium and, therefore, represents a reasonable time to calculate doses.

Table B-2 contains the releases at 2120, 12020, and 1,000,000 years for the pits and the soil vaults. Maheras (1993) contains the computer output for the calculations.

Table B-2. Atmospheric Releases for Pits and Soil Vaults for 2120, 12020, and 1,000,000 Years

	Atmospheric Releases for Pits (Ci)				Atmospheric Releases for Soil Vaults (Ci)		
Radionuclide	2120	12020	1,000,000	Radionuclide	2120	12020	1,000,000
H 3	2.9E-06	0.0E+00	0.0E+00	H 3	8.3E-03	0.0E+00	0.0E+00
C 14	2.4E-07	7.1E-08	6.9E-60	C 14	2.0E-04	6.2E-05	5.9E-57
NA22	1.2E-20	0.0E+00	0.0E+00	K 40	6.7E-07	6.7E-07	6.8E-07
K 40	2.3E-07	2.3E-07	2.3E-07	MN54	8.7E-38	0.0E+00	0.0E+00
MN54	4.9E-41	0.0E+00	0.0E+00	FE55	4.2E-14	0.0E+00	0.0E+00
FE55	5.5E-18	0.0E+00	0.0E+00	CO60	4.1E-07	0.0E+00	0.0E+00
CO60	2.9E-11	0.0E+00	0.0E+00	NI59	1.4E-03	1.2E-03	1.3E-07
NI63	2.9E-04	1.2E-36	0.0E+00	NI63	9.1E-02	3.7E-34	0.0E+00
SR90	7.9E-05	0.0E+00	0.0E+00	SR90	1.8E-04	0.0E+00	0.0E+00
Y 90	7.2E-06	0.0E+00	0.0E+00	Y 90	1.7E-05	0.0E+00	0.0E+00
ZR93	2.1E-17	2.1E-17	1.3E-17	NB94	2.2E-08	1.6E-08	3.2E-23
NB93M	2.1E-17	2.1E-17	1.4E-17	TC99	5.5E-06	5.3E-06	2.1E-07
NB94	1.8E-12	1.3E-12	2.7E-27	RU106	8.8E-38	0.0E+00	0.0E+00
TC99	5.3E-09	5.1E-09	2.0E-10	RH106	1.1E-37	0.0E+00	0.0E+00
RU106	4.3E-33	0.0E+00	0.0E+00	SN121M	2.7E-10	0.0E+00	0.0E+00
RH106	5.4E-33	0.0E+00	0.0E+00	SB125	9.0E-15	0.0E+00	0.0E+00
AG108	6.6E-12	2.3E-35	0.0E+00	TE125M	1.3E-15	0.0E+00	0.0E+00
AG108M	7.4E-11	2.5E-34	0.0E+00	I 129	4.5E-10	4.5E-10	4.3E-10
AG109M	5.8E-34	0.0E+00	0.0E+00	CS134	3.2E-21	0.0E+00	0.0E+00
CD109	7.2E-34	0.0E+00	0.0E+00	CS137	1.4E-04	0.0E+00	0.0E+00
SB125	1.7E-17	0.0E+00	0.0E+00	BA137M	1.6E-04	0.0E+00	0.0E+00
TE125M	2.4E-18	0.0E+00	0.0E+00	CE144	3.9E-46	0.0E+00	0.0E+00
I 129	7.2E-09	7.2E-09	6.9E-09	ND144	1.3E-20	1.3E-20	0.0E+00
CS134	1.4E-21	0.0E+00	0.0E+00	PM147	4.0E-19	0.0E+00	0.0E+00
CS137	2.2E-05	0.0E+00	0.0E+00	SM147	3.1E-17	3.1E-17	3.1E-17
BA133	1.4E-17	0.0E+00	0.0E+00	EU152	5.1E-10	0.0E+00	0.0E+00
BA137M	2.6E-05	0.0E+00	0.0E+00	EU154	3.2E-11	0.0E+00	0.0E+00
CE144	1.4E-45	0.0E+00	0.0E+00	EU155	3.3E-14	0.0E+00	0.0E+00
ND144	1.6E-20	1.6E-20	0.0E+00	GD152	1.7E-20	1.7E-20	1.7E-20
PM147	6.7E-26	0.0E+00	0.0E+00	RE187	1.9E-16	1.9E-16	1.9E-16
SM147	8.7E-21	8.7E-21	8.7E-21	TL207	1.0E-13	8.9E-12	4.7E-11
EU152	4.5E-10	0.0E+00	0.0E+00	TL208	1.1E-21	1.1E-19	1.2E-17
EU154	6.7E-11	0.0E+00	0.0E+00	TL209	4.6E-21	7.9E-17	4.4E-15
EU155	1.1E-13	0.0E+00	0.0E+00	PB209	2.5E-19	4.3E-15	2.4E-13
GD152	1.4E-20	1.4E-20	1.4E-20	PB210	1.1E-12	4.9E-09	7.6E-08
TL207	4.1E-10	1.9E-09	8.6E-09	PB211	1.2E-13	1.1E-11	5.5E-11
TL208	6.6E-08	2.1E-10	2.1E-10	PB212	3.6E-21	3.6E-19	3.9E-17
TL209	5.0E-14	3.4E-12	5.9E-11	PB214	1.8E-12	4.9E-09	7.6E-08
PB209	2.7E-12	1.8E-10	3.2E-09	BI210	1.0E-12	4.7E-09	7.3E-08
PB210	9.8E-08	1.9E-09	4.6E-07	BI211	1.2E-13	1.0E-11	5.3E-11
PB211	4.9E-10	2.2E-09	1.0E-08	BI212	3.4E-21	3.4E-19	3.8E-17
PB212	2.2E-07	6.9E-10	6.9E-10	BI213	2.4E-19	4.2E-15	2.3E-13
PB214	9.9E-08	1.9E-09	4.6E-07	BI214	1.7E-12	4.7E-09	7.3E-08
BI210	9.5E-08	1.8E-09	4.4E-07	PO210	9.1E-13	4.1E-09	6.5E-08
BI211	4.7E-10	2.1E-09	9.7E-09	PO211	2.9E-16	2.5E-14	1.3E-13
BI212	2.1E-07	6.7E-10	6.6E-10	PO212	1.9E-21	1.9E-19	2.1E-17
BI213	2.6E-12	1.8E-10	3.1E-09	PO213	2.1E-19	3.6E-15	2.0E-13
BI214	9.5E-08	1.8E-09	4.4E-07	PO214	1.5E-12	4.1E-09	6.5E-08
PO210	8.3E-08	1.6E-09	3.9E-07	PO215	1.0E-13	8.9E-12	4.7E-11
PO211	1.2E-12	5.2E-12	2.3E-11	PO216	3.0E-21	3.0E-19	3.3E-17
PO212	1.2E-07	3.7E-10	3.7E-10	PO218	1.5E-12	4.1E-09	6.5E-08
PO213	2.2E-12	1.5E-10	2.7E-09	AT217	1.1E-18	1.9E-14	1.1E-12
PO214	8.4E-08	1.6E-09	3.9E-07	RN219	1.0E-13	8.8E-12	4.6E-11
PO215	4.1E-10	1.8E-09	8.5E-09	RN220	3.0E-21	3.0E-19	3.3E-17
PO216	1.8E-07	5.8E-10	5.8E-10	RN222	1.5E-12	4.1E-09	6.4E-08
PO218	8.4E-08	1.6E-09	3.9E-07	FR221	2.3E-19	4.1E-15	2.2E-13
AT217	1.2E-11	8.1E-10	1.4E-08	FR223	1.6E-15	1.4E-13	7.2E-13
FR221	2.6E-12	1.7E-10	3.0E-09	RA223	1.1E-13	9.4E-12	4.9E-11
FR223	6.3E-12	2.8E-11	1.3E-10	RA224	3.2E-21	3.2E-19	3.5E-17
RA223	4.3E-10	1.9E-09	9.0E-09	RA225	2.2E-19	3.8E-15	2.1E-13

Table B-2. (continued).

Radionuclide	Atmospheric Releases for Pits (Ci) 2120	12020	1,000,000	Radionuclide	Atmospheric Releases for Soil Vaults (Ci) 2120	12020	1,000,000
RA224	1.9E-07	6.2E-10	6.1E-10	RA226	1.6E-12	4.3E-09	6.8E-08
RA225	2.4E-12	1.6E-10	2.9E-09	RA228	3.2E-21	3.2E-19	3.5E-17
RA226	8.8E-08	1.7E-09	4.1E-07	AC225	2.1E-19	3.7E-15	2.0E-13
RA228	6.2E-10	6.2E-10	6.1E-10	AC227	1.0E-13	8.9E-12	4.7E-11
AC225	2.3E-12	1.6E-10	2.7E-09	AC228	3.0E-21	3.0E-19	3.3E-17
AC227	4.1E-10	1.9E-09	8.5E-09	TH227	1.0E-13	8.7E-12	4.6E-11
AC228	5.9E-10	5.9E-10	5.9E-10	TH228	3.0E-21	3.0E-19	3.3E-17
TH227	4.0E-10	1.8E-09	8.3E-09	TH229	2.1E-19	3.6E-15	2.0E-13
TH228	1.8E-07	5.8E-10	5.8E-10	TH230	6.2E-11	5.2E-09	6.4E-08
TH229	2.3E-12	1.5E-10	2.7E-09	TH231	4.6E-11	4.6E-11	4.6E-11
TH230	5.2E-12	6.6E-10	3.9E-07	TH232	3.3E-21	3.0E-19	3.3E-17
TH231	8.5E-09	8.5E-09	8.5E-09	TH234	6.4E-08	6.4E-08	6.4E-08
TH232	5.8E-10	5.8E-10	5.8E-10	PA231	1.3E-13	8.9E-12	4.7E-11
TH234	4.2E-07	4.2E-07	4.2E-07	PA233	9.5E-14	2.6E-13	1.9E-13
PA231	2.9E-10	1.8E-09	8.5E-09	PA234M	6.5E-08	6.5E-08	6.5E-08
PA233	3.5E-09	3.5E-09	2.5E-09	PA234	8.4E-11	8.4E-11	1.0E-10
PA234M	4.3E-07	4.3E-07	4.3E-07	U 233	4.1E-17	1.1E-14	2.0E-13
PA234	5.5E-10	5.5E-10	6.8E-10	U 234	6.3E-08	6.3E-08	6.6E-08
U 232	1.8E-07	8.2E-49	0.0E+00	U 235	4.8E-11	4.8E-11	4.8E-11
U 233	1.8E-10	3.2E-10	2.8E-09	U 236	5.8E-13	6.6E-13	6.8E-13
U 234	1.8E-09	1.4E-08	4.1E-07	U 237	6.5E-16	0.0E+00	0.0E+00
U 235	8.8E-09	8.8E-09	8.7E-09	U 238	6.7E-08	6.7E-08	6.7E-08
U 236	1.2E-11	1.2E-11	1.2E-11	NP237	1.3E-13	3.7E-13	2.7E-13
U 237	6.6E-16	6.9E-18	0.0E+00	PU238	1.9E-08	2.0E-42	0.0E+00
U 238	4.4E-07	4.4E-07	4.4E-07	PU239	3.1E-09	2.3E-09	1.0E-21
U 240	2.0E-22	1.5E-20	6.6E-19	PU240	4.1E-10	1.5E-10	6.2E-56
NP237	5.0E-09	5.0E-09	3.6E-09	PU241	2.5E-11	0.0E+00	0.0E+00
NP239	1.9E-10	7.7E-11	3.1E-51	PU242	1.3E-14	1.2E-14	2.0E-15
NP240M	2.8E-22	2.1E-20	9.1E-19	AM241	8.3E-10	1.1E-16	0.0E+00
PU236	1.2E-27	0.0E+00	0.0E+00	CM244	3.1E-14	0.0E+00	0.0E+00
PU238	4.2E-10	4.5E-44	0.0E+00				
PU239	3.1E-08	2.3E-08	1.0E-20				
PU240	2.6E-09	9.0E-10	6.3E-19				
PU241	2.6E-11	2.7E-13	2.3E-48				
PU242	2.9E-11	2.8E-11	4.5E-12				
PU244	2.0E-22	1.5E-20	6.3E-19				
AM241	3.2E-08	2.8E-13	2.5E-48				
AM243	1.4E-10	5.5E-11	2.3E-51				
CM243	1.1E-15	0.0E+00	0.0E+00				
CM244	6.6E-12	0.0E+00	0.0E+00				
CM245	1.4E-13	2.7E-13	2.3E-48				
CM246	1.7E-14	3.9E-15	7.0E-78				
CM248	1.9E-16	1.9E-16	2.5E-17				
CF249	1.3E-11	4.0E-20	0.0E+00				
CF250	5.6E-15	0.0E+00	0.0E+00				
CF252	9.3E-27	0.0E+00	0.0E+00				

B-4 RESULTS

Table B-3 contains the doses for atmospheric releases resulting from biointrusion by harvester ants and plants. These doses represent the doses through the ingestion, inhalation, and external exposure pathways. For both pits and soil vaults, the maximum doses occurred in the year 2120, 100 years after the end of institutional control. The doses for pits ranged from 0.026 to 0.039 mrem/yr; the doses for soil vaults ranged from 0.079 to 0.13 mrem/yr. These doses were well below the 40 CFR 61 NESHAP standard of 10 mrem/yr. The dominant dose contributor for the pits was Cs-137, and the dominant dose contributors for the soil vaults were Cs-137 and Ni-63.

The doses from existing monitored and unmonitored emission points and existing diffuse emission sources at the INEL were reported to be 1.5E-3 mrem/yr in the INEL NESHAP Annual Report (DOE 1993). When the doses for pits were added to the doses from existing sources at the INEL, the INEL-wide doses ranged from 0.026 to 0.039 mrem/yr. When the doses from soil vaults were added to the doses from existing sources at the INEL, the INEL-wide doses ranged from 0.079 to 0.13 mrem/yr. When these doses were added to the dose from gaseous emissions of H-3 and C-14, doses ranged from 0.80 to 0.86 mrem/yr. These INEL-wide doses were also well below the 40 CFR 61 NESHAP standard of 10 mrem/yr.

Table B-3. Atmospheric doses because of biointrusion for pits and soil vaults.

Case	Year	EDE (mrem/yr)
Pits[a]	2120	0.039
Pits[b]	2120	0.026
Pits[a]	12,020	0.0064
Pits[b]	12,020	0.0046
Pits[a]	1,000,000	0.026
Pits[b]	1,000,000	0.019
Soil Vaults[a]	2120	0.13
Soil Vaults[b]	2120	0.079
Soil Vaults[a]	12,020	0.0033
Soil Vaults[b]	12,020	0.0021
Soil Vaults[a]	1,000,000	0.0035
Soil Vaults[b]	1,000,000	0.0024

a. Rupp diet, 8,030 m^3/yr inhalation rate, 0.7 shielding factor.

b. Yang and Nelson diet, 5,840 m^3/yr inhalation rate, 0.36 shielding factor.

B-3 REFERENCES

ASME (American Society of Mechanical Engineers), 1989, "Quality Assurance Program Requirements for Nuclear Facilities," NQA-1.

Baes, C. F., III et al., 1984, A Review and Analysis of Parameters for Assessing Transport of Environmentally Released Radionuclides through Agriculture, ORNL-5786.

Blom, P. E., W. H. Clark, J. B. Johnson, 1991, "Colony Densities of the Seed Harvesting Ant Pogonomyrmex salinus in Seven Plant Communities on the Idaho National Engineering Laboratory", Journal of the Idaho Academy of Science, 27, 1, pp. 28-36.

CFR (Code of Federal Regulations), 1992, "National Emission Standards for Hazardous Air Pollutants (Clean Air Act)," 40 CFR 61, U.S. Environmental Protection Agency, Office of the Federal Register.

Chew, E. W. and R. G. Mitchell, 1988, 1987 Environmental Monitoring Program Report for Idaho National Engineering Laboratory Site, IDO-12082(87).

Dodge, R. L. et al., 1991, Performance Assessment Review Guide for DOE Low-Level Radioactive Waste Disposal Facilities, DOE/LLW-93.

DOE (U.S. Department of Energy), 1988a, "Radioactive Waste Management," DOE Order 5820.2A, September 26.

DOE, 1988b, External Dose-Rate Conversion Factors for Calculation of Dose to the Public, DOE/EH-0070.

DOE, 1988c, Internal Dose Conversion Factors for Calculation of Dose to the Public, DOE/EH-0071.

DOE, 1993, 1992 INEL National Emission Standard for Hazardous Air Pollutants Annual Report, DOE/ID-10342(92).

EPA (U.S. Environmental Protection Agency), 1989, Risk Assessments Methodology, Environmental Impact Statement, NESHAPs for Radionuclides, Background Information Document-Volume 1, EPA/520/1-89-005.

Fraley, L., Jr., 1978, "Revegetation Following a 1974 Fire at the Idaho National Engineering Laboratory," in Ecological Studies on the Idaho National Engineering Laboratory Site 1978 Progress Report, O. D. Markham (ed.), IDO-12087, pp. 194-199.

Groves, C. R. and B. L. Keller, 1983, "Ecological Characteristics of Small Mammals on a Radioactive Waste Disposal Area in Southeastern Idaho," The American Midland Naturalist, 109, 2, pp. 253-265.

Hoff, D. L., E. W. Chew, R. L. Dickson, 1984, 1983 Environmental Monitoring Program Report for Idaho National Engineering Laboratory Site, IDO-12082(83).

Hoff, D. L., E. W. Chew, R. L. Dickson, 1985, 1984 Environmental Monitoring Program Report for Idaho National Engineering Laboratory Site, IDO-12082(84).

Hoff, D. L., E. W. Chew, S. K. Rope, 1986, 1985 Environmental Monitoring Program Report for Idaho National Engineering Laboratory Site, IDO-12082(85).

Hoff, D. L., E. W. Chew, S. K. Rope, 1987, 1986 Environmental Monitoring Program Report for Idaho National Engineering Laboratory Site, IDO-12082(86).

Hoff, D. L., R. G. Mitchell, R. Moore, 1989, The Idaho National Engineering Laboratory Site Environmental Report for Calendar Year 1988, IDO-12082(88).

Hoff, D. L. et al., 1990, The Idaho National Engineering Laboratory Site Environmental Report for Calendar Year 1989, IDO-12082(89).

Hoff, D. L. et al., 1991, The Idaho National Engineering Laboratory Site Environmental Report for Calendar Year 1990, IDO-12082(90).

Kennedy, W. E., Jr., L. L. Cadwell, D. H. McKenzie, 1985, "Biotic Transport of Radionuclides from a Low-Level Radioactive Waste Site," Health Physics, 49, 1, pp. 11-24.

Leonard, P. R., 1992, "Formal Documentation of 1987-1991 INEL Wind Files Used in GENII," EDF SEM-CX21-91-001, EG&G Idaho.

Maheras, S. J., 1993, "Revised RWMC Performance Assessment Atmospheric Pathway Analysis," EDF RWMC-617, Rev. 1, Science Applications International Corporation, November.

McKenzie, D. H. et al., 1982, Relevance of Biotic Pathways to the Long-Term Regulation of Nuclear Waste Disposal, Topical Report on Reference Western Arid Low-Level Sites, NUREG/CR-2675, Volume 2.

Napier, B. A. et al., 1988, GENII - The Hanford Environmental Radiation Dosimetry Software System, Volumes 1-3, PNL-6584.

Peterson, H. T., Jr., 1983, "Terrestrial and Aquatic Food Chain Pathways," Chapter 5 in Radiological Assessment: A Textbook on Environmental Dose Analysis, J. E. Till and H. R. Meyer (eds.), NUREG/CR-3332.

Reynolds, T. D. and L. Fraley, Jr., 1989, "Root Profiles of Some Native and Exotic Plant Species in Southeastern Idaho, Environmental and Experimental Botany, 29, pp. 241-248.

Reynolds, T. D. and W. L. Wakkinen, 1987, "Characteristics of the Burrows of Four Species of Rodents in Undisturbed Soils in Southeastern Idaho," The American Midland Naturalist, 118, 2, pp. 245-250.

Reynolds, T. D. and J. W. Laundre, 1988, "Vertical Distribution of Soil Removed by Four Species of Burrowing Rodents in Disturbed and Undisturbed Soils, Health Physics, 54, 4, pp. 445-450.

Rupp, E. M., 1980, "Age-Dependent Values of Dietary Intake for Assessing Human Exposures to Environmental Pollutants", Health Physics, 39, pp. 151-163.

Wood, D. E. et al., 1992, Performance Assessment Task Team Draft Progress Report, DOE/LLW-157, Rev. 0.

Yang, Y. Y. and C. B. Nelson, 1984, An Estimation of the Daily Average Food Intake by Age and Sex for Use in Assessing the Radionuclide Intake of Individuals in the General Population, EPA 520/1-84-021.

Yang, Y. Y. and C. B. Nelson, 1986, "An Estimation of Daily Food Usage factors for Assessing Radionuclide Intakes in the U.S. Population," Health Physics, 50, 2, pp. 245-257.

APPENDIX C

DOSES TO INADVERTENT INTRUDERS

APPENDIX C
DOSES TO INADVERTENT INTRUDERS

C-1 INTRODUCTION

This appendix contains detailed tables used in inadvertent intruder analyses. The analyses are described in Chapter 3, and the results are described in Chapter 4.

C-2 WASTE CONCENTRATIONS AND INVENTORIES FOR INTRUDER ANALYSES

Table C-1 contains the radionuclide concentrations in the waste and on the surface for intruder analyses for pits from 2120 through 12,020. Table C-2 contains the radionuclide concentrations in the waste and on the surface for intruder analyses for soil vault rows from 2120 through 12,020.

C-3 INADVERTENT INTRUDER RESULTS

Table C-3 contains the results for acute intruder-drilling and acute intruder-construction scenarios. Table C-4 contains the maximum chronic intruder agriculture results. Table C-5 contains the chronic intruder-agriculture results for pits, and Table C-6 contains the chronic intruder-agriculture results for soil vault rows.

Table C-1. Radionuclide waste concentration, surface concentration, and surface areal concentration for 2120 through 12,020 for pits.

	Waste Concentration (Ci/m^3)					Surface Concentration (Ci/m^3)[a]					Surface Areal Concentration (Ci/m^2)[a]				
Radionuclide	2120	3020	5020	7020	12020	2120[b]	3020[c]	5020[c]	7020[c]	12020[c]	2120[d]	3020[d]	5020[d]	7020[d]	12020[d]
H 3	3.1E-05	3.5E-27	0.0E+00	0.0E+00	0.0E+00	3.7E-09	1.3E-28	0.0E+00	0.0E+00	0.0E+00	2.1E-08	2.4E-30	0.0E+00	0.0E+00	0.0E+00
C 14	2.2E-06	2.0E-06	1.6E-06	1.2E-06	6.8E-07	2.7E-10	7.3E-08	5.7E-08	4.5E-08	2.5E-08	1.5E-09	1.4E-09	1.1E-09	8.4E-10	4.6E-10
NA22	2.1E-18	0.0E+00	0.0E+00	0.0E+00	0.0E+00	2.6E-22	0.0E+00	0.0E+00	0.0E+00	0.0E+00	1.5E-21	0.0E+00	0.0E+00	0.0E+00	0.0E+00
K 40	9.9E-06	9.9E-06	9.9E-06	9.9E-06	9.9E-06	1.2E-09	3.6E-07	3.6E-07	3.6E-07	3.6E-07	6.8E-09	6.8E-09	6.8E-09	6.8E-09	6.8E-09
MN54	5.5E-39	0.0E+00	0.0E+00	0.0E+00	0.0E+00	6.7E-43	0.0E+00	0.0E+00	0.0E+00	0.0E+00	3.8E-42	0.0E+00	0.0E+00	0.0E+00	0.0E+00
FE55	1.3E-15	0.0E+00	0.0E+00	0.0E+00	0.0E+00	1.5E-19	0.0E+00	0.0E+00	0.0E+00	0.0E+00	8.7E-19	0.0E+00	0.0E+00	0.0E+00	0.0E+00
CO60	6.4E-09	0.0E+00	0.0E+00	0.0E+00	0.0E+00	7.7E-13	0.0E+00	0.0E+00	0.0E+00	0.0E+00	4.3E-12	0.0E+00	0.0E+00	0.0E+00	0.0E+00
NI63	5.5E-02	6.2E-05	1.8E-11	5.1E-18	2.2E-34	6.6E-06	2.3E-06	6.5E-13	1.9E-19	8.1E-36	3.7E-05	4.2E-08	1.2E-14	3.5E-21	1.5E-37
ZN65	0.0E+00	0.0E+00	0.0E+00	0.0E+00	0.0E+00	0.0E+00	0.0E+00	0.0E+00	0.0E+00	0.0E+00	0.0E+00	0.0E+00	0.0E+00	0.0E+00	0.0E+00
SE75	0.0E+00	0.0E+00	0.0E+00	0.0E+00	0.0E+00	0.0E+00	0.0E+00	0.0E+00	0.0E+00	0.0E+00	0.0E+00	0.0E+00	0.0E+00	0.0E+00	0.0E+00
SR85	0.0E+00	0.0E+00	0.0E+00	0.0E+00	0.0E+00	0.0E+00	0.0E+00	0.0E+00	0.0E+00	0.0E+00	0.0E+00	0.0E+00	0.0E+00	0.0E+00	0.0E+00
SR89	0.0E+00	0.0E+00	0.0E+00	0.0E+00	0.0E+00	0.0E+00	0.0E+00	0.0E+00	0.0E+00	0.0E+00	0.0E+00	0.0E+00	0.0E+00	0.0E+00	0.0E+00
SR90	1.6E-03	7.8E-13	1.7E-33	0.0E+00	0.0E+00	1.9E-07	2.9E-14	6.1E-35	0.0E+00	0.0E+00	1.1E-06	5.3E-16	1.1E-36	0.0E+00	0.0E+00
Y 90	1.6E-03	7.8E-13	1.7E-33	0.0E+00	0.0E+00	1.9E-07	2.9E-14	6.1E-35	0.0E+00	0.0E+00	1.1E-06	5.3E-16	1.1E-36	0.0E+00	0.0E+00
ZR93	4.8E-15	4.8E-15	4.8E-15	4.8E-15	4.8E-15	5.8E-19	1.8E-16	1.8E-16	1.8E-16	1.8E-16	3.3E-18	3.3E-18	3.3E-18	3.3E-18	3.3E-18
ZR95	0.0E+00	0.0E+00	0.0E+00	0.0E+00	0.0E+00	0.0E+00	0.0E+00	0.0E+00	0.0E+00	0.0E+00	0.0E+00	0.0E+00	0.0E+00	0.0E+00	0.0E+00
NB93M	4.6E-15	4.6E-15	4.6E-15	4.6E-15	4.6E-15	5.5E-19	1.7E-16	1.7E-16	1.7E-16	1.7E-16	3.1E-18	3.1E-18	3.1E-18	3.1E-18	3.1E-18
NB94	4.0E-10	3.9E-10	3.6E-10	3.4E-10	2.8E-10	4.8E-14	1.4E-11	1.3E-11	1.2E-11	1.0E-11	2.7E-13	2.6E-13	2.5E-13	2.3E-13	1.9E-13
NB95	0.0E+00	0.0E+00	0.0E+00	0.0E+00	0.0E+00	0.0E+00	0.0E+00	0.0E+00	0.0E+00	0.0E+00	0.0E+00	0.0E+00	0.0E+00	0.0E+00	0.0E+00
NB95M	0.0E+00	0.0E+00	0.0E+00	0.0E+00	0.0E+00	0.0E+00	0.0E+00	0.0E+00	0.0E+00	0.0E+00	0.0E+00	0.0E+00	0.0E+00	0.0E+00	0.0E+00
TC99	2.9E-08	2.9E-08	2.9E-08	2.9E-08	2.8E-08	3.6E-12	1.1E-09	1.1E-09	1.1E-09	1.0E-09	2.0E-11	2.0E-11	2.0E-11	2.0E-11	1.9E-11
RU103	0.0E+00	0.0E+00	0.0E+00	0.0E+00	0.0E+00	0.0E+00	0.0E+00	0.0E+00	0.0E+00	0.0E+00	0.0E+00	0.0E+00	0.0E+00	0.0E+00	0.0E+00
RU106	7.7E-31	0.0E+00	0.0E+00	0.0E+00	0.0E+00	9.3E-35	0.0E+00	0.0E+00	0.0E+00	0.0E+00	5.2E-34	0.0E+00	0.0E+00	0.0E+00	0.0E+00
RH106	7.7E-31	0.0E+00	0.0E+00	0.0E+00	0.0E+00	9.3E-35	0.0E+00	0.0E+00	0.0E+00	0.0E+00	5.2E-34	0.0E+00	0.0E+00	0.0E+00	0.0E+00
AG108	5.7E-10	4.2E-12	7.6E-17	1.4E-21	1.9E-33	6.9E-14	1.5E-13	2.8E-18	5.0E-23	7.1E-35	3.9E-13	2.8E-15	5.2E-20	9.4E-25	1.3E-36
AG108M	6.4E-09	4.7E-11	8.5E-16	1.5E-20	2.2E-32	7.7E-13	1.7E-12	3.1E-17	5.7E-22	8.0E-34	4.3E-12	3.2E-14	5.8E-19	1.1E-23	1.5E-35
AG109M	5.0E-32	0.0E+00	0.0E+00	0.0E+00	0.0E+00	6.1E-36	0.0E+00	0.0E+00	0.0E+00	0.0E+00	3.4E-35	0.0E+00	0.0E+00	0.0E+00	0.0E+00
AG110	0.0E+00	0.0E+00	0.0E+00	0.0E+00	0.0E+00	0.0E+00	0.0E+00	0.0E+00	0.0E+00	0.0E+00	0.0E+00	0.0E+00	0.0E+00	0.0E+00	0.0E+00
AG110M	0.0E+00	0.0E+00	0.0E+00	0.0E+00	0.0E+00	0.0E+00	0.0E+00	0.0E+00	0.0E+00	0.0E+00	0.0E+00	0.0E+00	0.0E+00	0.0E+00	0.0E+00
CD109	5.0E-32	0.0E+00	0.0E+00	0.0E+00	0.0E+00	6.1E-36	0.0E+00	0.0E+00	0.0E+00	0.0E+00	3.4E-35	0.0E+00	0.0E+00	0.0E+00	0.0E+00
IN113M	0.0E+00	0.0E+00	0.0E+00	0.0E+00	0.0E+00	0.0E+00	0.0E+00	0.0E+00	0.0E+00	0.0E+00	0.0E+00	0.0E+00	0.0E+00	0.0E+00	0.0E+00
SN113	0.0E+00	0.0E+00	0.0E+00	0.0E+00	0.0E+00	0.0E+00	0.0E+00	0.0E+00	0.0E+00	0.0E+00	0.0E+00	0.0E+00	0.0E+00	0.0E+00	0.0E+00
SN117M	0.0E+00	0.0E+00	0.0E+00	0.0E+00	0.0E+00	0.0E+00	0.0E+00	0.0E+00	0.0E+00	0.0E+00	0.0E+00	0.0E+00	0.0E+00	0.0E+00	0.0E+00
SB124	0.0E+00	0.0E+00	0.0E+00	0.0E+00	0.0E+00	0.0E+00	0.0E+00	0.0E+00	0.0E+00	0.0E+00	0.0E+00	0.0E+00	0.0E+00	0.0E+00	0.0E+00
SB125	2.1E-15	0.0E+00	0.0E+00	0.0E+00	0.0E+00	2.6E-19	0.0E+00	0.0E+00	0.0E+00	0.0E+00	1.4E-18	0.0E+00	0.0E+00	0.0E+00	0.0E+00
TE125M	5.2E-16	0.0E+00	0.0E+00	0.0E+00	0.0E+00	6.3E-20	0.0E+00	0.0E+00	0.0E+00	0.0E+00	3.5E-19	0.0E+00	0.0E+00	0.0E+00	0.0E+00
I 129	1.0E-06	1.0E-06	1.0E-06	1.0E-06	1.0E-06	1.2E-10	3.7E-08	3.7E-08	3.7E-08	3.7E-08	7.0E-10	7.0E-10	7.0E-10	7.0E-10	6.9E-10
CS134	2.4E-19	0.0E+00	0.0E+00	0.0E+00	0.0E+00	3.0E-23	0.0E+00	0.0E+00	0.0E+00	0.0E+00	1.7E-22	0.0E+00	0.0E+00	0.0E+00	0.0E+00
CS137	3.9E-03	3.6E-12	3.1E-32	0.0E+00	0.0E+00	4.7E-07	1.3E-13	1.1E-33	0.0E+00	0.0E+00	2.7E-06	2.5E-15	2.1E-35	0.0E+00	0.0E+00
BA133	2.0E-15	1.2E-40	0.0E+00	0.0E+00	0.0E+00	2.5E-19	4.4E-42	0.0E+00	0.0E+00	0.0E+00	1.4E-18	8.2E-44	0.0E+00	0.0E+00	0.0E+00
BA137M	3.7E-03	3.4E-12	2.9E-32	0.0E+00	0.0E+00	4.5E-07	1.3E-13	1.1E-33	0.0E+00	0.0E+00	2.5E-06	2.3E-15	2.0E-35	0.0E+00	0.0E+00
BA140	0.0E+00	0.0E+00	0.0E+00	0.0E+00	0.0E+00	0.0E+00	0.0E+00	0.0E+00	0.0E+00	0.0E+00	0.0E+00	0.0E+00	0.0E+00	0.0E+00	0.0E+00
LA140	0.0E+00	0.0E+00	0.0E+00	0.0E+00	0.0E+00	0.0E+00	0.0E+00	0.0E+00	0.0E+00	0.0E+00	0.0E+00	0.0E+00	0.0E+00	0.0E+00	0.0E+00

Table C-1. (continued).

	Waste Concentration (Ci/m³)					Surface Concentration (Ci/m³)					Surface Areal Concentration (Ci/m²)				
Radionuclide	2120	3020	5020	7020	12020	2120	3020	5020	7020	12020	2120	3020	5020	7020	12020
CE144	3.2E-43	0.0E+00	0.0E+00	0.0E+00	0.0E+00	3.8E-47	0.0E+00	0.0E+00	0.0E+00	0.0E+00	2.1E-46	0.0E+00	0.0E+00	0.0E+00	0.0E+00
PR144	0.0E+00	0.0E+00	0.0E+00	0.0E+00	0.0E+00	0.0E+00	0.0E+00	0.0E+00	0.0E+00	0.0E+00	0.0E+00	0.0E+00	0.0E+00	0.0E+00	0.0E+00
ND144	3.5E-18	3.5E-18	3.5E-18	3.5E-18	3.5E-18	4.3E-22	1.3E-19	1.3E-19	1.3E-19	1.3E-19	2.4E-21	2.4E-21	2.4E-21	2.4E-21	2.4E-21
PM147	1.5E-23	0.0E+00	0.0E+00	0.0E+00	0.0E+00	1.8E-27	0.0E+00	0.0E+00	0.0E+00	0.0E+00	1.0E-26	0.0E+00	0.0E+00	0.0E+00	0.0E+00
SM147	1.9E-18	1.9E-18	1.9E-18	1.9E-18	1.9E-18	2.4E-22	7.1E-20	7.1E-20	7.1E-20	7.1E-20	1.3E-21	1.3E-21	1.3E-21	1.3E-21	1.3E-21
EU152	1.0E-07	1.2E-27	0.0E+00	0.0E+00	0.0E+00	1.2E-11	4.4E-29	0.0E+00	0.0E+00	0.0E+00	6.8E-11	8.2E-31	0.0E+00	0.0E+00	0.0E+00
EU154	1.5E-08	4.7E-40	0.0E+00	0.0E+00	0.0E+00	1.8E-12	1.7E-41	0.0E+00	0.0E+00	0.0E+00	1.0E-11	3.2E-43	0.0E+00	0.0E+00	0.0E+00
EU155	2.5E-11	0.0E+00	0.0E+00	0.0E+00	0.0E+00	3.0E-15	0.0E+00	0.0E+00	0.0E+00	0.0E+00	1.7E-14	0.0E+00	0.0E+00	0.0E+00	0.0E+00
GD152	3.1E-18	3.1E-18	3.1E-18	3.1E-18	3.1E-18	3.8E-22	1.1E-19	1.1E-19	1.1E-19	1.1E-19	2.1E-21	2.1E-21	2.1E-21	2.1E-21	2.1E-21
IR192	0.0E+00	0.0E+00	0.0E+00	0.0E+00	0.0E+00	0.0E+00	0.0E+00	0.0E+00	0.0E+00	0.0E+00	0.0E+00	0.0E+00	0.0E+00	0.0E+00	0.0E+00
HG203	0.0E+00	0.0E+00	0.0E+00	0.0E+00	0.0E+00	0.0E+00	0.0E+00	0.0E+00	0.0E+00	0.0E+00	0.0E+00	0.0E+00	0.0E+00	0.0E+00	0.0E+00
TL207	9.5E-08	1.0E-07	1.8E-07	2.5E-07	4.3E-07	1.2E-11	3.8E-09	6.6E-09	9.3E-09	1.6E-08	6.5E-11	7.0E-11	1.2E-10	1.7E-10	2.9E-10
TL208	1.5E-05	5.1E-08	4.9E-08	4.9E-08	4.9E-08	1.9E-09	1.9E-09	1.8E-09	1.8E-09	1.8E-09	1.0E-08	3.5E-11	3.3E-11	3.3E-11	3.3E-11
TL209	1.1E-11	8.3E-11	2.4E-10	4.0E-10	7.8E-10	1.4E-15	3.0E-12	8.8E-12	1.4E-11	2.8E-11	7.8E-15	5.7E-14	1.6E-13	2.7E-13	5.3E-13
PB209	5.3E-10	3.9E-09	1.1E-08	1.8E-08	3.6E-08	6.4E-14	1.4E-10	4.1E-10	6.7E-10	1.3E-09	3.6E-13	2.6E-12	7.6E-12	1.3E-11	2.4E-11
PB210	1.9E-05	1.3E-05	5.5E-06	2.3E-06	3.7E-07	2.3E-09	4.8E-07	2.0E-07	8.5E-08	1.3E-08	1.3E-08	8.9E-09	3.8E-09	1.6E-09	2.5E-10
PB211	9.5E-08	1.0E-07	1.8E-07	2.6E-07	4.3E-07	1.2E-11	3.8E-09	6.6E-09	9.3E-09	1.6E-08	6.5E-11	7.0E-11	1.2E-10	1.7E-10	2.9E-10
PB212	4.3E-05	1.4E-07	1.4E-07	1.4E-07	1.4E-07	5.2E-09	5.2E-09	4.9E-09	4.9E-09	4.9E-09	2.9E-08	9.7E-11	9.2E-11	9.2E-11	9.2E-11
PB214	1.9E-05	1.3E-05	5.5E-06	2.3E-06	3.7E-07	2.3E-09	4.8E-07	2.0E-07	8.5E-08	1.3E-08	1.3E-08	8.9E-09	3.8E-09	1.6E-09	2.5E-10
BI210	1.9E-05	1.3E-05	5.5E-06	2.3E-06	3.7E-07	2.3E-09	4.8E-07	2.0E-07	8.5E-08	1.3E-08	1.3E-08	8.9E-09	3.8E-09	1.6E-09	2.5E-10
BI211	9.5E-08	1.0E-07	1.8E-07	2.6E-07	4.3E-07	1.2E-11	3.8E-09	6.6E-09	9.3E-09	1.6E-08	6.5E-11	7.0E-11	1.2E-10	1.7E-10	2.9E-10
BI212	4.3E-05	1.4E-07	1.4E-07	1.4E-07	1.4E-07	5.2E-09	5.2E-09	4.9E-09	4.9E-09	4.9E-09	2.9E-08	9.7E-11	9.2E-11	9.2E-11	9.2E-11
BI213	5.3E-10	3.9E-09	1.1E-08	1.8E-08	3.6E-08	6.4E-14	1.4E-10	4.1E-10	6.7E-10	1.3E-09	3.6E-13	2.6E-12	7.6E-12	1.3E-11	2.4E-11
BI214	1.9E-05	1.3E-05	5.5E-06	2.3E-06	3.7E-07	2.3E-09	4.8E-07	2.0E-07	8.5E-08	1.3E-08	1.3E-08	8.9E-09	3.8E-09	1.6E-09	2.5E-10
PO210	1.9E-05	1.3E-05	5.5E-06	2.3E-06	3.7E-07	2.3E-09	4.8E-07	2.0E-07	8.5E-08	1.3E-08	1.3E-08	8.9E-09	3.8E-09	1.6E-09	2.5E-10
PO211	2.7E-10	2.9E-10	5.1E-10	7.1E-10	1.2E-09	3.2E-14	1.1E-11	1.8E-11	2.6E-11	4.4E-11	1.8E-13	2.0E-13	3.5E-13	4.9E-13	8.2E-13
PO212	2.7E-05	9.1E-08	8.7E-08	8.7E-08	8.7E-08	3.3E-09	3.3E-09	3.2E-09	3.2E-09	3.2E-09	1.9E-08	6.2E-11	5.9E-11	5.9E-11	5.9E-11
PO213	5.2E-10	3.8E-09	1.1E-08	1.8E-08	3.5E-08	6.3E-14	1.4E-10	4.0E-10	6.5E-10	1.3E-09	3.5E-13	2.6E-12	7.4E-12	1.2E-11	2.4E-11
PO214	1.9E-05	1.3E-05	5.5E-06	2.3E-06	3.7E-07	2.3E-09	4.8E-07	2.0E-07	8.5E-08	1.3E-08	1.3E-08	8.9E-09	3.8E-09	1.6E-09	2.5E-10
PO215	9.5E-08	1.0E-07	1.8E-07	2.6E-07	4.3E-07	1.2E-11	3.8E-09	6.6E-09	9.3E-09	1.6E-08	6.5E-11	7.0E-11	1.2E-10	1.7E-10	2.9E-10
PO216	4.3E-05	1.4E-07	1.4E-07	1.4E-07	1.4E-07	5.2E-09	5.2E-09	4.9E-09	4.9E-09	4.9E-09	2.9E-08	9.7E-11	9.2E-11	9.2E-11	9.2E-11
PO218	1.9E-05	1.3E-05	5.5E-06	2.3E-06	3.7E-07	2.3E-09	4.8E-07	2.0E-07	8.5E-08	1.3E-08	1.3E-08	8.9E-09	3.8E-09	1.6E-09	2.5E-10
AT217	5.3E-10	3.9E-09	1.1E-08	1.8E-08	3.6E-08	6.4E-14	1.4E-10	4.1E-10	6.7E-10	1.3E-09	3.6E-13	2.6E-12	7.6E-12	1.3E-11	2.4E-11
RN219	9.5E-08	1.0E-07	1.8E-07	2.6E-07	4.3E-07	1.2E-11	3.8E-09	6.6E-09	9.3E-09	1.6E-08	6.5E-11	7.0E-11	1.2E-10	1.7E-10	2.9E-10
RN220	4.3E-05	1.4E-07	1.4E-07	1.4E-07	1.4E-07	5.2E-09	5.2E-09	4.9E-09	4.9E-09	4.9E-09	2.9E-08	9.7E-11	9.2E-11	9.2E-11	9.2E-11
RN222	1.9E-05	1.3E-05	5.5E-06	2.3E-06	3.7E-07	2.3E-09	4.8E-07	2.0E-07	8.5E-08	1.3E-08	1.3E-08	8.9E-09	3.8E-09	1.6E-09	2.5E-10
FR221	5.3E-10	3.9E-09	1.1E-08	1.8E-08	3.6E-08	6.4E-14	1.4E-10	4.1E-10	6.7E-10	1.3E-09	3.6E-13	2.6E-12	7.6E-12	1.3E-11	2.4E-11
FR223	1.3E-09	1.4E-09	2.5E-09	3.5E-09	5.9E-09	1.6E-13	5.2E-11	9.1E-11	1.3E-10	2.2E-10	9.0E-13	9.7E-13	1.7E-12	2.4E-12	4.0E-12
RA223	9.5E-08	1.0E-07	1.8E-07	2.6E-07	4.3E-07	1.2E-11	3.8E-09	6.6E-09	9.3E-09	1.6E-08	6.5E-11	7.0E-11	1.2E-10	1.7E-10	2.9E-10
RA224	4.3E-05	1.4E-07	1.4E-07	1.4E-07	1.4E-07	5.2E-09	5.2E-09	4.9E-09	4.9E-09	4.9E-09	2.9E-08	9.7E-11	9.2E-11	9.2E-11	9.2E-11
RA225	5.3E-10	3.9E-09	1.1E-08	1.8E-08	3.6E-08	6.4E-14	1.4E-10	4.1E-10	6.7E-10	1.3E-09	3.6E-13	2.6E-12	7.6E-12	1.3E-11	2.4E-11
RA226	1.9E-05	1.3E-05	5.5E-06	2.3E-06	3.7E-07	2.3E-09	4.8E-07	2.0E-07	8.5E-08	1.3E-08	1.3E-08	8.9E-09	3.8E-09	1.6E-09	2.5E-10
RA228	1.4E-07	1.4E-07	1.4E-07	1.4E-07	1.4E-07	1.6E-11	4.9E-09	4.9E-09	4.9E-09	4.9E-09	9.2E-11	9.2E-11	9.2E-11	9.2E-11	9.2E-11
AC225	5.3E-10	3.9E-09	1.1E-08	1.8E-08	3.6E-08	6.4E-14	1.4E-10	4.1E-10	6.7E-10	1.3E-09	3.6E-13	2.6E-12	7.6E-12	1.3E-11	2.4E-11
AC227	9.5E-08	1.0E-07	1.8E-07	2.6E-07	4.3E-07	1.2E-11	3.8E-09	6.6E-09	9.3E-09	1.6E-08	6.5E-11	7.0E-11	1.2E-10	1.7E-10	2.9E-10
AC228	1.4E-07	1.4E-07	1.4E-07	1.4E-07	1.4E-07	1.6E-11	4.9E-09	4.9E-09	4.9E-09	4.9E-09	9.2E-11	9.2E-11	9.2E-11	9.2E-11	9.2E-11

Table C-1. (continued).

	Waste Concentration (Ci/m³)					Surface Concentration (Ci/m³)					Surface Areal Concentration (Ci/m²)				
Radionuclide	2120	3020	5020	7020	12020	2120	3020	5020	7020	12020	2120	3020	5020	7020	12020
TH227	9.4E-08	1.0E-07	1.8E-07	2.5E-07	4.2E-07	1.1E-11	3.7E-09	6.5E-09	9.2E-09	1.5E-08	6.4E-11	7.0E-11	1.2E-10	1.7E-10	2.9E-10
TH228	4.3E-05	1.4E-07	1.4E-07	1.4E-07	1.4E-07	5.2E-09	5.2E-09	4.9E-09	4.9E-09	4.9E-09	2.9E-08	9.7E-11	9.2E-11	9.2E-11	9.2E-11
TH229	5.3E-10	3.9E-09	1.1E-08	1.8E-08	3.6E-08	6.4E-14	1.4E-10	4.1E-10	6.7E-10	1.3E-09	3.6E-13	2.6E-12	7.6E-12	1.3E-11	2.4E-11
TH230	1.2E-09	5.4E-09	2.2E-08	4.8E-08	1.5E-07	1.5E-13	2.0E-10	8.0E-10	1.7E-09	5.6E-09	8.3E-13	3.7E-12	1.5E-11	3.3E-11	1.0E-10
TH231	2.0E-06	2.0E-06	2.0E-06	2.0E-06	2.0E-06	2.4E-10	7.2E-08	7.2E-08	7.2E-08	7.2E-08	1.3E-09	1.3E-09	1.3E-09	1.3E-09	1.3E-09
TH232	1.4E-07	1.4E-07	1.4E-07	1.4E-07	1.4E-07	1.6E-11	4.9E-09	4.9E-09	4.9E-09	4.9E-09	9.2E-11	9.2E-11	9.2E-11	9.2E-11	9.2E-11
TH234	9.9E-05	9.9E-05	9.9E-05	9.9E-05	9.9E-05	1.2E-08	3.6E-06	3.6E-06	3.6E-06	3.6E-06	6.7E-08	6.7E-08	6.7E-08	6.7E-08	6.7E-08
PA231	6.7E-08	1.0E-07	1.8E-07	2.6E-07	4.3E-07	8.2E-12	3.8E-09	6.6E-09	9.3E-09	1.6E-08	4.6E-11	7.0E-11	1.2E-10	1.7E-10	2.9E-10
PA233	8.1E-07	8.1E-07	8.1E-07	8.1E-07	8.1E-07	9.8E-11	3.0E-08	3.0E-08	3.0E-08	3.0E-08	5.5E-10	5.5E-10	5.5E-10	5.5E-10	5.5E-10
PA234M	9.9E-05	9.9E-05	9.9E-05	9.9E-05	9.9E-05	1.2E-08	3.6E-06	3.6E-06	3.6E-06	3.6E-06	6.7E-08	6.7E-08	6.7E-08	6.7E-08	6.7E-08
PA234	1.3E-07	1.3E-07	1.3E-07	1.3E-07	1.3E-07	1.6E-11	4.7E-09	4.7E-09	4.7E-09	4.7E-09	8.7E-11	8.7E-11	8.7E-11	8.7E-11	8.7E-11
U 232	4.1E-05	7.1E-09	3.1E-17	1.3E-25	1.8E-46	5.0E-09	2.6E-10	1.1E-18	4.9E-27	6.7E-48	2.8E-08	4.9E-12	2.1E-20	9.1E-29	1.3E-49
U 233	4.0E-08	4.3E-08	5.0E-08	5.6E-08	7.3E-08	4.8E-12	1.6E-09	1.8E-09	2.0E-09	2.6E-09	2.7E-11	2.9E-11	3.4E-11	3.8E-11	4.9E-11
U 234	4.0E-07	6.5E-07	1.2E-06	1.8E-06	3.1E-06	4.8E-11	2.4E-08	4.4E-08	6.4E-08	1.1E-07	2.7E-10	4.4E-10	8.2E-10	1.2E-09	2.1E-09
U 235	2.0E-06	2.0E-06	2.0E-06	2.0E-06	2.0E-06	2.4E-10	7.2E-08	7.2E-08	7.2E-08	7.2E-08	1.3E-09	1.3E-09	1.3E-09	1.3E-09	1.3E-09
U 236	2.7E-09	2.7E-09	2.7E-09	2.7E-09	2.8E-09	3.2E-13	9.8E-11	9.9E-11	1.0E-10	1.0E-10	1.8E-12	1.8E-12	1.8E-12	1.9E-12	1.9E-12
U 237	1.5E-13	2.8E-15	2.7E-15	2.3E-15	1.6E-15	1.8E-17	1.0E-16	1.0E-16	8.5E-17	5.7E-17	1.0E-16	1.9E-18	1.9E-18	1.6E-18	1.1E-18
U 238	9.9E-05	9.9E-05	9.9E-05	9.9E-05	9.9E-05	1.2E-08	3.6E-06	3.6E-06	3.6E-06	3.6E-06	6.7E-08	6.7E-08	6.7E-08	6.7E-08	6.7E-08
U 240	4.6E-20	3.6E-19	1.1E-18	1.7E-18	3.5E-18	5.6E-24	1.3E-20	3.8E-20	6.4E-20	1.3E-19	3.1E-23	2.5E-22	7.2E-22	1.2E-21	2.4E-21
NP237	8.1E-07	8.1E-07	8.1E-07	8.1E-07	8.1E-07	9.8E-11	3.0E-08	3.0E-08	3.0E-08	3.0E-08	5.5E-10	5.5E-10	5.5E-10	5.5E-10	5.5E-10
NP239	3.2E-08	2.9E-08	2.4E-08	2.0E-08	1.3E-08	3.9E-12	1.1E-09	8.8E-10	7.3E-10	4.6E-10	2.2E-11	2.0E-11	1.7E-11	1.4E-11	8.6E-12
NP240M	4.6E-20	3.6E-19	1.1E-18	1.7E-18	3.5E-18	5.6E-24	1.3E-20	3.8E-20	6.4E-20	1.3E-19	3.1E-23	2.5E-22	7.2E-22	1.2E-21	2.4E-21
PU236	2.7E-25	0.0E+00	0.0E+00	0.0E+00	0.0E+00	3.3E-29	0.0E+00	0.0E+00	0.0E+00	0.0E+00	1.9E-28	0.0E+00	0.0E+00	0.0E+00	0.0E+00
PU238	9.7E-08	7.9E-11	1.1E-17	1.5E-24	1.1E-41	1.2E-11	2.9E-12	4.0E-19	5.5E-26	3.8E-43	6.6E-11	5.4E-14	7.4E-21	1.0E-27	7.2E-45
PU239	7.2E-06	7.0E-06	6.6E-06	6.2E-06	5.4E-06	8.7E-10	2.6E-07	2.4E-07	2.3E-07	2.0E-07	4.9E-09	4.8E-09	4.5E-09	4.3E-09	3.7E-09
PU240	6.0E-07	5.5E-07	4.4E-07	3.6E-07	2.1E-07	7.3E-11	2.0E-08	1.6E-08	1.3E-08	7.7E-09	4.1E-10	3.7E-10	3.0E-10	2.4E-10	1.4E-10
PU241	6.1E-09	1.1E-10	1.1E-10	9.5E-11	6.3E-11	7.4E-13	4.1E-12	4.1E-12	3.5E-12	2.3E-12	4.2E-12	7.7E-14	7.6E-14	6.5E-14	4.3E-14
PU242	6.7E-09	6.7E-09	6.6E-09	6.6E-09	6.6E-09	8.1E-13	2.4E-10	2.4E-10	2.4E-10	2.4E-10	4.6E-12	4.5E-12	4.5E-12	4.5E-12	4.5E-12
PU244	4.6E-20	3.6E-19	1.1E-18	1.7E-18	3.5E-18	5.6E-24	1.3E-20	3.8E-20	6.4E-20	1.3E-19	3.1E-23	2.5E-22	7.2E-22	1.2E-21	2.4E-21
AM241	7.3E-06	1.7E-06	7.0E-08	2.9E-09	6.4E-11	8.9E-10	6.3E-08	2.6E-09	1.1E-10	2.3E-12	5.0E-09	1.2E-09	4.8E-11	2.0E-12	4.4E-14
AM243	3.2E-08	2.9E-08	2.4E-08	2.0E-08	1.3E-08	3.9E-12	1.1E-09	8.8E-10	7.3E-10	4.6E-10	2.2E-11	2.0E-11	1.7E-11	1.4E-11	8.6E-12
CM243	2.5E-13	7.7E-23	5.8E-44	0.0E+00	0.0E+00	3.0E-17	2.8E-24	2.1E-45	0.0E+00	0.0E+00	1.7E-16	5.3E-26	3.9E-47	0.0E+00	0.0E+00
CM244	1.5E-09	1.7E-24	0.0E+00	0.0E+00	0.0E+00	1.9E-13	6.1E-26	0.0E+00	0.0E+00	0.0E+00	1.0E-12	1.1E-27	0.0E+00	0.0E+00	0.0E+00
CM245	3.2E-11	1.1E-10	1.1E-10	9.5E-11	6.3E-11	3.9E-15	4.1E-12	4.1E-12	3.5E-12	2.3E-12	2.2E-14	7.7E-14	7.6E-14	6.5E-14	4.3E-14
CM246	3.9E-12	3.4E-12	2.5E-12	1.9E-12	9.1E-13	4.7E-16	1.2E-13	9.3E-14	6.9E-14	3.3E-14	2.6E-15	2.3E-15	1.7E-15	1.3E-15	6.2E-16
CM248	4.5E-14	4.5E-14	4.5E-14	4.5E-14	4.4E-14	5.5E-18	1.7E-15	1.6E-15	1.6E-15	1.6E-15	3.1E-17	3.1E-17	3.1E-17	3.1E-17	3.0E-17
CF249	2.5E-09	4.3E-10	8.2E-12	1.6E-13	8.0E-18	3.1E-13	1.6E-11	3.0E-13	5.8E-15	2.9E-19	1.7E-12	2.9E-13	5.6E-15	1.1E-16	5.5E-21
CF250	1.1E-12	2.2E-33	0.0E+00	0.0E+00	0.0E+00	1.4E-16	7.9E-35	0.0E+00	0.0E+00	0.0E+00	7.6E-16	1.5E-36	0.0E+00	0.0E+00	0.0E+00
CF252	1.8E-24	0.0E+00	0.0E+00	0.0E+00	0.0E+00	2.2E-28	0.0E+00	0.0E+00	0.0E+00	0.0E+00	1.3E-27	0.0E+00	0.0E+00	0.0E+00	0.0E+00

a. These data are based on ORIGEN2 calculations and may differ slightly from decay and ingrowth data derived from MICROSHIELD.
b. Surface concentration is based on bringing 0.2 m³ of contaminated cuttings to the surface while drilling an 8-in. well.
c. Surface concentration is based on bringing 60.2 m³ of contaminated cuttings to the surface while drilling an 8-in. well and excavating a basement.
d. Surface areal concentration is based on bringing 1.5 m³ of contaminated cuttings to the surface while drilling a 22-in. well.

Table C-2. Radionuclide waste concentration, surface concentration, and surface areal concentration for 2120 through 12,020 for soil vault rows.

	Waste Concentration (Ci/m³)					Surface Concentration (Ci/m³)[a]					Surface Areal Concentration (Ci/m²)[a]				
Radionuclide	2120	3020	5020	7020	12020	2120[b]	3020[b]	5020[b]	7020[b]	12020[b]	2120[c]	3020[c]	5020[c]	7020[c]	12020[c]
H 3	1.2E+00	1.4E-22	0.0E+00	0.0E+00	0.0E+00	7.3E-05	8.4E-27	0.0E+00	0.0E+00	0.0E+00	4.1E-04	4.7E-26	0.0E+00	0.0E+00	0.0E+00
C 14	2.6E-02	2.4E-02	1.8E-02	1.5E-02	7.9E-03	1.6E-06	1.4E-06	1.1E-06	8.7E-07	4.8E-07	9.0E-06	8.0E-06	6.3E-06	4.9E-06	2.7E-06
K 40	4.0E-04	4.0E-04	4.0E-04	4.0E-04	4.0E-04	2.4E-08	2.4E-08	2.4E-08	2.4E-08	2.4E-08	1.4E-07	1.4E-07	1.4E-07	1.4E-07	1.4E-07
CR51	0.0E+00	0.0E+00	0.0E+00	0.0E+00	0.0E+00	0.0E+00	0.0E+00	0.0E+00	0.0E+00	0.0E+00	0.0E+00	0.0E+00	0.0E+00	0.0E+00	0.0E+00
MN54	1.3E-34	0.0E+00	0.0E+00	0.0E+00	0.0E+00	7.9E-39	0.0E+00	0.0E+00	0.0E+00	0.0E+00	4.5E-38	0.0E+00	0.0E+00	0.0E+00	0.0E+00
FE55	1.3E-10	0.0E+00	0.0E+00	0.0E+00	0.0E+00	7.9E-15	0.0E+00	0.0E+00	0.0E+00	0.0E+00	4.5E-14	0.0E+00	0.0E+00	0.0E+00	0.0E+00
FE59	0.0E+00	0.0E+00	0.0E+00	0.0E+00	0.0E+00	0.0E+00	0.0E+00	0.0E+00	0.0E+00	0.0E+00	0.0E+00	0.0E+00	0.0E+00	0.0E+00	0.0E+00
CO58	0.0E+00	0.0E+00	0.0E+00	0.0E+00	0.0E+00	0.0E+00	0.0E+00	0.0E+00	0.0E+00	0.0E+00	0.0E+00	0.0E+00	0.0E+00	0.0E+00	0.0E+00
CO60	1.2E-03	0.0E+00	0.0E+00	0.0E+00	0.0E+00	7.1E-08	0.0E+00	0.0E+00	0.0E+00	0.0E+00	4.1E-07	0.0E+00	0.0E+00	0.0E+00	0.0E+00
NI59	3.4E+00	3.4E+00	3.3E+00	3.3E+00	3.1E+00	2.1E-04	2.0E-04	2.0E-04	2.0E-04	1.9E-04	1.2E-03	1.2E-03	1.1E-03	1.1E-03	1.1E-03
NI63	2.3E+02	2.6E-01	7.4E-08	2.1E-14	9.3E-31	1.4E-02	1.6E-05	4.5E-12	1.3E-18	5.6E-35	7.8E-02	8.9E-05	2.5E-11	7.3E-18	3.2E-34
ZN65	0.0E+00	0.0E+00	0.0E+00	0.0E+00	0.0E+00	0.0E+00	0.0E+00	0.0E+00	0.0E+00	0.0E+00	0.0E+00	0.0E+00	0.0E+00	0.0E+00	0.0E+00
SE75	0.0E+00	0.0E+00	0.0E+00	0.0E+00	0.0E+00	0.0E+00	0.0E+00	0.0E+00	0.0E+00	0.0E+00	0.0E+00	0.0E+00	0.0E+00	0.0E+00	0.0E+00
SR85	0.0E+00	0.0E+00	0.0E+00	0.0E+00	0.0E+00	0.0E+00	0.0E+00	0.0E+00	0.0E+00	0.0E+00	0.0E+00	0.0E+00	0.0E+00	0.0E+00	0.0E+00
SR90	4.9E-02	2.5E-11	5.2E-32	0.0E+00	0.0E+00	3.0E-06	1.5E-15	3.1E-36	0.0E+00	0.0E+00	1.7E-05	8.4E-15	1.8E-35	0.0E+00	0.0E+00
Y 90	4.9E-02	2.5E-11	5.2E-32	0.0E+00	0.0E+00	3.0E-06	1.5E-15	3.1E-36	0.0E+00	0.0E+00	1.7E-05	8.4E-15	1.8E-35	0.0E+00	0.0E+00
ZR95	0.0E+00	0.0E+00	0.0E+00	0.0E+00	0.0E+00	0.0E+00	0.0E+00	0.0E+00	0.0E+00	0.0E+00	0.0E+00	0.0E+00	0.0E+00	0.0E+00	0.0E+00
NB94	6.4E-05	6.2E-05	5.8E-05	5.4E-05	4.6E-05	3.8E-09	3.7E-09	3.5E-09	3.3E-09	2.7E-09	2.2E-08	2.1E-08	2.0E-08	1.8E-08	1.6E-08
NB95	0.0E+00	0.0E+00	0.0E+00	0.0E+00	0.0E+00	0.0E+00	0.0E+00	0.0E+00	0.0E+00	0.0E+00	0.0E+00	0.0E+00	0.0E+00	0.0E+00	0.0E+00
NB95M	0.0E+00	0.0E+00	0.0E+00	0.0E+00	0.0E+00	0.0E+00	0.0E+00	0.0E+00	0.0E+00	0.0E+00	0.0E+00	0.0E+00	0.0E+00	0.0E+00	0.0E+00
TC99	4.2E-04	4.2E-04	4.1E-04	4.1E-04	4.0E-04	2.5E-08	2.5E-08	2.5E-08	2.5E-08	2.4E-08	1.4E-07	1.4E-07	1.4E-07	1.4E-07	1.4E-07
RU103	0.0E+00	0.0E+00	0.0E+00	0.0E+00	0.0E+00	0.0E+00	0.0E+00	0.0E+00	0.0E+00	0.0E+00	0.0E+00	0.0E+00	0.0E+00	0.0E+00	0.0E+00
RU106	2.1E-34	0.0E+00	0.0E+00	0.0E+00	0.0E+00	1.3E-38	0.0E+00	0.0E+00	0.0E+00	0.0E+00	7.2E-38	0.0E+00	0.0E+00	0.0E+00	0.0E+00
RH106	2.1E-34	0.0E+00	0.0E+00	0.0E+00	0.0E+00	1.3E-38	0.0E+00	0.0E+00	0.0E+00	0.0E+00	7.2E-38	0.0E+00	0.0E+00	0.0E+00	0.0E+00
AG110	0.0E+00	0.0E+00	0.0E+00	0.0E+00	0.0E+00	0.0E+00	0.0E+00	0.0E+00	0.0E+00	0.0E+00	0.0E+00	0.0E+00	0.0E+00	0.0E+00	0.0E+00
AG110M	0.0E+00	0.0E+00	0.0E+00	0.0E+00	0.0E+00	0.0E+00	0.0E+00	0.0E+00	0.0E+00	0.0E+00	0.0E+00	0.0E+00	0.0E+00	0.0E+00	0.0E+00
IN113M	0.0E+00	0.0E+00	0.0E+00	0.0E+00	0.0E+00	0.0E+00	0.0E+00	0.0E+00	0.0E+00	0.0E+00	0.0E+00	0.0E+00	0.0E+00	0.0E+00	0.0E+00
SN113	0.0E+00	0.0E+00	0.0E+00	0.0E+00	0.0E+00	0.0E+00	0.0E+00	0.0E+00	0.0E+00	0.0E+00	0.0E+00	0.0E+00	0.0E+00	0.0E+00	0.0E+00
SN117M	0.0E+00	0.0E+00	0.0E+00	0.0E+00	0.0E+00	0.0E+00	0.0E+00	0.0E+00	0.0E+00	0.0E+00	0.0E+00	0.0E+00	0.0E+00	0.0E+00	0.0E+00
SN119M	0.0E+00	0.0E+00	0.0E+00	0.0E+00	0.0E+00	0.0E+00	0.0E+00	0.0E+00	0.0E+00	0.0E+00	0.0E+00	0.0E+00	0.0E+00	0.0E+00	0.0E+00
SN121M	7.5E-07	2.9E-12	2.6E-24	2.3E-36	0.0E+00	4.5E-11	1.7E-16	1.5E-28	1.4E-40	0.0E+00	2.6E-10	9.7E-16	8.7E-28	7.8E-40	0.0E+00
SB124	0.0E+00	0.0E+00	0.0E+00	0.0E+00	0.0E+00	0.0E+00	0.0E+00	0.0E+00	0.0E+00	0.0E+00	0.0E+00	0.0E+00	0.0E+00	0.0E+00	0.0E+00
SB125	1.5E-11	0.0E+00	0.0E+00	0.0E+00	0.0E+00	9.2E-16	0.0E+00	0.0E+00	0.0E+00	0.0E+00	5.2E-15	0.0E+00	0.0E+00	0.0E+00	0.0E+00
TE125M	3.7E-12	0.0E+00	0.0E+00	0.0E+00	0.0E+00	2.2E-16	0.0E+00	0.0E+00	0.0E+00	0.0E+00	1.3E-15	0.0E+00	0.0E+00	0.0E+00	0.0E+00
I 129	8.7E-07	8.7E-07	8.7E-07	8.7E-07	8.7E-07	5.2E-11	5.2E-11	5.2E-11	5.2E-11	5.2E-11	3.0E-10	3.0E-10	3.0E-10	3.0E-10	3.0E-10
CS134	7.4E-18	0.0E+00	0.0E+00	0.0E+00	0.0E+00	4.5E-22	0.0E+00	0.0E+00	0.0E+00	0.0E+00	2.5E-21	0.0E+00	0.0E+00	0.0E+00	0.0E+00
CS137	3.3E-01	3.1E-10	2.7E-30	0.0E+00	0.0E+00	2.0E-05	1.9E-14	1.6E-34	0.0E+00	0.0E+00	1.1E-04	1.1E-13	9.0E-34	0.0E+00	0.0E+00
BA137M	3.2E-01	2.9E-10	2.5E-30	0.0E+00	0.0E+00	1.9E-05	1.8E-14	1.5E-34	0.0E+00	0.0E+00	1.1E-04	1.0E-13	8.6E-34	0.0E+00	0.0E+00
BA140	0.0E+00	0.0E+00	0.0E+00	0.0E+00	0.0E+00	0.0E+00	0.0E+00	0.0E+00	0.0E+00	0.0E+00	0.0E+00	0.0E+00	0.0E+00	0.0E+00	0.0E+00
LA140	0.0E+00	0.0E+00	0.0E+00	0.0E+00	0.0E+00	0.0E+00	0.0E+00	0.0E+00	0.0E+00	0.0E+00	0.0E+00	0.0E+00	0.0E+00	0.0E+00	0.0E+00
CE141	0.0E+00	0.0E+00	0.0E+00	0.0E+00	0.0E+00	0.0E+00	0.0E+00	0.0E+00	0.0E+00	0.0E+00	0.0E+00	0.0E+00	0.0E+00	0.0E+00	0.0E+00
CE144	1.2E-42	0.0E+00	0.0E+00	0.0E+00	0.0E+00	7.2E-47	0.0E+00	0.0E+00	0.0E+00	0.0E+00	4.1E-46	0.0E+00	0.0E+00	0.0E+00	0.0E+00
PR144	0.0E+00	0.0E+00	0.0E+00	0.0E+00	0.0E+00	0.0E+00	0.0E+00	0.0E+00	0.0E+00	0.0E+00	0.0E+00	0.0E+00	0.0E+00	0.0E+00	0.0E+00
ND144	4.0E-17	4.0E-17	4.0E-17	4.0E-17	4.0E-17	2.4E-21	2.4E-21	2.4E-21	2.4E-21	2.4E-21	1.4E-20	1.4E-20	1.4E-20	1.4E-20	1.4E-20
PM147	1.2E-15	0.0E+00	0.0E+00	0.0E+00	0.0E+00	7.4E-20	0.0E+00	0.0E+00	0.0E+00	0.0E+00	4.2E-19	0.0E+00	0.0E+00	0.0E+00	0.0E+00
SM147	9.5E-14	9.5E-14	9.5E-14	9.5E-14	9.5E-14	5.7E-18	5.7E-18	5.7E-18	5.7E-18	5.7E-18	3.2E-17	3.2E-17	3.2E-17	3.2E-17	3.2E-17
EU152	1.6E-06	1.9E-26	0.0E+00	0.0E+00	0.0E+00	9.4E-11	1.1E-30	0.0E+00	0.0E+00	0.0E+00	5.3E-10	6.4E-30	0.0E+00	0.0E+00	0.0E+00

Table C-2. (continued).

Radionuclide	Waste Concentration (Ci/m^3)					Surface Concentration (Ci/m^3)					Surface Areal Concentration (Ci/m^2)				
	2120	3020	5020	7020	12020	2120	3020	5020	7020	12020	2120	3020	5020	7020	12020
EU154	9.7E-08	3.0E-39	0.0E+00	0.0E+00	0.0E+00	5.8E-12	1.8E-43	0.0E+00	0.0E+00	0.0E+00	3.3E-11	1.0E-42	0.0E+00	0.0E+00	0.0E+00
EU155	1.0E-10	0.0E+00	0.0E+00	0.0E+00	0.0E+00	6.1E-15	0.0E+00	0.0E+00	0.0E+00	0.0E+00	3.4E-14	0.0E+00	0.0E+00	0.0E+00	0.0E+00
GD152	5.1E-17	5.1E-17	5.1E-17	5.1E-17	5.1E-17	3.0E-21	3.0E-21	3.0E-21	3.0E-21	3.0E-21	1.7E-20	1.7E-20	1.7E-20	1.7E-20	1.7E-20
GD153	0.0E+00	0.0E+00	0.0E+00	0.0E+00	0.0E+00	0.0E+00	0.0E+00	0.0E+00	0.0E+00	0.0E+00	0.0E+00	0.0E+00	0.0E+00	0.0E+00	0.0E+00
TA182	0.0E+00	0.0E+00	0.0E+00	0.0E+00	0.0E+00	0.0E+00	0.0E+00	0.0E+00	0.0E+00	0.0E+00	0.0E+00	0.0E+00	0.0E+00	0.0E+00	0.0E+00
W 185	0.0E+00	0.0E+00	0.0E+00	0.0E+00	0.0E+00	0.0E+00	0.0E+00	0.0E+00	0.0E+00	0.0E+00	0.0E+00	0.0E+00	0.0E+00	0.0E+00	0.0E+00
W 187	0.0E+00	0.0E+00	0.0E+00	0.0E+00	0.0E+00	0.0E+00	0.0E+00	0.0E+00	0.0E+00	0.0E+00	0.0E+00	0.0E+00	0.0E+00	0.0E+00	0.0E+00
RE187	8.1E-14	8.1E-14	8.1E-14	8.1E-14	8.1E-14	4.9E-18	4.9E-18	4.9E-18	4.9E-18	4.9E-18	2.8E-17	2.8E-17	2.8E-17	2.8E-17	2.8E-17
IR192	0.0E+00	0.0E+00	0.0E+00	0.0E+00	0.0E+00	0.0E+00	0.0E+00	0.0E+00	0.0E+00	0.0E+00	0.0E+00	0.0E+00	0.0E+00	0.0E+00	0.0E+00
HG203	0.0E+00	0.0E+00	0.0E+00	0.0E+00	0.0E+00	0.0E+00	0.0E+00	0.0E+00	0.0E+00	0.0E+00	0.0E+00	0.0E+00	0.0E+00	0.0E+00	0.0E+00
TL207	3.2E-10	3.2E-09	9.1E-09	1.5E-08	2.8E-08	1.9E-14	1.9E-13	5.4E-13	8.8E-13	1.7E-12	1.1E-13	1.1E-12	3.1E-12	5.0E-12	9.5E-12
TL208	3.4E-18	3.2E-17	9.8E-17	1.7E-16	3.4E-16	2.0E-22	1.9E-21	5.9E-21	9.9E-21	2.0E-20	1.2E-21	1.1E-20	3.3E-20	5.6E-20	1.2E-19
TL209	1.4E-17	1.9E-15	2.3E-14	6.6E-14	2.5E-13	8.6E-22	1.1E-19	1.4E-18	3.9E-18	1.5E-17	4.9E-21	6.5E-19	7.7E-18	2.2E-17	8.4E-17
PB209	6.6E-16	8.9E-14	1.1E-12	3.0E-12	1.1E-11	4.0E-20	5.3E-18	6.3E-17	1.8E-16	6.9E-16	2.2E-19	3.0E-17	3.6E-16	1.0E-15	3.9E-15
PB210	2.9E-09	3.3E-07	2.3E-06	5.1E-06	1.3E-05	1.7E-13	2.0E-11	1.4E-10	3.0E-10	7.7E-10	9.7E-13	1.1E-10	7.8E-10	1.7E-09	4.4E-09
PB211	3.2E-10	3.2E-09	9.1E-09	1.5E-08	2.8E-08	1.9E-14	1.9E-13	5.5E-13	8.9E-13	1.7E-12	1.1E-13	1.1E-12	3.1E-12	5.0E-12	9.5E-12
PB212	9.5E-18	9.0E-17	2.7E-16	4.6E-16	9.5E-16	5.7E-22	5.4E-21	1.6E-20	2.8E-20	5.7E-20	3.2E-21	3.1E-20	9.3E-20	1.6E-19	3.2E-19
PB214	4.8E-09	3.3E-07	2.3E-06	5.1E-06	1.3E-05	2.9E-13	2.0E-11	1.4E-10	3.0E-10	7.7E-10	1.6E-12	1.1E-10	7.8E-10	1.7E-09	4.4E-09
BI210	2.9E-09	3.3E-07	2.3E-06	5.1E-06	1.3E-05	1.7E-13	2.0E-11	1.4E-10	3.0E-10	7.7E-10	9.7E-13	1.1E-10	7.8E-10	1.7E-09	4.4E-09
BI211	3.2E-10	3.2E-09	9.1E-09	1.5E-08	2.8E-08	1.9E-14	1.9E-13	5.5E-13	8.9E-13	1.7E-12	1.1E-13	1.1E-12	3.1E-12	5.0E-12	9.5E-12
BI212	9.5E-18	9.0E-17	2.7E-16	4.6E-16	9.5E-16	5.7E-22	5.4E-21	1.6E-20	2.8E-20	5.7E-20	3.2E-21	3.1E-20	9.3E-20	1.6E-19	3.2E-19
BI213	6.6E-16	8.9E-14	1.1E-12	3.0E-12	1.1E-11	4.0E-20	5.3E-18	6.3E-17	1.8E-16	6.9E-16	2.2E-19	3.0E-17	3.6E-16	1.0E-15	3.9E-15
BI214	4.8E-09	3.3E-07	2.3E-06	5.1E-06	1.3E-05	2.9E-13	2.0E-11	1.4E-10	3.0E-10	7.7E-10	1.6E-12	1.1E-10	7.8E-10	1.7E-09	4.4E-09
PO210	2.9E-09	3.3E-07	2.3E-06	5.1E-06	1.3E-05	1.7E-13	2.0E-11	1.4E-10	3.0E-10	7.7E-10	9.7E-13	1.1E-10	7.8E-10	1.7E-09	4.4E-09
PO211	9.0E-13	8.9E-12	2.5E-11	4.1E-11	7.8E-11	5.4E-17	5.3E-16	1.5E-15	2.5E-15	4.7E-15	3.1E-16	3.0E-15	8.7E-15	1.4E-14	2.7E-14
PO212	6.1E-18	5.8E-17	1.7E-16	2.9E-16	6.1E-16	3.6E-22	3.5E-21	1.0E-20	1.8E-20	3.6E-20	2.1E-21	2.0E-20	5.9E-20	1.0E-19	2.1E-19
PO213	6.5E-16	8.7E-14	1.0E-12	3.0E-12	1.1E-11	3.9E-20	5.2E-18	6.2E-17	1.8E-16	6.7E-16	2.2E-19	3.0E-17	3.5E-16	1.0E-15	3.8E-15
PO214	4.8E-09	3.3E-07	2.3E-06	5.1E-06	1.3E-05	2.9E-13	2.0E-11	1.4E-10	3.0E-10	7.7E-10	1.6E-12	1.1E-10	7.8E-10	1.7E-09	4.4E-09
PO215	3.2E-10	3.2E-09	9.1E-09	1.5E-08	2.8E-08	1.9E-14	1.9E-13	5.5E-13	8.9E-13	1.7E-12	1.1E-13	1.1E-12	3.1E-12	5.0E-12	9.5E-12
PO216	9.5E-18	9.0E-17	2.7E-16	4.6E-16	9.5E-16	5.7E-22	5.4E-21	1.6E-20	2.8E-20	5.7E-20	3.2E-21	3.1E-20	9.3E-20	1.6E-19	3.2E-19
PO218	4.8E-09	3.3E-07	2.3E-06	5.1E-06	1.3E-05	2.9E-13	2.0E-11	1.4E-10	3.0E-10	7.7E-10	1.6E-12	1.1E-10	7.8E-10	1.7E-09	4.4E-09
AT217	6.6E-16	8.9E-14	1.1E-12	3.0E-12	1.1E-11	4.0E-20	5.3E-18	6.3E-17	1.8E-16	6.9E-16	2.2E-19	3.0E-17	3.6E-16	1.0E-15	3.9E-15
RN219	3.2E-10	3.2E-09	9.1E-09	1.5E-08	2.8E-08	1.9E-14	1.9E-13	5.5E-13	8.9E-13	1.7E-12	1.1E-13	1.1E-12	3.1E-12	5.0E-12	9.5E-12
RN220	9.5E-18	9.0E-17	2.7E-16	4.6E-16	9.5E-16	5.7E-22	5.4E-21	1.6E-20	2.8E-20	5.7E-20	3.2E-21	3.1E-20	9.3E-20	1.6E-19	3.2E-19
RN222	4.8E-09	3.3E-07	2.3E-06	5.1E-06	1.3E-05	2.9E-13	2.0E-11	1.4E-10	3.0E-10	7.7E-10	1.6E-12	1.1E-10	7.8E-10	1.7E-09	4.4E-09
FR221	6.6E-16	8.9E-14	1.1E-12	3.0E-12	1.1E-11	4.0E-20	5.3E-18	6.3E-17	1.8E-16	6.9E-16	2.2E-19	3.0E-17	3.6E-16	1.0E-15	3.9E-15
FR223	4.4E-12	4.4E-11	1.3E-10	2.0E-10	3.9E-10	2.7E-16	2.6E-15	7.5E-15	1.2E-14	2.3E-14	1.5E-15	1.5E-14	4.3E-14	7.0E-14	1.3E-13
RA223	3.2E-10	3.2E-09	9.1E-09	1.5E-08	2.8E-08	1.9E-14	1.9E-13	5.5E-13	8.9E-13	1.7E-12	1.1E-13	1.1E-12	3.1E-12	5.0E-12	9.5E-12
RA224	9.5E-18	9.0E-17	2.7E-16	4.6E-16	9.5E-16	5.7E-22	5.4E-21	1.6E-20	2.8E-20	5.7E-20	3.2E-21	3.1E-20	9.3E-20	1.6E-19	3.2E-19
RA225	6.6E-16	8.9E-14	1.1E-12	3.0E-12	1.1E-11	4.0E-20	5.3E-18	6.3E-17	1.8E-16	6.9E-16	2.2E-19	3.0E-17	3.6E-16	1.0E-15	3.9E-15
RA226	4.8E-09	3.3E-07	2.3E-06	5.1E-06	1.3E-05	2.9E-13	2.0E-11	1.4E-10	3.0E-10	7.7E-10	1.6E-12	1.1E-10	7.8E-10	1.7E-09	4.4E-09
RA228	9.5E-18	9.0E-17	2.7E-16	4.6E-16	9.5E-16	5.7E-22	5.4E-21	1.6E-20	2.8E-20	5.7E-20	3.2E-21	3.1E-20	9.3E-20	1.6E-19	3.2E-19
AC225	6.6E-16	8.9E-14	1.1E-12	3.0E-12	1.1E-11	4.0E-20	5.3E-18	6.3E-17	1.8E-16	6.9E-16	2.2E-19	3.0E-17	3.6E-16	1.0E-15	3.9E-15
AC227	3.2E-10	3.2E-09	9.1E-09	1.5E-08	2.8E-08	1.9E-14	1.9E-13	5.5E-13	8.9E-13	1.7E-12	1.1E-13	1.1E-12	3.1E-12	5.0E-12	9.5E-12
AC228	9.5E-18	9.0E-17	2.7E-16	4.6E-16	9.5E-16	5.7E-22	5.4E-21	1.6E-20	2.8E-20	5.7E-20	3.2E-21	3.1E-20	9.3E-20	1.6E-19	3.2E-19
TH227	3.2E-10	3.1E-09	9.0E-09	1.5E-08	2.8E-08	1.9E-14	1.9E-13	5.4E-13	8.7E-13	1.7E-12	1.1E-13	1.1E-12	3.1E-12	5.0E-12	9.4E-12
TH228	9.5E-18	9.0E-17	2.7E-16	4.6E-16	9.5E-16	5.7E-22	5.4E-21	1.6E-20	2.8E-20	5.7E-20	3.2E-21	3.1E-20	9.3E-20	1.6E-19	3.2E-19
TH229	6.6E-16	8.9E-14	1.1E-12	3.0E-12	1.1E-11	4.0E-20	5.3E-18	6.3E-17	1.8E-16	6.9E-16	2.2E-19	3.0E-17	3.6E-16	1.0E-15	3.9E-15

Table C-2. (continued).

Radionuclide	Waste Concentration (Ci/m³)					Surface Concentration (Ci/m³)					Surface Areal Concentration (Ci/m²)				
	2120	3020	5020	7020	12020	2120	3020	5020	7020	12020	2120	3020	5020	7020	12020
TH230	2.0E-07	1.7E-06	5.2E-06	8.5E-06	1.7E-05	1.2E-11	1.0E-10	3.1E-10	5.1E-10	1.0E-09	6.7E-11	6.0E-10	1.8E-09	2.9E-09	5.7E-09
TH231	1.5E-07	1.5E-07	1.5E-07	1.5E-07	1.5E-07	8.8E-12	8.8E-12	8.8E-12	8.8E-12	8.8E-12	5.0E-11	5.0E-11	5.0E-11	5.0E-11	5.0E-11
TH232	1.0E-17	9.0E-17	2.7E-16	4.6E-16	9.5E-16	6.2E-22	5.4E-21	1.6E-20	2.8E-20	5.7E-20	3.5E-21	3.1E-20	9.3E-20	1.6E-19	3.2E-19
TH234	2.0E-04	2.0E-04	2.0E-04	2.0E-04	2.0E-04	1.2E-08	1.2E-08	1.2E-08	1.2E-08	1.2E-08	6.9E-08	6.9E-08	6.9E-08	6.9E-08	6.9E-08
PA231	4.2E-10	3.2E-09	9.1E-09	1.5E-08	2.8E-08	2.5E-14	1.9E-13	5.5E-13	8.9E-13	1.7E-12	1.4E-13	1.1E-12	3.1E-12	5.0E-12	9.5E-12
PA233	3.0E-10	6.9E-10	8.1E-10	8.2E-10	8.1E-10	1.8E-14	4.2E-14	4.9E-14	4.9E-14	4.9E-14	1.0E-13	2.4E-13	2.8E-13	2.8E-13	2.8E-13
PA234M	2.0E-04	2.0E-04	2.0E-04	2.0E-04	2.0E-04	1.2E-08	1.2E-08	1.2E-08	1.2E-08	1.2E-08	6.9E-08	6.9E-08	6.9E-08	6.9E-08	6.9E-08
PA234	2.6E-07	2.6E-07	2.6E-07	2.6E-07	2.6E-07	1.6E-11	1.6E-11	1.6E-11	1.6E-11	1.6E-11	9.0E-11	9.0E-11	9.0E-11	9.0E-11	9.0E-11
U 233	1.3E-13	2.3E-12	9.0E-12	1.6E-11	3.3E-11	7.6E-18	1.4E-16	5.4E-16	9.6E-16	2.0E-15	4.3E-17	7.7E-16	3.1E-15	5.5E-15	1.1E-14
U 234	1.9E-04	1.9E-04	1.9E-04	1.9E-04	1.9E-04	1.2E-08	1.2E-08	1.2E-08	1.2E-08	1.2E-08	6.6E-08	6.6E-08	6.6E-08	6.6E-08	6.6E-08
U 235	1.5E-07	1.5E-07	1.5E-07	1.5E-07	1.5E-07	8.8E-12	8.8E-12	8.8E-12	8.8E-12	8.8E-12	5.0E-11	5.0E-11	5.0E-11	5.0E-11	5.0E-11
U 236	1.8E-09	1.8E-09	1.9E-09	1.9E-09	2.0E-09	1.1E-13	1.1E-13	1.1E-13	1.2E-13	1.2E-13	6.1E-13	6.2E-13	6.4E-13	6.6E-13	6.9E-13
U 237	2.0E-12	3.0E-31	0.0E+00	0.0E+00	0.0E+00	1.2E-16	1.8E-35	0.0E+00	0.0E+00	0.0E+00	6.7E-16	1.0E-34	0.0E+00	0.0E+00	0.0E+00
U 238	2.0E-04	2.0E-04	2.0E-04	2.0E-04	2.0E-04	1.2E-08	1.2E-08	1.2E-08	1.2E-08	1.2E-08	6.9E-08	6.9E-08	6.9E-08	6.9E-08	6.9E-08
NP237	3.0E-10	6.9E-10	8.1E-10	8.2E-10	8.1E-10	1.8E-14	4.2E-14	4.9E-14	4.9E-14	4.9E-14	1.0E-13	2.4E-13	2.8E-13	2.8E-13	2.8E-13
PU238	6.0E-05	4.9E-08	6.7E-15	9.2E-22	6.5E-39	3.6E-09	2.9E-12	4.0E-19	5.5E-26	3.9E-43	2.0E-08	1.7E-11	2.3E-18	3.1E-25	2.2E-42
PU239	9.7E-06	9.4E-06	8.9E-06	8.4E-06	7.3E-06	5.8E-10	5.7E-10	5.3E-10	5.0E-10	4.4E-10	3.3E-09	3.2E-09	3.0E-09	2.9E-09	2.5E-09
PU240	1.3E-06	1.2E-06	9.7E-07	7.8E-07	4.6E-07	7.9E-11	7.2E-11	5.8E-11	4.7E-11	2.8E-11	4.5E-10	4.1E-10	3.3E-10	2.7E-10	1.6E-10
PU241	8.1E-08	1.2E-26	0.0E+00	0.0E+00	0.0E+00	4.8E-12	7.4E-31	0.0E+00	0.0E+00	0.0E+00	2.7E-11	4.2E-30	0.0E+00	0.0E+00	0.0E+00
PU242	4.0E-11	4.0E-11	4.0E-11	4.0E-11	4.0E-11	2.4E-15	2.4E-15	2.4E-15	2.4E-15	2.4E-15	1.4E-14	1.4E-14	1.4E-14	1.4E-14	1.3E-14
AM241	2.6E-06	6.1E-07	2.5E-08	9.9E-10	3.3E-13	1.5E-10	3.6E-11	1.5E-12	6.0E-14	2.0E-17	8.8E-10	2.1E-10	8.4E-12	3.4E-13	1.1E-16
CM242	0.0E+00	0.0E+00	0.0E+00	0.0E+00	0.0E+00	0.0E+00	0.0E+00	0.0E+00	0.0E+00	0.0E+00	0.0E+00	0.0E+00	0.0E+00	0.0E+00	0.0E+00
CM244	9.7E-11	1.1E-25	0.0E+00	0.0E+00	0.0E+00	5.8E-15	6.4E-30	0.0E+00	0.0E+00	0.0E+00	3.3E-14	3.6E-29	0.0E+00	0.0E+00	0.0E+00

a. These data are based on ORIGEN2 calculations and may differ slightly from decay and ingrowth data derived from MICROSHIELD.

b. Surface concentration is based on bringing 0.099 m³ of contaminated cuttings to the surface while drilling an 8-in. well.

c. Surface areal concentration is based on bringing 0.75 m³ of contaminated cuttings to the surface while drilling a 22-in. well.

Table C-3. Acute intruder-drilling and acute intruder-construction doses for pits and soil vault rows.

Scenario and year	Internal dose (mrem)	External dose (mrem)	Total dose (mrem)
Acute drilling--pits (2120)	5.8	2.5	8.3
Acute drilling--soil vault rows (2120)	80	110	190
Acute construction--pits (5020)[a]	0.69	0.68	1.4
Acute construction--pits (12,020)	0.75	0.25	1.0
Acute construction--pits (1,000,000 years)	3.0	8.2	11

a. Basement excavation is not possible in 2120.

Table C-4. Maximum chronic intruder-agriculture doses.

Case	EDE (mrem/yr)
Year 1,000,000 pits	
8,030 m^3/yr inhalation rate Rupp diet, 0.7 shielding factor	28
5,840 m^3/yr inhalation rate Yang and Nelson diet, 0.36 shielding factor	15
Year 2120 soil vault rows	
8,030 m^3/yr inhalation rate Rupp diet, 0.7 shielding factor	53
5,840 m^3/yr inhalation rate Yang and Nelson diet, 0.36 shielding factor	28

Table C-5. Chronic intruder-agriculture doses for pits.

Year	Internal dose (mrem)	External dose (mrem)	Total dose (mrem)
2120[a]	0.21	0.98	1.2
2120[b]	0.13	0.50	0.63
5020[a]	0.68	2.0	2.7
5020[b]	0.43	1.0	1.4
12020[a]	0.46	0.71	1.2
12020[b]	0.30	0.37	0.67
U-238 equilibrium[a]	5.4	23	28
U-238 equilibrium[b]	3.4	12	15

a. Rupp diet, 8,030 m^3/yr inhalation rate, 0.7 shielding factor.

b. Yang and Nelson diet, 5,840 m^3/yr inhalation rate, 0.36 shielding factor.

Table C-6. Chronic intruder-agriculture doses for soil vault rows.

Year	Internal dose (mrem)	External dose (mrem)	Total dose (mrem)
2120[a]	13	40	53
2120[b]	7.8	20	28
3020[a]	0.073	0.042	0.12
3020[b]	0.040	0.022	0.062
12020[a]	0.060	0.041	0.10
12020[b]	0.034	0.021	0.055
U-238 equilibrium[a]	0.023	0.098	0.12
U-238 equilibrium[b]	0.014	0.050	0.064

a. Rupp diet, 8,030 m^3/yr inhalation rate, 0.7 shielding factor.

b. Yang and Nelson diet, 5,840 m^3/yr inhalation rate, 0.36 shielding factor.

APPENDIX D

DESCRIPTION OF COMPUTER CODES USED IN THE RWMC LLW RADIOLOGICAL PERFORMANCE ASSESSMENT ANALYSES

APPENDIX D
DESCRIPTION OF COMPUTER CODES
USED IN THE RWMC LLW RADIOLOGICAL PERFORMANCE ASSESSMENT ANALYSES

This appendix provides a brief description of computer codes used for the analyses supporting the RWMC LLW radiological performance assessment.

D-1 MICROSHIELD 4

MICROSHIELD Version 4 is the personal computer version of ISOSHLD, which is a computer code that performs gamma-ray shielding calculations for radioactive sources with a wide variety of source and shield configurations. Attenuation calculations are performed by point kernel integrations (i.e., the dose at the exposure point is the contribution from a large number of point sources). A numerical integration is carried out over the source volume to obtain the total dose. Build-up factors are used and are calculated by the code based on the number of mean free paths of material between the source and exposure point locations, the effective atomic number of a particular shield region, and the point isotropic NDA build-up data available as Taylor coefficients in the effective atomic number range of 4 to 82. For most problems, the user need only supply (a) the geometry and material composition of the source and of the shields and (b) the thicknesses and distances involved. Other data needed to complete the calculations are contained in data libraries used by the code.

The MICROSHIELD code was chosen for the external exposure analyses because it contains the source and shielding geometries appropriate for buried waste, it contains a transparent decay and ingrowth data base, and it meets appropriate quality assurance requirements. MICROSHIELD can also incorporate site-specific data, which enables more realistic dose assessments to be performed. MICROSHIELD is also used extensively at the INEL for shielding calculations, and the radiological performance assessment preparers had extensive experience using the code.

A comprehensive verification of MICROSHIELD has been conducted (Negin and Worku 1992) and a comparison to both American National Standards Institute (ANSI) and European Shielding Information Service (ESIS) benchmark shielding

problems have been published (ANSI 1979; ESIS 1981; Negin and Worku 1992). The MICROSHIELD computer code is maintained by Grove Engineering, Inc., which is responsible for configuration management.

D-2 GENII

The GENII computer code is an environmental radiological assessment code that calculates doses from acute and chronic release to, or initial contamination of, air, water, or soil. GENII also implements a Gaussian plume atmospheric dispersion model and terrestrial pathway models similar to the models in U.S. Nuclear Regulatory Commission (NRC) Regulatory Guide 1.109 (NRC 1977). GENII meets the American Society of Mechanical Engineers (ASME) NQA-1 Base and Supplementary Requirements for Design Control contained in Basic Requirement 3, "Design Control," and Supplementary Requirement 3S-1, "Supplementary Requirements for Design Control," which include requirements for verification and validation of computer codes (ASME 1989).

The output from the GENII computer code is the effective dose equivalent (EDE), which includes the 50-year committed effective dose equivalent (CEDE) from internal exposures through the ingestion (including soil) and inhalation pathways and the external EDE from the ground surface and air immersion pathways. The dose conversion factors in GENII are consistent with the internal dose conversion factors contained in DOE/EH-0071 (DOE 1988a) and the external dose conversion factors contained in DOE/EH-0070 (DOE 1988b).

The GENII code was chosen for the intruder and atmospheric analyses because it has several advanced features such as a transparent decay and ingrowth data base, it models applicable exposure pathways, and it meets appropriate quality assurance requirements. The GENII computer code was the subject of an extensive code selection process for the New Production Reactor Environmental Impact Statement, where it was found to meet the code selection criteria. GENII has been benchmarked to the CAP-88 and PATHRAE computer codes. GENII can incorporate site-specific data, which enables more realistic dose assessments to be performed. It has a large user population across the U.S. and has been used at the INEL in environmental impact statements and other environmental analyses, so the radiological performance assessment preparers had extensive experience using the code. The GENII computer code is

maintained by Pacific Northwest Laboratories, which is responsible for configuration management.

D-3 GWSCREEN

GWSCREEN is a groundwater assessment code that was developed for the assessment of the groundwater pathway from leaching of radioactive and nonradioactive substances from surface or buried sources. The code was designed for implementation in the Track I and Track II assessment of Comprehensive Environmental Response, Compensation, and Liability Act (CERCLA) sites identified as low probability hazard at the INEL (DOE-ID 1992a, 1992b). In addition, the code methodology has been applied to numerous other sites and problems.

The code calculates the limiting soil concentration and inventory so that after leaching and transport of the contaminant to the aquifer, regulatory contaminant levels in groundwater are not exceeded. Groundwater concentrations and dose results are also output at user-specified times. The code uses a mass conservation approach to model three processes: (1) contaminant release from a source volume, (2) contaminant transport in the unsaturated zone, and (3) contaminant transport in the aquifer. The source model considers the sorptive properties and solubility of the contaminant. Transport in the unsaturated zone is described by a plug flow model. Transport in the aquifer is calculated with a semianalytical solution to the advection dispersion equation in groundwater.

The GWSCREEN code, Version 2.0 and higher, includes transport, decay, and ingrowth of radioactive progeny. The simplifying but conservative assumption was made that progeny travel at the same rate as their parent. Version 2.02 was used for all performance assessment calculations.

GWSCREEN results are comparable with results from other codes using similar algorithms and have also been shown to provide bounding estimates of groundwater concentrations when compared to results from numerical codes. GWSCREEN is not intended to be a predictive tool; rather, it provides a framework to calculate bounding impacts to groundwater from the leaching of surficial and buried contamination.

Two codes were used to perform the numerical calculations of groundwater flow and contaminant transport needed for the RWMC LLW radiological performance assessment. The primary code used was GWSCREEN and the secondary code was PORFLOW.

The GWSCREEN code was used because it was developed to solve for unsaturated and saturated transport under the conditions that were described in the conceptual model in Section 3. The code was developed to perform screening of a large number of nuclides under simplistic flow assumptions, namely one-dimensional, predefined infiltration down to an aquifer undergoing uniform horizontal flow. With the limited understanding of water movement in the complicated subsurface beneath the SDA, it was also appropriate to use the GWSCREEN code for the fate and transport predictions for the RWMC LLW radiological performance assessment. GWSCREEN is currently being used for CERCLA groundwater assessment at the INEL and is approved for use on these tasks by the State of Idaho and U.S. Environmental Protection Agency, Region VIII. GWSCREEN is relatively simple to use and interfaces well with other codes used in this radiological performance assessment such as PORFLO.

GWSCREEN meets the requirements of Quality Level B documentation. Quality Level B documentation includes a software configuration management plan (Matthews 1992), verification and validation test plan (Rood 1993), and verification and validation report (Smith 1993).

D-4 PORFLOW

The PORFLOW computer code, Version 2.39 (Runchal and Sagar 1991) was developed to evaluate hazardous and radioactive waste problems. The computer code is based on the numerical solution of the general equations for (a) time-dependent, porous flow, (b) transport of a reactive solute, and (c) coupled heat transport. The governing equations describing these processes are approximated by an integrated finite-difference technique. Both direct and iterative solution approaches are available and can be used to solve the finite-difference equations.

The code is capable of solving for fluid flow, heat, and mass transport in porous media, which can be heterogenous, anisotropic, variably saturated,

and/or discreetly fractured. Specific capabilities of the code include the ability to simulate the following: multiple phases, up to four species at a time, chemical reactions, four-member chain decay with differential transport of daughters, arbitrary sources and sinks, and variable density as a function of either concentration or temperature.

Limitations of the model include (a) single temperature for all phases, (b) one-phase heat and mass transport so that there is no heat transfer between phases, (c) reversible linear Freundlich isotherm to describe partitioning, and (d) one-way chain decay so that daughter products can only occur along one chain per simulation.

An earlier version of the PORFLOW code, called PORFLO-3, was verified against a number of known analytical solutions and benchmark tested by making code-to-code comparisons for several flow and transport simulations. The results of the verification and benchmark testing are documented in Magnuson et al. (1990).

The PORFLOW code is written in standard FORTRAN-77 and is easy to install on most mainframe computer systems. The code is relatively easy to convert to different computer systems. However, practical applications of the PORFLOW code to realistic flow and transport problems in multidimensions require the availability of a scientific workstation or mainframe computer. At the INEL, the PORFLOW code resides in a configuration controlled environment on the INEL Cray XMP (Maheras 1993).

In addition to the GWSCREEN code, the PORFLOW code was used to perform the numerical calculations of groundwater flow and contaminant transport during flooding. The PORFLOW code was used for simulating the transient nature of water movement under flooding conditions because it had the capability of solving the governing equation for unsaturated flow under conditions of varying water infiltration rates. In addition, the PORFLOW code had the capability of solving the transport equations for this time-varying flow field with a time-varying mass loading rate.

D-5 ORIGEN2

ORIGEN is a computer code for calculating the buildup, decay, and processing of radioactive materials. ORIGEN2 is a revised version of ORIGEN and incorporates updates of the reactor models, cross sections, fission product yields, decay data, decay photon data, as well as the source code. ORIGEN2.1 replaces ORIGEN2 and includes additional libraries for standard and extended-burnup pressurized water reactor and boiling water reactor calculations, which are documented in Croff (1982).

The ORIGEN2 computer code was chosen to perform the ingrowth and decay calculations because it is the industry standard for these types of calculations. It also has an extensive user population across the U.S. at commercial power plants and DOE facilities. ORIGEN2 was the only computer code available that could perform the iterative ingrowth and decay calculations required in the RWMC LLW radiological performance assessment.

A number of verification activities have been undertaken, including comparison of (a) ORIGEN2 decay heat results with both calculated and experimental values and (b) predicted spent fuel compositions with measured values. The agreement between ORIGEN2 and the comparison bases is generally very good. Future work concerning ORIGEN2 will involve continued maintenance and user support along with additional verification studies and limited modifications to enhance its flexibility and usability. The ORIGEN2 computer code is maintained by Oak Ridge National Laboratory, which is responsible for configuration management.

D-6 RESRAD

RESRAD is a computer code developed at Argonne National Laboratory for DOE to calculate site-specific RESidual RADioactive material guidelines and radiation dose to an onsite resident.

The RESRAD computer code was chosen for the radon exposure analyses because it includes a radon pathway suitable for buried waste, it is approved for residual radioactive material analyses (see DOE 1990 and Gilbert et al. 1989), and it meets appropriate quality assurance requirements. RESRAD also

can incorporate site-specific data, which enables more realistic dose assessments to be performed. The RESRAD computer code is maintained by Argonne National Laboratory-East, which is responsible for configuration management.

D-7 REFERENCES

ANSI (American National Standards Institute), 1979, American National Standard for Calculation and Measurement of Direct and Scattered Gamma Radiation from LWR Nuclear Power Plants, ANSI/ANS-6.6.1-1979, January.

ASME (American Society of Mechanical Engineers), 1989, "Quality Assurance Program Requirements for Nuclear Facilities," NQA-1.

Croff, A. G., 1982, ORIGEN2: A Versatile Computer Code for Calculating the Nuclide Compositions and Characteristics of Nuclear Materials, ORNL/TM-11018.

DOE (U.S. Department of Energy), 1988a, Internal Dose Conversion Factors for Calculation of Dose to the Public, DOE/EH-0071.

DOE, 1988b, External Dose-Rate Conversion Factors for Calculation of Dose to the Public, DOE/EH-0070.

DOE, 1990, "Radiation Protection of the Public and the Environment," DOE Order 5400.5, February 8.

DOE-ID (U.S. Department of Energy Idaho Field Office), 1992a, Track 1 Sites: Guidance for Assessing Low Probability Hazard Sites at the INEL, DOE/ID-10340(92), Revision 1, July.

DOE-ID, 1992b, Track 2 Sites: Guidance for Assessing Low Probability Hazard Sites at the INEL, Draft, Revision 4, DOE/ID-10389, March.

ESIS (European Shielding Information Service), 1981, "Specification for Gamma Ray Shielding Benchmark Applicable to a Nuclear Radwaste Facility," Newsletter #37, ISPRA Establishment, Italy, April.

Gilbert, T. L. et al., 1989, A Manual for Implementing Residual Radioactive Material Guidelines, A Supplement to the U.S. Department of Energy Guidelines for Residual Radioactive Material at FUSRAP and SFMP Sites," DOE/CH-8901, June.

Magnuson, S. O, R. G. Baca, A. J. Sondrup, 1990, Independent Verification and Benchmark Testing of the PORFLO-3 Computer Code, Version 1.0, EGG-BG-9175, August.

Maheras, S. J., 1993, Software Quality Assurance Plan for PORFLOW, EGG-EELS-003, January.

Matthews, S. D., 1992, Software Configuration Management Plan for Controlled Code Support System, EGG-CATT-10196, April.

NRC (U.S. Nuclear Regulatory Commission), 1977, Regulatory Guide 1.109 Calculation of Annual Doses to Man From Routine Releases of Reactor Effluents for the Purpose of Evaluating Compliance With 10 CFR Part 50 Appendix I, Revision 1.

Negin, C. A. and G. Worku, 1992, MICROSHIELD Version 4 User's Manual, Grove 92-2, Grove Engineering, Inc. Rockville, MD.

Rood, A. S., 1993, Software Verification and Validation Plan for the GWSCREEN Code, EGG-GEO-10798, May.

Runchal, A. K. and B. Sagar, 1991, PORFLOW - A Model for Fluid Flow, Heat and Mass Transport in Multifluid, Multiphase, Fractured or Porous Media, User's Manual, Version 2.39, ACRi/016/Rev. F, Analytic and Computational Research, Inc., Los Angeles, CA, June.

Smith, C. S., 1993, Independent Verification and Limited Benchmarking of the GWSCREEN Computer Code Version 2.0, EGG-GEO-10799, June.

APPENDIX E

DATA QUALITY

APPENDIX E
DATA QUALITY

E-1 WASTE INVENTORY

The quality of the inventory data that has been collected over the years for waste disposed of at the RWMC has continually improved. Initially, records were collected; however, individual radionuclides were not identified, and the curie content was estimated not measured. Improved radionuclide identification procedures have resulted in improved estimates of container activity. In addition, data on physical and chemical characteristics are now collected. Waste management records have been computerized and incorporated into the Radioactive Waste Management Information System (RWMIS).

Recent studies have been performed to improve knowledge of the waste disposal inventory buried at the RWMC. During 1991 and 1992, a study was performed to improve the information about radionuclides in LLW buried at the RWMC (Plansky and Hoiland 1992). A questionnaire and an RWMIS LLW inventory printout was sent to LLW generators, requesting their review of that data. The questionnaire included questions related to past processes, disposed wastes, radionuclides, activities, weights, and the existence of other sources of information or disposal records. If differences in disposal data were identified as a result of this study, generators either indicated agreement with their RWMIS inventory data or noted changes on the questionnaire and inventory data printout. The generators also provided the needed changes to RWMIS personnel for update of the RWMIS data base.

In 1992, a task verified the shipment-specific waste information in the historical data electronic data bases with the RWMIS data base (Barnard 1992). This task was accomplished by comparing the original shipping manifests that accompanied the waste shipments for the years 1961 through 1984 with fields on printouts of the RWMIS data base. Inconsistencies were noted, and proposed amendments to the RWMIS data base were reviewed and resolved. The RWMIS data base was updated to incorporate the new information from this task.

To ship LLW to the RWMC, waste generators must be approved and the waste stream must be authorized to ensure compliance with requirements of the INEL

Reusable Property, Recyclable Materials, and Waste Acceptance Criteria. The waste stream is characterized to ensure the physical and chemical characteristics and radionuclide content are known and recorded during all stages of the waste management process. The waste characterization and certification process is a controlled process that uses records, statements, reports, and data along with a waste certification statement signed by the waste generator. Waste shipment information is input into the RWMIS, which includes data checks and edit routines to assure the quality of the input data. RWMC personnel perform receipt inspection of incoming LLW shipments to verify waste generator compliance with the WAC, and they periodically conduct audits of the generator's facility.

E-2 PERFORMANCE ASSESSMENT ANALYSES AND CALCULATIONS

The requirements for documenting analyses at EG&G Idaho come from several sources: (a) DOE orders, (b) NQA-1, (c) the EG&G Idaho Quality Manual, (d) the EG&G Idaho Company Procedures Manual, (e) EG&G Idaho Engineering Standard Practices, and (f) Subsurface and Environmental Modeling Unit guidance (see Figure E-1). The primary guidance used to document the RWMC LLW radiological performance assessment analyses is contained in EG&G Idaho Company Procedures Manual, Number 2.17, "Engineering Analysis." This procedure requires that the analysis be documented in a report. The following items should be included as appropriate:

1. Calculations, by subject.

2. The author, reviewer, and approver of the analysis.

3. The computer programs used to perform the analysis, computer type, revision identification, inputs, and outputs.

4. Evidence that computer programs have been verified and validated. In the context used in this procedure, validation means compliance with software requirements.

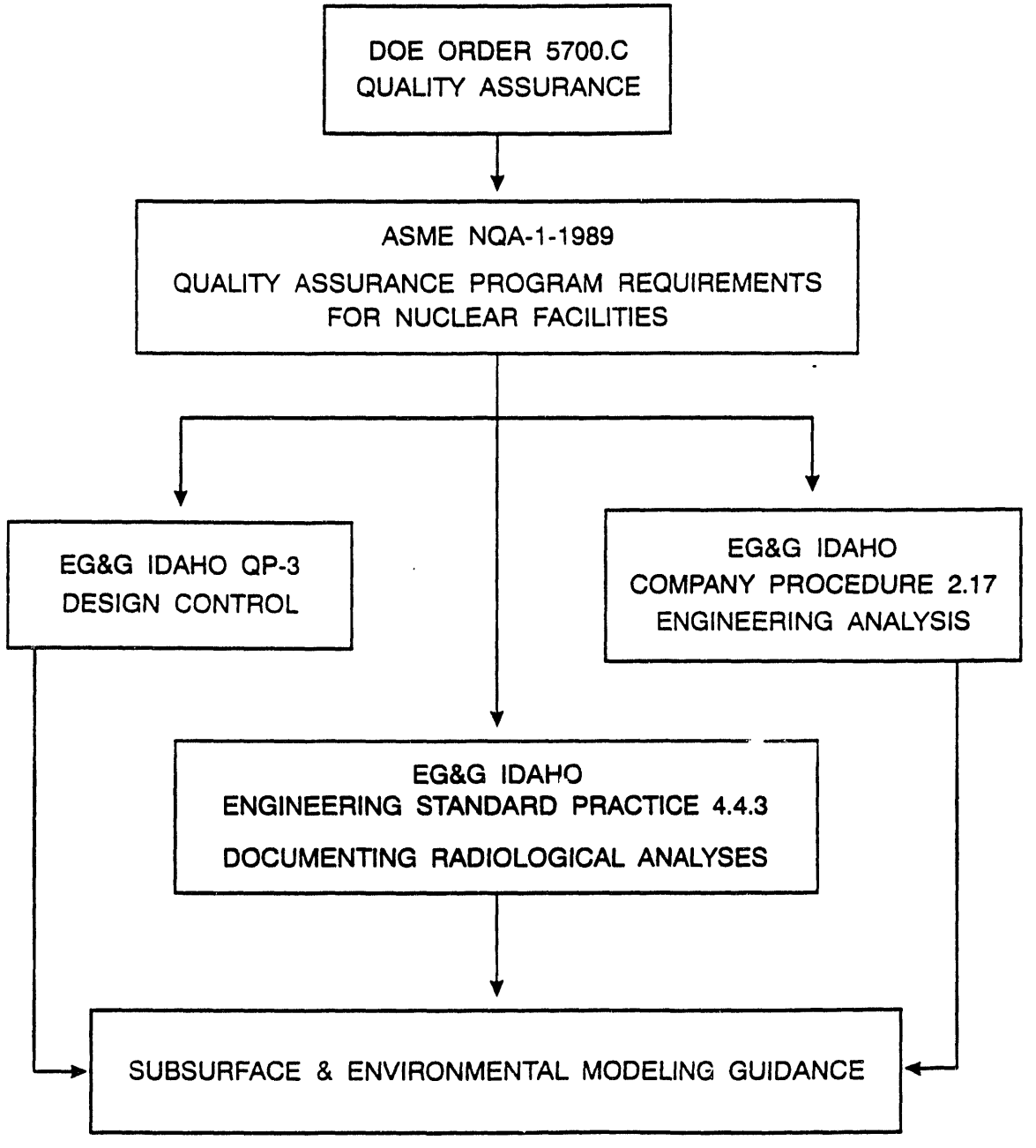

Figure E-1. Document hierarchy for documenting analyses.

5. Results of literature or background data searches.

6. All assumptions.

The primary mechanism used to document the analyses in the RWMC LLW radiological performance assessment was through engineering design files (EDFs) (EG&G Idaho Form EGG-2631). The EDF is a method of documenting analyses that provides a formal review and approval process. The author originates the EDF and forwards it to a technical reviewer, who performs a review and comments on the EDF. Comments are resolved and incorporated into the EDF as appropriate, and the EDF is forwarded to an approver, who also reviews and comments on the EDF. After resolution of comments from the approver, the EDF is finalized. The EDF cover page contains the signatures of the author, reviewer, and approver. Copies of the EDF are distributed, and a copy is kept in the EDF project file.

E-3 COMPUTER CODE QUALITY ASSURANCE

Computer code quality assurance requirements are divided into two major areas: (1) configuration management and (2) verification and validation. Configuration management requirements at EG&G Idaho come from several sources: (a) DOE orders, (b) NQA-1, (c) the EG&G Idaho Quality Manual, and (c) other codes and standards, such as those developed by the American National Standards Institute (ANSI) and the Institute of Electrical and Electronics Engineers (IEEE) (see Figure E-2). Often, the developer of a computer code distributes executable code and not source code; this means that the developer of the computer code is responsible for configuration management. This was the case for GENII, MICROSHIELD, ORIGEN2, and RESRAD. Other times, the developer distributes source code, which is then compiled on the user's computer system, and EG&G Idaho is responsible for configuration management. This was the case for PORFLOW and GWSCREEN (EG&G Idaho-developed computer codes). These computer codes are kept under configuration management according to configuration management plans (Baca 1990, Miller 1991, Matthews 1992), which contain the details on how configuration management is performed for these codes.

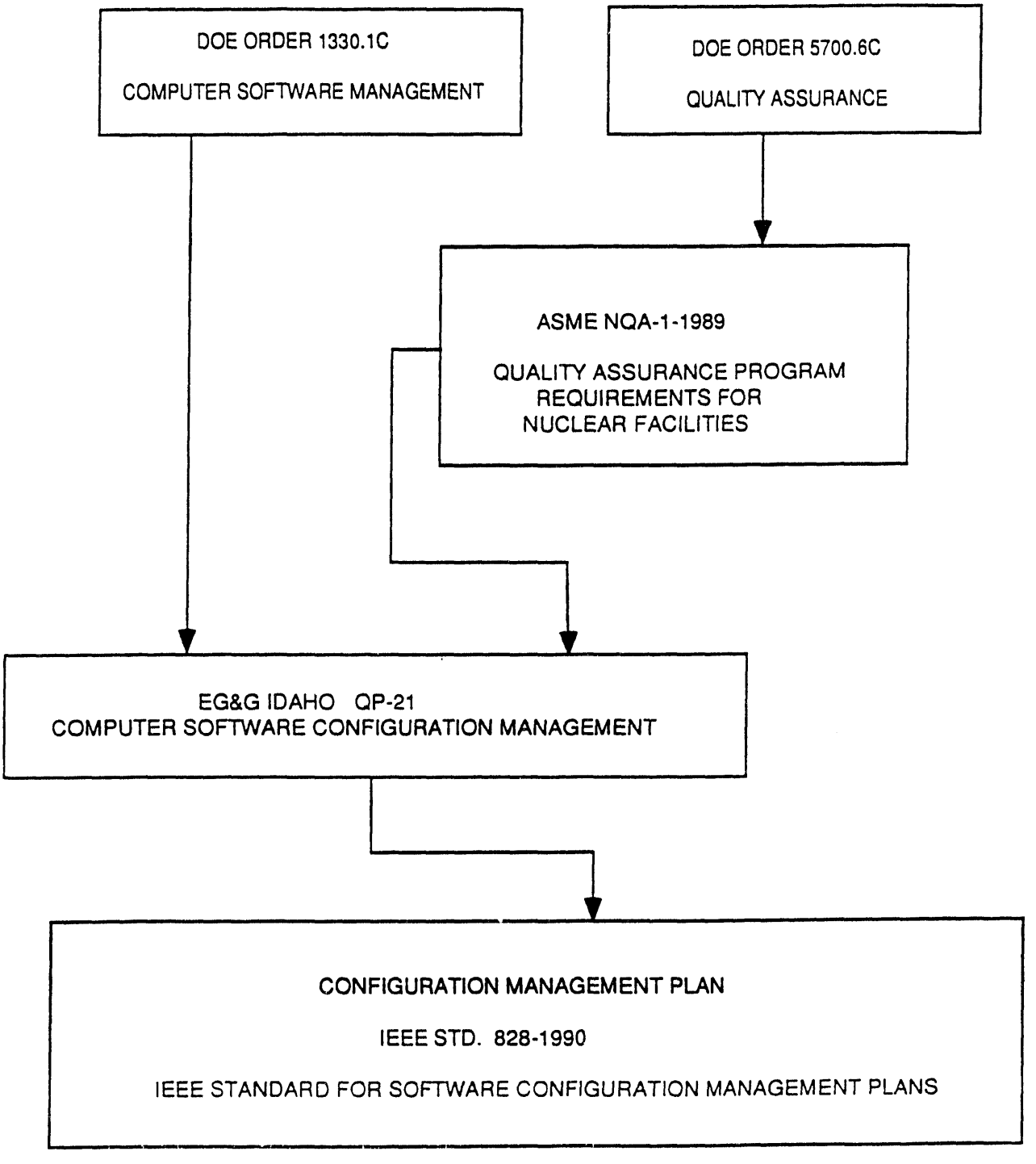

Figure E-2. Document hierarchy for configuration management requirements.

Verification and validation requirements at EG&G Idaho also come from (a) DOE orders, (b) NQA-1, (c) the EG&G Idaho Quality Manual, (d) the EG&G Idaho Company Procedures Manual, and (e) other codes and standards, such as those developed by ANSI and IEEE (see Figure E-3). The code documentation summarizes the verification and validation status:

1. GENII - GENII meets the ASME NQA-1 Basic and Supplementary Requirements for Design Control contained in Basic Requirement 3, "Design Control," and Supplementary Requirement 3S-1, "Supplementary Requirements for Design Control," which include requirements for verification and validation of computer codes.

2. MICROSHIELD - A comprehensive verification of MICROSHIELD has been performed, and comparisons to both ANSI and European Shielding Information Service benchmark shielding problems have been published.

3. RESRAD - A formal verification and validation of RESRAD has not been published by the code developers, Argonne National Laboratory. However, RESRAD is approved by the U.S. Department of Energy (DOE) for calculating site-specific residual radioactive material guidelines and radiation doses to onsite residents (see DOE Order 5400.5).

4. ORIGEN2 - A formal verification and validation of ORIGEN2 has not been published by the code developers, Oak Ridge National Laboratory. However, a number of verification activities have been undertaken, including comparison of ORIGEN2 decay heat results with both calculated and experimental values and a comparison of predicted spent fuel compositions with measured values. ORIGEN2 is used widely at DOE facilities and in the commercial nuclear industry, and it is an industry standard for calculations of the production, decay, and ingrowth of radionuclides.

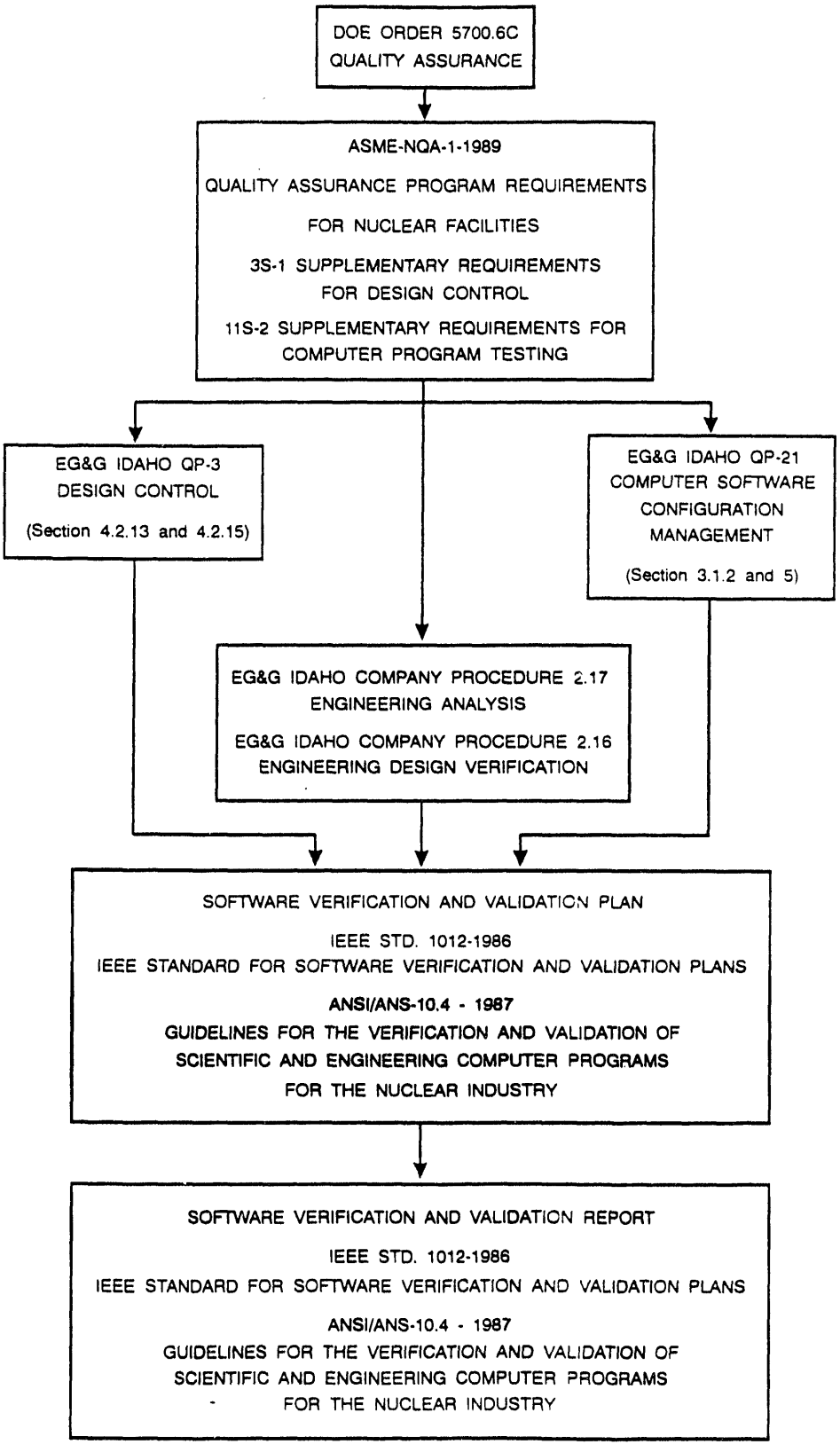

Figure E-3. Document hierarchy for verification and validation requirements.

5. GWSCREEN - Quality assurance requirements that have been completed include documentation of software requirements, theory of operation, and user documentation. Verification and validation test plans and a verification and validation report have been completed.

6. PORFLOW - An earlier version of PORFLOW, called PORFLO-3, was verified against a number of known analytical solutions and benchmark tested by making code-to-code comparisons for several flow and transport solutions. The results of the verification and benchmark testing are documented in Magnuson et al. (1990).

E-4 MONITORING DATA

Quality assurance for the environmental monitoring and surveillance programs use data quality objectives (DQOs) that provide the overall quality requirements for each data collection activity. The quantitative and qualitative DQOs are used to screen environmental data before interpreting and reporting the data. The DQOs are contained in the standard operating procedures used by the monitoring program to collect and analyze the environmental samples and data.

E-5 REFERENCES

Baca, R. G., 1990, Configuration Management and Software Control Procedure for Subsurface Flow and Transport Simulation Codes, EGG-WM-9103.

Barnard, C. J., 1992, Verification and Updating of Radioactive Waste Management Information System for the Inactive TRU and non-TRU Pits and Trenches at the RWMC SDA, EGG-ER-10519, November.

DOE (U.S. Department of Energy), 1990, "Radiation Protection of the Public and the Environment," Order 5400.5, February 8.

Magnuson, S. O., R. G. Baca, A. J. Sondrup, 1990, Independent Verification and Benchmark Testing of the PORFLO-3 Computer Code, Version 1.0, EGG-BG-9175.

Matthews, S. D., 1992, Software Configuration Plan for Controlled Code Support System, EGG-CATT-10196.

Miller, G. V., 1991, Software Configuration Plan for FLASH, FLAME, DOSTOMAN, and CAP88 Codes, EGG-CATT-9838.

Plansky, L. E. and S. A. Hoiland, 1992, Analysis of the Low-Level Waste Radionuclide Inventory for the Radioactive Waste Management Complex Performance Assessment, EGG-WM-9857, Rev. 1, June.

APPENDIX F

PERFORMANCE ASSESSMENT REVIEWS

APPENDIX F
PERFORMANCE ASSESSMENT REVIEWS

F-1 DOE-HQ PERFORMANCE ASSESSMENT PEER REVIEW PANEL PRELIMINARY REVIEW OF THE JUNE 1990 DRAFT RWMC PERFORMANCE ASSESSMENT DOCUMENT

The U.S. Department of Energy Headquarters (DOE-HQ) Performance Assessment Peer Review Panel performed a preliminary review of the June 1990 draft Radioactive Waste Management Complex (RWMC) Low-Level Radioactive Waste (LLW) Radiological Performance Assessment during August 1990. Written comments from this review were received in October 1990, and several studies were performed during FY 1991 and FY 1992 to address key concerns from the comments. These included development and documentation of site-specific hydrology models and parameters and analyses of the waste inventory data to improve knowledge of the inventory used for the performance assessment modeling. During 1993, several iterations of review and comment of the performance assessment document have been conducted. Two reviews were performed by EG&G Idaho personnel, and two reviews were performed by external subcontractor personnel to provide an independent review.

The following is a list of the comments from the DOE-HQ Performance Assessment Peer Review Panel's preliminary review of the June 1990 draft RWMC LLW radiological performance assessment document. Each comment is followed with a discussion of how the comment was resolved in this performance assessment document.

1. Assumptions made and scenarios used should be stated more clearly and justified. For example, the draft performance assessment did not clearly portray the closure scenario analyzed (5 m of earth) as a baseline case that will be compared with other alternatives as they are developed.

   RESOLUTION: Additional information has been added to Sections 1, 2, 3, and 4 to clarify the baseline closure scenario that was analyzed. Assumptions used for each scenario are described in Section 3. The sensitivity/uncertainty analysis in Section

4.2.2.2 explicitly addresses the dose impact of no closure cover during institutional control.

2. The Panel cautions the INEL about undue conservatism in the analysis. The Panel suggests that two analyses be presented: a best estimate and a health conservative analysis.

   RESOLUTION: To avoid undue conservatism in the performance assessment analyses, the base case analyses for intruder, atmospheric, and ground water were performed using available site-specific parameters. Where site-specific data were not available, conservative, but reasonable, parameters were used. In the uncertainty analysis for the performance assessment scenarios, a broader range of key parameters was used.

3. The discussion of the results of the analysis should be amplified to put into context the period of analysis (about 2 million years) and the magnitude of dose estimates. The Panel recommends including a plot of total dose versus time.

   RESOLUTION: Analyses for intruder, atmospheric, and ground water dose calculations were performed for various points in time. Peak doses were calculated for times after 10,000 years and are discussed in the text.

4. The inventory of radionuclides analyzed needs to be further refined and explained. Apparently, waste disposed of before the effective date of DOE Order 5820.2A was included in the analysis, even though such wastes are not required to be in compliance with the order. Some nuclides, such as I-129, were omitted from the inventory. Also, certain nuclides (such as Cs-137 and Sr-90) do not seem to be represented in the analysis in the proper proportions.

   RESOLUTION: Sections 2.2 and 2.3 and Appendix A contain information about the inventory that was used for the analyses. All radionuclides were explicitly evaluated for the intruder and atmospheric analyses. Key radionuclides, such as I-129 and Tc-99,

were evaluated in the ground water analyses using a screening methodology.

The primary source of I-129 at the INEL, the Idaho Chemical Processing Plant (ICPP), sends little I-129 to the RWMC. At present, I-129 is released to the atmosphere during calcining of liquid high-level waste. This iodine is not recovered or filtered; therefore, little iodine is sent to the RWMC. Previously, iodine was disposed of in the ICPP injection well.

Strontium-90 and Cs-137 will not necessarily be in fission yield proportions in INEL waste because of the large number of reactor research activities performed compared to production activities. For example, during destructive testing of nuclear fuel, Cs-137, a semivolatile radionuclide, would tend to be released from the fuel, while Sr-90 would tend to be retained. In addition, waste streams such as irradiators would also not have Cs-137 and Sr-90 in fission yield proportions. However, because a 50% Cs-137, 50% Sr-90 mix was chosen for unidentified beta-gamma (mixed fission product) activity, the quantities of Sr-90 and Cs-137 are more nearly in fission yield proportion.

Plansky and Hoiland (1992) performed a comprehensive analysis of the RWMC LLW inventory based on historical records and generator surveys; the analysis contains a more detailed discussion of the inventory associated with INEL facilities.

5. The analysis of uncertainty should discuss, to the extent possible, future activities at the Idaho National Engineering Laboratory (INEL), such as decontamination and decommissioning (D&D) of facilities.

RESOLUTION: The Environmental Restoration and D&D programs have submitted radionuclide forecast information for waste projected to be disposed of at the RWMC to the RWMIS. This information was included in the radiological performance assessment forecast inventory and, therefore, included in the performance assessment calculations. Funding is planned for future years to periodically

update and revise the RWMC performance assessment, and as additional disposal forecast information for D&D and ER activities becomes available, it will be assessed for inclusion in the performance assessment.

6. Screening of isotopes for more detailed analysis should include mobility and pathways considerations such as external exposure, as well as hazard index. Certain radionuclides, such as I-129, should be included in the detailed analysis even though excluded by the screening methodology.

RESOLUTION: The screening methodology used for the ground water pathway analysis considered the nuclide's inventory, mobility, and relative hazard (dose conversion factor). These properties are the same properties that were considered in the detailed analysis. The detailed analysis also considered dispersion in the saturated zone. Therefore, a relative ranking of the nuclide's committed effective dose equivalent using the detailed analysis will yield the same results as the ranking generated by the screening methodology. Screening analyses were not performed for the atmospheric and intruder analyses; all radionuclides were analyzed.

7. The potential for surface water impacts on the RWMC, such as localized flooding from snow melt and flooding from the Big Lost River, should be discussed in detail. The Panel sees the potential for such impacts to be significant after loss of institutional control.

RESOLUTION: The potential for flooding from the Big Lost River has been addressed by Koslow and Van Haaften (1986). They showed that the RWMC was hydraulically separated from the Big Lost River and that there was no possibility of flooding as a result of the most extreme event imaginable, the combined maximum precipitation event and the failure of Mackay Dam. This topic is addressed in Section 2.1.

Flooding from a hypothetical failure of Dike No. 2 was studied by Martineau (1990). He found that there was potential for overtopping the berm around the SDA from this hypothetical failure.

Numerical simulations of past flooding (Baca et al. 1992) have been conducted to investigate the effect of flooding pits that were open during the floods. Studies such as these will be used to continue to gain insight into the proper methodology to simulate water movement in the vadose zone.

In the uncertainty and sensitivity analysis section in Chapter 4, an explicitly time-dependent case was performed. This time-dependent analysis was performed with PORFLOW, which matches the base case scenario for the water travel time through the vadose zone, consisting of the sedimentary interbeds. These interbeds were grouped together for the purposes of simulation. A flooding event was modeled to occur shortly after the end of the institutional control period. An additional amount of water was added to the source release model over a 0.1-year period. The time-dependent leachate from the source term was assumed to immediately reach the top of the B-C interbed. The amount of water added was treated as variable. Three amounts of water were assessed corresponding to approximately 3, 5, and 10 times the annual estimated infiltration rate of 7 cm/yr. Two contaminants were considered in the flooding analysis: C-14 and I-129. These contaminants were chosen based on mobility, relatively long half-lives, and dose contributions in the base case.

8. The issue of volcanism should be presented in a descriptive and qualitative manner.

RESOLUTION: A description of volcanism has been included in Section 2.1.

9. The analysis of ground water flow is a major area for improvement of the draft performance assessment. Better modeling of ground water,

particularly the unsaturated zone, is needed to incorporate all available site-specific data.

RESOLUTION: Improvements have been made in understanding the hydraulic properties of the subsurface beneath the RWMC. These improvements have been associated primarily with the sedimentary materials and with the basalts. Studies that have been completed in recent years include

McElroy, D. L. and J. M. Hubbell, 1990, Hydrologic and Physical Properties of Sediments at the RWMC, EGG-BG-9147.

Hubbell, J. M., 1990, Perched Water at the RWMC, EGG-ER-8779.

Hubbell, J. M., 1992, "Perched Water at the Radioactive Waste Management Complex," Engineering Design File (EDF) VVED-ER-098, EG&G Idaho, Inc., December.

Hubbell, J. M., 1993, "Perched Ground Water Monitoring in the Subsurface Disposal Area of the Radioactive Waste Management Complex, FY-1993," EDF ER&WM-EDF-002293, EG&G Idaho, Inc., November.

Bishop, C. W., 1991, Hydraulic Properties of Vesicular Basalts, MS Thesis, University of Arizona, Tucson, Arizona.

Knutson, C. F., K. A. McCormick, J. C. Crocker, M. A. Glenn, M. L. Fisher, 1992, 3D RWMC Vadose Zone Model (Including FY-89-90 Basalt Characterization Results), EGG-GEO-9943.

McElroy, D. L., 1993, Soil Moisture Monitoring Results at the Radioactive Waste Management Complex of the Idaho National Engineering Laboratory, FY-1993, EGG-WM-11066, November.

Magnuson, S. O. and D. L. McElroy, 1993, "Estimation of Infiltration From In Situ Moisture Contents and Representative Moisture Characteristic Curves for the 30', 110', and 240' Interbeds," EDF RWM-93-001.1, EG&G Idaho, August.

Magnuson, S. O., 1993, A Simulation Study of Moisture Movement in Proposed Barriers for the Subsurface Disposal Area, INEL, EGG-WM-10947, September.

Wylie, A. H. and J. M. Hubbell, 1993, "Aquifer testing of wells M1S, M3S, M4D, M6S, M7S, and M10S at the Radioactive Waste Management Complex," EDF ER-WAG7-26, EG&G Idaho, Inc.

Burgess, J. D., B. D. Higgs, T. R. Wood, 1993, WAG 7 Groundwater Pathway Draft Track 2 Summary Report, EGG-ER-10731.

These studies represent a good start on understanding water movement in the subsurface. Hydrologic properties such as hydraulic conductivity, effective porosity, and moisture characteristic curves have been developed using these data sources. These hydrologic properties were used in performing the calculations for ground water transport.

However, the data that have been used can only be said to be part of the information necessary to understand water movement in the subsurface. This understanding is necessary before detailed simulations of water movement and contaminant transport can be used in the performance assessment process. To summarize from Chapter 3, there are many complex questions regarding water movement that cannot currently be answered, such as what is the amount and timing of water that infiltrates into surficial sediments inside the SDA, how does this water move from the surficial sediments into the underlying basalts, what is the role of fractures in water movement into and through the basalts, what is the role of the interbeds in creating perched water, and what is the net travel time of infiltrating water down to the aquifer?

Field measurements of moisture content and matric potential will need to be measured at multiple depths and multiple locations as a function of time in order to get answers to some of the questions listed above. Two studies are currently being funded to collect this type of much-needed data. The first consists of monitoring moisture content and matric potential in the surficial sediments at two separate locations inside the SDA. These two locations were also monitored for three years from 1987 to 1989. This data base is being expanded to allow estimates to be made of rates of water infiltration, its timing, and spatial distribution. The number and locations of sample points may provide a basis for answering questions about infiltration for the whole SDA.

A second ongoing study consists of a perched water monitoring network. Six wells that either have or are known to occasionally have perched water in them are being monitored with downhole

pressure transducers connected to data loggers. Measurements will be made on these perched water bodies above both the 110- and 240-ft interbeds. Past measurements of perched water levels have shown transient responses. The objective of this study is to improve the consistency of these measurements and thereby have a possibility of correlating background infiltration events from snowmelt at the surface to rises in perched water levels at depth. If this correlation can be made, realistic estimates of water travel times under background conditions can be made. Data collected during the study may also necessitate changes in the current conceptual model of water movement at the RWMC.

A study has been proposed but not funded to look at the movement of water from the surficial sediments into the basalts. This study would consist of using an existing exposed face of the active disposal pit. Instrumentation would monitor moisture movement in both sediments and basalts to measure water movement in response to a series of induced and background infiltration events. This instrumentation would have to be innovative in order to determine the effect of fractures in the basalt. A study such as this would dramatically improve the understanding of movement of water in the subsurface.

The current modeling approach contained in the RWMC performance assessment has made improvements over the previous draft RWMC performance assessment in that more site-specific information was used. Studies are under way or proposed that should improve our understanding of subsurface water movement, and updates to this RWMC performance assessment are planned to incorporate the results.

10. Regulatory references throughout the document should be updated. Examples are 40 CFR 61, 40 CFR 141, BEIR IV.

RESOLUTION: Regulatory references have been updated throughout the document (primarily in Sections 1, 3, 4, and 5).

11. The source term analysis in the June 1990 draft performance assessment presented an apparent correlation between container lifetime and leach rate from the waste, which is not intuitive. This should be investigated and justified.

RESOLUTION: Release from waste containers in this revision to the performance assessment document was analyzed as part of the hydrologic transport conceptual model. The discussion on container lifetime and release rate has been expanded and is contained in Section 3.3.1.

12. The treatment of erosion of the final cover (following institutional control) should be expanded and clarified.

RESOLUTION: Information on soils and the potential for erosion has been expanded and is discussed in Section 2.1.2. Section 3.1 discusses erosion of the final cover.

13. The technical validity of AIRDOSE for estimating impacts to a receptor far from the RWMC should be examined. If AIRDOSE is not technically appropriate, results from a more technically valid code (such as MESODIF) should be presented as well as those from AIRDOSE.

RESOLUTION: The GENII computer code was used for atmospheric and intruder analyses in the RWMC radiological performance assessment instead of the AIRDOS (CAP-88) or MESODIF computer codes. GENII was chosen because it has several advanced features such as a transparent decay and ingrowth data base, models applicable exposure pathways, and meets the appropriate quality assurance requirements. GENII also has an extensive user population across the U.S. and has been used in other projects at the INEL, such as the New Production Reactor Environmental Impact Statement and the INEL Environmental Restoration and Waste Management Environmental Impact Statement. Although GENII does not use site-specific formulations for σ_y and σ_z, the Pasquill-Gifford formulations of σ_y

and σ_z used in GENII yield results close to the site-specific formulations.

14. The appendix on computer codes (Appendix B in the June 1990 draft RWMC LLW radiological performance assessment; Appendix D in the April 1994 document) should include all computer codes used in the performance assessment. The quality assurance program for computer codes should also be discussed.

    RESOLUTION: Appendix D of this performance assessment contains a description of all computer codes used in the performance assessment, including quality assurance.

15. The quality assurance program for each aspect of the performance assessment should be discussed.

    RESOLUTION: Quality assurance for the performance assessment is discussed in Appendix E.

16. Figures used to portray pathways analysis by the DOSTOMAN code should be clarified. The use of artistic conceptual diagrams in addition to the technical figures should be considered.

    RESOLUTION: The use of conceptual diagrams and figures has been included in the performance assessment to portray pathways analyses. The majority of these are contained in Section 3, where the methodology and assumptions are described for the various pathways. In addition, DOSTOMAN was not used in the revision of the performance assessment.

17. Appropriate credit should be taken for engineered barriers used at the RWMC. Justification for the credit taken must be provided in the performance assessment.

    RESOLUTION: The performance assessment has been revised to assess an engineered cover during the institutional control period and

used simulated estimates of cover performance completed in September 1993. Engineered barrier/closure cover test plots are planned to be constructed in future years to provide these test data. The proposed closure configuration as currently planned is discussed in Chapter 3.

18. The Panel noted a lack of consistency in the application of intruder scenarios for different waste streams. INEL should strive for consistent use of intruder scenarios as the performance assessment is finalized.

RESOLUTION: The discussion of intruder scenarios has been significantly expanded, and the site-specific attributes have been included. Consistent application of intruder scenarios for RWMC LLW has been achieved by performing a more rigorous suite of site-specific analyses.

19. All activities at the RWMC, even though not regulated by DOE Order 5820.2A, Chapter 3, should be presented as information. In particular, the potential for chemicals to cause enhanced migration of radionuclides should be considered.

RESOLUTION: On December 9, 1991, a Federal Facility Agreement and Consent Order (FFA/CO) for the INEL was signed. The FFA/CO is a comprehensive environmental cleanup agreement between the DOE, U.S. Environmental Protection Agency, and the State of Idaho. The FFA/CO requires DOE to perform specific remediation activities and meet certain legally-enforceable deadlines. Major INEL facilities and waste management units scheduled for environmental restoration by the DOE Idaho Field Office are identified as Waste Area Groups (WAGs) and are generally grouped by facility. Environmental restoration activities include an assessment phase to characterize the nature and extent of contamination and a cleanup/remediation phase. The cleanup/remediation phase is implemented when the extent and nature of the contamination constitutes a potential threat to human health and safety or the environment.

The environmental restoration projects for the RWMC are currently in the planning or assessment phase. Data on chemical inventories that were disposed of in the RWMC are being compiled; however, at the time of these performance assessment analyses, the inventories had not been finalized. A particular concern is the interaction between the chemicals and the actinides. In general, most actinides adsorb highly and are relatively immobile. However, under some conditions, actinides may be complexed with organic chemicals, and under these conditions, actinides are mobile.

Mobility of radionuclides is typically modeled through the use of sorption coefficients that describe the equilibrium partitioning between the solid (immobile) and liquid (mobile) phase. The impacts of chemical complexing agents in the RWMC are planned to be evaluated using the sorption coefficient of K_d. In this revision of the performance assessment, we have attempted to address this problem in the uncertainty/sensitivity analysis by evaluating the effects of using K_d values from different literature sources. These K_d values varied significantly from the K_d values used for the base case. For example, in one of the uncertainty/sensitivity cases, the plutonium K_d value was reduced from 200 to 6 mL/g.

It is currently unknown what complexing agents are in the RWMC SDA and how effectively these agents increase the mobility of actinides in the SDA. The first step was taken in this performance assessment--evaluating the sensitivity of the results to changes in the actinide mobility by changing the K_d value. As information becomes available from studies and risk assessments associated with the environmental restoration projects, the information will be evaluated and judged for consistency with the assumptions in the RWMC LLW performance assessment.

The RWMC LLW radiological performance assessment is planned to be updated periodically; therefore, new information can be incorporated as appropriate.

20. Supporting data, such as detailed input data, results of intermediate calculations, etc., should be contained in a separate document that is referenced in the performance assessment.

RESOLUTION: Supporting data, such as detailed input data, computer output, etc., for the various performance assessment scenarios are contained in separate EDFs. These EDFS are referenced in the performance assessment document.

21. The title of the performance assessment document should be revised to reflect that the scope of the analysis is limited to low-level waste.

RESOLUTION: The title has been changed to reflect that this radiological performance assessment is limited to LLW.

22. The discussion of the use of factorial design in uncertainty analysis should be clarified.

RESOLUTION: The factorial design used in the June 1990 RWMC performance assessment document has been changed. The uncertainty analyses have been expanded in Chapter 4, and they are presented in terms of projected doses. In addition, sensitivity analyses were used to identify important parameters.

F-2 INDEPENDENT PEER REVIEW OF THE APRIL 1993 DRAFT RWMC PERFORMANCE ASSESSMENT DOCUMENT

DOE Order 5820.2A requires that each DOE facility with a radioactive waste disposal facility complete a radiological performance assessment to project long-term impacts from the facility and to determine whether the facility is in compliance with DOE's objectives for long-term performance.

DOE Order 5820.2A also requires the formation of a Performance Assessment Peer Review Panel (PRP). The PRP is comprised of representatives from each DOE site with a waste disposal facility and an additional representative from the DOE waste generators. The PRP also has interfacing advisors from EPA and NRC. The PRP is tasked with reviewing all performance assessments to ensure that they are technically adequate. The PRP makes a determination and communicates its opinion to DOE-HQ (EM-35), which makes a final decision on acceptability.

The radiological performance assessment for the RWMC at the INEL has undergone several iterations. The PRP completed its preliminary review of the document in August 1990. Since that time, EG&G Idaho has been modifying the performance assessment to incorporate the Panel's recommendations. In preparation for submission to the PRP for a "final" review, DOE-ID tasked the Environmental Resources Management-Program Management Company and their subcontractor, Rogers and Associates Engineering Corporation (RAE), to conduct an independent peer review of the RWMC radiological performance assessment. A team of technical experts was proposed and approved by DOE-ID in March 1993. Members of the review team were given copies of the performance assessment document in late April. After a 6-week review period, the team met in mid-June with DOE-ID and EG&G Idaho to discuss their findings. This section summarizes the major issues and comments raised at the meeting and makes recommendations for possible resolution of the identified issues.

F-2.1 Review Team Recommendations

S-1. In the PA document, all four performance objectives in DOE Order 5820.2A must be addressed.

POSSIBLE APPROACH FOR RESOLUTION: DOE Order 5820.2A contains four performance objectives for the disposal of low-level radioactive waste. Each of these should be addressed in the performance assessment document. The text should include a discussion of the performance objective and where it fits in the assessment or the reasoning/justification for not including a particular performance objective should be presented.

EG&G RESOLUTION: The regulatory section of the performance assessment document has been revised and expanded to show specifically to which regulations the performance assessment is assessing compliance.

S-2. The assessment of compliance with DOE Order 5820.2A performance objectives should be presented at 10,000 years. Additional discussion of peak dose beyond 10,000 years should also be presented.

POSSIBLE APPROACH FOR RESOLUTION: EG&G Idaho should indicate that, to assess compliance with the performance objectives related to potential doses to hypothetical individuals or inadvertent intruders, they developed credible exposure scenarios for a variety of pathways. Based on these exposure scenarios and pathways, they calculated conservative estimates of potential doses for a time period of 10,000 years for most radionuclides. For certain of the more mobile, longer-lived radionuclides (including daughter products), they carried the analyses out for longer time periods to determine the times of occurrence and the peak potential doses from the radionuclides.

The emphasis should be placed on the first 1,000 or 10,000 years since it becomes increasingly difficult to have confidence in the assumptions underlying the analyses for significantly longer periods of time. The performance assessment should clearly state that the calculations determine potential doses rather than expected doses. Expected doses should be significantly lower due to the conservatism in the analyses.

EG&G RESOLUTION: The performance assessment has been revised so that assessment of compliance with DOE Order 5820.2A performance objectives is presented at 10,000 years. Additional discussion of peak dose beyond 10,000 years is also presented.

S-3. Analysis of facility performance should start at a contemporary time and proceed with the inventory as presently projected from 1964 onward.

POSSIBLE APPROACH FOR RESOLUTION: EG&G Idaho should start the analysis at the present time to provide an adequate basis for reasonable assurance that the ongoing disposal of LLW will not result in failure to meet the performance objectives. Monitoring should be used to confirm the analyses; however, monitoring should not be used in place of a current performance assessment. If the review team's recommendation on splitting the pre- and post-1988 inventories is implemented, a good point to begin the analysis would be 1988.

The waste inventory should be updated each year to account for additional disposed LLW, radioactive decay, and daughter in-growth. EG&G Idaho should provide a concise explanation of why the waste inventory projected from 1964 onward was used in the performance assessments.

EG&G RESOLUTION: The waste inventory for assessment in the performance assessment has been revised to include buried LLW since mid-1984 and LLW projected for the future. Although DOE Order 5820.2A applies only to LLW disposed of after September 26, 1988, LLW disposed of before this date was included in the radiological performance assessment. The Environmental Restoration (ER) Program at the INEL will assess waste buried in the SDA from 1952 through 1983 in accordance with the National Contingency Plan under CERCLA. The year 1983 was selected as the cutoff date for waste to be assessed under CERCLA because waste containing the hazardous materials mercury and cadmium were disposed of in the SDA as late as June 1983. Therefore, the trenches, pits, and soil vault rows that were open before this

date could potentially contain mixed waste, which falls under the domain of the ER program and will be assessed under CERCLA. Because it is impractical to remediate only part of a pit or soil vault row, all waste buried in Pit 16 and Soil Vault Row 13 will be assessed under CERCLA even though Pit 16 closed October 25, 1984, and Soil Vault Row 13 closed on December 21, 1984. Soil Vault Row 14 opened on October 13, 1984, and Pit 17 opened on May 5, 1984; they should only contain LLW not the mixed waste described previously. Therefore, that is a logical point from which to begin the radiological performance assessment, and it provides an effective point of interface with the ER program. This will ensure that all waste is accounted for either in the radiological performance assessment performed under DOE Order 5820.2A or in the baseline risk assessments performed under CERCLA. Although current plans are to replace the existing RWMC by approximately 2002, anticipated disposals of LLW through CY 2020 are included in the RWMC radiological performance assessment to provide future flexibility because of uncertain funding levels needed to support the development of a new disposal capacity.

For mobile nuclides, such as H-3, C-14, and I-129, the waste emplacement rate from 1984 to 2020 will be modeled. For nuclides with little mobility, such as plutonium and uranium isotopes, the total inventory at 2020 will be used because little of the nuclide will migrate from the waste site during the emplacement process.

S-4. Expand the discussion of the assumed site configuration at closure used as the basis for this assessment and discuss any planned refinements to the closure configuration in future assessments.

POSSIBLE APPROACH FOR RESOLUTION: The performance assessment makes the assumption of long-term stability over the period of interest such that the final site grade is reduced to original ground elevation. Under this assumption, trench covers remain intact. Exposure of the waste because of wind or water erosion or intrusion by burrowing animals is not analyzed. EG&G Idaho should

make a clear commitment that the design of the trench covers and the site closure plan will provide sufficient long-term protection so as to ensure that this assumption continues to be valid. This should include a commitment to evaluate the design of the trench covers and the site closure plan for the various failure modes that were eliminated from the performance assessment.

EG&G RESOLUTION: The performance assessment has been revised to assess an engineered closure cover during the institutional control period because much of the modeling work on the cover performance was completed in September 1993. There are presently no site-specific test data to support the theory of an intact cover after institutional control; however, engineered barrier/closure cover test plots are planned to be constructed in future years to provide this test data. The proposed closure configuration as currently planned is discussed in Chapter 3.

S-5. Clarify the discussion of what waste is included in the performance assessment. Specifically state that this performance assessment applies to all wastes (operations, D&D, ER, and reclassified TRU) as long as the physical, chemical, and radiological characteristics specified in the assessment are met.

POSSIBLE APPROACH FOR RESOLUTION: Explain that the RWMC will accept low-level radioactive waste regardless of its programmatic origination, as long as the waste meets the waste acceptance criteria (and therefore radionuclide inventory limits) for the facility. If new waste streams develop that have physical, chemical, or radiological characteristics different from those allowed in the Waste Acceptance Criteria (and therefore not projected by the performance assessment) the waste cannot be accepted for disposal until the performance assessment can be modified to determine if the new waste will cause the facility to exceed its radiological performance objectives.

EG&G RESOLUTION: The discussion of the Waste Acceptance Criteria in Chapter 2 has been revised to include this point.

S-6. It is recommended that the results of the assessment be presented in terms of pre- and post-1988 inventories. The post-1988 inventory should be used to demonstrate compliance with DOE Order 5820.2A. The pre-1988 assessment results may then be combined (with the post-1988) as appropriate.

POSSIBLE APPROACH F· RESOLUTION: Because DOE Order 5820.2A only requires the performance assessment to include waste disposed of since 1988 (the effective date of the order), it is appropriate to separate the performance assessment for the RWMC into two parts--one using the inventory before 1988 and one using the inventory from 1988 on. Compliance with the performance objectives would only need to consider the inventory from 1988 and later. A combined run using the entire inventory may also be helpful for comparing calculated results with monitoring data.

EG&G RESOLUTION: The inventory for use in the performance assessment has been changed to be from mid-1984 through 2020. Because there is only a small amount of pre-1988 waste, it does not make sense to separate the inventory into pre-1988 and 1988-2020 results to show compliance; therefore, compliance will be assessed for the entire inventory (mid-1984 through 2020).

S-7. We believe that the biointrusion scenarios are nonconservative, especially with respect to animal intrusion (rodents and ants).

POSSIBLE APPROACH FOR RESOLUTION: The report would be improved by a stronger discussion on why biointrusion was ruled out or provide such an analysis. It is important that the criteria used to include/exclude biointrusion in the performance assessment should be consistently applied to both plants and animals. There are references such and Reynolds and Laundre (1988, Health Physics, 54,4) cited in the report which need more in-depth discussion and comparison to situations at the RWMC. Because the above reference studied both disturbed and undisturbed sites, the report should provide a detailed discussion of Reynold's data to justify exclusion of rodent intrusion. Finally, a look at the literature

on harvester ant burrowing would be prudent. Perhaps a calculation or two may be needed to justify the exclusion of ants as biointruders. In summary, the information is available to exclude biointrusion as a significant contributor to dose but a more organized and thorough discussion needs to be made so it is clear to the reader.

EG&G RESOLUTION: The analyses have been revised to incorporate biointrusion by ants, but not rodents. Site-specific studies on disturbed and undisturbed areas near the SDA have shown that rodent biointrusion is not credible. The text has been revised, as suggested, to more thoroughly discuss the ant and rodent studies.

S-8. Need to further justify the choice of a 100-year unsaturated zone ground water travel time. Include comparisons with regional models, discussion or explanation of the contamination at the 110- and 240-foot interbeds including reasons that these incidents should not be used as an argument against the 100-year unsaturated zone travel time. Sensitivity analyses should be used to address the potential impacts of unsaturated zone travel times of less than 100 years.

POSSIBLE APPROACH FOR RESOLUTION: EG&G Idaho should clearly indicate that the 100-year ground water travel time in the unsaturated zone was used for two purposes, namely (1) to determine a conservative estimate of the amount of infiltration that may contact the disposed LLW and then reach the water table and (2) to provide for decay of dissolved radionuclides during the transport through the unsaturated zone to the water table.

With respect to the latter usage, EG&G Idaho should vary the ground water travel time in the vadose zone over a range of 10 to 1,000 years in a sensitivity analysis in order to determine the effect significantly shorter and longer ground water travel times in the unsaturated zone would have on the analysis demonstrating compliance with the performance objectives.

EG&G RESOLUTION: The hydrologic conceptual model used in the performance assessment has been revised, and a draft has been reviewed by independent peers (personnel from the U.S. Geological Survey, EG&G Idaho Chemical and Radiological Risk Assessment, RAE, Environmental Resources Management Program Management Company, and Science Applications International Corporation) so that the approach will be technically defensible. The revised model has resulted in different travel times, which are less than 100 years.

S-9. The performance assessment should include a time-dependent infiltration case based on a pulsed infiltration event.

POSSIBLE APPROACH FOR RESOLUTION: The current modeling of the vadose zone, which assumes a 100-year ground water travel time, could be strengthened by evaluating the effects of time-dependent precipitation/infiltration events. An assumption of steady state constant infiltration could lead to very different travel times than a case where spring runoff is included in the simulation.

Because most infiltration is likely to occur in the spring, the effects of the time-dependent surface boundary conditions could provide insight into the vadose zone flow system. The PORFLOW code should be capable of such a simulation. The results could provide valuable supporting information for the 100-year travel time assumption.

EG&G RESOLUTION: The base case ground water scenario in the April 1994 performance assessment document consisted of a constant infiltration rate of 7 cm/yr at depth. The assumption in the hydrological conceptual model was that this infiltration occurred primarily at the surface during the spring and infiltrated rapidly down to the first interbed (B-C). In effect, this was a mini-flood every year during spring snowmelt. The near field source release model assumed a constant infiltration rate throughout the year, which resulted in a higher overall mass release than would

be expected from the pulse infiltration event. In the base case, an explicitly time-dependent case was not included.

However, in the uncertainty and sensitivity analysis section in Chapter 4, an explicitly time-dependent case was performed. This time-dependent analysis was performed with PORFLOW, which matches the base case scenario for the water travel time through the vadose zone, consisting of the sedimentary interbeds. These interbeds were grouped together for the purposes of simulation. A flooding event was modeled to occur shortly after the end of the institutional control period. An additional amount of water was added to the source release model over a 0.1-year period. The time-dependent leachate from the source term was assumed to immediately reach the top of the B-C interbed. The amount of water added was treated as variable. Three amounts of water were assessed corresponding to approximately 3, 5, and 10 times the annual estimated infiltration rate of 7 cm/yr. Two contaminants were considered in the flooding analysis: C-14 and I-129. These contaminants were chosen based on mobility, relatively long half-lives, and dose contributions in the base case.

S-10. It is recommended that the fractured flow analysis be corrected or removed.

POSSIBLE APPROACH FOR RESOLUTION: Lamb (1) presents the following simplified equation for estimating the quantity of fluid flow through fractures:

$$Q = (G f_s a_f^3 H)/(12\ ) \qquad \text{(F-1)}$$

where

Q = fluid flow through the fracture (m^3/s)
G = specific weight of water (kg/m^2s^2)
  = dynamic viscosity (kg/ms)
f_s = fracture length normal to flow (m)

a_f = fracture width (m)

H = gradient of piezometric head (dimensionless).

Neuzil and Tracy (2) have extended Lamb's model for different widths within the fracture. Equation (F-1) can also be expressed in terms of the fluid velocity through the fracture zones, using the relation

$$Q = V_f f_s a_f \qquad \text{(F-2)}$$

where V_f is the fracture flow velocity. Combining Equations (F-1) and (F-2) gives

$$Vf = (Ga_f^2)/(12\ ). \qquad \text{(F-3)}$$

Equation (F-3) is a more realistic presentation of flow through fracture and should give more realistic fracture widths than the V_f equation in the report.

EG&G RESOLUTION: The hydrology conceptual model has been revised as previously indicated in the planned resolution for Comment S-8, and the fracture flow analysis has been removed. The revised hydrological conceptual model assumes flow through the fracture basalt system is instantaneous. This assumption supersedes the fracture flow analysis from the April 1993 draft performance assessment document.

S-11. Dispersion of contamination in the saturated ground water zone should be incorporated in the saturated transport model used to demonstrate ground water protection.

POSSIBLE APPROACH FOR RESOLUTION: One of the comments about the performance assessment was that the analysis did not consider the protection of ground water resources. As discussed above, the authors must determine the relevance of existing ground water protection standards to the Snake River Plain Aquifer in the

vicinity of the RWMC. The need for a quantitative analysis demonstrating compliance with relevant ground water protection standards will be decided upon as part of that determination.

If further analyses are required to demonstrate compliance with ground water protection standards, the existing ground water modeling analysis should be modified to account for radionuclide dispersion in the aquifer. Lack of consideration of dispersion will tend to underestimate contaminant travel time to offsite users of ground water and tend to overestimate radionuclide concentrations in the ground water. These effects will generally be small over short distances, e.g., to a 100-m well. However, dispersive effects over distances relevant to the protection of regional ground water supplies may be significant and should be considered in a realistic assessment of the impacts of the RWMC.

EG&G RESOLUTION: Dispersion was included in the saturated zone transport model (see page 3-17, number 5 and Equations (D-28) through (D-31) in Appendix D of April 1993 draft performance assessment document). However, text has been added to Section 3.4 of the performance assessment to clarify this point.

S-12. The radon calculations associated with intruders should be reviewed. It appears that an order-of-magnitude error may be contained in the present analysis.

POSSIBLE APPROACH FOR RESOLUTION: The indoor radon intruder scenario description in the report does not contain sufficient information to reproduce the results. As an independent check on the analysis, the following calculation was made.

1. It was assumed that there is 22 Ci of Ra-226 in the waste at the time of exposure.

2. It was assumed that the volume of the waste is 470,000 m^3.

3. It was assumed that the waste density is about 1.5 g/cm^3 at the time of the exposure.

4. This gives an average Ra-226 concentration of 31.2 pCi/g in the waste that is in contact with the foundation of the house.

5. Generic studies relating the concentration of Rn-222 inside a dwelling to the Ra-226 concentration in the subsoil give a range of .2 to 1 pCi Rn-222/L in the house per pCi Ra-226/g in the soil (1-4). These values are obtained with a two-dimensional, elliptical geometry diffusive-advective code written explicitly for estimating indoor radon concentrations (2,5). This analysis assumes a value of 0.33 for this ratio.

6. The estimated indoor radon concentration is 10 pCi/L, based on items 4 and 5.

7. NCRP 77 gives an indoor radon and radon-daughter lung dose conversion factor of 1.2 x 10^3 mrem per pCi/L of radon in the dwelling. This assumes a 50 percent equilibrium between radon and its short-lived, alpha-emitting daughters.

8. Applying the dose conversion factor in item 7 to the estimated indoor radon concentration in item 6, gives annual lung dose of 12,000 mrem/year. Applying a weighting factor of .12 for the lung (NCRP 91) gives an effective dose equivalent of 1,400 mrem/yr.

9. Thus, I obtain a result that is very nearly a factor of 1000 greater than the effective dose equivalent given in the report. Could it be a rem-mrem conversion?

References

1. V. C. Rogers and K. K. Nielson. "Benchmark and Application of the RAETRAD Model," 1990 International Symposium on Radon and Radon Reduction Technology EPA/609/9-90/005c.

2. K. K. Nielson, et al. RAETRAD Version 3.1 Users Manual, RAE report for the State of Florida Department of Community Affairs and the Environmental Protection Agency. RAE-9127/10 2, October 1992.

3. W. W. Nazaroff and A.V. Nero, Radon and Its Decay Products in Indoor Air, New York: Wiley & Sons 1988.

4. K. K. Nielson, et al. "Development of a Lumped Parameter Model of Indoor Radon Concentrations," RAE report for the State of Florida Department of Community Affairs and the Environmental Protection Agency, RAE-9127/10-6.

5. V. C. Rogers and K. K. Nielson, 1992, "Multiphase Radon Generation and Transport in porus materials," Health Physics 60, pp. 807-815, 1992.

EG&G RESOLUTION: The difference between the radon calculation in the April 1993 performance assessment document and the RAE calculation is the degree of penetration of the waste by the basement. The RAE calculation appears to be based on a complete penetration of the waste; the April 1993 performance assessment calculation is based on a 0.6-m penetration of the waste. The calculations in the April 1993 performance assessment were revised in this performance assessment to incorporate the geometry of the soil vaults and to use measured data from instrumented basement structures at Colorado State University.

F-2.2 General Comments

G-1. The presentation of information in the performance assessment document needs to be reorganized to group like information and analyses together (e.g., geochemical information is now presented in three different locations).

POSSIBLE APPROACH FOR RESOLUTION: This comment is self explanatory. An additional example is the discussion of local flooding in under meteorology rather than under hydrology.

EG&G RESOLUTION: Performance assessment text has been revised; the conceptual model is described in Chapter 3.

G-2. The sensitivity/uncertainty analysis needs to be expanded. To be of more use, express the results of the sensitivity/uncertainty analyses in terms of compliance (i.e., dose).

POSSIBLE APPROACH FOR RESOLUTION: A number of items are unclear from the current presentation of the uncertainty analysis. These include 1) how the analysis was conducted, 2) whether all potentially important sources and ranges of uncertainty have been considered, and 3) what impacts the parameter uncertainties considered in the analysis have on the performance assessment results.

A clear description of the approach taken in conducting the uncertainty analysis is missing from the performance assessment report. For instance, it is not clear how the parameters considered in the uncertainty analysis were selected. It also is not clear how values for these parameters were chosen. As currently presented, the analysis appears a bit haphazard.

The parameters chosen for consideration in the uncertainty analysis should be those having the greatest potential effect on the results of the performance assessment. One way in which these parameters may be identified is through a sensitivity analysis. It is not clear whether such an analysis was conducted, although it appears that it was not.

Once selected, the parameters considered in the uncertainty analysis should be varied over a reasonable range to assess the effect uncertainty in its value may have on the performance assessment results. Two values were considered in defining the uncertainty for many of the parameters considered in the RWMC performance assessment. It is not clear what the selected values are intended to represent. Explicit justification for these selections should be included in the report.

It appears that potentially important sources of uncertainty are omitted from the uncertainty analysis. The current report

discusses uncertainties in portions of the inventory considered in the analysis yet it is unclear what impact these uncertainties may have on dose projections. Based on information presented during the review meeting with EG&G Idaho personnel, it appears this omission is to be addressed with respect to assignment of mixed fission product to specific radionuclides. The authors are cautioned, however, to carefully consider uncertainties in other portions of the source term that can be reliably bounded.

Another potentially important source of uncertainty concerns the potential for small mammals to intrude into the waste during the construction of burrowing. Specific guidance has been provided elsewhere with respect to this source of uncertainty.

The ranges of uncertainty considered in the analysis for selected parameters appear questionable, most notably with respect to ground water travel time. Data provided in the performance assessment report supports ground water travel times much less than the 100 and 1,000-year travel times considered in the assessment. While one can argue all day about what the range of parameters should be, the important point is to define a range of parameter values that is supported by the available data.

The results of the uncertainty analysis should be reported consistently for all parameters. For example, the effect of uncertainties in inhalation and food ingestion rates are provided in terms of doses. In contrast, uncertainties associated with distribution coefficients are discussed in terms of changes in radionuclide concentrations but are not reported in terms of the effect on projected ground water doses. Here, then, the reader is left to decide what the impact uncertainties in these coefficients have upon the projected doses.

It is recommended that all results of the uncertainty analysis be presented in terms of projected doses. This is consistent with the fact that the performance objectives are stated in terms of doses to the general public and the intruder. Furthermore, this

approach provides the most concise summary of the analysis for the reader, while eliminating the need for interpretation on his or her part.

EG&G RESOLUTION: The uncertainty analyses in the performance assessment have been expanded in Chapter 4, and they are presented in terms of projected doses. In addition, sensitivity analysis was used to identify important parameters.

G-3. Revise the presentation of the conceptual model to include both the elements of the model and how each element functions.

POSSIBLE APPROACH FOR RESOLUTION: EG&G Idaho needs to provide better descriptions of the elements of the conceptual model, how these elements fit together, how each of these elements function, and the interdependence of the elemental functions.

EG&G RESOLUTION: Performance assessment text has been revised with the conceptual model described in Chapter 3.

G-4. Expand the justification for selecting the various computer codes used in the performance assessment. Expand the description of how each code is used to implement the elements and functions of the components of the conceptual models.

POSSIBLE APPROACH FOR RESOLUTION: Self explanatory.

EG&G RESOLUTION: Performance assessment text has been revised to expand the rationale on using the computer codes.

F-3 REFERENCES

Baca, R. G. et al., 1992, A Modeling Study of Water Flow in the Vadose Zone Beneath the Radioactive Waste Management Complex, EGG-GEO-10068.

Koslow, K. N. and D. H. Van Haaften, 1986, Flood Routing Analysis for a Failure of Mackay Dam, EGG-EP-7184, June.

Martineau, R. C. et al., 1990, Hydrologic Modeling Study of Potential Flooding at the Subsurface Disposal Area from a Hypothetical Breach of Dike 2 at the Idaho National Engineering Laboratory, EGG-WM-9502.

Plansky L. E. and S.A. Hoiland, 1992, Analysis of the Low-Level Waste Radionuclide Inventory for the Radioactive Waste Management Complex Performance Assessment, EGG-WM-9857, Revision 1, June.

DATE
FILMED
9/8/94

END